SFERA-III

Solar Facilities for the European Research Area

Training for Industries, Almería, 26. – 29.04.2022:
“Optimization of CST plant output by optical and thermal characterization and target-oriented O&M”

as part of SFERA-III Networking Activities
Daniel Benítez, DLR

NETWORKING

THIS PROJECT HAS RECEIVED FUNDING FROM THE EUROPEAN UNION’S HORIZON 2020 RESEARCH AND INNOVATION PROGRAMME UNDER GRANT AGREEMENT NO **823802**

SFERA-III
Solar Facilities for the European Research Area

SFERA-III

- Networking Activities
- Transnational Access
- Joint Research Activities

SFERA-III
Solar Facilities for the European Research Area

SFERA-III

- **Networking Activities**
  - **Capacity building and training activities:** Doctoral Colloquia, Summer schools and On-Site Training for Industries
  - **Scientific and Technological Exchanges:** Workshops, Exchange of personnel, Short-term training for technical staff and scientists within SFERA-III partners
  - **Advanced Integrating Activities:** Research infrastructure needs, Clustering and coordination with other international initiatives, Alignment of funding sources and Support to establish the CST European RIs as a legal structure (EU-SOLARIS ESFRI)
- **Transnational Access**
- **Joint Research Activities**

For more information, visit: https://sfera3.sollab.eu/

SFERA-III: NA1 Capacity building and training activities

On-Site Training for Industries

Industrial knowledge,
skills and capacities

SFERA III
→
Training

INNOVATION

→ Training about CST technology design, optimization and O&M through knowledge transfer by research experts with their infrastructures

- **Target Group:** Industrial researchers and developers
- **Objective:** Gain practical experience on different aspects of CST technologies
- **Approach:** Theory basis and emphasis on practical skills

SFERA-III: NA1 Capacity building and training activities

On-Site Training for Industries; Proposed courses

No.	Topic	Local Course Management	Location	Date
1	Central receivers and heliostat field	CNRS (+FRA, DLR)	France	July 2019
2	**Optimization of CST plant output by optical & thermal characterization and target-oriented O&M**	**DLR (+CIEMAT)**	**Spain PSA**	**26th – 29th April 2022**
3	Testing the durability of solar materials and systems	CEA (+DLR)	France	8th -10th June 2022
4	Process heat application for CST technologies: system integration, design and performance assessment	Fraunhofer	Germany	2023
5	Use of molten salt as HTF and/or HSM in CST plant that employ linear focussing systems	ENEA (+DLR)	Portugal	2023

SFERA-II Training for industries courses (offered 2014-2017)

- **CIEMAT, 2014:** Operation & testing of direct steam generation in linear focusing collectors, Reflector Characterization
- **ENEA, 2015:** Molten Salt Systems: Collector Loop, Thermal Storage and Heat Transfer Fluids
- **CNRS, 2016:** Central Receivers: Operation of Heliostat Fields
- **DLR, 2017:** Thermal component testing of parabolic troughs with oil as HTF (Receivers, Facets, Module Qualification, Connectors)

Organization:

Overall Programme Manager (DLR)

Benitez/Röger
Kruschinski

- Defines the frame of the course program
- Announces course program, using homepages (SFERA, ESTELA, etc.) & Mailing lists
- Communication to the course participants

Local Course Managers

E. Guillot (CNRS)

Benitez, Röger (DLR)

Estelle Le Baron (CEA)

Fraunhofer (Germany)

ENEA (Italy)

- Prepares details of course program
- Prepares courses and educational materials
- Gives access to research infrastructure during course
- Implements courses with its trainers/scientists

Course Program

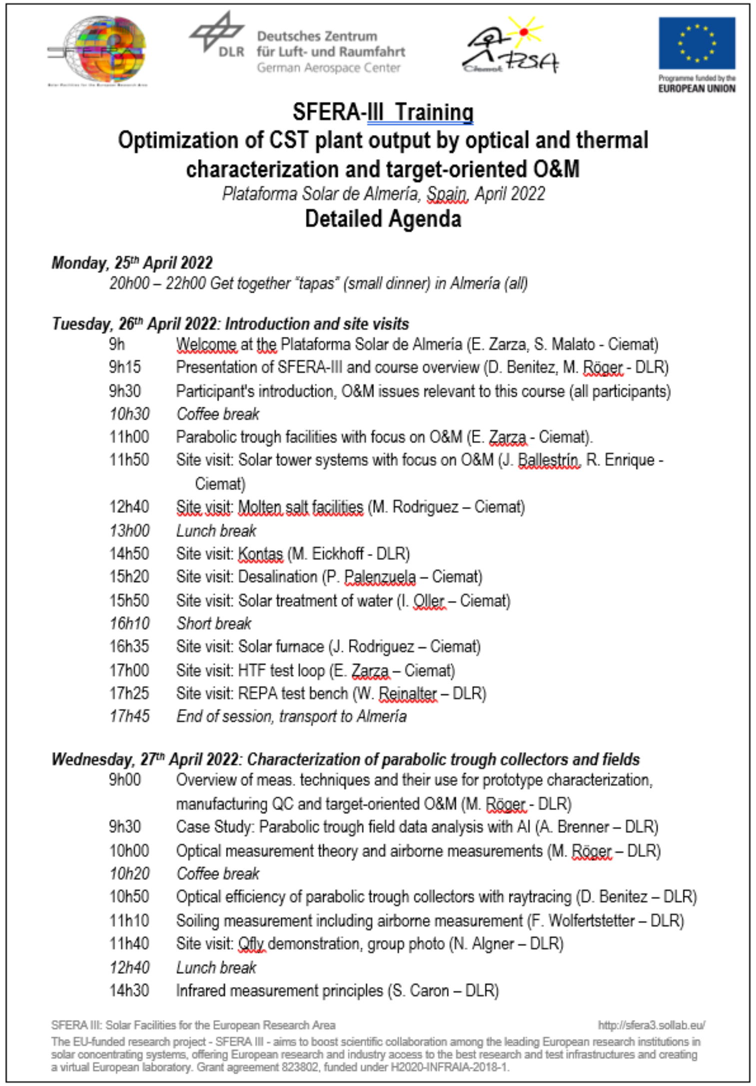

SFERA-III Training
Optimization of CST plant output by optical and thermal characterization and target-oriented O&M
Plataforma Solar de Almería, Spain, April 2022
Detailed Agenda

Monday, 25th April 2022
20h00 – 22h00 Get together "tapas" (small dinner) in Almería (all)

Tuesday, 26th April 2022: Introduction and site visits
9h Welcome at the Plataforma Solar de Almería (E. Zarza, S. Malato - Ciemat)
9h15 Presentation of SFERA-III and course overview (D. Benitez, M. Röger - DLR)
9h30 Participant's introduction, O&M issues relevant to this course (all participants)
10h30 Coffee break
11h00 Parabolic trough facilities with focus on O&M (E. Zarza - Ciemat).
11h50 Site visit: Solar tower systems with focus on O&M (J. Ballestrín, R. Enrique - Ciemat)
12h40 Site visit: Molten salt facilities (M. Rodriguez – Ciemat)
13h00 Lunch break
14h50 Site visit: Kontas (M. Eickhoff - DLR)
15h20 Site visit: Desalination (P. Palenzuela – Ciemat)
15h50 Site visit: Solar treatment of water (I. Oller – Ciemat)
16h10 Short break
16h35 Site visit: Solar furnace (J. Rodriguez – Ciemat)
17h00 Site visit: HTF test loop (E. Zarza – Ciemat)
17h25 Site visit: REPA test bench (W. Reinalter – DLR)
17h45 End of session, transport to Almería

Wednesday, 27th April 2022: Characterization of parabolic trough collectors and fields
9h00 Overview of meas. techniques and their use for prototype characterization, manufacturing QC and target-oriented O&M (M. Röger - DLR)
9h30 Case Study: Parabolic trough field data analysis with AI (A. Brenner – DLR)
10h00 Optical measurement theory and airborne measurements (M. Röger – DLR)
10h20 Coffee break
10h50 Optical efficiency of parabolic trough collectors with raytracing (D. Benitez – DLR)
11h10 Soiling measurement including airborne measurement (F. Wolfertstetter – DLR)
11h40 Site visit: Qfly demonstration, group photo (N. Algner – DLR)
12h40 Lunch break
14h30 Infrared measurement principles (S. Caron – DLR)

SFERA III: Solar Facilities for the European Research Area http://sfera3.sollab.eu/
The EU-funded research project - SFERA III - aims to boost scientific collaboration among the leading European research institutions in solar concentrating systems, offering European research and industry access to the best research and test infrastructures and creating a virtual European laboratory. Grant agreement 823802, funded under H2020-INFRAIA-2018-1.

15h00 Airborne IR measurement on parabolic trough receivers (N. Algner – DLR)
15h40 Site visit: Dishes, aging at dishes (S. Caron – DLR, J. Rodriguez – Ciemat)
16:10 Short break
16h35 Case study: Techno-economic evaluation of receiver repair/replacement scenarios (M. Röger – DLR)
17:05 Clamp-on measurements and evaluation by parameterized dynamic performance model (N. Janotte – DLR, online)
17h35 End of session, transport to Almería

Thursday, 28th April 2022
The solar resource and operation
9h00 Solar resource: measurement and extinction (S. Wilbert / N. Blum – DLR)
10h00 Solar resource: nowcasting (S. Wilbert / N. Blum – DLR)
10h30 Coffee break
11h00 Case study: Use of nowcasting system to optimize the yield in parabolic trough power plants (T. Kotzab – DLR)
11h30 Field visit: METAS
12h50 Lunch break
Component aging
14h30 Measurement of optical properties (reflectance, absorptance, transmittance) (F. Sutter – DLR)
15h30 Component aging: Mirrors (A. Fernández – Ciemat)
16h00 Component aging: Receiver coatings (S. Caron / F. Sutter – DLR)
16:30 Short break
16h55 Field visit: Optical ageing characterization lab OPAC (A. Fernández – Ciemat, F. Sutter – DLR)
17h55 End of session, transport to Almería

Friday, 29th April 2022
Operation and maintenance of central receiver systems
9h00 Heliostat calibration (R. Monterreal – Ciemat)
9h30 Recent development in airborne heliostat calibration (J. Krauth – DLR)
10h00 Flux density measurement (C. Raeder – DLR, online)
10h30 Coffee break
11h00 Case study: Techno-economic evaluation of soiling, optimization of mirror cleaning (F. Wolfertstetter – DLR)
11h40 "CSP markets worldwide" and workshop about practical experiences, problems, suggestions, etc. (Gonzalo Martín – Protermosolar and all participants)
13:40 Feedback, Certificate and Closing (all)
14h00 Lunch
15:30 End of event, transport to Almería

SFERA III: Solar Facilities for the European Research Area http://sfera3.sollab.eu/
The EU-funded research project - SFERA III - aims to boost scientific collaboration among the leading European research institutions in solar concentrating systems, offering European research and industry access to the best research and test infrastructures and creating a virtual European laboratory. Grant agreement 823802, funded under H2020-INFRAIA-2018-1.

THANK YOU FOR YOUR ATTENTION!

WE WISH YOU AN INTERESTING AND INSPIRING WEEK!

GOBIERNO DE ESPAÑA
MINISTERIO DE CIENCIA, INNOVACIÓN Y UNIVERSIDADES
Ciemat
Centro de Investigaciones Energéticas, Medioambientales y Tecnológicas
ENEA
DLR Deutsches Zentrum für Luft- und Raumfahrt
UNIVERSIDADE DE ÉVORA
ESTELA
The Cyprus Institute
instituto imdea energía
Fraunhofer ISE
euronovia
LNEG
METU
ETH zürich
IN LUMINE SAPIENTIA · UNIVERSITAS ALMERIENSIS
UNIVERSIDAD DE ALMERÍA
cnrs dépasser les frontières
DE LA RECHERCHE À L'INDUSTRIE cea
SFERA
Solar Facilities for the European Research Area

SFERA

Solar Facilities for the European Research Area

Training course on:
“Optimization of CST plant output by optical and thermal characterization and target-oriented O&M”
(Almería, April 26th- 29th, 2022)

Operation & Maintenance of Parabolic Trough Solar Fields

Dr. Eduardo Zarza
Plataforma Solar de Almería – CIEMAT
E-mail: eduardo.zarza@psa.es

GOBIERNO DE ESPAÑA

MINISTERIO DE CIENCIA E INNOVACIÓN

Ciemat
Centro de Investigaciones Energéticas, Medioambientales y Tecnológicas

Ciemat PSA

Content

- ☐ **Solar plants with parabolic trough collectors**
- ☐ **O&M of solar fields with PTCs**

O&M of Parabolic Trough solar fields

Content

- ☐ **Solar plants with parabolic trough collectors**
- ☐ **O&M of solar fields with PTCs**

Solar Plants with Parabolic-trough Collectors

Parabolic-trough collectors

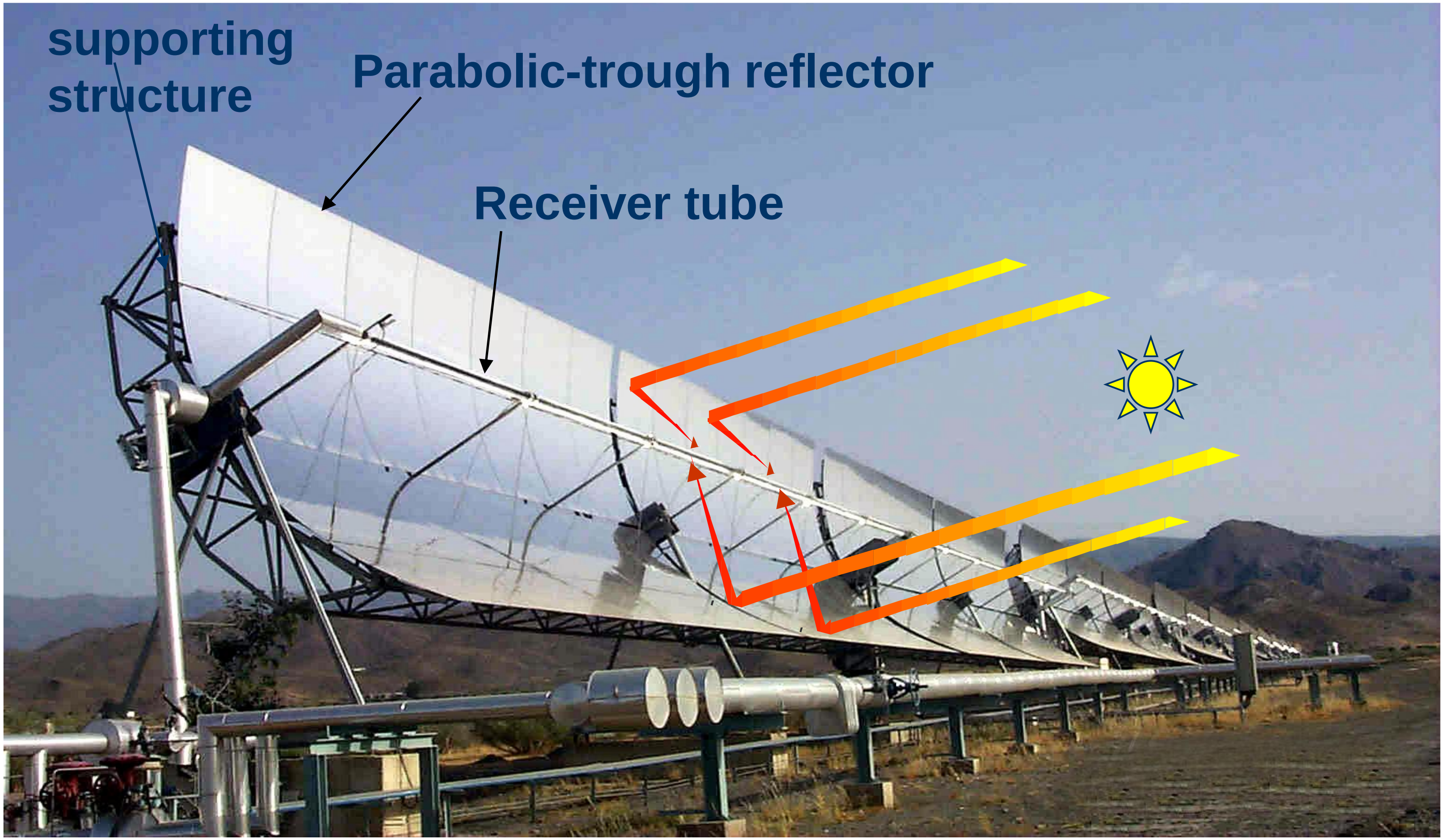

supporting structure

Parabolic-trough reflector

Receiver tube

Solar Plants with Parabolic-trough Collectors

Working Fluids for Parabolic Trough Collectors

- Pressurized liquid wáter (up to 225°C)
- Thermal oil (up to 398°C)
- Liquid water/steam (Direct Steam Generation)

Solar Plants with Parabolic-trough Collectors

Solar Field Lay-out

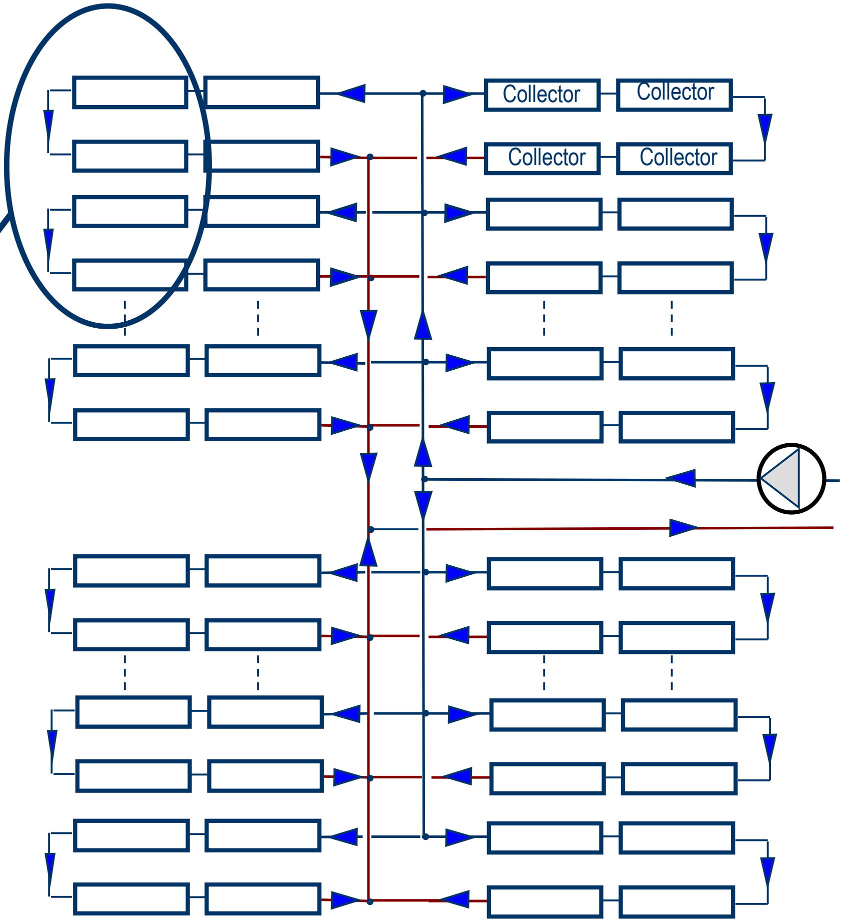

The so-called ***Central Feed*** configuration

Solar Plants with Parabolic-trough Collectors

- Main applications for parabolic trough solar fields are:

Industrial process heat: the thermal energy is used to feed industrial processes demanding heat in the range 125ºC - 450ºC. These applications are internationally known as “**SHIP”** applications

Electricity Generation: it is the most important commercial application at present, with more than 5000 MWe currently in operation. These solar systems are called *Solar Thermal Power Plants* and are internationally known as “**CSP**” or “**STE**” plants

Solar Plants with Parabolic-trough Collectors

Simplified scheme of a solar thermal power plant with PTCs

The most complex application of parabolic-trough collectors are the solar thermal power plants

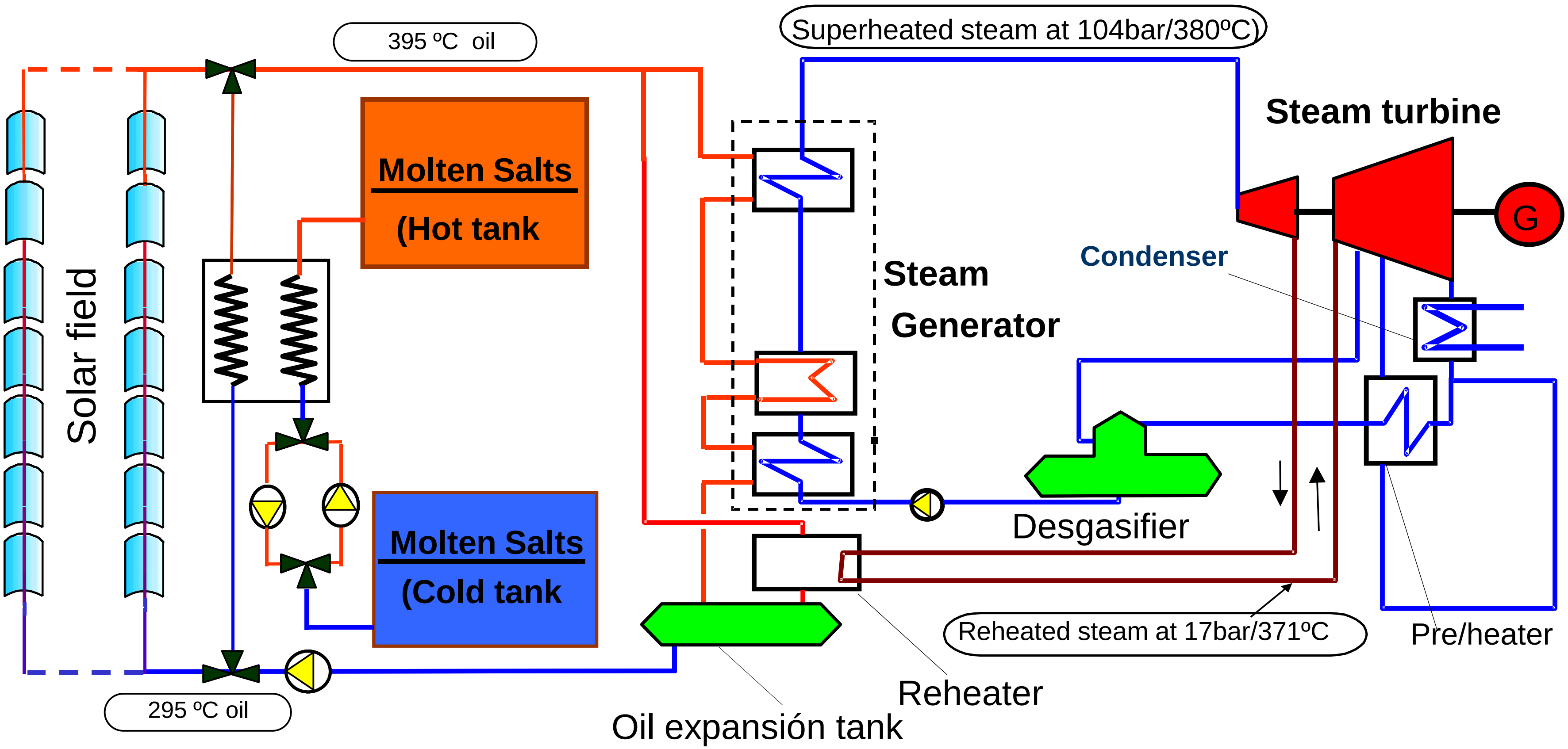

O&M of Parabolic Trough solar fields

Content

- Solar plants with parabolic trough collectors
- **O&M of solar fields with PTCs**

Operation and Maintenance of Solar Fields with parabolic-trough collectors

- *The performance of the solar fields not only depends on the quality of the O&M, but also on the quality control during the construction*

The solar field collects and transforms the direct solar radiation into thermal energy. It is composed of: solar collectors, piping and auxiliary elements (ball-joints, valves and instrumentation, among others)

A good quality control is essential during the assembly process, because any error or mistake will be very difficult and costly to repair once the collectors are assembled.

Assembly jigs used for commercial parabolic trough collectors

Operation and Maintenance of Solar Fields with parabolic-trough collectors

Solar Field Operating Modes

- ***Long shut-down:*** Solar collectors must be put in “Stow” position; Take measures to avoid working fluid freezing in the piping and receiver tubes.

- ***Overnight stop:*** Solar collectors are kept in “Stow” position and a low fluid flow is kept to avoid fluid freezing, during cold winter nights

- ***Stand-by:*** Solar field operating with the solar collectors in “Desteer” position (defocused 5º).

- ***Pre-heating:*** Solar field increasing the working fluid temperature until the nominal value. High thermal gradients in the equipment must be avoided to reduce thermal stress.

- ***Routine operation:*** solar collectors in “Track” position and the nominal solar field temperatures are maintained.

Operation and Maintenance of Solar Fields with parabolic-trough collectors

Critical issues during the solar field operation with thermal oil

There are three critical issues in solar fields using thermal oil as working fluid that must be continuously taken into consideration:

- *Oil freezing must be avoided when ambient temperature is low*
- *Oil must be pressurized at a pressure over the vapour pressure at the maximum working temperature to avoid fluid evaporation in the oil piping and vessels*
- *Keep all the elements of the oil circuit inertized to avoid fire hazards*

Operation and Maintenance of Solar Fields with parabolic-trough collectors

Threshold level of Direct Solar Radiation

It is the minimum value of the direct solar radiation to have a positive net energy balance in the solar field (thermal energy absorbed > thermal losses)

$$\dot{Q}_{net} = \cdot A_c \cdot G_b \cdot \mathrm{Cos}(\theta) \cdot \eta_{opt,\ 0^o} \cdot K(\theta) \cdot F_c - \dot{Q}_{loss}$$

$$\dot{Q}_{net} = q_m \times \left(h_{out} - h_{in}\right)$$

$$G_b = [q_m \cdot (h_{out} - h_{in}) + \dot{Q}_{loss}] \big/ A_c \cdot \mathrm{Cos}(\theta) \cdot \eta_{opt.,0^o} \cdot K(\theta) \cdot F_c$$

q_m = minimum mass flowrate required to operate the solar field (kg/s)

$T_{out} = T_{in} + 5^oC$

$$G_{b,\ threshold} = 1{,}05 x G_b$$

Operation and Maintenance of Solar Fields with parabolic-trough collectors

Curve of ***Direct Radiation Threshold Level*** for a solar field East-West oriented and ΔT = 5ºC in the solar field

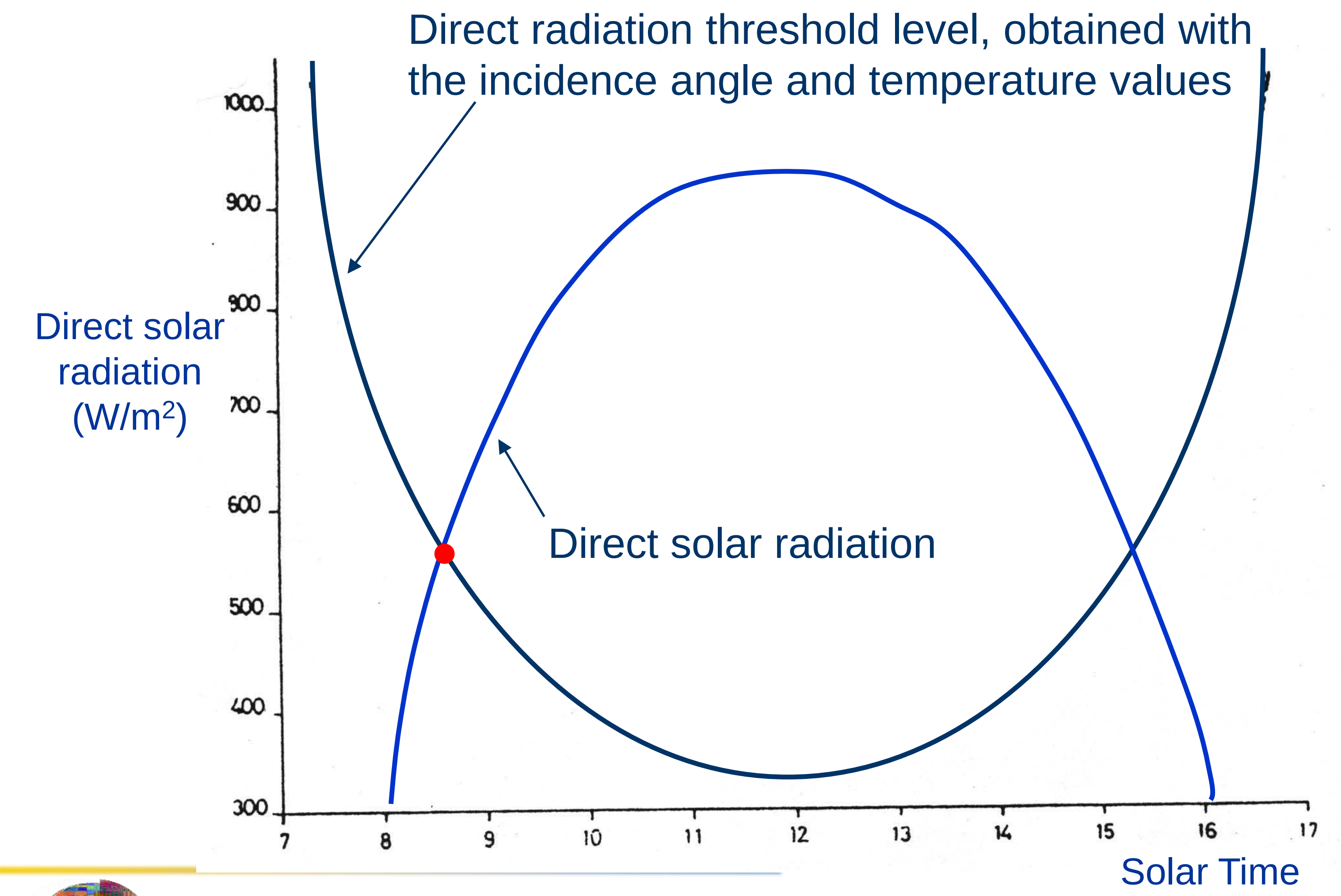

Operation and Maintenance of Solar Fields with parabolic-trough collectors

Maintenance of plants with Parabolic-trough collectors

- **SOLAR FIELD:**
  - Washing of solar collectors

Operation and Maintenance of Solar Fields with parabolic-trough collectors

Maintenance of plants with Parabolic-trough collectors

Solar collectors washing

Operation and Maintenance of Solar Fields with parabolic-trough collectors

Maintenance of plants with Parabolic-trough collectors

- **SOLAR FIELD:**
  - Washing of solar collectors
  - Periodic reflectance measurement

Operation and Maintenance of Solar Fields with parabolic-trough collectors

Maintenance of plants with Parabolic-trough collectors

Measuring the reflectance in a parabolic-trough collector

Operation and Maintenance of Solar Fields with parabolic-trough collectors

Maintenance of plants with Parabolic-trough collectors

- **SOLAR FIELD:**
  - Washing of solar collectors
  - Periodic reflectance measurement
  - Replacement of broken mirrors (less than 0.1% per year)
  - Yearly revision of the receiver tubes alignment

Operation and Maintenance of Solar Fields with parabolic-trough collectors

Maintenance of plants with Parabolic-trough collectors

Bending of a receiver tube

Operation and Maintenance of Solar Fields with parabolic-trough collectors

Maintenance of plants with Parabolic-trough collectors

- **SOLAR FIELD:**
  - Washing of solar collectors
  - Periodic reflectance measurement
  - Replacement of broken mirrors (less than 0.1% per year)
  - Yearly revision of the receiver tubes alignment
  - Refiling of the ball-joints graphite sealing (~ 3 years)

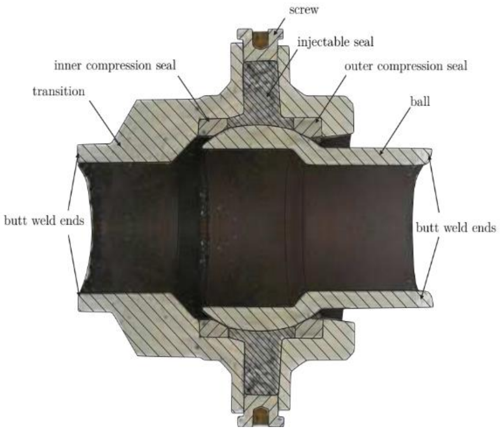

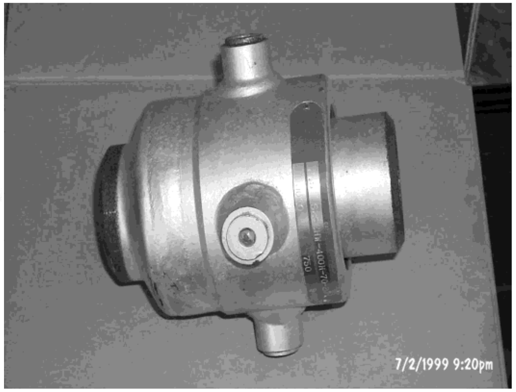

Maintenance of plants with Parabolic-trough collectors

SOLAR FIELD:

- Washing of solar collectors
- Periodic reflectance measurement
- Replacement of broken mirrors (less than 0.1% per year)
- Yearly revision of the receiver tubes alignment
- Refiling of the ball-joints graphite sealing (every 3 years)
- Verification of the receiver tubes vacuum

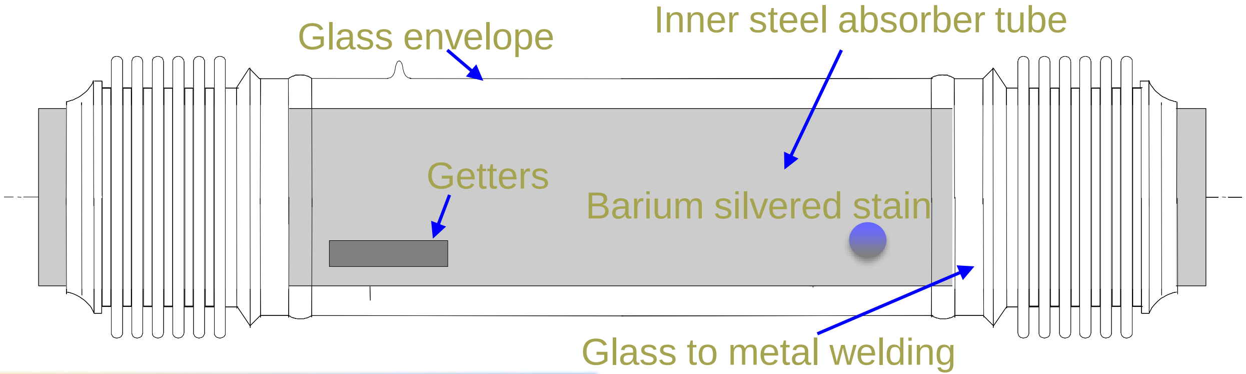

Operation and Maintenance of Solar Fields with parabolic-trough collectors

Maintenance of plants with Parabolic-trough collectors

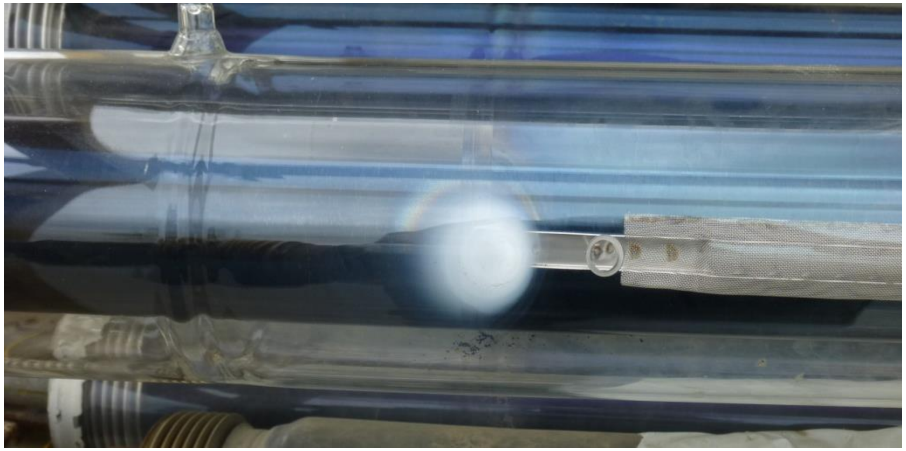

Receiver tube with vacuum loss

Receiver tube with good vacuum

Vacuum indicator with Barium

Operation and Maintenance of Solar Fields with parabolic-trough collectors

Maintenance of plants with Parabolic-trough collectors

SOLAR FIELD:

- Washing of solar collectors
- Periodic reflectance measurement
- Replacement of broken mirrors (less than 0.1% per year)
- Yearly revision of the receiver tubes alignment
- Refiling of the ball-joints graphite sealing (every 3 years)
- Verification of the receiver tubes vacuum
- Yearly verification of the sun tracking system

Operation and Maintenance of Solar Fields with parabolic-trough collectors

Maintenance of plants with Parabolic-trough collectors

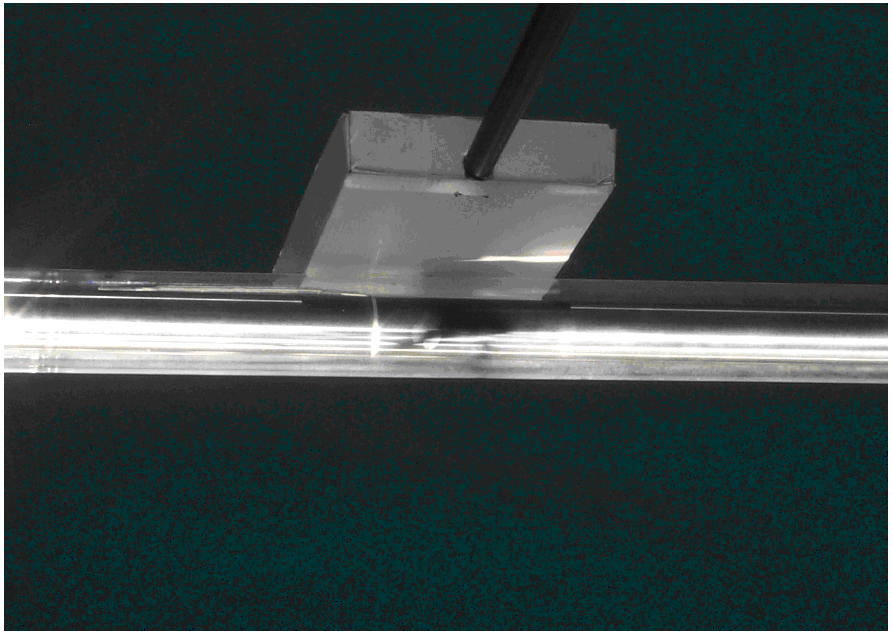

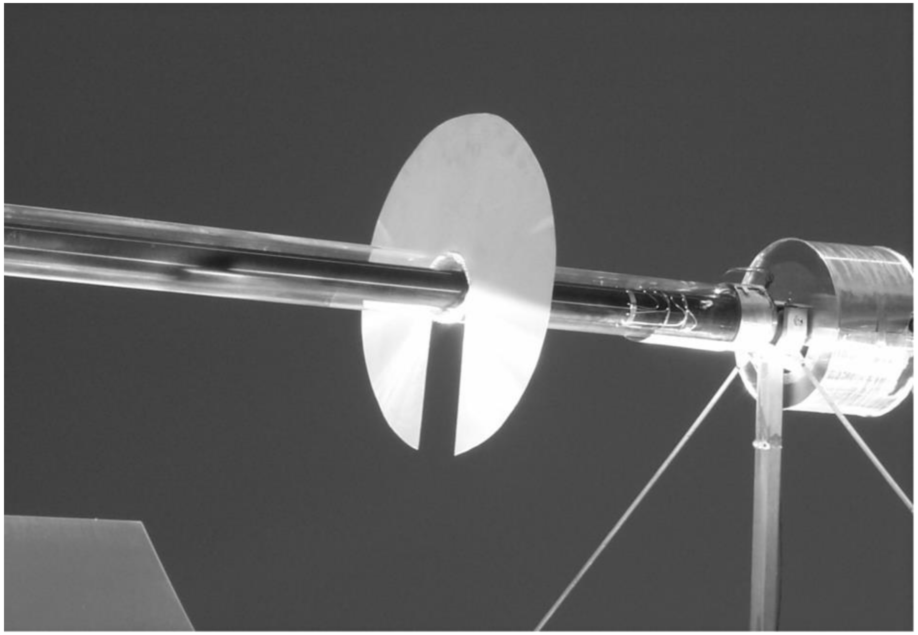

Hand-checking of the correct positioning of the receiver tubes

Maintenance of plants with Parabolic-trough collectors

SOLAR FIELD:

- Washing of solar collectors
- Periodic reflectance measurement
- Replacement of broken mirrors (less than 0.1% per year)
- Yearly revision of the receiver tubes alignment
- Refiling of the ball-joints graphite sealing (2-3 years)
- Verification of the receiver tubes vacuum
- Yearly verification of the sun tracking system

OIL CIRCUIT:

- Yearly analysis of the thermal oil
- Yearly oil make-up (3 – 4% yearly)

Operation and Maintenance of Solar Fields with parabolic-trough collectors

Expected improvements for O&M in plants with Parabolic-trough collectors in a short term

There will be two major improvements in future plants with PTCs:

- Mirrors with an anti-soiling coating (less frequent mirrors cleaning and lower water consumption)
- The replacement of thermal oil currently used (Biphenyl-diphenil oxide) by a silicone-based oil (less environmental hazards, less H_2 permeation in the receiver tubes, higher working temperatures and no freezing problem)

SFERA

Solar Facilities for the European Research Area

Operation & Maintenance of Parabolic Trough Solar Fields

! Thank you for your attention ¡

Dr. Eduardo Zarza
Plataforma Solar de Almería – CIEMAT
E-mail: eduardo.zarza@psa.es

GOBIERNO DE ESPAÑA

MINISTERIO DE CIENCIA E INNOVACIÓN

Ciemat
Centro de Investigaciones Energéticas, Medioambientales y Tecnológicas

Ciemat PSA

SFERA-III

Solar Facilities for the European Research Area

2nd Training for Industries “Optimization of CST plant output by optical and thermal characterization and target-oriented O&M”
26 – 29 April 2022, Plataforma Solar de Almería, Spain

Overview of measurement techniques

and their use for prototype characterization,
manufacturing quality control and target-oriented O&M

Marc Röger, DLR

NETWORKING

THIS PROJECT HAS RECEIVED FUNDING FROM THE EUROPEAN UNION’S HORIZON 2020 RESEARCH AND INNOVATION PROGRAMME UNDER GRANT AGREEMENT NO **823802**

Overview

Motivation: Why do we need metrology?

Metrology in Different Phases

Qualification and Monitoring of

1. Meteorological Parameters
2. Concentrators
3. Receivers
4. System Performance
5. Materials and Fluids

Motivation: Why do we need metrology ?

- Solar field has a high share of the total investment
- It is a *long-term* investment
- It is of *big extent* (corrections are expensive)
- Yearly *plant output* strongly depends on
  - optical and thermal quality of collector field
  - and the operation & maintenance strategy
- *Quality assurance* and *final acceptance tests* of collector fields are necessary for control of subcontractors and warranty claims
- Optimized operation & maintenance needs viable data of the plant and the meteorological conditions.

Motivation: Why do we need metrology ?

Importance of high quality and durable components

Example 1: Possible degradation of mirror panels in a 200-MW_{el} power plant with annual capacity factor of 40% and revenue of 0.14 US$/kWh

Exemplary degradation of mirrors

→ 0.3% less reflectance/year
→ 0.45% less thermal efficiency/year
→ ~ 4% less energy production on average over 20 years

➔ **Loss of revenues of 78 Million US$ can be avoided with high quality and durable components**

Motivation: Why do we need metrology ?
Improved Performance by Proper Implementation of Construction

Example 2: Instead of having achieved an optical efficiency of 76%, we have achieved only 75% (Andasol-type 50MW plant)

Results in:
- 0.5 million € less revenues per year
- 10 million € less revenues during the lifetime

➔ **Quality assurance to achieve high optical effiency in a collector field makes sense economically**

Sources for Losses

EuroTrough Geometry

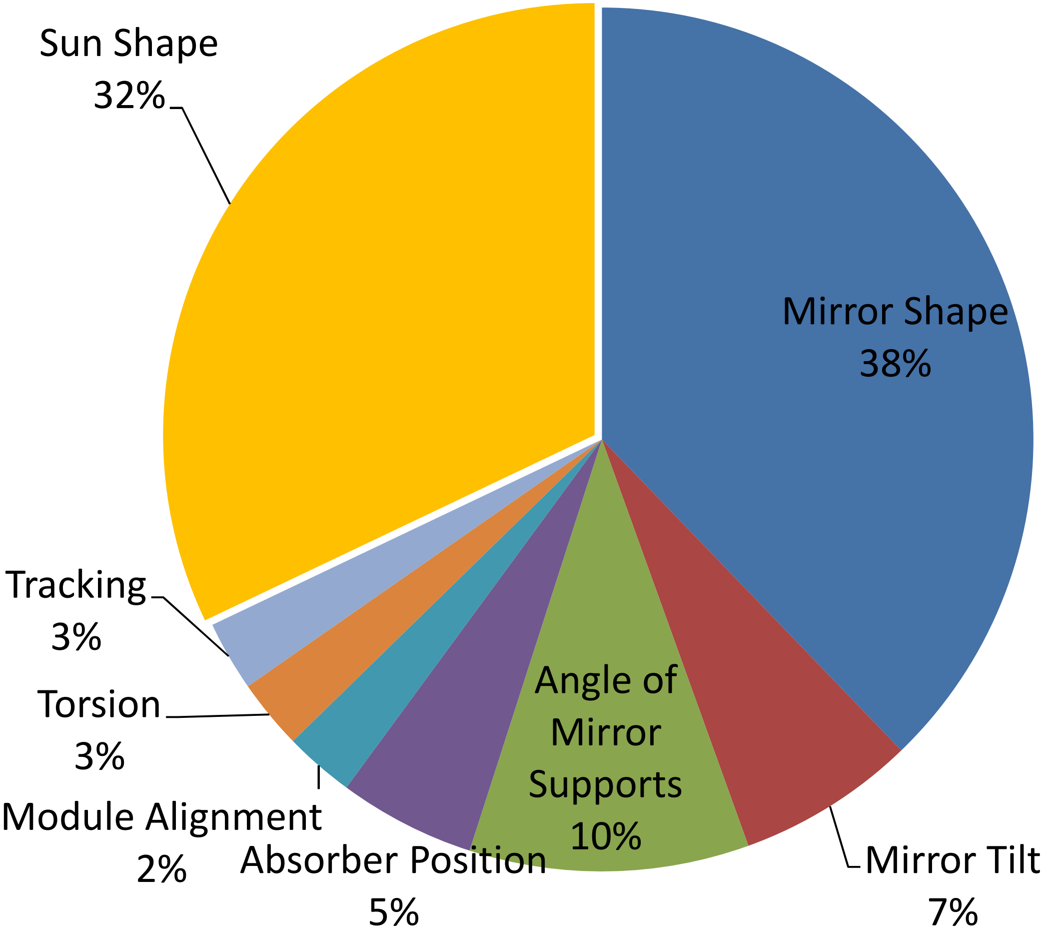

Graph for good collector quality:

- Total beam spread σ_{total} : 6.2 mrad
- Sun shape effect is fixed
- Currently: largest impact from mirror shape and supports

In case of poor collector quality other error types may dominate!

Metrology in Different Phases

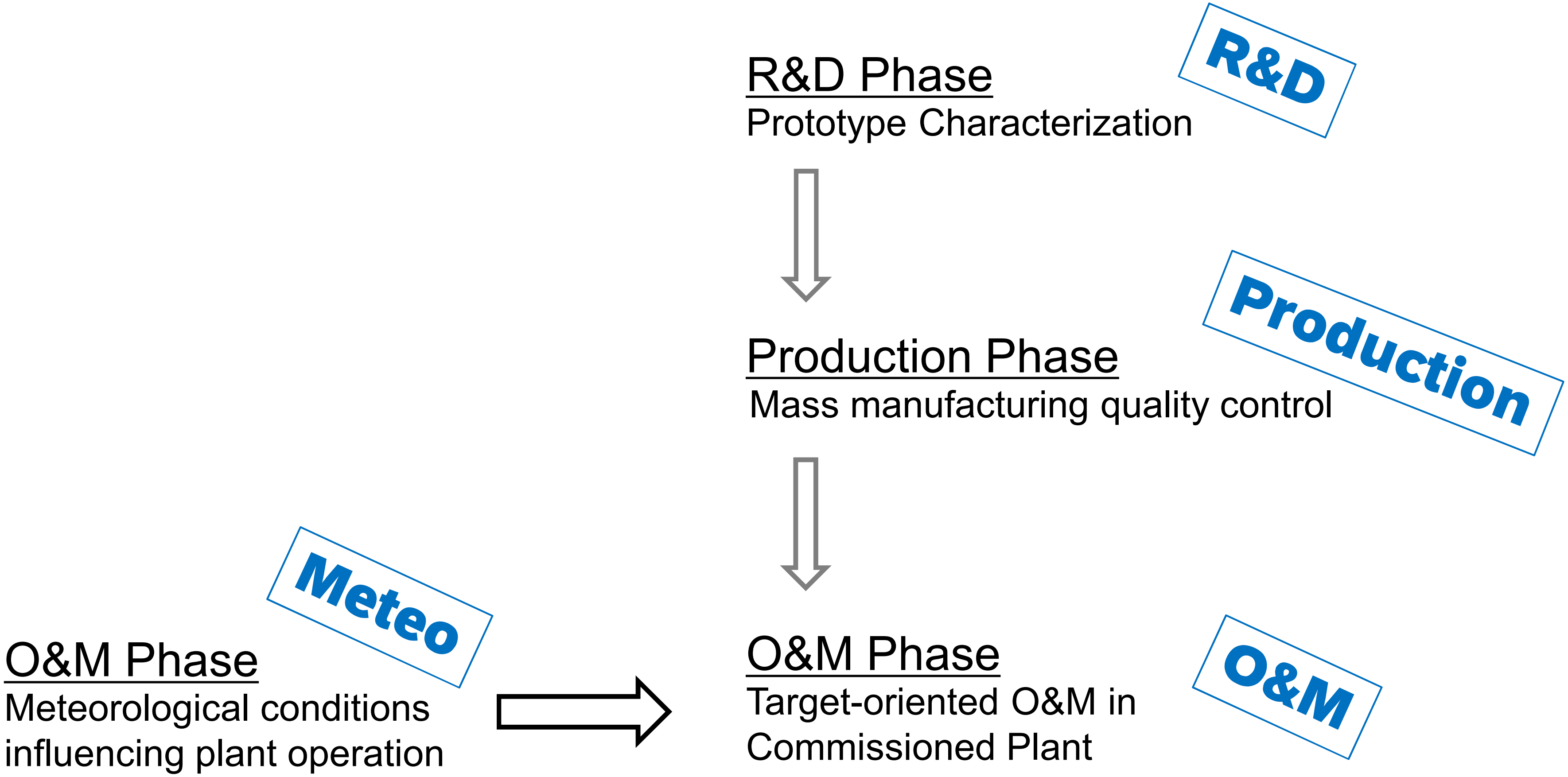

R&D Phase
Prototype Characterization

R&D

Production Phase
Mass manufacturing quality control

Production

Meteo

O&M Phase
Meteorological conditions influencing plant operation

O&M Phase
Target-oriented O&M in Commissioned Plant

O&M

→ Specific talks on Thursday

Meteo

1 Monitoring of Meteorological Parameters

Measurements:
- Solar Radiation
- Soiling of components
- Aerosols
- Beam attenuation, Extinction
- Sunshape
- Nowcasting (prediction of DNI for next 30 min.)

Services:
- Calibration of sensors
- Analysis of effects on Plant design, Operation, System performance

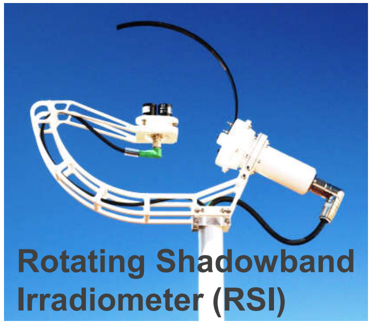

2 Mirror / Collector Shape Accuracy

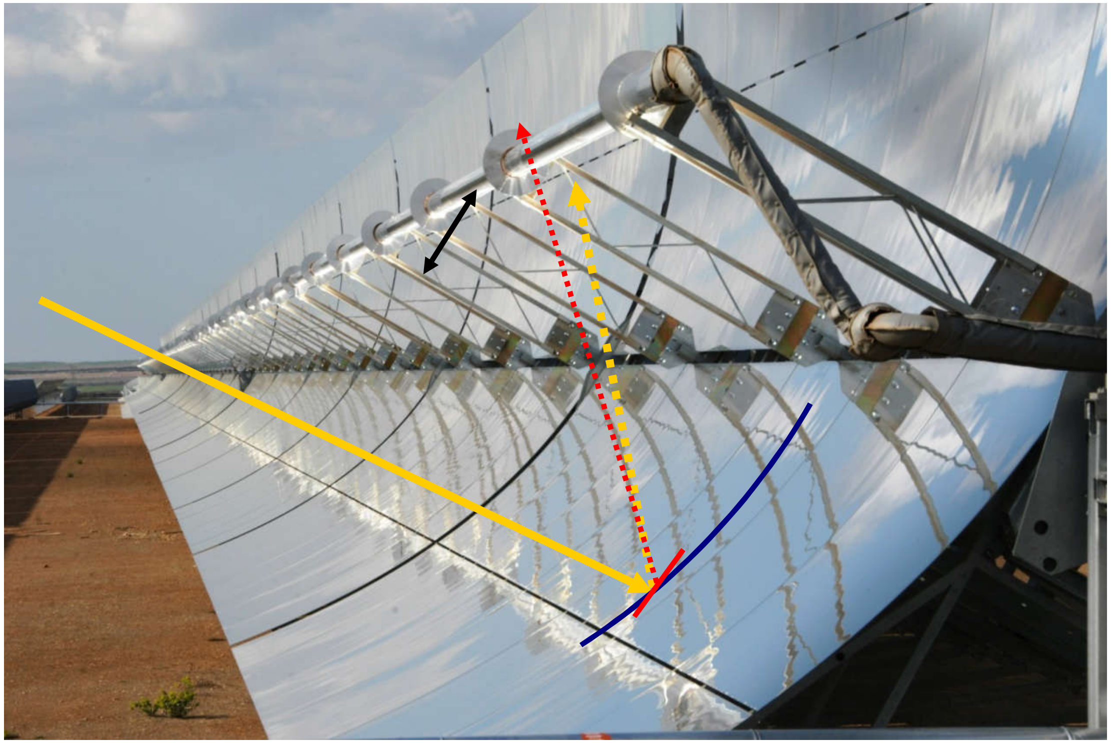

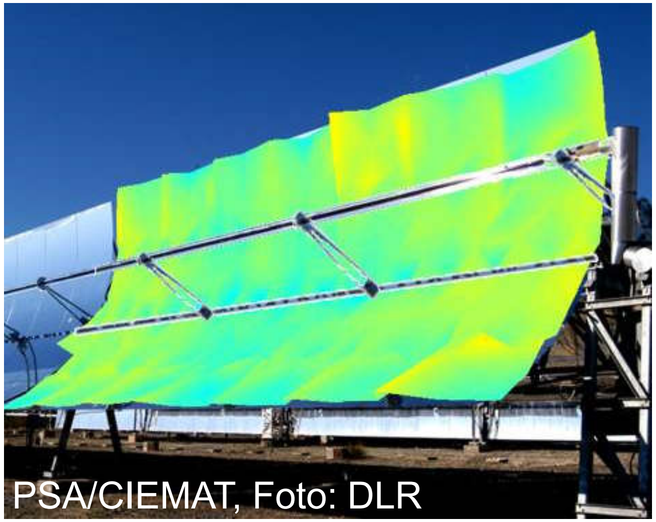

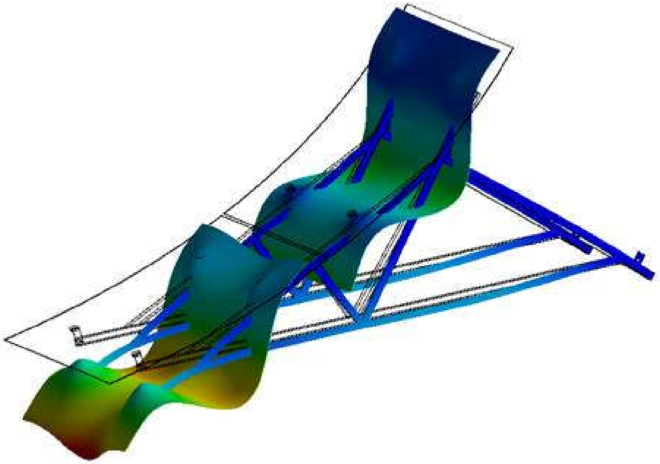

Evaluation of quality and performance parameters:
- Methods: deflectometry, photogrammetry (in laboratory, in the collector, in the solar field)
- Analysis of reflector/collector deformation and receiver positioning (sag, interaction with support structure)

2 Qualification of Concentrators

optical

Photogrammetry: Collector Shape and Deformation

From photos to coordinates

- **Image acquisition:** several photos of measurement object are taken form different angles
- **Point recognition:** clearly recognizable points of object are determined in all photos
- **Evaluation:** calculation of 3D point geometry via initial orientation, intersection and bundle adjustment
- **Scaling:** inclusion of known distances between targets

Result: all object coordinates, camera positions and orientations together with their precisions are known

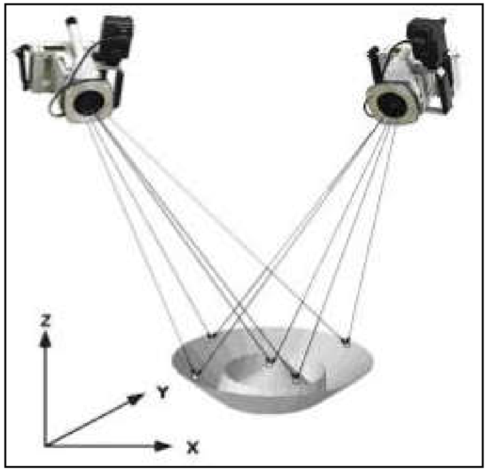

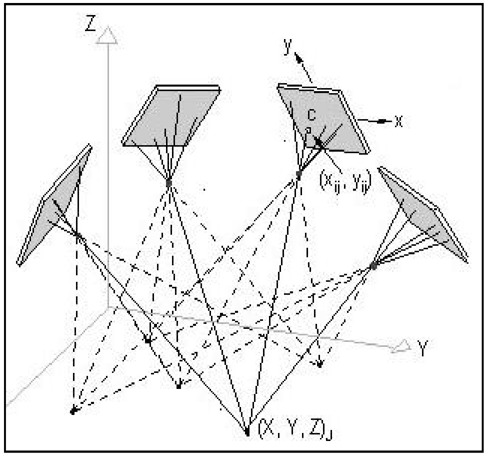

R&D
optical

2 Qualification of Concentrators

Photogrammetry: Collector Shape and Deformation

Object Preparation

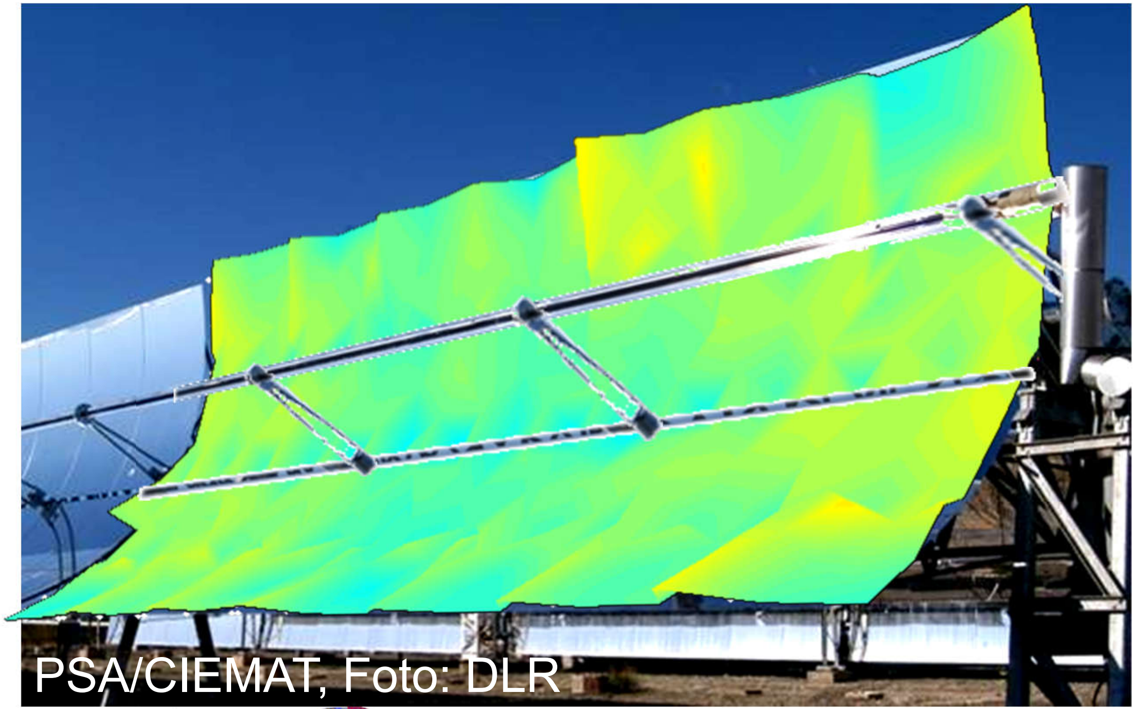
PSA/CIEMAT, Foto: DLR

Results
- 3D Coordinates
  - Coordinate Deviations
  - Angle Deviations
- Shape and Deformation Studies

R&D

optical

2 Qualification of Concentrators

Photogrammetry: Heliostat Shape and Deformation

Object Preparation

- 216 targets on 12 facets (18 each)

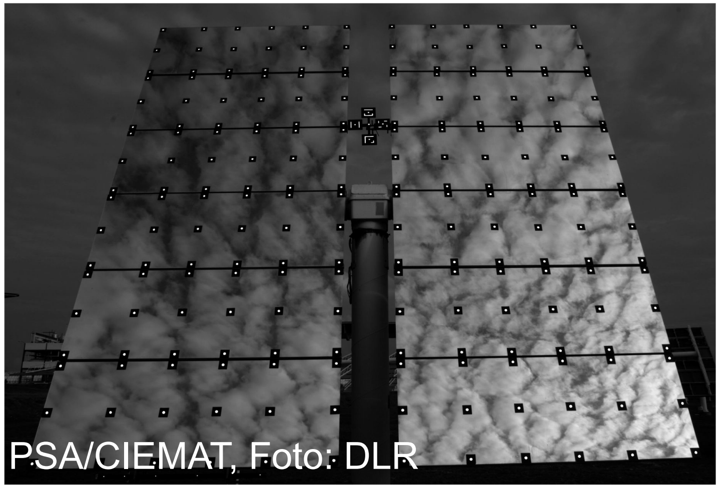

PSA/CIEMAT, Foto: DLR

Photogrammetric measurement

- 9 orientations with different elevations
- 20 photos for each orientation

PSA/CIEMAT, Foto: DLR

Measurement uncertainty

mean over 9 orientations:

- σ=0.3 mm
- Δ_{max} = 0.6 mm

R&D

optical

2 Qualification of Concentrators

Photogrammetry: Heliostat Shape and Deformation

Measured displacements

Δ between 10° and 90° :

- $\Delta = 1.1 \pm 1.9$ mm
- $\Delta_{max} < 5.5$ mm

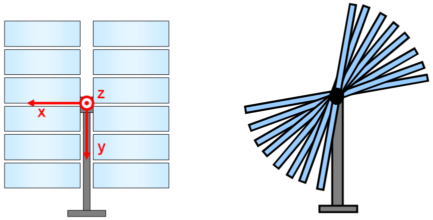

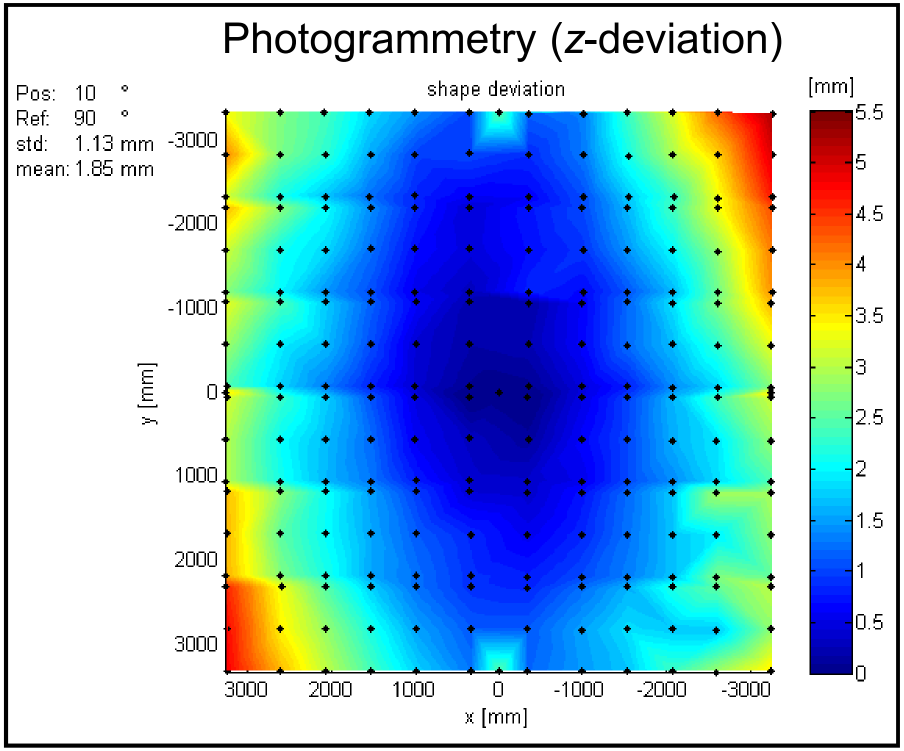
Photogrammetry (z-deviation)

Production

optical

2 Qualification of Concentrators

QFoto: Photogrammetry Setup for Collector/Heliostat Structures

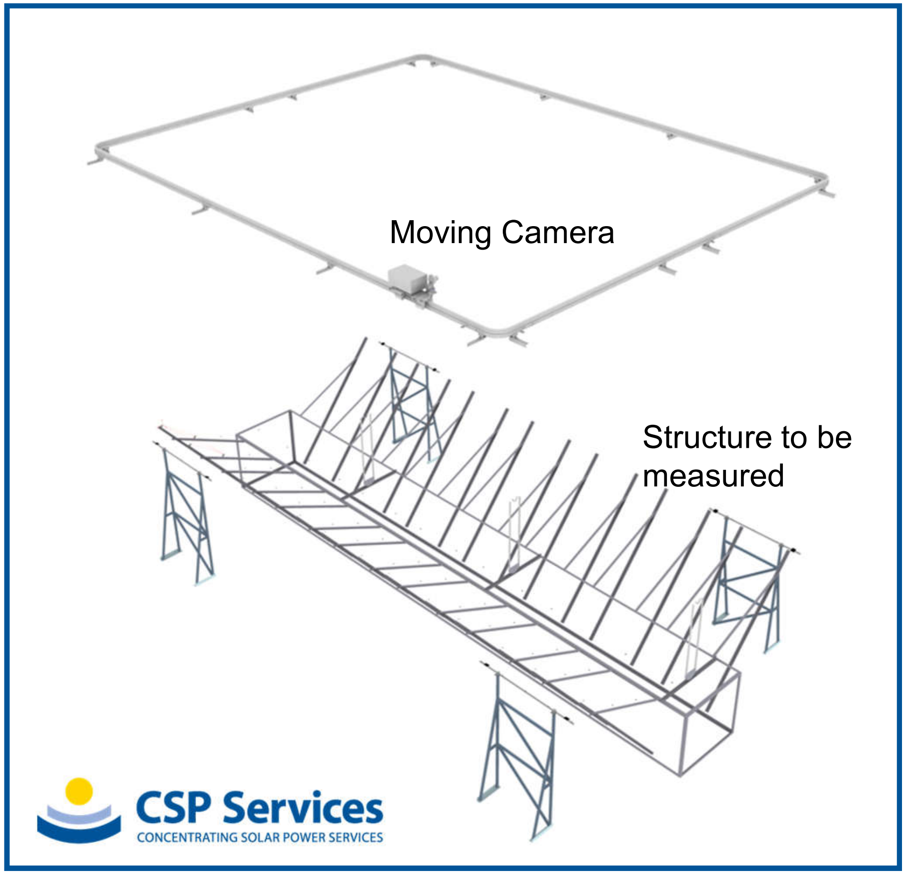

<u>QFoto:</u> Automated System for *<u>Collector Structures</u>*

Moving Camera

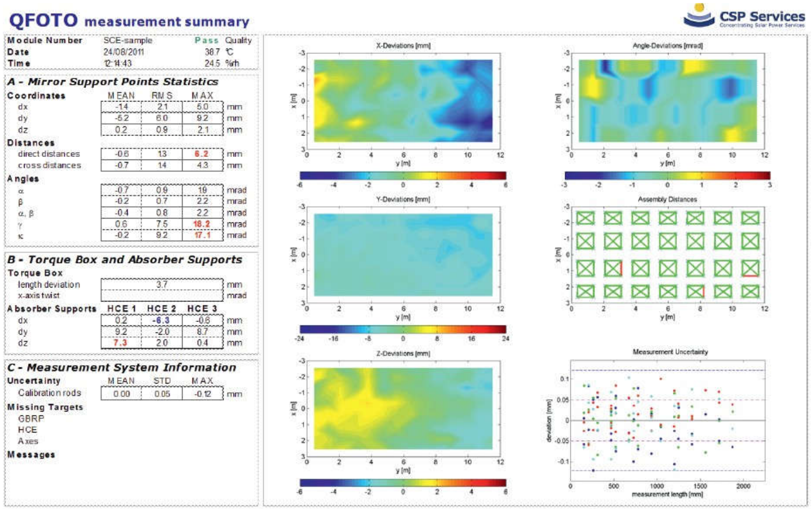

QFOTO measurement summary

Module Number	SCE-sample	Pass	Quality
Date	24/08/2011	38.7	°C
Time	12:14:43	24.5	%rh

A - Mirror Support Points Statistics

Coordinates	MEAN	RMS	MAX	
dx	-1.4	2.1	5.0	mm
dy	-5.2	6.0	9.2	mm
dz	0.2	0.9	2.1	mm
Distances				
direct distances	-0.6	1.3	6.2	mm
cross distances	-0.7	1.4	4.3	mm
Angles				
α	-0.7	0.9	1.9	mrad
β	-0.2	0.7	2.2	mrad
α, β	-0.4	0.8	2.2	mrad
γ	0.6	7.5	18.2	mrad
κ	-0.2	9.2	17.1	mrad

B - Torque Box and Absorber Supports

Torque Box		
length deviation	3.7	mm
x-axis twist		mrad

Absorber Supports	HCE 1	HCE 2	HCE 3	
dx	0.2	-6.3	-0.6	mm
dy	9.2	-2.0	8.7	mm
dz	7.3	2.0	0.4	mm

C - Measurement System Information

Uncertainty	MEAN	STD	MAX	
Calibration rods	0.00	0.05	-0.12	mm

Missing Targets
GBRP
HCE
Axes

Messages

QFoto-Module Quality Report

Production

optical

2 Qualification of Concentrators

QDec: Deflectometry Systems for Mirror Panels & Modules

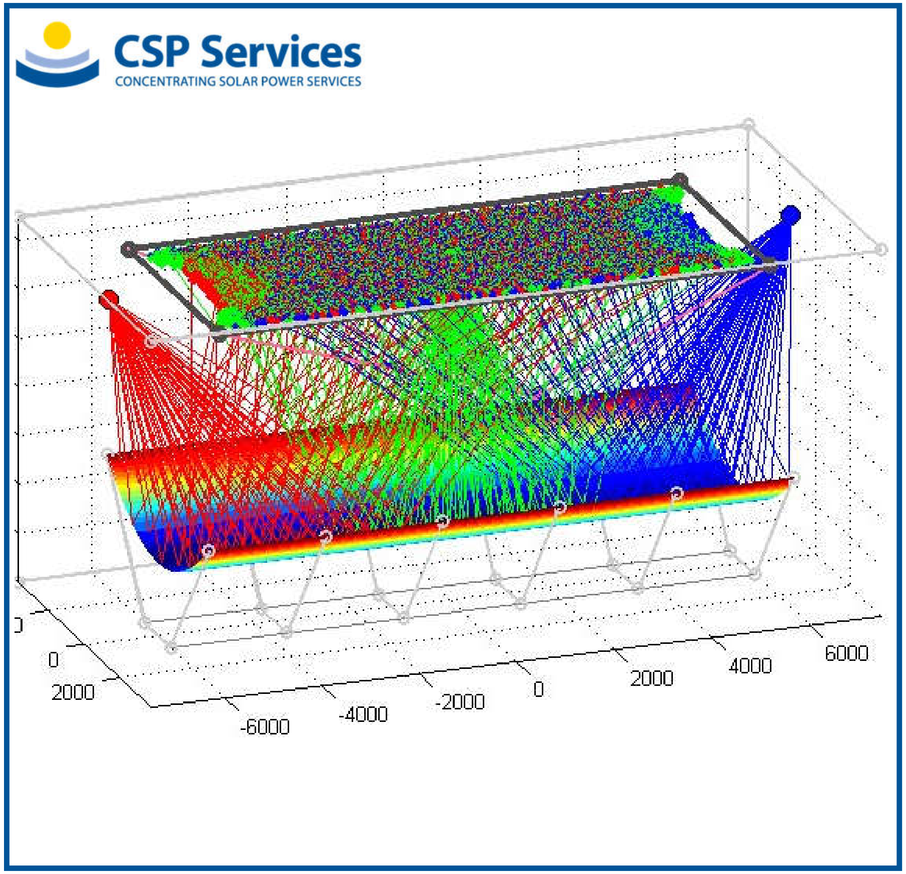

QDec: Automated System for Horizontal and Vertical *Mirror Panels*

QDec-M: Automated System for *12m-Collector Module*

R&D

&

O&M

2 Deflectometry in the field

For heliostats

For troughs

→ Part of other talks today

3 Receiver Performance

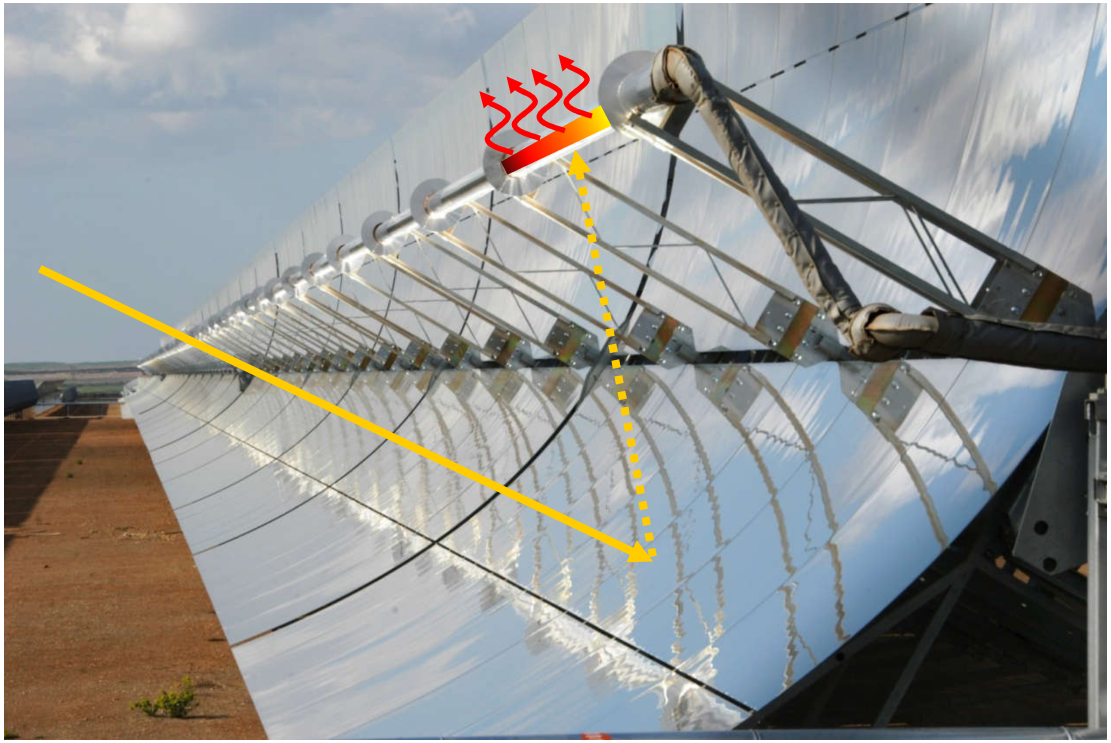

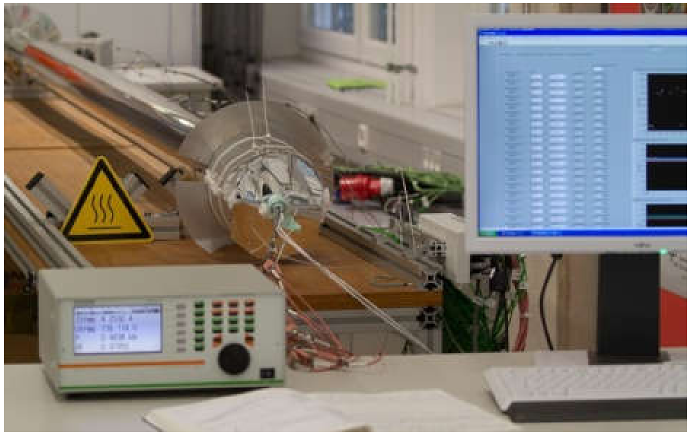

Receiver performance parameters:

- Optical efficiency $\eta_{opt,rec}(T)$
- Thermal loss power $P_{th,loss}(T)$

(non-destructive measurements)

3 Receiver Durability

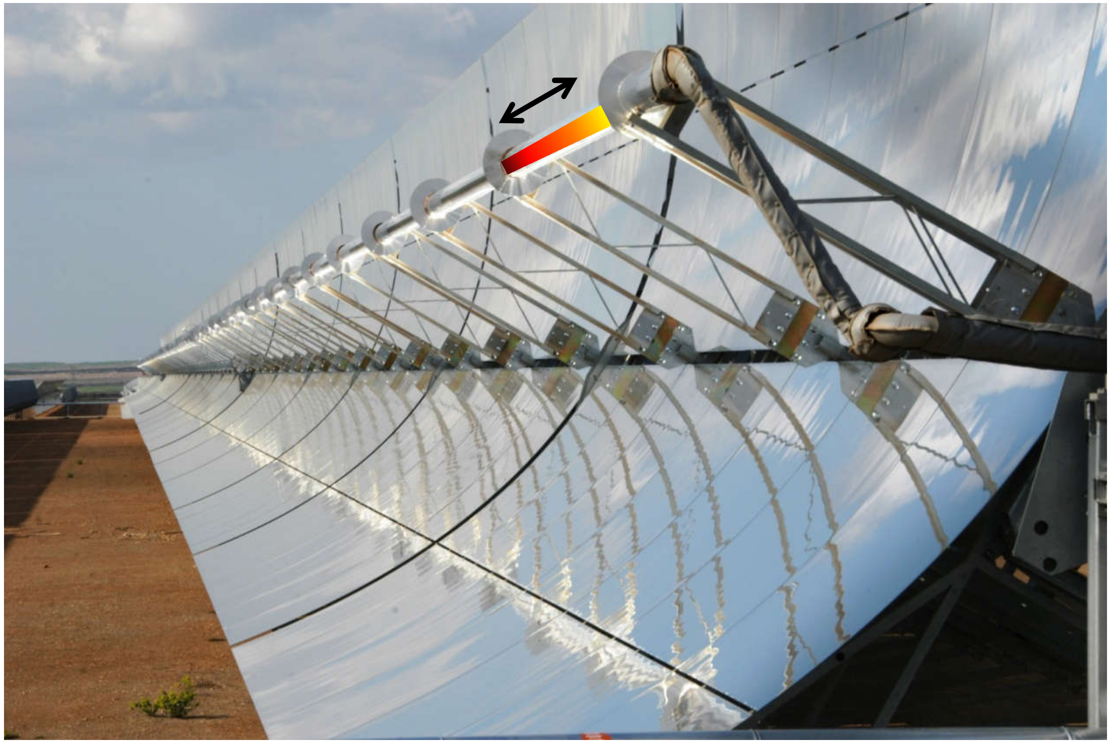

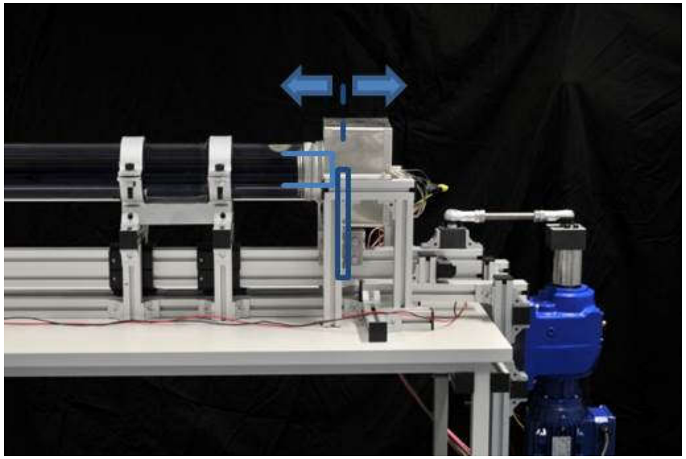

Durability tests:
- Overheating and Thermal Cycling
- Bellow fatigue tests
- Operability tests under real solar conditions (Kontas at PSA, Spain)

4 Performance testing – collector module

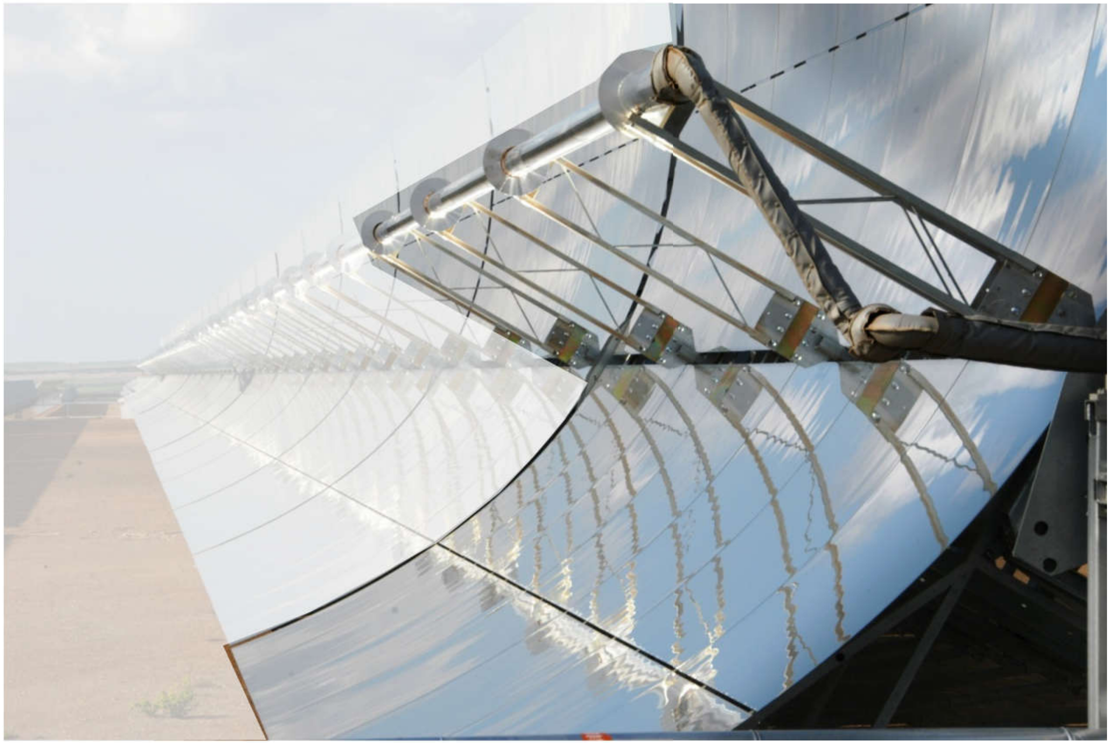

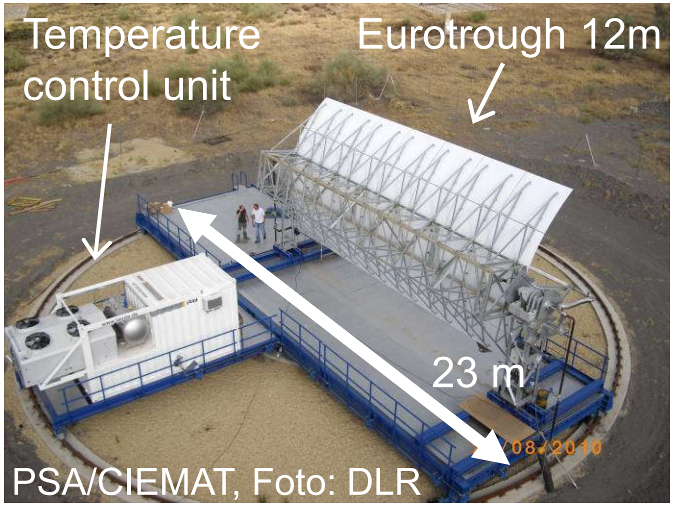

PSA/CIEMAT, Foto: DLR

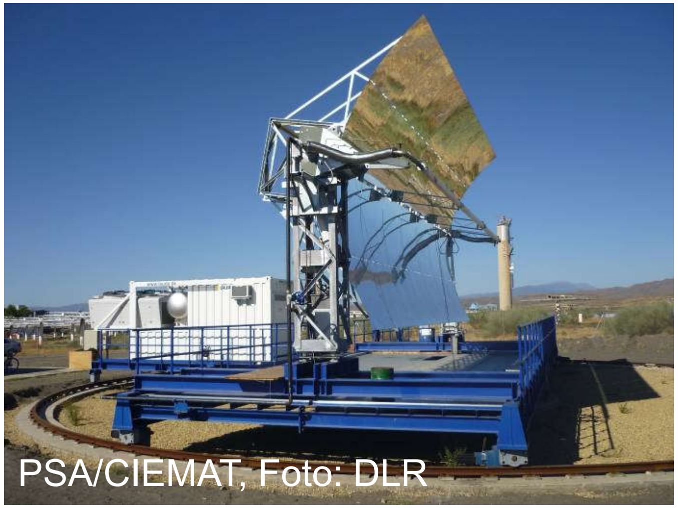

PSA/CIEMAT, Foto: DLR

Collector quality features:
- Peak efficiency, thermal losses
- Behavior under different load conditions (tracking quality, deformation, torsion)

R&D O&M

→ Specific talk today

4 Performance testing – collector loop

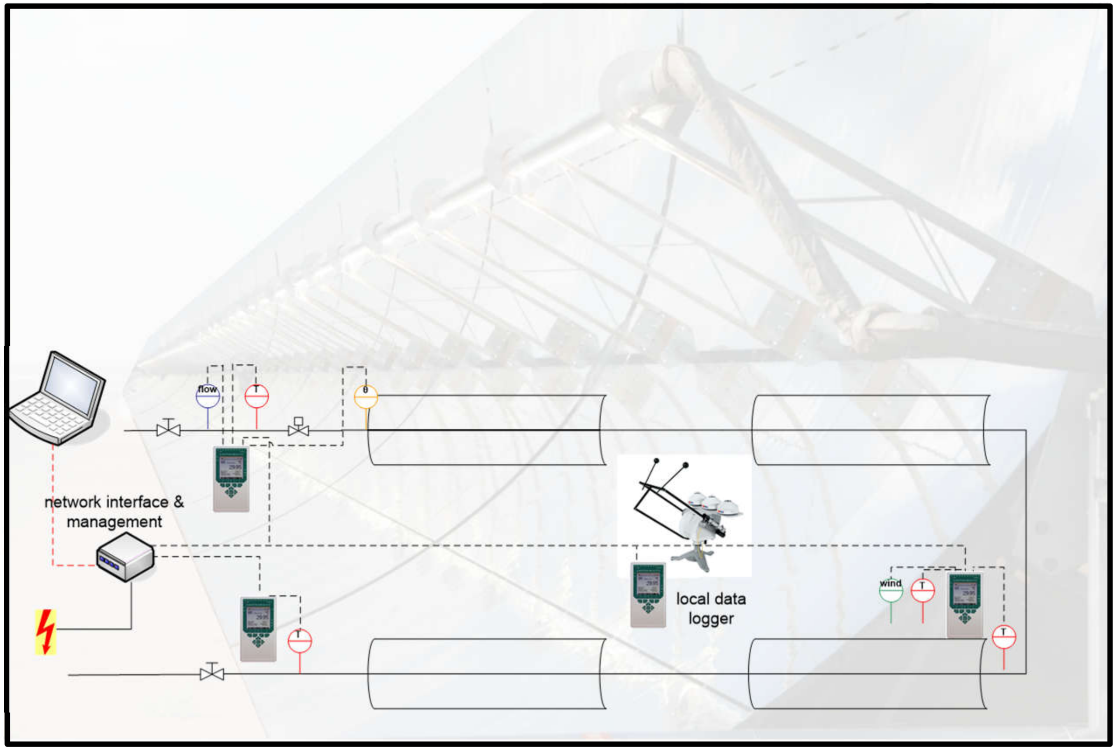

Mobile Field Laboratory:
- Clamp-on ultrasonic flow meter
- Clamp-on temperature sensors
- Irradiance measurement station
- Camera equipped quadrocopter


PSA/CIEMAT, Foto: DLR

Benefits
- Detecting optimization potential of solar field
- Failure Detection, Quality Control
- Accurate performance parameters lead to reliable results of system simulations

4 Performance testing – collector field (optical & thermal)

→ Specific talk today

O&M

*) Measurement Volume per day, of a 50 MW PTC solar field


PSA/CIEMAT, Foto: DLR

QFly Classic
- Mirror shape (high resolution)
- Absorber Tube

QFly Survey
- Alignment
- Torsion, Tracking
- Mirror shape (low resolution)

QFly Thermo
- Defective absorber
- Heat loss detection

DLR Spin-Offs: Volateq and CSP Services

Benefits
- Failure Detection
- Quality Control
- Optimization of parabolic trough collector Fields

→ Specific talk on Friday

4 Performance Testing / CRS Receivers

Flux Density Measurement

optical

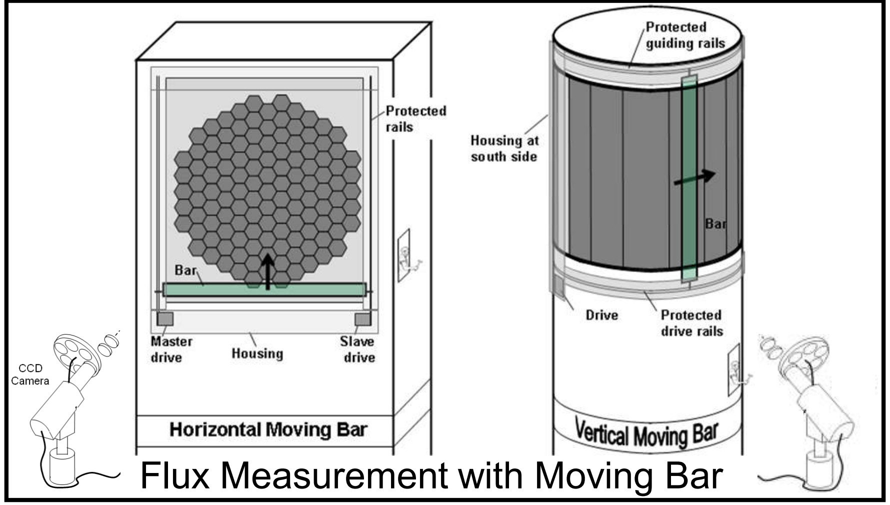

Flux Measurement with Moving Bar

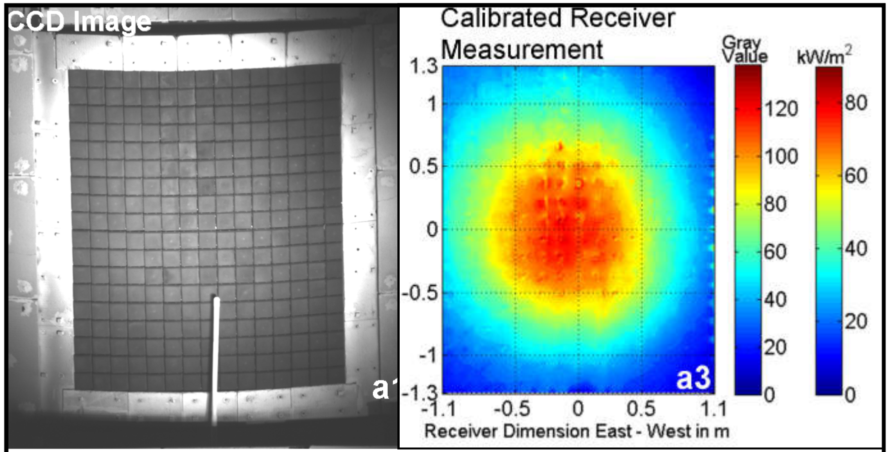

Flux Measurement on Receiver Surface

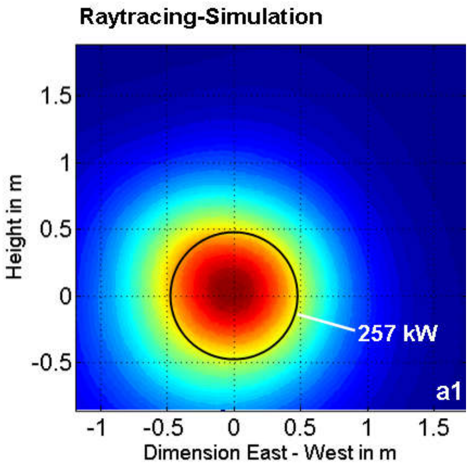

Flux Density by Raytracing-Simulation

5 Materials: Mirror Reflectance

→ Specific talk on Thursday

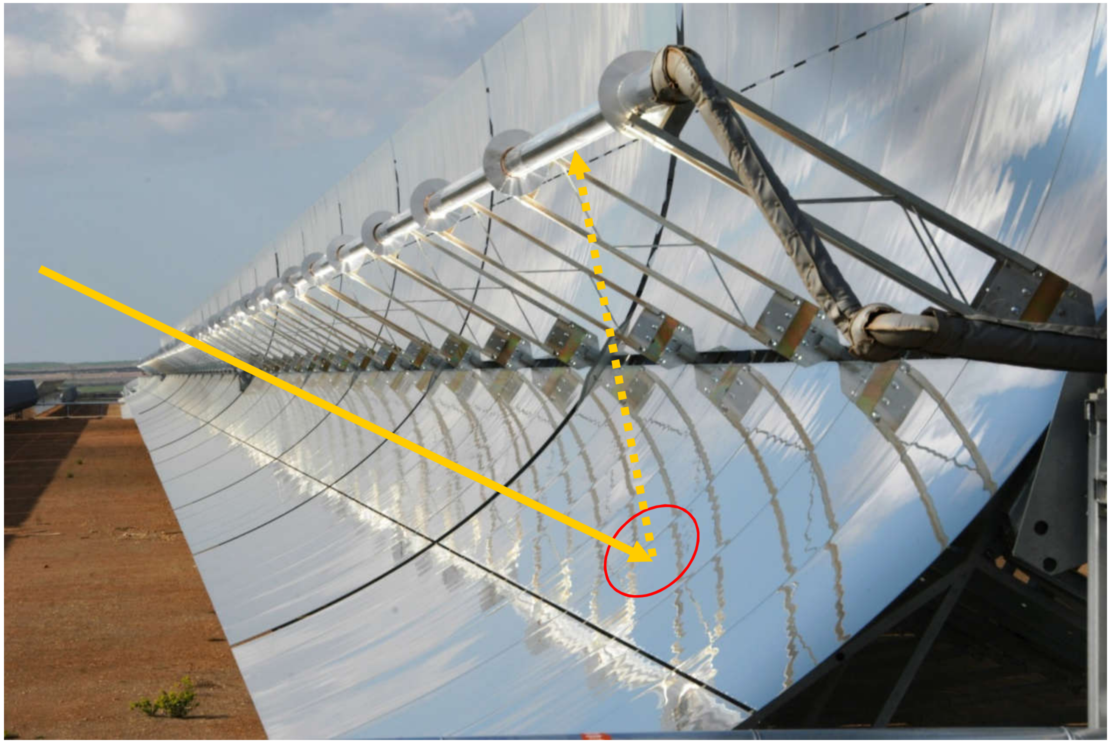

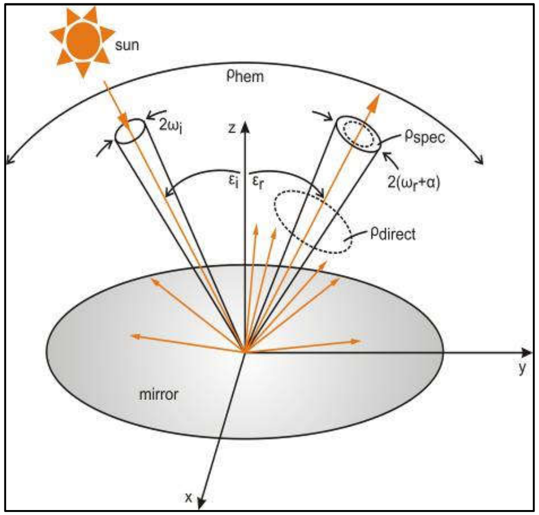

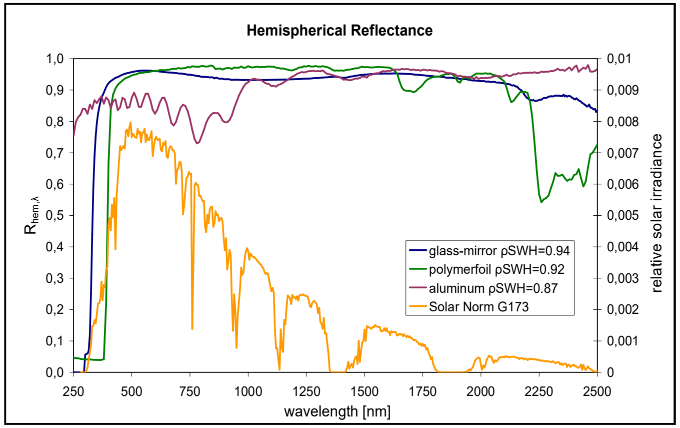

Evaluation of quality and performance parameters:
- Spectral hemispherical reflectance
- Specular reflectance

5 Materials: Mirror Durability

→ Specific talk on Thursday

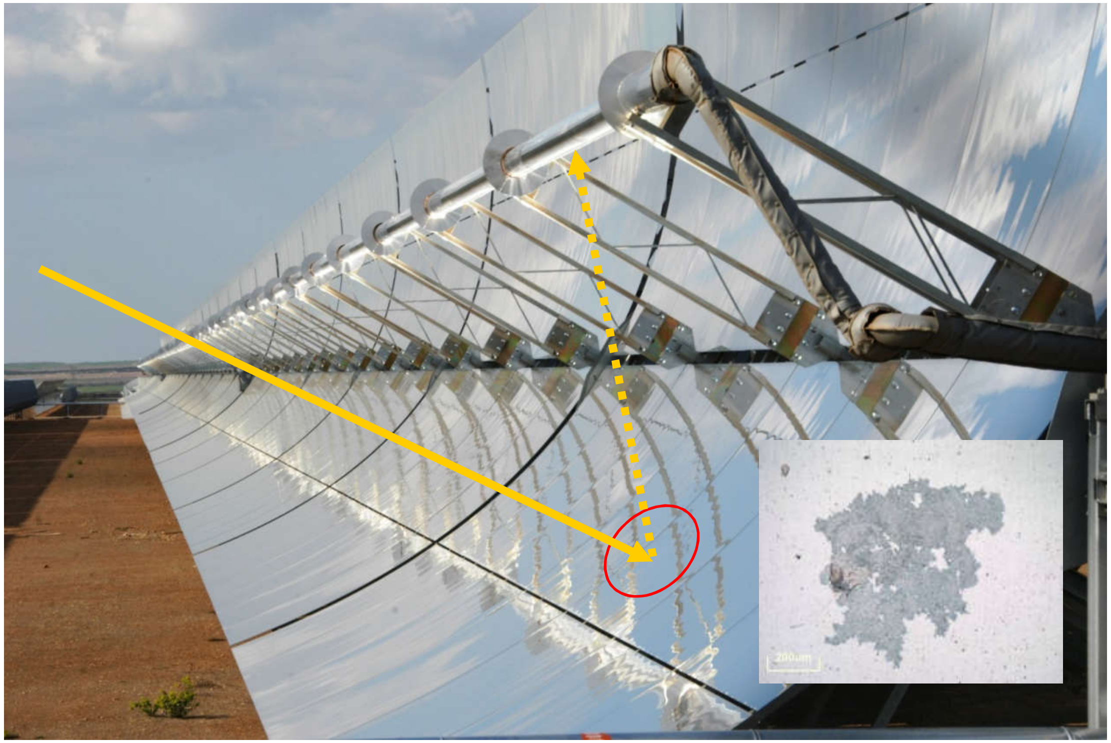

PSA/CIEMAT, Foto: DLR

Accelerated ageing tests
- Laboratory: humidity, salt spray, UV, temp. cycling, aggressive corrosion
- Outdoor ageing tests in different climatic regions

O&M

5 Qualification of Fluids

Measurement of hydrogen in oil samples in solar field

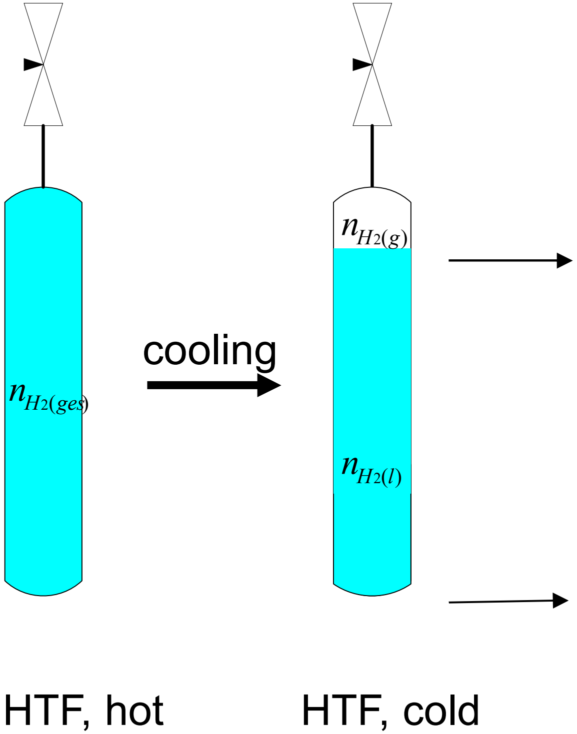

Hydrogen in gas phase

$$n_{H2(g)} = \frac{p_{H2}\left(V_{ges} - \frac{m_{HTF}}{\rho_{HTF}}\right)}{RT}$$

$p_{H2} = p_{ges} x_{H2}$ x_{H2} - *via GC*

Hydrogen in liquid phase

$$p_{H2} = \frac{n_{H2(l)}}{n_{HTF}} H_{H2}$$

$$n_{H2(l)} = \frac{p_{H2} n_{HTF}}{H_2}$$

- Sampling of <u>liquid and gas phase</u> with steel cylinders inline (pressurized & hot)
- Analysis of (all) dissolved gases offline (lab)

O&M

5 Qualification of Fluids

Reduced H2-Formation using Silicone Fluids

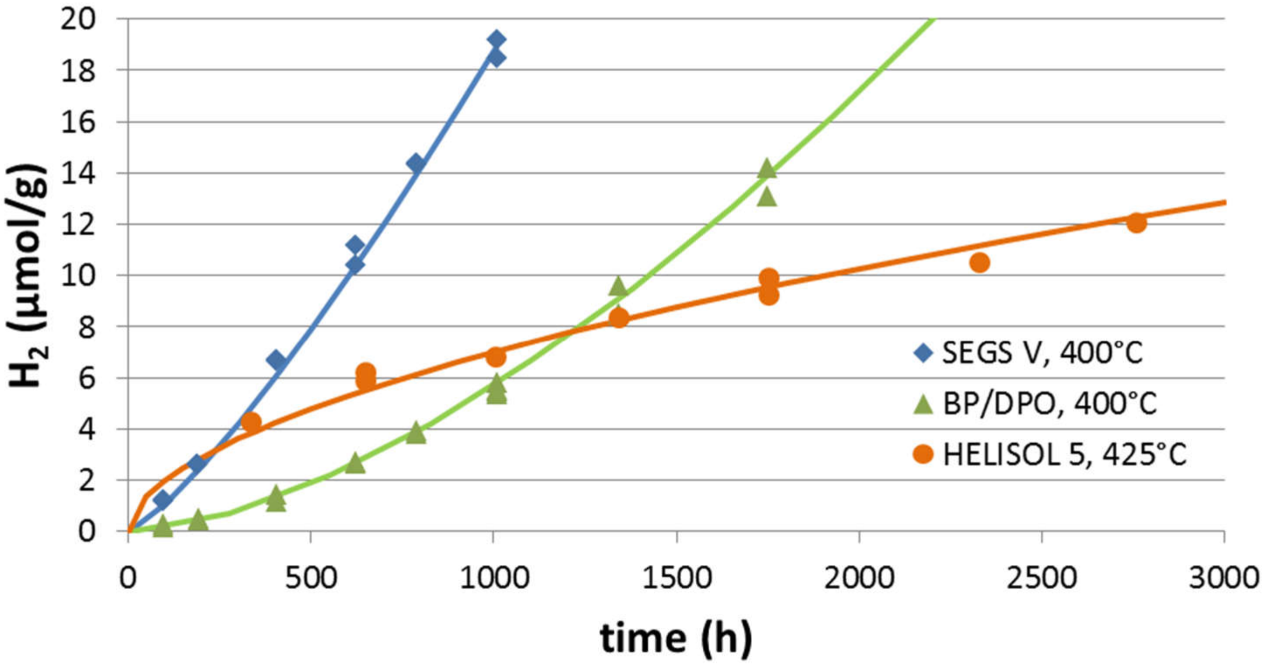

- Eutectic mixture of biphenyl (BP) and diphenyl oxide (DPO) forms hydrogen at increasing rate on prolonged operation
- New silicone fluids form less hydrogen on prolonged operation at elevated temperature

O&M

Qualification using Artificial Intelligence

Analysis of optical images and vector data streams

We use machine learning methods for:
- image processing
  (e.g. cloud images or concentrator recognition)
- and for data-driven failure detection for preventive maintenance.

→ Next talk:
Case Study - Parabolic trough field data analysis with AI (A. Brenner)

SFERA-III
Solar Facilities for the European Research Area

-THANK YOU FOR YOUR ATTENTION!
-ANY QUESTIONS?

GOBIERNO DE ESPAÑA MINISTERIO DE CIENCIA, INNOVACIÓN Y UNIVERSIDADES Ciemat
ENEA
DLR Deutsches Zentrum für Luft- und Raumfahrt
UNIVERSIDADE DE ÉVORA
ESTELA
THE CYPRUS INSTITUTE
instituto IMdea energía
Fraunhofer ISE
euronovia
LNEG
METU
ETH zürich
UNIVERSIDAD DE ALMERÍA
cnrs
cea

Marc Röger, DLR
marc.roeger@dlr.de

DLR SFERA

SFERA-III
Solar Facilities for the European Research Area

Solar Facilities for the European Research Area

2nd Training for Industries “Optimization of CST plant output by optical and thermal characterization and target-oriented O&M”
26 – 29 April 2022, Plataforma Solar de Almería, Spain

Parabolic trough field data analysis with artificial intelligence (AI)

Alex Brenner, DLR (alex.brenner@dlr.de)

NETWORKING

THIS PROJECT HAS RECEIVED FUNDING FROM THE EUROPEAN UNION’S HORIZON 2020 RESEARCH AND INNOVATION PROGRAMME UNDER GRANT AGREEMENT NO **823802**

Motivation

- Data analysis: Use available measurements from solar field and artificial intelligence tools to get **useful** and **understandable** information about solar field condition
- Quantify the goodness of operation, calculate additional parameters which are difficult/expensive to measure

- **Optimize power output** of the solar field with:
  - Early detection of degradations (Predictive Maintenance)
  - Reduction of down times
  - Optimize control parameters
- Reduction of **operation costs**:
  - Reduced personnel costs
  - Maintenance follows requirements not strict time interval
  - Increase in component lifetime

Satellite image of La Africana

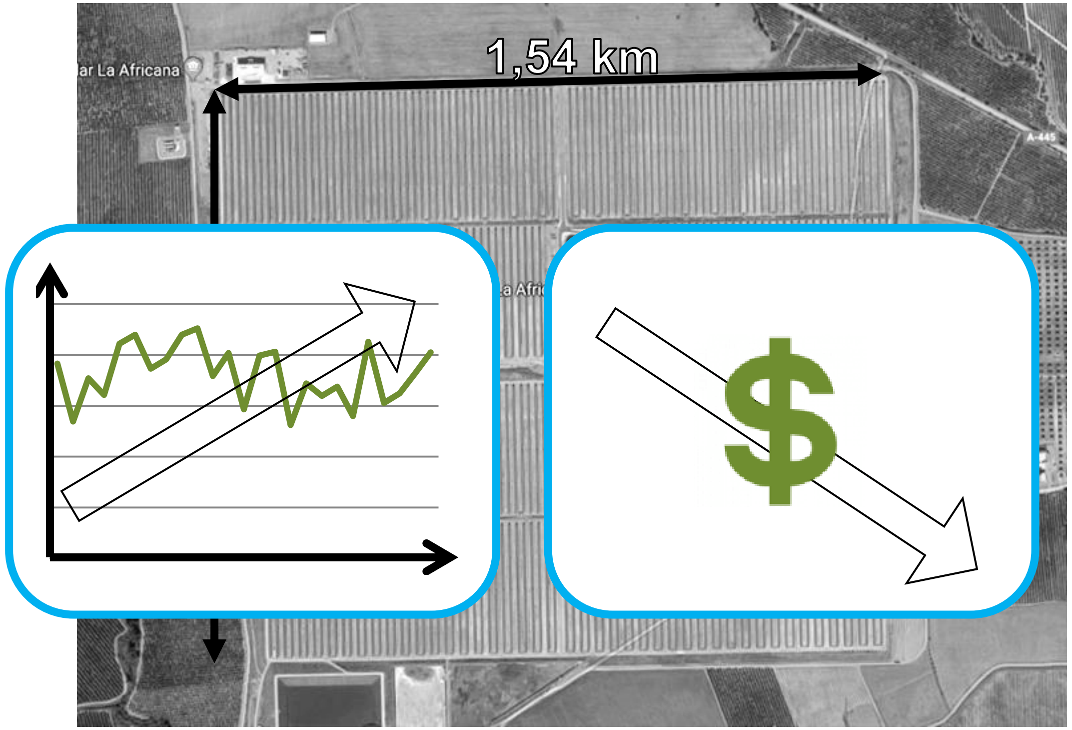

Google. Google Maps. 2019 [cited 2019 18. September]; Available from: https://www.google.com/maps/@37.7544897,-5.0605687,2216m/data=!3m1!1e3.

Motivation

> *„How can we use the available data in a parabolic trough solar field to maximize the information about the solar field condition?“*

Data analysis applications: Anomaly detection

- Find unusual behaviour in measurment data from solar field
- Locate collectors with unusual behaviour

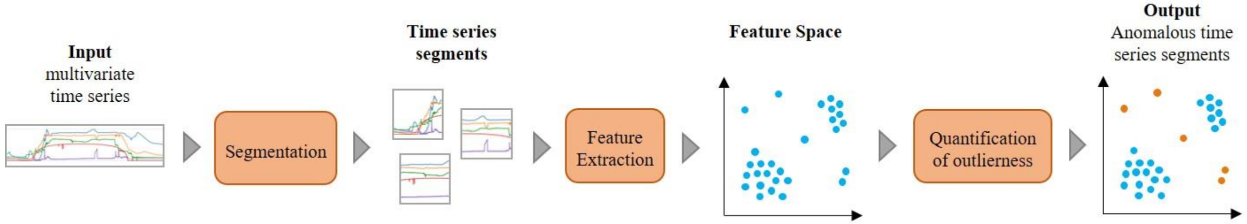

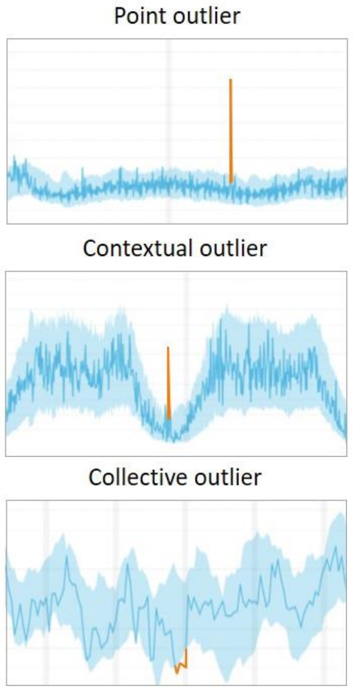

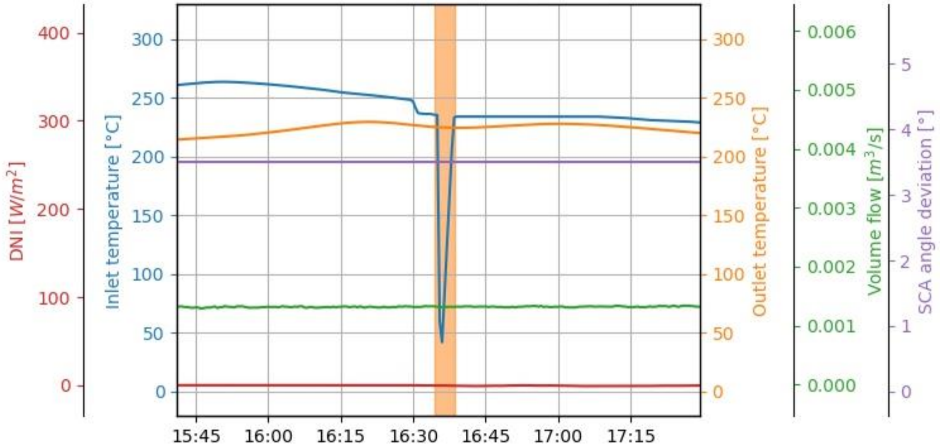

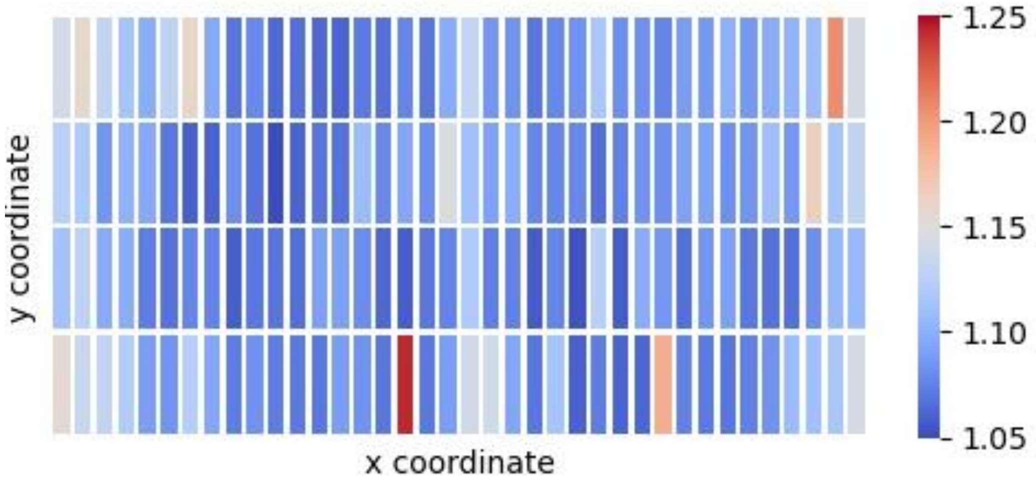

Images from Braun 2020; https://elib.dlr.de/139874/

Data analysis applications: Loop flow determination

- Use the temperature sensors at collectors to determine the loop flow from fluid runtime
- Loop flow helpful for: hydraulic balancing, control tasks,…

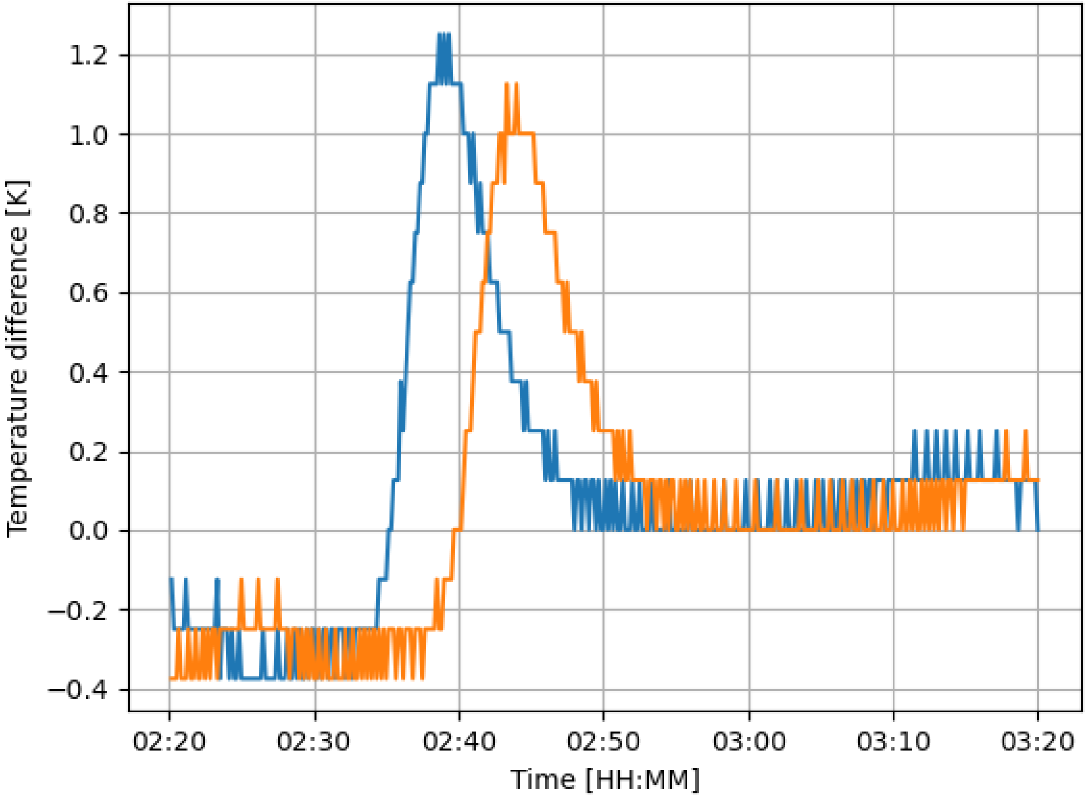

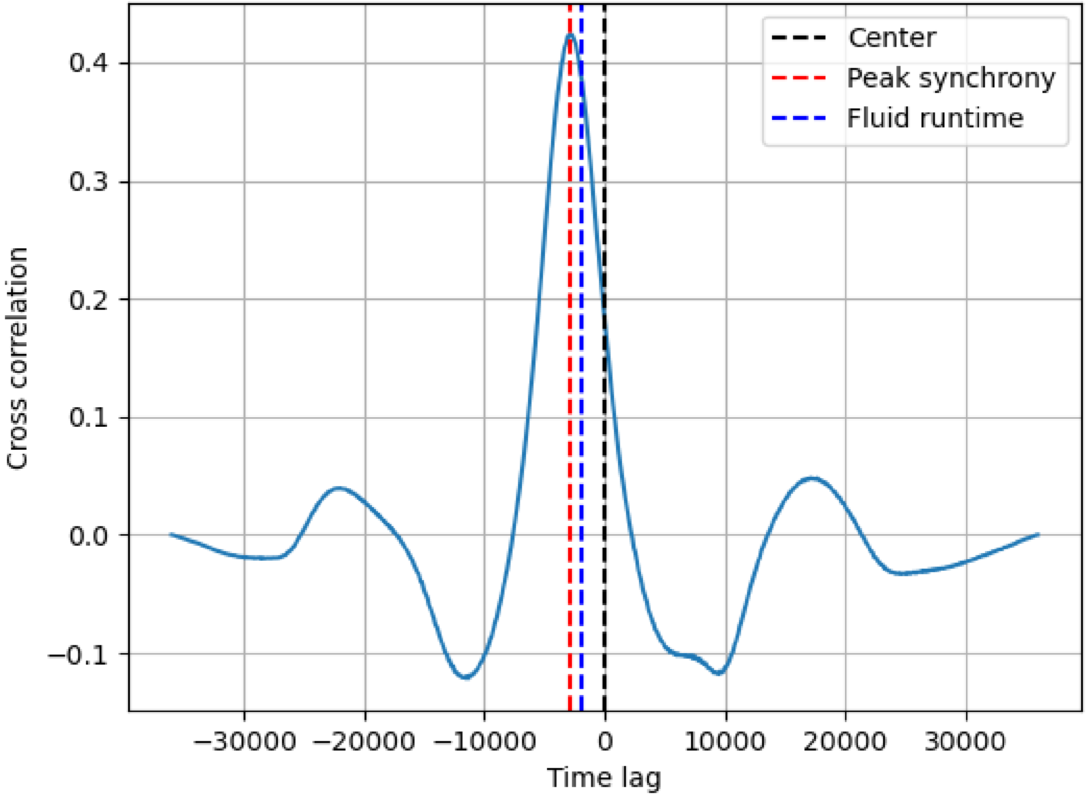

Data analysis applications: Soiling estimation

Soiling

- Dust particle deposition on the mirrors
- Highly dependent on the location
- Power output directly influenced → less irradiation on the receiver

Parabolic trough at Plataforma Solar de Almería
(Owned by the Spanish research center CIEMAT), Source DLR

Operational data

- Used and recorded in regular power plant operation
- Only certain measured variables at specific positions in the field

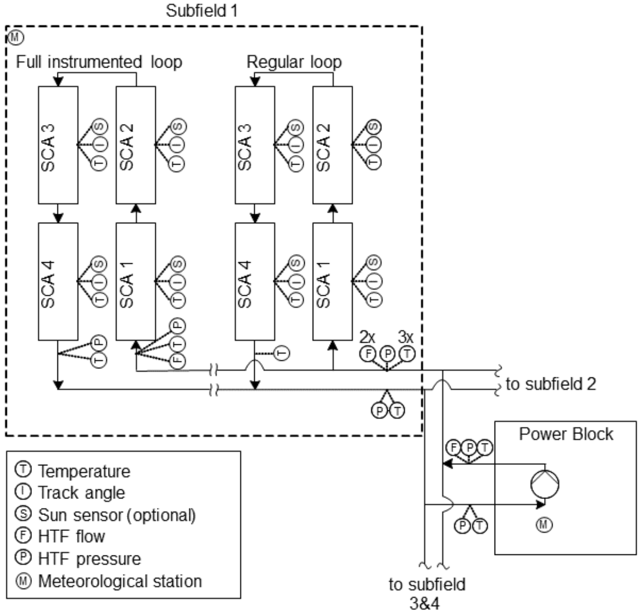

Brenner, A. et al. 2021; https:// doi.org/10.3390/en14217166

Meteorological data

- Time-series data
- Measuring stations already available in the solar field
- Only certain measured variables at specific positions in the field
- Direct soiling measurement usualy not available

Approach

Aim:

- Determine soiling level directly from operational + meteorological data for each collector in the field
    - Improvements in cleaning schedule
    - Supplement to reflection measurements in the field
    - Detect influence of soiling on single collectors

Approach:

Soiling reason

Meteorological factors

Wind, rain, particle concentration,…

Soiling influence

Position in the field

Higher soiling impact on collectors at solar field edge,…

Plant operation

Time since the last cleaning,…

Operational data

Temperature, focus, dumping,…

Soiling measurements

Ground-truth data, target values

Effects

Soiling model uses reasons, influences and effects to determine current soiling level

Approach

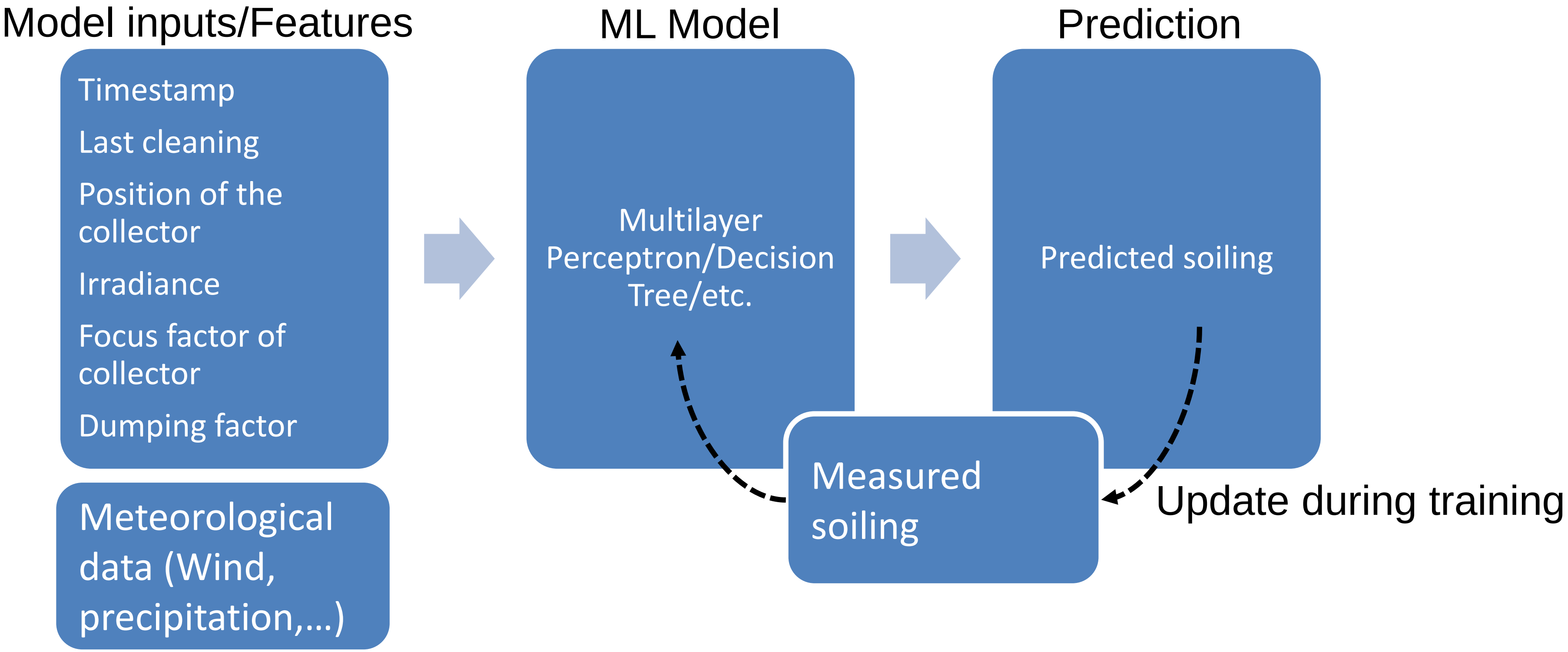

Model inputs/Features

- Timestamp
- Last cleaning
- Position of the collector
- Irradiance
- Focus factor of collector
- Dumping factor

Meteorological data (Wind, precipitation,…)

ML Model

Multilayer Perceptron/Decision Tree/etc.

Prediction

Predicted soiling

Measured soiling

Update during training

Models

Decision Tree: Regression

- Supervised Learning
- Decision Trees are interpretable models
- Split of tree in a new branch is made if model performance can be increased
- Further model improvement with adaptive boosting procedure

Model inputs/Features

Timestamp

Last cleaning

Position of the collector

Irradiance

Focus factor of collector

Dumping factor

Meteorological data (Wind, precipitation,…)

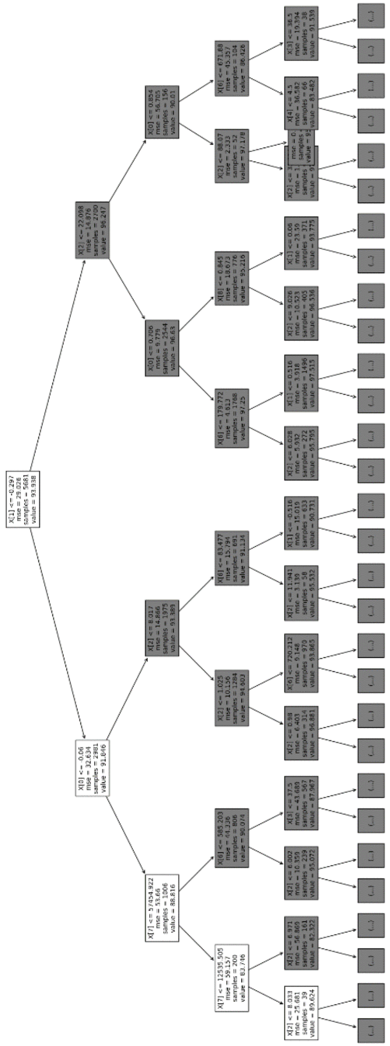

Models

Decision Tree: Regression

- Supervised Learning
- Decision Trees are interpretable models
- Split of tree in a new branch is made if model performance can be increased
- Further model improvement with adaptive boosting procedure

- Coefficient of determination: R^2 = 74.8%
- MSE: 6.36
- RMSE: 2.52
- MAE: 1.56

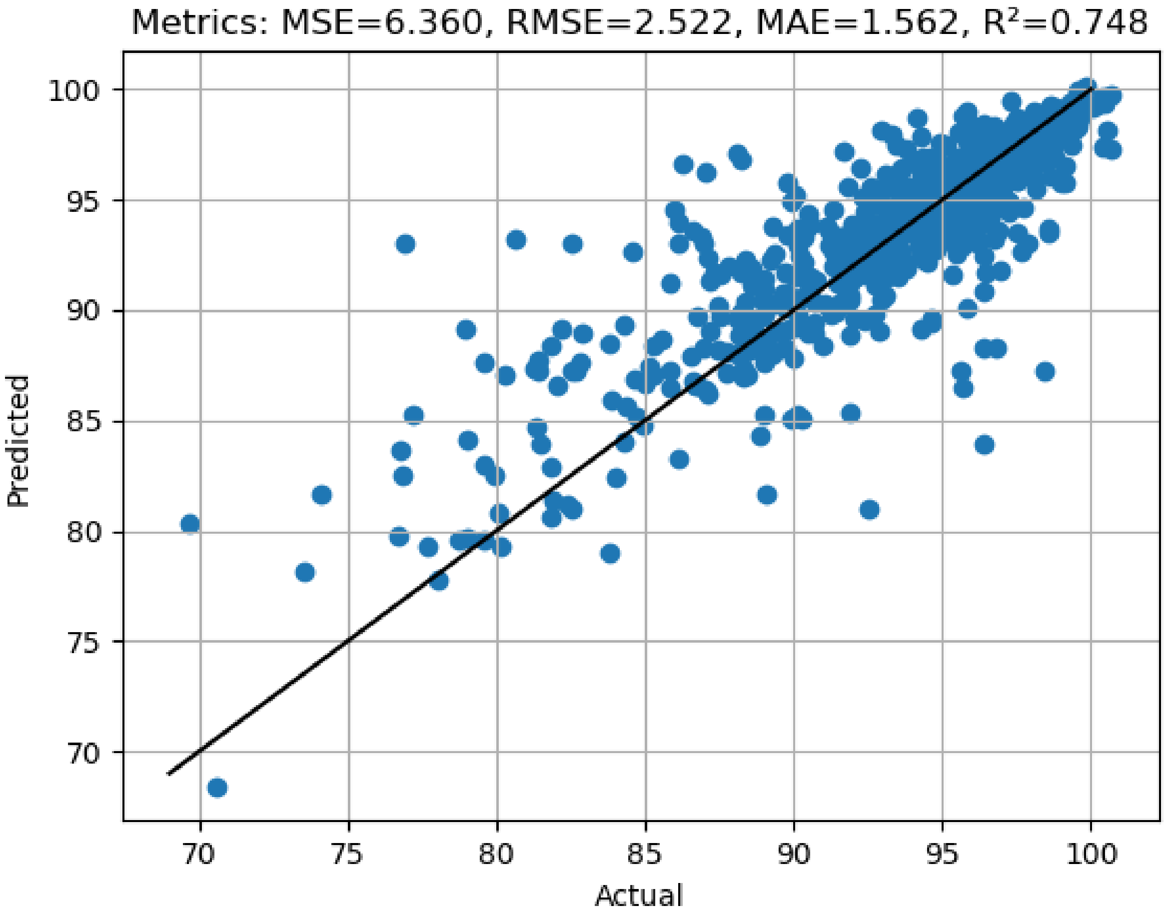

Models

Neural network: Regression

- Supervised Learning
- Simple Feed-forward network
- 4 hidden layers
- Output layer initialized with average soiling value
- Dropout layer between hidden layers

Model inputs/Features

- Timestamp
- Last cleaning
- Position of the collector
- Irradiance
- Focus factor of collector
- Dumping factor

Meteorological data (Wind, precipitation,…)

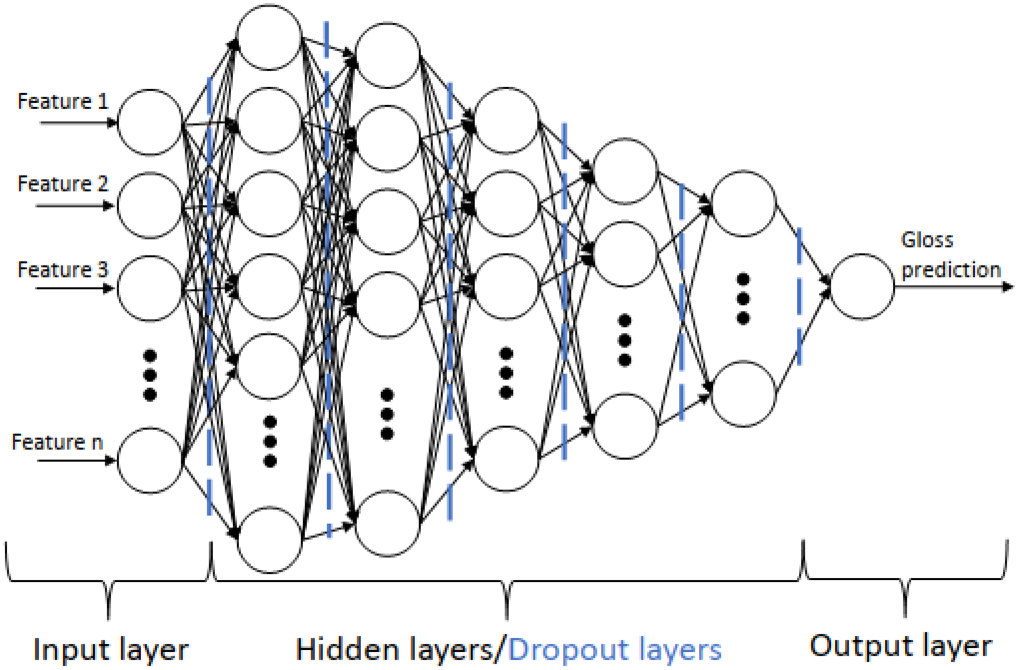

Models

Neural network: Regression

- Supervised Learning
- Simple Feed-forward network
- 4 hidden layers
- Output layer initialized with average soiling value
- Dropout layer between hidden layers

Coefficient of determination: $R^2 = 73.5\%$
MSE: 6.67
RMSE: 2.58
MAE: 1.74

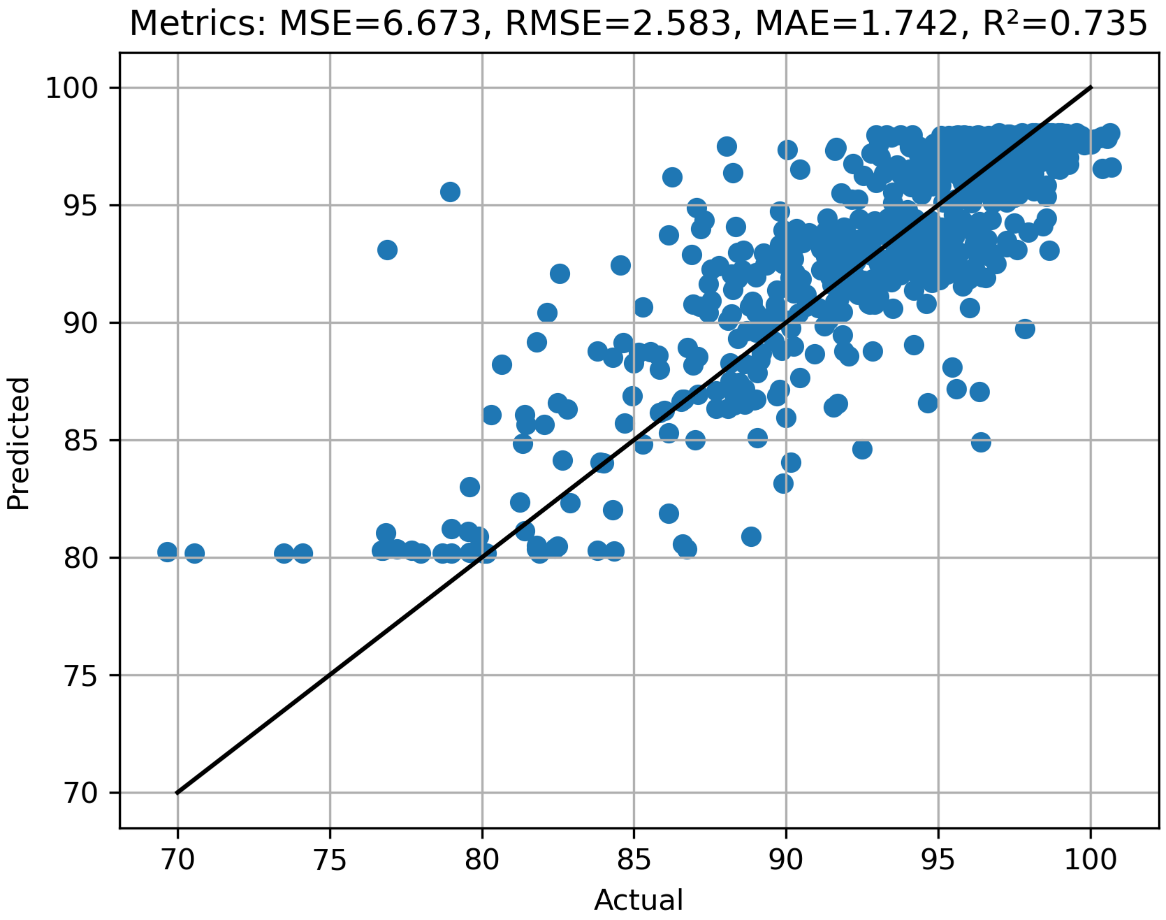

Models

Neural network: Results optimization of cleaning schedule

- If we want to use the results only for the optimization of the cleaning schedule we do not need a precise measurement
- Question to be answered for this purpose: Is collector soiling **above** or **below** a certain cleaning threshold

→ Prediction needs to be sufficiently good in order to reliably decide whether cleaning is necessary or not

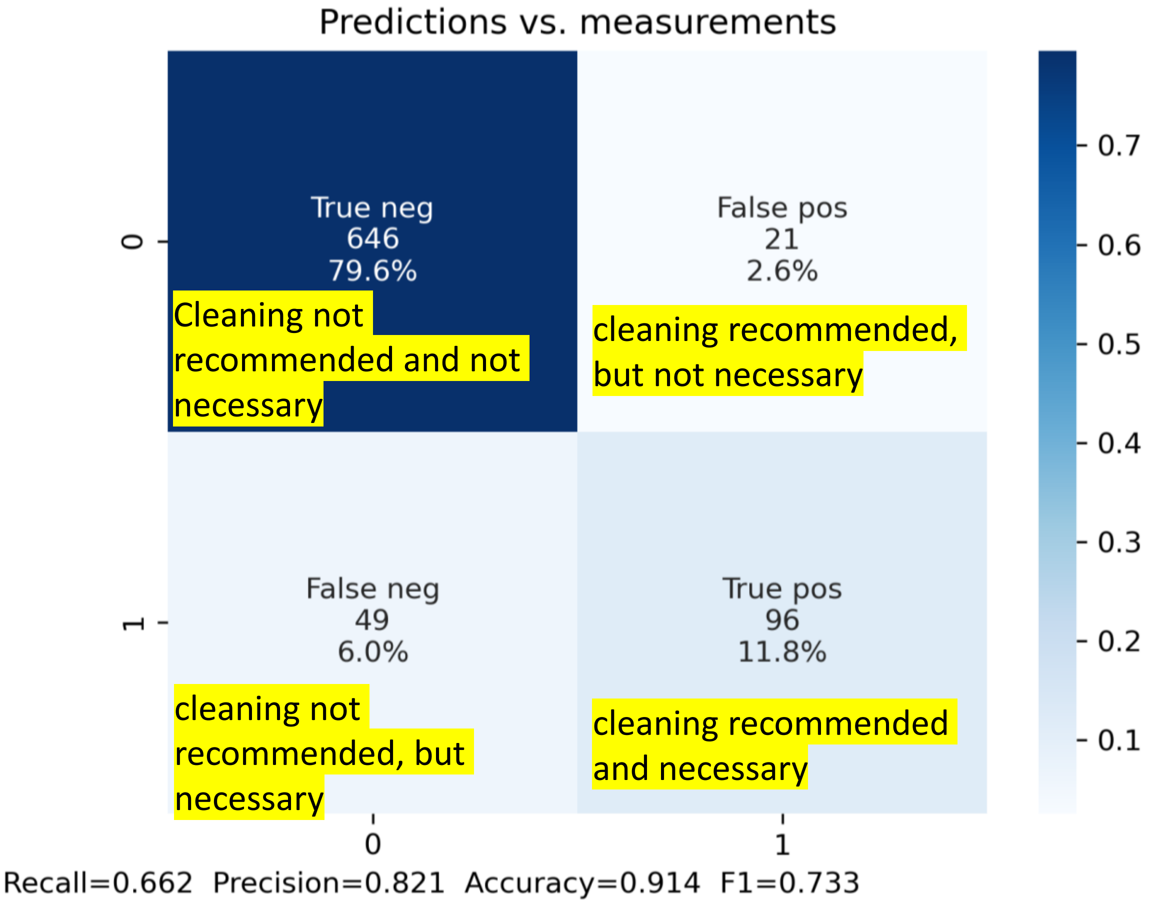

Cleaning not recommended and not necessary

cleaning recommended, but not necessary

cleaning not recommended, but necessary

cleaning recommended and necessary

Recall=0.662 Precision=0.821 Accuracy=0.914 F1=0.733

Conclusion

Method for the determination of soiling from operational and meteorological data for parabolic trough fields

Potentials of the method :

- Reduction of the necessary soiling measurements for the collectors in the field
    - About 75 % of the measurements can be explained with the use of the soiling regression model
- Optimization of the cleaning schedule through soiling determination on collector levels
    - Useful cleanings increased by 12.2 %, too early cleanings reduced by 14.5 %
- Determine power of each collector independently of the soiling state

Any questions regarding the presented applications?

Discussion

- Where do you see further potential for data analysis in CSP applications?
  - Where are the problems?
  - Are there enough measurement data available?

Anomaly detection in parabolic trough fields/heliostat fields?

Digital twin for (sub)components in CSP plant?

Operation strategy recommendation?

THANK YOU FOR YOUR ATTENTION!
ANY QUESTIONS?

Contact:

Alex Brenner, alex.brenner@dlr.de

GOBIERNO DE ESPAÑA
MINISTERIO DE CIENCIA, INNOVACIÓN Y UNIVERSIDADES
Ciemat
Centro de Investigaciones Energéticas, Medioambientales y Tecnológicas

ENEA

DLR Deutsches Zentrum für Luft- und Raumfahrt

UNIVERSIDADE DE ÉVORA

ESTELA

The Cyprus Institute

instituto IMDEA energía

Fraunhofer ISE

euronovia

LNEG

METU

ETH zürich

IN LUMINE SAPIENTIA · UNIVERSITAS ALMERIENSIS
UNIVERSIDAD DE ALMERÍA

cnrs dépasser les frontières

DE LA RECHERCHE À L'INDUSTRIE cea

DLR

SFERA
Solar Facilities for the European Research Area

SFERA-III

Solar Facilities for the European Research Area

2nd Training for Industries “Optimization of CST plant output by optical and thermal characterization and target-oriented O&M”
26 – 29 April 2022, Plataforma Solar de Almería, Spain

Optical measurement theory and airborne measurements

Marc Röger, DLR

NETWORKING

THIS PROJECT HAS RECEIVED FUNDING FROM THE EUROPEAN UNION’S HORIZON 2020 RESEARCH AND INNOVATION PROGRAMME UNDER GRANT AGREEMENT NO **823802**

Overview

1. Efficiency chain
2. Deflectometric measurement principle (Heliostats, trough)
3. Use of UAVs in CSP
4. Examples (Methods already applied and under development)
5. Conclusions & Outlook

1. Efficiency Chain

Example: Parabolic Trough

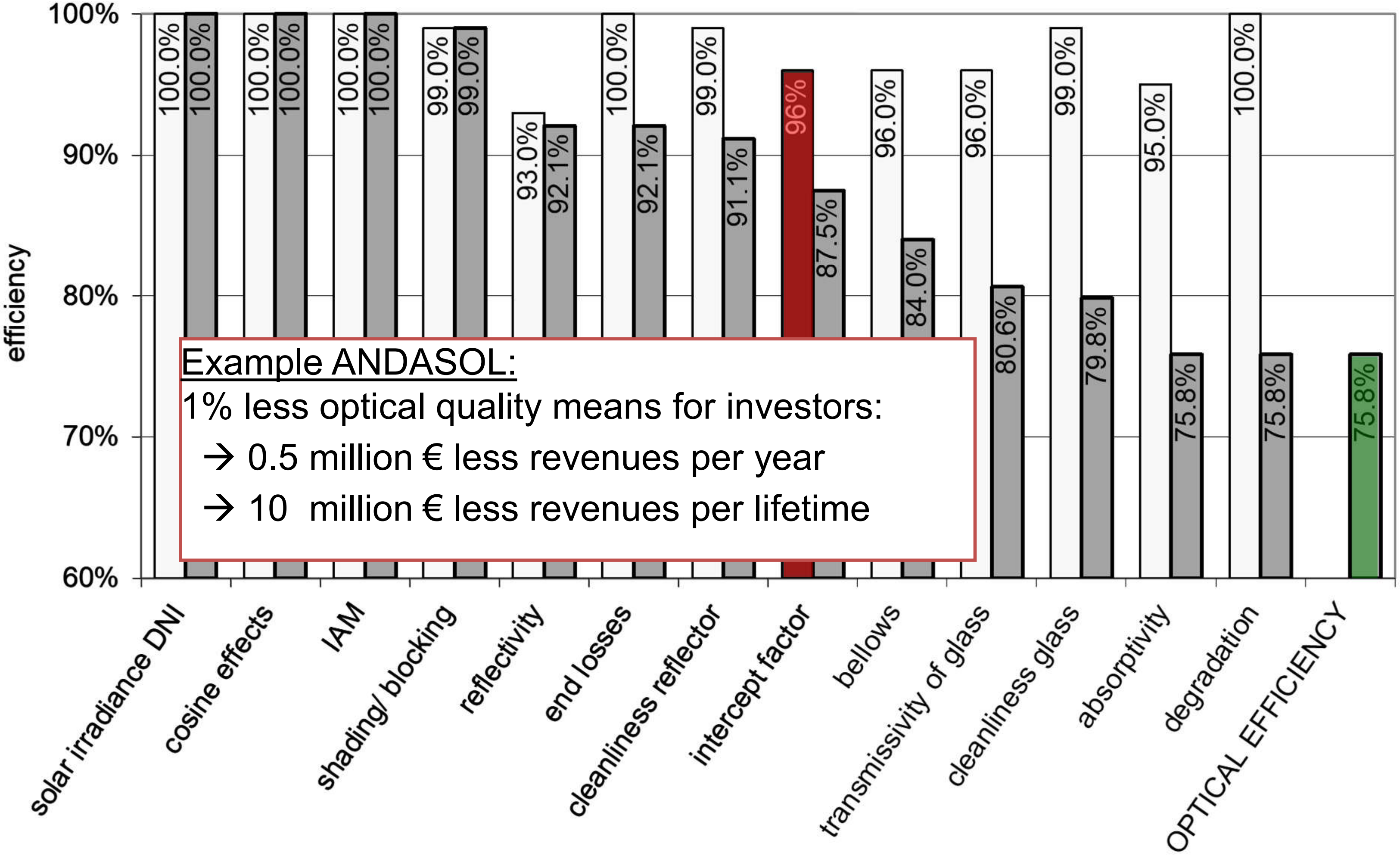

Example ANDASOL:

1% less optical quality means for investors:

→ 0.5 million € less revenues per year

→ 10 million € less revenues per lifetime

1. Efficiency Chain

Possible Concentrator Errors

- **Microscopic surface errors** (roughness, deterioration, scratches, …)
- **Macroscopic surface deviations** (waviness, mirror contour errors, deformations, structural errors, …)
- **Positioning of the receiver tube** (position of supports, bending of tube, …)
- **Tracking errors** (tracking, module alignment, collector torsion, …)
- **(Meteo: Sun Shape, Soiling,…)**
- **(Material: Reflectance Degradation, H2 diffusion,..)**

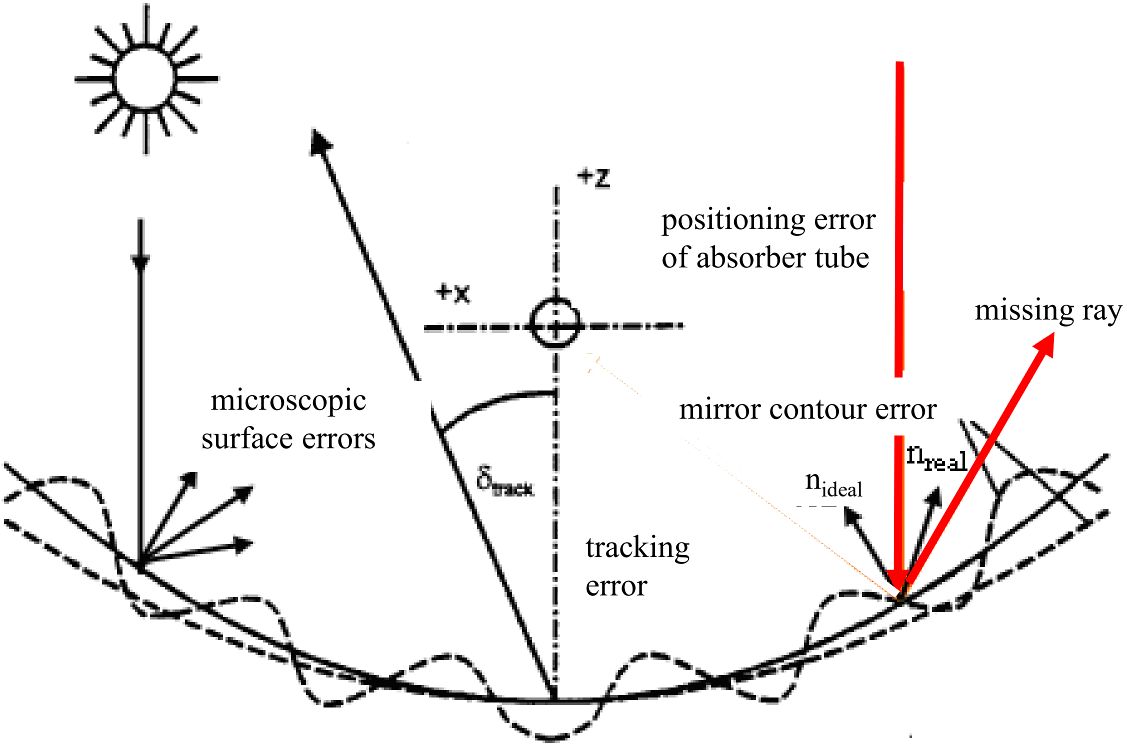

3. Deflectometric measurement principle

Parabolic Trough

- **We have to know**: the position and orientation of the camera relative to the concentrator, and the position of our target (here: the absorber tube)
- **Then**, we can calculate the slope deviation SDx

PSA/CIEMAT, Foto: DLR

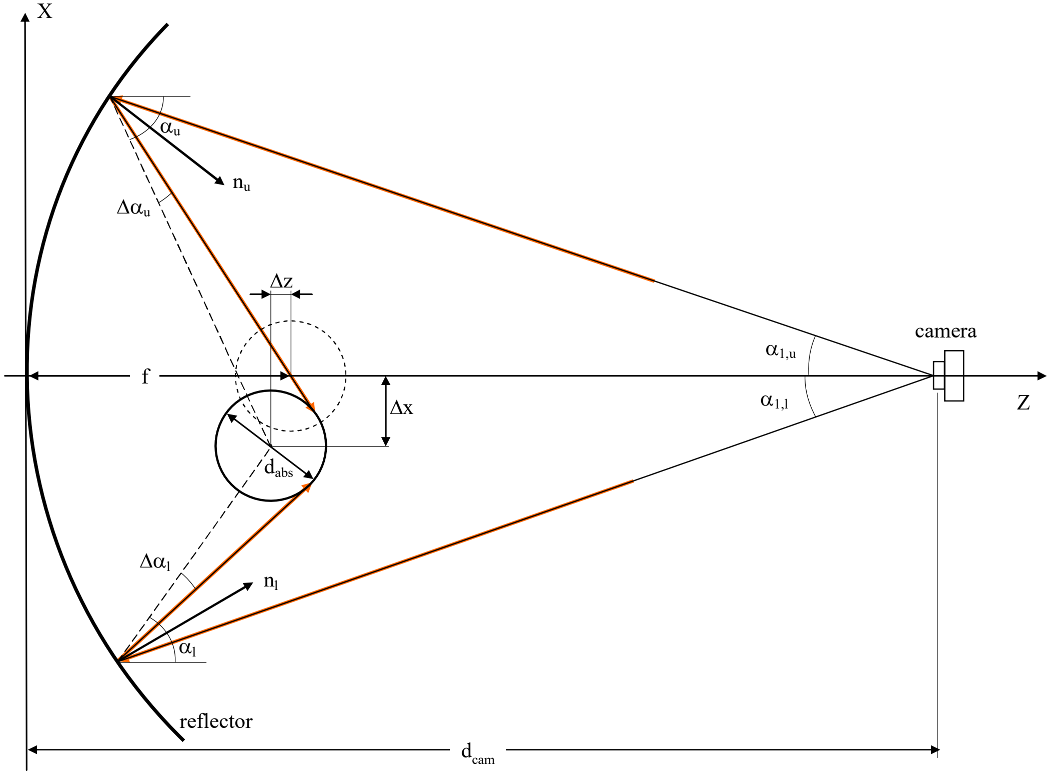

2. Deflectometric Measurement Principle

Parabolic Trough – Image Acquisition

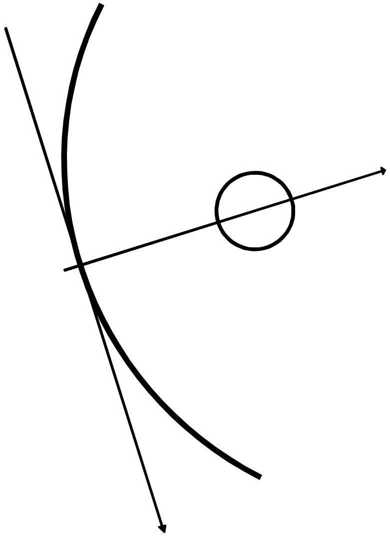

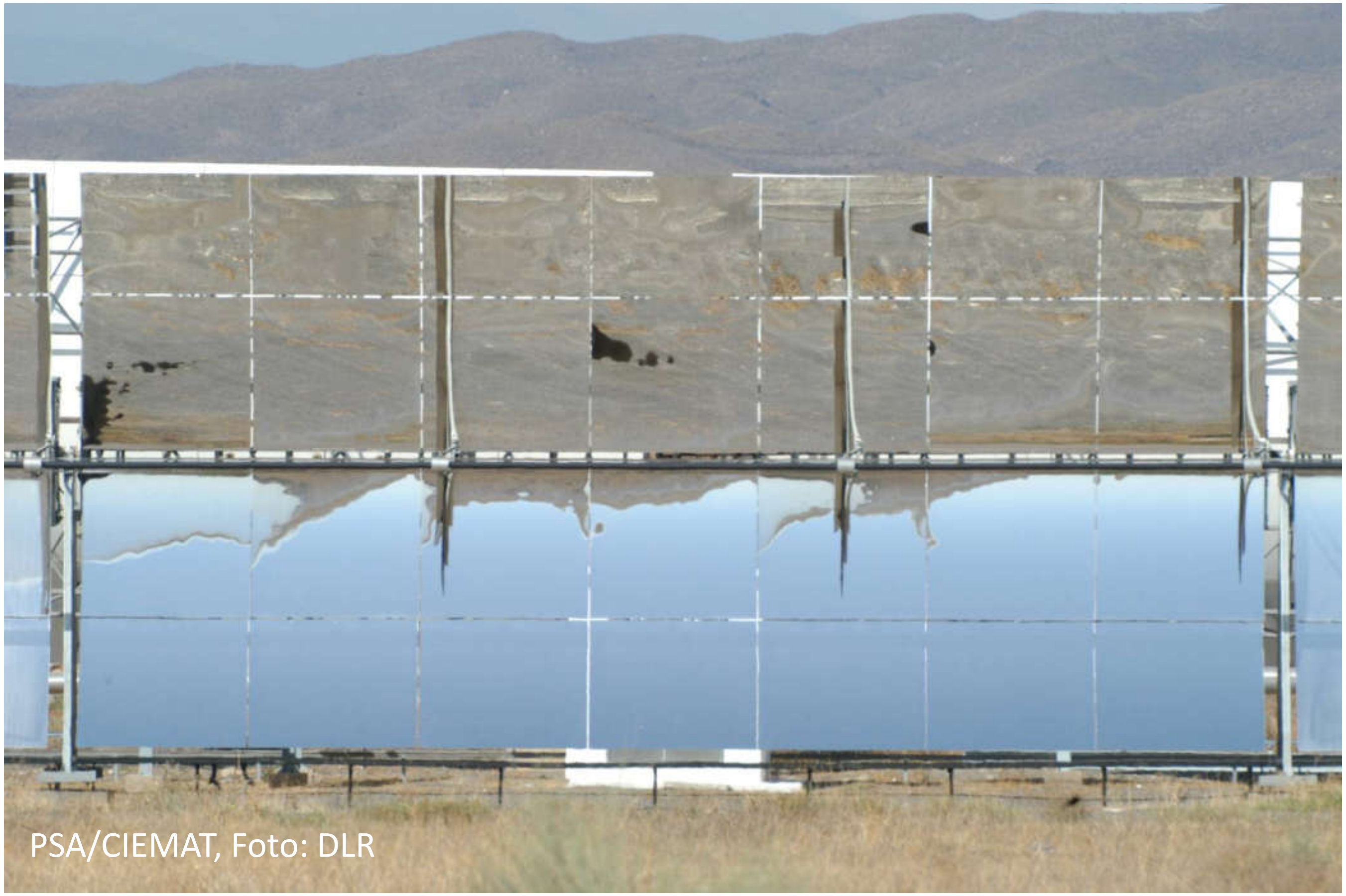

PSA/CIEMAT, Foto: DLR

2. Deflectometric Measurement Principle

Parabolic Trough – Result

Focus deviation in mm of reflected ideal rays

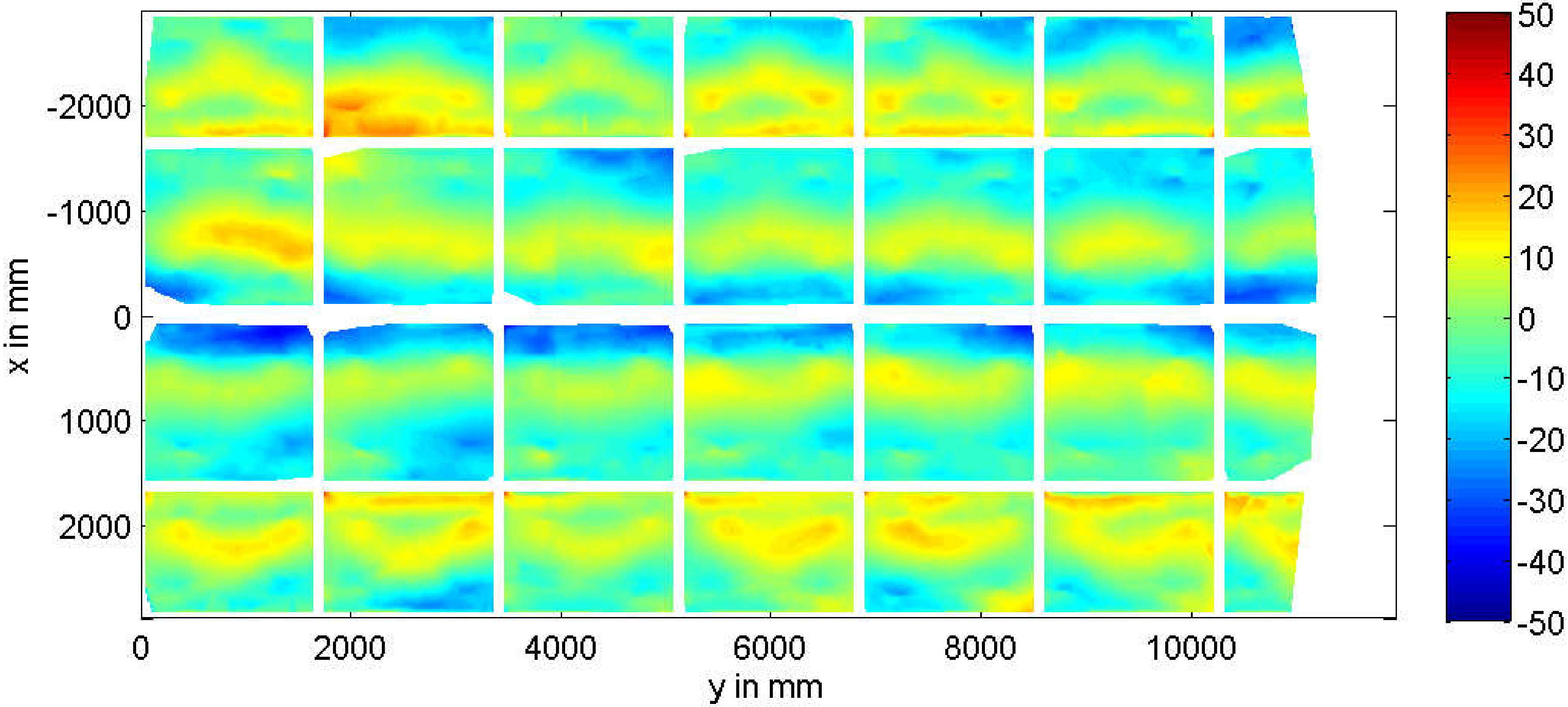

Interpretation of Results

Deflectometry + Intercept Calculation – Result

optical

Local intercept factor in percent with consideration of degraded sunshape

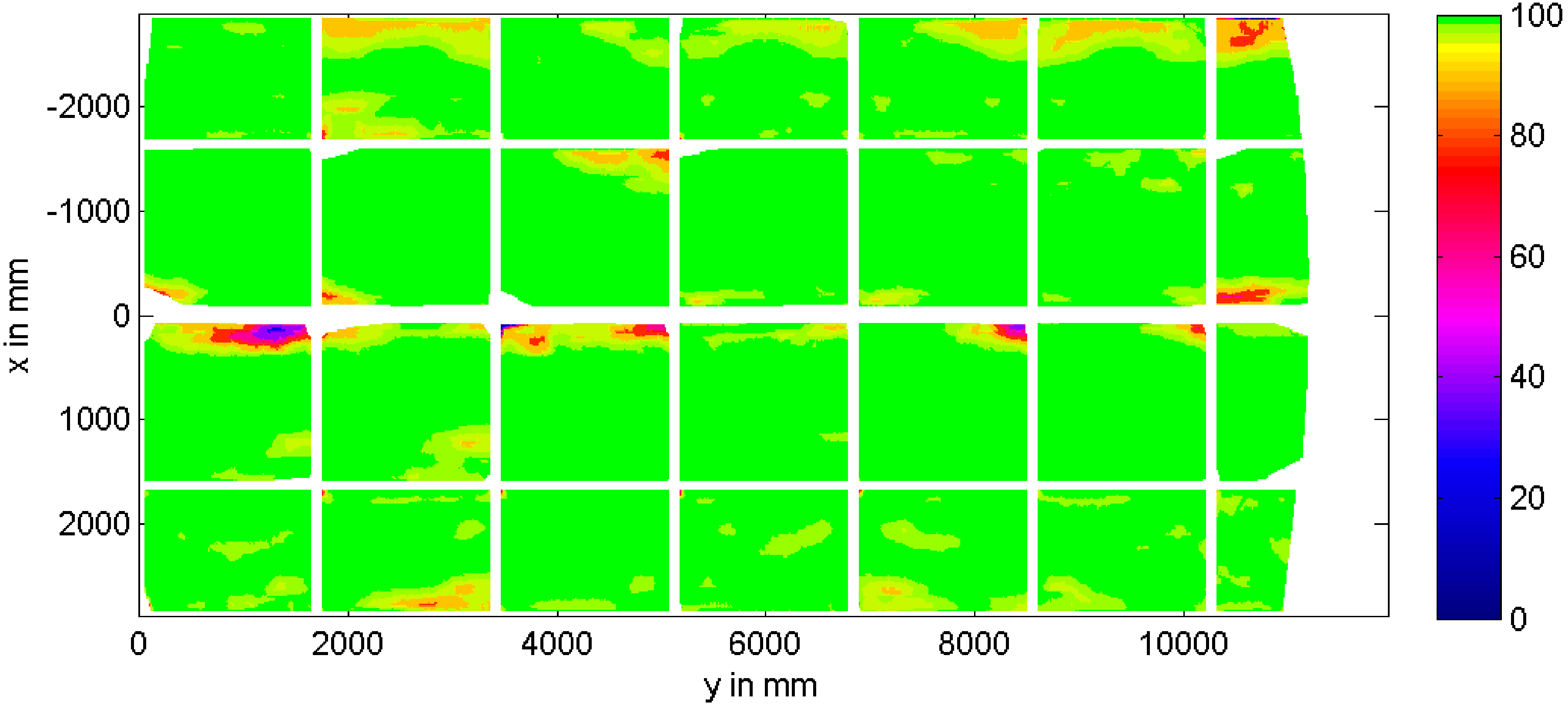

2. Deflectometric Measurement Principle

Solar Tower – Measurement Setup for Heliostats

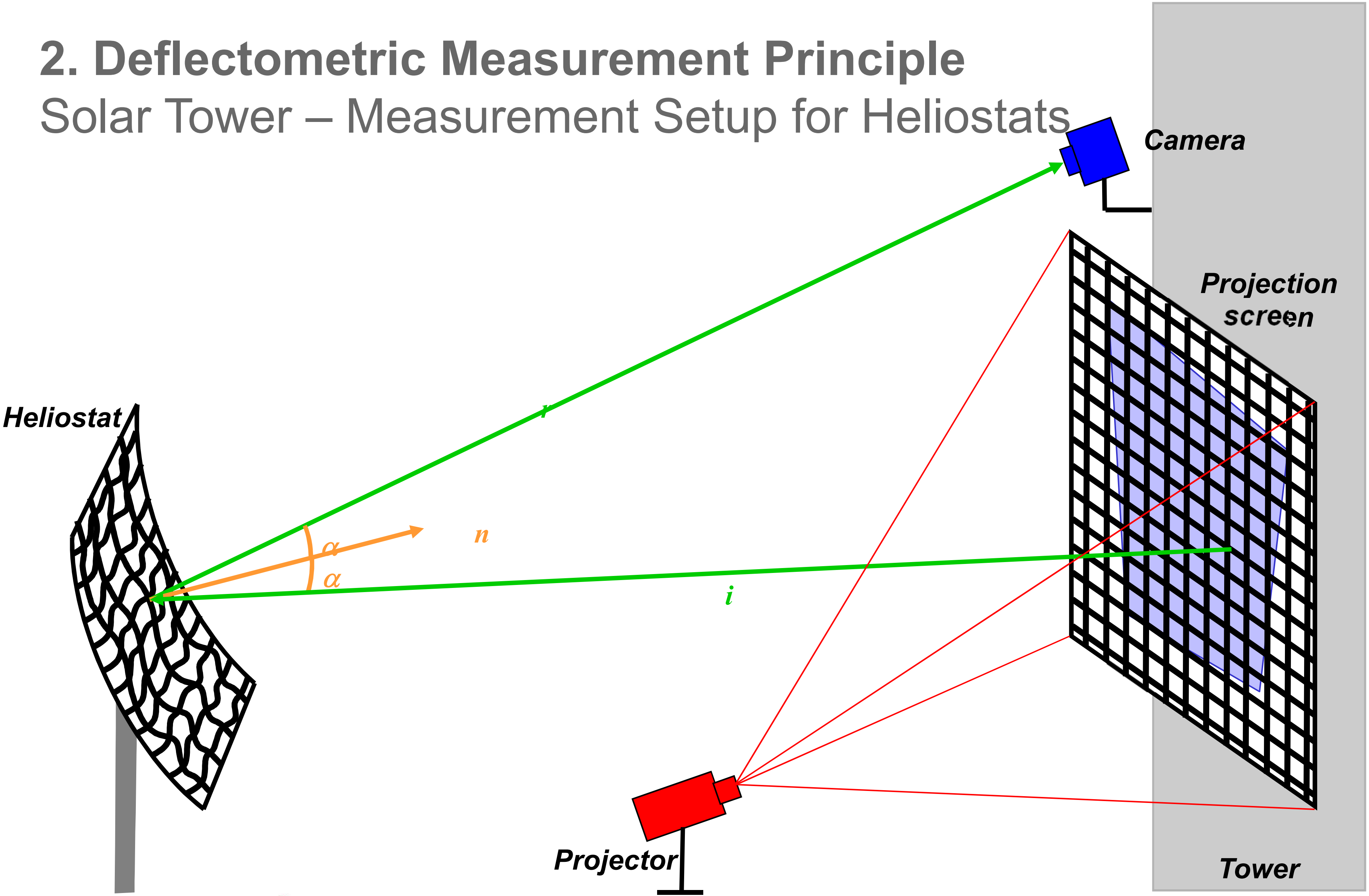

2. Deflectometric Measurement Principle

Solar Tower – Reflected Patterns in Heliostat

optical

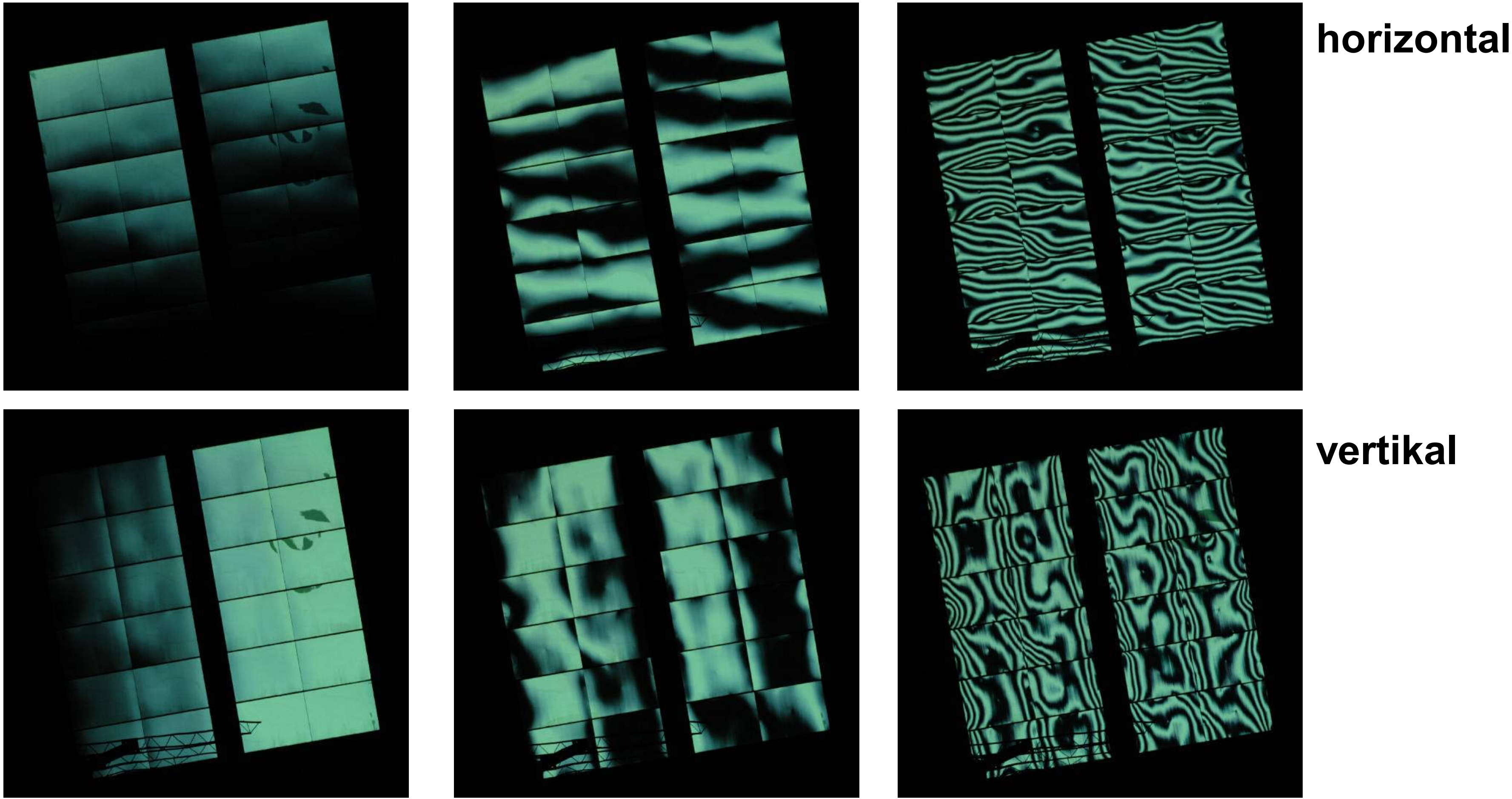

PSA/CIEMAT, Foto: DLR

2. Deflectometric Measurement Principle

Solar Tower – Results Heliostat CESA-1, PSA

optical

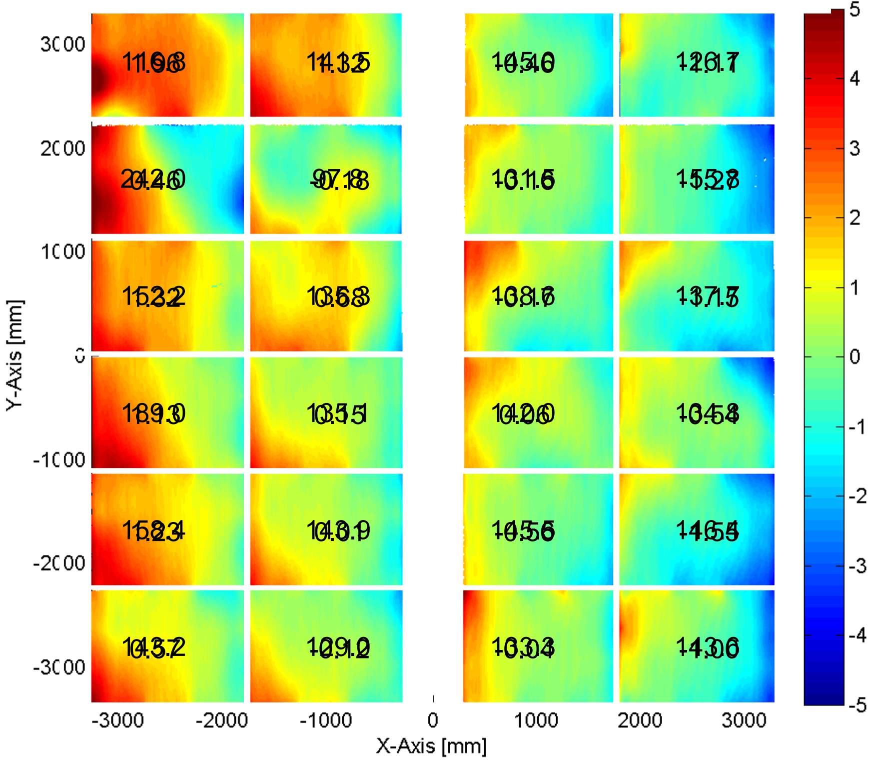

Slope deviation in *x*-direction in mrad

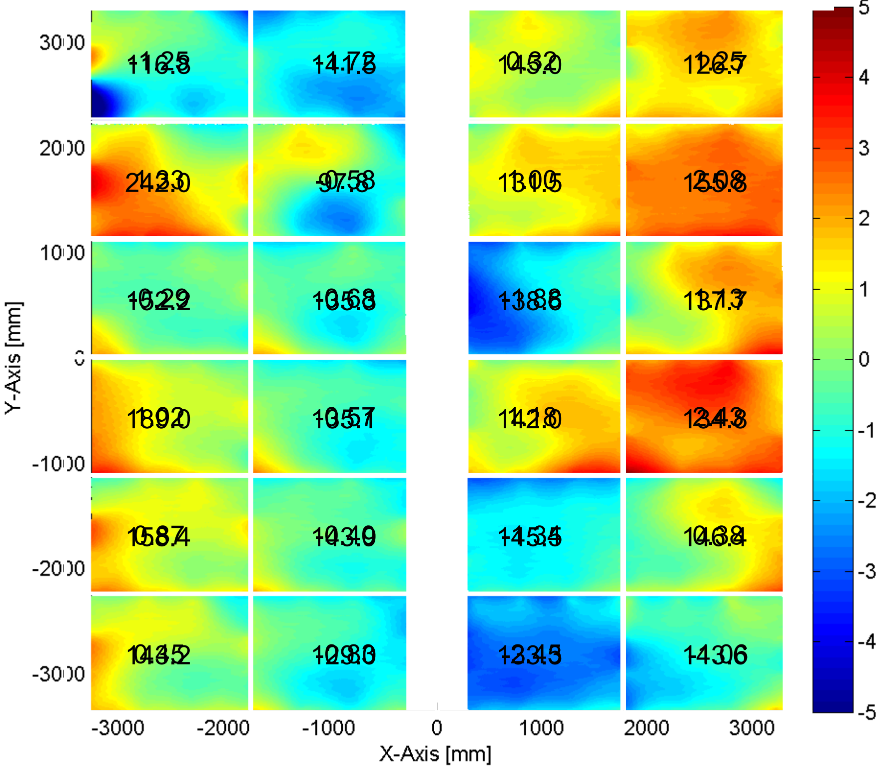

Slope deviation in *y*-direction in mrad

Results on heliostat level:

RMS slope deviation = 1.98 mrad

Heliostat design focal length = 104.1 m

Measured focal length = 116.2 m

Measured focal length

⇨ adjustments of focal length

→ canting

2. Deflectometric Measurement Principle

optical

Solar Tower – Raytracing Heliostats CESA-1, PSA

- STRAL, DLR-Raytracing program which can Use Deflectometry Results
- Code Validation by Simulation of a Group of Heliostats with Blocking and Shading
- Comparison with Flux Measurement

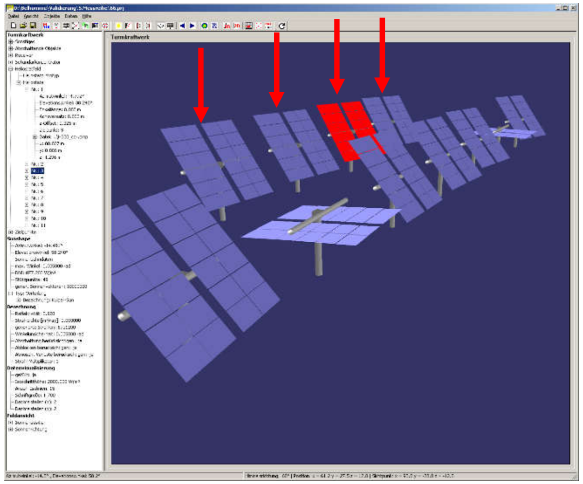

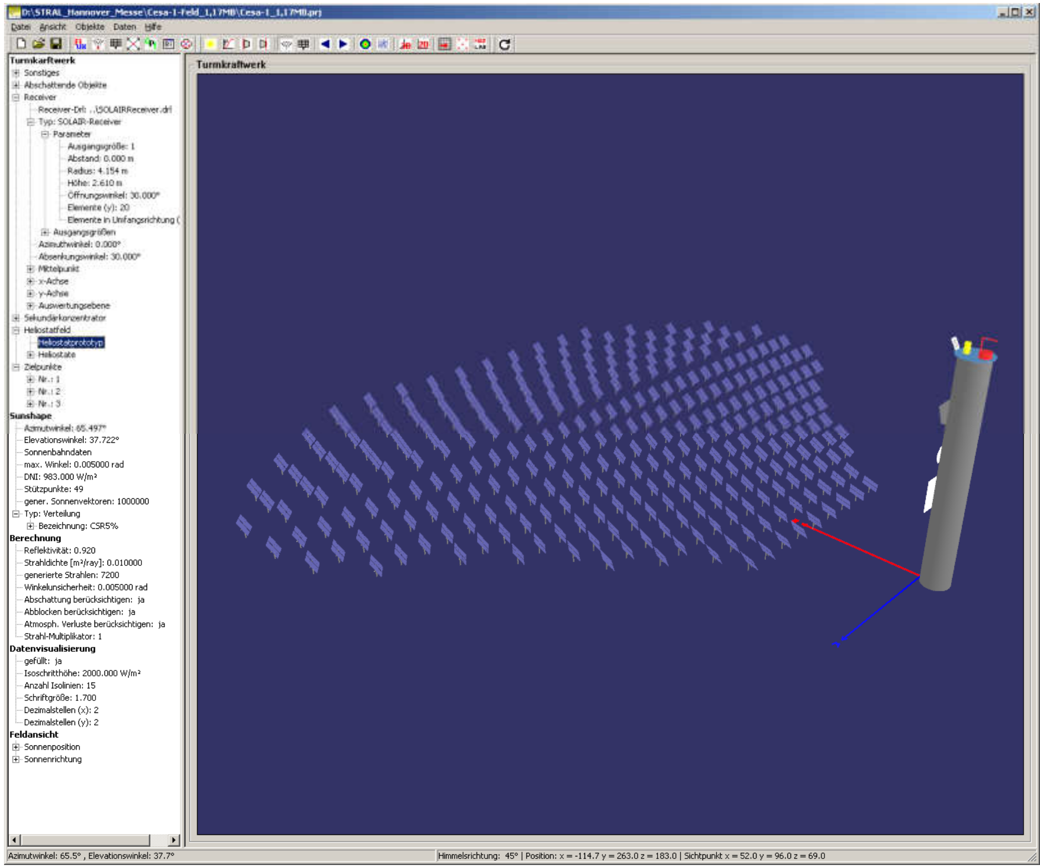

```
Turmkarftwerk
  Sonstiges
  Abschattende Objekte
  Receiver
    Receiver-Drl: ..\SOLAIRReceiver.drl
    Typ: SOLAIR-Receiver
      Parameter
        Ausgangsgröße: 1
        Abstand: 0.000 m
        Radius: 4.154 m
        Höhe: 2.610 m
        Öffnungswinkel: 30.000°
        Elemente (y): 20
        Elemente in Umfangsrichtung (
      Ausgangsgrößen
    Azimuthwinkel: 0.000°
    Absenkungswinkel: 30.000°
    Mittelpunkt
    x-Achse
    y-Achse
    Auswertungsebene
  Sekundärkonzentrator
  Heliostatfeld
    Heliostatprototyp
    Heliostate
  Zielpunkte
    Nr.: 1
    Nr.: 2
    Nr.: 3
Sunshape
  Azimutwinkel: 65.497°
  Elevationswinkel: 37.722°
  Sonnenbahndaten
  max. Winkel: 0.005000 rad
  DNI: 983.000 W/m²
  Stützpunkte: 49
  gener. Sonnenvektoren: 1000000
  Typ: Verteilung
    Bezeichnung: CSR5%
Berechnung
  Reflektivität: 0.920
  Strahldichte [m²/ray]: 0.010000
  generierte Strahlen: 7200
  Winkelunsicherheit: 0.005000 rad
  Abschattung berücksichtigen:  ja
  Abblocken berücksichtigen:  ja
  Atmosph. Verluste berücksichtigen:  ja
  Strahl-Multiplikator: 1
Datenvisualisierung
  gefüllt:  ja
  Isoschritthöhe: 2000.000 W/m²
  Anzahl Isolinien: 15
  Schriftgröße: 1.700
  Dezimalstellen (x): 2
  Dezimalstellen (y): 2
Feldansicht
  Sonnenposition
  Sonnenrichtung

Azimutwinkel: 65.5° , Elevationswinkel: 37.7°
Himmelsrichtung:  45° | Position: x = -114.7 y = 263.0 z = 183.0 | Sichtpunkt x = 52.0 y = 96.0 z = 69.0
```

2. Deflectometric Measurement Principle

Solar Tower – Raytracing Heliostats CESA-1, PSA

optical

Flux Measurement

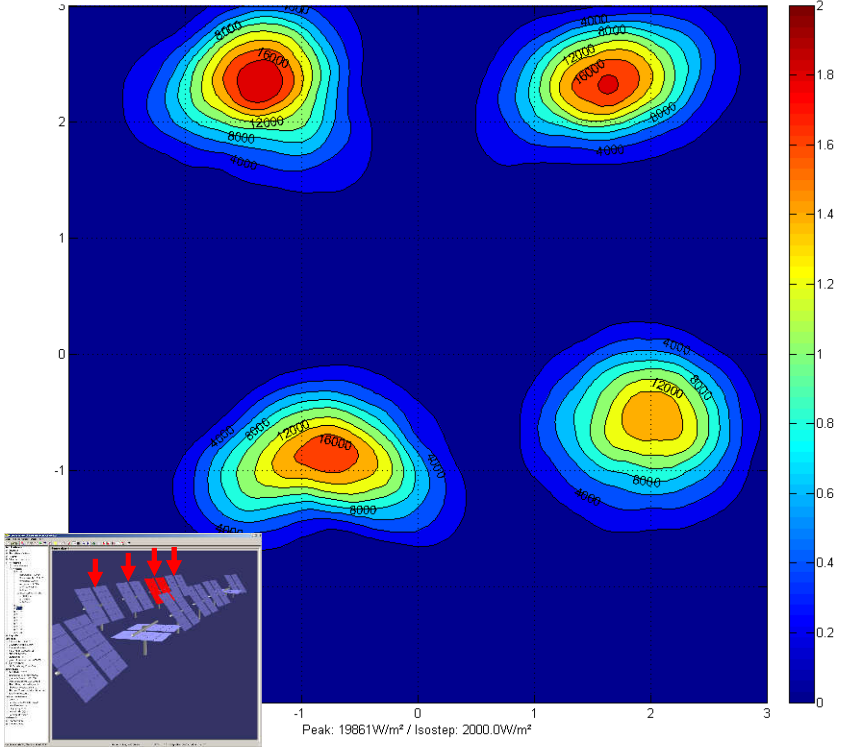

Simulation

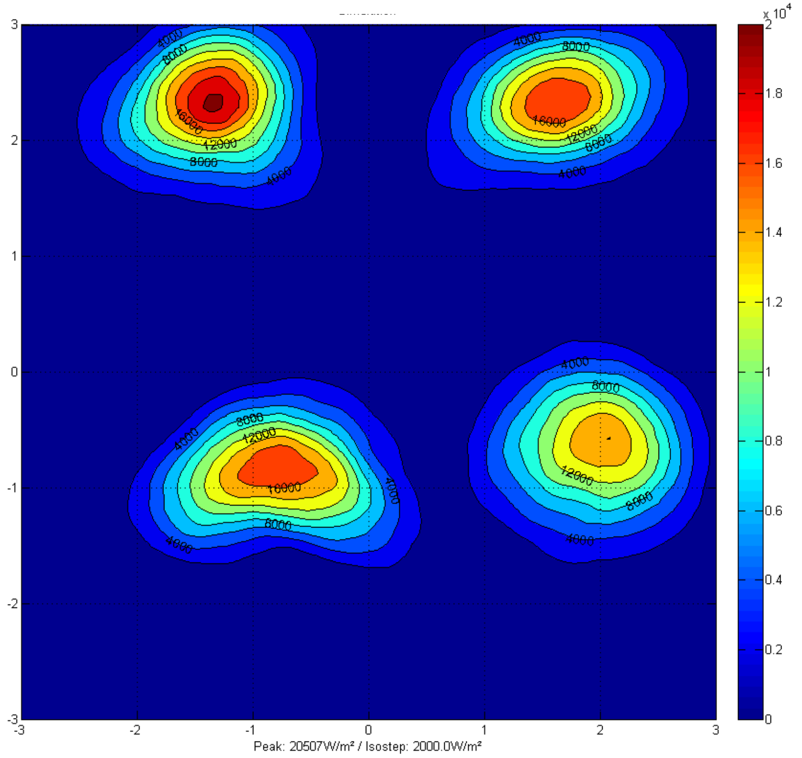

→ Detailed Simulation of Solar Flux Possible by Using Deflecometry Data

2 Use of UAVs (Unmanned Aerial Vehicles) in CSP

Motivation

- Solar fields are of **big extent**
- UAVs allow to position and move the camera **above ground** in almost any place
- Today's UAVs are **cheap**, **easy-to-fly**, **programmable**, have **reasonable flight-times** and carry **good-quality cameras**
- **Challenge**: For optical measurements like slope deviations, the positioning (x,y,z) and orientation of the camera (ω,φ,κ) has to be known within mm/cm range accuracy

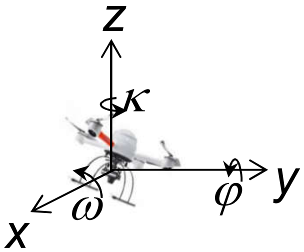

- **Techn. Development in Drones:** Allow simplyfing methods while reaching higher quality results

3 Use of UAVs in CSP

For which CSP systems?

- UAVs are used both for **parabolic troughs** and **central receiver systems**
- **To consider**: Different optics → different flight routes and measurement approaches

Parabolic Trough
(Linear Fresnel)

- Line focus
  (1 axis tracking)
- Small focal length of troughs

→ **This talk**

Central Receiver

CESA-1, PSA

- Point focus
  (2 axis tracking)
- Large focal length of heliostats

→ **Specific talks on Friday**

DLR Spin-Offs:
Volateq and CSP Services

3 Use of UAVs in CSP
Several groups work with UAV for inspection of CSP plants

NREL, SANDIA
Distant Observer (DO), NIO for heliostats

https://www.nrel.gov/csp/field-characterization.html

Jorgensen, G. et.al Assess the Efficacy of an Aerial Distant Observer Tool Capable of Rapid Analysis of Large Sections of Collector Fields, Tech. Report NREL/MP-550-44332, 2009

DLR
QFly: Deflectometry, Photogrammetry, IR, …

Prahl, C. et al, Airborne shape measurement of parabolic trough collector fields. Solar Energy, 91, 2013

Prahl, C. et al, Airborne Characterization of the Andasol-3 SolarField, SolarPACES, Santiago de Chile, 2017

University of Cordoba
Open Hardware and Software System

Mesas-Carrascosa, F.J. et al. The Development of an Open Hardware and Software System Onboard Unmanned Aerial Vehicles to Monitor Concentrated Solar Power Plants, Sensors, 2017

CIEMAT, ENEA, etc

3 Use of UAVs in CSP: DLR-QFly system

Separation of (i) **flight planning** (software)
(ii) data **acquisition** (UAV+hardware), and
(iii) data **processing and evaluation** (software)

Hardware

- UAV
  - MD4-1000
  - DJI Phantom
  - DJI Matrice
- PAYLOAD
  - Camera VIS
  - Camera IR
  - Gas sensor

Software:

- MATLAB
  - Waypoints
  - Image processing and evaluations
- AICON 3D Studio
  - Close-range photogrammetry
- SPRAY/STRAL
  - Ray-traycing

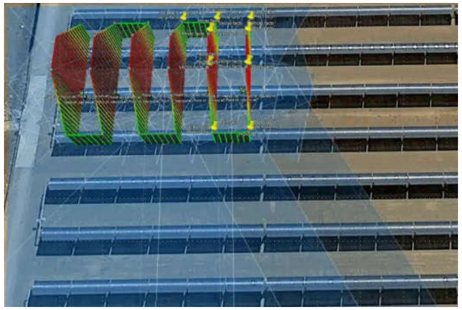

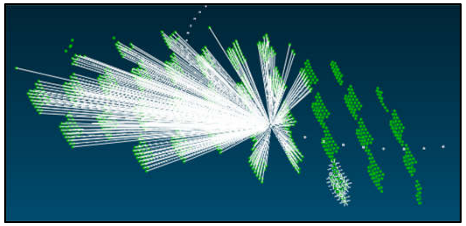

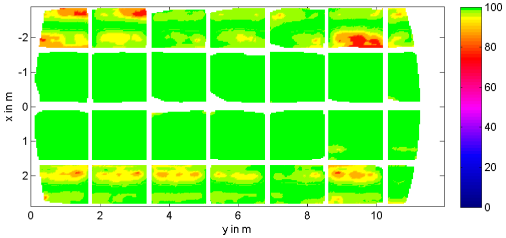

4. Examples

Performance testing – collector field

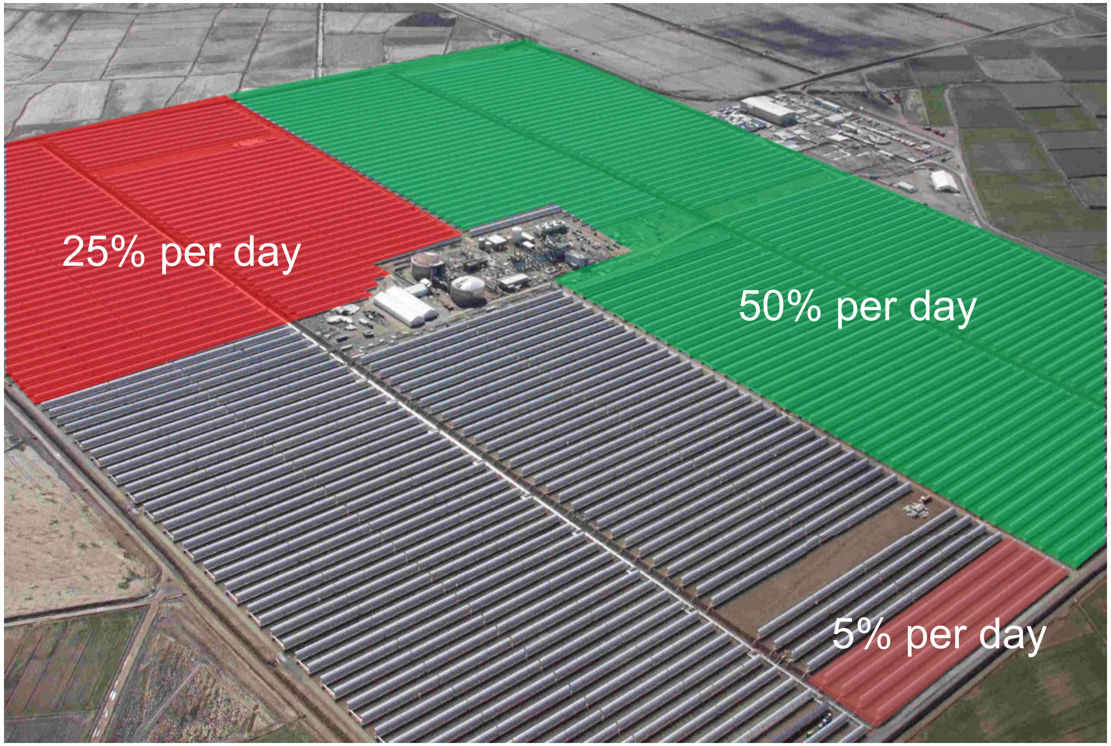

*) Measurement Volume per day, of a 50 MW PTC solar field

QFly Classic

- Mirror shape (high resolution)
- Absorber Tube

QFly Survey

- Alignment
- Torsion, Tracking
- Mirror shape (low resolution)

QFly Thermo

- Defective absorber
- Heat loss detection

Benefits

- Failure Detection
- Quality Control
- Optimization of parabolic trough collector Fields

4. Example ① Parabolic Trough Shape Accuracy

Performance testing – collector field, validation

PSA/CIEMAT, Foto: DLR

a) Airborne camera vehicle during a test flight at KONTAS test facility (PSA)

b) Automatic creation of flight routes (DISS, PSA)

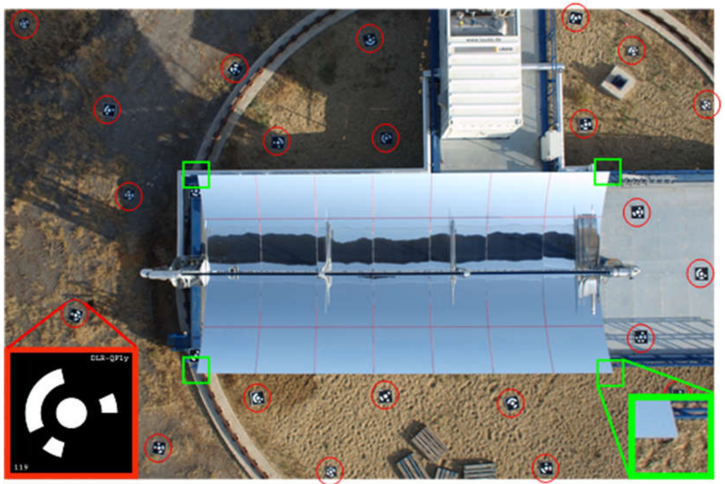

c) Photogrammetric determination of camera and collector position

- System successfully **validated** for single module (against TARMES and Photogrammetrie)
- **Measurement uncertainty**:
  local slope deviation.: 0.6 – 1.1 mrad
  RMS whole module: ca. 0.1 mrad

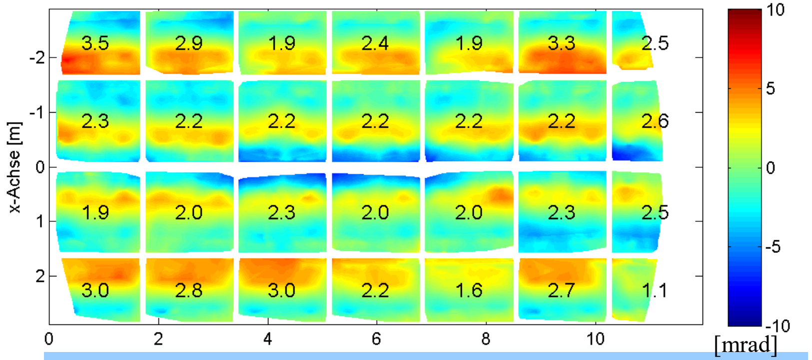

d) Slope deviation measured by QFly for KONTAS collector

Example ① Parabolic Trough Shape Accuracy

Airborne Data Acquisition

PSA/CIEMAT, Foto: DLR

Mode: High Res
Flight Height: < 30 m
Volume 50-MW Field: 5%/day

Example ① Parabolic Trough Shape Accuracy

QFly Results: Collector Module (SCE)

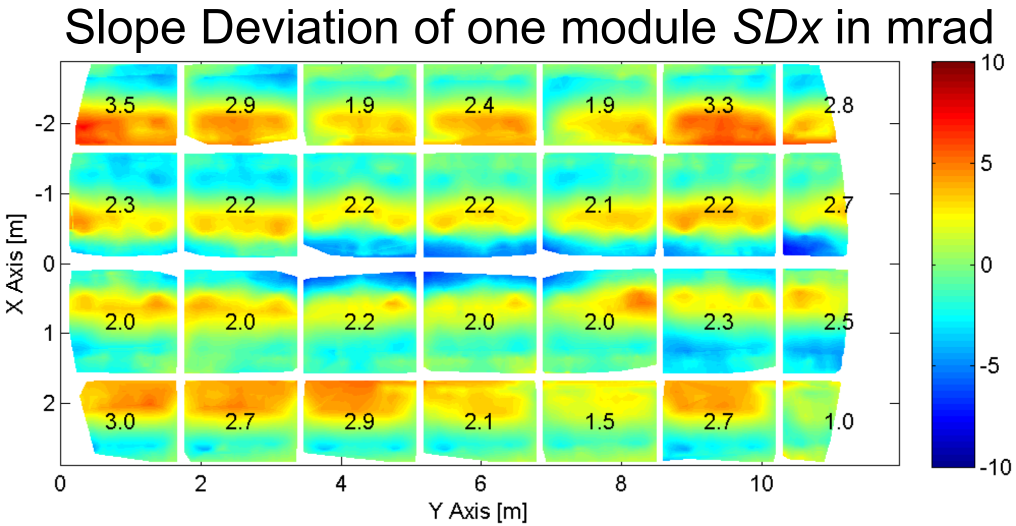
Slope Deviation of one module *SDx* in mrad

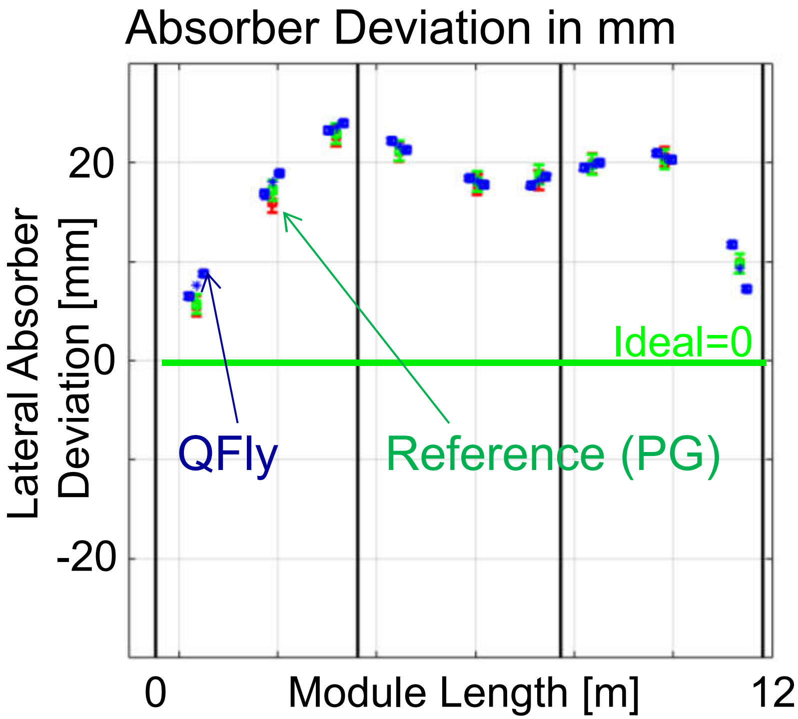
Absorber Deviation in mm

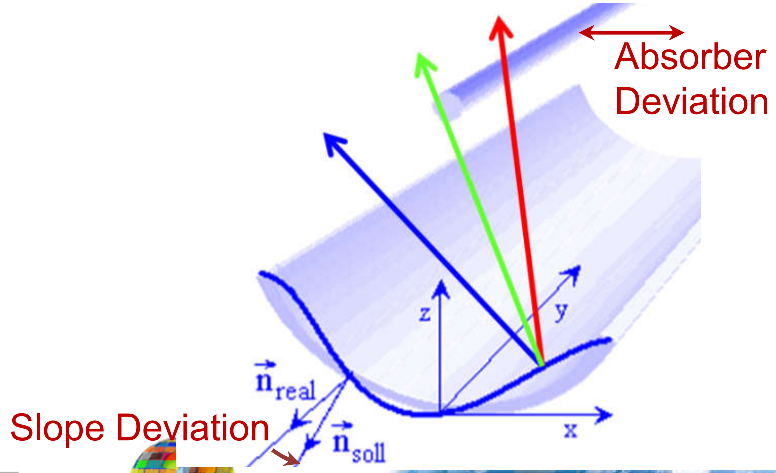

Mode: Survey
Flight Height: < 250 m
Volume 50-MW Field: 100%/4h

Example ① Parabolic Trough Shape Accuracy

Results: Solar Field

Slope Deviation *SDx,eff* for the whole collector (SCA) in mrad

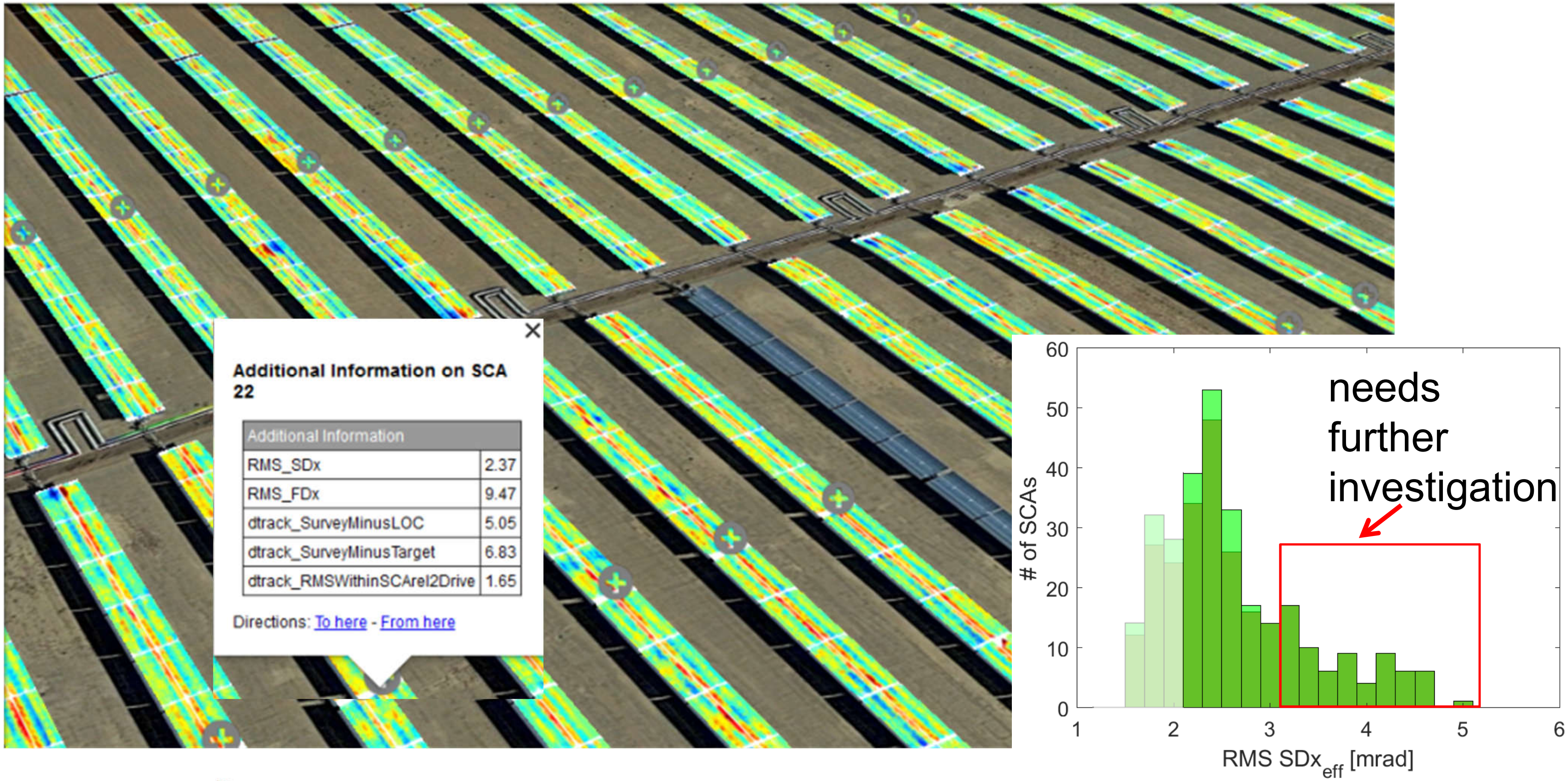

Additional Information on SCA 22

Additional Information	
RMS_SDx	2.37
RMS_FDx	9.47
dtrack_SurveyMinusLOC	5.05
dtrack_SurveyMinusTarget	6.83
dtrack_RMSWithinSCArel2Drive	1.65

Directions: To here - From here

Mode: Survey
Flight Height: < 250 m
Volume 50-MW Field: 100%/4h

Example ② Parabolic Trough Torsion/Tracking

Results: Collector (SCA)

PSA/CIEMAT, Foto: DLR

Mode: Survey
Flight Height: < 250 m
Volume 50-MW Field: 100%/4h

Example ② Parabolic Trough Torsion/Tracking

QFly Results: Collector (SCA)

Torsion and module alignment along collector (SCA) in mrad

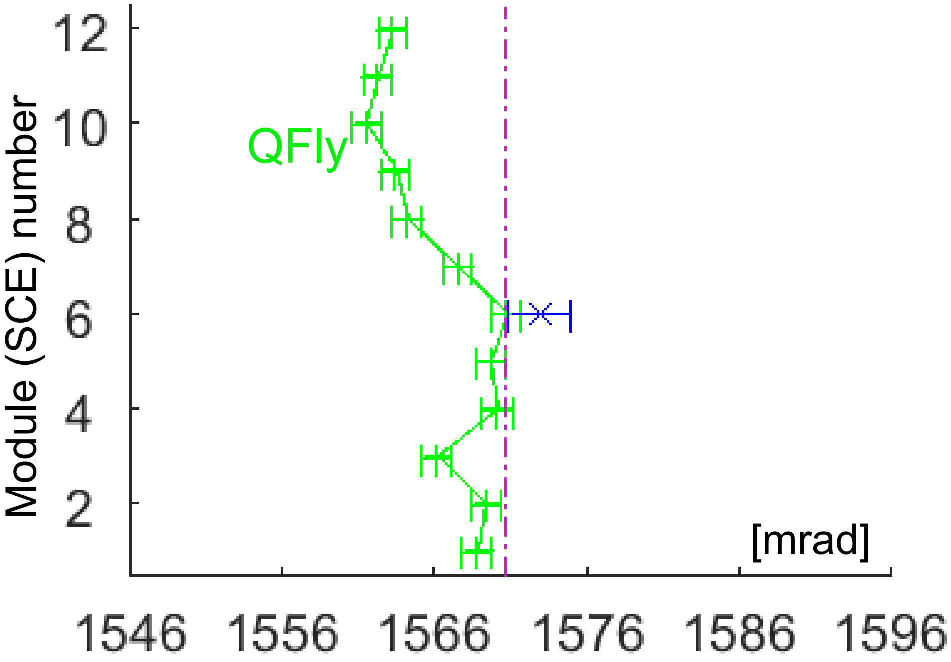

Mode: Survey
Flight Height: < 250 m
Volume 50-MW Field: 100%/4h

Example ② Parabolic Trough Torsion/Tracking

QFly Results: Collector (SCA)

Torsion and module alignment along collector (SCA) / Tracking mrad

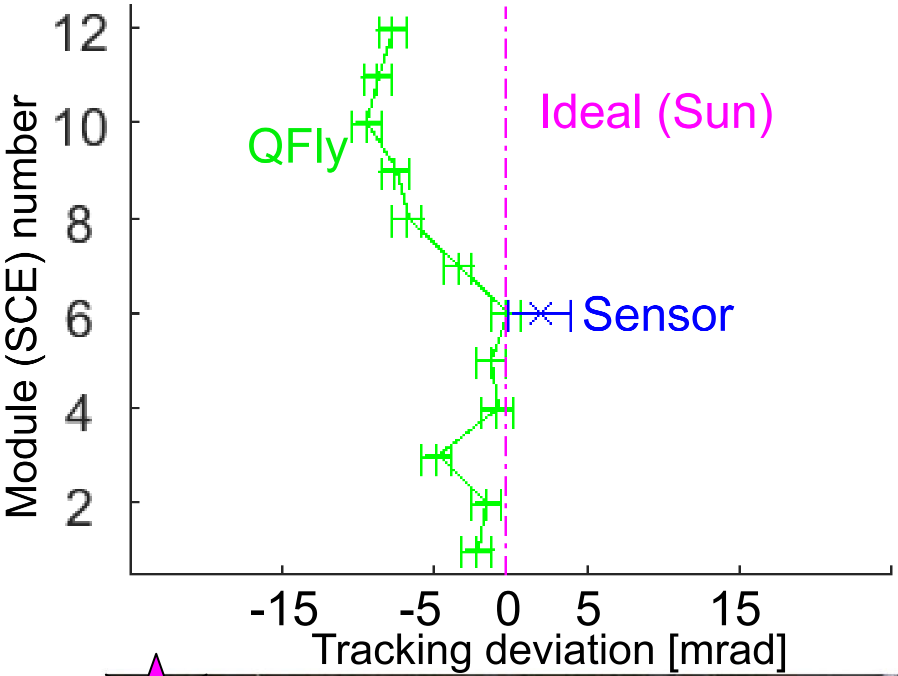

Tracking in mrad

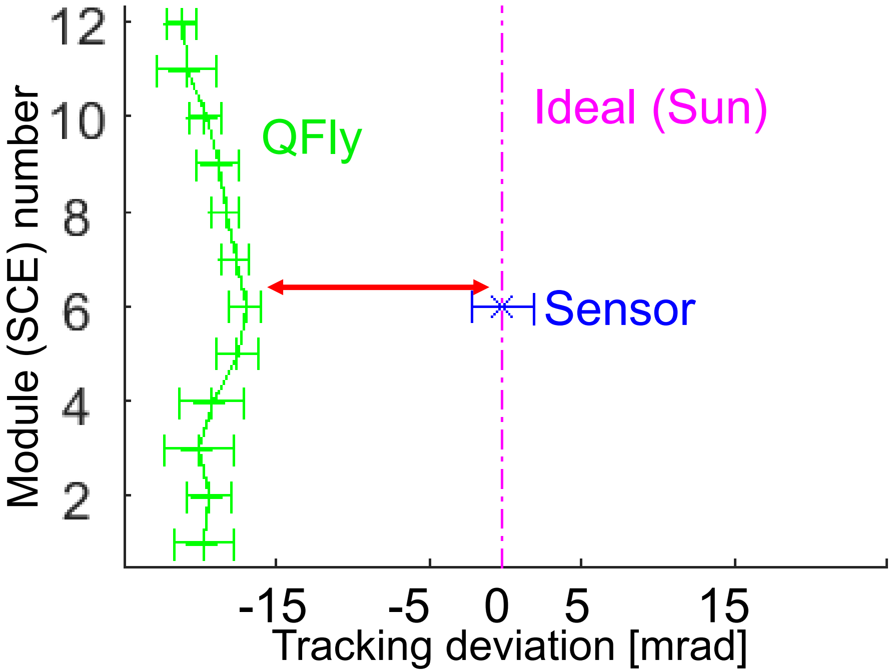

Mode: IR
Flight Height: < 15 m
Volume 50-MW Field: 25%/day

Example ③ Parabolic Trough HCE Quality Screening

- Measurement of glass envelope temperature by IR camera
- Measurement accuracy ~2K

→ Specific talk of Niels Algner today, 15:00h,

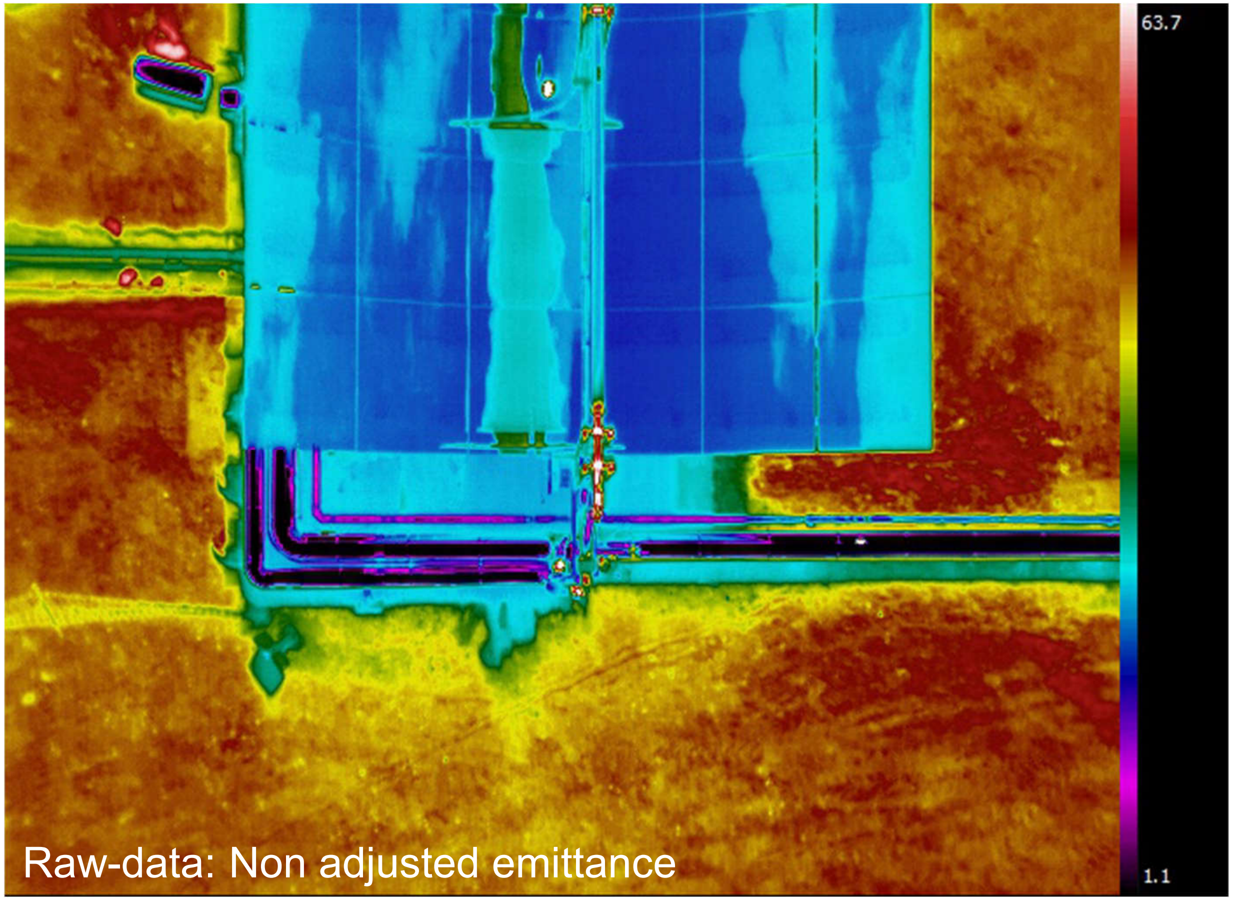

Raw-data: Non adjusted emittance

PROMETEO, PSA

In development ④ Central Receiver Heliostat Offset /Shape

④

*Heliostat **Calibration of Orientation***

- **Accurate tracking** of **heliostats** is system-relevant for tower power plants
  - Safety
  - performance
- Need for new methods for **initial calibration** of the heliostat field
  - Fast, independent of environmental conditions and add. infrastructure
  - Using **UAV only**

- Airborne camera data acquisition using mainly **deflectometry**

→ Specific talk of Julian Krauth, Friday, 9:30h

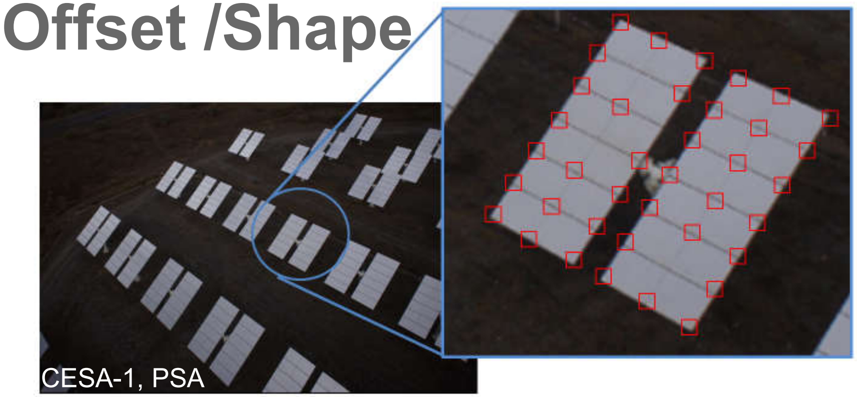

CESA-1, PSA

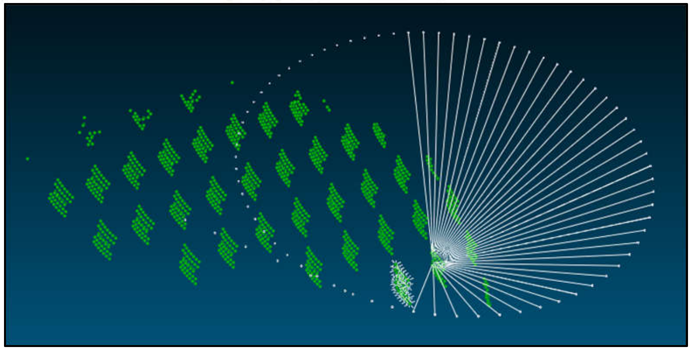

Example ⑤ Parabolic Trough and Heliostat Soiling

⑤

Soiling / Cleanlines Measurement

- Promising proof-of-concept for airborne soiling measurement
- **Spatially resolved cleanliness maps**

PSA/CIEMAT, Foto: DLR

→ Specific talk of Fabian Wolfertstetter today, 11:10h

In development ⑥ Parabolic Trough HTF leakage detection

*Drone for **HTF leakage detection ?*** ⑥

- Will be probably looked at in future research project “AuDroMon”

5 Conclusions

- **Airborne measurement** systems offer a wide range of measurement methods
- They serve the characterization and optimization of solar concentrators
  - from **prototype developments**
  - to whole **solar fields** during **construction**, **operation**, **maintenance**
  - and **optical acceptance testing**

- They can cover nearly all operation-relevant parameters of the solar field
- **Airborne measurement** systems are **very fast** and allow **fully automatic** data acquisition and evaluation and have **low influence** on power plant **operation**

- **Experience** has been gained in prototype and commercial power plants, e.g. in Spain, Israel, Portugal, and Germany

5 Outlook

- Airborne data acquisition will also play a role in **central receiver plants** for both **heliostats** and **receiver inspections**
- It is good practice to **separate** data acquisition **(UAV flight)** and data processing step **(software)**
- Further **automation** using **cloud based solutions** and **interactive custom-tailored reporting** will be used

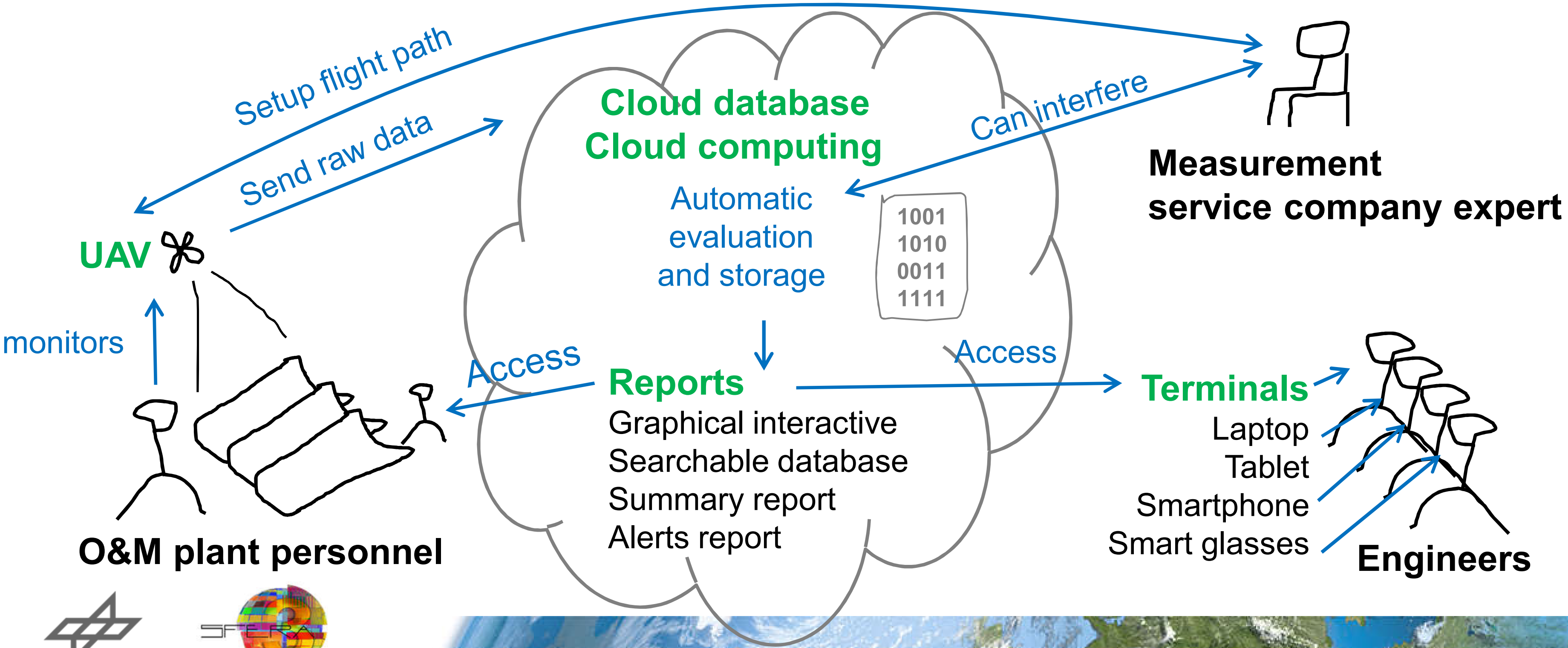

THANK YOU FOR YOUR ATTENTION!
ANY QUESTIONS?

Marc Röger, DLR
marc.roeger@dlr.de

We gratefully acknowledge funding by the German Federal Foreign Office, German Federal Ministry of Economic Affairs, German Federal State North Rhine-Westphalia and DLR Technology Marketing.

We thank the whole QFly team and the CIEMAT-PSA for permitting QFly flights over their premises.

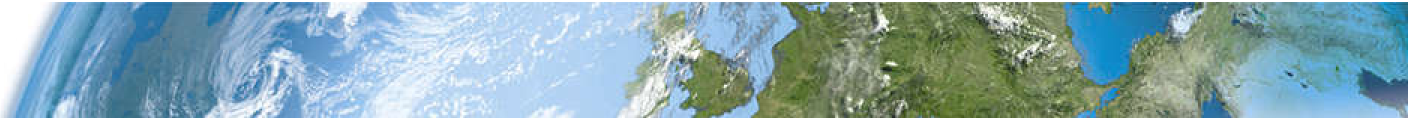

SFERA-III
Solar Facilities for the European Research Area

Solar Facilities for the European Research Area

2nd Training for Industries on optimization of CST plant output by optical and thermal characterization and target-oriented O&M

25 April 2022, Plataforma Solar de Almería, Spain

“Optical Efficiency of Parabolic Trough Collectors with Raytracing”

Daniel Benitez, DLR, System Qualification

NETWORKING

THIS PROJECT HAS RECEIVED FUNDING FROM THE EUROPEAN UNION’S HORIZON 2020 RESEARCH AND INNOVATION PROGRAMME UNDER GRANT AGREEMENT NO **823802**

Content

Raytracing Overview

Raytracing is used to calculate the flux density distribution and the incoming thermal power on a surface (e.g. receiver). It simulates the path of the sun rays through the different elements such as mirrors, blocking and shading elements (beams, other collectors) and receiver considering their optical properties, position and shape.

The rays that reach the surface of interest are then added up to obtain a flux map and the incoming power.

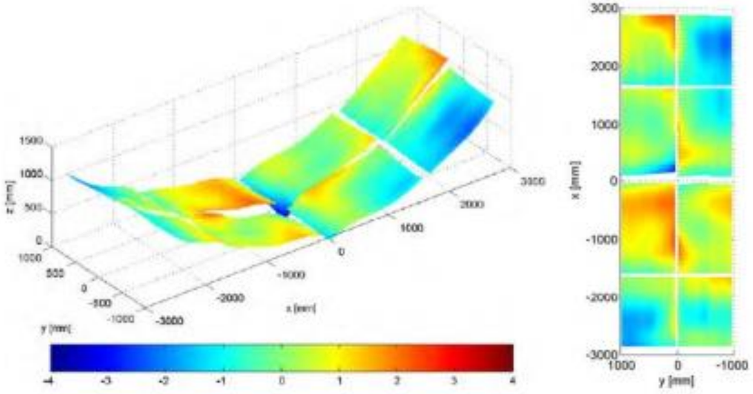

Pottler K.; Deutsches Zentrum für Luft- und Raumfahrt; 2005

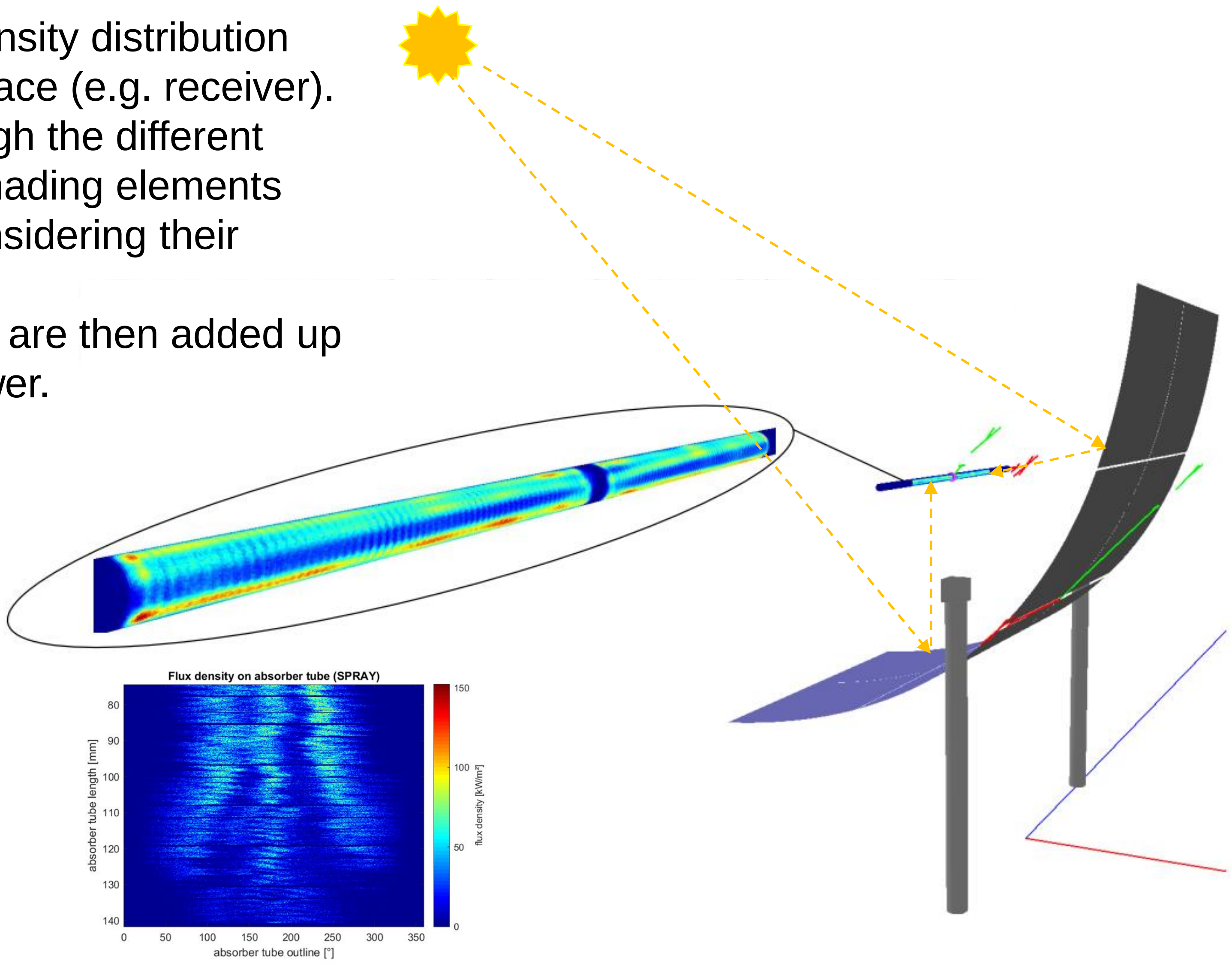

Optical efficiency of a parabolic trough collector

1- Available Solar Power $\dot{Q}_{\text{avail}}$

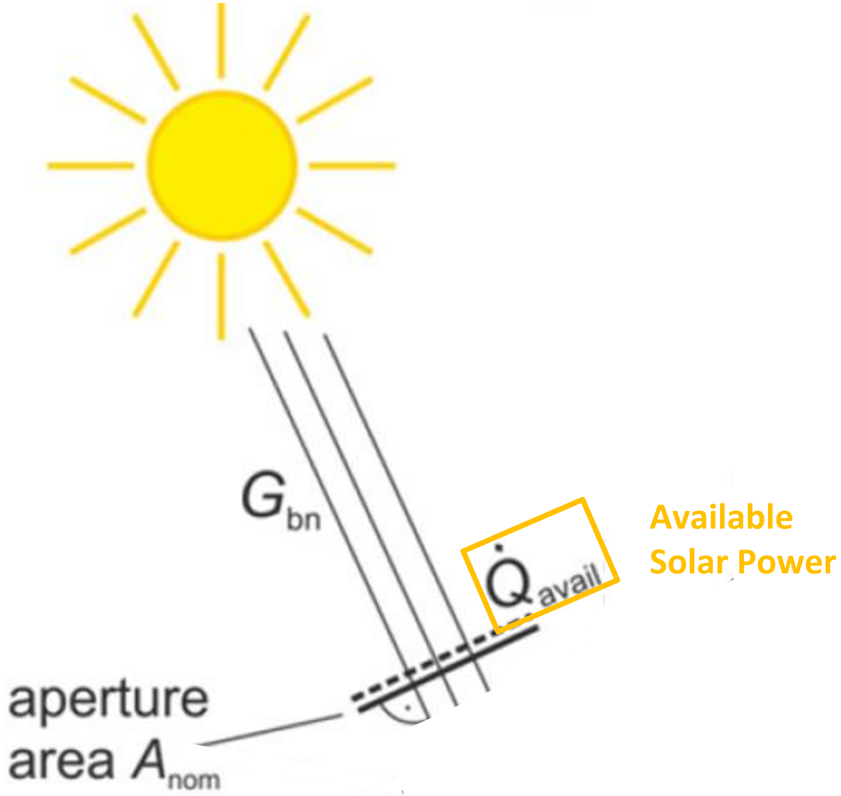

Optical efficiency of parabolic trough collector

1- Available Solar Power $\dot{Q}_{\text{avail}}$

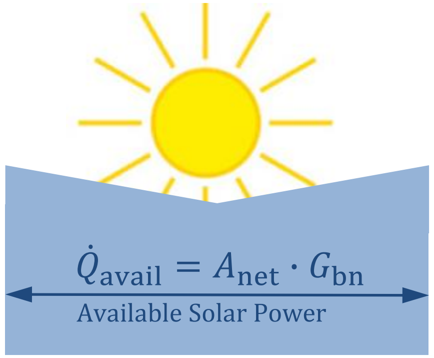

$$\dot{Q}_{\text{avail}} = A_{\text{net}} \cdot G_{\text{bn}}$$

Optical efficiency of parabolic trough collector

2- Projected Solar Power $\dot{Q}_{\mathrm{proj}}$

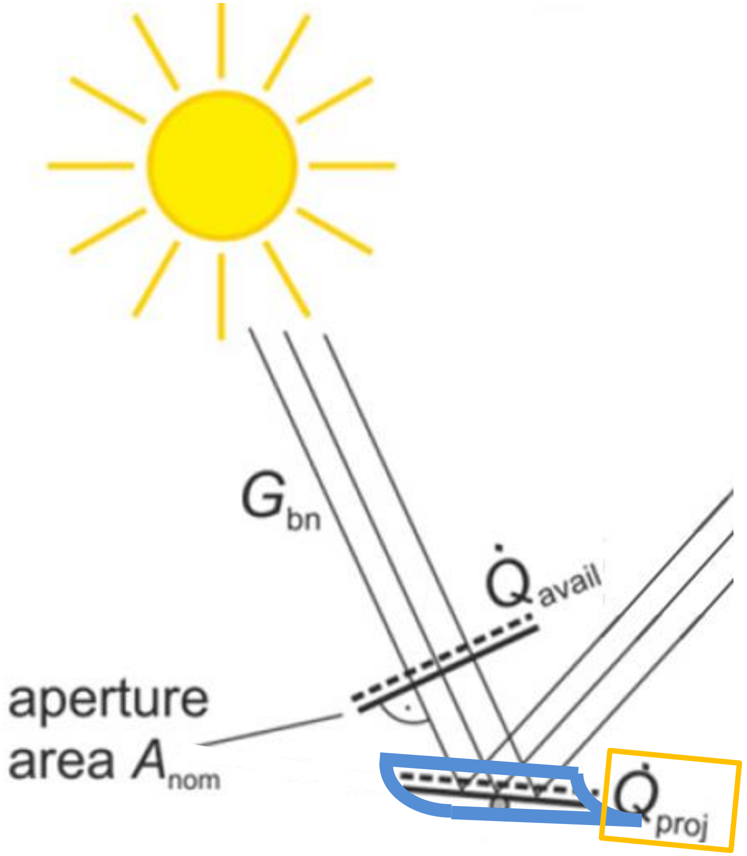

Projected Solar Power

Optical efficiency of parabolic trough collector

2- Projected Solar Power $\dot{Q}_{\mathrm{proj}}$

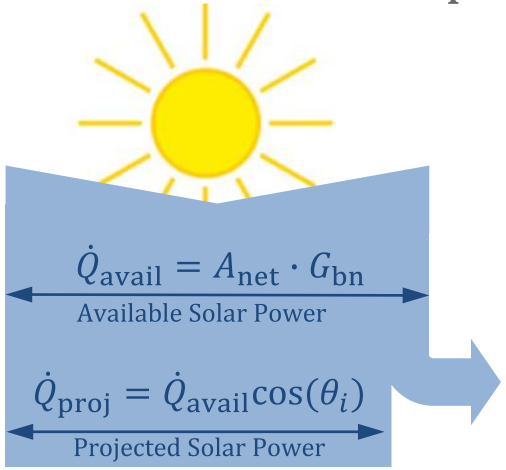

$\dot{Q}_{\mathrm{avail}} = A_{\mathrm{net}} \cdot G_{\mathrm{bn}}$

Available Solar Power

$\dot{Q}_{\mathrm{proj}} = \dot{Q}_{\mathrm{avail}} \cos(\theta_i)$

Projected Solar Power

Cosine losses 1-cos (θ_i)

Optical efficiency of parabolic trough collector

3- Intercepted Radiant Power $\dot{Q}_{\text{inter}}$

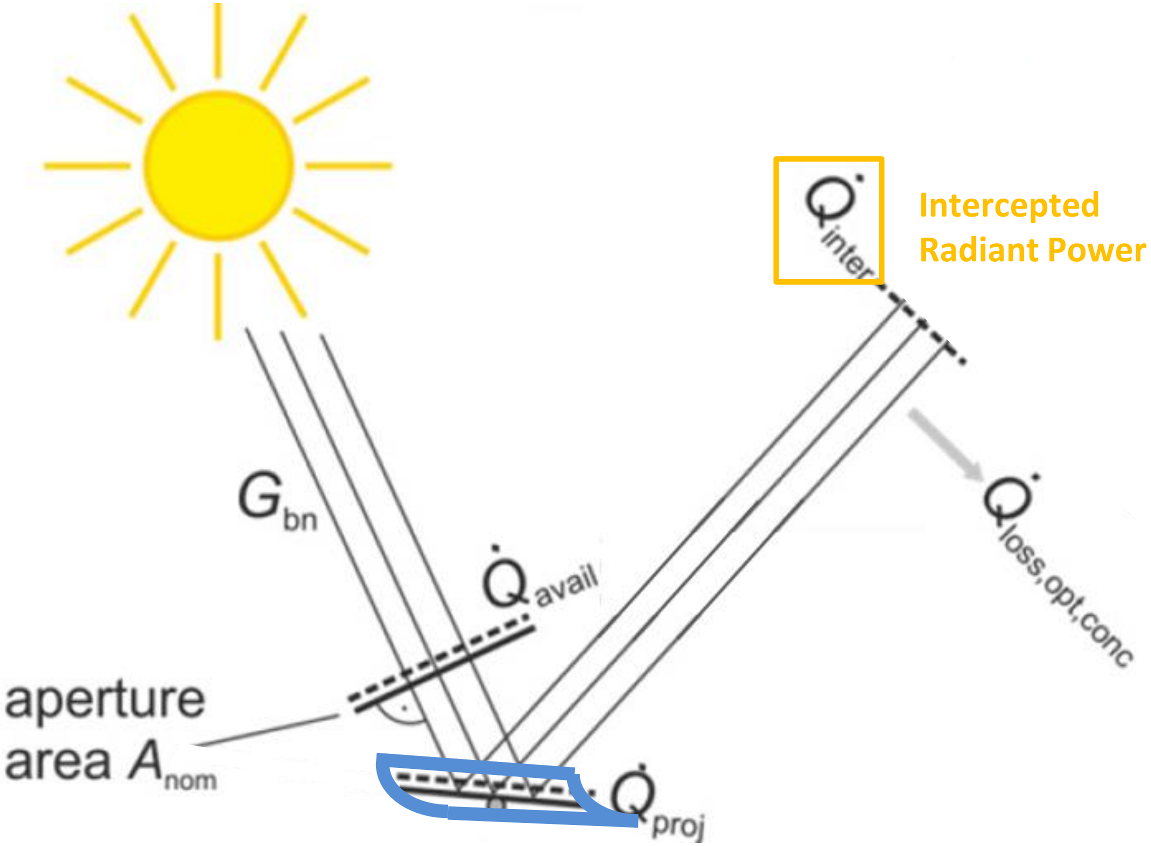

Optical efficiency of parabolic trough collector

3- Intercepted Radiant Power $\dot{Q}_{\text{inter}}$

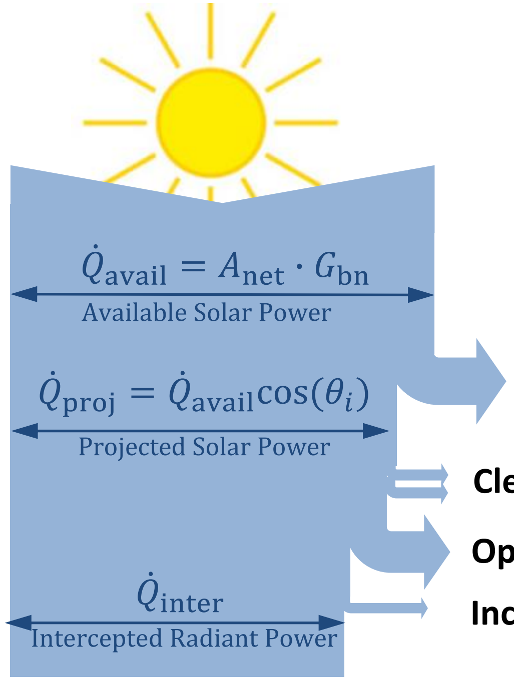

$\dot{Q}_{\text{avail}} = A_{\text{net}} \cdot G_{\text{bn}}$

Available Solar Power

$\dot{Q}_{\text{proj}} = \dot{Q}_{\text{avail}} \cos(\theta_i)$

Projected Solar Power

$\dot{Q}_{\text{inter}}$

Intercepted Radiant Power

Cosine losses 1-cos (θ_i)

Cleanliness, endloss and shading factor (1-η_{clean}), (1-η_{endloss}), (1-η_{shad})

Optical + geometric concentrator losses $(1 - \rho \cdot IC)$ (reflectance, intercept)

Incidence angle modifier (1-$K(\theta_i)$) (add. losses by non-perpendicular rays)

Optical efficiency of parabolic trough collector

4- Thermal Power induced by absorption at surface $\dot{Q}_{\mathrm{abs}}$

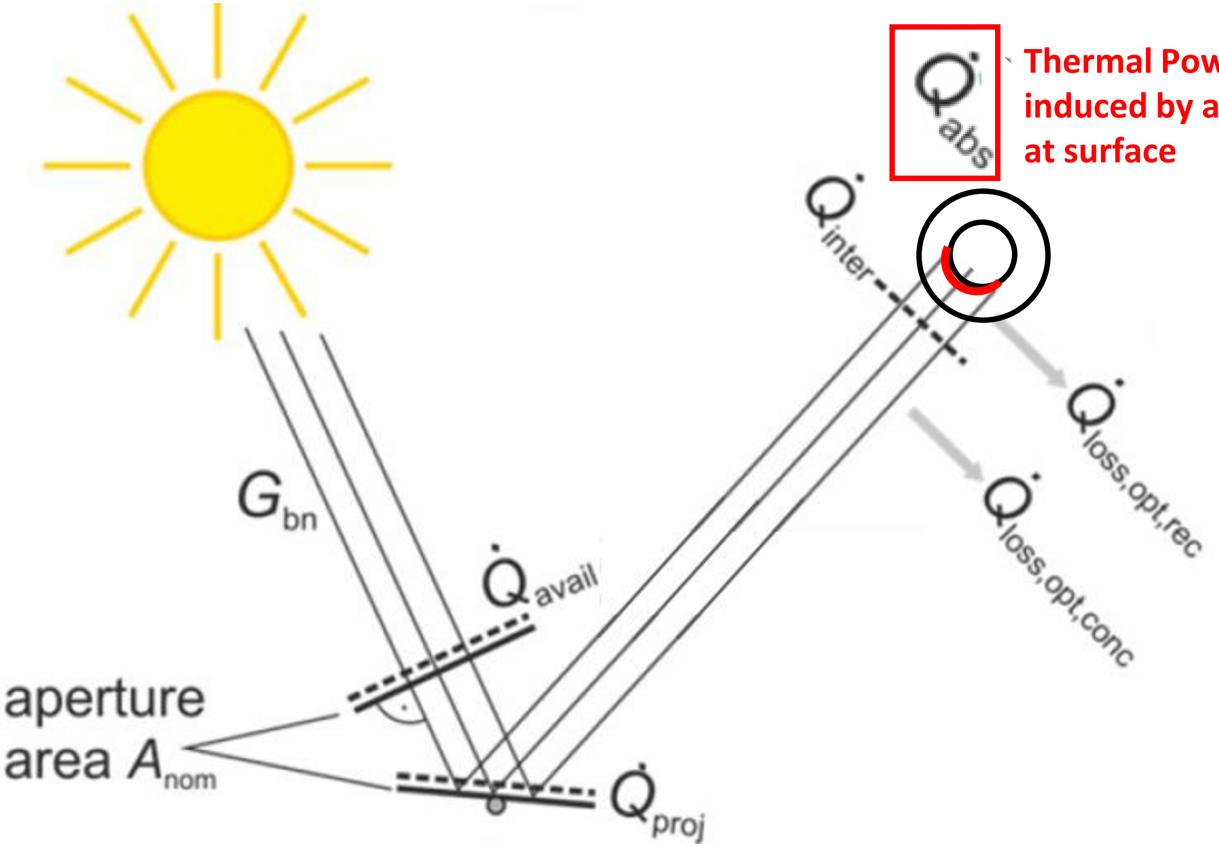

Thermal Power induced by absorption at surface

Optical efficiency of parabolic trough collector

4- Thermal Power induced by absorption at surface $\dot{Q}_{\mathrm{abs}}$

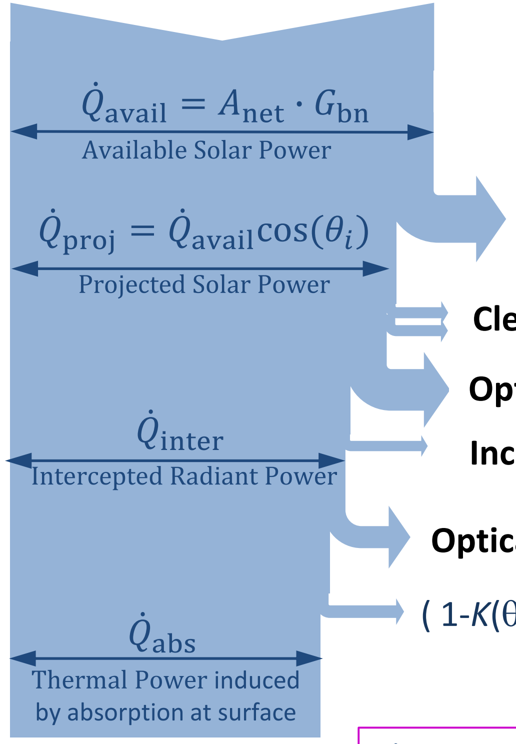

$\dot{Q}_{\mathrm{avail}} = A_{\mathrm{net}} \cdot G_{\mathrm{bn}}$

Available Solar Power

$\dot{Q}_{\mathrm{proj}} = \dot{Q}_{\mathrm{avail}} \cos(\theta_i)$

Projected Solar Power

$\dot{Q}_{\mathrm{inter}}$

Intercepted Radiant Power

$\dot{Q}_{\mathrm{abs}}$

Thermal Power induced by absorption at surface

Cosine losses 1-cos (θ_i)

Cleanliness, end losses and shading factor (1-η_{clean}), (1-η_{endloss}), (1-η_{shad})

Optical + geometric concentrator losses $(1 - \rho \cdot IC)$ (reflectance, intercept)

Incidence angle modifier (IAM) (1-$K(\theta_i)$) (add. losses by non-perpendicular rays)

Optical receiver losses $1 - \tau\alpha \frac{L_{\mathrm{act}}}{L_{\mathrm{rec}}}$ (transmittance, absorptance, eff. length)

(1-$K(\theta_i)$)

$$\eta_{\mathrm{opt},0} = \rho \cdot \tau \cdot \alpha \cdot \frac{L_{\mathrm{act}}}{L_{\mathrm{rec}}} \cdot IC$$

$$\dot{Q}_{abs} = G_{\mathrm{bn}} \cdot A_{\mathrm{net}} \cdot \cos(\theta_i) \cdot K(\theta_i) \cdot \eta_{\mathrm{opt},0} \cdot \eta_{\mathrm{clean}} \cdot \eta_{\mathrm{endloss}} \cdot \eta_{\mathrm{shad}}$$

$$\eta_{\mathrm{opt}} = \frac{\dot{Q}_{abs}}{\dot{Q}_{avail}} = \cos(\theta) \cdot K(\theta_i) \cdot \eta_{\mathrm{opt},0} \cdot \eta_{\mathrm{clean}} \cdot \eta_{\mathrm{endloss}} \cdot \eta_{\mathrm{shad}}$$

Nomenclature according T.Hirsch, SolarPACES Guideline for Bankable STE Yield Assessment, Appendix T - Terminology, 2017 http://www.solarpaces.org/images/SolarPACES_Guideline_for_Bankable_STE_Yield_Assessment_-_Appendix_Terminology_-_Version_2017.pdf

Optical efficiency of parabolic trough collector

With simulation of the IAM, receiver temperature and collector tracking accuracy

$$\boxed{\eta_{opt} = \cos(\theta) \cdot IAM \cdot \eta_{opt,0} \cdot \eta_{clean} \cdot \eta_{endloss} \cdot \eta_{shad} \cdot \eta_{\mathbf{opt,temp}} \cdot \eta_{\mathbf{opt,track}}}$$

$$K(\theta_i) = IAM \; (common\ nomenclature)$$

$$IAM = 1 - \frac{a_1 \cdot \theta + a_2 \cdot \theta^2 + a_3 \cdot \theta^3}{cos\,\theta}$$

$$\eta_{opt,temp} = 1 + temp_1 \cdot dT + temp_2 \cdot dT^2 + temp_3 \cdot dT^3$$

mit $dT = |T_{mean,coll} - T_{mean,coll,nom}|$

$$\eta_{opt,track} = 1 + track_1 \cdot dTrack + track_2 \cdot dTrack^2 + track_3 \cdot dTrack^3$$

mit $dTrack = |trackError| - trackNom$

IAM: incidence angle modifier
$\eta_{opt,temp}$: HCE temperature correction factor
$\eta_{opt,track}$: tracking error correction factor

Measurement data required for raytracing

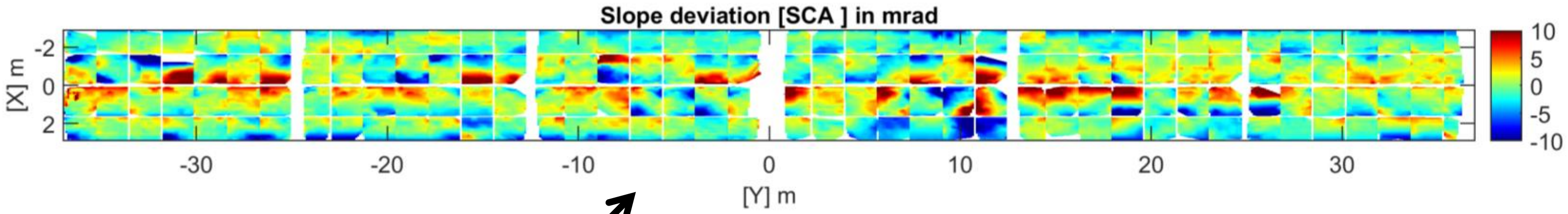

QFly slope deviation results

Raw images → Slope Deviations,
Tracking error,
Receiver temperatures

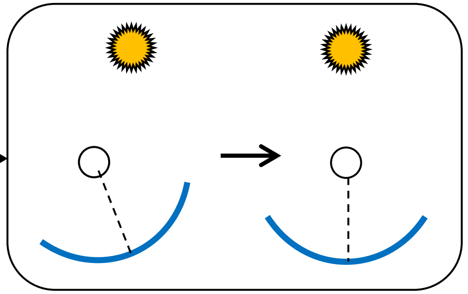

Tracking error is measured by QFly in High Resolution Mode

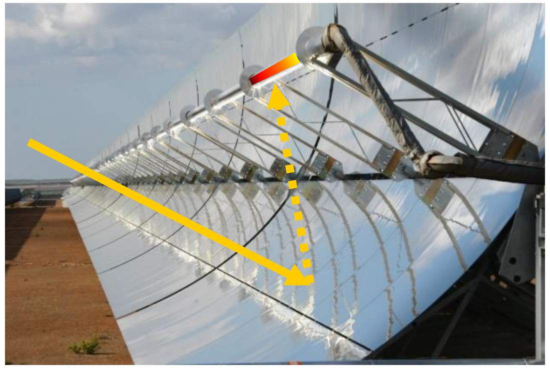

HCE receiver temperatures can be obtained from the solar field data acquisition system

Methodology for optical efficiency simulation

Measurement and raytracing with collector on zenith position

⇩

Optical efficiency (η_{opt}) at **perpendicular incidence angle (0°)**

⇩

Results correspond to **nominal conditions**

⇩

Power at "12h noon" in MW

Raytracing simulations with different conditions

η_{opt} for non-perpendicular incidence angle

η_{opt} for different receiver temperatures

η_{opt} for different tracking errors

⇩

Results closer to "**real conditions**"

⇩

Power plant simulation for a complete year:

Energy Yield in MWh/a

⇩

Plant earnings in Mio €/a

Raytracing simulations – Incidence Angles

Measurement and raytracing with collector on zenith position

Flux density distribution on the receiver for perpendicular incidence angle (0°)

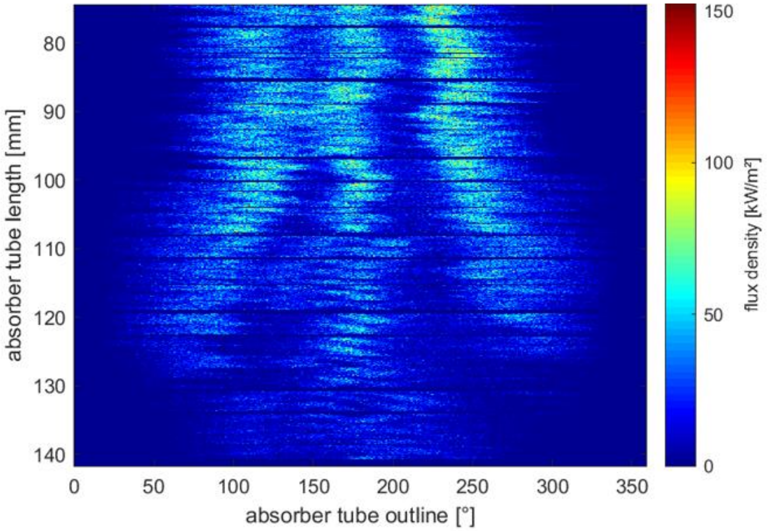

Raytracing simulations with different conditions

Flux density distribution on the receiver for incidence angle: 50°

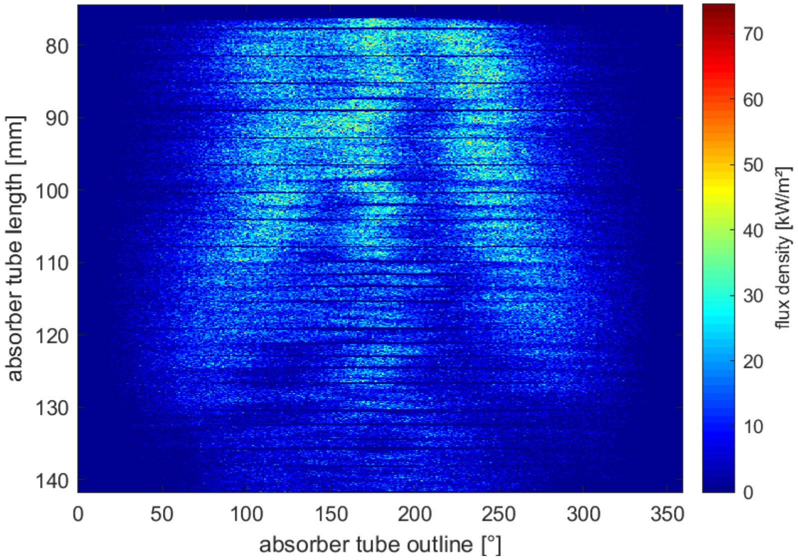

Raytracing simulations – Incidence Angles

Optical efficiency varies depending on the incidence angle due to material properties and geometrical effects

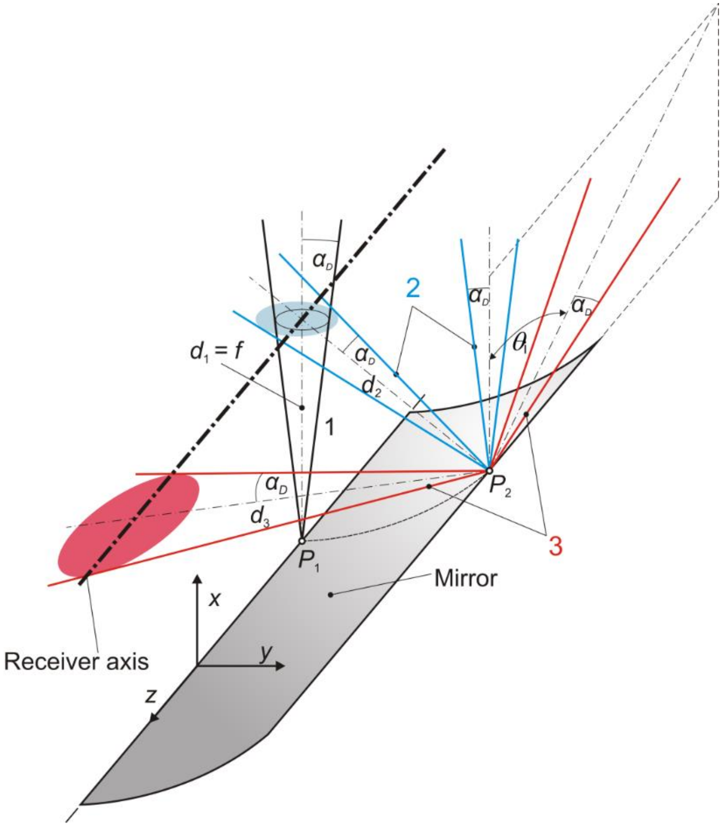

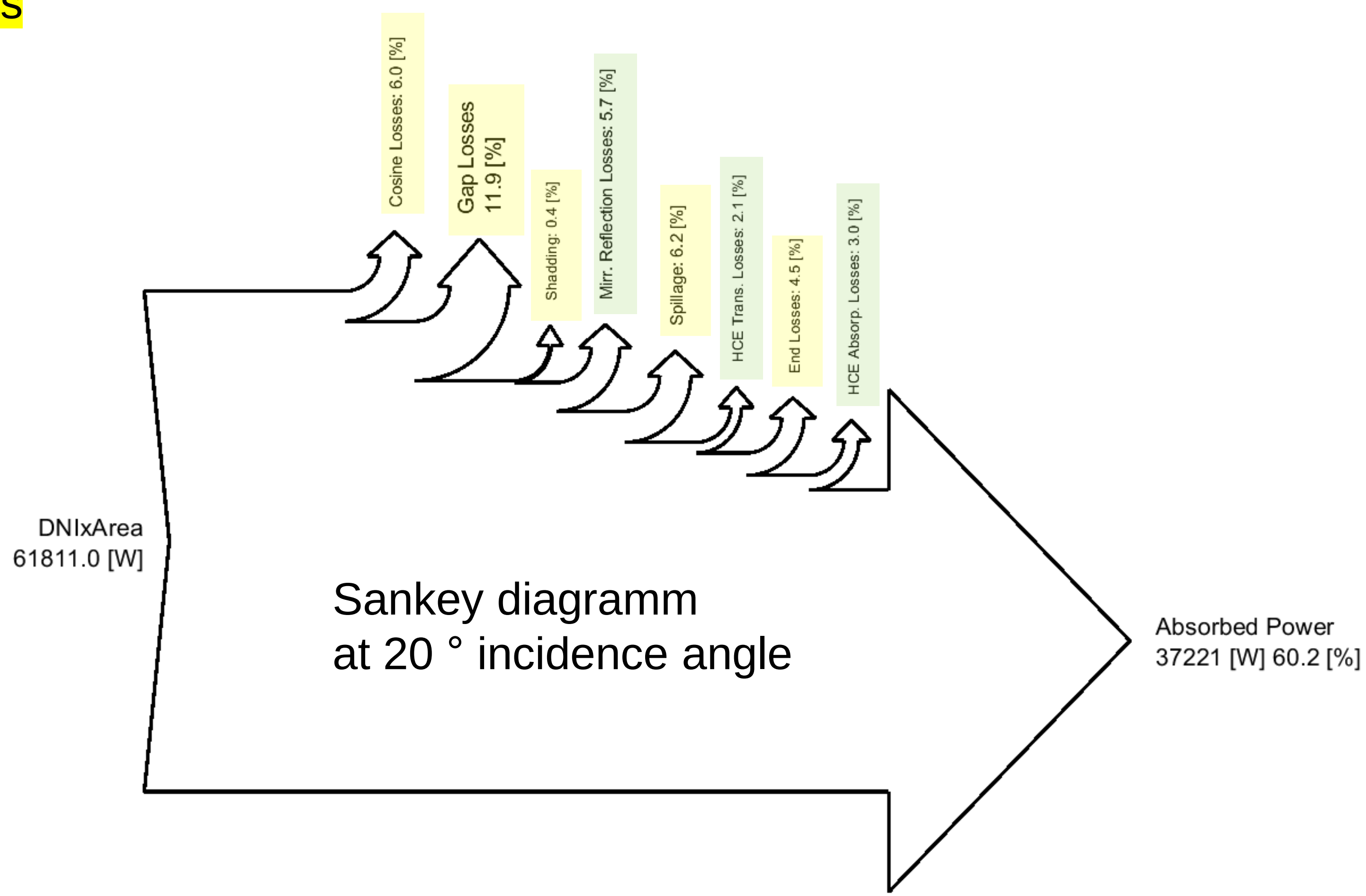

Sankey diagramm
at 20 ° incidence angle

Raytracing simulations – Incidence Angles

Optical efficiency varies depending on the incidence angle due to material properties and geometrical effects

⇩ Raytracing at 0,10,…50°

η_{opt} for different incidence angles

Goal is to extend the power and efficiency from the nominal conditions into all conditions during the year

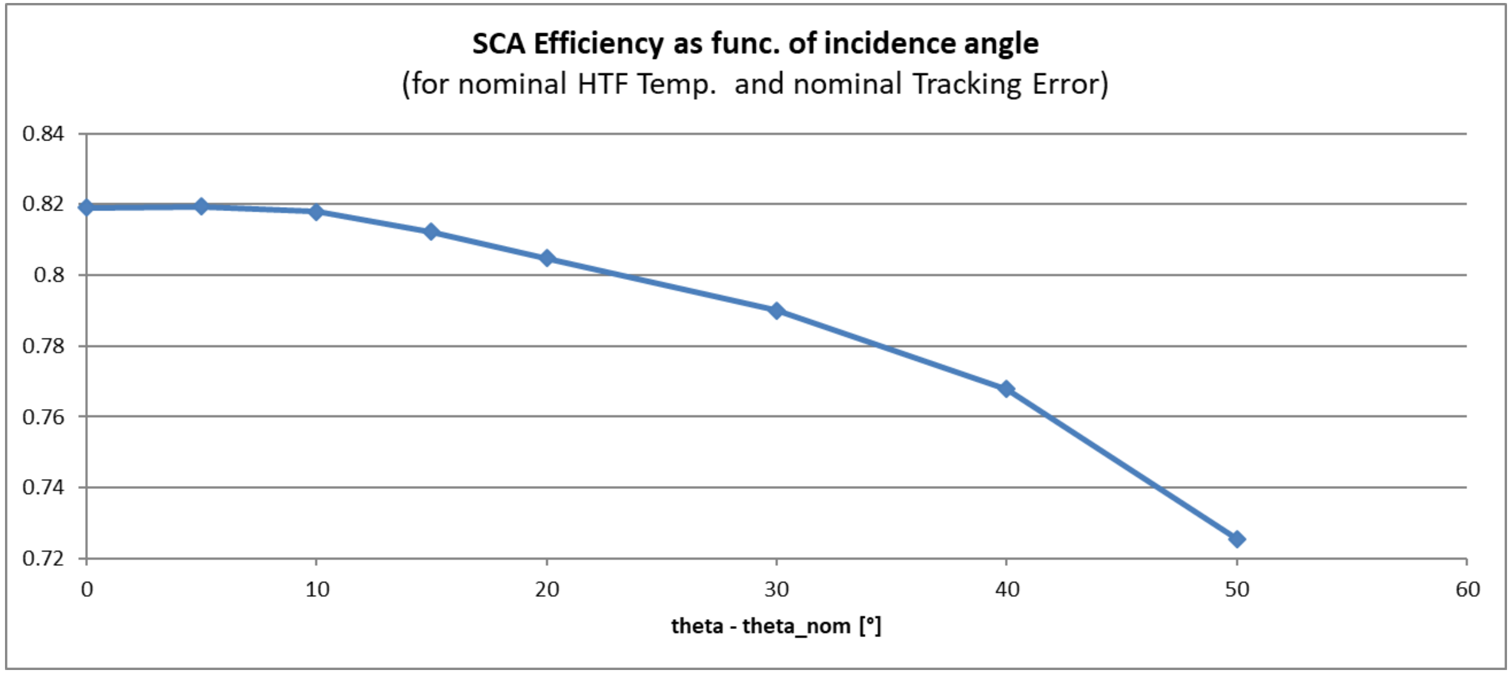

Incidence Angle Modifier Validation

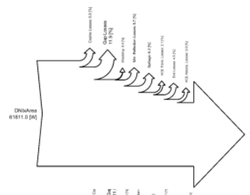

0° Incidence

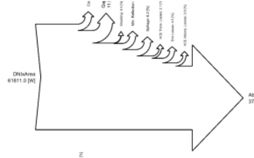

10° Incidence

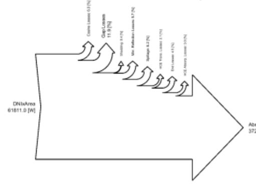

20° Incidence

.
.
.

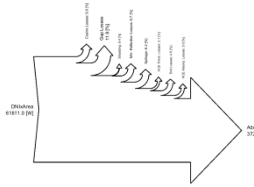

70° Incidence

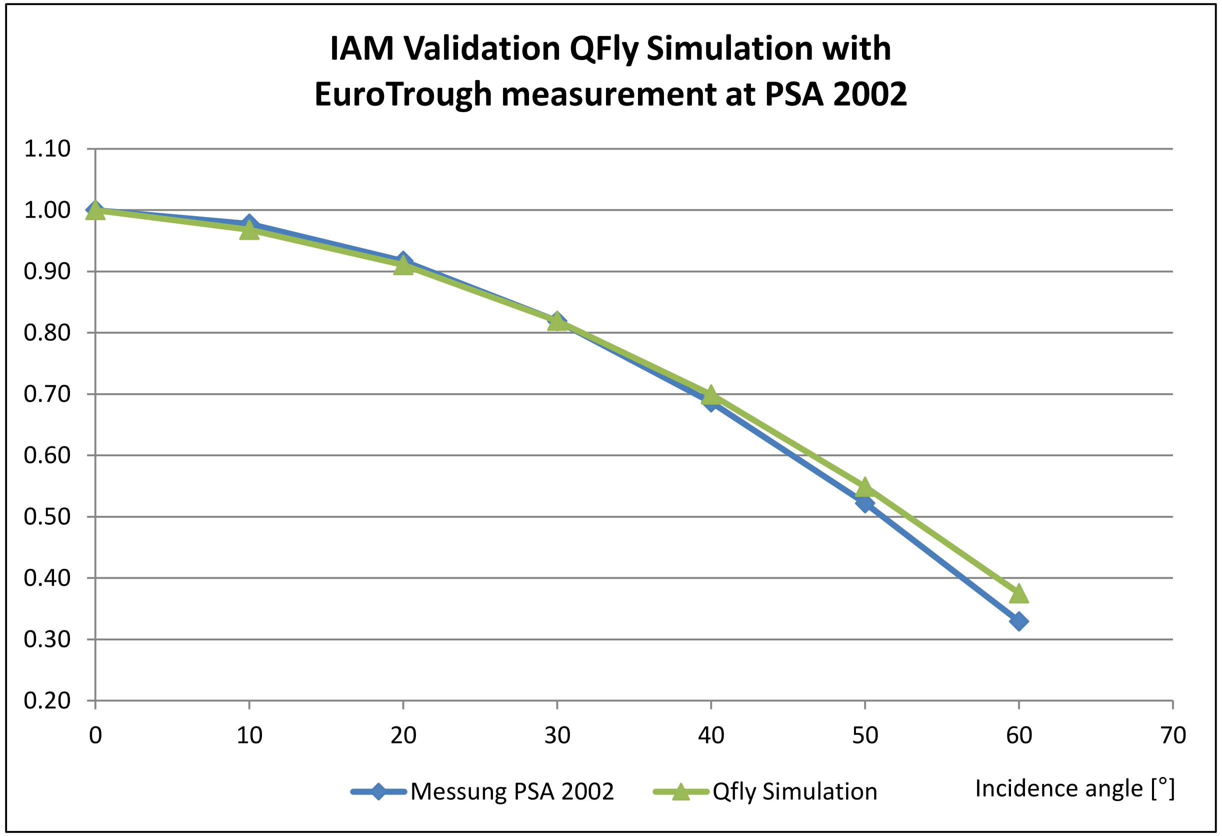

Raytracing simulations – Receiver Temperatures

- For temperatures different than designed, the receiver moves out of the parabola’s focal line. Due to thermal expansion on design temperature it is ideally located on the focal line.
- Additional shading, blocking and end losses occur due to the non-vertical position of the HCE supports and the shorter length of the absorber tube.

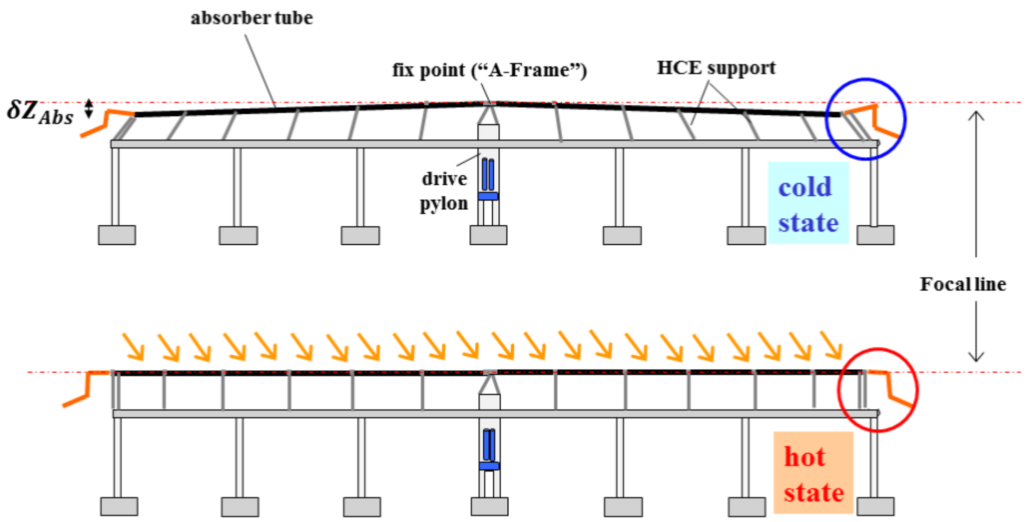

C. Prahl (2019). PhD. Thesis: "Photogrammetric Measurement of the Optical Performance of Parabolic Trough Solar Fields"

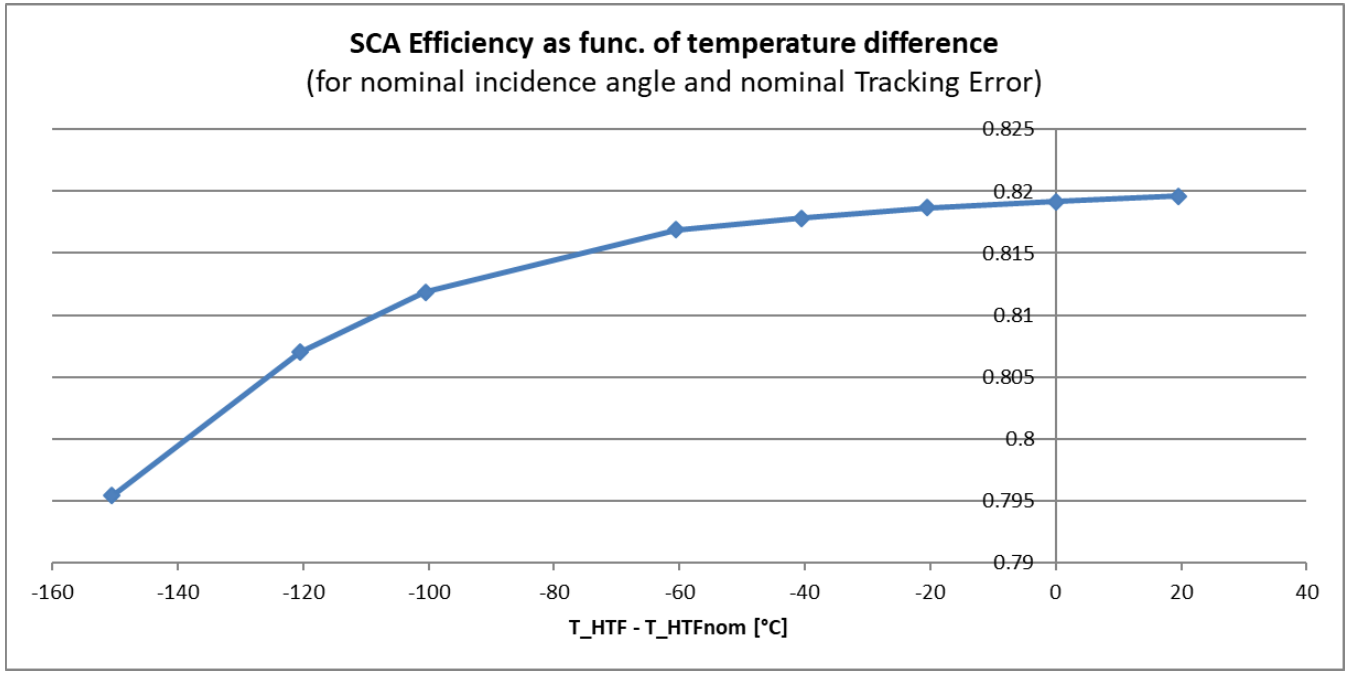

Raytracing simulations – Tracking Error

- Due to tracking error the trough's aperture area would not be perpendicular to the incoming beam radiation, therefore the reflected rays will not hit the receiver tube as designed.

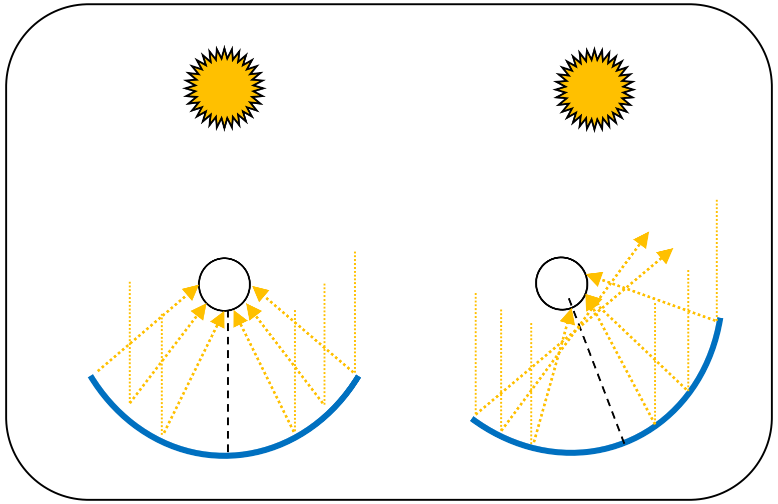

Ideal collector tracking

Collector with tracking error

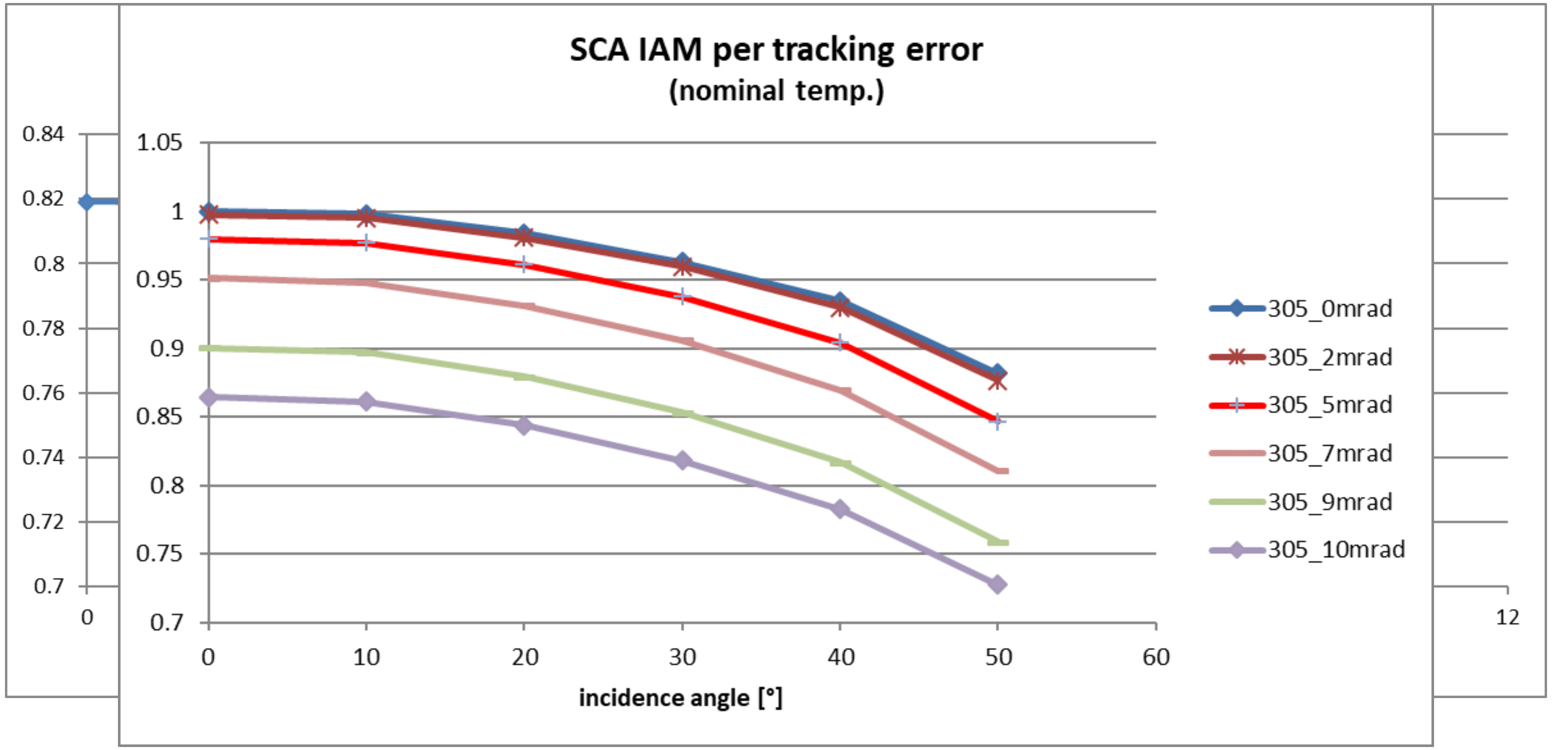

Parametrization of analized effects

$$\eta_{\mathrm{opt}} = \cos(\theta) \cdot IAM \cdot \eta_{\mathrm{opt\_0}} \cdot \eta_{\mathrm{clean}} \cdot \eta_{\mathrm{endloss}} \cdot \eta_{\mathrm{shad}} \cdot \boldsymbol{\eta_{\mathrm{opt\_temp}}} \cdot \boldsymbol{\eta_{\mathrm{opt\_track}}}$$

$$IAM = 1 - \frac{a_1 \cdot \theta + a_2 \cdot \theta^2 + a_3 \cdot \theta^3}{\cos\theta}$$

$$\eta_{opt,temp} = 1 + temp_1 \cdot dT + temp_2 \cdot dT^2 + temp_3 \cdot dT^3$$

mit $dT = |T_{mean,coll} - T_{mean,coll,nom}|$

$$\eta_{opt,track} = 1 + track_1 \cdot dTrack + track_2 \cdot dTrack^2 + track_3 \cdot dTrack^3$$

mit $dTrack = |trackError| - trackNom$

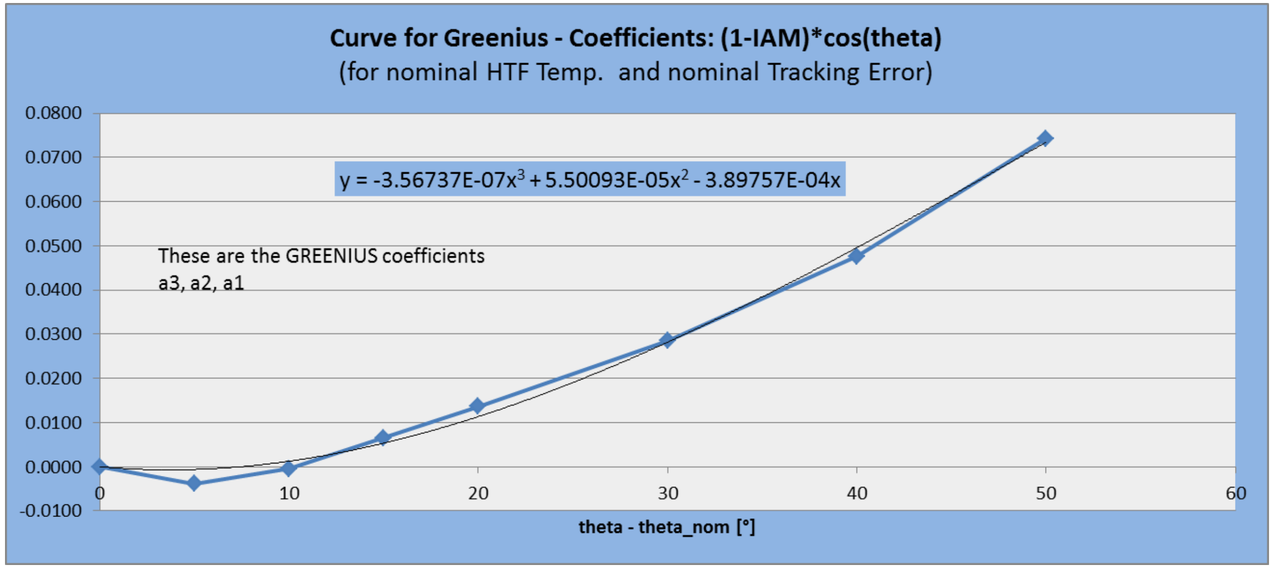
Curve for Greenius - Coefficients: (1-IAM)*cos(theta)
(for nominal HTF Temp. and nominal Tracking Error)

y = -3.56737E-07x³ + 5.50093E-05x² - 3.89757E-04x

These are the GREENIUS coefficients
a3, a2, a1

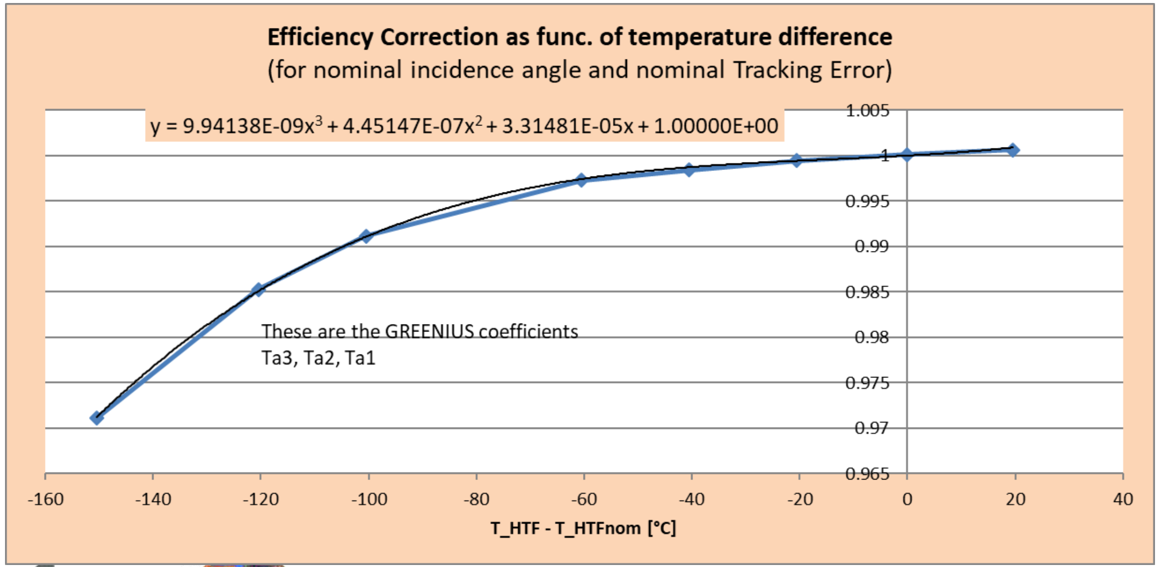
Efficiency Correction as func. of temperature difference
(for nominal incidence angle and nominal Tracking Error)

y = 9.94138E-09x³ + 4.45147E-07x² + 3.31481E-05x + 1.00000E+00

These are the GREENIUS coefficients
Ta3, Ta2, Ta1

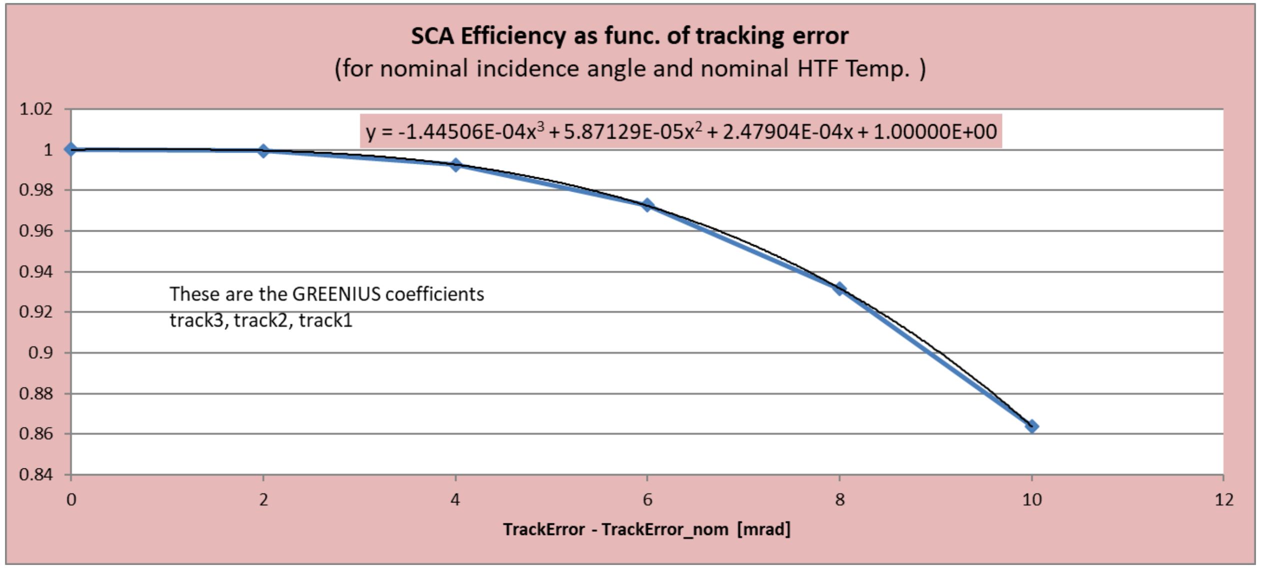
SCA Efficiency as func. of tracking error
(for nominal incidence angle and nominal HTF Temp.)

y = -1.44506E-04x³ + 5.87129E-05x² + 2.47904E-04x + 1.00000E+00

These are the GREENIUS coefficients
track3, track2, track1

Coupling with performance model

greenius
THE GREEN ENERGY SYSTEM ANALYSIS TOOL

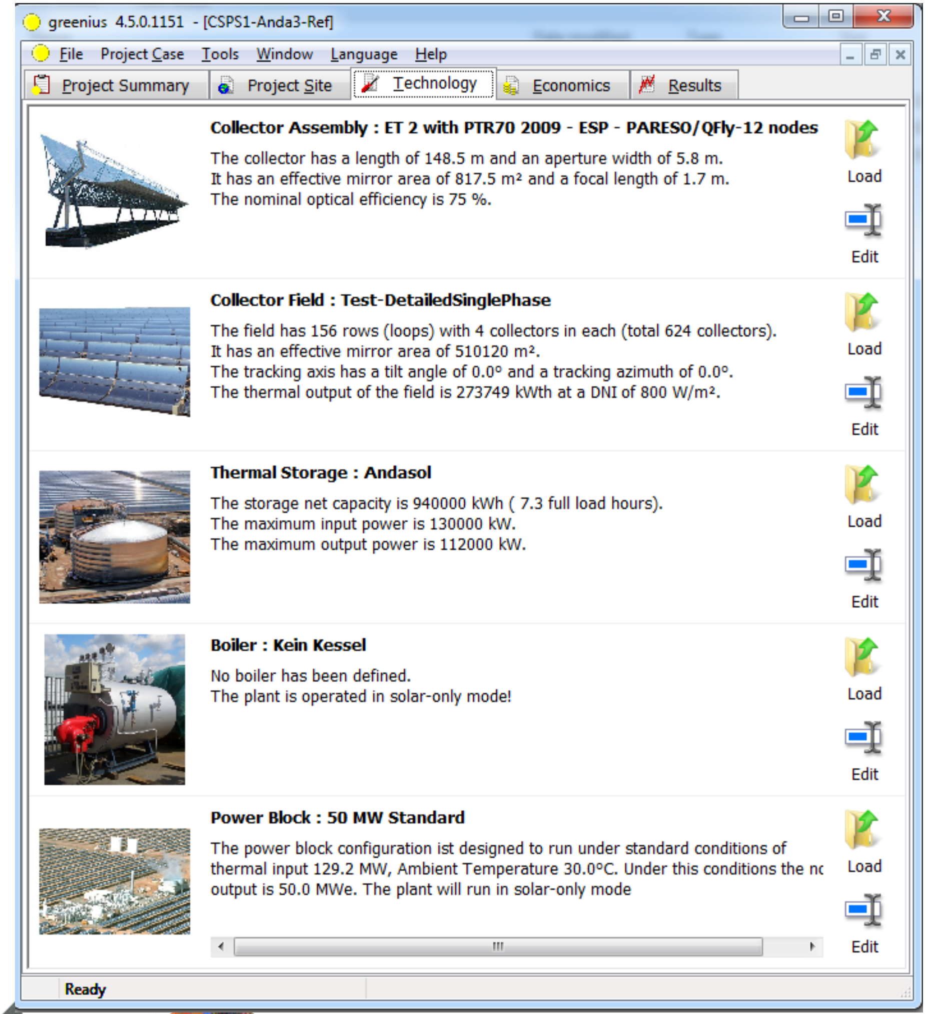

Collector Assembly : ET 2 with PTR70 2009 - ESP - PARESO/QFly-12 nodes

The collector has a length of 148.5 m and an aperture width of 5.8 m.
It has an effective mirror area of 817.5 m² and a focal length of 1.7 m.
The nominal optical efficiency is 75 %.

Collector Field : Test-DetailedSinglePhase

The field has 156 rows (loops) with 4 collectors in each (total 624 collectors).
It has an effective mirror area of 510120 m².
The tracking axis has a tilt angle of 0.0° and a tracking azimuth of 0.0°.
The thermal output of the field is 273749 kWth at a DNI of 800 W/m².

Thermal Storage : Andasol

The storage net capacity is 940000 kWh (7.3 full load hours).
The maximum input power is 130000 kW.
The maximum output power is 112000 kW.

Boiler : Kein Kessel

No boiler has been defined.
The plant is operated in solar-only mode!

Power Block : 50 MW Standard

The power block configuration ist designed to run under standard conditions of
thermal input 129.2 MW, Ambient Temperature 30.0°C. Under this conditions the nc
output is 50.0 MWe. The plant will run in solar-only mode

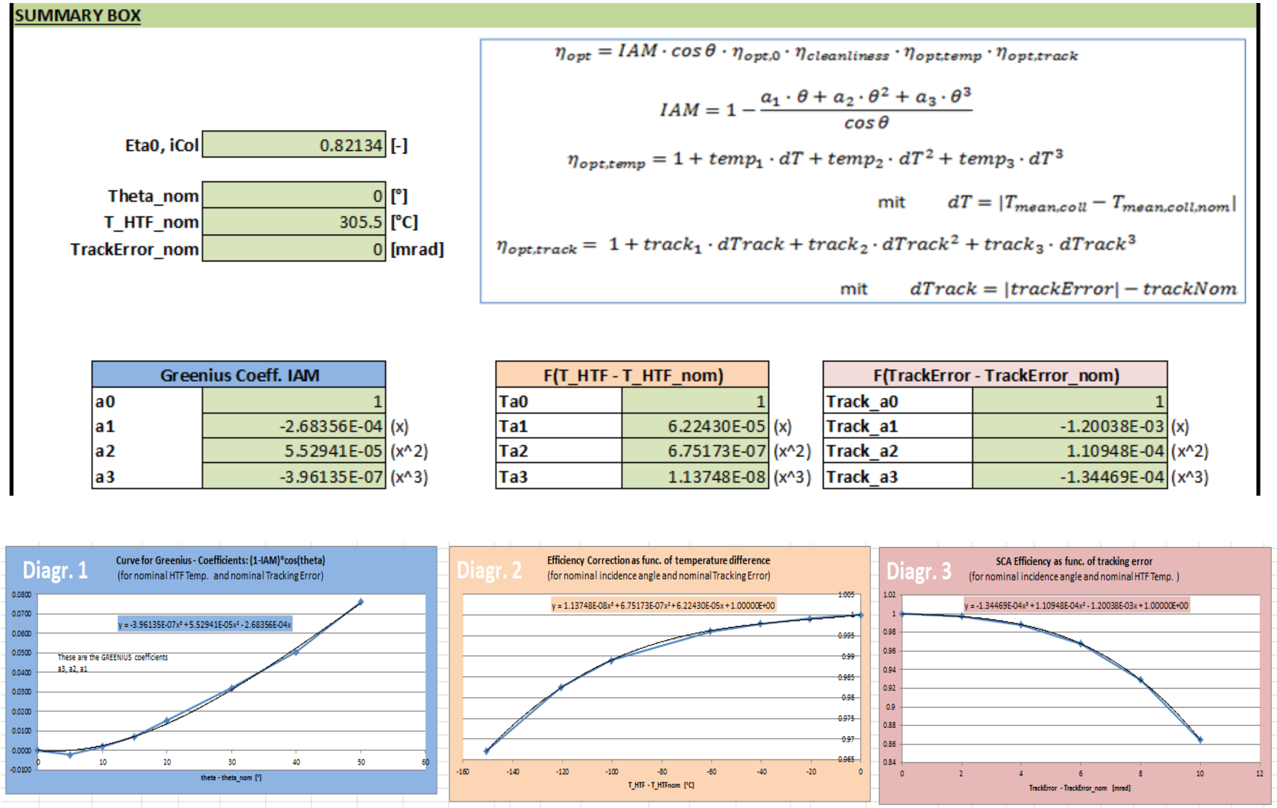

SUMMARY BOX

Eta0, iCol	0.82134	[-]
Theta_nom	0	[°]
T_HTF_nom	305.5	[°C]
TrackError_nom	0	[mrad]

$$\eta_{opt} = IAM \cdot \cos\theta \cdot \eta_{opt,0} \cdot \eta_{cleanliness} \cdot \eta_{opt,temp} \cdot \eta_{opt,track}$$

$$IAM = 1 - \frac{a_1 \cdot \theta + a_2 \cdot \theta^2 + a_3 \cdot \theta^3}{\cos\theta}$$

$$\eta_{opt,temp} = 1 + temp_1 \cdot dT + temp_2 \cdot dT^2 + temp_3 \cdot dT^3$$

$$\text{mit} \quad dT = |T_{mean,coll} - T_{mean,coll,nom}|$$

$$\eta_{opt,track} = 1 + track_1 \cdot dTrack + track_2 \cdot dTrack^2 + track_3 \cdot dTrack^3$$

$$\text{mit} \quad dTrack = |trackError| - trackNom$$

Greenius Coeff. IAM		
a0	1	
a1	-2.68356E-04	(x)
a2	5.52941E-05	(x^2)
a3	-3.96135E-07	(x^3)

F(T_HTF - T_HTF_nom)		
Ta0	1	
Ta1	6.22430E-05	(x)
Ta2	6.75173E-07	(x^2)
Ta3	1.13748E-08	(x^3)

F(TrackError - TrackError_nom)		
Track_a0	1	
Track_a1	-1.20038E-03	(x)
Track_a2	1.10948E-04	(x^2)
Track_a3	-1.34469E-04	(x^3)

Greenius‘ information and free download:
[DLR - Institute of Solar Research - greenius - The Green Energy System Analysis Tool]

Coupling with performance model

greenius
THE GREEN ENERGY SYSTEM ANALYSIS TOOL

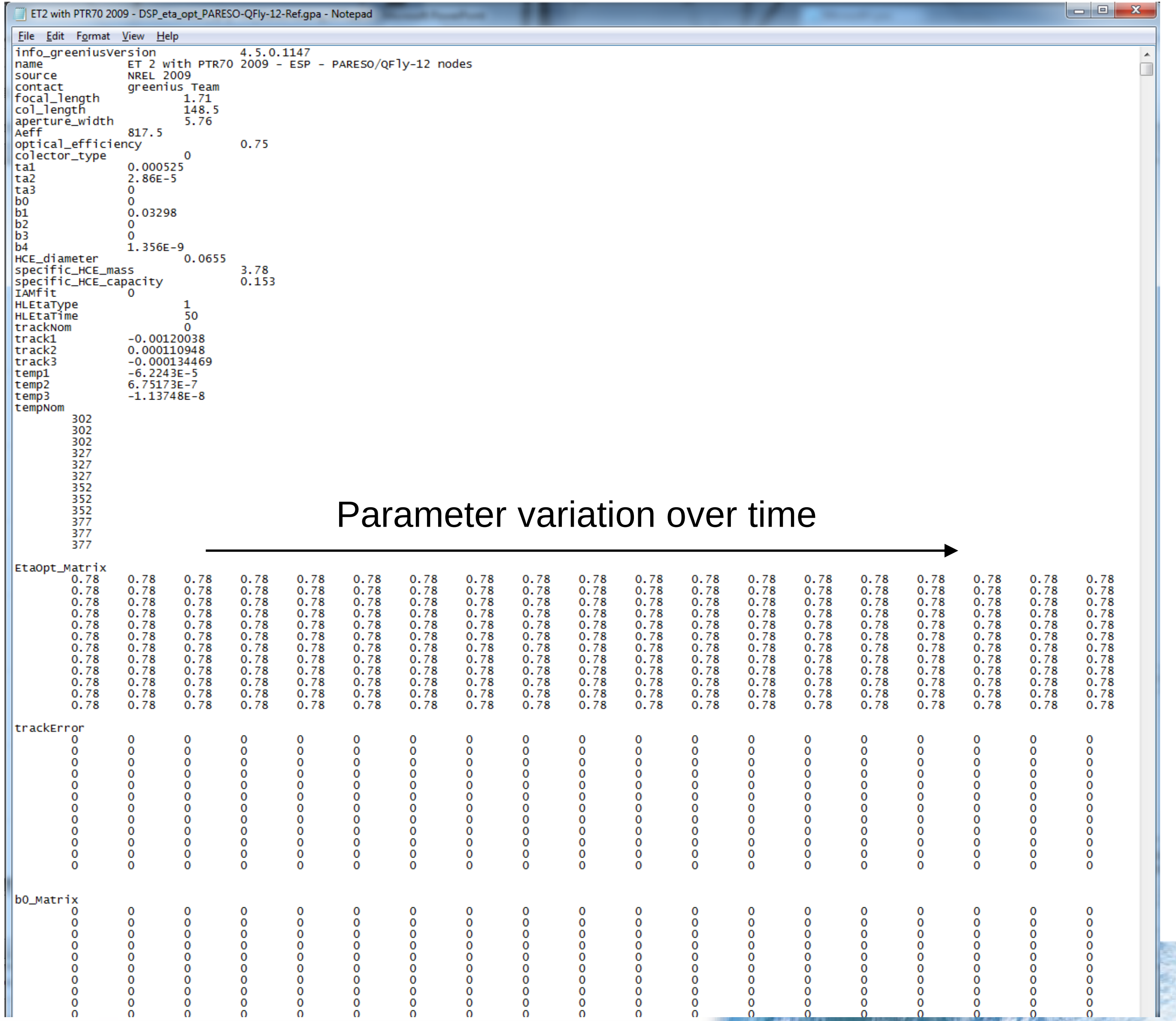

```
info_greeniusVersion            4.5.0.1147
name            ET 2 with PTR70 2009 - ESP - PARESO/QFly-12 nodes
source          NREL 2009
contact         greenius Team
focal_length            1.71
col_length              148.5
aperture_width          5.76
Aeff            817.5
optical_efficiency              0.75
colector_type           0
ta1             0.000525
ta2             2.86E-5
ta3             0
b0              0
b1              0.03298
b2              0
b3              0
b4              1.356E-9
HCE_diameter            0.0655
specific_HCE_mass               3.78
specific_HCE_capacity           0.153
IAMfit          0
HLEtaType               1
HLEtaTime               50
trackNom                0
track1          -0.00120038
track2          0.000110948
track3          -0.000134469
temp1           -6.2243E-5
temp2           6.75173E-7
temp3           -1.13748E-8
tempNom
        302
        302
        302
        327
        327
        327
        352
        352
        352
        377
        377
        377

EtaOpt_Matrix
        0.78    0.78    0.78    0.78    0.78    0.78    0.78    0.78    0.78    0.78    0.78    0.78    0.78    0.78    0.78    0.78    0.78    0.78    0.78
        0.78    0.78    0.78    0.78    0.78    0.78    0.78    0.78    0.78    0.78    0.78    0.78    0.78    0.78    0.78    0.78    0.78    0.78    0.78
        0.78    0.78    0.78    0.78    0.78    0.78    0.78    0.78    0.78    0.78    0.78    0.78    0.78    0.78    0.78    0.78    0.78    0.78    0.78
        0.78    0.78    0.78    0.78    0.78    0.78    0.78    0.78    0.78    0.78    0.78    0.78    0.78    0.78    0.78    0.78    0.78    0.78    0.78
        0.78    0.78    0.78    0.78    0.78    0.78    0.78    0.78    0.78    0.78    0.78    0.78    0.78    0.78    0.78    0.78    0.78    0.78    0.78
        0.78    0.78    0.78    0.78    0.78    0.78    0.78    0.78    0.78    0.78    0.78    0.78    0.78    0.78    0.78    0.78    0.78    0.78    0.78
        0.78    0.78    0.78    0.78    0.78    0.78    0.78    0.78    0.78    0.78    0.78    0.78    0.78    0.78    0.78    0.78    0.78    0.78    0.78
        0.78    0.78    0.78    0.78    0.78    0.78    0.78    0.78    0.78    0.78    0.78    0.78    0.78    0.78    0.78    0.78    0.78    0.78    0.78
        0.78    0.78    0.78    0.78    0.78    0.78    0.78    0.78    0.78    0.78    0.78    0.78    0.78    0.78    0.78    0.78    0.78    0.78    0.78
        0.78    0.78    0.78    0.78    0.78    0.78    0.78    0.78    0.78    0.78    0.78    0.78    0.78    0.78    0.78    0.78    0.78    0.78    0.78
        0.78    0.78    0.78    0.78    0.78    0.78    0.78    0.78    0.78    0.78    0.78    0.78    0.78    0.78    0.78    0.78    0.78    0.78    0.78
        0.78    0.78    0.78    0.78    0.78    0.78    0.78    0.78    0.78    0.78    0.78    0.78    0.78    0.78    0.78    0.78    0.78    0.78    0.78

trackError
        0       0       0       0       0       0       0       0       0       0       0       0       0       0       0       0       0       0       0
        0       0       0       0       0       0       0       0       0       0       0       0       0       0       0       0       0       0       0
        0       0       0       0       0       0       0       0       0       0       0       0       0       0       0       0       0       0       0
        0       0       0       0       0       0       0       0       0       0       0       0       0       0       0       0       0       0       0
        0       0       0       0       0       0       0       0       0       0       0       0       0       0       0       0       0       0       0
        0       0       0       0       0       0       0       0       0       0       0       0       0       0       0       0       0       0       0
        0       0       0       0       0       0       0       0       0       0       0       0       0       0       0       0       0       0       0
        0       0       0       0       0       0       0       0       0       0       0       0       0       0       0       0       0       0       0
        0       0       0       0       0       0       0       0       0       0       0       0       0       0       0       0       0       0       0
        0       0       0       0       0       0       0       0       0       0       0       0       0       0       0       0       0       0       0
        0       0       0       0       0       0       0       0       0       0       0       0       0       0       0       0       0       0       0
        0       0       0       0       0       0       0       0       0       0       0       0       0       0       0       0       0       0       0

b0_Matrix
        0       0       0       0       0       0       0       0       0       0       0       0       0       0       0       0       0       0       0
        0       0       0       0       0       0       0       0       0       0       0       0       0       0       0       0       0       0       0
        0       0       0       0       0       0       0       0       0       0       0       0       0       0       0       0       0       0       0
        0       0       0       0       0       0       0       0       0       0       0       0       0       0       0       0       0       0       0
        0       0       0       0       0       0       0       0       0       0       0       0       0       0       0       0       0       0       0
        0       0       0       0       0       0       0       0       0       0       0       0       0       0       0       0       0       0       0
        0       0       0       0       0       0       0       0       0       0       0       0       0       0       0       0       0       0       0
        0       0       0       0       0       0       0       0       0       0       0       0       0       0       0       0       0       0       0
        0       0       0       0       0       0       0       0       0       0       0       0       0       0       0       0       0       0       0
        0       0       0       0       0       0       0       0       0       0       0       0       0       0       0       0       0       0       0
```

Parameter variation over time →

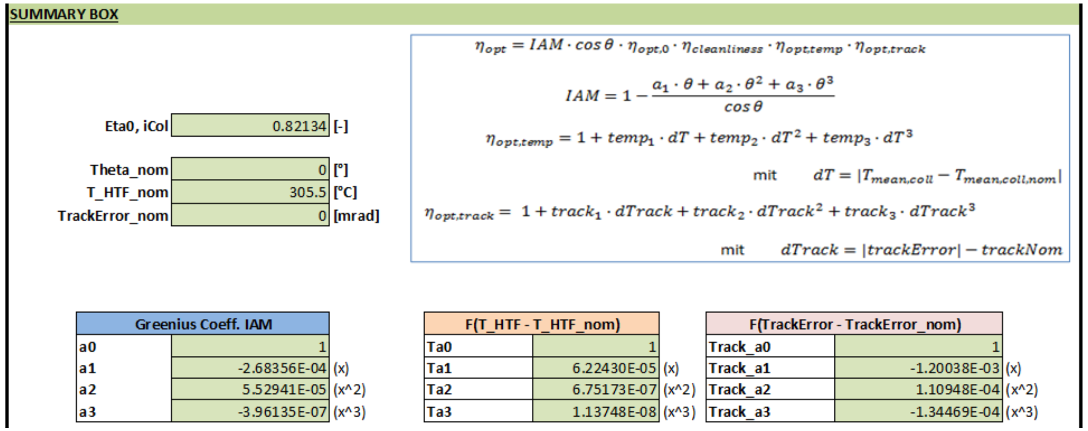

SUMMARY BOX

Eta0, iCol	0.82134	[-]
Theta_nom	0	[°]
T_HTF_nom	305.5	[°C]
TrackError_nom	0	[mrad]

$$\eta_{opt} = IAM \cdot \cos\theta \cdot \eta_{opt,0} \cdot \eta_{cleanliness} \cdot \eta_{opt,temp} \cdot \eta_{opt,track}$$

$$IAM = 1 - \frac{a_1 \cdot \theta + a_2 \cdot \theta^2 + a_3 \cdot \theta^3}{\cos\theta}$$

$$\eta_{opt,temp} = 1 + temp_1 \cdot dT + temp_2 \cdot dT^2 + temp_3 \cdot dT^3$$

$$\text{mit} \quad dT = |T_{mean,coll} - T_{mean,coll,nom}|$$

$$\eta_{opt,track} = 1 + track_1 \cdot dTrack + track_2 \cdot dTrack^2 + track_3 \cdot dTrack^3$$

$$\text{mit} \quad dTrack = |trackError| - trackNom$$

Greenius Coeff. IAM		
a0	1	
a1	-2.68356E-04	(x)
a2	5.52941E-05	(x^2)
a3	-3.96135E-07	(x^3)

F(T_HTF - T_HTF_nom)		
Ta0	1	
Ta1	6.22430E-05	(x)
Ta2	6.75173E-07	(x^2)
Ta3	1.13748E-08	(x^3)

F(TrackError - TrackError_nom)		
Track_a0	1	
Track_a1	-1.20038E-03	(x)
Track_a2	1.10948E-04	(x^2)
Track_a3	-1.34469E-04	(x^3)

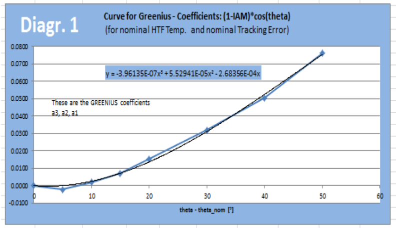

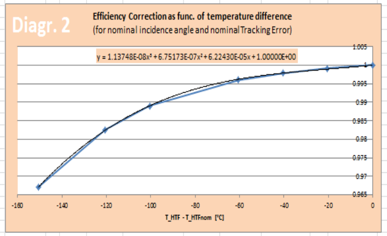

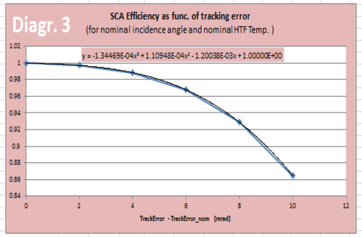

Performance mode is under construction…
Yield analysis results are not available yet.

THANK YOU FOR YOUR ATTENTION!
ANY QUESTIONS?

GOBIERNO DE ESPAÑA MINISTERIO DE CIENCIA, INNOVACIÓN Y UNIVERSIDADES Ciemat Centro de Investigaciones Energéticas, Medioambientales y Tecnológicas

ENEA

DLR Deutsches Zentrum für Luft- und Raumfahrt

UNIVERSIDADE DE ÉVORA

ESTELA

The Cyprus Institute

instituto IMDEA energía

Fraunhofer ISE

euronovia

LNEG

METU

ETH zürich

UNIVERSIDAD DE ALMERÍA

cnrs

cea

SFERA-III
Solar Facilities for the European Research Area

Solar Facilities for the European Research Area

2nd Training for Industries “Optimization of CST plant output by optical and thermal characterization and target-oriented O&M”
26 – 29 April 2022, Plataforma Solar de Almería, Spain

Soiling measurement on mirrors including airborne soiling measurement
Dr.-Ing. Fabian Wolfertstetter, DLR

NETWORKING

THIS PROJECT HAS RECEIVED FUNDING FROM THE EUROPEAN UNION’S HORIZON 2020 RESEARCH AND INNOVATION PROGRAMME UNDER GRANT AGREEMENT NO **823802**

Agenda

- Introduction to the soiling issue
- Measurement of soiling
    - Laboratory instruments
    - Handheld field measurement devices
    - Automatic field measurements
    - Airborne drone measurement principle
- Mitigation and cleaning optimization

Introduction

- Soiling is the **accumulation of particles** (mineral dust, soot, pollen, bird droppings etc.) on the optical surfaces of a solar field
- Soiling reduces efficiency of a solar field
- Operators have to find the best trade-off between reduced **cleaning costs** and increased optical **solar field efficiency**
- **Time resolved** analysis and **realistic soiling** rate dataset is crucial to optimize cleaning procedures

=> Soiling measurements and predictions are necessary as a decision basis

Soiled CSP collector at PSA
(Infrastructure owned by the Spanish research centre CIEMAT)

Cleaning truck in action
Image courtesy of Abengoa Solar

Introduction

Soiling optical losses occur due to:

- Diffuse reflection
- Scattering
- Absorption

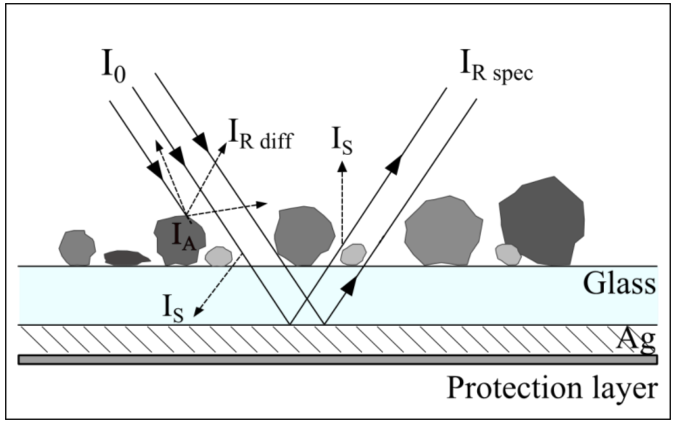

- 2 passages through the soiling layer
- 1 passage through the (soiled) absorber tubes glass cover
- Most forward scattered light is lost

Soiled collector at PSA

Collector during Saharan dust event, March `22

(Infrastructure owned by the Spanish research centre CIEMAT)

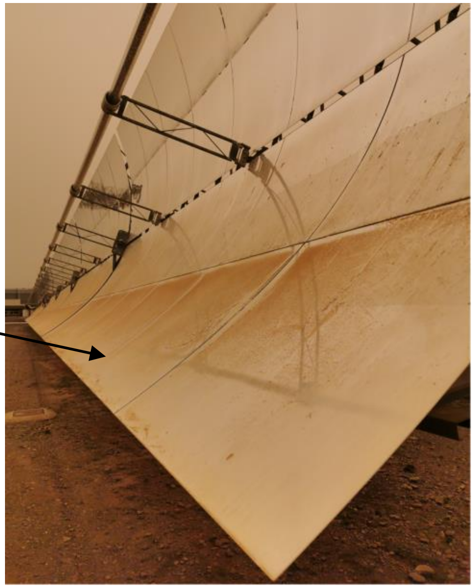

Note: **In PV the issue is less severe** for same amounts of soiling:

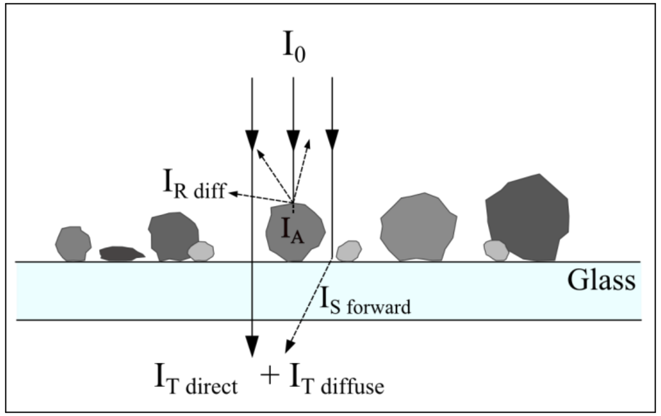

Soiled PV modules at PSA
(Infrastructure owned by the Spanish research centre CIEMAT)

PV:

- 1 passage through the (soiled) glass cover
- Most forward scattered light is NOT lost

Optical properties of dust

- Optical properties of dust influence its scattering behavior
- Dust types vary with site and time
    - Local dust types depending on wind and humidity
    - Pollen
    - Long range dust transport
- Accurate determination of soiling requires optical measurement representative of power plant

Total dust load today

Screenshot from https://forecast.uoa.gr/en/forecast-maps/dust/europe

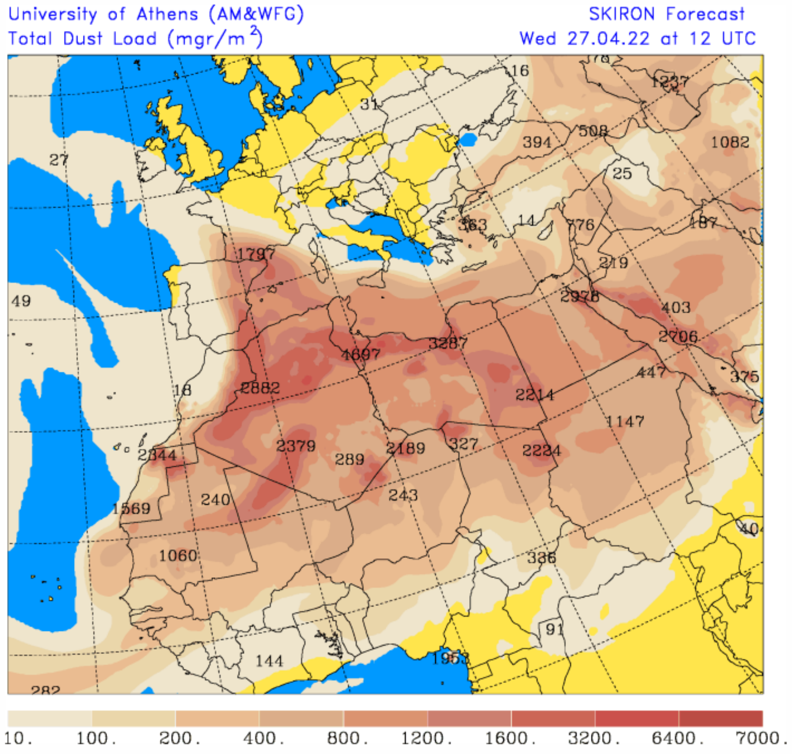

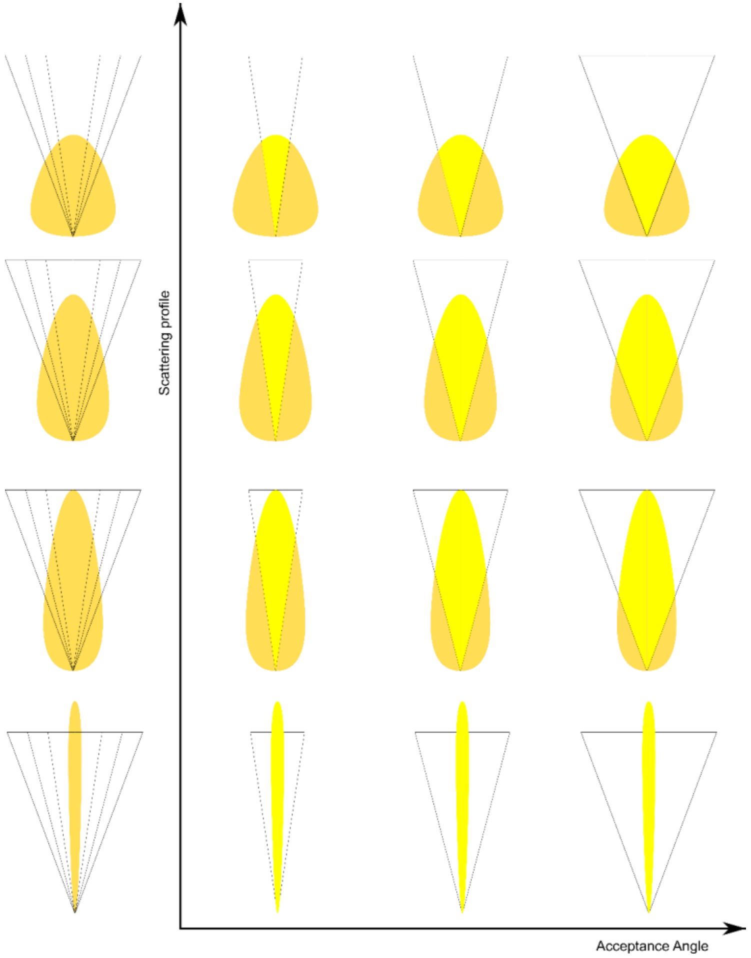

Schematic representation of different dust scattering profiles and instrument acceptance angles

from soiling reflectance measurement guideline

Soiling optical effects and solar field layout

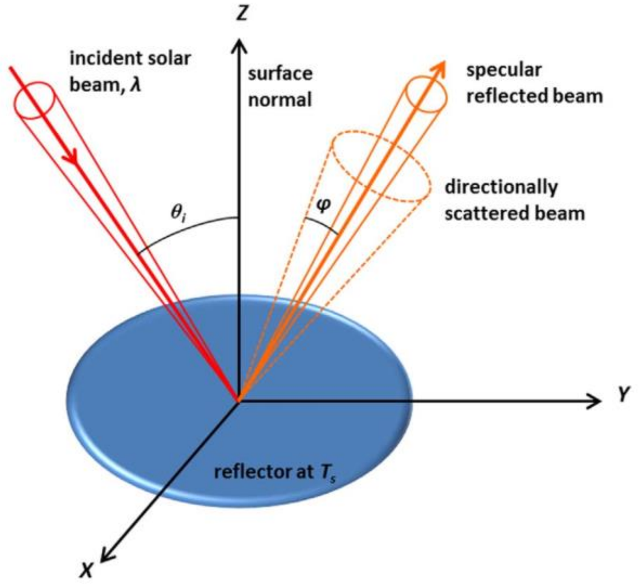

- Each solar field has specific optical boundary conditions:
  - Acceptance angle
  - Incidence angle
  - Spectral limitations
- Soiling has an influence on all
- The „ideal soiling measurement instrument“ should measure with the plant optical parameters

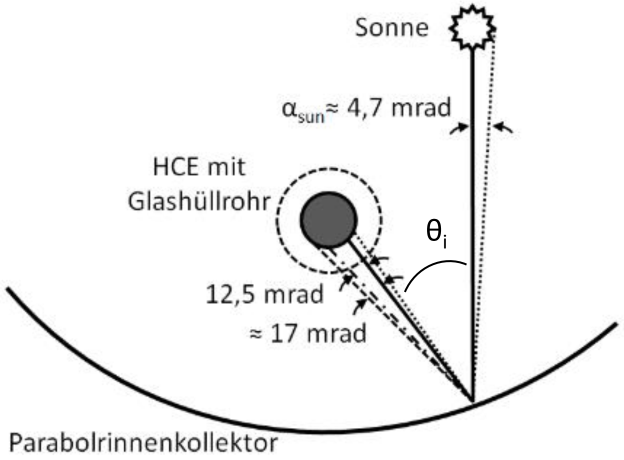

Acceptance and incidence angles in a parabolic trough

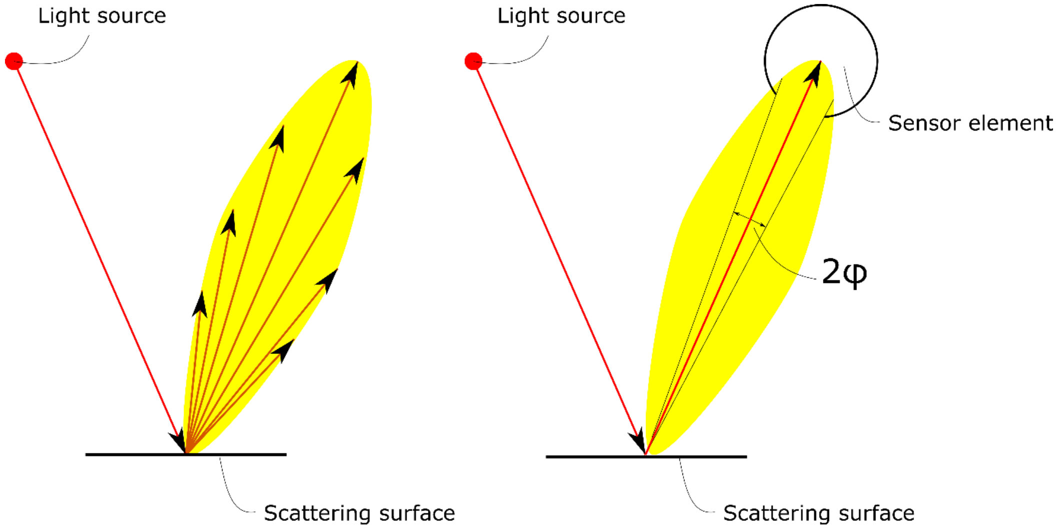

Optical effects of a soiling layer on a point like light source

Laboratory measurement instruments

- Spectrally resolved
- High precision
- Only small samples, no application in solar field

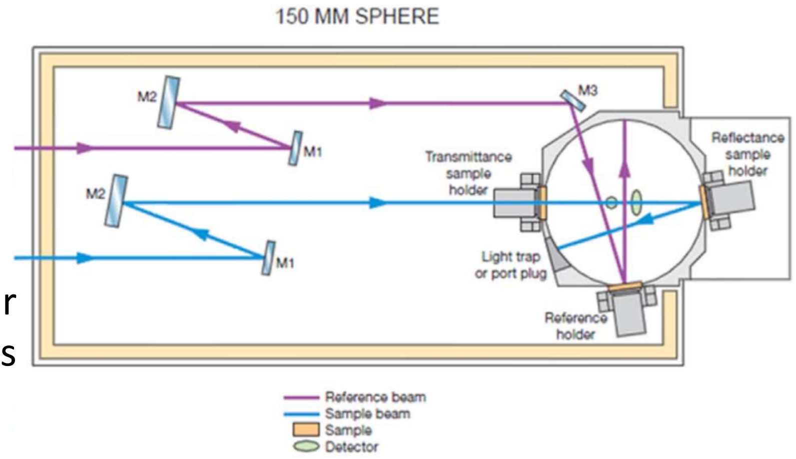

Spectrophotometer optical pathways

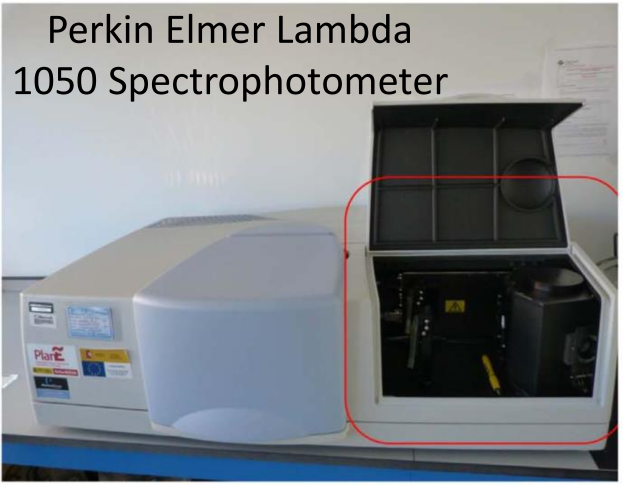

Perkin Elmer Lambda 1050 Spectrophotometer

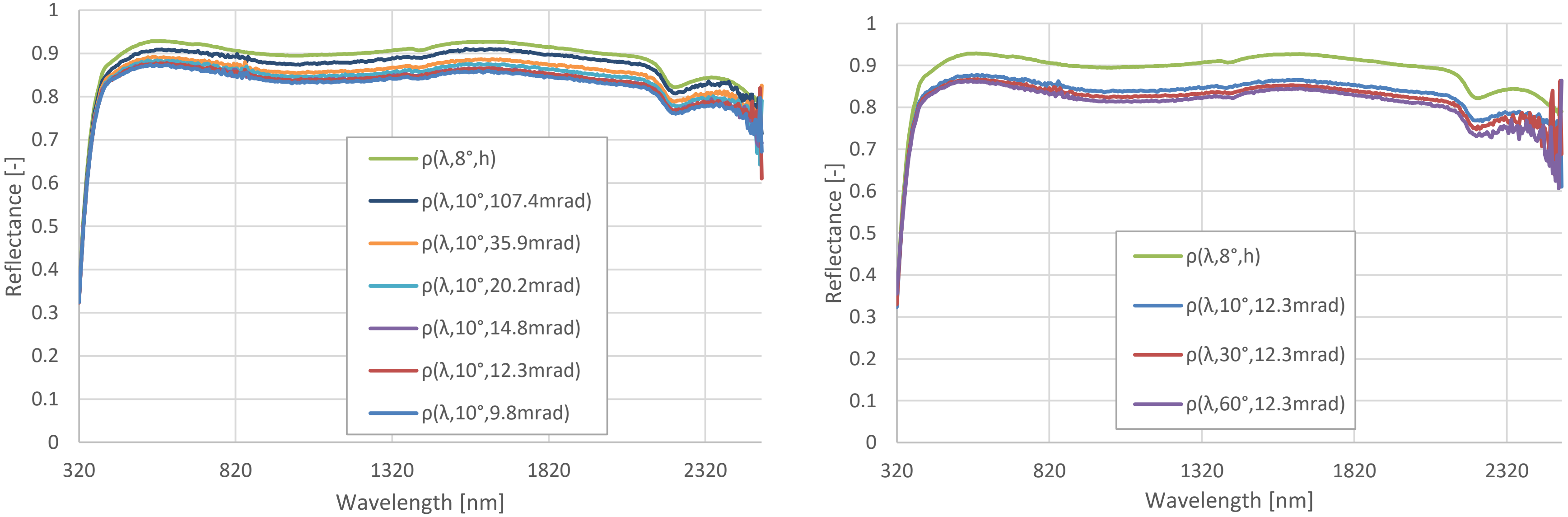

S2R example measurements of soiled sample for different acceptance and incidence angles. Taken in PSA-OPAC-laboratory

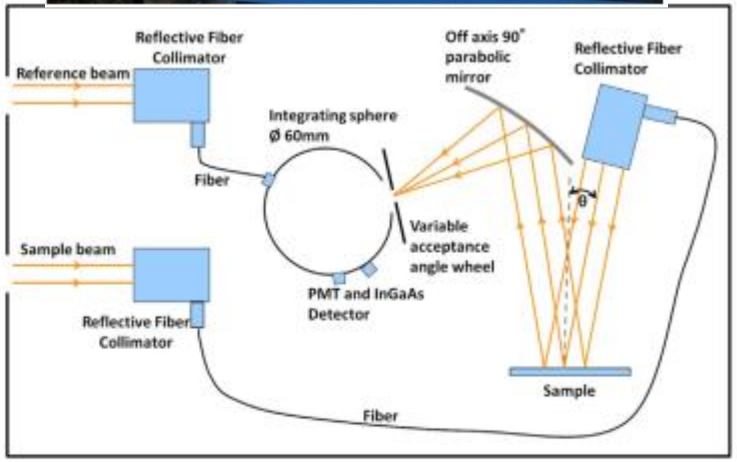

S2R pathway. Accessory to Spectrophotometer

Handheld reflectometers

- Currently, mainly handheld reflectometers are used in CSP solar fields
- The soiling guideline lists the properties of a selection of handheld instruments:
  - High variation of incidence and acceptance angles

=> Know your instrument!

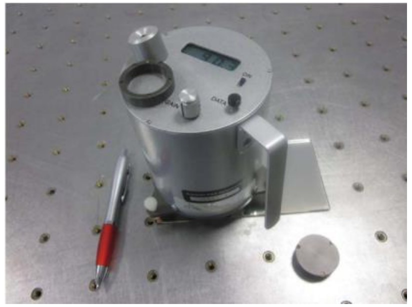

Devices&Services R15

Condor, Abengoa

SOC 410, Solar Surface Optics

Fraunhofer/PSE pFlex

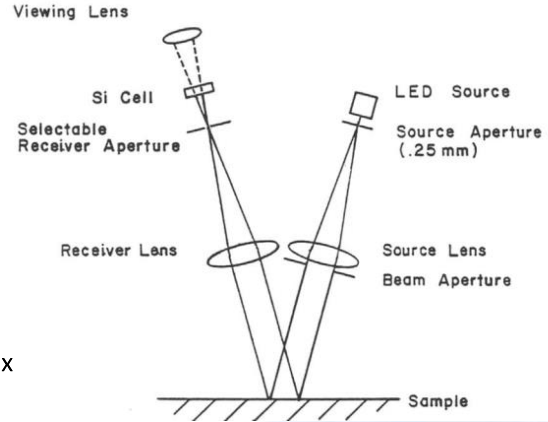

Manufacturer	Surface Optics	Devices & Services Co		Aragon Photonics	Konica Minolta	PSE AG
Developer	Surface Optics	Devices & Services Co		Abengoa & University of Zaragoza	Konica Minolta	Fraunhofer ISE
Model	**410 Solar**	**15R-USB**	**15R- RGB**	**Condor**	**CM-700d/600d**	**PFlex**
Measurement principle	Integrating sphere unit where the specular port can be opened	A source lamp and a detector positioned in incidence and outgoing angles		6 different beam sources and 6 detectors	Integrating sphere unit where the specular port can be opened	1 light source for each λ and 1 detector
Measurement type	Hemispherical and diffuse reflectance (specular calculated)	Monochromatic specular reflectance at selected acceptance angles		Monochromatic specular reflectance and solar-weighted specular reflectance (from the six wavelengths)	Hemispherical and diffuse reflectance and colour	Monocromatic specular reflectance and cleanliness
Incidence angle, θ_i (º)	20	15		12	8	8
Beam spot size (diameter in mm)	6.35	10.00		1.00, each of six spots	3 (700d model) 8 (700d and 600d models)	10.00
Wavelength range, λ (nm)	7 bands between 300 and 2500	Peak at 660	Band red, green, blue, white and IR filters: 460 (±50), 550 (±50), 650 (-40 +150), 720 (-40 +100)	435, 525, 650, 780, 940 and 1050, solar-weighted according to ISO 9050	400-700 (10nm steps)	470, 525, 625
(Half) acceptance angle, ϕ (mrad)	52.4	3.5, 7.5, 12.5, 23.0	2.3, 3.5, 7.5, 12.5, 23.0	145.0	*	67.2
Weight (kg)	2.13	1.10		1.40	0.55 (without calibration cap and batteries)	1.45
Operating temp. (ºC)	0 - 40	0 - 50		-20 - 55	5 - 40	-15 - 60
Autonomy	2 hours	49 - 52 hours		1,200 measurements	2,000 measurements	> 12 hours
Type of calibration	Two external reference mirrors	One external reference mirror		One external reference mirror	Two references (one black and one white)	Black reference (offset) and one external reference mirror
Beam aligment	No	Yes		No	No	No
Adaptable to mirror curvature	Yes, 15.24 mm radius minimum	Yes (two screws to adapt the curvature)		Yes, up to 300 mm radius within 99.5 % tolerance, without adapting anything in the reflectometer	*	Yes

Handheld reflectometers

- Advantages:
  - Portable
  - Measurements on the actual mirror surfaces
  - Medium to high accuracy
- Disadvantage:
  - Manual operation -> time consuming
  - Many different instrument types
  - Not comparable among each other

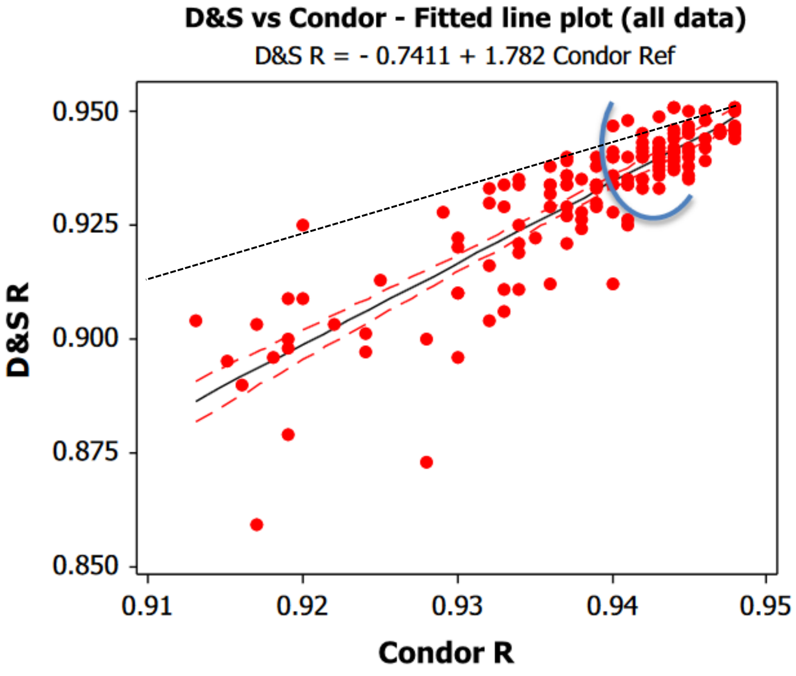

Comparison of soiling measurements with two instruments on same samples. Perfect agreement shown as dashed line.

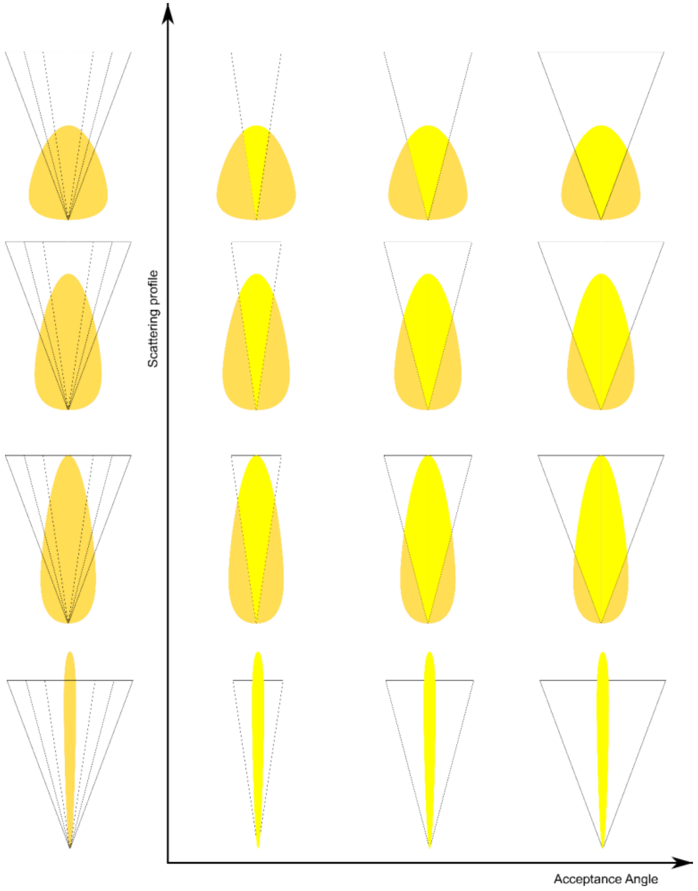

Schematic representation of different dust scattering profiles and instrument acceptance angles

from soiling reflectance measurement guideline

Sansom, C., A. Fernández-García, P. King, F. Sutter, and A. Garcia Segura. Reflectometer Comparison for Assessment of Back-Silvered Glass Solar Mirrors. Sol Energy 2017;155: 496-505

TraCS measurement instrument

- TraCS is an accessory to a meteorological station comprising a solar tracker
- Automatic, high time resolution measurement
- Minimal additional maintenance requirements
- Cleanliness, ξ: Comparison of reflected and direct DNI measured with pyrheliometers
- Soiling Rate $\hat{\xi}$ from fit curve

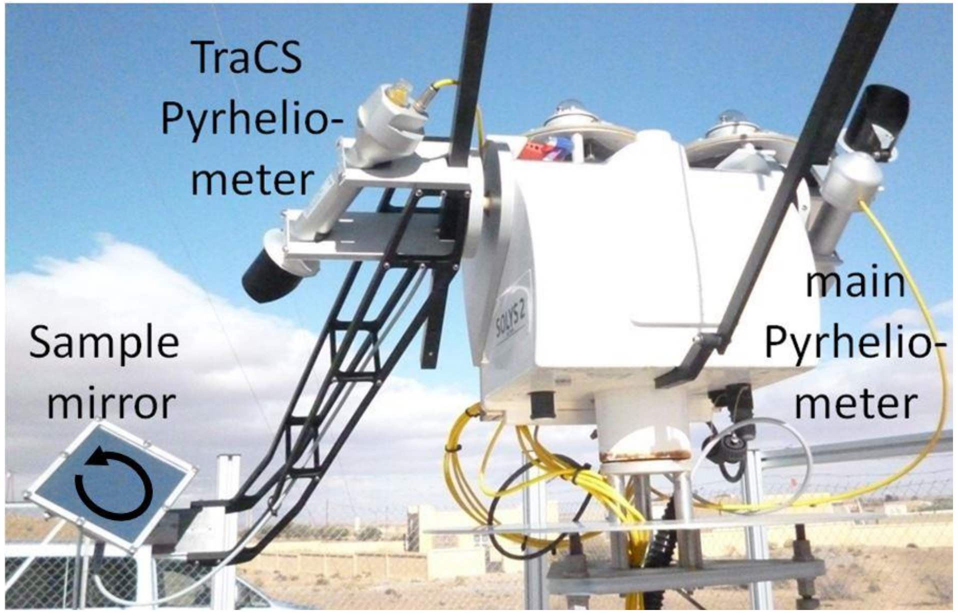

Tracs Instrument

$$\xi(t) = \frac{DNI_{refl}(t)}{k_c \cdot DNI_{dir}(t)}\Bigg| DNI_{dir} > DNI_{lim}$$

$$\hat{\xi}\,(t) = \frac{d\xi(t)}{dt}$$

$$k_c = \frac{1}{N}\sum_{n=1}^{N}\frac{DNI_{refl}^{clean}(t_n)}{DNI_{dir}(t_n)} = constant$$

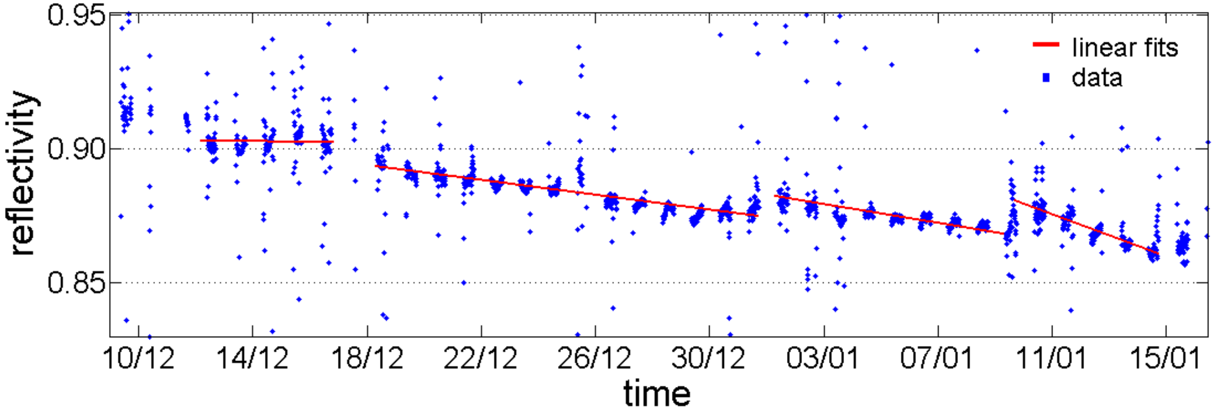

Tracs measurement time series

Wolfertstetter, F., Hanrieder, N., Bellmann, P., Ghennioui, A., Wette, J., & Fernandez-Garcia, A. (2020, December). Parallel soiling measurements for 4 mirror samples during outdoor exposure with TraCS. In *AIP Conference Proceedings* (Vol. 2303, No. 1, p. 100009). AIP Publishing LLC.

Glass tube transmission measurement T-TraCS

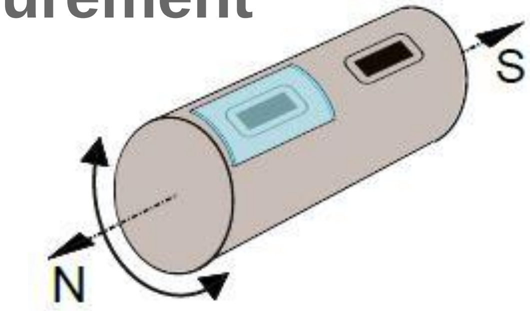

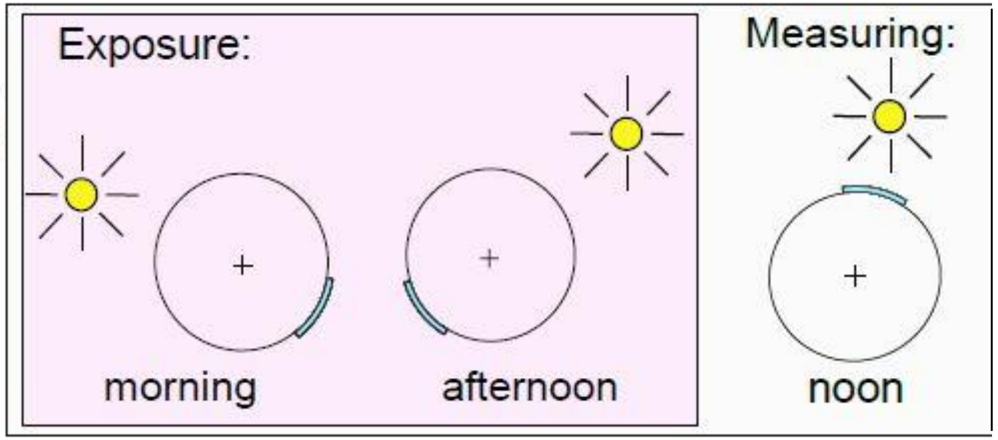

- Similar measurement principle as TraCS applied to soiling of absorber tubes
- Transmission τ is ratio of pyranometer signals I

$$\tau = \frac{I_{\text{glass}}}{I_0}$$

- Cleanliness: $$\xi = \frac{\tau_{\text{soiled}}}{\tau_{\text{clean}}},$$

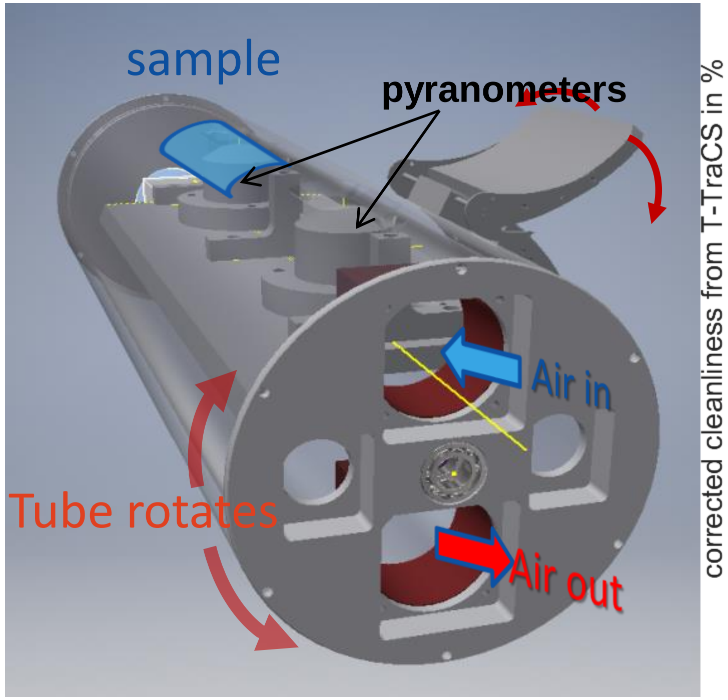

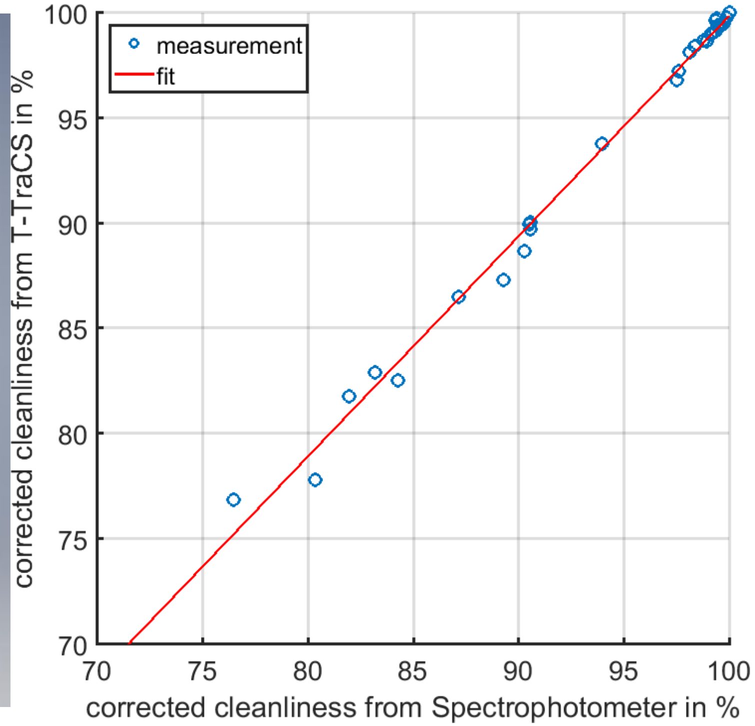

Wolfertstetter, F., Wilbert, S., Bellmann, P., Rodriguez, S. G., Navarro, T. R., Keller, L., & Fernandez-Garcia, A. (2020, December). T-TraCS–An automated method to measure soiling losses at parabolic trough receiver tubes. In *AIP Conference Proceedings* (Vol. 2303, No. 1, p. 210006). AIP Publishing LLC.

Automatic field sensors

- Scattering based sensors to detect the amount of soiling deposited on a surface
  - Prototype status for CSP
  - More common in PV: DustIQ, MARS
- Advantages:
  - Automatic, no maintenance
  - High time resolution
- Disadvantages:
  - Soiling measured on a separate surface
  - Scattering is dependent on dust particles' optical properties

Tekniker CSP soiling sensor

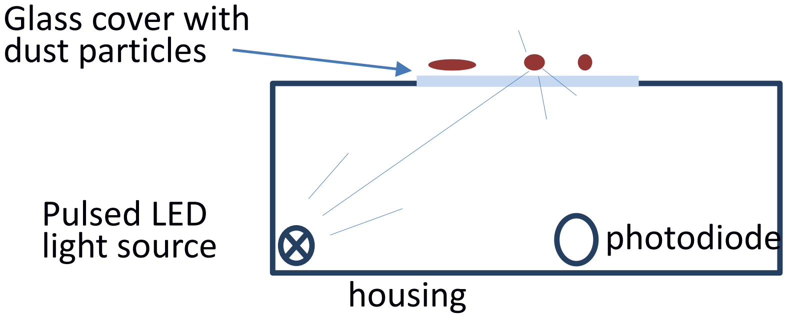

DustIQ PV soiling sensor

MARS PV soiling sensor

QFly soiling measurement principle

- Dirt on windows can be seen with the naked eye
- Reason: Incident light is scattered at soiling layer
- Scattering can be seen as “brighter areas” in front of background
- **Quantitative soiling measurement possible from drone images?**

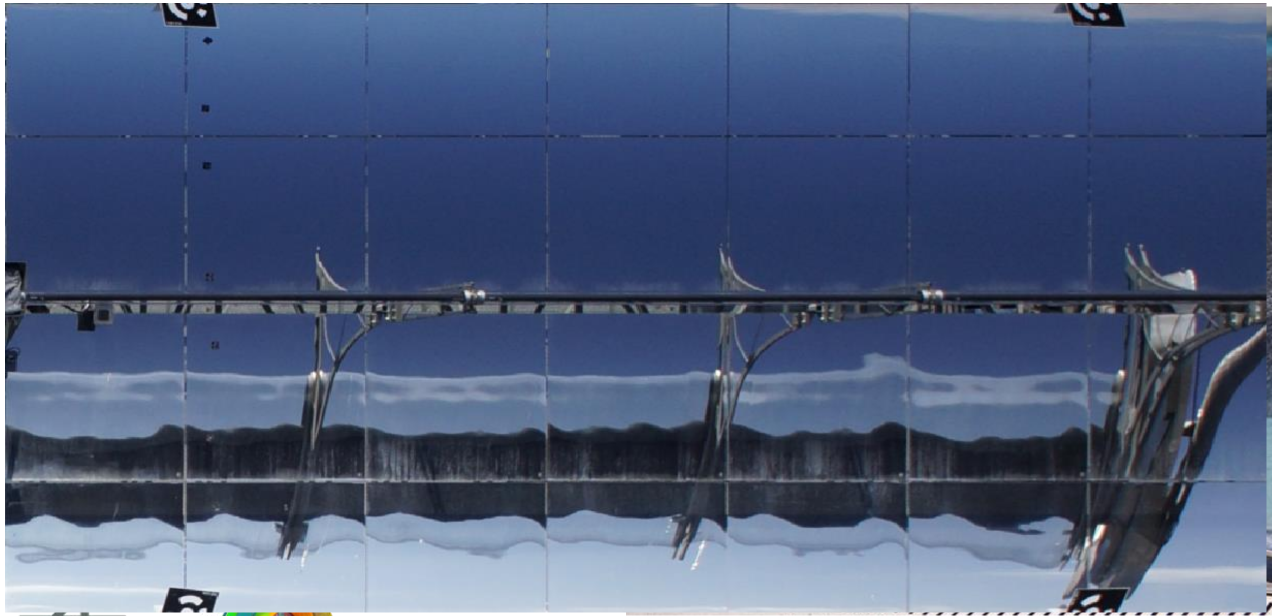

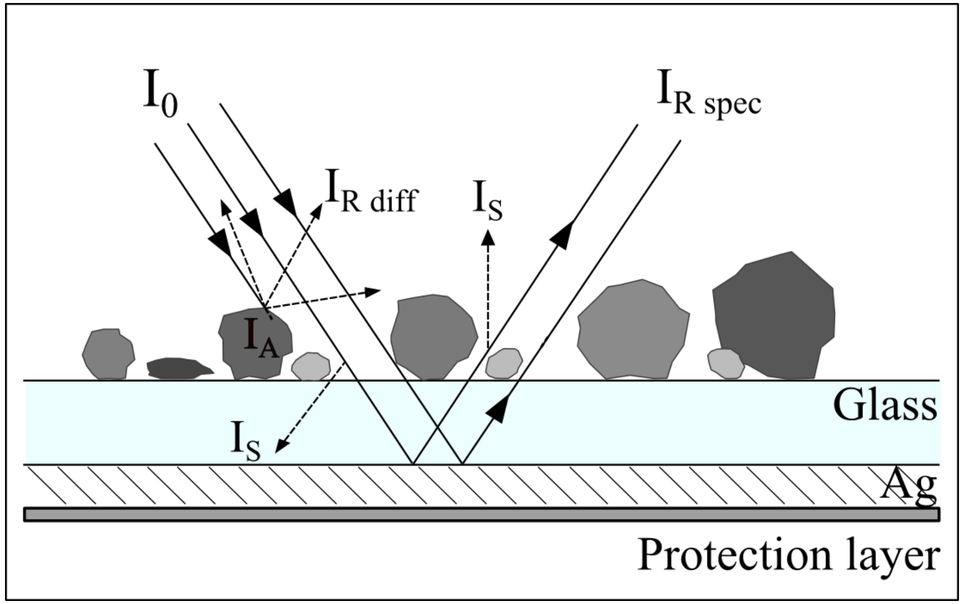

Wolfertstetter, F., Fonk, R., Prahl, C., Röger, M., Wilbert, S., & Fernández-Reche, J. (2020, December). Airborne soiling measurements of entire solar fields with Qfly. In *AIP Conference Proceedings* (Vol. 2303, No. 1, p. 100008). AIP Publishing LLC.

Soiling measurement: RGB contributions

Contributions to Camera RGB signal

- **Scattering** – solar irradiance scattered by particles in the direction of the camera; depending on:
  - Viewing angle of camera
  - Solar spectrum
  - Particle size distribution and optical properties
- **Background**-contribution
- **Camera**-corrections taken into account:
  - RAW image format
  - Gamma correction
  - Color-balancing
  - Camera chip signature (Vignetting effect)

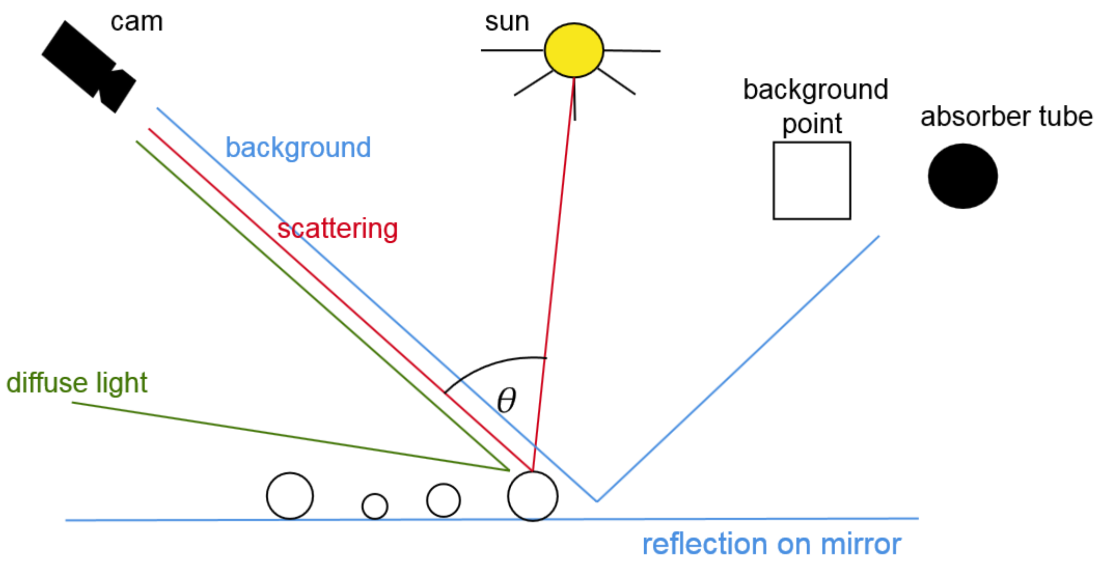

Measurement campaign

- UAV flight on a sunny day
- Collector left to soil for weeks before
- Reference measurements taken with handheld reflectometer after flight
- Locations of measurements digitalized

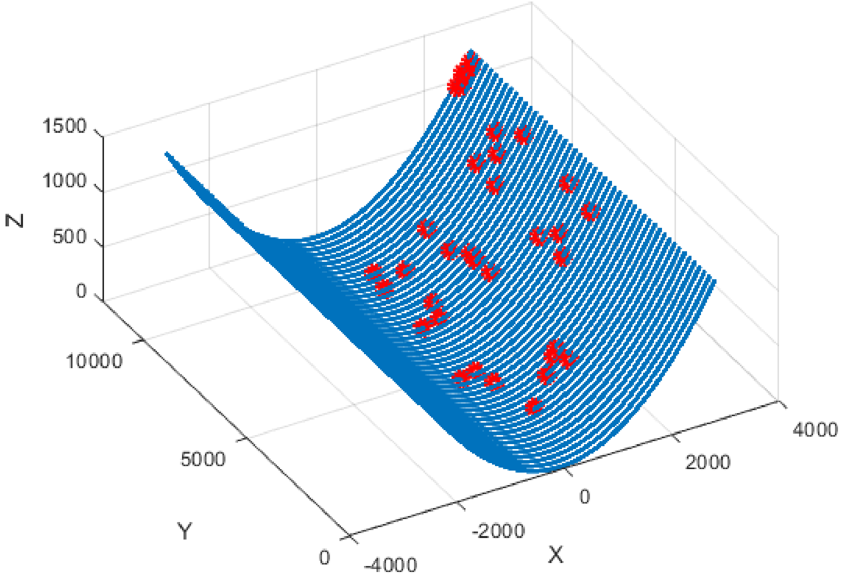

Collector geometry with measurement points

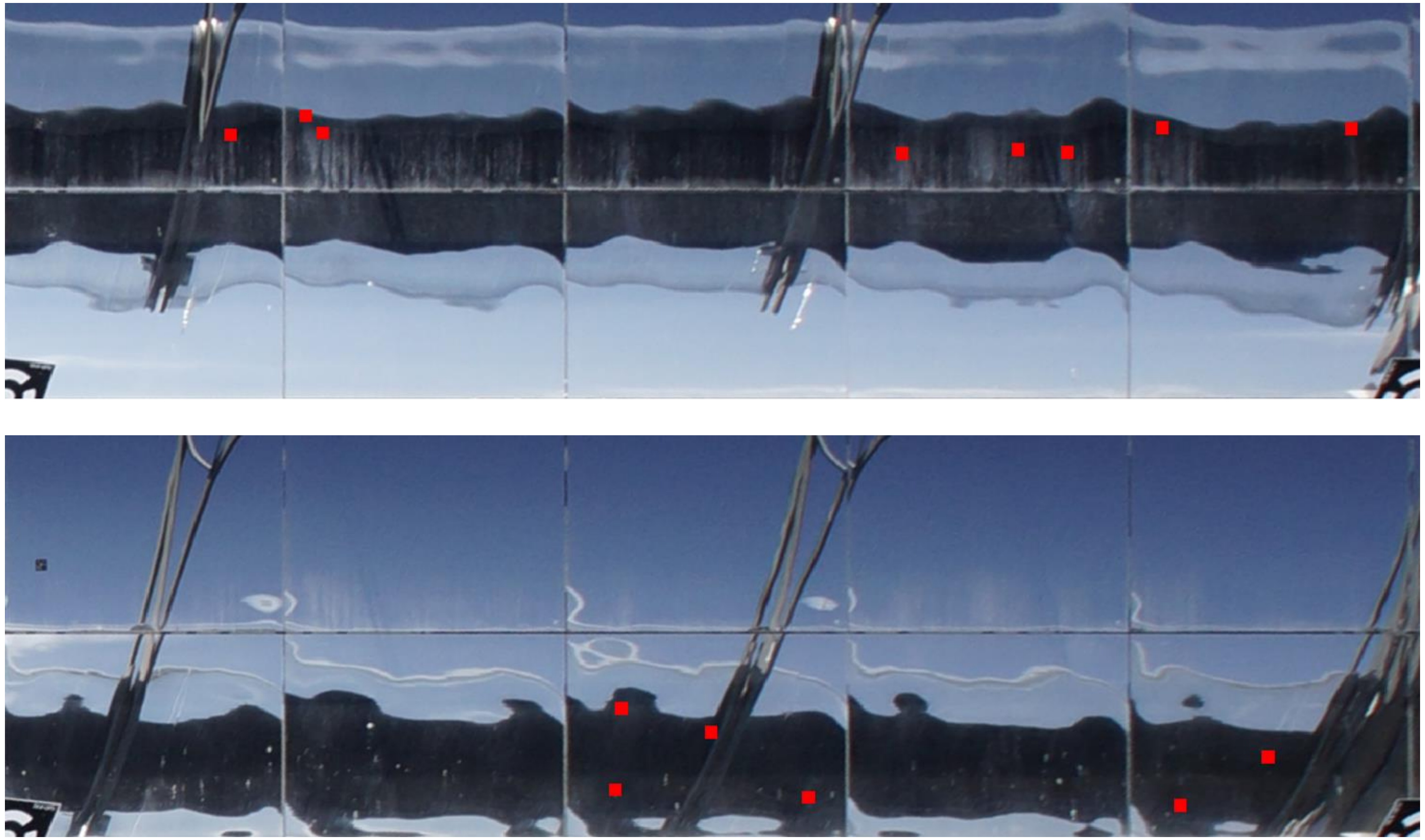

Two orthogonalized images with measurement points in red at tube reflection

Results

- Correlation improves significantly with the scattering correction
- Promising results
- Currently working on refinement of the method

Uncorrected grey values

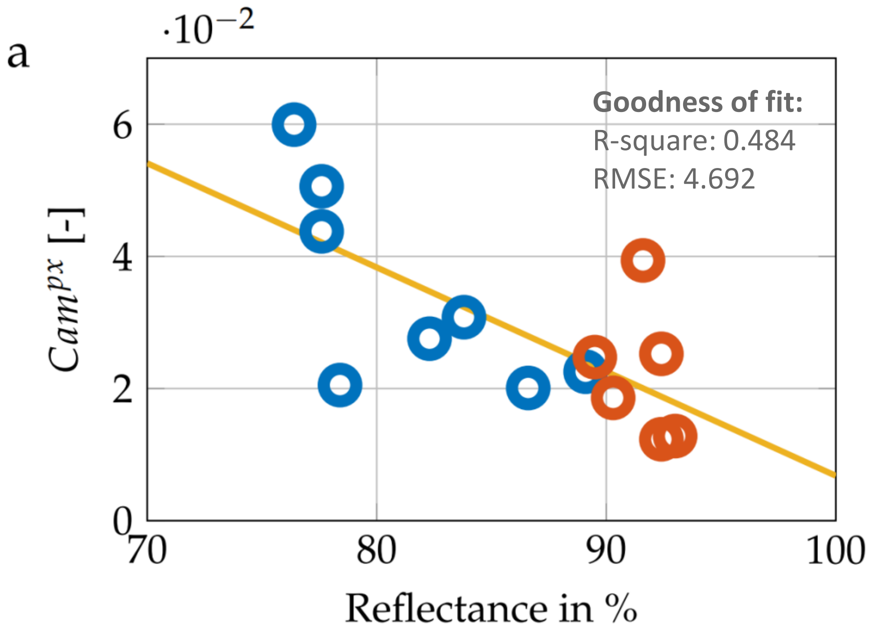

Scattering corrected grey values

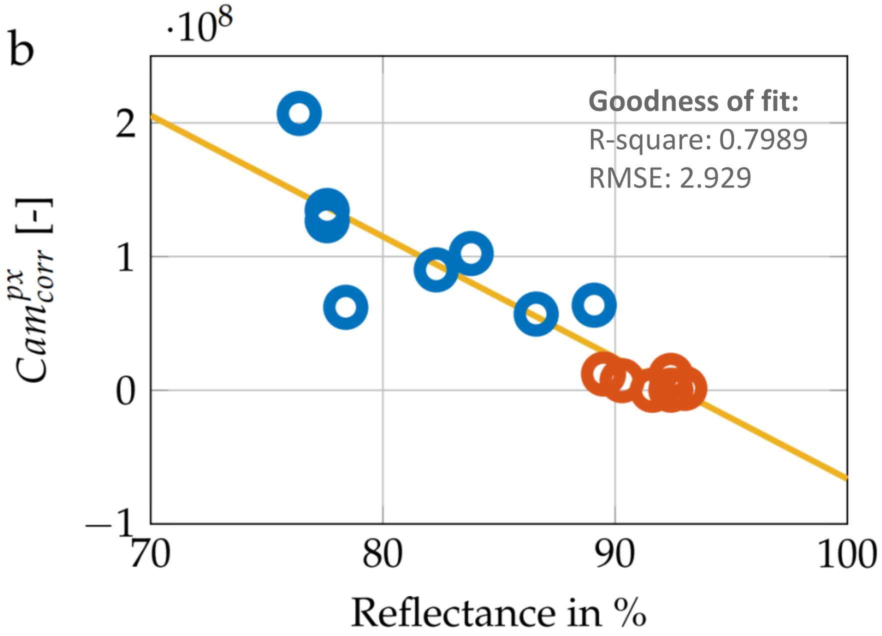

Wolfertstetter, F., Fonk, R., Prahl, C., Röger, M., Wilbert, S., & Fernández-Reche, J. (2020, December). Airborne soiling measurements of entire solar fields with Qfly. In *AIP Conference Proceedings* (Vol. 2303, No. 1, p. 100008). AIP Publishing LLC.

Summary soiling measurements

- Many types of measurements exist
- No perfect measurement
- Best method depends on use case:
    - Every field has different optical properties
- Currently, handheld reflectometers are most commonly used in solar fields
- The first SolarPACES „Soiling reflectance measurement guideline“ will be published very soon here: https://www.solarpaces.org/csp-research-tasks/task-annexes-iea/task-iii-solar-technology-and-advanced-applications/reflectance-measurement-guidelines/
  it summarizes the information given above

So what to do with soiling measurements?

Cleaning optimization: technical and financial inputs

- 50 MW plant with 7.5 h storage
- Water and brush based cleaning vehicles
- Collect cleaning related technical and financial parameters
- Cleaning costs:
    - Labor, water, fuel, depreciation of cleaning vehicles


COURTESY OF ABENGOA

Parameter	**Value**
Nominal turbine power	$49,9MW$
Number of loops in Solar Field	156
Aperture area of solar field	510.000 m^2
Thermal storage	7.5 h
Cooling	water
Planned lifetime	25 years
DNI-yearly sum at PSA	2388 $kWh/m^2/a$
Equity ratio	30 %
Specific operating costs	1.8 $EUR/m^2/a$
Feed-in tariff	0.27 EUR/kWh
Cleaning velocity for one unit	9 loops / shift
Number of personnel per vehicle	1
Cleaning vehicle fuel consumption	6 – 8 l/loop
Cleanliness after cleaning	0.986
Demin. water consumption of cleaning unit	1 m^3/loop
Estimated lifetime of cleaning unit	15 years

Wolfertstetter, F., Wilbert, S., Dersch, J., Dieckmann, S., Pitz-Paal, R., & Ghennioui, A. (2018). Integration of Soiling-Rate Measurements and Cleaning Strategies in Yield Analysis of Parabolic Trough Plants. *Journal of Solar Energy Engineering*, *140*(4), 041008.

Cleaning optimization: policy comparison

- A **reference cleaning strategy** is chosen as a reference point: constant, daily cleaning in one shift with 1 vehicle
- Cleaning policies are compared to reference by **relative profit increase (RPI)**
- Condition based cleaning policies:
    - Vary number of vehicles and cleanliness threshold

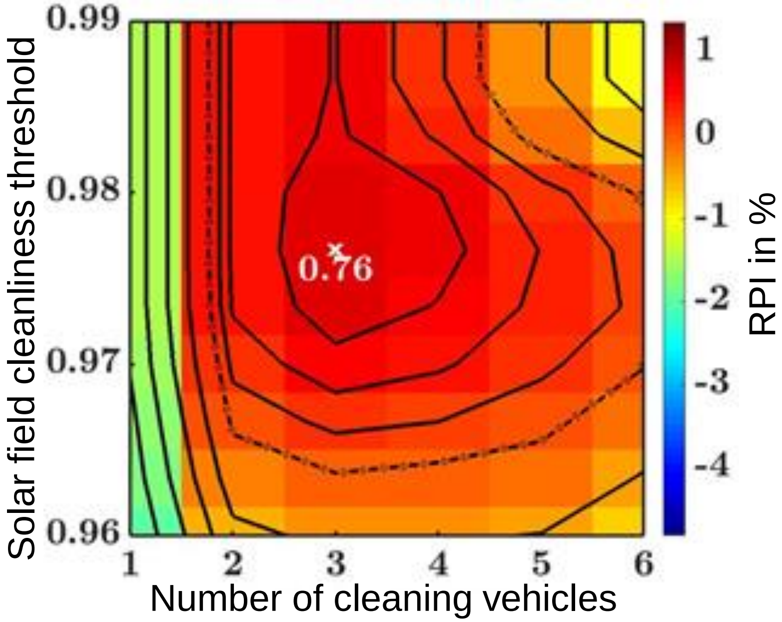

Wolfertstetter, F., Wilbert, S., Dersch, J., Dieckmann, S., Pitz-Paal, R., & Ghennioui, A. (2018). Integration of Soiling-Rate Measurements and Cleaning Strategies in Yield Analysis of Parabolic Trough Plants. *Journal of Solar Energy Engineering*, *140*(4), 041008.

Application of soiling forecast in cleaning policy: results

- Reinforcement learning strategy nearly doubles the RPI of the condition based strategy if no forecast is provided
- Reinforcement learning strategies achieve RPI of 1.3 % if no forecast is provided
- RPI of 1.4% with forecast information

- Note: PSA is not a heavy soiling location
- Much higher results are expected for regions with higher dust loads

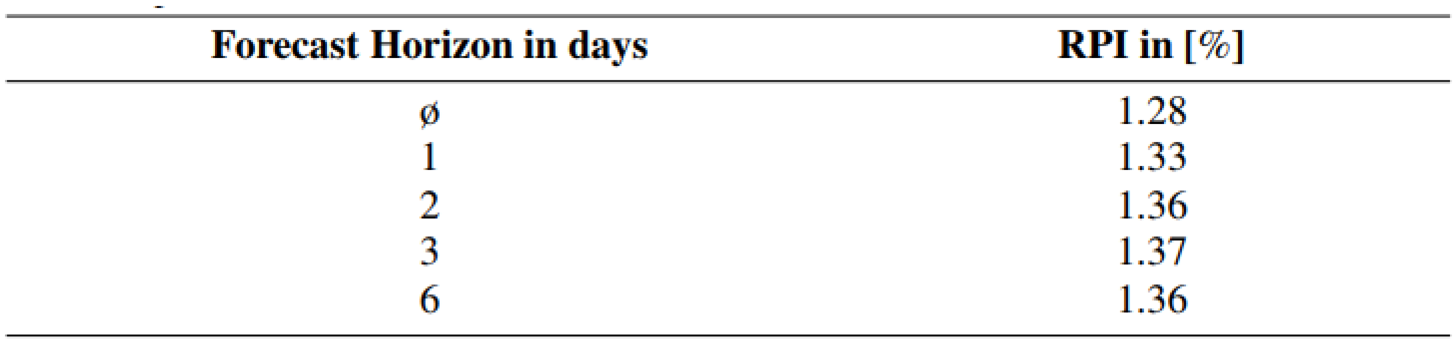

Forecast Horizon in days	**RPI in [%]**
ø	1.28
1	1.33
2	1.36
3	1.37
6	1.36

Terhag, F., Wolfertstetter, F., Wilbert, S., Hirsch, T., & Schaudt, O. (2019, July). Optimization of cleaning strategies based on ANN algorithms assessing the benefit of soiling rate forecasts. In *AIP Conference Proceedings* (Vol. 2126, No. 1, p. 220005). AIP Publishing LLC.

THANK YOU FOR YOUR ATTENTION!
ANY QUESTIONS?

SFERA-III
Solar Facilities for the European Research Area

Solar Facilities for the European Research Area

2nd Training for Industries "Optimization of CST plant output by optical and thermal characterization and target-oriented O&M"
26 – 29 April 2022, Plataforma Solar de Almería, Spain

Infrared measurement principles
Simon Caron (DLR)

NETWORKING

THIS PROJECT HAS RECEIVED FUNDING FROM THE EUROPEAN UNION'S HORIZON 2020 RESEARCH AND INNOVATION PROGRAMME UNDER GRANT AGREEMENT NO **823802**

Outline

- **Infrared Physics**
  - Blackbody radiation
  - Surface emittance
  - Atmosphere transmittance
  - Radiometric chain
- **Applications in CSP industry**
  - Parabolic trough receivers
  - Central receiver systems
- **How to select an IR camera**
- **Calibration and measurement**

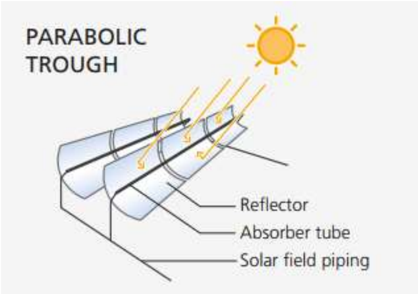

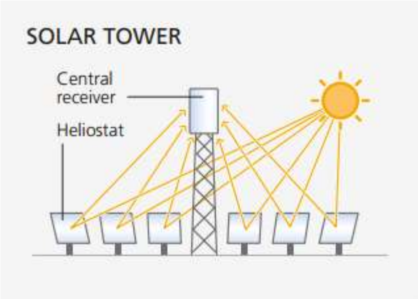

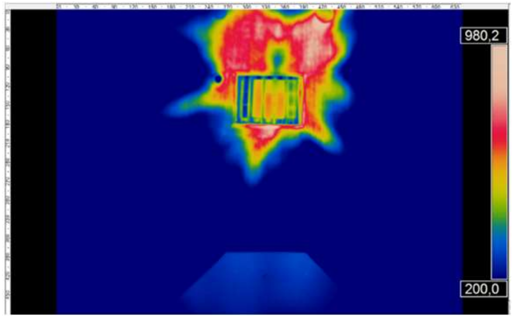

What is infrared radiation ?

- **Electromagnetic radiation spectrum**
  - Any object above 0 K emits thermal radiation.

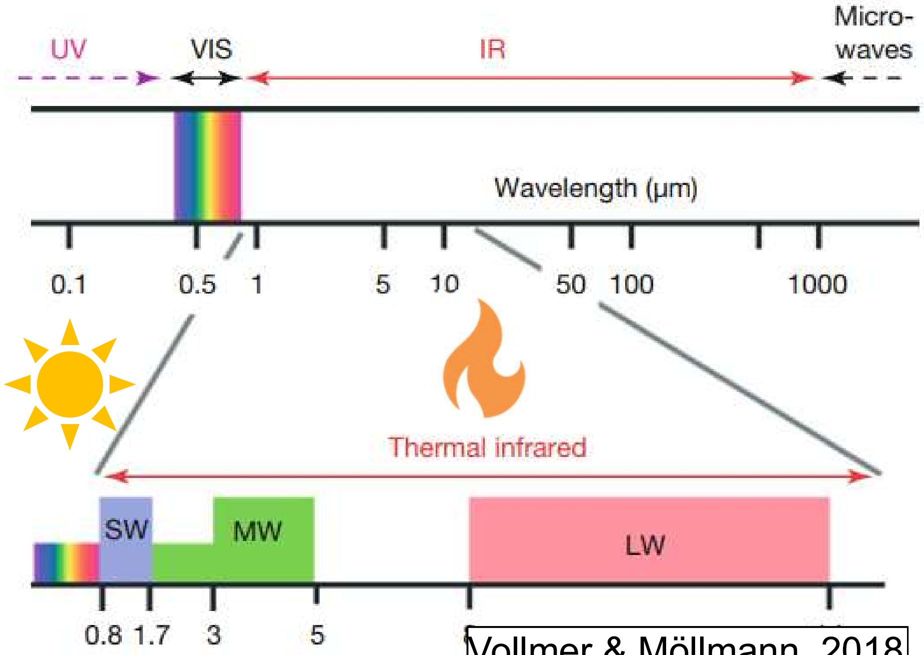

Vollmer & Möllmann, 2018

- **Different IR spectral ranges exist**
  - Shortwave (SW): 0.8 … 2.5 µm
  - Midwave (MW): 1.5 …5.5 µm
  - Longwave (LW): 8 … 14 µm

- There are two main categories of detectors:
  - Photon vs. Thermal

- Photon detectors ~ semiconductor materials InGaAs, InSb, HgCdTe

- Thermal detectors ~ microbolometer arrays (a-Si, VOx with black coating)

What is infrared thermography ?

- **Infrared thermography**
    - Remote sensing/mapping of thermal radiation
    - Thermal radiation is a function of temperature T

    >> Radiometric temperature measurements

- Accurate temperature measurements are important for in situ plan monitoring and control.
    - *Process efficiency* vs. *Material degradation*

- Several factors affect IR measurements:
    - Surface **emittance**
    - Atmospheric **transmittance**
    - Reflections of **solar radiation**
    - Detector **temperature drifts**
    - Optical effects (focus, FOV, etc.)

- IR cameras are available in many formats:

Portable camera
Source: FLIR

UAV camera
Source: FLIR

Industrial camera
Source: InfraTec

Scientific cameras
Source: InfraTec

Infrared Physics

Blackbody radiation (1)

- **Definition of a blackbody**
- A blackbody absorbs all radiation, for any wavelength and direction.
- For a given temperature and wavelength, no surface can emit more radiation than a blackbody.
- Radiation emitted by a blackbody depends on wavelength, it behaves like a Lambertian radiator.

- **Blackbody = radiometric calibration source**
  - Known emissivity (> 99%)
  - Known temperature (PID control)
  - Different geometries (cavity vs. extended)

- Example of blackbody calibration sources

Left: Mikron M305 (Cavity blackbody)
Right: HGH ECN 100 (Extended area blackbody)

Infrared Physics

Blackbody radiation (2)

- Planck, Wien, Stefan-Boltzmann

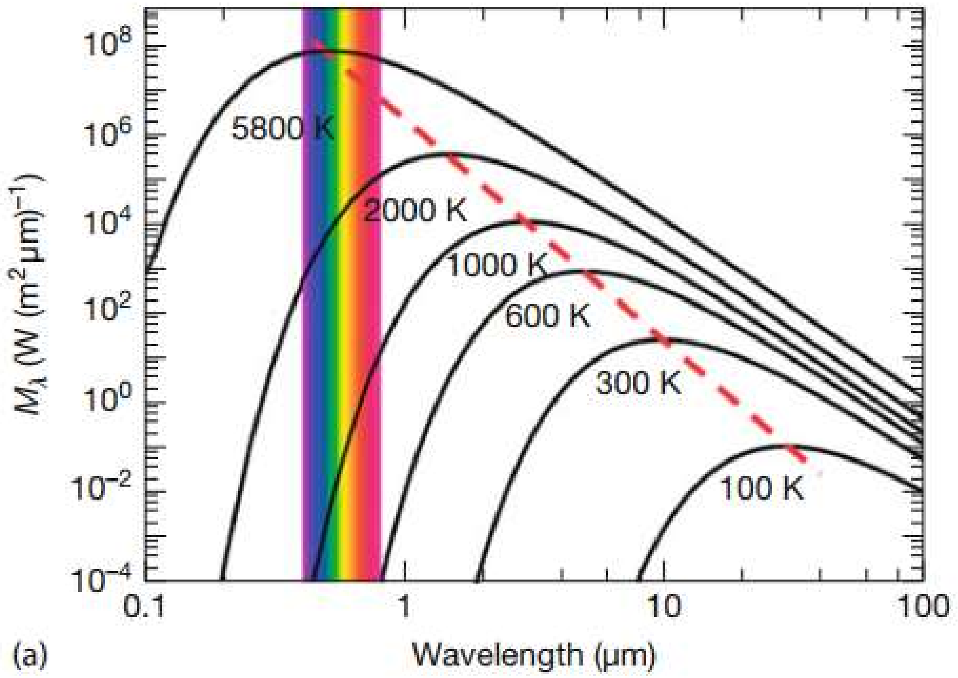

Vollmer & Möllmann, 2018

- Planck radiation law

$$M_\lambda(T)\,\mathrm{d}\lambda = \frac{2\pi hc^2}{\lambda^5}\frac{1}{e^{hc/(\lambda kT)}-1}\,\mathrm{d}\lambda$$

- Wien's displacement law

$$\lambda_{\max}\cdot T = 2897.8\ \mu\mathrm{m\,K} \qquad (1.16)$$

- Stefan-Boltzmann law

The excitance of a blackbody source is calculated from

$$M(T) = \int_0^\infty M_\lambda(T)\,\mathrm{d}\lambda = \int_0^\infty M_\nu(T)\,\mathrm{d}\nu = \sigma T^4 \qquad (1.19)$$

Here, $\sigma = 5.67\cdot 10^{-8}\ \mathrm{W\,m^{-2}\,K^{-4}}$ denotes the Stefan–Boltzmann constant.

Infrared Physics

Surface emissivity

- The directional emissivity of ε (λ,θ,φ,T) of a surface S is defined as a ratio. The ratio compares the radiation emitted by this surface to the radiation emitted by a blackbody at the same temperature.

- $\varepsilon(\lambda, \theta, \varphi, T) = \dfrac{L_S(\lambda,\theta,\varphi,T)}{L_B(\lambda,T)}$

→ Surface radiation

→ Blackbody radiation

No surface can emit more radiation than a blackbody:

- $0 \leq \varepsilon(\lambda, \theta, \varphi, T) \leq 1$

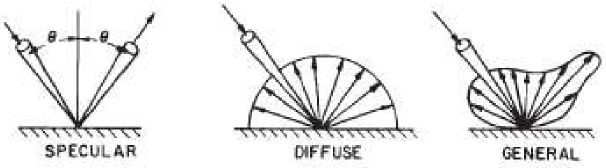

Figure 4.3.1 Reflection from surfaces.

Duffie & Beckman, 2013

- The emissivity is a thermophysical material property. It depends on several factors:
  - Wavelength (grey vs. selective coating)
  - Surface micro-structure (roughness)
  - It may depends on temperature

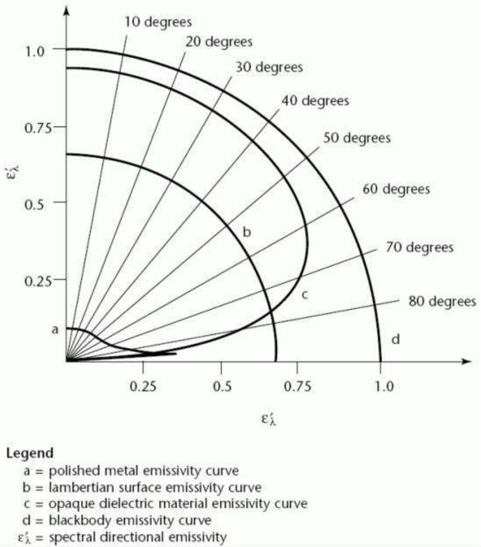

Duffie & Beckman, 2013

Leslie cube

Infrared Physics

Optical properties

- **Optical properties**:
  - Reflectivity: $\rho(\lambda,\theta,\varphi,T)$
  - Transmissivity: $\tau(\lambda,\theta,\varphi,T)$
  - Absorptivity: $\alpha(\lambda,\theta,\varphi,T)$
  - **Kirchhoff's radiation law:**
    - $\alpha(\lambda,\theta,\varphi,T)= \varepsilon(\lambda,\theta,\varphi,T)$
  - **Opaque materials (τ=0):**
    - $\rho(\lambda,\theta,\varphi,T) +\alpha(\lambda,\theta,\varphi,T) =1$;
    - $\varepsilon(\lambda,\theta,\varphi,T) = 1-\rho(\lambda,\theta,\varphi,T)$
  - **Transparent materials ($0<\tau<1$)**:
    - $\rho+\tau+\alpha=1$

- **Measurements of reflectivity @ ambient temp.**
  - Spectrophotometers (@ OPAC)
  - Portable reflectometers (Surface Optics)

Lambda1050 spectrophotometer

Source: OPAC (CIEMAT-DLR)

Portable reflectometers

Source: Surface Optics

Infrared Physics
Surface emittance

- **Example**: Absorber coatings
  - Selective coating vs. black paint

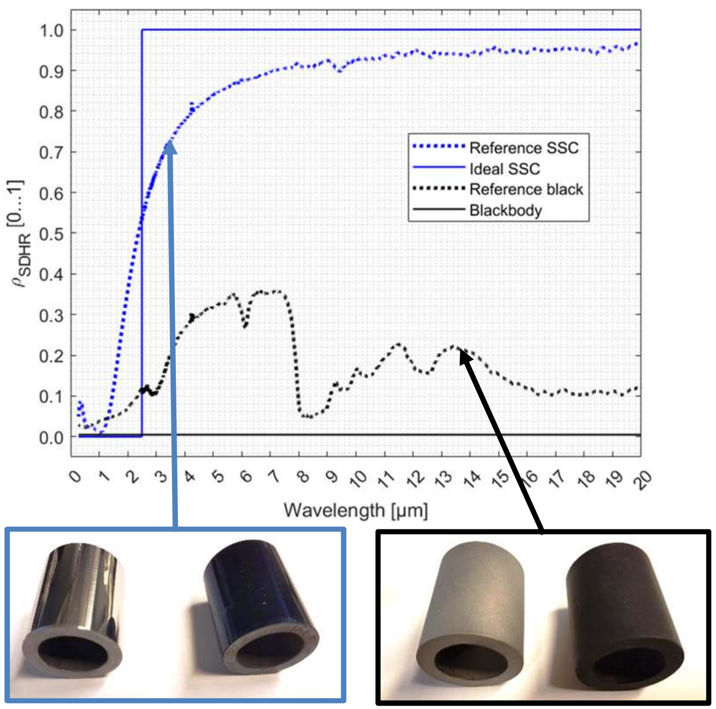

- Thermal emittance calculation (broadband):

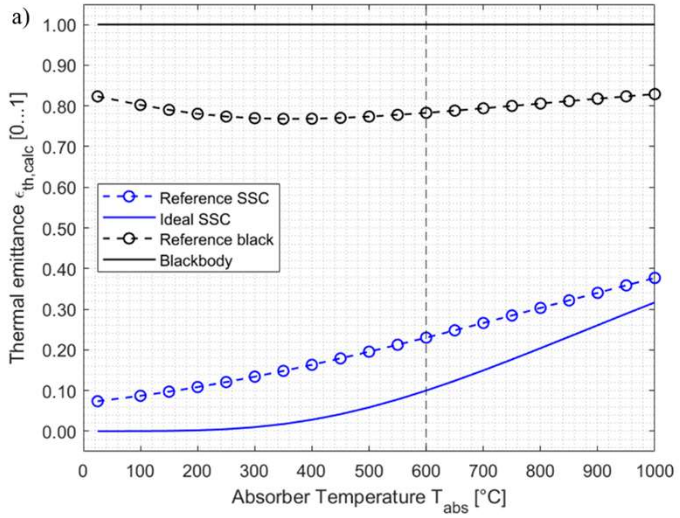

$$\varepsilon_{th,calc}(T_{abs}) = \frac{\int_{\lambda_1}^{\lambda_2}[1-\rho_{SDHR}(\lambda,\theta,T_{amb})]E_{bb}(\lambda,T_{abs})d\lambda}{\int_{\lambda_1}^{\lambda_2}E_{bb}(\lambda,T_{abs})d\lambda}$$

Infrared Physics
Atmospheric transmittance

- MODTRAN® (spectral.com)

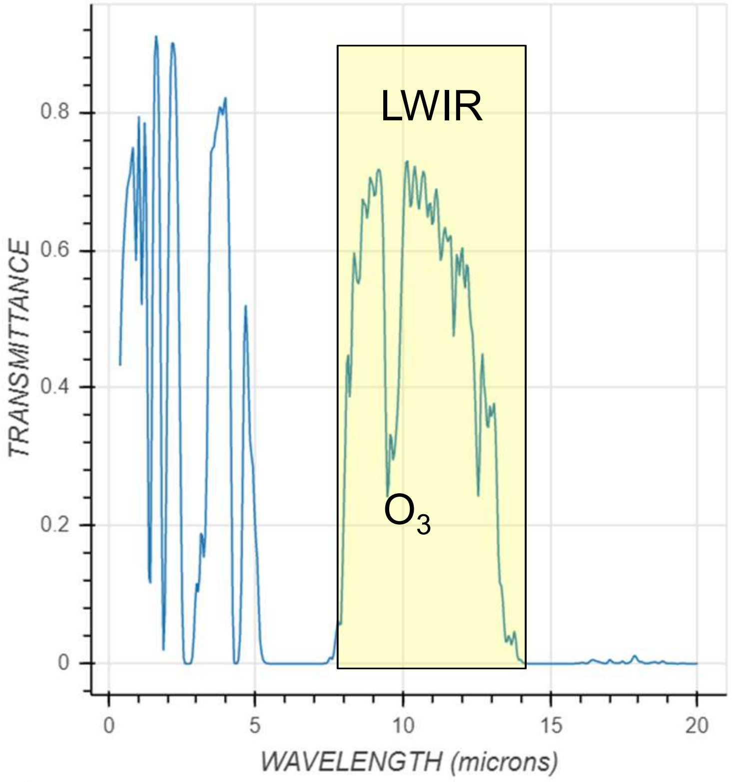

- **Atmospheric Radiative Transfer Codes**
    - Atom and molecule lines catalogs
    - Atmosphere models (vertical profiles)
        - Temperature
        - Water Vapor Column (H_2O)
        - Carbone Dioxide (CO_2), Ozone (O_3)
        - Aerosols and trace gases
        - Distance to measuremenrt object

- Atmospheric transmittance τ can play an important role on the measurement accuracy:
    - Especially at longer ranges
    - Especially for absorption bands

Infrared Physics
Radiometric chain (1)

- Case specific radiometric chain (windows, mirrors)

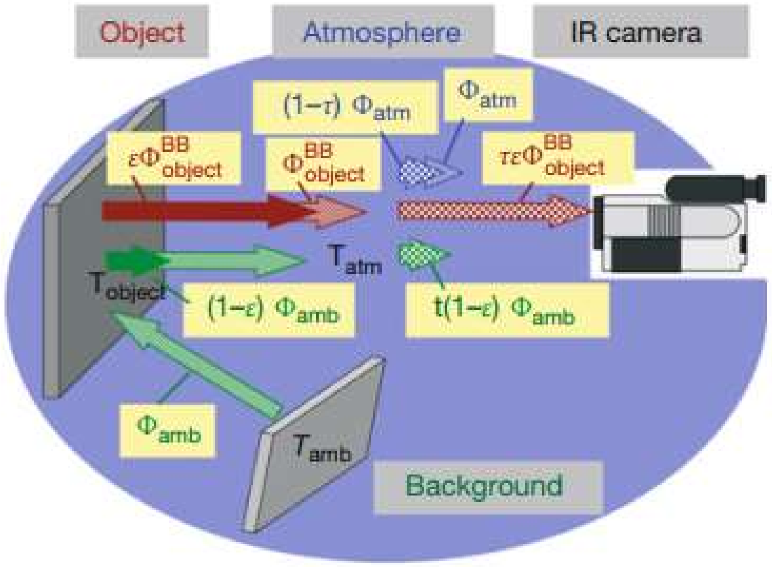

Figure 2.24 Radiometric chain – basic measurement process for opaque objects.

Vollmer & Möllmann, 2018

- „Solar-blind“ temperature measurements
  - Selection of narrow bandpass filters
  - Avoid solar parasitics (background radiation)

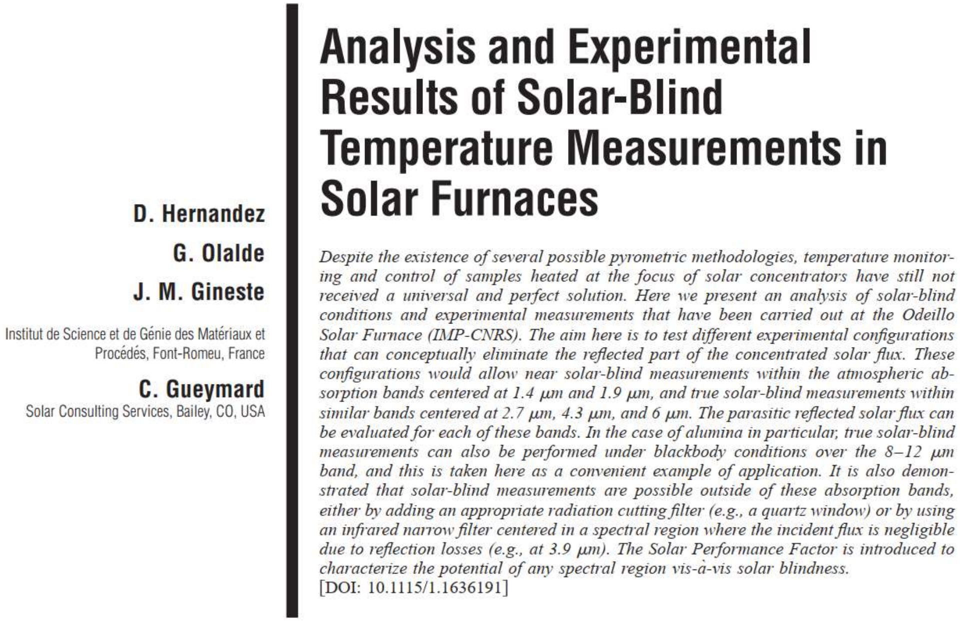

Analysis and Experimental Results of Solar-Blind Temperature Measurements in Solar Furnaces

D. Hernandez
G. Olalde
J. M. Gineste
Institut de Science et de Génie des Matériaux et Procédés, Font-Romeu, France
C. Gueymard
Solar Consulting Services, Bailey, CO, USA

Despite the existence of several possible pyrometric methodologies, temperature monitoring and control of samples heated at the focus of solar concentrators have still not received a universal and perfect solution. Here we present an analysis of solar-blind conditions and experimental measurements that have been carried out at the Odeillo Solar Furnace (IMP-CNRS). The aim here is to test different experimental configurations that can conceptually eliminate the reflected part of the concentrated solar flux. These configurations would allow near solar-blind measurements within the atmospheric absorption bands centered at 1.4 μm and 1.9 μm, and true solar-blind measurements within similar bands centered at 2.7 μm, 4.3 μm, and 6 μm. The parasitic reflected solar flux can be evaluated for each of these bands. In the case of alumina in particular, true solar-blind measurements can also be performed under blackbody conditions over the 8–12 μm band, and this is taken here as a convenient example of application. It is also demonstrated that solar-blind measurements are possible outside of these absorption bands, either by adding an appropriate radiation cutting filter (e.g., a quartz window) or by using an infrared narrow filter centered in a spectral region where the incident flux is negligible due to reflection losses (e.g., at 3.9 μm). The Solar Performance Factor is introduced to characterize the potential of any spectral region vis-à-vis solar blindness.
[DOI: 10.1115/1.1636191]

https://doi.org/10.1115/1.1636191

Infrared Physics

Radiometric chain (2)

- Case specific radiometric chain (windows, mirrors)

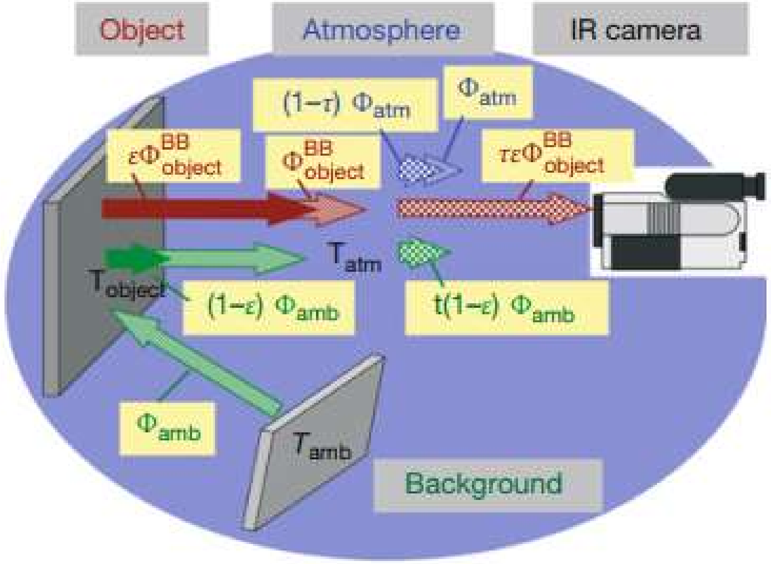

Figure 2.24 Radiometric chain – basic measurement process for opaque objects.

Vollmer & Möllmann, 2018

- **Radiometric terms**:
- Emission:

$$E = \int_{\lambda 1}^{\lambda 2} (\varepsilon(\lambda, T_{obj}).\tau(\lambda, T_{atm}).\phi(\lambda, T_{obj}).S(\lambda).d\lambda$$

- Reflection:

$$R = \int_{\lambda 1}^{\lambda 2} ([1-\varepsilon(\lambda, T_{obj})].\tau(\lambda, T_{atm}).\phi(\lambda, T_{amb}).S(\lambda).d\lambda$$

- Atmosphere:

$$A = \int_{\lambda 1}^{\lambda 2} [1-(\tau(\lambda, T_{atm})].\phi(\lambda, T_{atm}).S(\lambda).d\lambda$$

Radiometric balance:

Signal = **E**+**R**+A

Note 1: S is the camera response.

Note 2: The camera detector housing may also contribute to the radiometric balance.

Infrared Physics

Radiometric chain (3)

- Case specific radiometric chain (windows, mirrors)

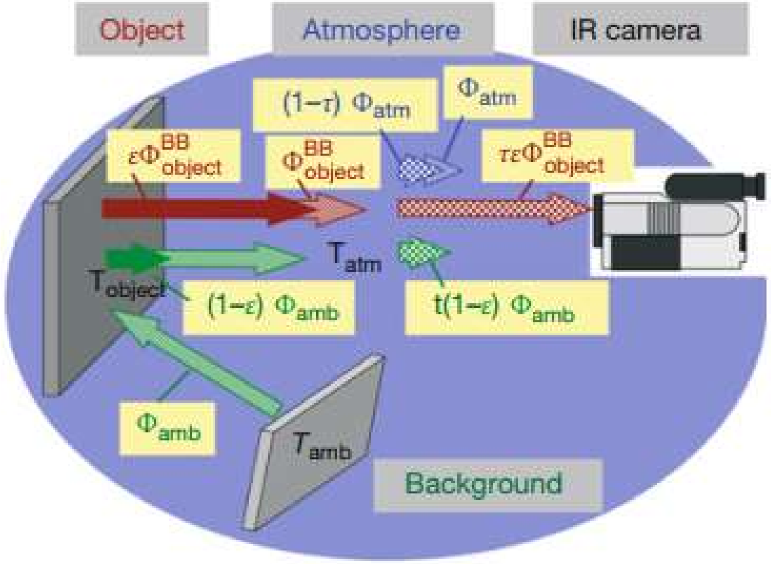

Figure 2.24 Radiometric chain – basic measurement process for opaque objects.

Vollmer & Möllmann, 2018

- **Lumped form:**

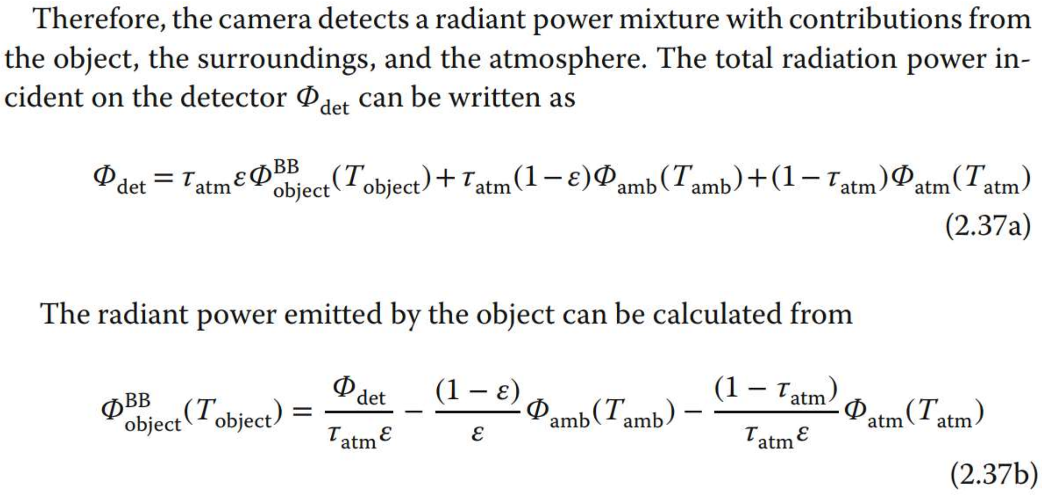

Therefore, the camera detects a radiant power mixture with contributions from the object, the surroundings, and the atmosphere. The total radiation power incident on the detector Φ_{det} can be written as

$$\Phi_{\text{det}} = \tau_{\text{atm}}\varepsilon\Phi^{\text{BB}}_{\text{object}}(T_{\text{object}}) + \tau_{\text{atm}}(1-\varepsilon)\Phi_{\text{amb}}(T_{\text{amb}}) + (1-\tau_{\text{atm}})\Phi_{\text{atm}}(T_{\text{atm}}) \tag{2.37a}$$

The radiant power emitted by the object can be calculated from

$$\Phi^{\text{BB}}_{\text{object}}(T_{\text{object}}) = \frac{\Phi_{\text{det}}}{\tau_{\text{atm}}\varepsilon} - \frac{(1-\varepsilon)}{\varepsilon}\Phi_{\text{amb}}(T_{\text{amb}}) - \frac{(1-\tau_{\text{atm}})}{\tau_{\text{atm}}\varepsilon}\Phi_{\text{atm}}(T_{\text{atm}}) \tag{2.37b}$$

Vollmer & Möllmann, 2018

Applications in CSP industry

Parabolic trough receivers

- State of the art: UAV based inspection
- Measurement objects: Glass envelope
- Camera type: LWIR, uncooled bolometer

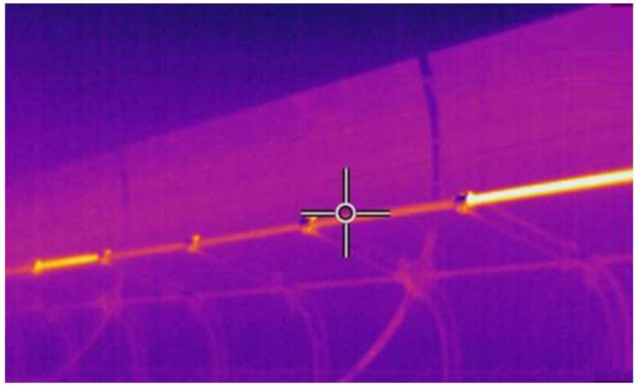

Fig. 8. Thermocamera image from the receiver monitoring.

https://doi.org/10.1016/j.solener.2016.09.017

- Field survey of parabolic trough receivers
- Classification in different categories

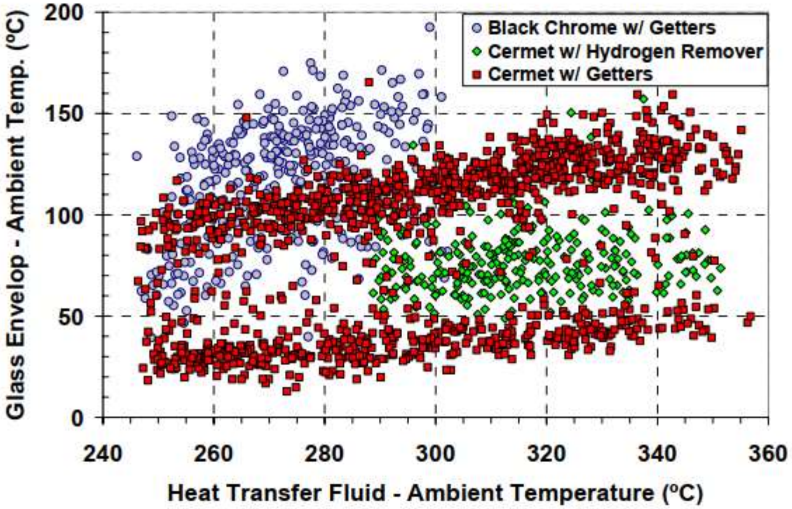

Figure 10. SEGS VI Receiver Survey Results

NREL/CP-550-39459 (2006)

Applications in CSP industry

Central Receiver Systems

- **State of the art**: Ground based monitoring
- InfraTec Solar Power Tower Control (SPTC)
- **Measurement object**: Receiver

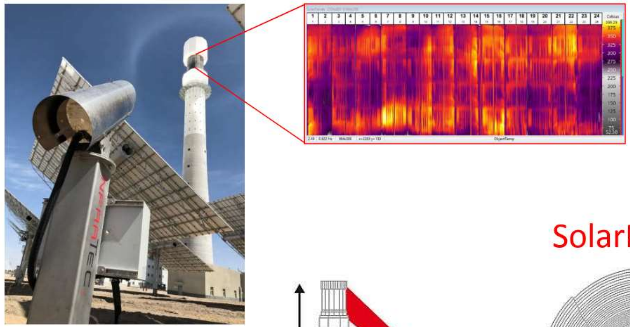

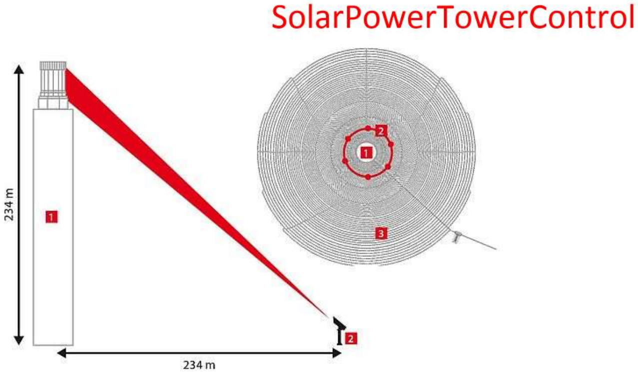

Solar Power Tower Check - SPTC | InfraTec

- The IR camera measurement system is used for real time operation and monitoring in the plant.

- Interaction with flux control (aiming strategy)
- Monitoring of receiver pre-heating with molten salts

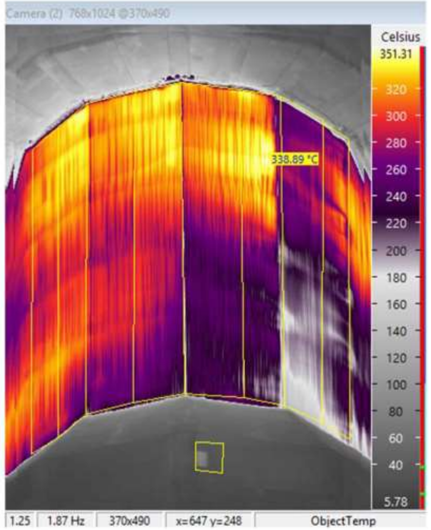

How to select your IR camera

Block diagram:

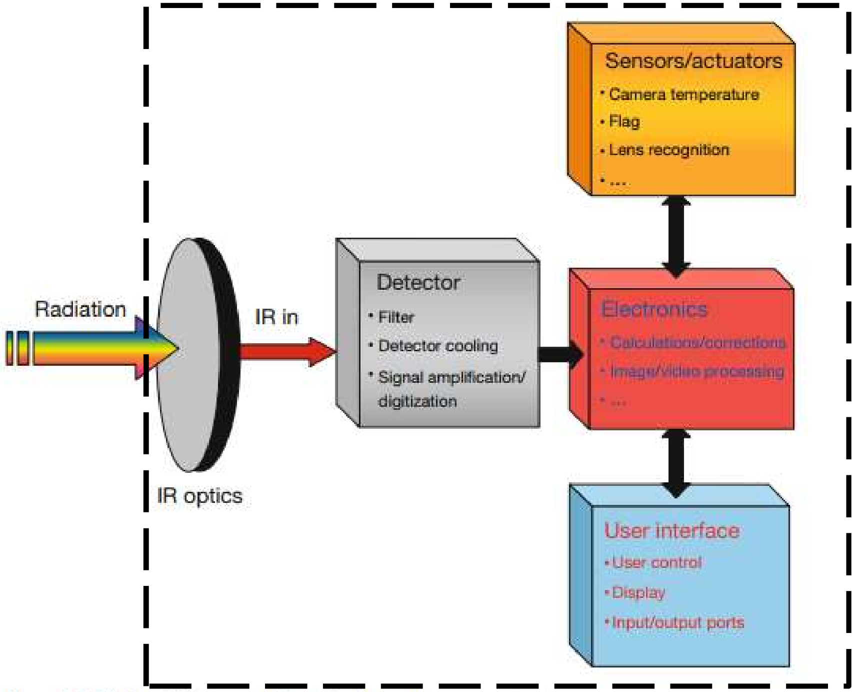

Figure 2.53 Block diagram with main IR camera components.

Vollmer & Möllmann, 2018

- **Sophistical opto-electronical device**
  - Detector
  - Objective lens
  - Optionally, filters
  - Software user interface

- Depending on the specific measurement task, the hardware price may range from 1 to 100 k€, including radiometric calibration.

- **Objective**: The measurement object must be „visible“ and its temperature range must be measured by the camera.

How to select your IR camera

- **Detector specifications**:
  - Wavelength band & filters (SW/MW/LW)
  - Meas. temperature range for your application
  - NETD: Noise Equivalent Temp. Difference (mK)
  - Radiometric accuracy (blackbody calibration)

- **Optical specifications:**
  - IR detector resolution (pixels)
    - 320x256; 640x512; 1280x1024 …
  - Optical lens
    - Aperture f/
    - Focal length (f:mm)
    - FOV (see diagram)
  - Focus type
    - Manual / Motorized
- Note: Each lens must be calibrated separately.

- **Electronics**:
  - Image acquisition rate (Hz) for moving objects

- **Image processing**:
  - Non Uniformity Correction (NUC) algorithm

- **Thermal management**:
  - Detector cooling / Housing athermalization

- **Software user interface**:
  - Image format, post-processing options
  - Radiometric corrections (ε,τ)

- **Peripherical components**:
  - Cabling, data transfer
  - Outdoor protection housing

How to select your IR camera

Detector types and spectral responses

- Photon vs. thermal detector

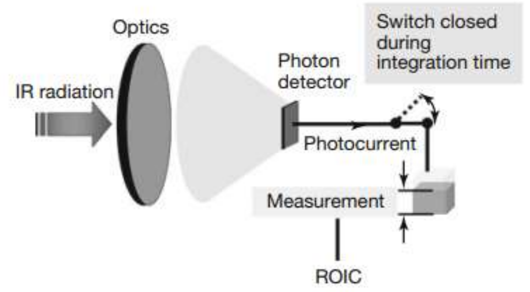

Figure 2.67 Signal generation process and signal readout in a photon detector camera.

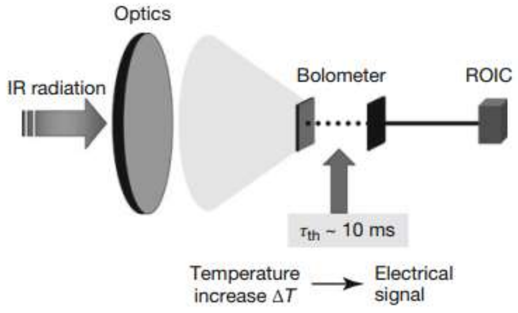

Figure 2.66 Signal generation process and signal readout in a bolometer camera (dotted line illustrates the time delay of bolometer temperature increase with τ_{th}).

Vollmer & Möllmann, 2018

- Spectral response

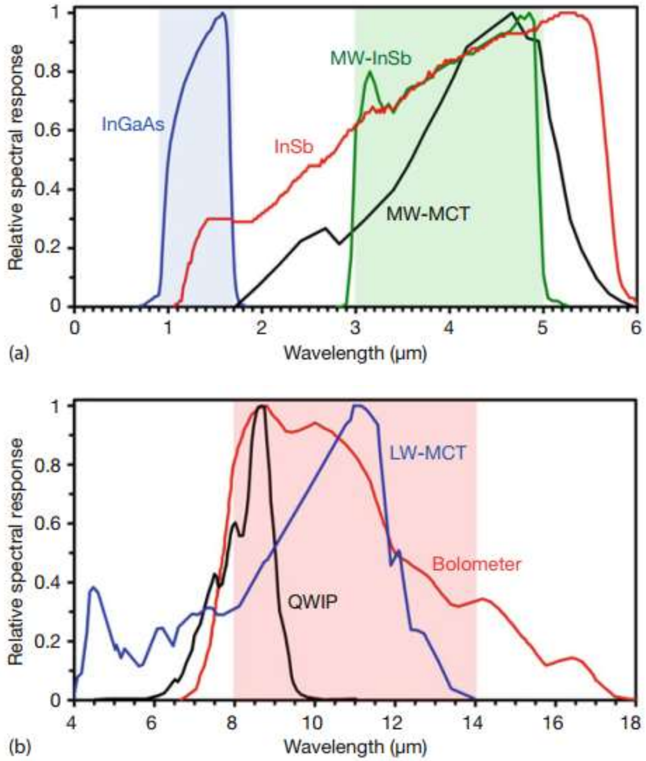

Vollmer & Möllmann, 2018

How to select your IR camera
Optical resolution

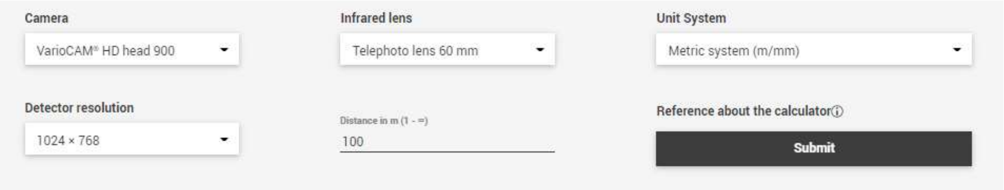

Camera: VarioCAM® HD head 900

Infrared lens: Telephoto lens 60 mm

Unit System: Metric system (m/mm)

Detector resolution: 1024 × 768

Distance in m (1 - ∞): 100

- IFOV: Instant Field of View
- MFOV: Measurement Field of View

[Use the field of view calculator from InfraTec | FOV calculator (infratec-infrared.com)]

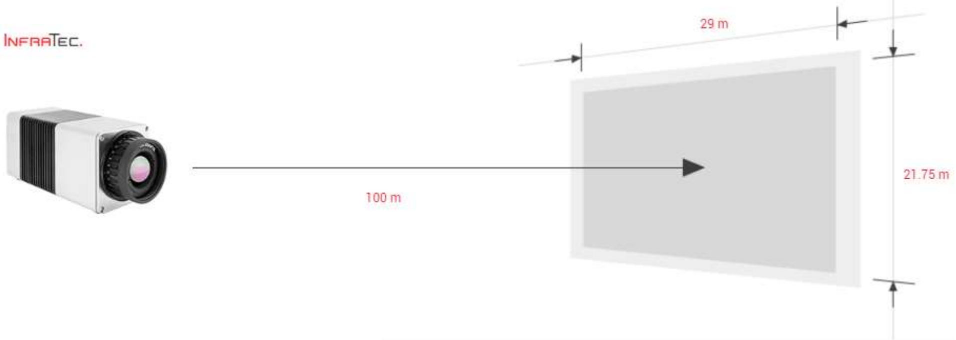

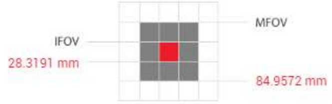

Calculated field of view	Value
Width	29 m
Height	21.75 m
Pixel grid / IFOV	28.3191 mm
Pixel grid with opto-mechanical MicroScan	14.1595 mm
MFOV	84.9572 mm

Calibration and measurement

Selecting a blackbody source

- **Important specifications**:
    - Temperature range + uncertainty
    - Heated emitter shape + aperture diameter
    - Standard Calibration method
    - Emissivity in Calibration Spectral Range
    - Control unit (PID), Warm-up time, etc.
    - Dimensions, Weight, Power supply

[Temperature Calibration Sources - Highly accurate calibration equipment for thermal imaging cameras, radiometers, heatflux, and spectrographic measurement systems (advancedenergy.com)]

Mid Temperature Versions up to 1150°C (2102°F)

Type	M300	M305	M360
Temperature Ranges	200 to 1150°C (392 to 2102°F)	100 to 1000°C (212 to 1832°F)	50 to 1100°C (122 to 2012°F)
Benefits	Medium calibration source with high emissivity for calibration indipendent of the wavelength.	Compact design of the M300 with smaller cavity shape and temperature range.	Medium temp. blackbody calibration source with two separate portable modules and a wide temperature range.
Heated Emitter Shape	Spherical	Spherical	Spherical
Standard Calibration Method	Pyrometric	Pyrometric	Pyrometric
Emissivity (ε_{eff}=effective / ε=real)[1] in Calibration Spectral Range[2]	ε_{eff} = 1.00 0.65 to 15 µm	ε_{eff} = 1.00 8 to 14 µm (<230°C); 0.7 to 1.8 µm (>230°C)	ε_{eff} = 1.00 8 to 14 µm (< 230°C); 0.7 to 1.8 µm (> 230°C)
Aperture Diameter	51 mm (2")	25.4 mm (1.0")	25 mm (1")
Temperature Uncertainty	0.25% of reading ±1°C	±0.2% of reading ±1°C	±0.2% of reading ±1°C
Average Warm-up Time	60 min from ambient to 1000°C	~60 min from ambient to 700°C	60 min from ambient to 700°C
Dimensions (H x W x D)	640 mm x 500 mm x 572 mm	270 mm x 430 mm x 370 mm	Cal. Source: 345 mm x 277 mm x 425 mm Controller: 168 mm x 280 mm x 280 mm
Weight	80 kg (175 lb)	25 kg (55 lb)	Cal. source: 17.8 kg (39.3 lb) Controller: 5 kg (10.7 lb)

Calibration and measurement
Performing a blackbody calibration

- **Test procedure**
    - Mount camera incl. housing on a tripod.
    - Position and align camera in front of blackbody aperture. Take into accound the camera resolution and optics to select the distance.

    - Define calibration points
    - Increase temperature gradually and stabilize
    - Record IR image and source temperature

- **Uncertainty budget**
    - [ASTM E2847-14]

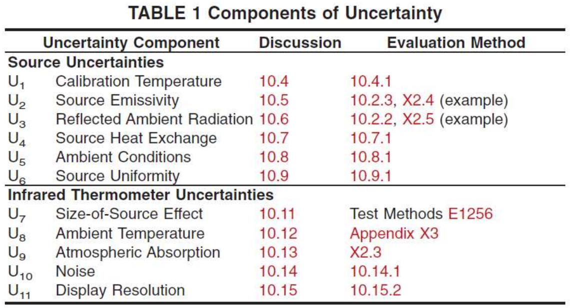

TABLE 1 Components of Uncertainty

Uncertainty Component		Discussion	Evaluation Method
Source Uncertainties			
U_1	Calibration Temperature	10.4	10.4.1
U_2	Source Emissivity	10.5	10.2.3, X2.4 (example)
U_3	Reflected Ambient Radiation	10.6	10.2.2, X2.5 (example)
U_4	Source Heat Exchange	10.7	10.7.1
U_5	Ambient Conditions	10.8	10.8.1
U_6	Source Uniformity	10.9	10.9.1
Infrared Thermometer Uncertainties			
U_7	Size-of-Source Effect	10.11	Test Methods E1256
U_8	Ambient Temperature	10.12	Appendix X3
U_9	Atmospheric Absorption	10.13	X2.3
U_{10}	Noise	10.14	10.14.1
U_{11}	Display Resolution	10.15	10.15.2

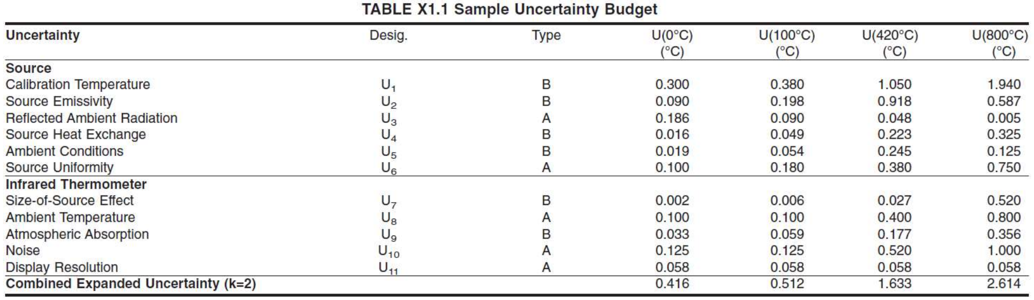

TABLE X1.1 Sample Uncertainty Budget

Uncertainty	Desig.	Type	U(0°C) (°C)	U(100°C) (°C)	U(420°C) (°C)	U(800°C) (°C)
Source						
Calibration Temperature	U_1	B	0.300	0.380	1.050	1.940
Source Emissivity	U_2	B	0.090	0.198	0.918	0.587
Reflected Ambient Radiation	U_3	A	0.186	0.090	0.048	0.005
Source Heat Exchange	U_4	B	0.016	0.049	0.223	0.325
Ambient Conditions	U_5	B	0.019	0.054	0.245	0.125
Source Uniformity	U_6	A	0.100	0.180	0.380	0.750
Infrared Thermometer						
Size-of-Source Effect	U_7	B	0.002	0.006	0.027	0.520
Ambient Temperature	U_8	A	0.100	0.100	0.400	0.800
Atmospheric Absorption	U_9	B	0.033	0.059	0.177	0.356
Noise	U_{10}	A	0.125	0.125	0.520	1.000
Display Resolution	U_{11}	A	0.058	0.058	0.058	0.058
Combined Expanded Uncertainty (k=2)			0.416	0.512	1.633	2.614

Calibration and measurement

Calibration curve S = f(T)

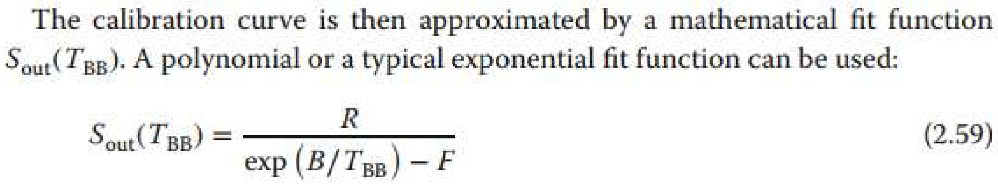

The calibration curve is then approximated by a mathematical fit function $S_{\mathrm{out}}(T_{\mathrm{BB}})$. A polynomial or a typical exponential fit function can be used:

$$S_{\mathrm{out}}(T_{\mathrm{BB}}) = \frac{R}{\exp\left(B/T_{\mathrm{BB}}\right) - F} \tag{2.59}$$

- R: Response factor
- B: Spectral factor
- F: Form factor

- Knowing the camera signal S_{out}, the blackbody temperature can be extracted:

$$T_{BB} = \frac{B}{\ln[\frac{R}{S_{out}} + F]}$$

- Alternative formulas are available in Sakuma-Hattori function catalog: Sakuma–Hattori equation - Wikipedia

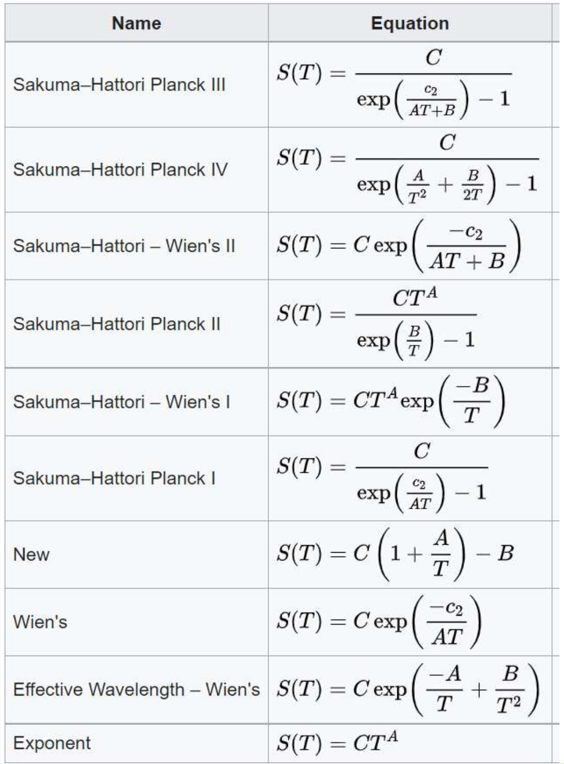

Name	Equation
Sakuma–Hattori Planck III	$S(T) = \frac{C}{\exp\left(\frac{c_2}{AT+B}\right) - 1}$
Sakuma–Hattori Planck IV	$S(T) = \frac{C}{\exp\left(\frac{A}{T^2} + \frac{B}{2T}\right) - 1}$
Sakuma–Hattori – Wien's II	$S(T) = C\exp\left(\frac{-c_2}{AT+B}\right)$
Sakuma–Hattori Planck II	$S(T) = \frac{CT^A}{\exp\left(\frac{B}{T}\right) - 1}$
Sakuma–Hattori – Wien's I	$S(T) = CT^A\exp\left(\frac{-B}{T}\right)$
Sakuma–Hattori Planck I	$S(T) = \frac{C}{\exp\left(\frac{c_2}{AT}\right) - 1}$
New	$S(T) = C\left(1 + \frac{A}{T}\right) - B$
Wien's	$S(T) = C\exp\left(\frac{-c_2}{AT}\right)$
Effective Wavelength – Wien's	$S(T) = C\exp\left(\frac{-A}{T} + \frac{B}{T^2}\right)$
Exponent	$S(T) = CT^A$

Calibration and measurement
Measurement

- For the measurement of a real scene, the radiometric balance is used applying the calibration curve on the one hand and defining ε, $\tau_{atm,}$ T_{amb}, T_{atm}.

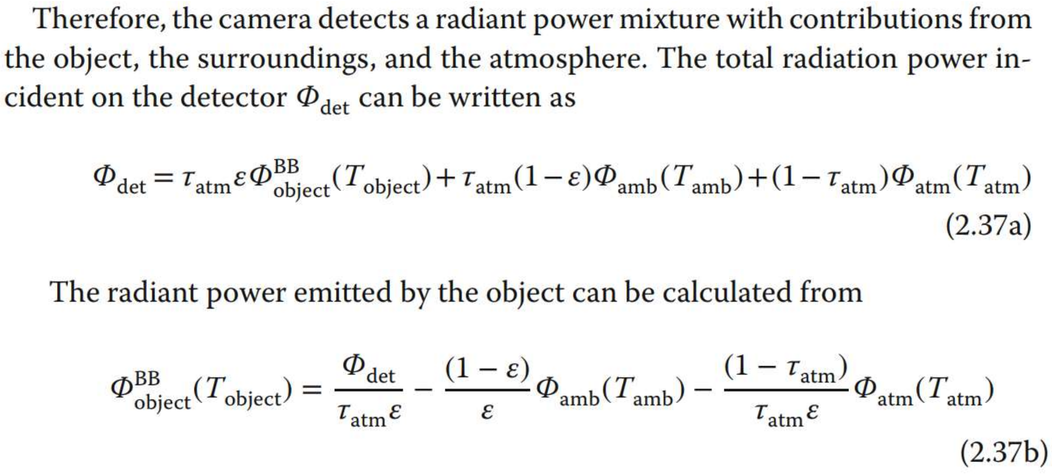

Therefore, the camera detects a radiant power mixture with contributions from the object, the surroundings, and the atmosphere. The total radiation power incident on the detector Φ_{det} can be written as

$$\Phi_{\text{det}} = \tau_{\text{atm}}\varepsilon\Phi^{\text{BB}}_{\text{object}}(T_{\text{object}}) + \tau_{\text{atm}}(1-\varepsilon)\Phi_{\text{amb}}(T_{\text{amb}}) + (1-\tau_{\text{atm}})\Phi_{\text{atm}}(T_{\text{atm}}) \tag{2.37a}$$

The radiant power emitted by the object can be calculated from

$$\Phi^{\text{BB}}_{\text{object}}(T_{\text{object}}) = \frac{\Phi_{\text{det}}}{\tau_{\text{atm}}\varepsilon} - \frac{(1-\varepsilon)}{\varepsilon}\Phi_{\text{amb}}(T_{\text{amb}}) - \frac{(1-\tau_{\text{atm}})}{\tau_{\text{atm}}\varepsilon}\Phi_{\text{atm}}(T_{\text{atm}}) \tag{2.37b}$$

Vollmer & Möllmann, 2018

- These equations can be used further to assess the sensitivity of the temperature measurement w.r.t. to input parameters.

- Calibration curve: S=f(T)

- Reciprocal calibration curve: $T=f^{-1}(S)$

SFERA-III
Solar Facilities for the European Research Area

THANK YOU FOR YOUR ATTENTION!
ANY QUESTIONS?

Reference textbooks

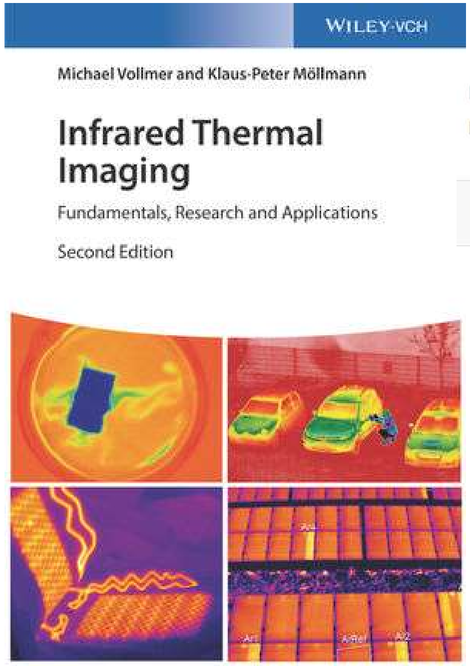

Vollmer & Möllmann, 2018

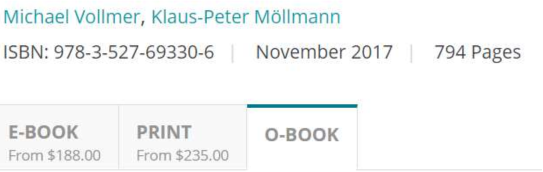

Michael Vollmer, Klaus-Peter Möllmann

ISBN: 978-3-527-69330-6 | November 2017 | 794 Pages

[Infrared Thermal Imaging: Fundamentals, Research and Applications, 2nd Edition | Wiley]

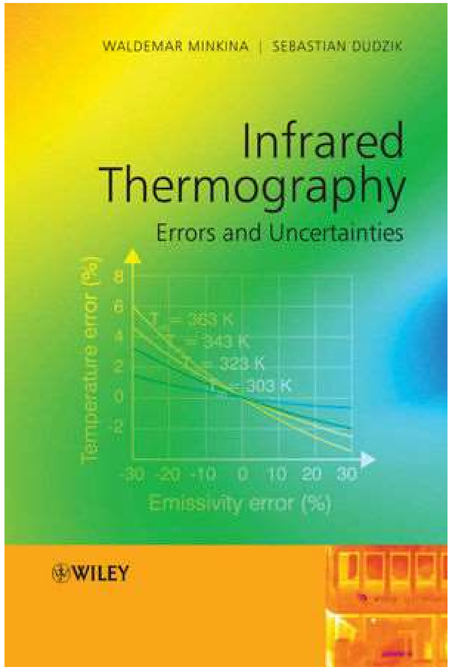

Minkina & Dudzik 2009

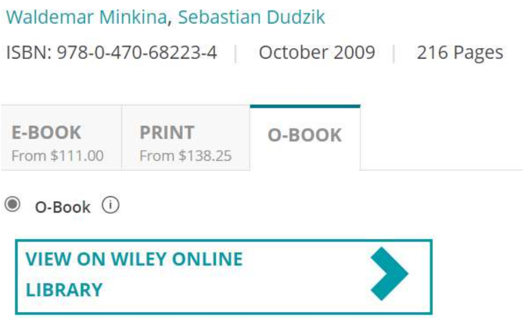

Waldemar Minkina, Sebastian Dudzik

ISBN: 978-0-470-68223-4 | October 2009 | 216 Pages

[Infrared Thermography: Errors and Uncertainties | Wiley]

SFERA-III
Solar Facilities for the European Research Area

Solar Facilities for the European Research Area

2nd Training for Industries "Optimization of CST plant output by optical and thermal characterization and target-oriented O&M"
26 – 29 April 2022, Plataforma Solar de Almería, Spain

Airborne IR measurement on parabolic trough receivers
Niels Algner, DLR

NETWORKING

THIS PROJECT HAS RECEIVED FUNDING FROM THE EUROPEAN UNION'S HORIZON 2020 RESEARCH AND INNOVATION PROGRAMME UNDER GRANT AGREEMENT NO **823802**

Overview

- Motivation
- Choose the right Measurement Equipment
- Calibrate IR and RGB (visual) camera
- Build a digital twin of the solar field
- Programming Flight Routes
- Measurement Procedure
- Outlook

Motivation for drone based thermal measurements of receiver tubes in CSP plants

- 10-40% receiver tubes in significantly bad conditions due to vacuum loss or broken receiver glass envelopes
- **Potential savings of half a million euro annually for a 100 MW CSP plant**
- Old method is time consuming! Operator with IR measurement pistol needs months to measure the whole plant – with 1 measpoint per tube
- fastest IR measurement by drone: 100 MW in 1 h
- IR cameras on drones are constantly improving –
    - cheap, easy to use and available worldwide

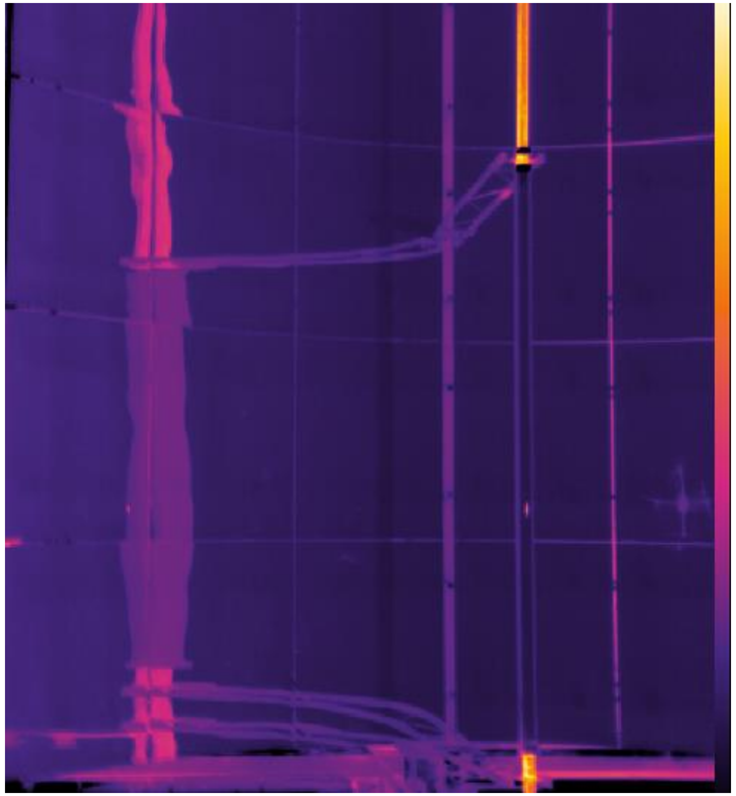

- Right: Broken glass envelope tube and intact receiver tube
- Left: reflection of absorber tubes (enlarges with flight height)

Choose the right Measurement Equipment

- Dual Camera with IR and RGB (visual)
- **Our method: detect the tubes in RGB videoframes (high resolution) and synchronize it with the corresponding IR videoframe to find the exact same spot and tube**
- IR Resolution 640 x 512 px, optional: radiometric (measures absolute temperatures)
- 9 Hz is sufficient, 30 Hz travel & export restrictions due to dual use
- No optical zoom, because camera has to be calibrated. With zoom calibration is not stable
- Development of IR code was done with now outdated small & cheap DJI Mavic 2 Enterprise Dual (120 px)

DJI Mavic Enterprise Advanced

DJI Matrice M30

Autel EVO II Dual 640T

Calibrate IR and RGB (visual) camera

- Both cameras have to be calibrated to avoid lens distortion
- For RGB camera AICON 3D Studio recognizes ~50 unique QLFY targets and calculates a calibration file with all parameters to describe the inner orientation of the camera

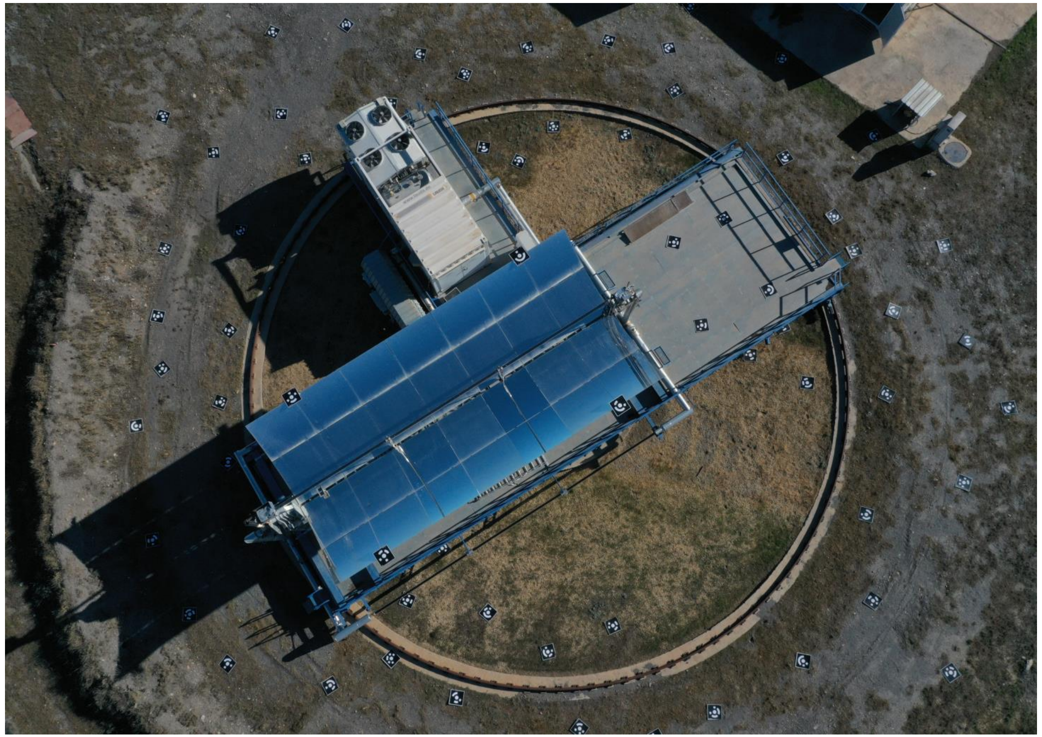

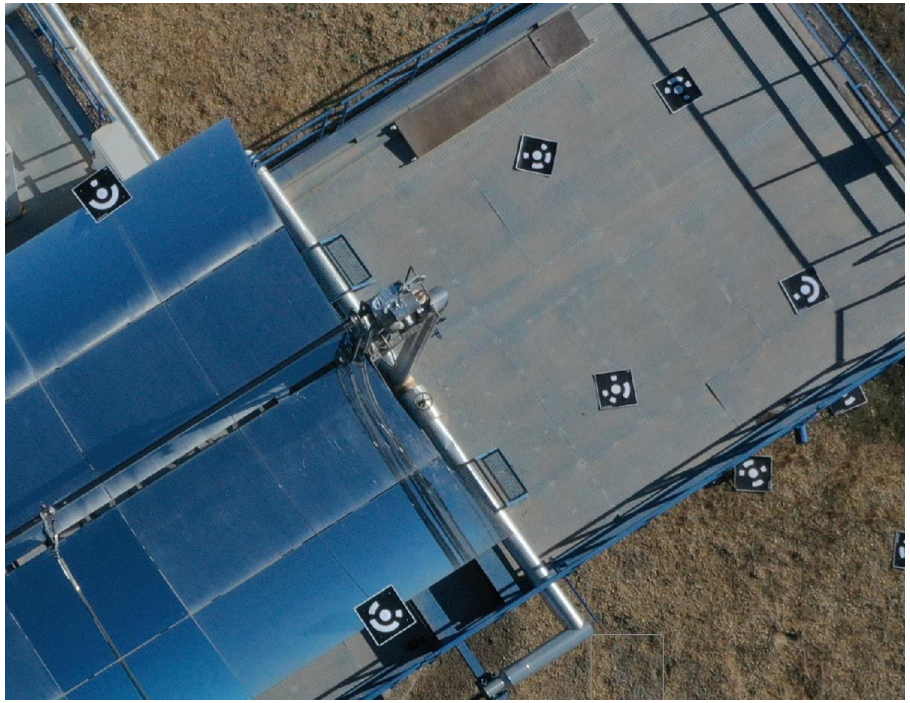

Image shows KONTAS Installation @ Plataforma Solar de Almeria. (Owned by the Spanish research centre CIEMAT.) Source: DLR

Calibrate IR and RGB (visual) camera

Calibrate IR and RGB (visual) camera

- IR calibration is more difficult due to bad resolution and calibration setup (hot circles in cold background)
- 120 px IR camera (left)
- Camera is calibrated by clicking the middle of the circle in both images

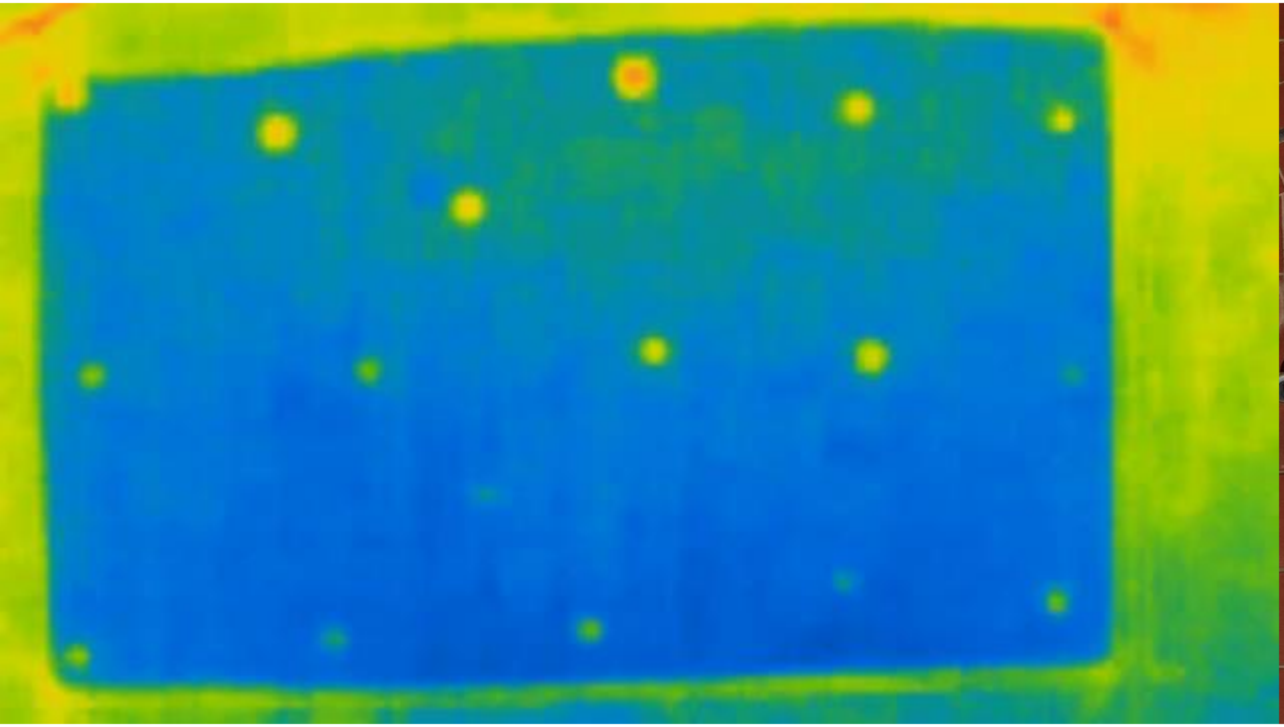

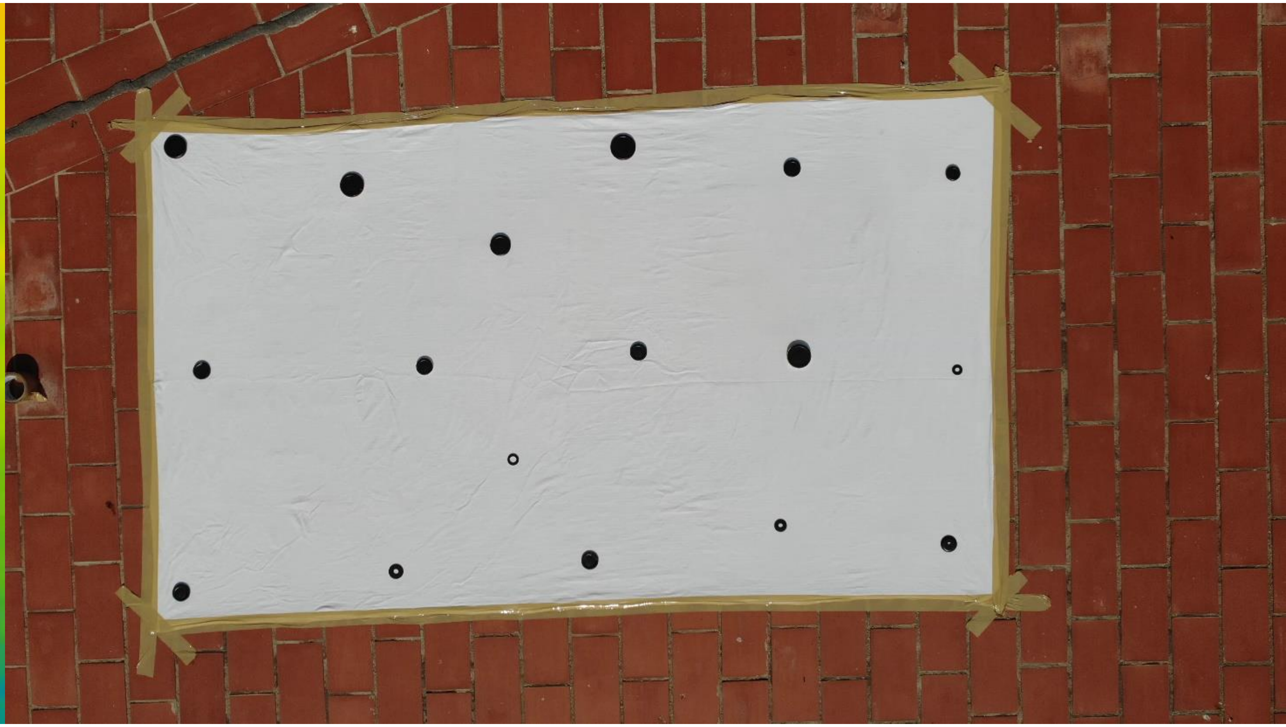

Synchronization of IR and RGB videoframes

- IR and RGB camera have a different framerate
- Synchronization depends on camera manufacturer and can be changed due to software updates (DJI)
- Synchronization has to be better, the higher the flight speed

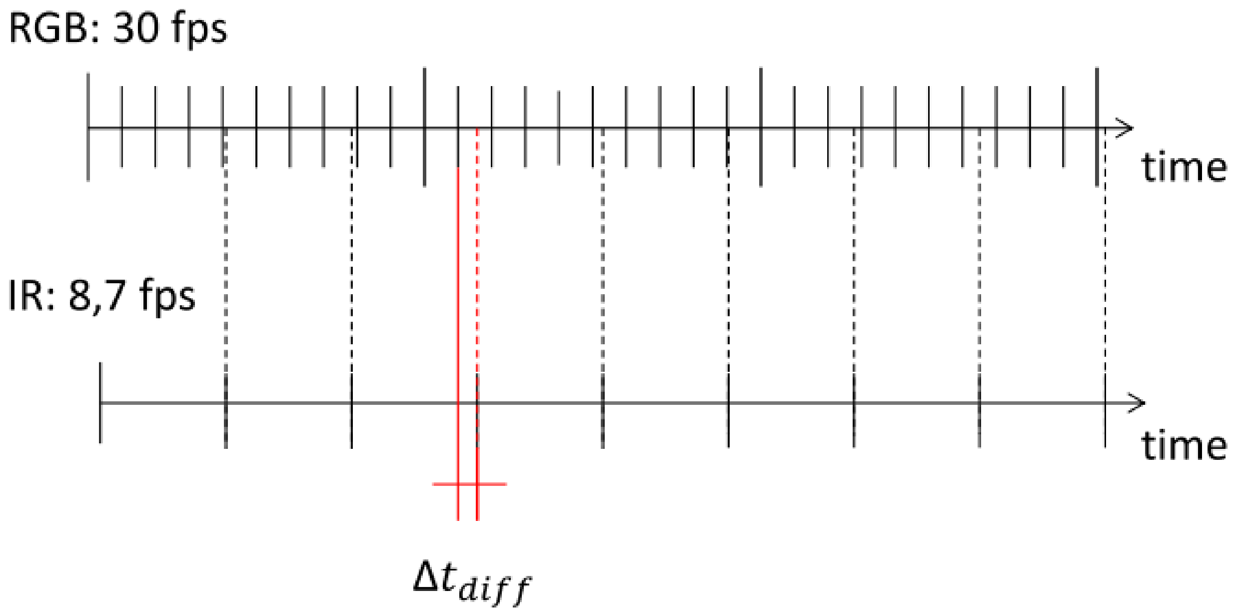

Build a digital twin of the solar field

- To easily program flight routes over areas of interest, evaluate data and visualize result
- Includes:
  - GPS location of every SCA and SCE which has to be measured
  - Every mirror facette corner, every drive pylon included in point cloud where every point has a unique ID
  - May include: No fly zones (power lines, wind fences, salt tanks)
  - Possible to include KKS nomenclature to identify each tube with specific code

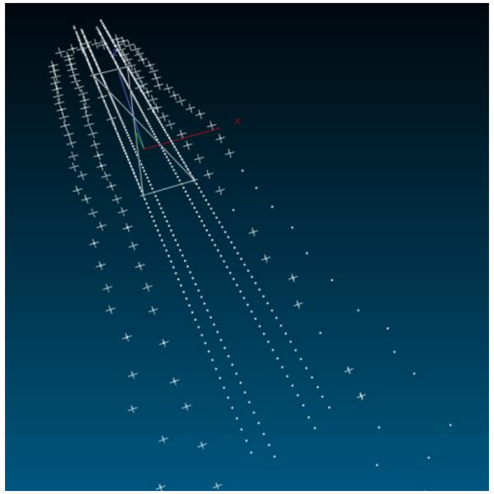

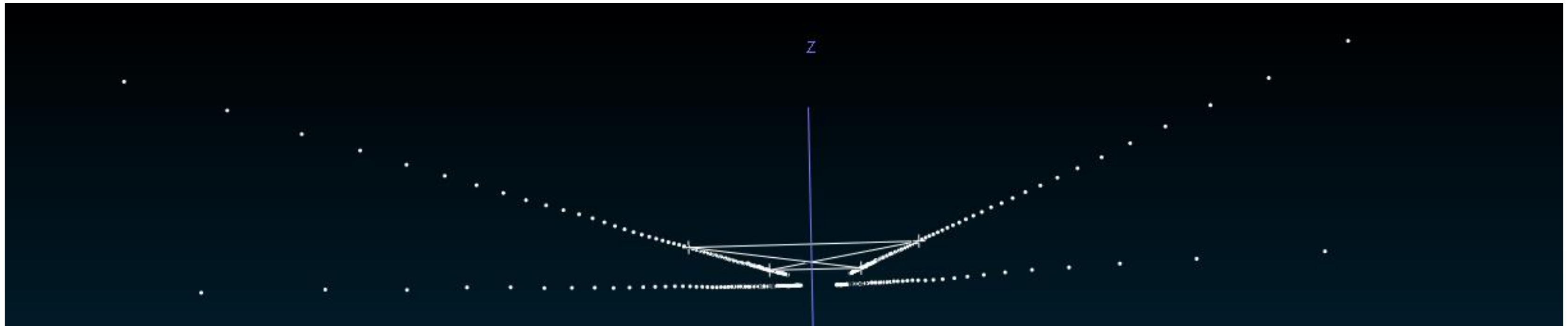

Programming Flight Routes

- Examples:
    - LITCHI: 2D Software only for DJI drones
    - UGCS: 3D Software for DJI and MAVLink
- Flight routes are generated automatically out of MATLAB with the info from the digital twin
- Upload flight routes as .csv or .kml to LITCHI/ UGCS

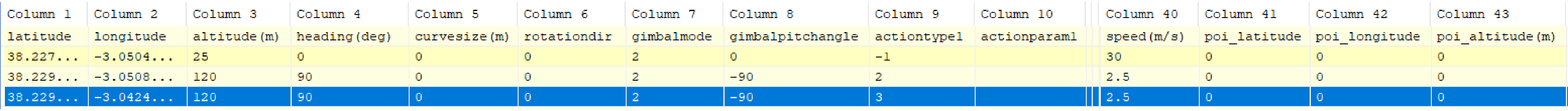

Column 1	Column 2	Column 3	Column 4	Column 5	Column 6	Column 7	Column 8	Column 9	Column 10	Column 40	Column 41	Column 42	Column 43
latitude	longitude	altitude(m)	heading(deg)	curvesize(m)	rotationdir	gimbalmode	gimbalpitchangle	actiontype1	actionparam1	speed(m/s)	poi_latitude	poi_longitude	poi_altitude(m)
38.227...	-3.0504...	25	0	0	0	2	0	-1		30	0	0	0
38.229...	-3.0508...	120	90	0	0	2	-90	2		2.5	0	0	0
38.229...	-3.0424...	120	90	0	0	2	-90	3		2.5	0	0	0

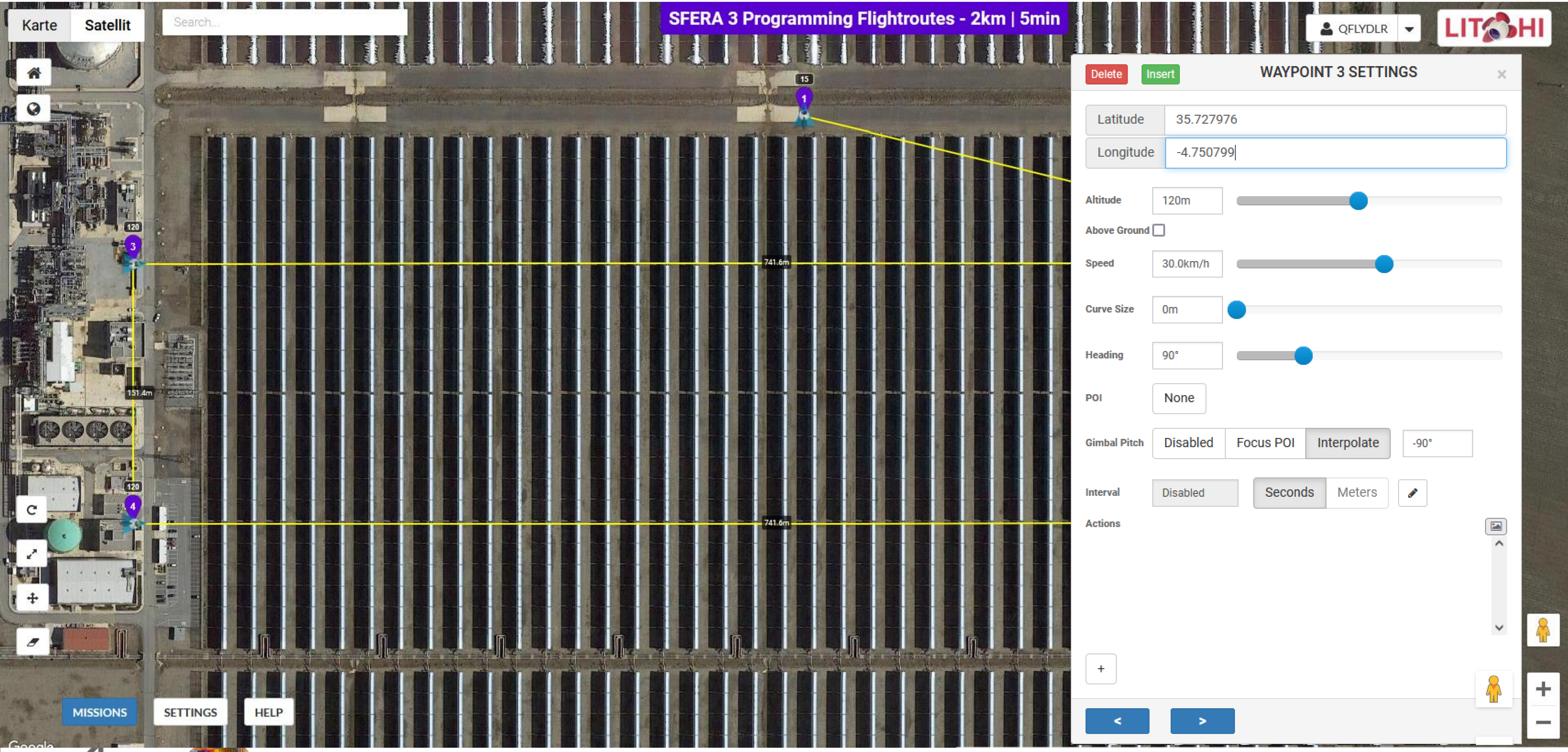

SFERA 3 Programming Flightroutes - 2km | 5min

WAYPOINT 3 SETTINGS

Latitude 35.727976
Longitude -4.750799
Altitude 120m
Above Ground ☐
Speed 30.0km/h
Curve Size 0m
Heading 90°
POI None
Gimbal Pitch Disabled | Focus POI | Interpolate -90°
Interval Disabled Seconds | Meters
Actions

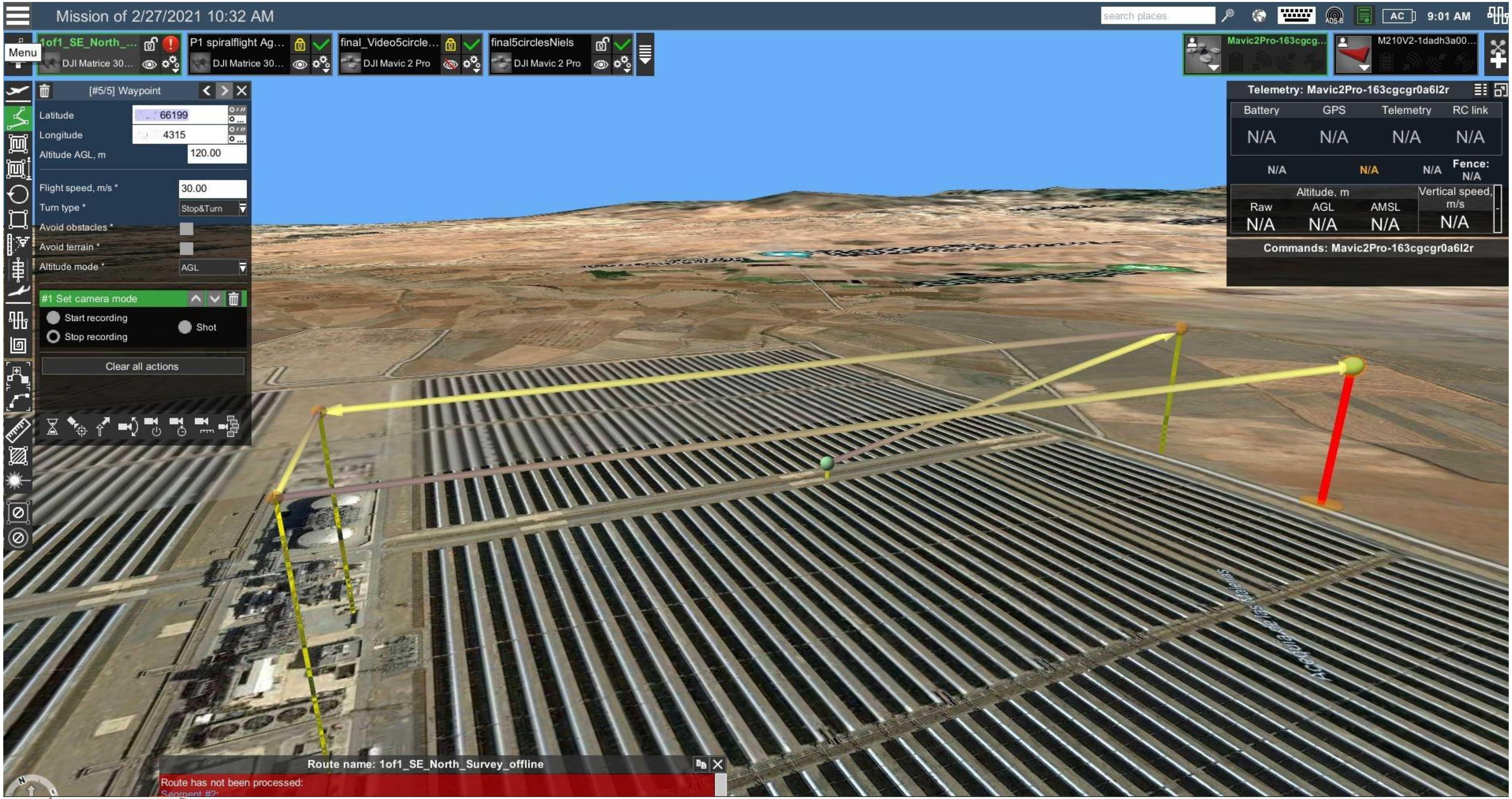

Mission of 2/27/2021 10:32 AM

[#5/5] Waypoint

Latitude: 66199

Longitude: 4315

Altitude AGL, m: 120.00

Flight speed, m/s *: 30.00

Turn type *: Stop&Turn

Avoid obstacles *: ☐

Avoid terrain *: ☐

Altitude mode *: AGL

#1 Set camera mode

○ Start recording ● Stop recording ○ Shot

Telemetry: Mavic2Pro-163cgcgr0a6l2r

Battery	GPS	Telemetry	RC link
N/A	N/A	N/A	N/A

N/A N/A N/A Fence: N/A

Altitude, m			Vertical speed, m/s
Raw	AGL	AMSL	
N/A	N/A	N/A	N/A

Commands: Mavic2Pro-163cgcgr0a6l2r

Route name: 1of1_SE_North_Survey_offline

Route has not been processed:

Measurement methods: 10 m vs 120 m flight altitude

- Start:
  - high accuracy IR measurements with 10 m flight altitude above tube
  - Get the absolute temperature of each tube measuring on glass envelope
  - flying along all tubes is too slow for 90 km of tubes in a 50 MW plant
- Solution:
  - 120 m survey flights without seeing the tube itself, but the reflection in the parabolic trough mirror
  - not as accurate as directly measured, but good relative results between healthy and broken tubes
  - By few absolute reference temperatures measured from ground, these relative results are improved and rise to a level of good absolute temperatures

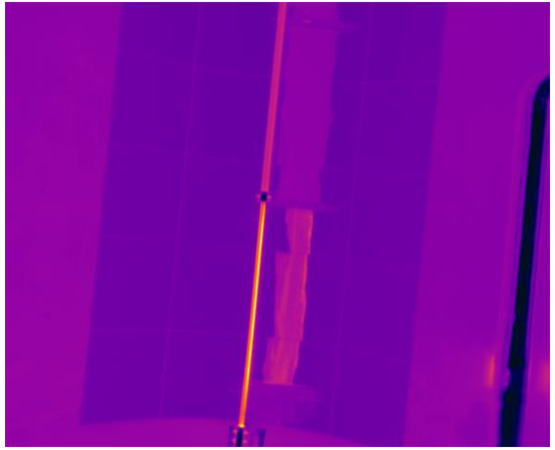

10 m altitude

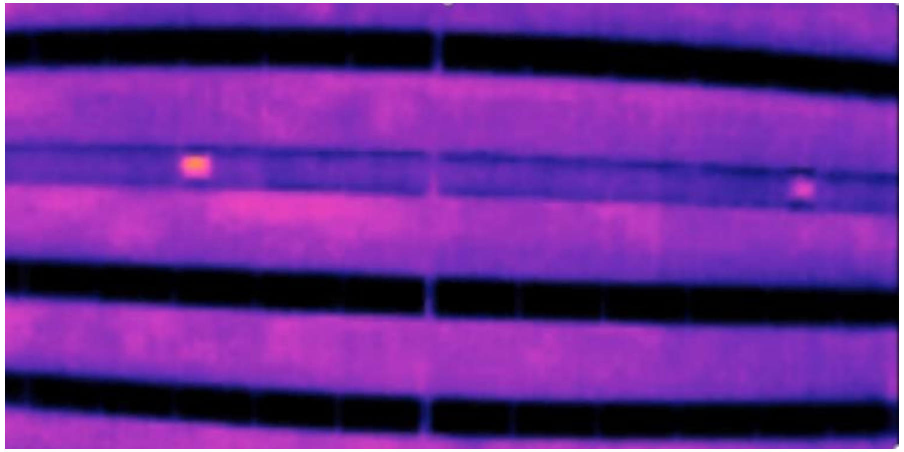

120 m altitude

Measurement Procedure & Data Acquisition

- Solar field requirements:
  - HTF @ operation temperature (200 – 400°C) must be continuously cycled through all measured loops
  - Collectors in zenith position (90°)

- Optimal measurement time to not affect plant operation (taking loops out of tracking):
  - 1 h around solar noon
  - 30 min before and after sunset or
- measurement speed: 100 MW/h @ 120 m flight altitude & flight speed over ground: ~8 m/s

Data Acquisition

Detection of:

- Broken/ bad vacuum tubes
- Missing mirrors
- torsion & alignment errors
- Slope deviations (less accurate)

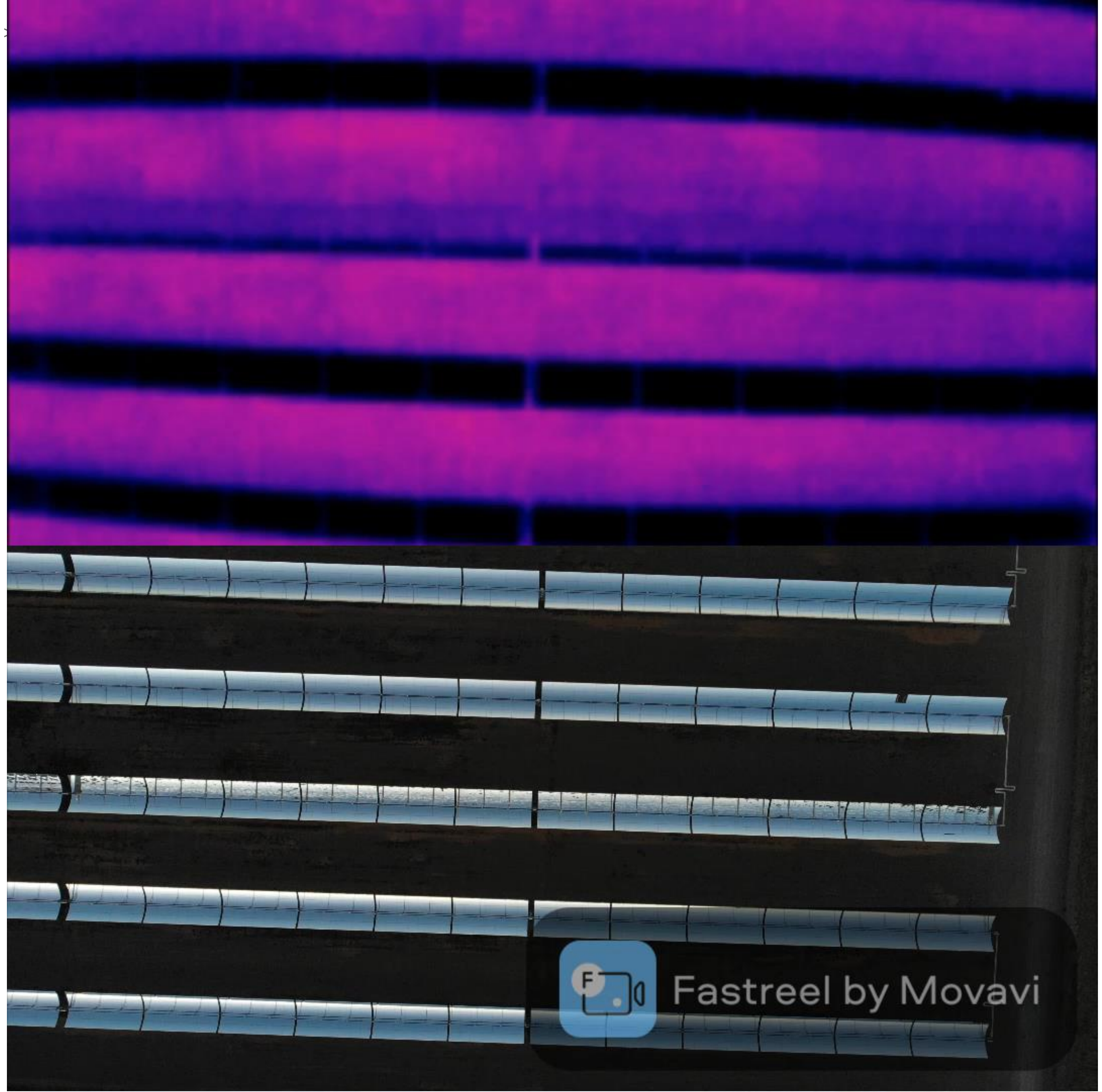

Outlook

- QFLY IR method is patented by DLR
- Fully automated maintenance by Drone in a box solutions like DJI Dock (available end 2022)

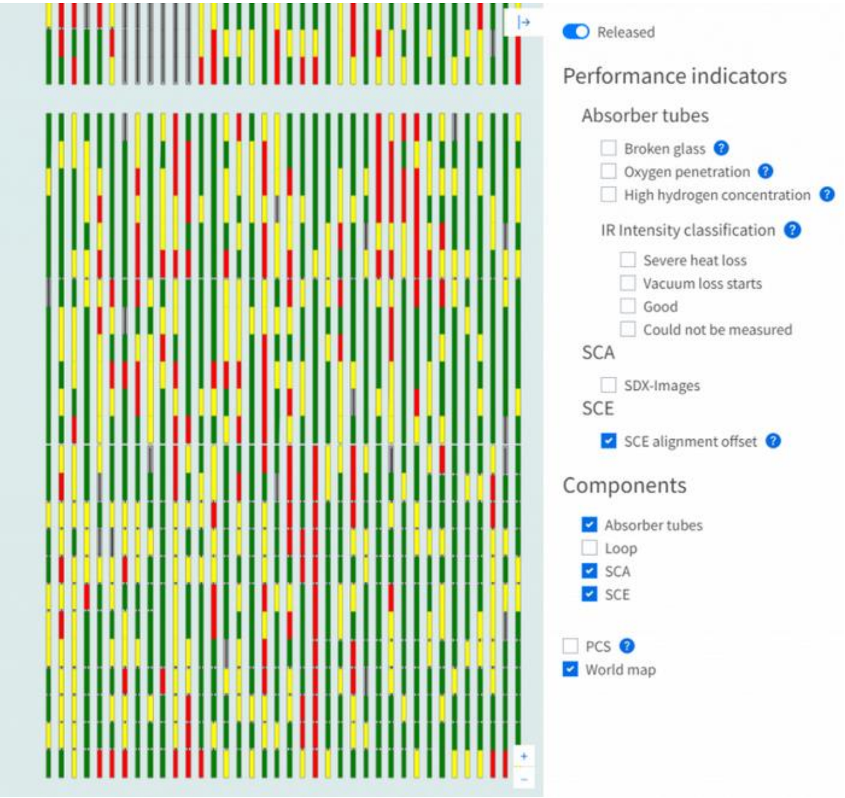

● Released

Performance indicators

Absorber tubes

☐ Broken glass

☐ Oxygen penetration

☐ High hydrogen concentration

IR Intensity classification

☐ Severe heat loss

☐ Vacuum loss starts

☐ Good

☐ Could not be measured

SCA

☐ SDX-Images

SCE

☑ SCE alignment offset

Components

☑ Absorber tubes

☐ Loop

☑ SCA

☑ SCE

☐ PCS

☑ World map

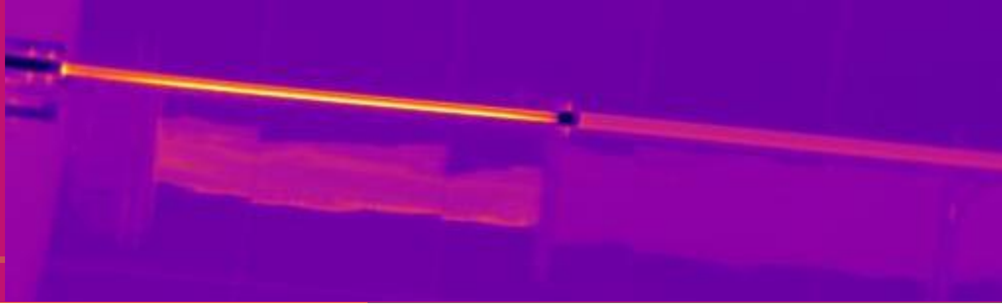

THANK YOU FOR YOUR ATTENTION!
ANY QUESTIONS?

GOBIERNO DE ESPAÑA
MINISTERIO DE CIENCIA, INNOVACIÓN Y UNIVERSIDADES
Ciemat
Centro de Investigaciones Energéticas, Medioambientales y Tecnológicas

ENEA

DLR
Deutsches Zentrum für Luft- und Raumfahrt

UNIVERSIDADE DE ÉVORA

ESTELA

The Cyprus Institute

instituto imdea energía

Fraunhofer ISE

euronovia

LNEG

METU

ETH zürich

IN LUMINE SAPIENTIA · UNIVERSITAS ALMERIENSIS
UNIVERSIDAD DE ALMERÍA

cnrs
dépasser les frontières

DE LA RECHERCHE À L'INDUSTRIE
cea

SFERA-III

Solar Facilities for the European Research Area

2nd Training for Industries “Optimization of CST plant output by optical and thermal characterization and target-oriented O&M”
26 – 29 April 2022, Plataforma Solar de Almería, Spain

Techno-Economic Analysis of Receiver Repair/Replacement Scenarios in a Parabolic Trough Field

Marc Röger, DLR

NETWORKING

THIS PROJECT HAS RECEIVED FUNDING FROM THE EUROPEAN UNION’S HORIZON 2020 RESEARCH AND INNOVATION PROGRAMME UNDER GRANT AGREEMENT NO **823802**

Overview

1. **MOTIVATION** of Study
2. **REFERENCE** Parabolic Trough Plant
3. **SCENARIOS** for Receiver Performance Loss
4. **METHODOLOGY**
5. **RESULTS**
6. **CONCLUSIONS**

1. MOTIVATION of Study

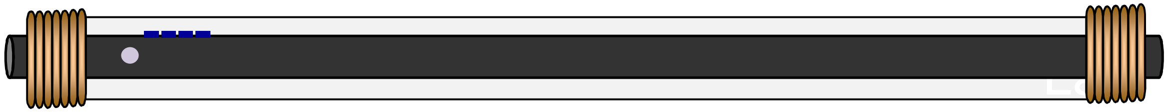

- **Field heat losses** are between **7%** (Jordan, Ma'an) and **10%** (Guadix, Spain) of the collected solar energy (Eurotrough-type, 70mm absorber, HTF: Oil)

- Receiver design lifetime is **20-40 years**
- However, lifetime may be reduced by
  - Different maturity of products
  - Limited experience in operation, H_2 accumulation in HTF
  - Increasing temperatures and new fluids
  - Wind events with glass breakage

- In case of failure, receiver heat loss may be increased by a **factor 5 to 10**

- **Objective of study**: Energetic and economic impact of different receiver performance loss scenarios

2. REFERENCE Parabolic Trough Plant

Technology

- Modern **150-MW$_{el}$ parabolic trough plant** in **Ma’an**, Jordan (DNI 2820 kWh/m^{2}a)
- **7.5h**-molten salt storage
- 360 loops of **high-quality collectors** (η_{opt}= 0.78) (Eurotrough-geometry)
- **51’840 receivers** (totaling 207 km), either standard or with Xe-capsule (+1.3% solar field cost est.)
- **Turbine 150 MW**, efficiency 38.5%
- **Dry cooling**, no fossil firing

Economy

- Investment costs 4 M€/MW$_{el}$
- Annual O&M + Ins.: 2.4%*I
- Discount rate 6%, 25% equity, 75% debt (5% interest rate), 25 yrs operation

→ **LEC 11.3 €cent/kWh$_{el}$**

3. SCENARIOS for Receiver Performance Loss

Event

- “**Wind A/B**” Wind event destroying glass envelopes
- “**H_2**” Hydrogen accumulation
- “**AR**” Anti-reflection coating degradation

Affected Field

- **50%** (H_2) or **100%** (AR) of field
- Limits of field (**5.6%**, Wind)

Variation of *point in time* when damage occurs

- **sudden** event year ***t*=5**, **10**, or **15** (Wind, H_2)
- **gradual** damage (AR) **1..5**, **1..10**, **1..15**

Different counter measures (full performance in year t+2)

- “**Leave**” damaged receivers (do nothing)
- “**Replace**” damaged receivers
- Activate “**Xenon**” capsule (H_2 accumulation)
- “**Fix**” receivers (H_2 accumulation)

3. SCENARIOS for Receiver Performance Loss

Heat Loss of Considered Receivers

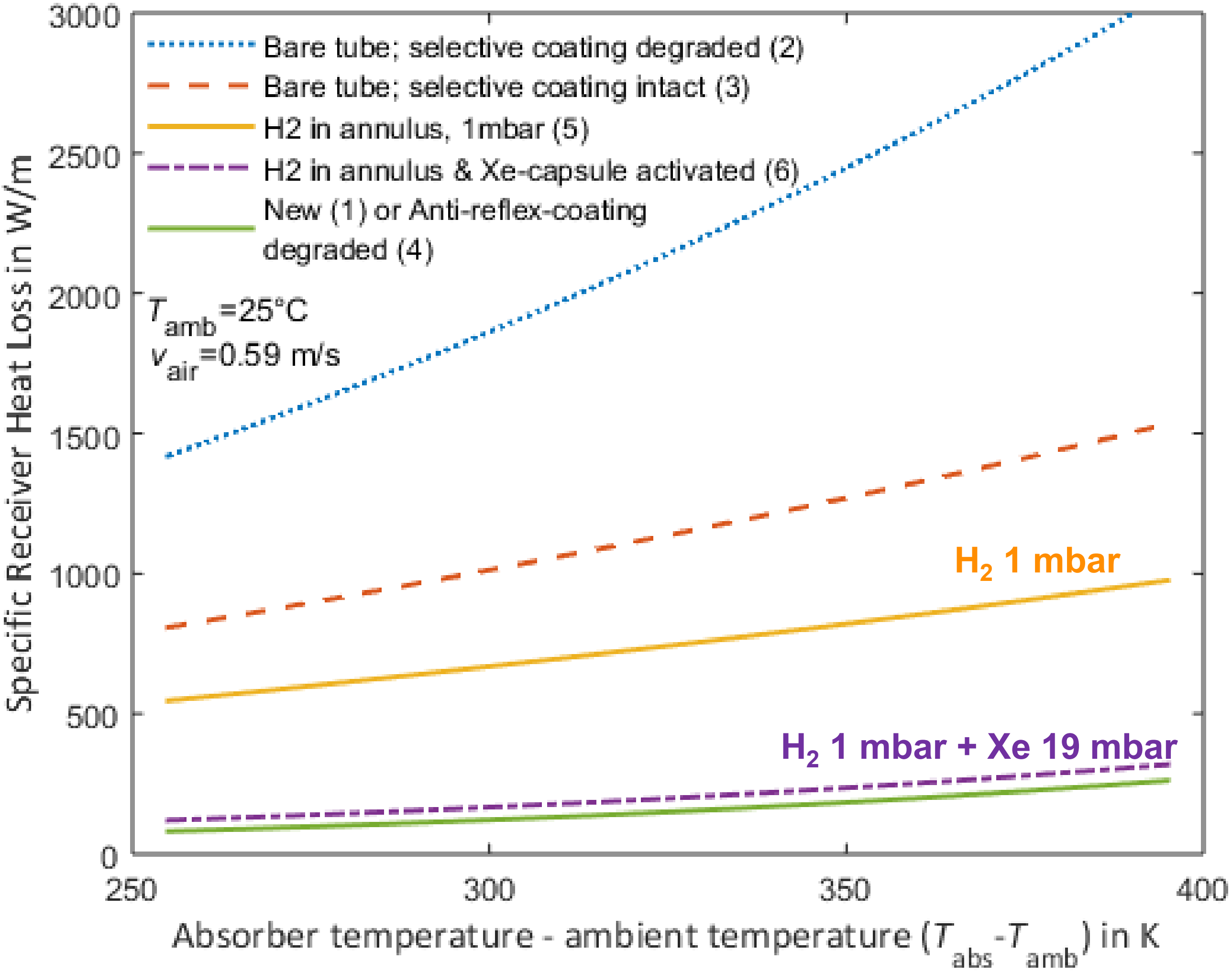

τ=100%; α_{sol} = **55%**,
ε=65%, **free convection**

τ=100%; α_{sol} = 96%,
ε=8-9%, **free convection**

τ=97%; α_{sol} = 96%,
ε=8-9%, h_{ann}=**12.4 W/m²K**

τ=97%; α_{sol} = 96%,
ε=8-9%, h_{ann}=**0.8 W/m²K**

τ=97/92%; α_{sol} = 96%,
ε=8-9%, h_{ann}=0.0 W/m²K

3. SCENARIOS for Receiver Performance Loss

Heat Loss of Regarded Receivers

Wind strongly influences bare and H_2 receivers. Increase of air speed near receivers from 0.6 to 3.0 m/s leads to higher heat losses:

- **With intact envelope** + 6 W/m
- **H_2 accumulation** +100 W/m
- **Bare tubes with broken envelope** +1000-2000 W/m

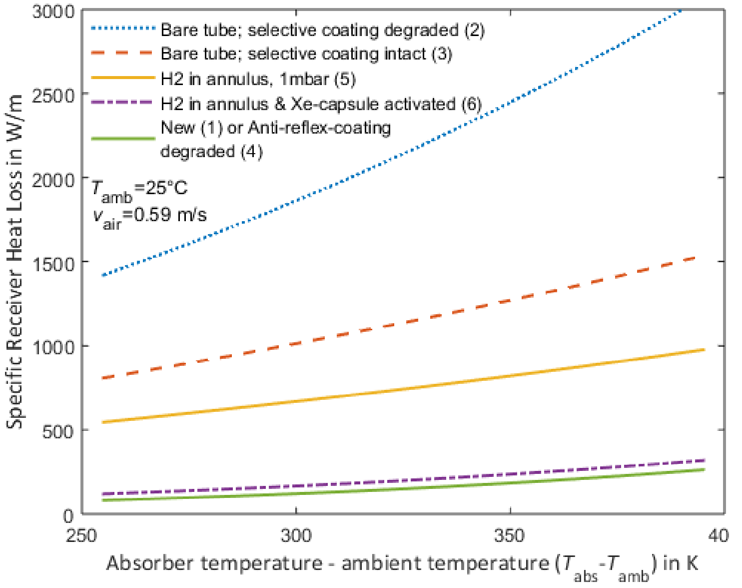

Relation between air speed interacting with receivers and 10m wind speed derived from measurements of [Dudley]

- 10m wind speed of 3.8 m/s (Ma'an) → 0.6 m/s air speed near receivers

V. Dudley, G. Kolb, M. Sloan, D. Kearney, "Test Results, SEGS LS-2 Solar Collector," Sandia National Laboratories, Report SAND94-1884, Dec. 1994

4. METHODOLOGY

greenius + Matlab

Software ***greenius*** (http://freegreenius.dlr.de)

- Performance calculations of CSP & other renewable systems based on hourly plant performance simulations

Special version created to represent

- **Spatially inhomogeneous** collector loops
- **Temporal variation** of optical and thermal receiver quality
- **Additional investments** for repair at specific points in time ***t*+1** possible
- Calculation of **each** year
- greenius start from **DOS / Matlab prompt** and preparation of input files and post-processing with Matlab

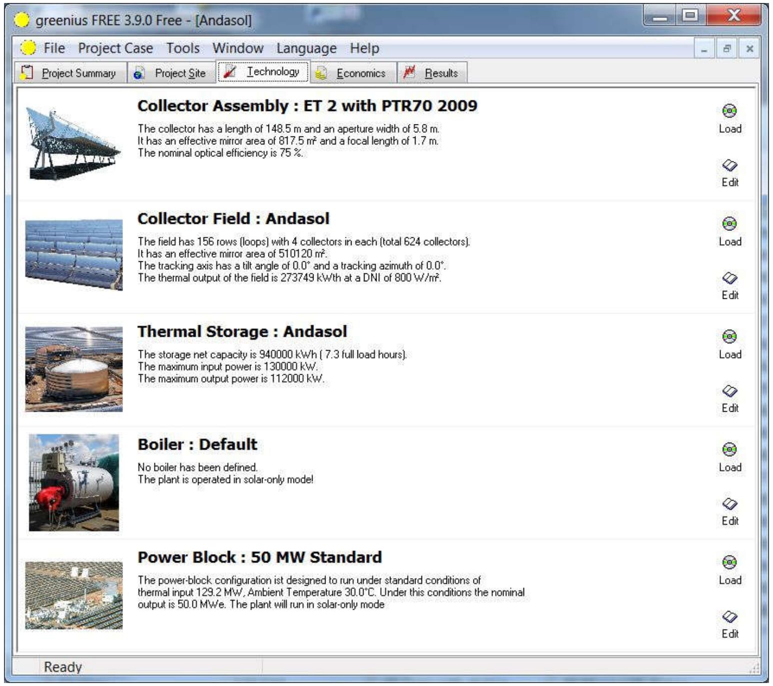

Collector Assembly : ET 2 with PTR70 2009

The collector has a length of 148.5 m and an aperture width of 5.8 m.
It has an effective mirror area of 817.5 m^2 and a focal length of 1.7 m.
The nominal optical efficiency is 75 %.

Collector Field : Andasol

The field has 156 rows (loops) with 4 collectors in each (total 624 collectors).
It has an effective mirror area of 510120 m^2.
The tracking axis has a tilt angle of 0.0° and a tracking azimuth of 0.0°.
The thermal output of the field is 273749 kWth at a DNI of 800 W/m^2.

Thermal Storage : Andasol

The storage net capacity is 940000 kWh (7.3 full load hours).
The maximum input power is 130000 kW.
The maximum output power is 112000 kW.

Boiler : Default

No boiler has been defined.
The plant is operated in solar-only mode!

Power Block : 50 MW Standard

The power-block configuration ist designed to run under standard conditions of thermal input 129.2 MW, Ambient Temperature 30.0°C. Under this conditions the nominal output is 50.0 MWe. The plant will run in solar-only mode

greenius

THE GREEN ENERGY SYSTEM ANALYSIS TOOL

4. METHODOLOGY

greenius + Matlab

Definition Collector Efficiency

$$\eta_{collector} = K \cdot \eta_{opt,0} \cdot \eta_{cleanliness} - \left(K \cdot b_0 \cdot \Delta T + \frac{b_1 \cdot \Delta T + b_2 \cdot \Delta T^2 + b_3 \cdot \Delta T^3 + b_4 \cdot \Delta T^4}{DNI} \right)$$

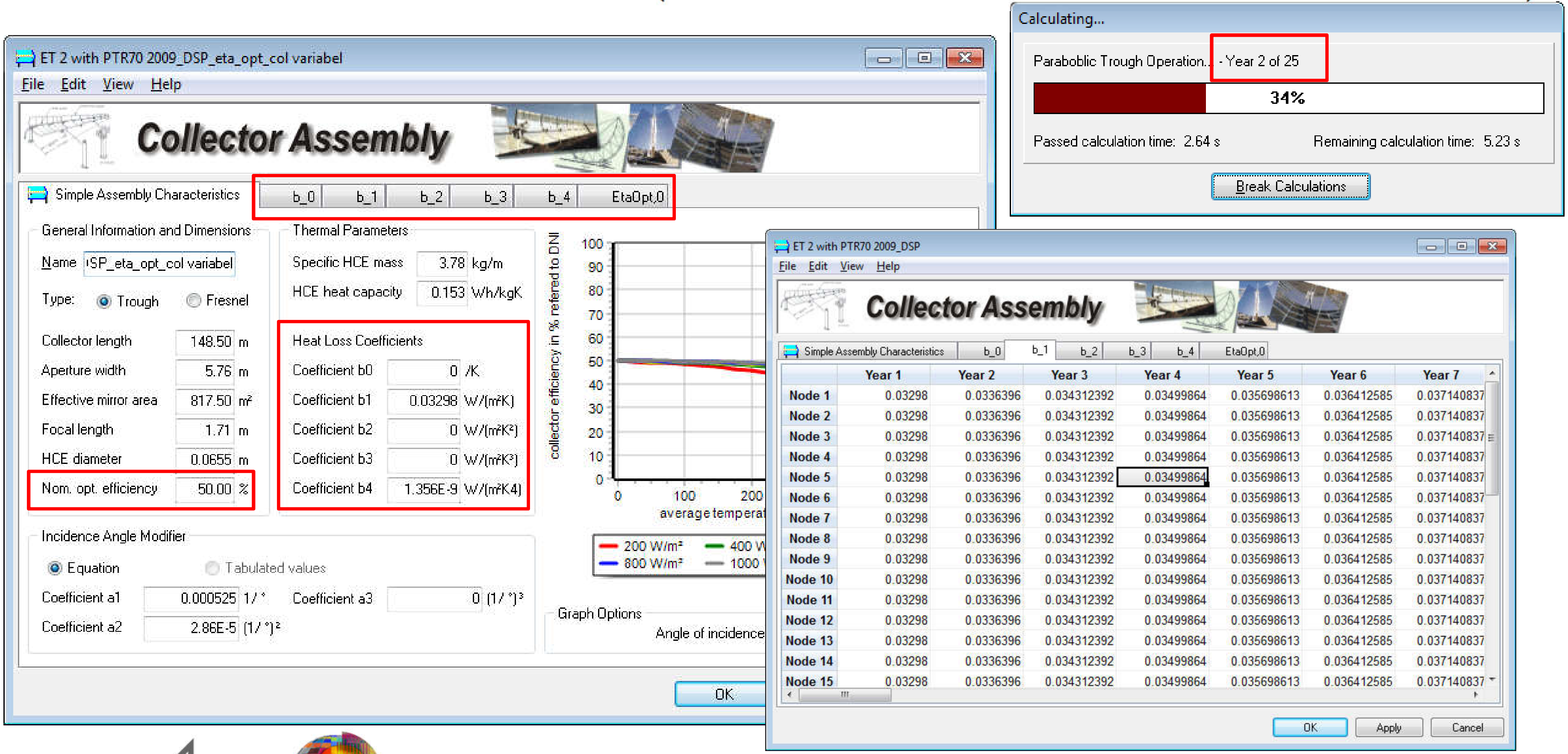

General Information and Dimensions

Name: ıSP_eta_opt_col variabel

Type: ● Trough ○ Fresnel

Collector length	148.50	m
Aperture width	5.76	m
Effective mirror area	817.50	m²
Focal length	1.71	m
HCE diameter	0.0655	m
Nom. opt. efficiency	50.00	%

Thermal Parameters

Specific HCE mass	3.78	kg/m
HCE heat capacity	0.153	Wh/kgK

Heat Loss Coefficients

Coefficient b0	0	/K
Coefficient b1	0.03298	W/(m²K)
Coefficient b2	0	W/(m²K²)
Coefficient b3	0	W/(m²K³)
Coefficient b4	1.356E-9	W/(m²K4)

Incidence Angle Modifier

● Equation ○ Tabulated values

Coefficient a1	0.000525	1/ °
Coefficient a2	2.86E-5	(1/ °)²
Coefficient a3	0	(1/ °)³

Graph Options

Angle of incidence

Paraboblic Trough Operation... - Year 2 of 25

34%

Passed calculation time: 2.64 s

Remaining calculation time: 5.23 s

	Year 1	Year 2	Year 3	Year 4	Year 5	Year 6	Year 7
Node 1	0.03298	0.0336396	0.034312392	0.03499864	0.035698613	0.036412585	0.037140837
Node 2	0.03298	0.0336396	0.034312392	0.03499864	0.035698613	0.036412585	0.037140837
Node 3	0.03298	0.0336396	0.034312392	0.03499864	0.035698613	0.036412585	0.037140837
Node 4	0.03298	0.0336396	0.034312392	0.03499864	0.035698613	0.036412585	0.037140837
Node 5	0.03298	0.0336396	0.034312392	0.03499864	0.035698613	0.036412585	0.037140837
Node 6	0.03298	0.0336396	0.034312392	0.03499864	0.035698613	0.036412585	0.037140837
Node 7	0.03298	0.0336396	0.034312392	0.03499864	0.035698613	0.036412585	0.037140837
Node 8	0.03298	0.0336396	0.034312392	0.03499864	0.035698613	0.036412585	0.037140837
Node 9	0.03298	0.0336396	0.034312392	0.03499864	0.035698613	0.036412585	0.037140837
Node 10	0.03298	0.0336396	0.034312392	0.03499864	0.035698613	0.036412585	0.037140837
Node 11	0.03298	0.0336396	0.034312392	0.03499864	0.035698613	0.036412585	0.037140837
Node 12	0.03298	0.0336396	0.034312392	0.03499864	0.035698613	0.036412585	0.037140837
Node 13	0.03298	0.0336396	0.034312392	0.03499864	0.035698613	0.036412585	0.037140837
Node 14	0.03298	0.0336396	0.034312392	0.03499864	0.035698613	0.036412585	0.037140837
Node 15	0.03298	0.0336396	0.034312392	0.03499864	0.035698613	0.036412585	0.037140837

5. RESULTS

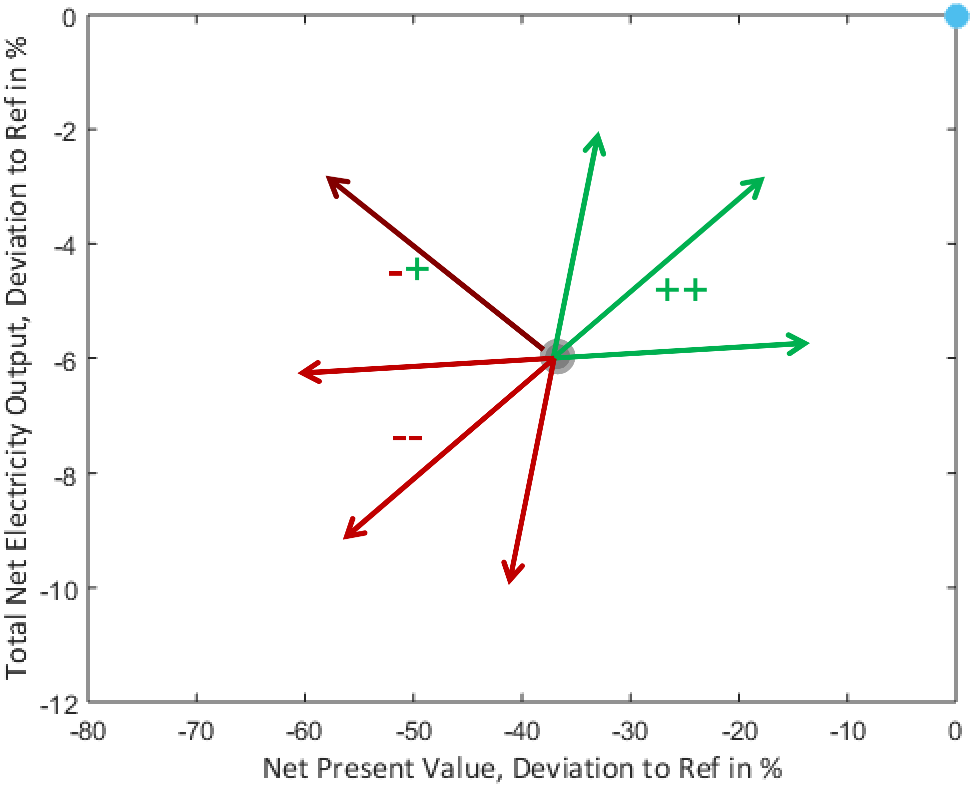

Net Present Value *(x-axis)*

- is the discounted value of the cumulated project cash flows at time zero
- is a **measure for economic success** of a project

Total Net Electricity Output *(y-axis)*

- is the total net electrical output of the plant **over 25 years**

Plotted is the **deviation to the reference scenarios** ('Ref' or 'Ref-Xe')

For maximum electricity production and maximum economic success

→ move right and up

5. RESULTS

Wind (‘A’/’B’) and Anti-reflection Coating (‘AR’) Scenarios

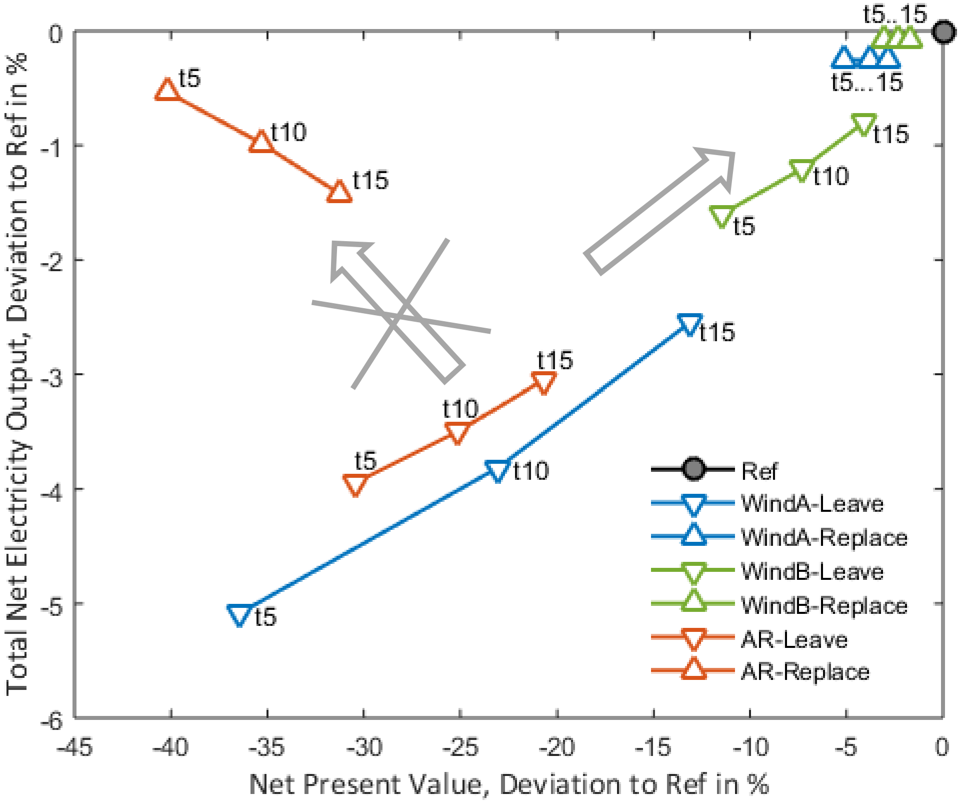

*Replace: ~1 k€/rec. (rec. 600€ + labour 400€ + Loop outage)

- **WindA** (degr. coating) event may reduce **net present value up to 36%** and total generated **electricity up to 5%** over plant lifetime
- **Replacement*** is both economically and energetically **viable**
- **WindB** (stable coating) is similar but less pronounced
- **AR** scenario may reduce **net present value up to 30%** and **electr. up to 4%**
- **Replacement*** is energetically viable, but **economically <u>NOT</u> viable**

5. RESULTS

Hydrogen Scenarios (‘H2’)

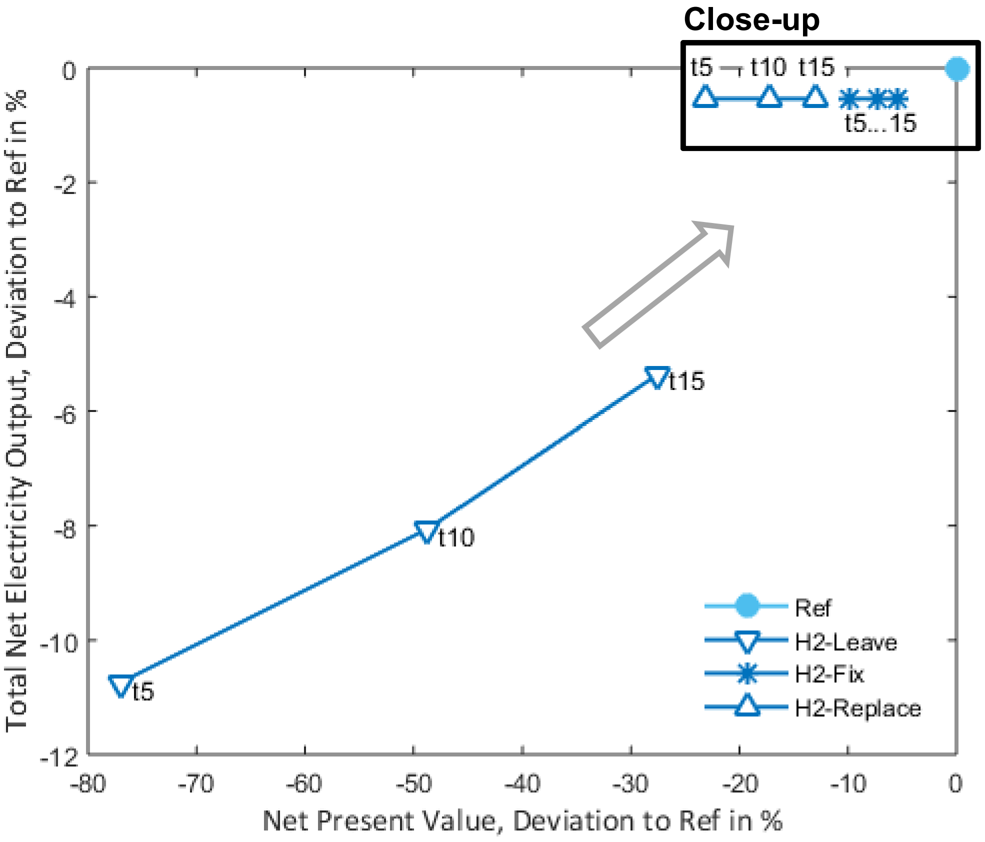

- H_2 may reduce **net present value up to 77%** and total generated **electricity up to 11%** over plant lifetime
- **Replacement*** is both economically and energetically **viable**
- **Fixing**:** The **repair** solution for standard receivers, is the **most viable solution**

*Replace: ~1 k€/rec. (rec. 600€ + labour 400€ + Loop outage)

**Repair/Fix : 200€/rec. assumed

5. RESULTS

Hydrogen Scenarios (‘H2’)

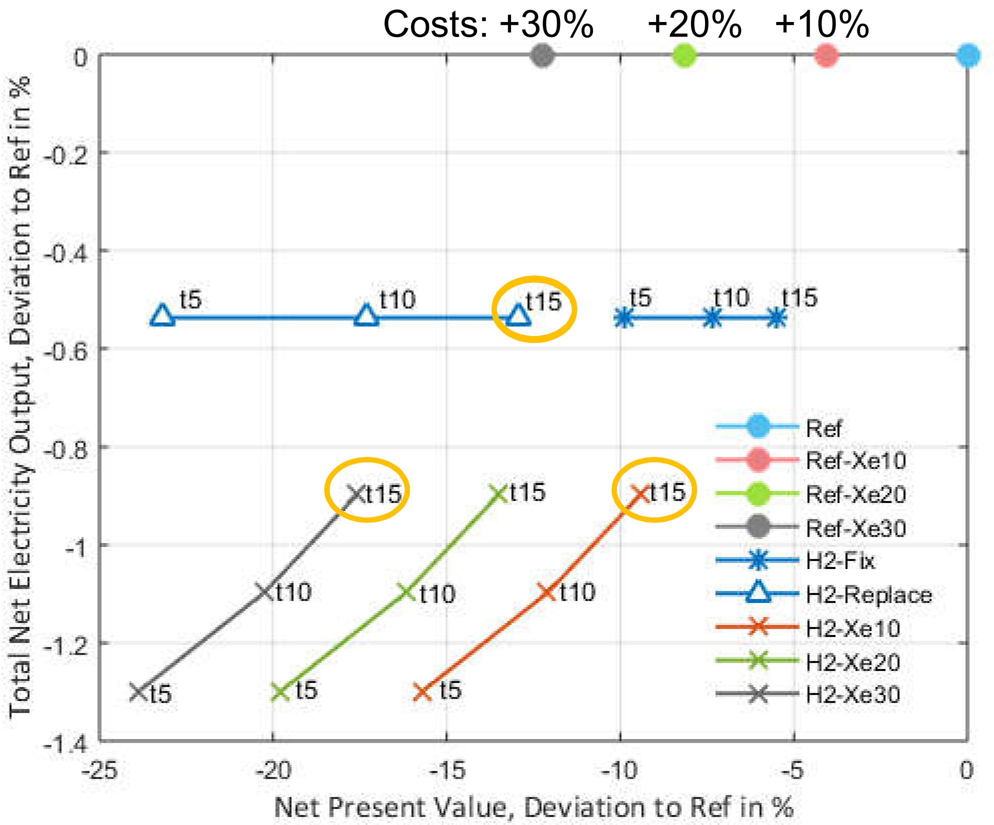

*Replace: ~1 k€/rec. (rec. 600€ + labour 400€ + Loop outage)

**Repair/Fix : 200€/rec. assumed

Xe receivers:

- Reference ‘Ref-Xe’ scenarios have lower net present value, because of higher initial investment
- Xe10 / Xe20 / X30: surplus of +10% / 20% / 30% costs compared to standard receivers
- Xe10: In case of H_2 accumulation, ‘H2-Xe10’ more viable than standard receiver replacement ‘H2-Replace’
- Xe30: Not viable comp. to ‘H2-Replace’
- Xe20: Depends on point of time of damage

5. RESULTS

Mean Solar Field Efficiency and LEC

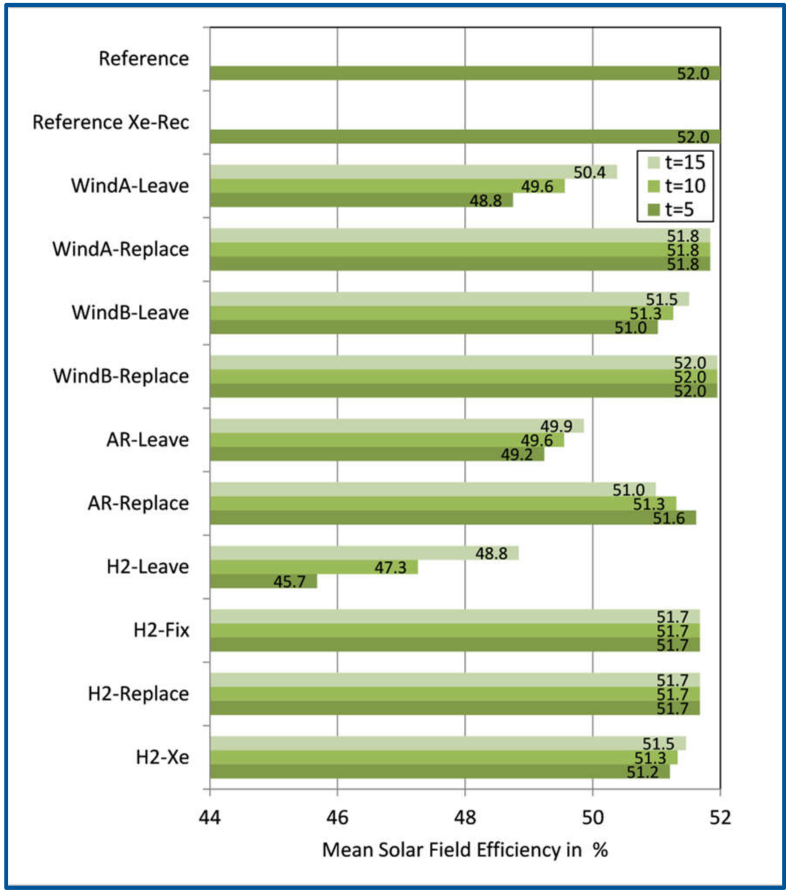

Mean Solar Field Efficieny in %

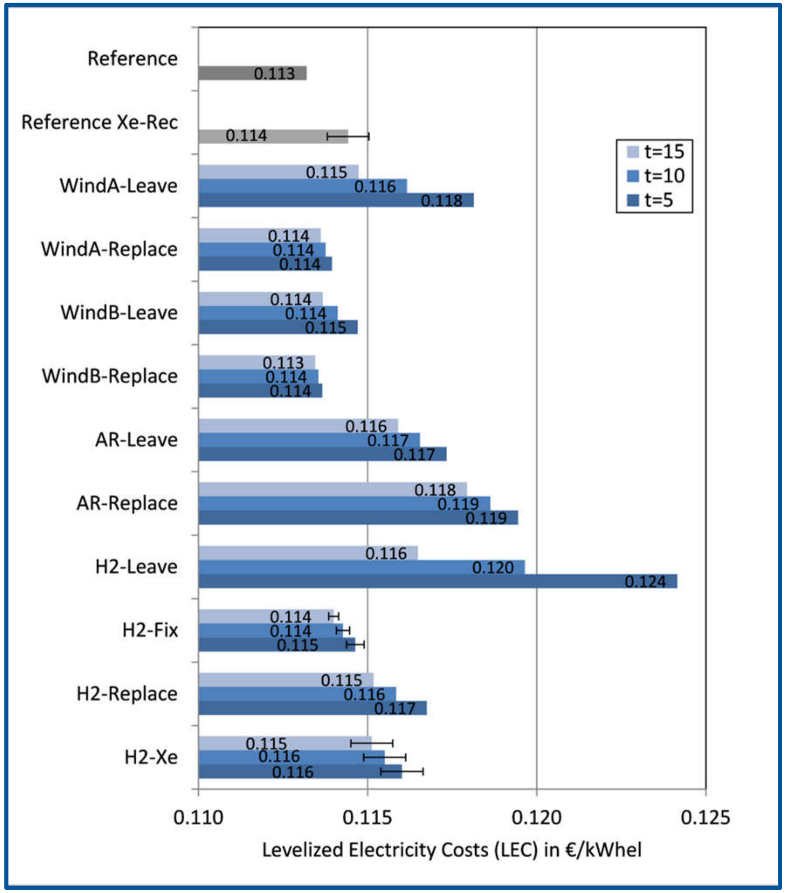

Levelized Electricity Costs in €/kWh_{el}

5. RESULTS

Discounted Payback Period

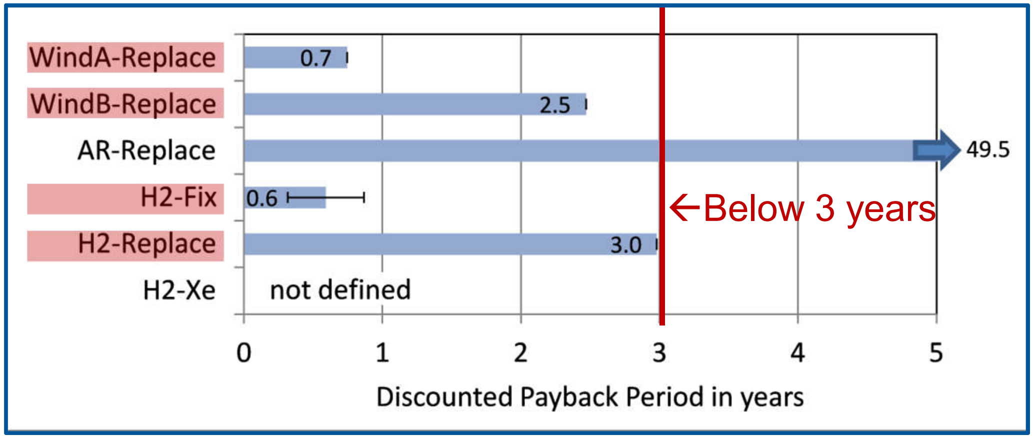

Discounted Payback Period

=Time after which the additional investment has been amortized by the additional revenues

Payback period is **below 3 years** for all measures except for Replacement in AR case

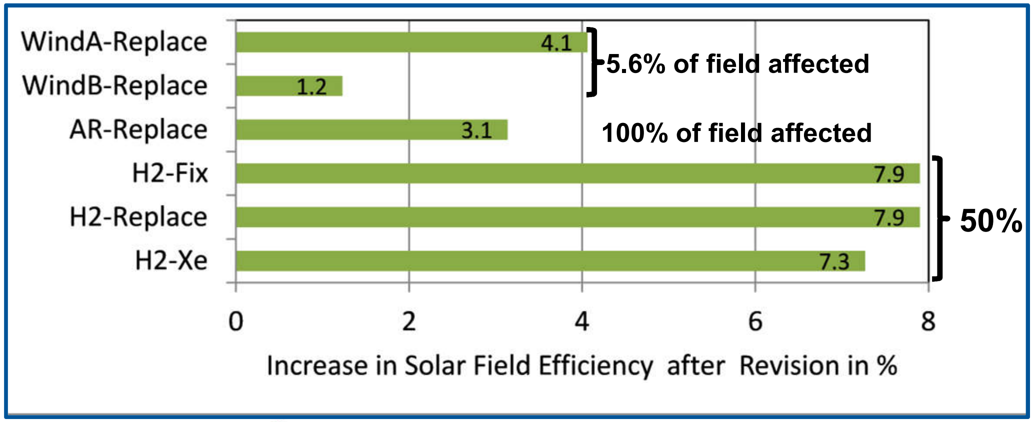

50% of field affected

Efficiency Increase of Counter Measure

6. Conclusions (I)

- A **method** to investigate the **energetic and economic impact** of different **receiver performance loss scenarios** was presented.
- The software tool **greenius** was extended and coupled to Matlab

More Details:

Röger, M.; Lüpfert E.; Caron, S.; Dieckmann, S.: Techno-economic analyses of receiver replacement scenarios in a parabolic trough field, AIP Conf. Proc. 1734, 030030 (2016); http://dx.doi.org/10.1063/1.4949082

6. Conclusions (II)

The following results are of exemplary character and only valid under the assumed boundary conditions. Plant Owner should repeat the calculations for their own conditions with the proposed method.

- ***Reference***: **150-MW_{el}-parabolic trough** plant with **7.5-h**-molten-salt-storage
- ***Scenarios***: **Wind** breakage, **H_2** accumulation, anti-reflection coating degradation (**AR**) in event year **5**, **10**, or **15** and **counter-measures**

- ***Wind***: **Receiver replacement** of receivers with broken glass envelope has a **payback period of 0.7 to 2.5 years** and hence replacement is strongly recommended
- ***H2***: Hydrogen accumulation has the highest impact, reducing output up to 11% and net present value by 77%. Receiver **replacement** (**payback 3 years**) or **repair** (**payback 0.6 years**) is economically and energetically required.
- ***H2-Xe***: The option of investing in receivers with **Xe-capsule** is a viable option, only if the **surplus cost is lower than 10 to 20%** and H_2 accumulation occurs.
- ***AR***: **Replacement is NOT viable**.

SFERA-III

Solar Facilities for the European Research Area

THANK YOU FOR YOUR ATTENTION!
ANY QUESTIONS?

GOBIERNO DE ESPAÑA MINISTERIO DE CIENCIA, INNOVACIÓN Y UNIVERSIDADES Ciemat

ENEA

DLR Deutsches Zentrum für Luft- und Raumfahrt

UNIVERSIDADE DE ÉVORA

ESTELA

The Cyprus Institute

instituto imdea energía

Fraunhofer ISE

euronovia

LNEG

METU

ETH zürich

UNIVERSIDAD DE ALMERÍA

cnrs

cea

The speaker gratefully acknowledges the financial support from the German Federal Ministry for Economic Affairs and Energy for the two projects PARESO (0325412) and FreeGreenius (0325427)

DLR

SFERA

SFERA-III

Solar Facilities for the European Research Area

2nd Training for Industries "Optimization of CST plant output by optical and thermal characterization and target-oriented O&M"
26 – 29 April 2022, Plataforma Solar de Almería, Spain

Clamp-On Measurements and Evaluation by Parameterized Dynamic Performance Model

Nicole Janotte, Marc Röger, DLR

NETWORKING

THIS PROJECT HAS RECEIVED FUNDING FROM THE EUROPEAN UNION'S HORIZON 2020 RESEARCH AND INNOVATION PROGRAMME UNDER GRANT AGREEMENT NO **823802**

Overview

- **Motivation** for in situ performance evaluation of CSP systems
- **Principle** of thermal performance evaluation
- **In situ Performance Testing**
    - Measurement Approaches
    - Clamp-On Equipment (Mobile Field Laboratory)
- **Data Analysis and Evaluation** using Parameterized Dynamic Solar Field Model
- **Practical Application**: Loop Performance Testing AndaSol-3
- **Summary**

Motivation for in situ Performance Evaluation of CSP Systems

Thermal performance characterizes the capacity of a system to convert available solar irradiance into useful heat under specific boundary conditions.

- Assessment of thermal overall performance of a particular
  - collector design
  - complete system/loop/field

  under actual /specific operating conditions

- Application and Potential
  - Collector / system / solar field characterisation
  - Acceptance testing
  - Long-term characterisation

CHARACTERIZATION
VERIFICATION
MONITORING

Principle of Thermal Performance Evaluation

Calorimetric evaluation of HTF flow

$$\dot{Q}_{field} = \dot{m}_{HTF} \cdot \int_{T_{in}}^{T_{out}} c_p(T)dT$$

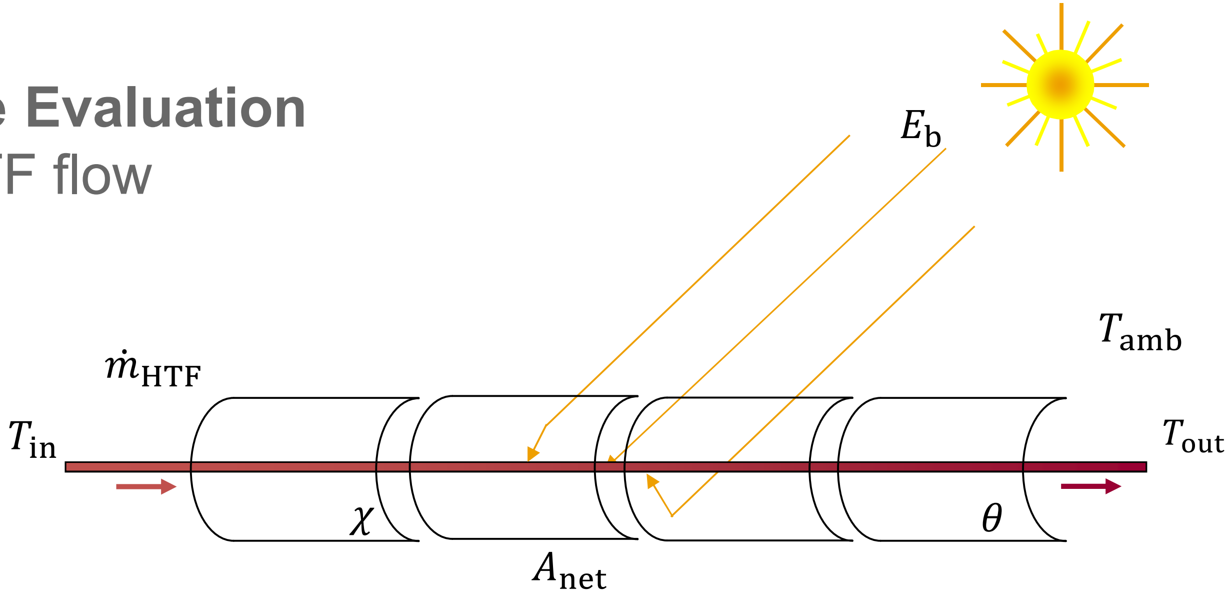

For given solar input at prevailing boundary conditions

- Solar irradiance E_b
- Angle of incidence θ
- Mirror cleanliness χ
- Ambient temperature T_amb

$$\eta_{th} = \frac{\dot{Q}_{th}}{\dot{Q}_{Solar}} = \frac{\dot{m} \cdot c_p (T_\text{out} - T_\text{in})}{A_\text{net} \cdot E_\text{b} \cdot \cos(\theta) \cdot \chi^{3/2}}$$

Principle of Thermal Performance Evaluation

System Scales –Test Operation Conditions

KONTAS

Rotary test bench

KONTAS at PSA (PSA is owned by Ciemat)

- Sophisticated HTF temperature and flow control
- Wide range of operating conditions
- Adjustable angle of incidence
- Replacable HTF
- Precision measurement equipment

→ greatest possible control of test conditions

→ very limited system dimensions

⇩

High „preparatory“ effort,
easy access to desired performance characteristic

SolarField

AndaSol 1 (Spain)

- Individual solar field operating conditions and HTF determined by plant operation
- Typically limited variation
- Different approaches for determining relevant (HTF bound) measurement quantities

⇩

Any existing collector system in regular operation,
High analytical effort to access to desired performance characteristic

In situ Performance Testing

Non Fluid Bound Measurement Quantities

- Monitoring and Documentation of Test/Operation conditions
  - Irradiance
  - Tracking angle (tracking + incidence angle)
  - cleanliness
  - Wind velocity and ambient temperature (not depicted)
  - Aperture area
  - Specific heat capacity of HTF
- Implementation in DLR’s Mobile Field Laboratory

$$\eta_{th} = \frac{\dot{Q}_{th}}{\dot{Q}_{Solar}} = \frac{\dot{m}\cdot \boxed{c_p}(T_{out}-T_{in})}{\boxed{A_{net}}\cdot\boxed{E_b}\cdot\boxed{\cos(\theta)}\cdot\boxed{\chi^{3/2}}}$$

HP irradiance station

Differential scanning calorimeter

Reflektometer

Inclinometer

In situ Performance Testing

Fluid Bound Measurement Quantities

- Volumetric/mass flow rate
- HTF temperature
  - Inlet
  - Outlet
  - Flow measurement

$$\eta_{th} = \frac{\dot{Q}_{th}}{\dot{Q}_{Solar}} = \frac{\boxed{\dot{m}} \cdot c_{p} \left(\boxed{T_{\mathrm{out}} - T_{\mathrm{in}}}\right)}{A_{\mathrm{net}} \cdot E_{\mathrm{b}} \cdot \cos(\theta) \cdot \chi^{3/2}}$$

➢ Different measurement approaches

➢ Eligibility criteria

Measurement uncertainty
Mounting effort
Flexibilitly
Leakage risk

Cost
Independence
Adaptability
Interference with process operation

Measurement Approaches

Regular Plant Instrumentation

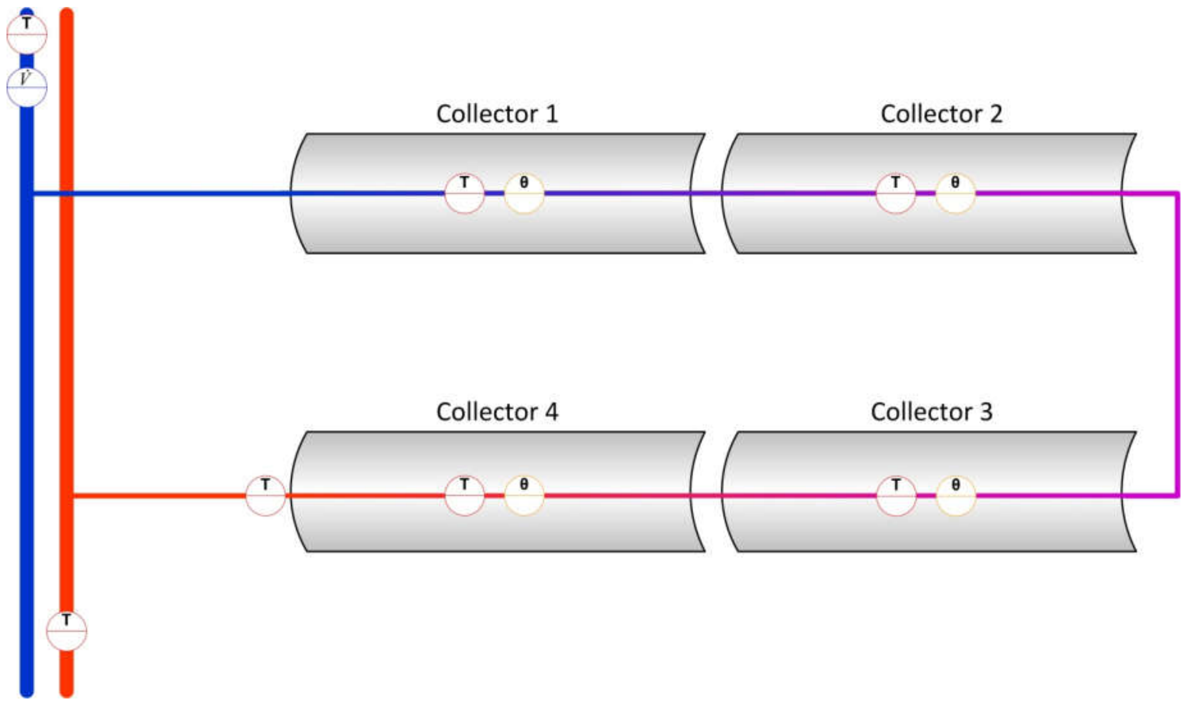

	Regular Plant Instrumentation
Measurement Uncertainty	– –
Cost	+ +
Mounting Effort	+ +
Independence	– –
Flexibility	– –
Adaptability	– –
Leakage Risk	+ +
Interference with Process Operation	+ +

Measurement Approaches

Embeded calibrated Instrumentation

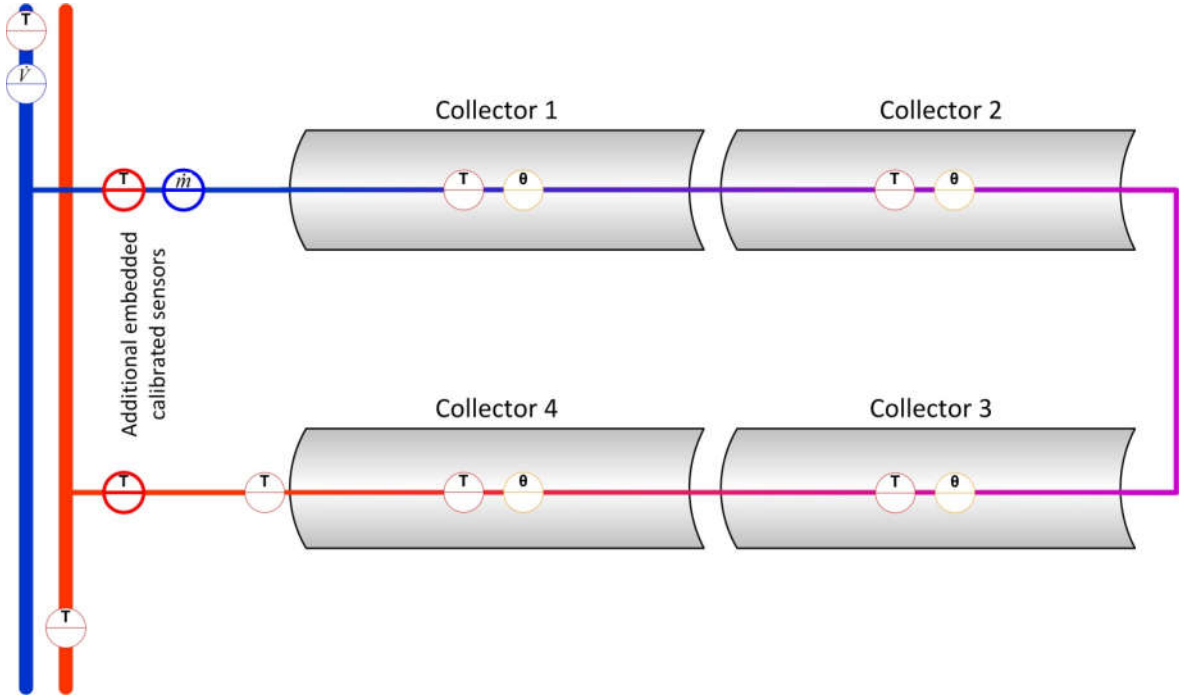

	Embedded Calibrated Instrumentation
Measurement Uncertainty	++
Cost	–
Mounting Effort	o
Independence	++
Flexibility	– –
Adaptability	++
Leakage Risk	–
Interference with Process Operation	o

Measurement Approaches

Bypass

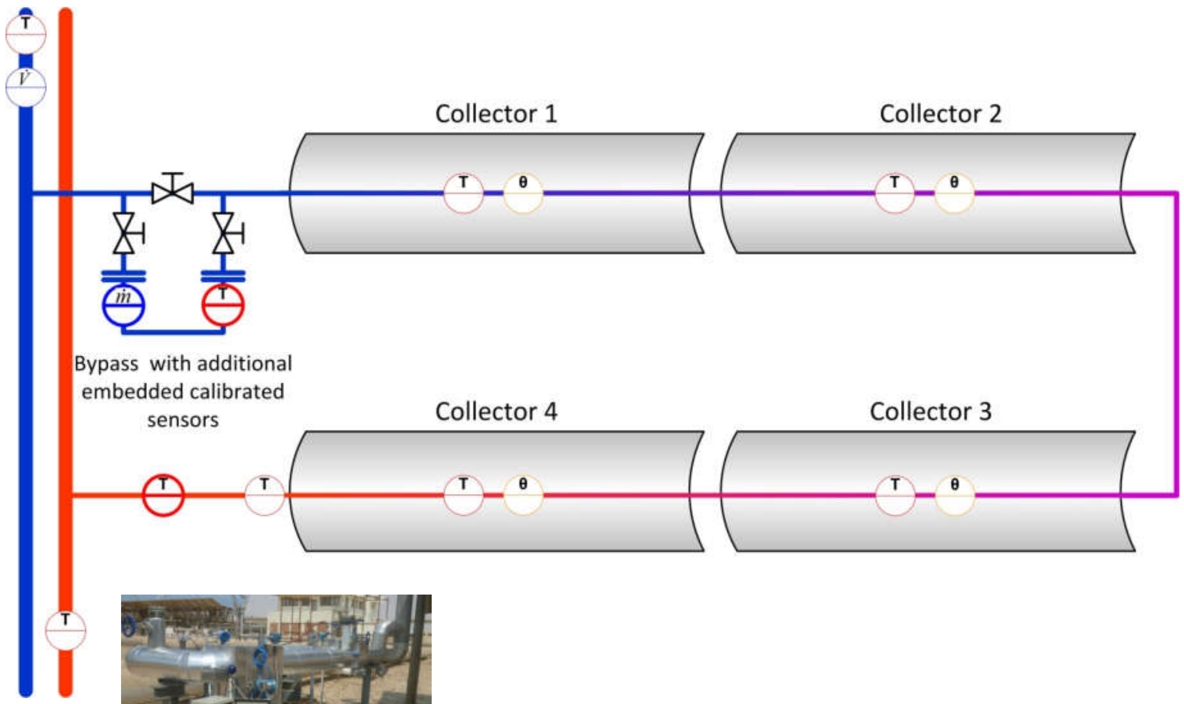

Bypass with additional embedded calibrated sensors

	Bypass
Measurement Uncertainty	+ +
Cost	–
Mounting Effort	+
Independence	+ +
Flexibility	– –
Adaptability	– –
Leakage Risk	o
Interference with Process Operation	+

Measurement Approaches

Mobile Heat Unit

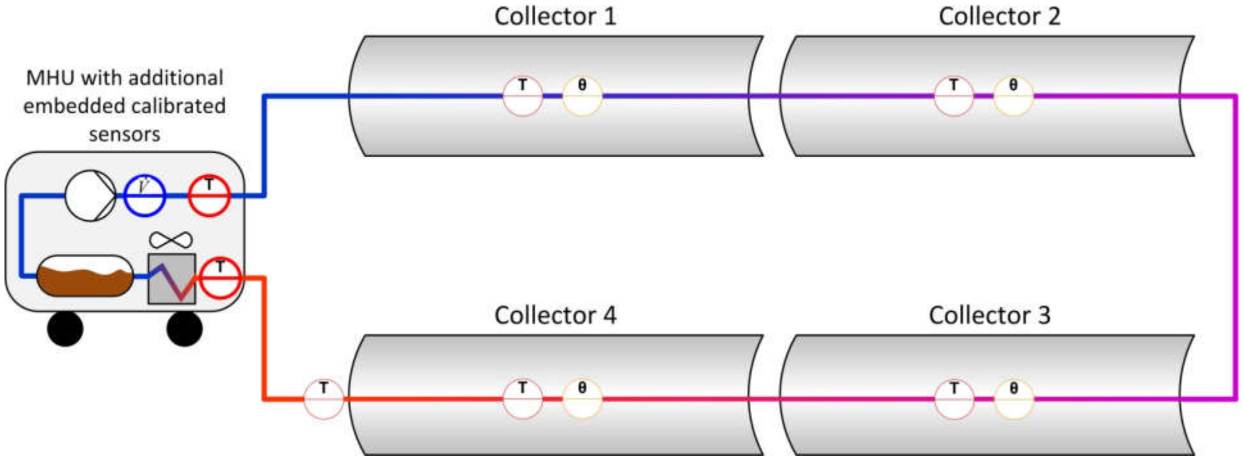

	Mobile Heat Unit
Measurement Uncertainty	+
Cost	o
Mounting Effort	+
Independence	o
Flexibility	–
Adaptability	–
Leakage Risk	o
Interference with Process Operation	o

Measurement Approaches

Mobile Field Laboratory

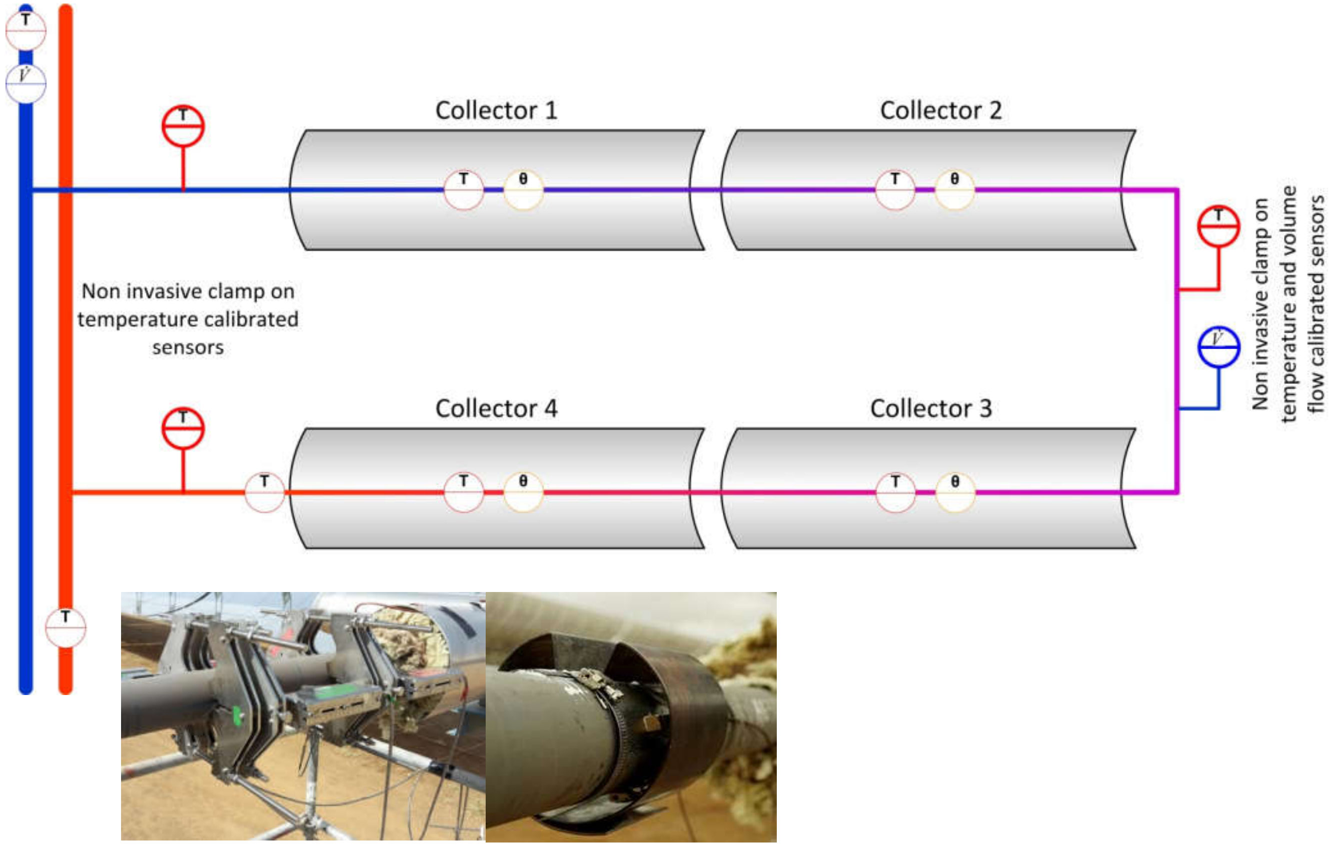

Non invasive clamp on temperature calibrated sensors

Non invasive clamp on temperature and volume flow calibrated sensors

	Mobile Field Laboratory
Measurement Uncertainty	+
Cost	– –
Mounting Effort	–
Independence	+ +
Flexibility	+ +
Adaptability	o
Leakage Risk	+ +
Interference with Process Operation	+ +

Measurement Approaches

Overview and Comparison

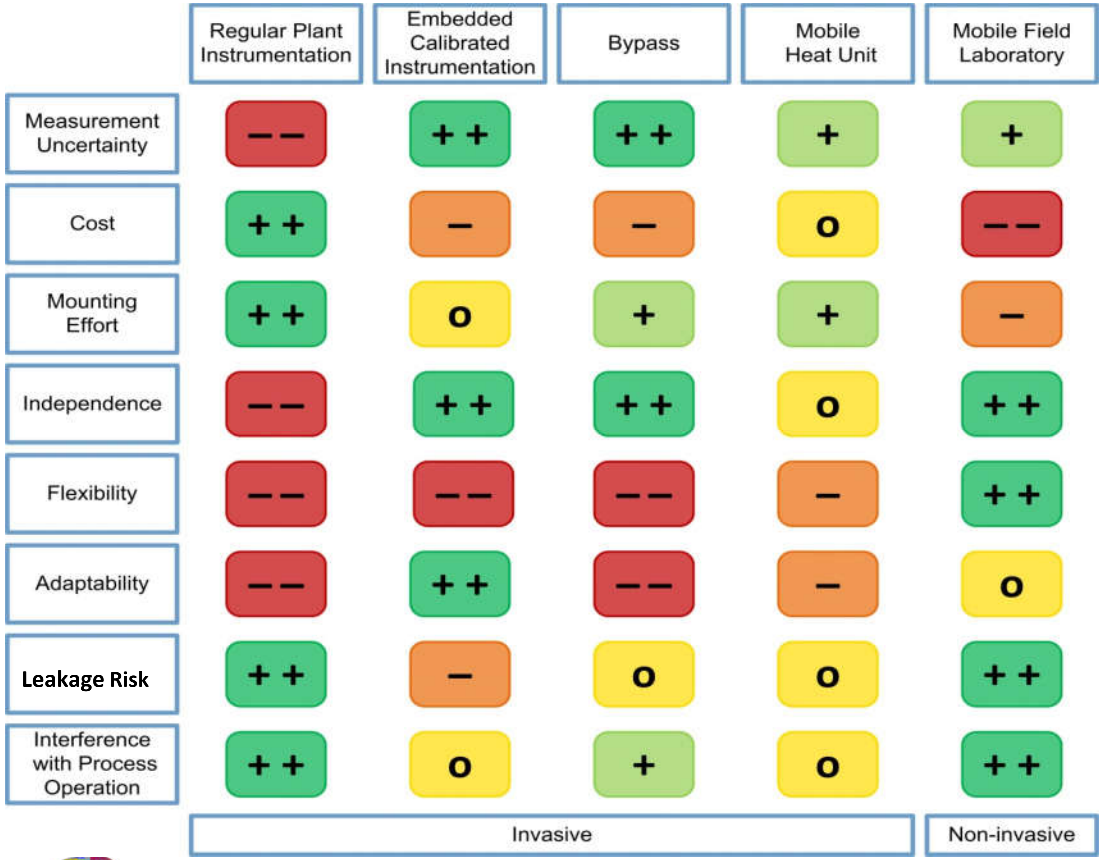

	Regular Plant Instrumentation	Embedded Calibrated Instrumentation	Bypass	Mobile Heat Unit	Mobile Field Laboratory
Measurement Uncertainty	– –	+ +	+ +	+	+
Cost	+ +	–	–	o	– –
Mounting Effort	+ +	o	+	+	–
Independence	– –	+ +	+ +	o	+ +
Flexibility	– –	– –	– –	–	+ +
Adaptability	– –	+ +	– –	–	o
Leakage Risk	+ +	–	o	o	+ +
Interference with Process Operation	+ +	o	+	o	+ +
	Invasive				Non-invasive

Trend of cost and mounting effort increasing with increasing flexibility and adaptability

Individual choice depends on prioritization of eligibility criteria

DLR‘s choice as independent research institution:
Mobile Field Laboratory

Mobile Field Laboratory

Challenges in Measuring Fluid Bound Quantities with clamp on Sensors

- High fluid temperatures (300-400°C)
    - Mounting of sensors
    - need for monitoring
    - temperature gradient to surroundings (temperature measurement)
    - sensor durability (flow rate measurement)
    - Contact/Coupling
- Choice of measurement location
    - At system boundaries
    - Fully developed flow profile
    - Accessibility restrictions in practice
- off-shelf solutions scarcely available for specific application
- Data quality and uncertainty determined by sensor and mounting quality
- Tendency of underestimation of temperature and flow rate

$$\eta_{th} = \frac{\dot{Q}_{th}}{\dot{Q}_{Solar}} = \frac{\dot{m} \cdot c_p (T_{\text{out}} - T_{\text{in}})}{A_{\text{net}} \cdot E_{\text{b}} \cdot \cos(\theta) \cdot \chi^{3/2}}$$

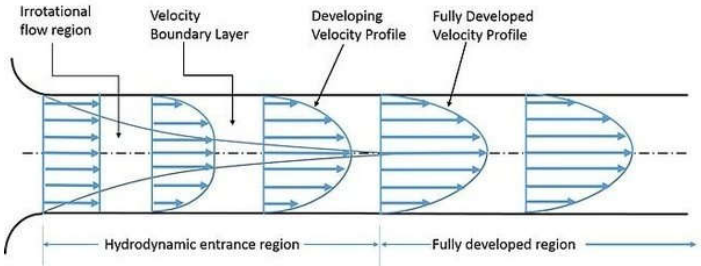

Mobile Field Laboratory

Volume Flow Measurement

- Clamp-on ultrasonic flow meter with WaveInjector (by Flexim)
    - Travel time difference measurement
    - Clamp-on HTF temperature measurement → mass flow rate calculation
- WaveInjector
    - Thermal decoupling of ultrasonic sensors from hot pipe
    - Increase in measurement uncertainty
- Qualification:

in comparison to inline reference Coriolis measurement at KONTAS test facility (PSA) shows an underestimation of measurements by about 1%

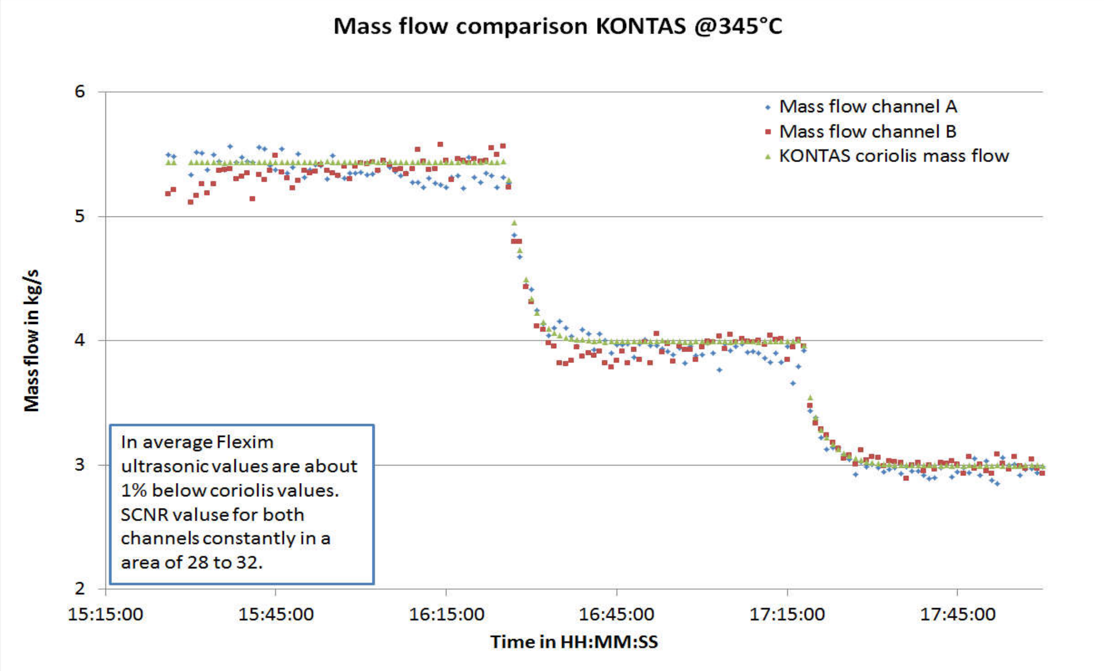

In average Flexim ultrasonic values are about 1% below coriolis values. SCNR value for both channels constantly in a area of 28 to 32.

Mobile Field Laboratory

Fluid Temperature Measurement

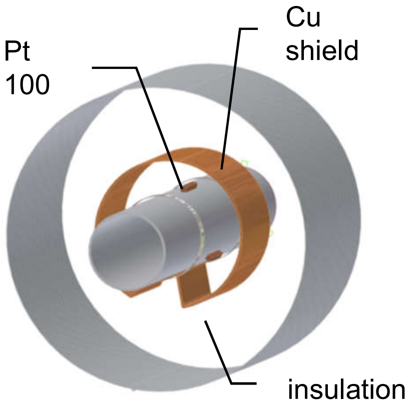

Measurement Set-Up

Clamp-on temperature measurement using PT100 sensors with brass blocks, copper shields, heat conductive paste and insulation)

- Minimization of temperature gradient across sensor setup by creating hot surroundings
- 2-3 sensors

Qualification

In comparison to inline reference temperature sensors at KONTAS test facility (PSA) clamp on sensors show some variation and remaining temperature differences increasing with temperature (up to about 1K)

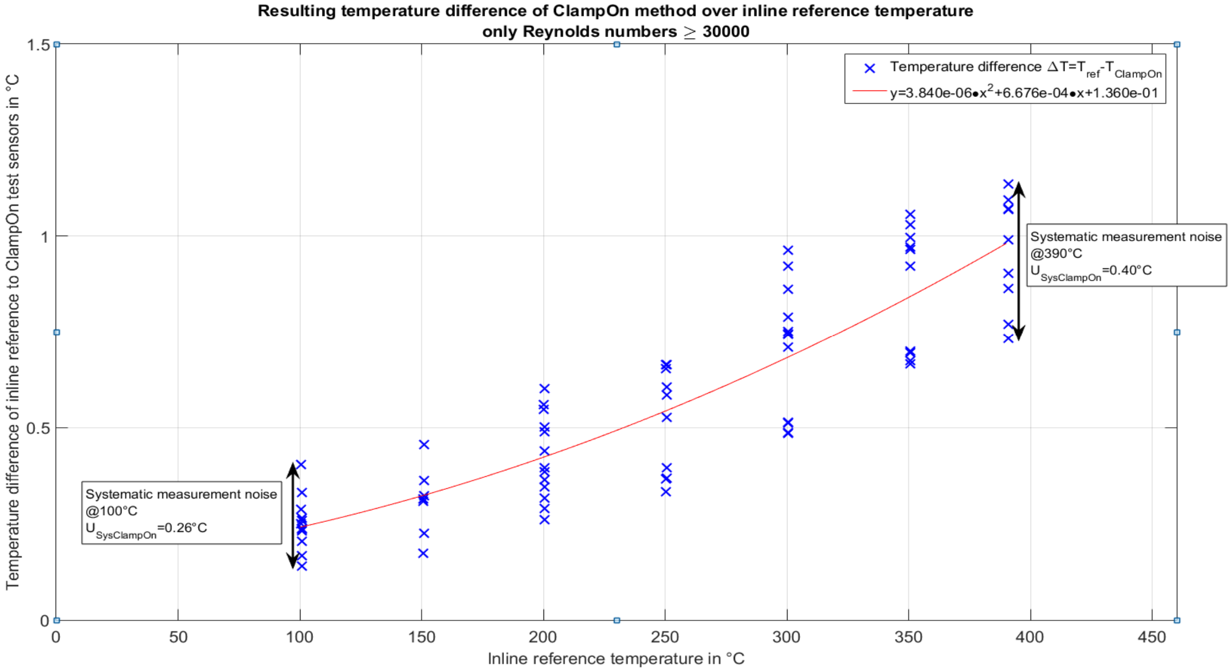

Systematic measurement noise @100°C $U_{SysClampOn}$=0.26°C

Systematic measurement noise @390°C $U_{SysClampOn}$=0.40°C

Data Analysis + Evaluation

Requirements

- Collected data base:
    - Synchronous
    - Complete including all relevant signals
    - checked

- Parameterized validated performance model capable of mapping dynamics of the solar field/loop under investigation

- Adequate Tool for numerical parameter identification by optimization

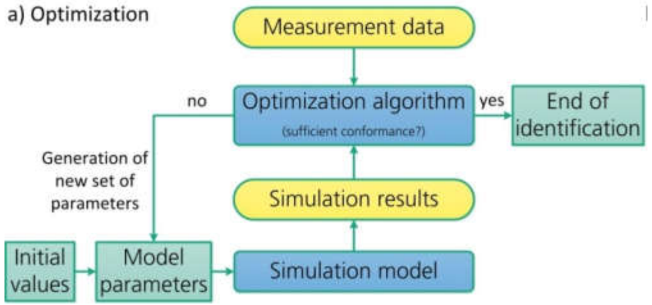

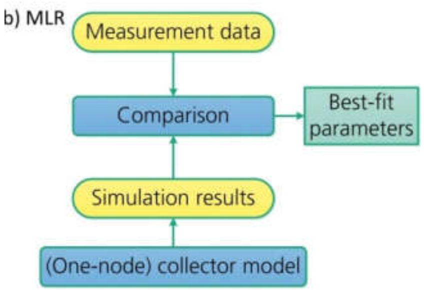

A. Zirkel-Hofer, 2018: Enhanced dynamic performance testing method for line-concentrating solar thermal collectors. Dissertation, Cuvillier Verlag, 2018

Data Analysis + Evaluation

Parameterized Dynamic Solar Field Performance Model

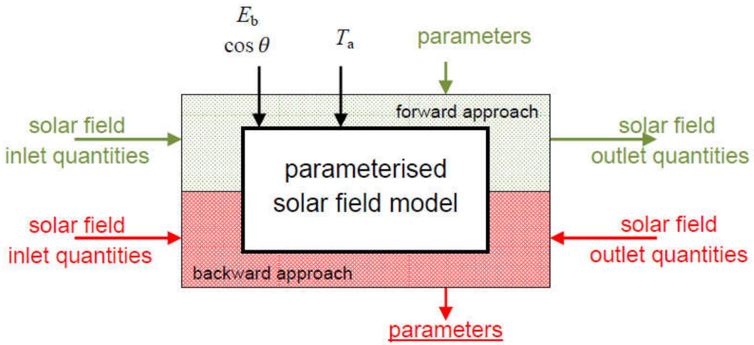

Modelling approach for parameter identification from test data for field performance prediction for given field parameters and ambient conditions.

$$\dot{Q}_{th} = \chi^{3/2} \cdot A_{net} \cdot E_b \cdot \cos(\theta) \cdot \eta_{opt,0} \cdot \kappa(\theta) \cdot f_{endloss} \cdot f_{shade} \cdot f_{focus} - c_1 \cdot (T_m - T_{amb}) - c_2 \cdot (T_m - T_{amb})^2 - c_3 \frac{dT_m}{dt}$$

with

$$\kappa(\theta) = 1 - b_1\theta - b_2\theta^2$$

coefficients	definition
$\eta_{opt,0}$	optical efficiency
b_1, b_2	IAM coefficients
c_1, c_2	thermal loss coefficients
c_3	specific heat capacity coefficient

Residence time effects are considered through a CSTR model (continuous stirred tank reactor)

Perfect mixing of fluid in each tank is assumed

Time stamp i-1

Time stamp i

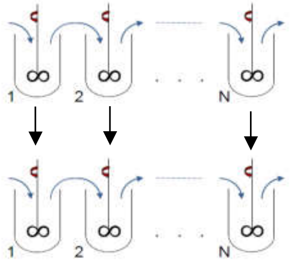

$$m_i^j = (m_{i-1}^j - \Delta m_{i-1}^j) + \Delta m_i^{j-1}$$

$$h_i^j = \frac{m_{i-1}^j h_{i-1}^j + \Delta m_i^{j-1} h_i^{j-1}}{m_i^j}$$

$$T_i^j = f(h_i^j), \quad \rho_i^j = g(h_i^j)$$

$$\Delta m_i^j = \rho_i^j \cdot V_i$$

Data Analysis + Evaluation

Model Performance ↔ Measured Performance

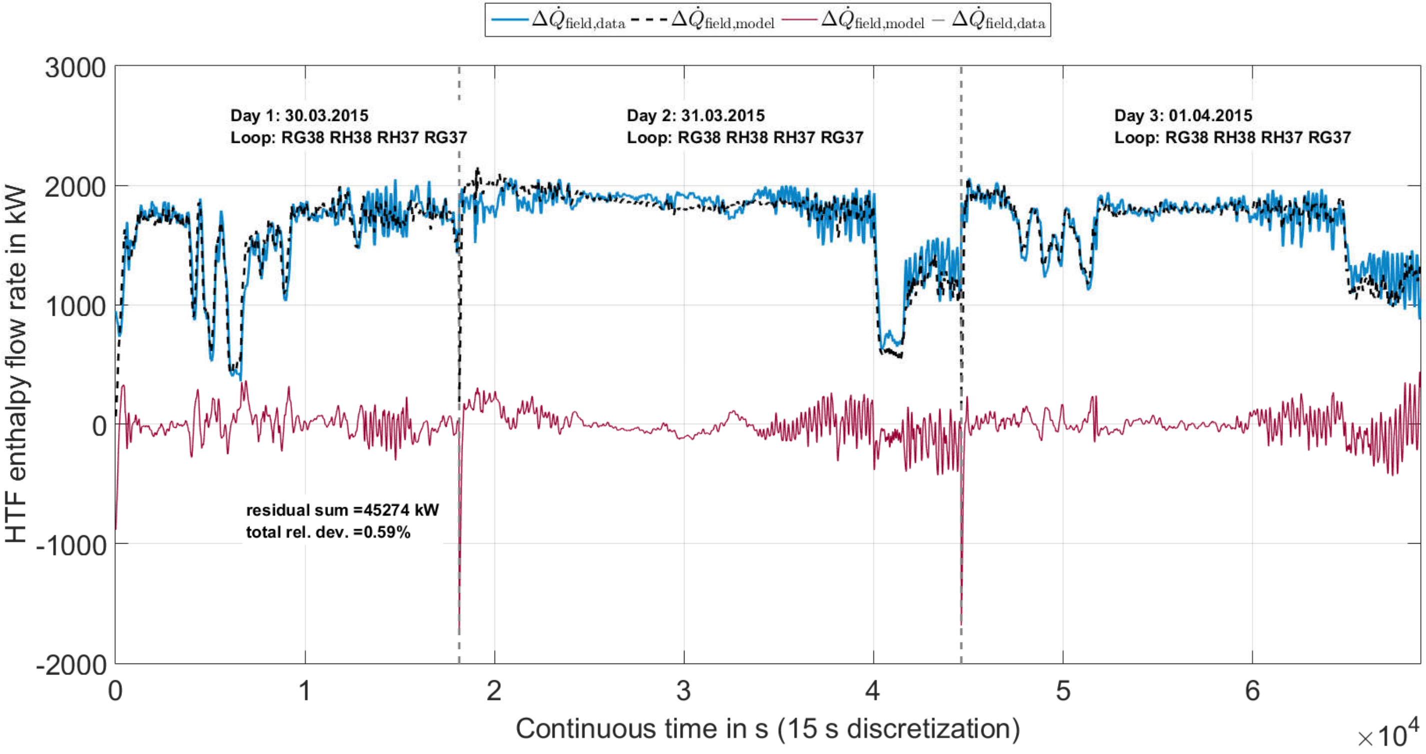

Data Analysis + Evaluation

PDPM for subfields

- Condensing all parallel loops into one average loop
- Only overall performance characteristics no individual loop characteristics
- Target quantity: Thermal power of solar subfield

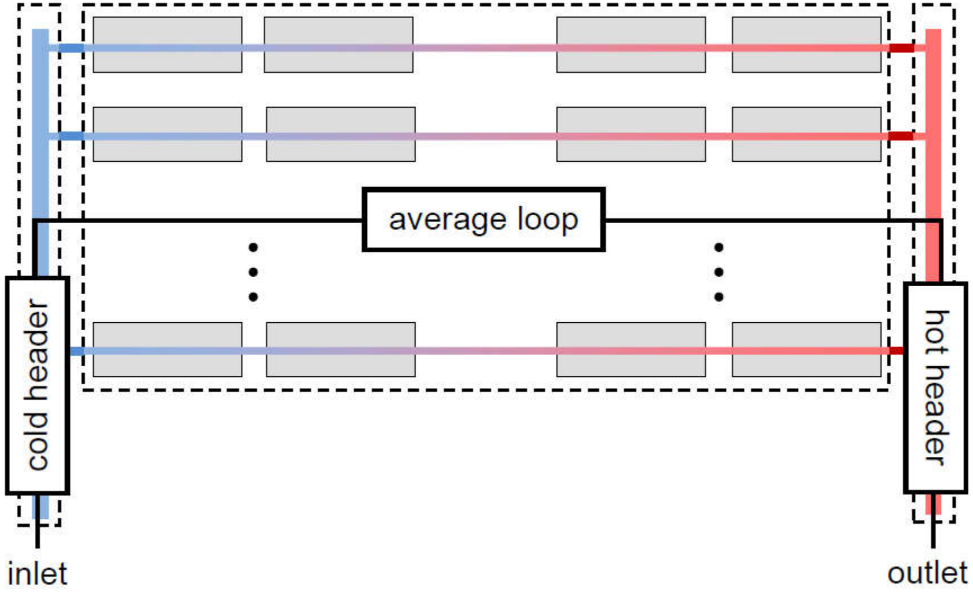

Practical Application

AS3 Loop Performance Testing

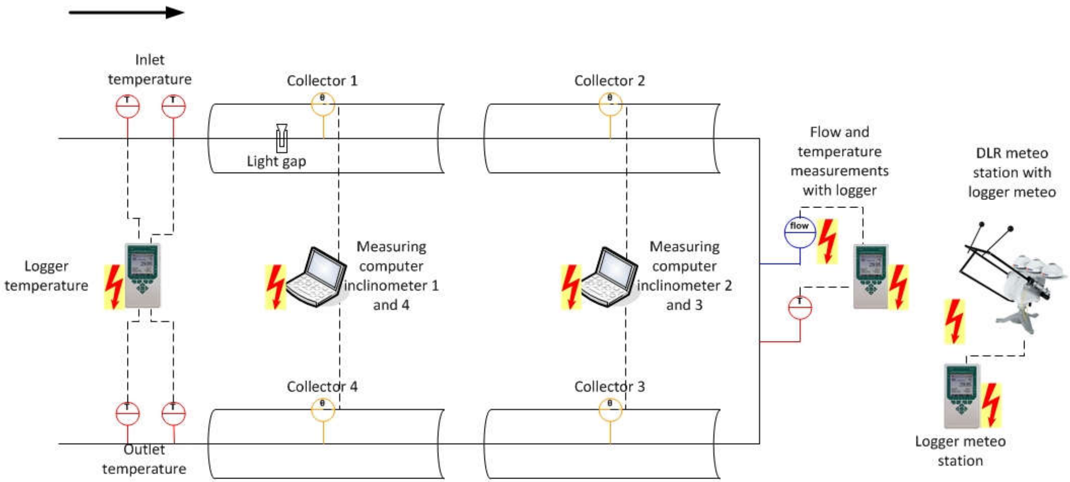

- Performance Measurements of several loops in AndaSol3 in 2015
- Mobile Field Laboratory (clamp-on sensors, weather station + DAS network)
- Evaluation using PDPM

Practical Example

Loop Analysis Results

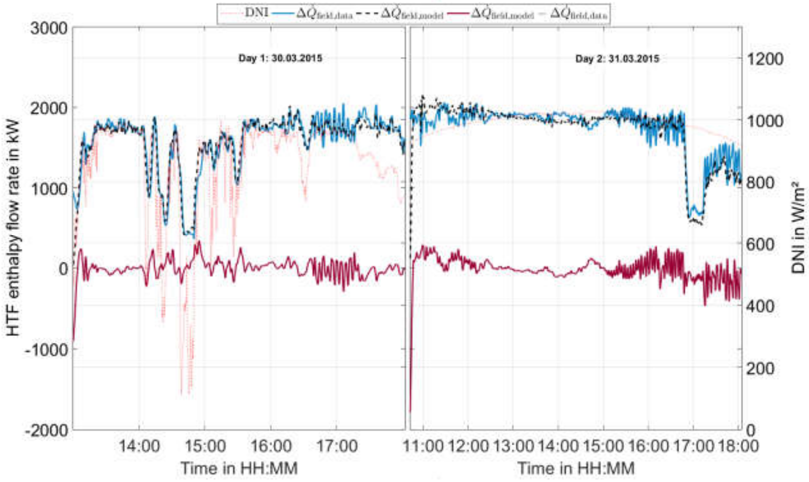

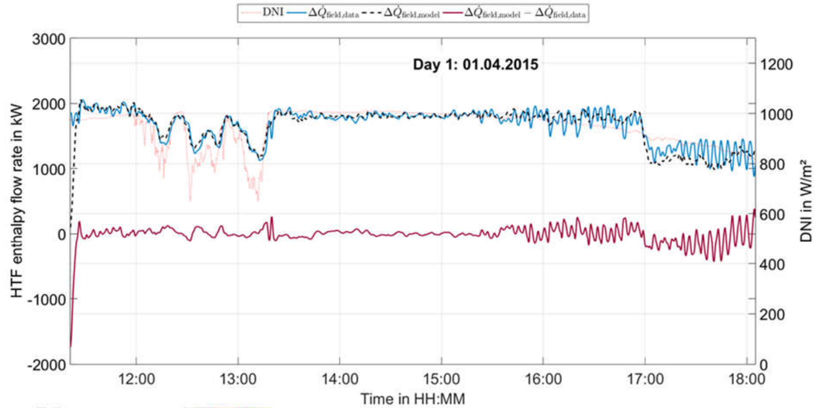

- Parameter Identification based on data of 2 test days

	value	unit
$\eta_{opt,0}$	0,804	-
b_1	2,7433E-04	1/°
b_2	1,4295E-04	1/°²
c_1	6,6941E+02	W/(m²K)
c_2	4,3108E-03	W/(m²K²)
c_3	5,3379E-08	J/(m² K)

- Deviation between measured and modeled thermal performance -0,39%
- Validation on data of third measurement day

→ deviation between measured and modeled thermal performance 0,4%

Practical Application

Results + Interpretation

- Different quality loops distinguishable from evaluation results
- Thermal performance results in good agreement with previous optical characterization
- Confirmation of hypothesis of differing actual overall performance of structurally identical loops in the field

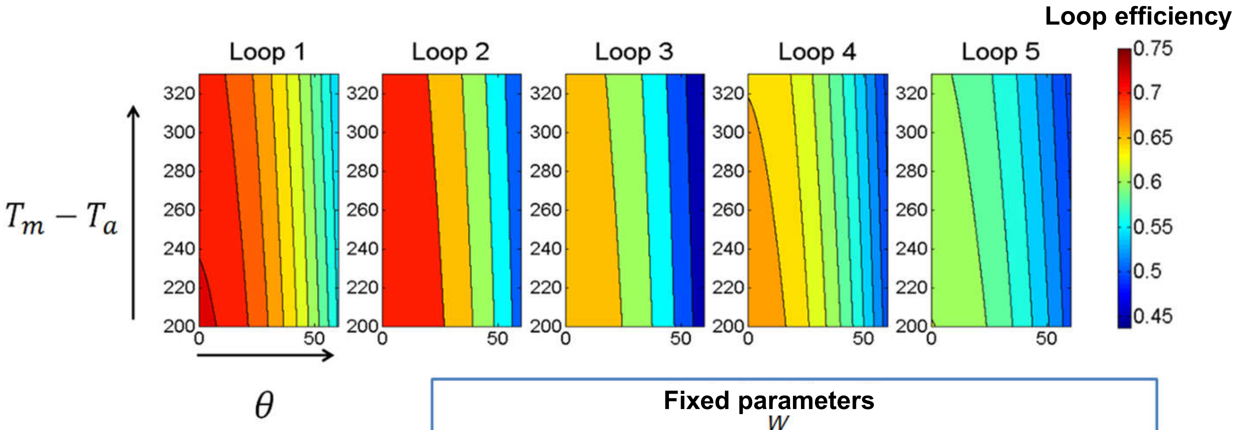

Fixed parameters

$$DNI = 800\frac{W}{m^2}, \qquad \chi = 0,97$$

Summary

- In situ performance testing as means of characterizing, veryfying and monitoring solar collector systems at their site of installation
- Various measurement approaches available according to testing requirements and legal / financial / technical framework or conditions
- Mobile Field Laboratory as DLR‘s favoured option introduced in detail
- Application of Mobile Field Laboratory for loop performance evaluation demonstrated

- Official references for in situ performance testing
    - SolarPACES Best Practice Guideline DisPAT - Dynamic in situ Performance and Acceptance Testing of Line-Focus Solar Thermal Collectors and Fields (under preparation)
    - UNE 201614:2017 Tests for the determination of the solar field efficiency of solar thermal power plants with parabolic trough collector technology
    - IEC 62862-3-4: Code for the solar field performance test of parabolic trough solar thermal electric plants (under preparation)

THANK YOU FOR YOUR ATTENTION!
ANY QUESTIONS?

SFERA-III
Solar Facilities for the European Research Area

Solar Facilities for the European Research Area

2nd Training for Industries *"Optimization of CST plant output by optical and thermal characterization and target-oriented O&M"*
26 – 29 April 2022, Plataforma Solar de Almería, Spain

Solar Resource Measurement

Stefan Wilbert, DLR

NETWORKING

THIS PROJECT HAS RECEIVED FUNDING FROM THE EUROPEAN UNION'S HORIZON 2020 RESEARCH AND INNOVATION PROGRAMME UNDER GRANT AGREEMENT NO ***823802***

Measurement of Solar Radiation

Overview

1. Solar Radiation in the Atmosphere: Definitions
2. Measurement principles
3. Sensor calibration
4. Other measurands
5. Quality control

Stefan Wilbert

- Team leader of the research group “Solar Energy Meteorology” within the department “Qualification” of DLR’s Institute of Solar Research
- >15 years of professional experience in solar energy and solar radiation measurement
- Degree Dr. rer. nat. for the thesis “Determination of Circumsolar Radiation and its Effect on Concentrating Solar Power”, RWTH Aachen
- Degree as Physicist (Dipl.-Phys.), University of Bonn; thesis “Further Development of an Optical Measurement System for the Determination of Shape Inaccuracies of Concentrating Solar Power Collectors Under Dynamic Wind Influence”
- Leader of subtask 1 “Resource assessment methodologies” in IEA PVPS task 16 “Solar Resource for High Penetration and Large Scale Applications” (mirrored to SolarPACES T5)
- Main topics
    - irradiance and other meteo data for solar energy
    - measurement and modelling of soiling of solar collectors
    - nowcasting of irradiance and soiling
    - standardization of solar resource assessment
- stefan.wilbert@dlr.de
- http://www.dlr.de/sf/en/desktopdefault.aspx/tabid-8724/14207_read-35930/

Solar Radiation in the Atmosphere: Definitions

DNI

… is what's interesting for CST

DNI = Direct Normal Irradiance

- Irradiance (W/m²)
  - caused by light coming "directly from the sun"
  - measured in a plane normal to the beams coming from the center of the sun

- Tracking imperfections of DNI measurement instruments exist

⟶ WMO defines opening angle of 2.5° for DNI measurements

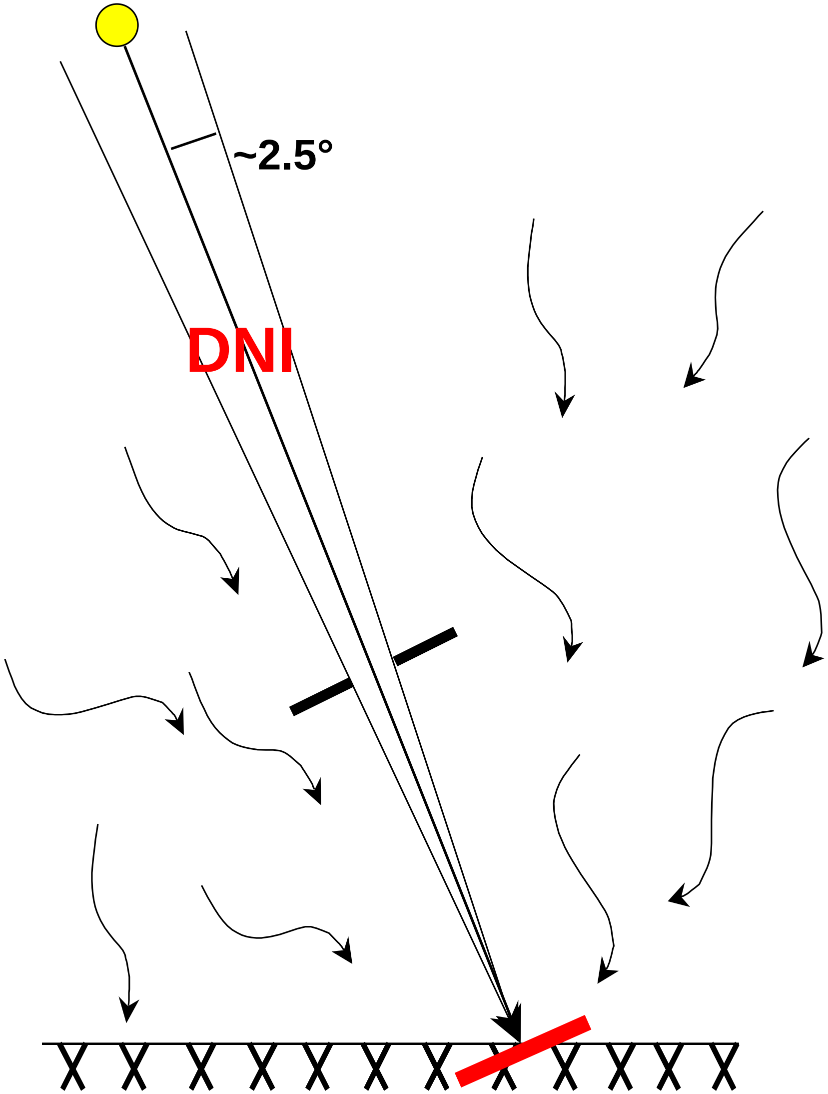

Solar Radiation in the Atmosphere: Definitions

DHI

- DHI = Diffuse Horizontal Irradiance
- Irradiance (W/m²)
  - caused by light coming from the upper half sphere
  - but excluding light which is coming “directly from the sun“
  - measured in a horizontal plane
- Caused by Atmospheric Scattering
- WMO:
  - Exclude 2.5° around the sun

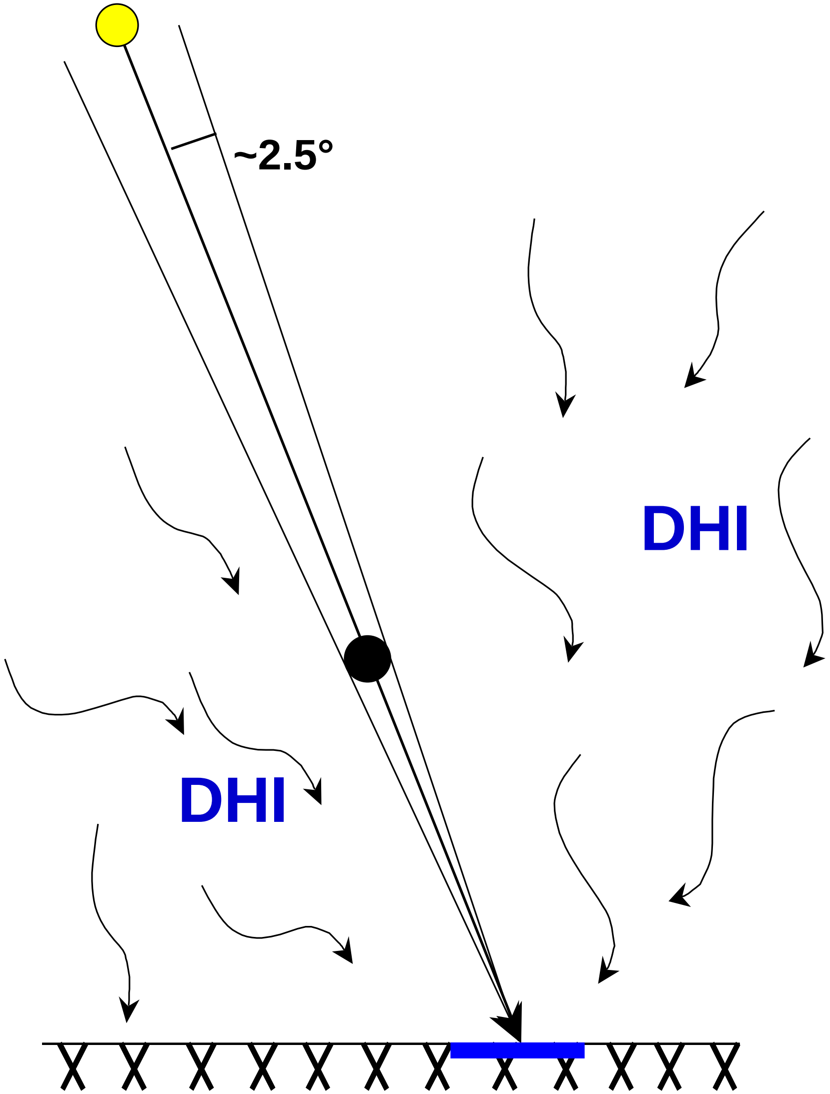

Solar Radiation in the Atmosphere: Definitions

GHI

- GHI = Global Horizontal Irradiance
- Irradiance (W/m²)
    - caused by direct and scattered light which is coming from the upper half sphere
    - measured in a horizontal plane

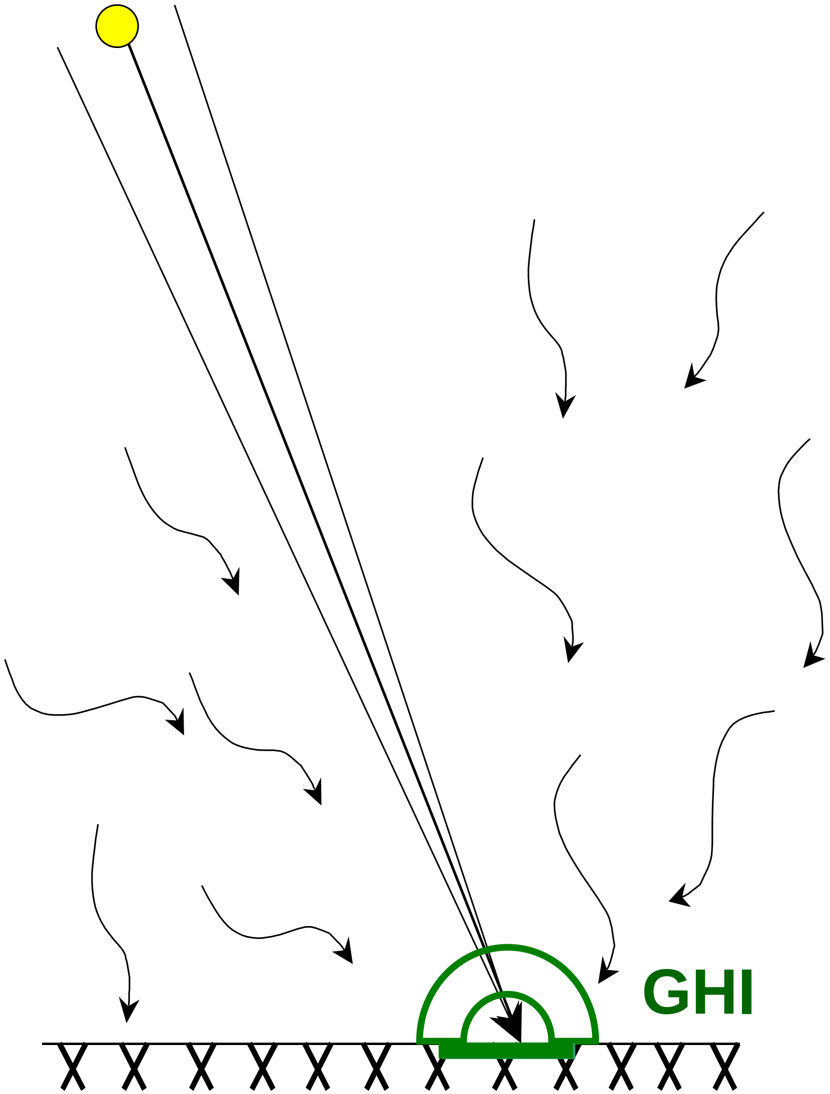

Solar Radiation in the Atmosphere: Definitions

GHI, DHI and DNI

- GHI = Global Horizontal Irradiance
- DHI = Diffuse Horizontal Irradiance
- DNI = Direct Normal Irradiance

GHI = DHI + DNI *cos(SZA)

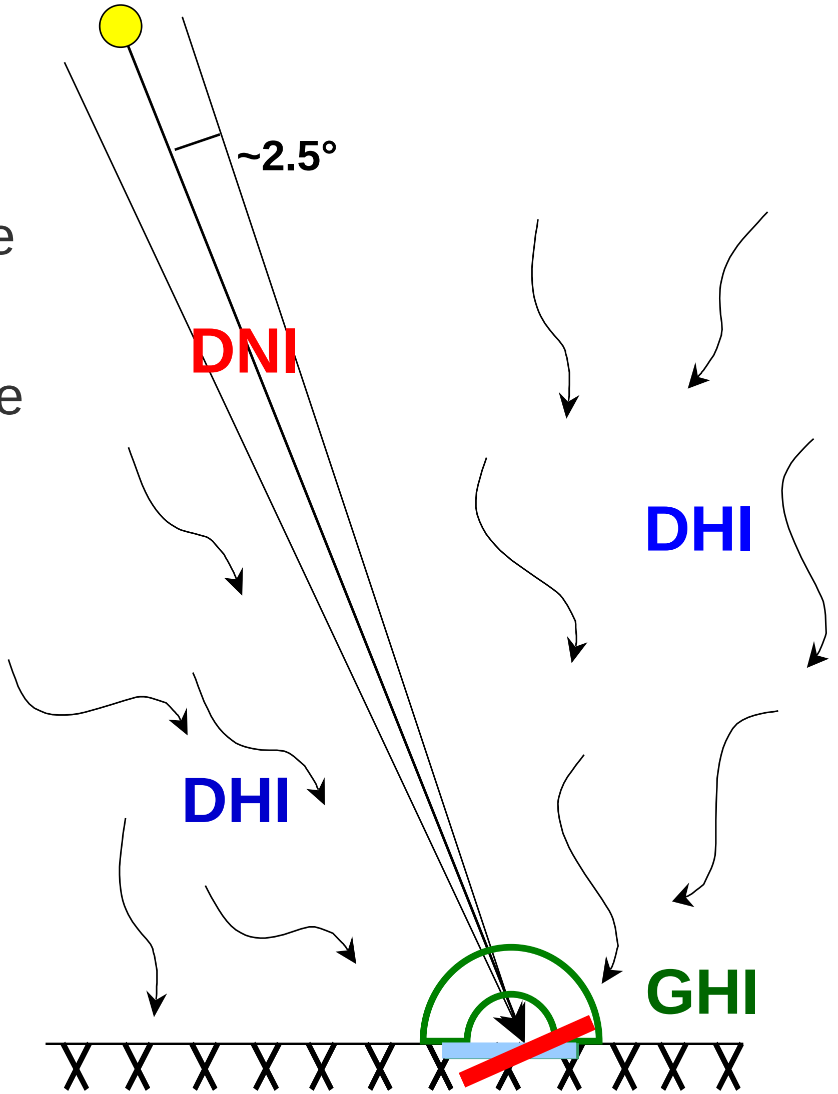

Measurement principles – **Examples and Challenges**

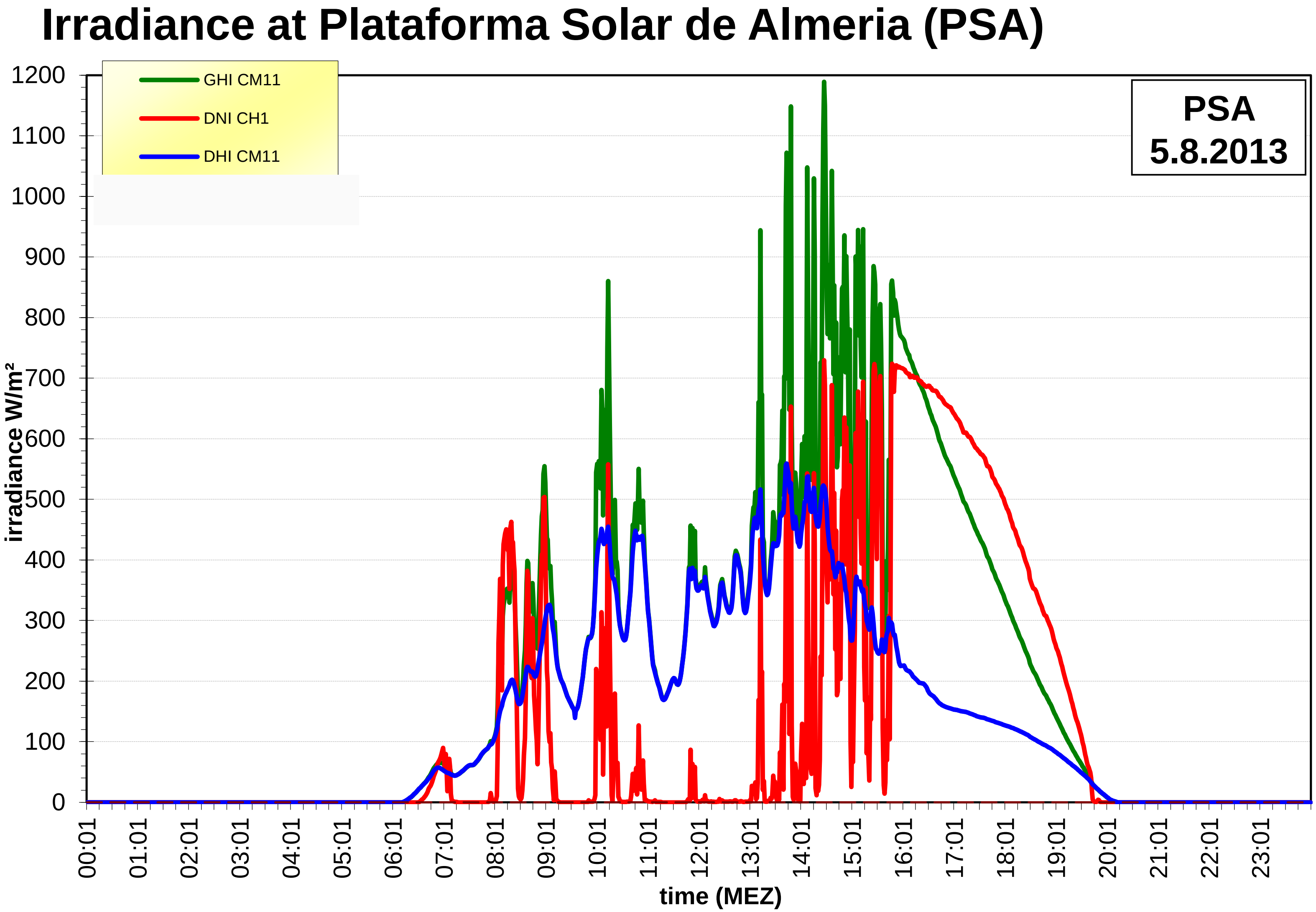

Solar Radiation in the Atmosphere: Definitions

GTI

- Is what is used by PV and flat plate collectors
- GTI = Global Tilted Irradiance
  - Plane of array POA
- Irradiance (W/m²)
  - caused by direct and scattered light which is coming from the half sphere above the surface
  - measured in a tilted plane

- For bifacial PV now also of interest:
  - Rear side POA (not shown)

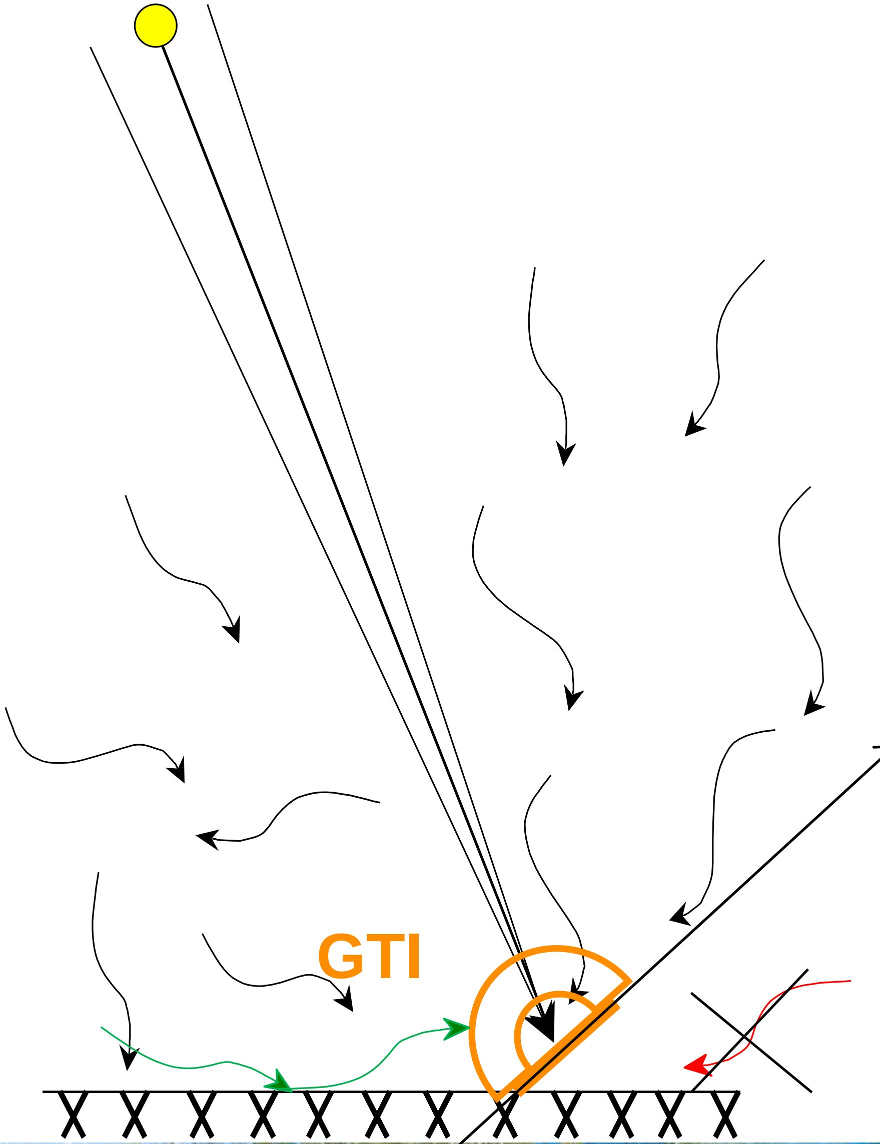

Measurement principles – **Thermopile sensors**

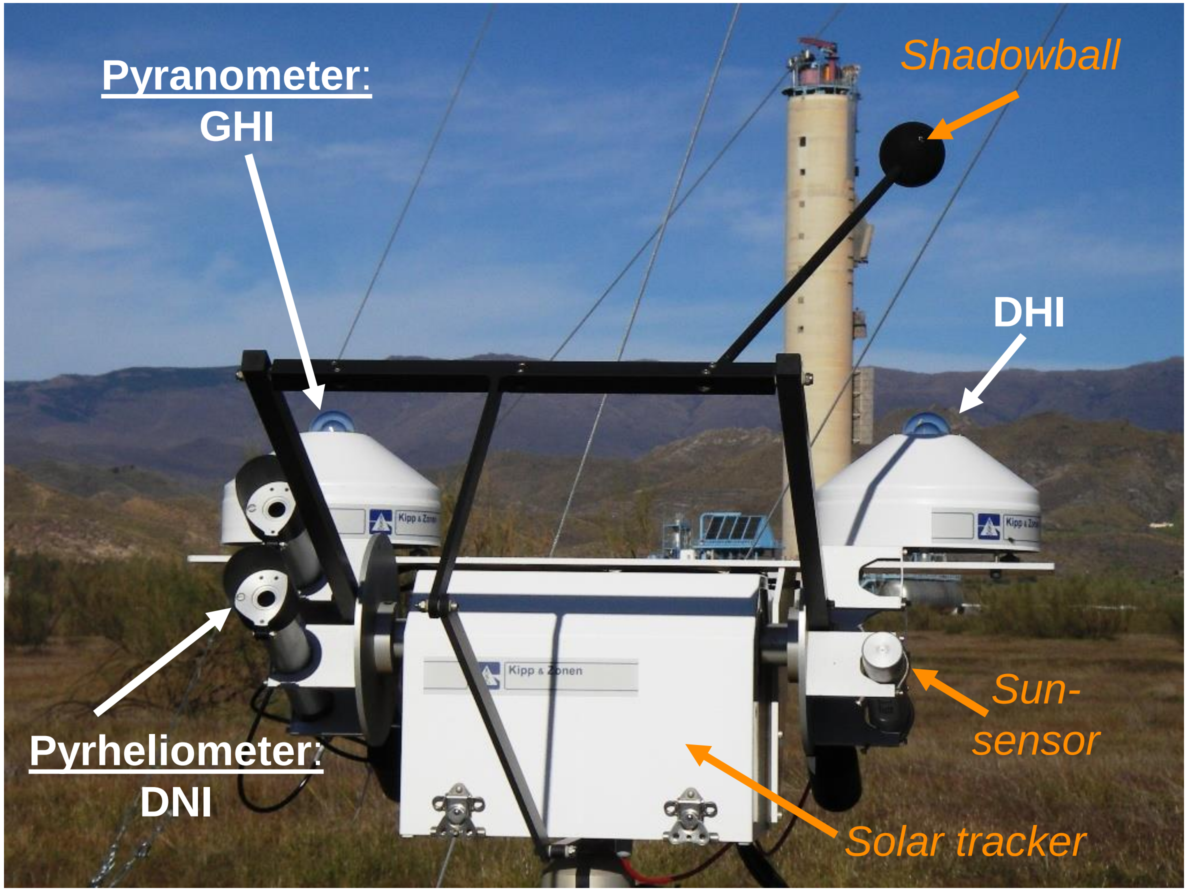

- Tracker follows the sun:

Algorithm (lon, lat, height/pressure) +

Sun sensor (4 quadrant sensor, gives four signals, equal signals if tracked)

→ Controls tracker

DNI: Directly from sun, measured normal to central beam → Pyrheliometer

GHI: Total power on horizontal plane → Pyranometer

DHI: Total power on horizontal plane without direct radiation → Pyranometer + Shadowball

Measurement principles – **Thermopile sensors**

Summary: thermal sensors: Pyrheliometer and Pyranometer

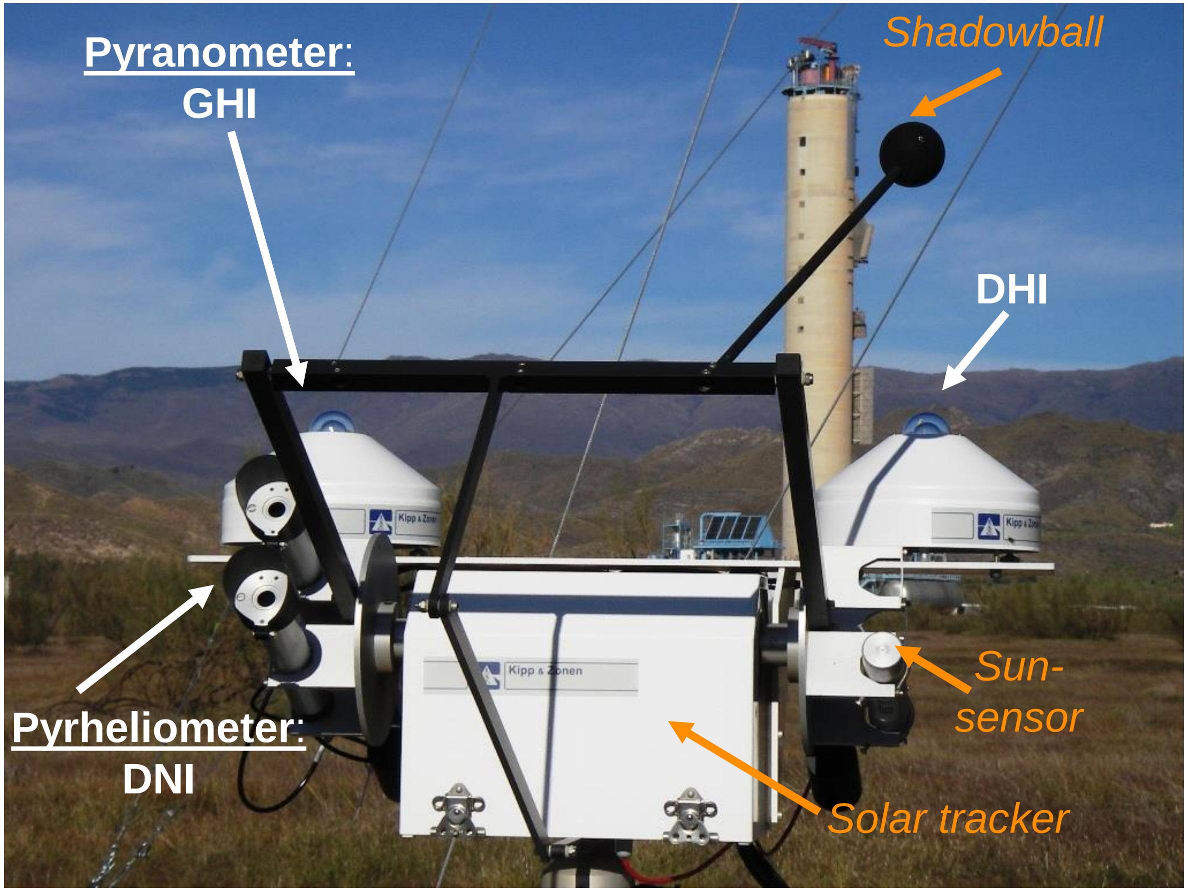

on a solar 2-axis tracker

Advantage:

+ high accuracy (1 to 2%, DNI)

+ separate sensors for GHI, DNI and DHI *(cross-check through redundancy)*

Disadvantages:

- high costs *(also O&M)*
- high susceptibility for soiling
- high power supply

Measurement principles – **Photodiode pyranometer**

- Photodiodes below diffusor disk
- Often higher temperature dependence of sensitivity
- Often higher cosine errors (incidence angle dependency of sensitivity)
- Spectral response of photoelectric sensors
  - is not flat and does not match solar spectrum
- Higher uncertainty than thermal sensors
- Less affected by soiling!

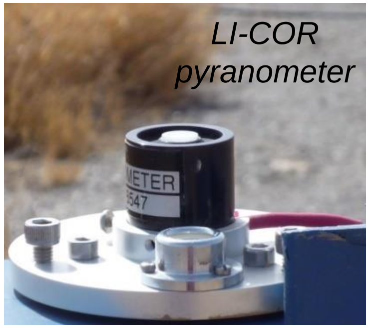

LI-COR pyranometer

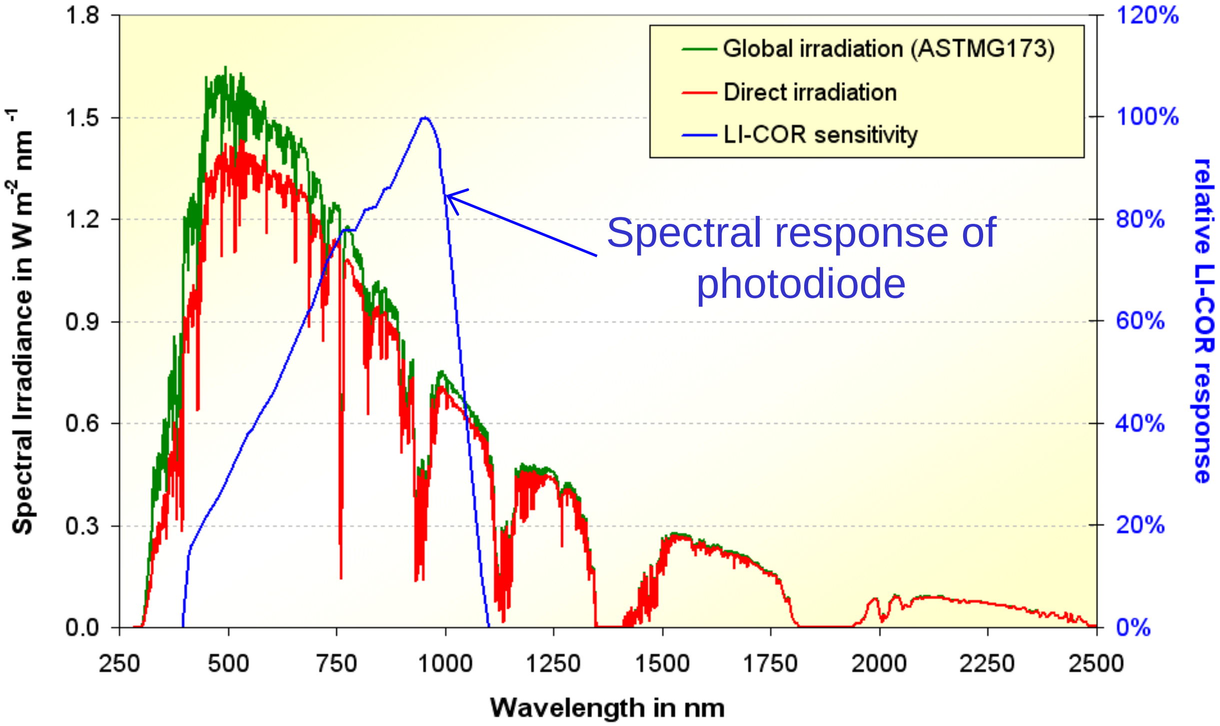

Correction functions – incidence angle correction

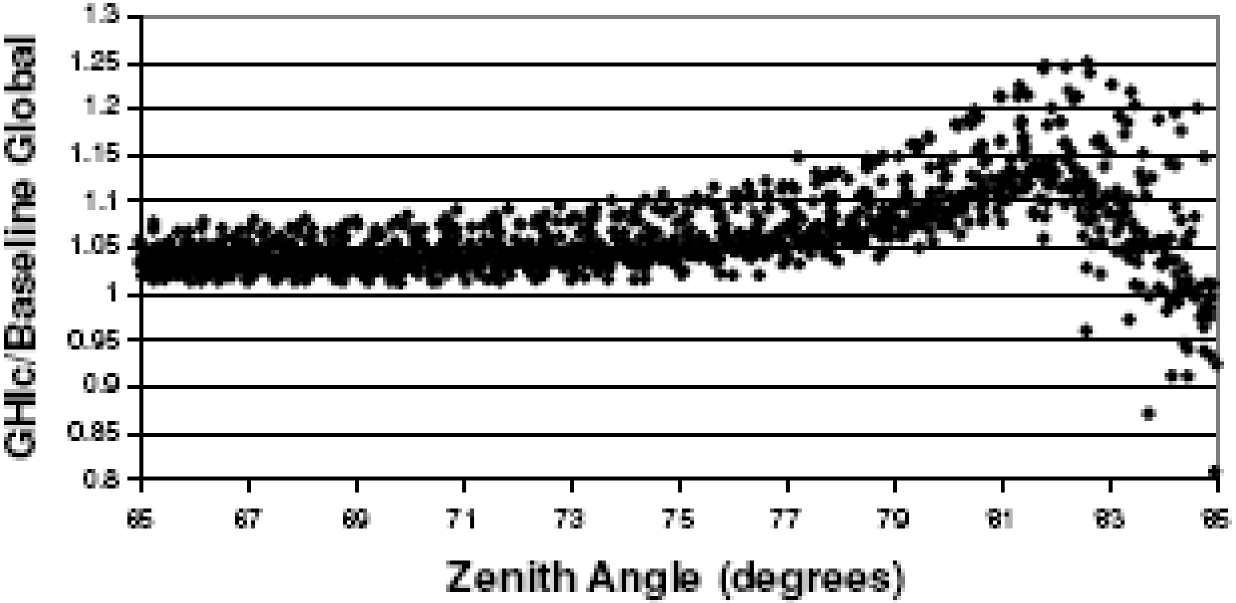

Correction functions – Temperature correction

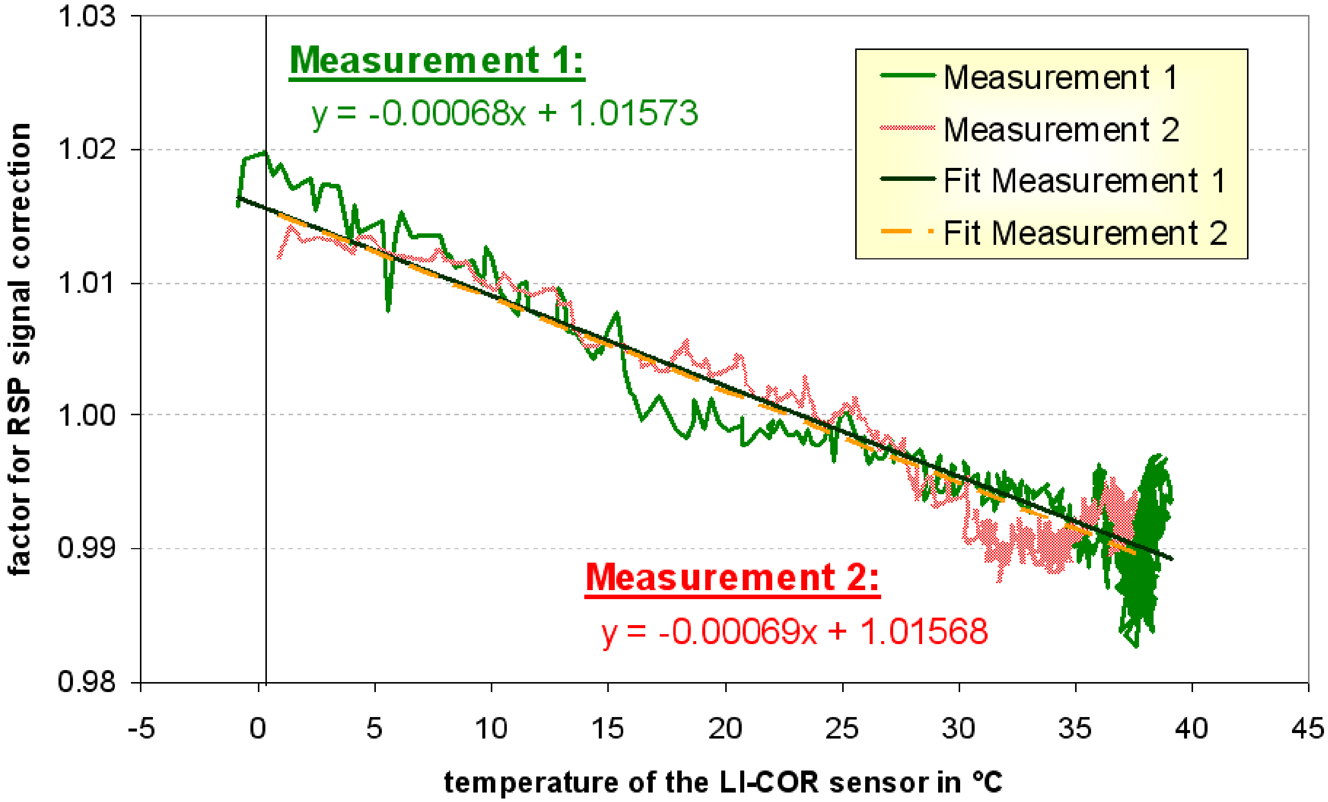

$$\boxed{CF_{temp} = (1 - 0.0007 \cdot (T_{LI-COR} - 25°C))}$$

Most important difference between thermopile sensors and photodiode sensors (RSI) – spectral error

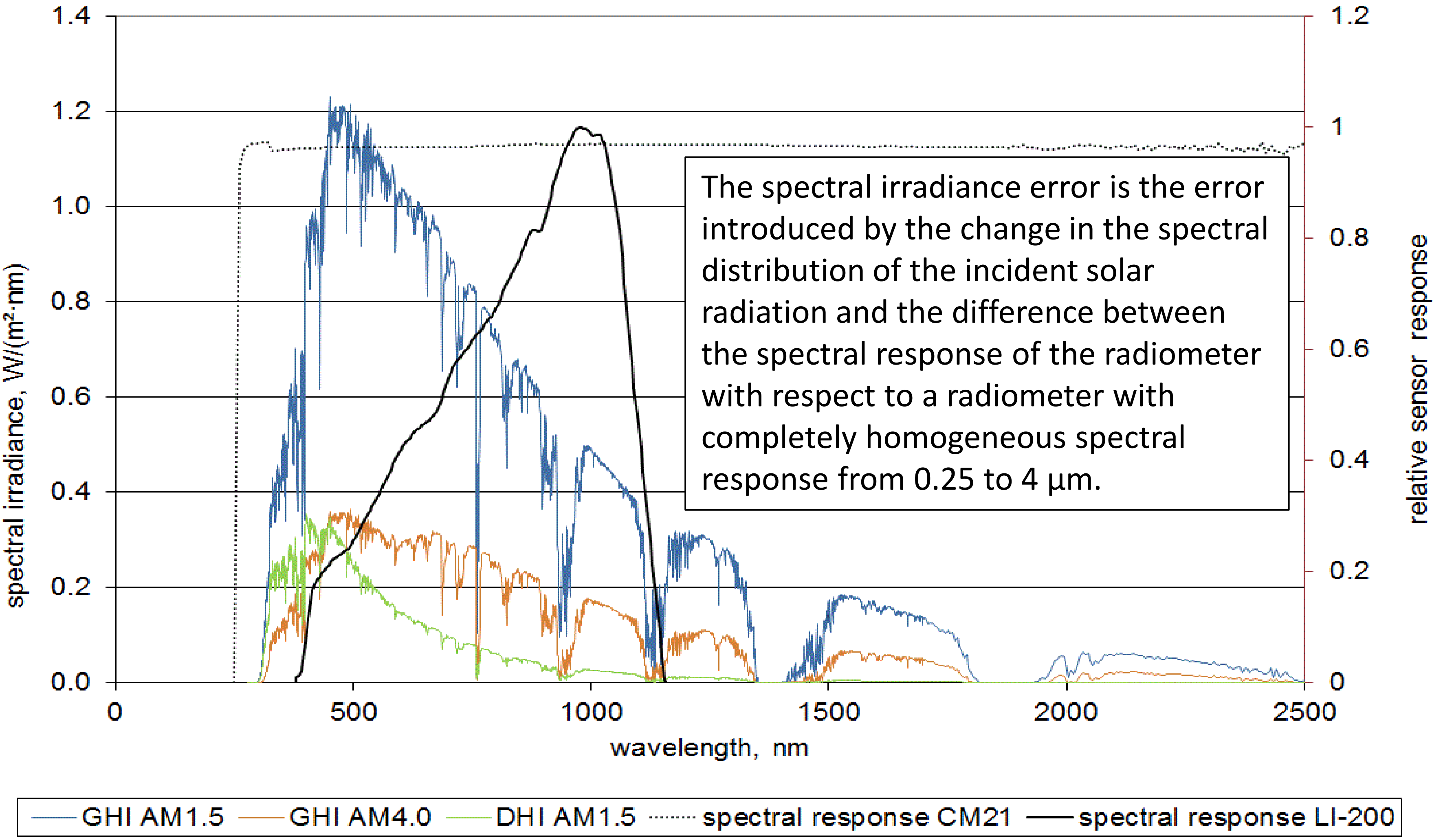

The spectral irradiance error is the error introduced by the change in the spectral distribution of the incident solar radiation and the difference between the spectral response of the radiometer with respect to a radiometer with completely homogeneous spectral response from 0.25 to 4 µm.

Measurement principles – Rotating Shadowband Irradiometer (RSI)

- Pyranometer measures Global Horizontal Irradiance (GHI)
  - photodiode

- Shadowband rotates every minute

- During rotation the signal is logged with high frequency
  - When shadow falls on the sensor Diffuse Horizontal Irradiance (DHI) is measured

- Alternative names: RSR (Rotating Shadowband Radiometer) and RSP (Rotating Shadowband Pyranometer)

Measurement principles – Rotating Shadowband Irradiometer (RSI)

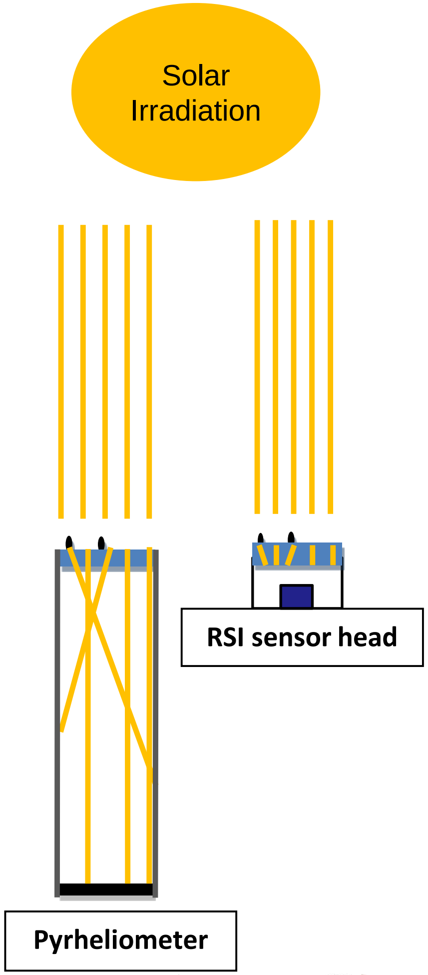

Soiling characteristics of pyrheliometers and RSIs

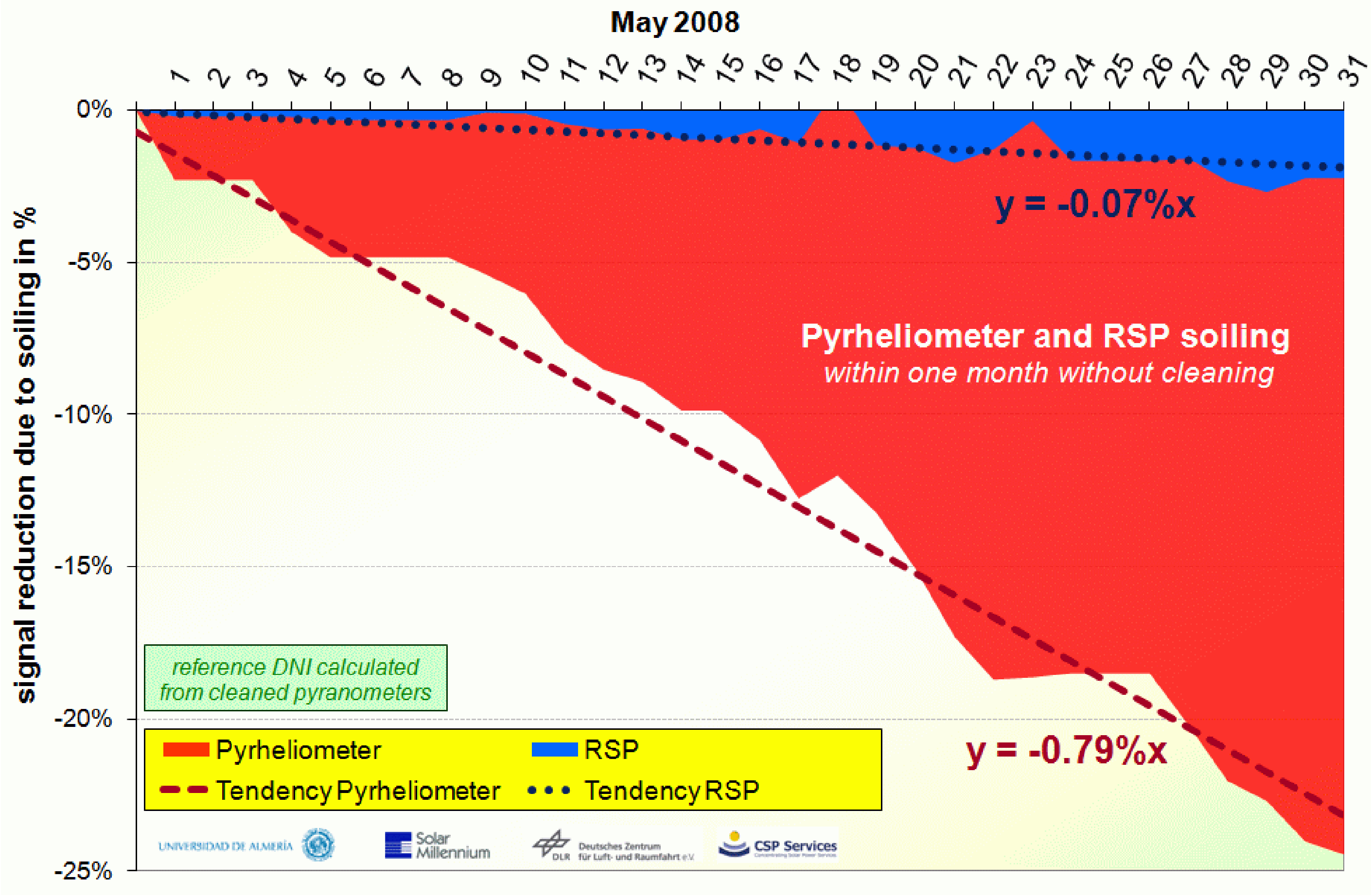

Measurement principles – Rotating Shadowband Irradiometer (RSI)

Advantages of RSI:

+ fair acquisition costs
+ low maintenance
+ low soiling sensitivity
+ low power demand *(PV panel)*

Disadvantages:

- systematic deviations of the measurement signal (Si diode)

Systematic errors can be corrected

2-3% uncertainty for DNI, 10min

Delta-T Devices, Ltd., SPN1

- The detectors are positioned under diffuser disks and a special shadow mask.
- The shape of the mask is selected such that for any position of the sun in the sky
  - there is always **one or more detectors that are fully shaded** from the sun
    - those are **exposed to approximately half of the diffuse radiation** (for completely overcast skies)
  - **and one or more detectors are exposed to the full solar beam**
- Diffuse = 2 * MIN
- Direct = MAX – MIN
- Global = Direct + Diffuse = MAX + MIN

Delta-T Devices, Ltd., SPN1

- Accuracy: Badosa et al. (2014)

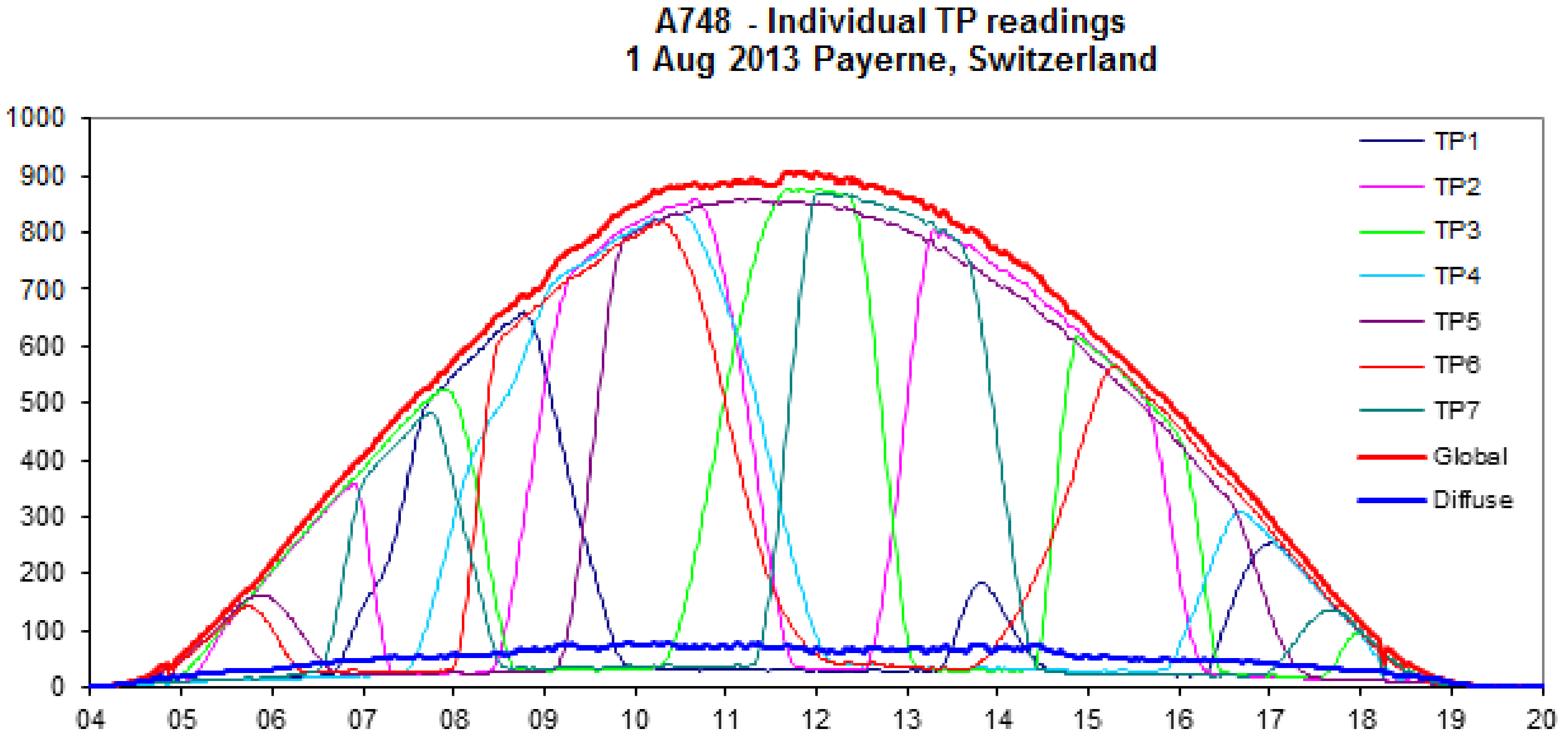

Radiometer choices

- (Thermopile) pyranometers for GTI, GHI, rear-side POA
- Solar trackers with pyrheliometers (DNI) & shaded pyranometers (DHI)
  - Accurate if well maintained, but expensive, complex (less robust)
- DNI or DHI measurements without solar trackers
  - RSIs, SPN1, some sunshine duration sensors, all sky imagers…
- *ISO 9060 (Radiometer classification)*
- *Which instruments & how many? -> see monitoring standards*
- For PV reference cells are also of relevance

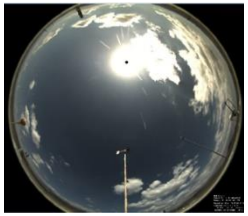

Which radiation components must be measured?

Project phase /standards	Accuracy case	Fixed PV, thermal non-concentrating	Tracked PV	Bifacial PV	Concentrating Solar Technology
Before construction of large solar plant (~IEC TS 62862-1-2)	Basic	GHI	GHI	GHI, RHI (albedo), DifHI	GHI, „DNI or DifHI“
	Enhanced (big plants, complex atmosphere, terrain, technology)	GHI, GTI for specific tilt that has been selected as best option, DNI*, DifHI*, RHI (albedo)**	GHI, DNI, DifHI, RHI (albedo)	GHI, DNI, DifHI, RHI (albedo), GTI	DNI, GHI, DifHI
Monitoring & forecasting for large (& medium) solar plant (IEC 61724-1 for PV, IEC 62862-3-2 et al. for CSP, ISO9806 thermal collectors)	Basic	GHI, GTI	GHI, GTI tracked	GHI, GTI, rearside POA or „RHI (albedos)+DifHI“	DNI or for medium plants „DifHI & GHI“
	Enhanced	GHI, GTI, DNI*, DifHI*, RHI (albedo)**	GHI, GTI tracked, DNI*, DifHI*, RHI (albedos)	GHI, GTI, rearside POA, RHI (albedos), DifHI, DNI*	DNI, GHI, DifHI

- ** for big power plants ~50MW*
- *** high latitude*
- *Best selection of measurements and instruments depends on investment/complexity of site/…*

Maintenance of the station

Stefan Wilbert
DLR
Institute of Solar Research
Qualification
Solar Energy Meteorology

Measurement best practices – O&M

- ISO TR 9901, ASTM G183 = standards for radiometer operation
- All inspections must be documented
- (Week-)daily:
  - cleaning according to ISO TR 9901, ASTM G183
  - alignment
  - condensation on window/dome/lens, damage or wear (cable(s), connector(s), windows, wind vane, …)
  - proper working condition of the ventilator
  - data control (later more)

Measurement best practices – O&M

- Weekly:
  - Pyranometer cleaning according to IEC 61724-1 (debatable, not pyrheliometer)
  - Desiccant (ASTM G 183, monthly or quarterly)
  - Ventilator filter check (monthly ok for clean environment)
- Monthly
  - Azimuth and tilt angles (ASTM G 183 semi-annually)
  - Cabling in more detail
  - Datalogger clock (if 10s error and logger are ok, otherwise more often e.g. daily automatic)
- ~yearly or 2-yearly:
  - Calibration (ISO 9059, 9847, 9846 + ASTM equivalents)

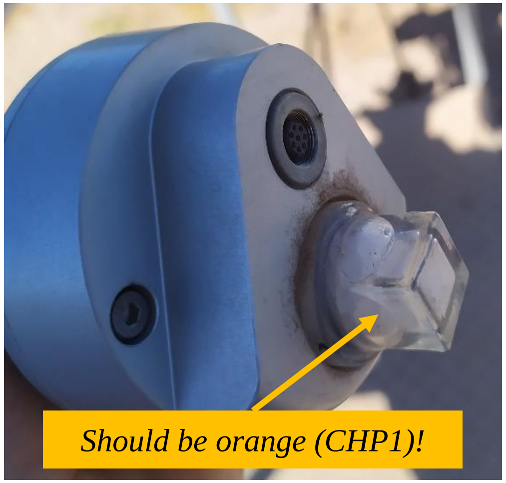

Should be orange (CHP1)!

CIEMAT's calibration bench at PSA

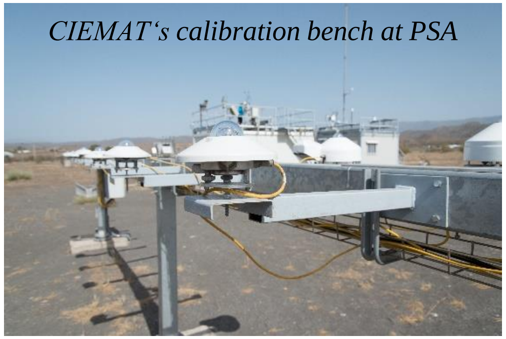

Measurement field protocol

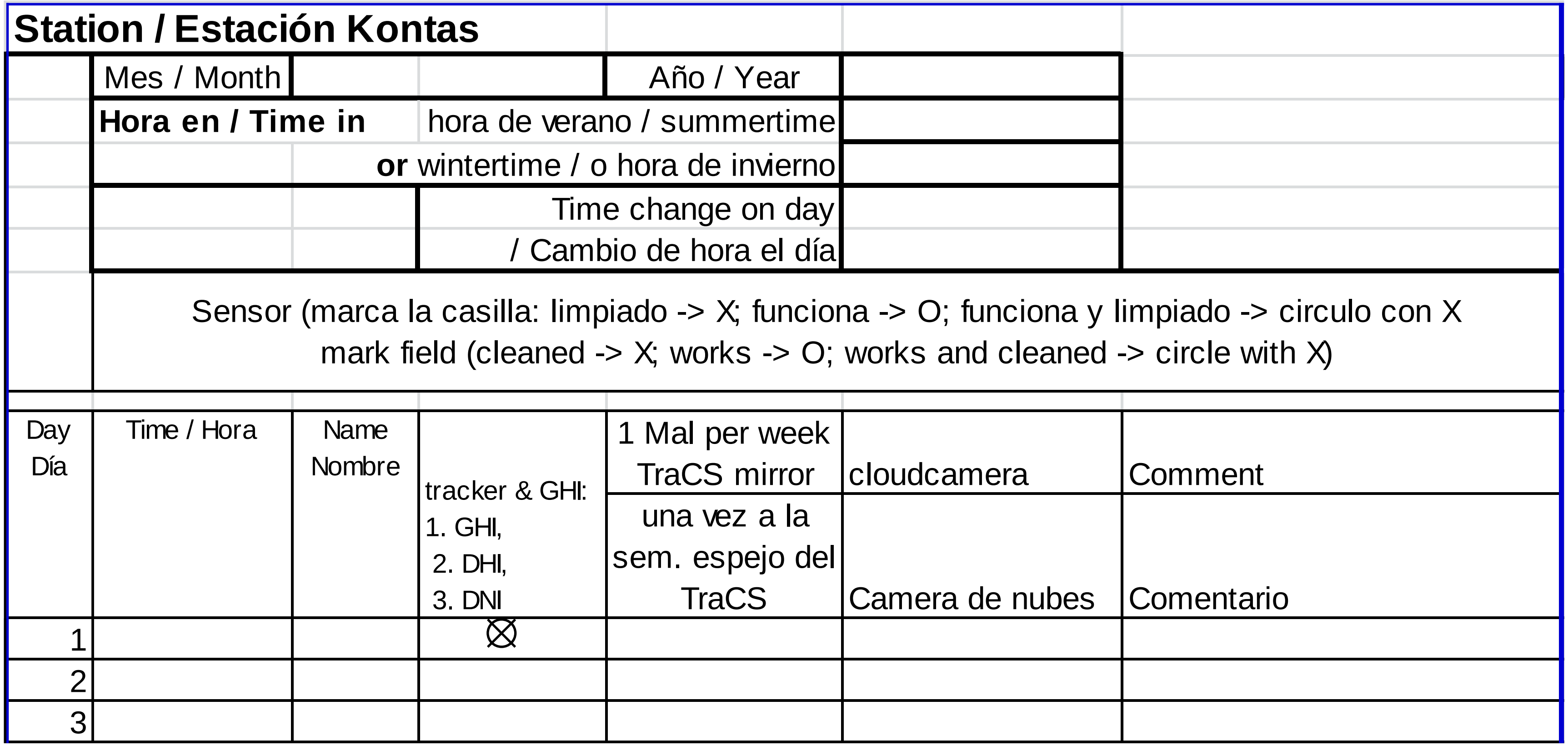

Station / Estación Kontas						
	Mes / Month			Año / Year		
	Hora en / Time in		hora de verano / summertime			
		or wintertime / o hora de invierno				
			Time change on day			
			/ Cambio de hora el día			
	Sensor (marca la casilla: limpiado -> X; funciona -> O; funciona y limpiado -> circulo con X mark field (cleaned -> X; works -> O; works and cleaned -> circle with X)					
Day Día	Time / Hora	Name Nombre	tracker & GHI: 1. GHI, 2. DHI, 3. DNI	1 Mal per week TraCS mirror una vez a la sem. espejo del TraCS	cloudcamera Camera de nubes	Comment Comentario
1			⊗			
2						
3						

- Direct contact is required between those who maintain a station and those who work with the data
- Digital information is required at some point (evlt. cumbersome copying is required)

Calibration of Solar Radiometers

Stefan Wilbert
DLR
Institute of Solar Research
Qualification
Solar Energy Meteorology

DLR

Sensor Calibration

- Thermal sensors: Factor between output voltage of thermopile and irradiance needed
- Pyranometer and pyrheliometer calibration scales are traced to the World Radiometric Reference (WRR)
  - Represented by the World Standard Group (WSG)
    - Group of absolute cavity pyrheliometers (next slide)
  - WRR/WSG maintained by the World Radiation Centre (WRC) in Davos

Image: PMOD-WRC

Sensor Calibration - *Absolute Cavity Radiometer*

Principle of operation

- Track instrument to the sun
- Open phase: Light heats up absorber, temperature difference created by light
- Closed phase: close aperture and create same temperature difference with electrical heating
- With this power and the size of the absorber one obtains the DNI

Characteristics:

- Uncertainty ~0.3%
- Not weatherproof
- expensive (35k€)
  - >10 x price field-pyrheliometer
- Only chopped measurements

To be discussed later at METAS station

Sensor Calibration – Pyrheliometers & Pyranometers

- Necessary at least every 2 years for each sensor (most manufacturer’s recommendation)
- Calibration following ISO standards
  - Parallel outdoor measurements of test and reference instruments under certain meteorological conditions
    - Test pyrheliometer(s) vs. reference pyrheliometer(s)
    - Reference pyrheliometer vs test DNI from consecutively shaded and unshaded pyranometer
    - Unshaded pyranometers vs. reference GHI
      - Reference GHI from unshaded ref. pyranometer
      - Reference GHI from shaded reference pyranometer and reference pyrheliometer
  - Indoor calibration:
    - Comparison of test and reference sensor signals to light from a lamp (for pyrheliometers only included in upcoming, still unpublished ISO standard)

To be discussed later at METAS station

Sensor Calibration - **RSI**

- RSI-calibration is more complicated
- Reasons:
    - dependent on wavelength distribution of irradiation!
      Not independent like thermal sensors…
- Result:
    - Calibration result depends on atmospheric conditions during the calibration campaign (Aerosols, solar elevation, …)
    - Solution:
        - Calibration time much higher (2 months)
        - On site calibration
        - Observation of calibration conditions

Other Measurements For Resource Assessment

Further meteorological parameters

- Many further meteo. parameters required for solar energy besides broadband irradiance
  - Wind
  - Ambient temperature and relative humidity
  - Atm. pressure
  - Precipitation
  - Solar spectra, UV irradiance, aerosols & water vapor
  - Soiling
  - Surface albedo ((bifacial-)PV)
  - Circumsolar radiation
  - Beam attenuation between heliostats & receivers of tower plants

Chapter 5

Further reading: Best Practices Handbook for the Collection and Use of Solar Resource Data for Solar Energy Applications: Third Edition - IEA-PVPS

To be discussed later at METAS station

Additional Instrumentation

Temperature and Humidity

- Radiation shield
- Sensor under ceramic head
  - CMOS Sensor

- Temperature affects PV efficiency!
- Temperature and humidity are relevant for CSP
  - Thermal losses
  - Thermodynamic processes need T_{cold}
  - Dew/soiling of mirrors

To be discussed later at METAS station

Additional Instrumentation

Precipitation

Principle of operation:

- rain collected with a defined aperture
- collected rain water enters slowly into a mechanism that gives a pulse when filled to a defined level
- pulses are counted

Might clean the plant (heavy rain)

To be discussed later at METAS station

Additional Instrumentation

Ambient Pressure

- E.g. capacitive sensor
- Hose connection

- Thermodynamic processes (turbine, …) require air pressure information
- Radiative transfer modelling requires pressure input

To be discussed later at METAS station

Additional Instrumentation

Wind

- Vane (direction)
- 10m height (also 5m, 20m…)
- Anemometer (speed)

- Wind loads have to be considered for plant design
- Tracked collectors cannot operate at high wind velocities (design dependent)
- For CST: Wind might cause mirror deformation/vibration

  mirror concentrates worse

Additional Instrumentation

Sunshape and circumsolar radiation

DLR/PSA

Sunshapes and circumsolar radiation

- Sunshapes are used in raytracing
- Sunshapes are complex to measure and require lots of disk space
- -> scalar parameters describing the sunshapes are of interest (circumsolar ratio, circumsolar contribution -> used in simpler CSP models)

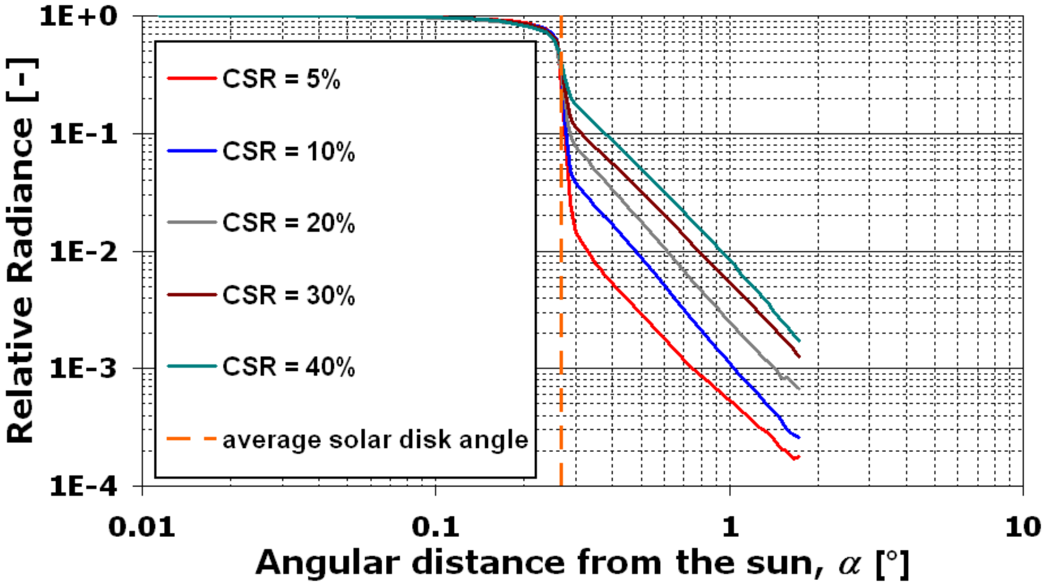

Additional Instrumentation

Soiling

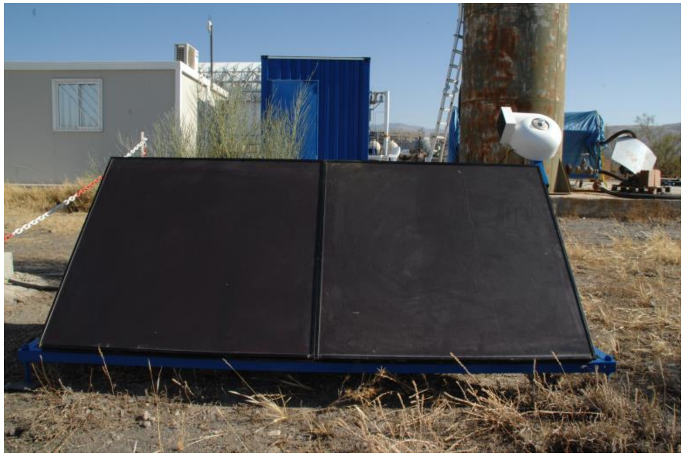

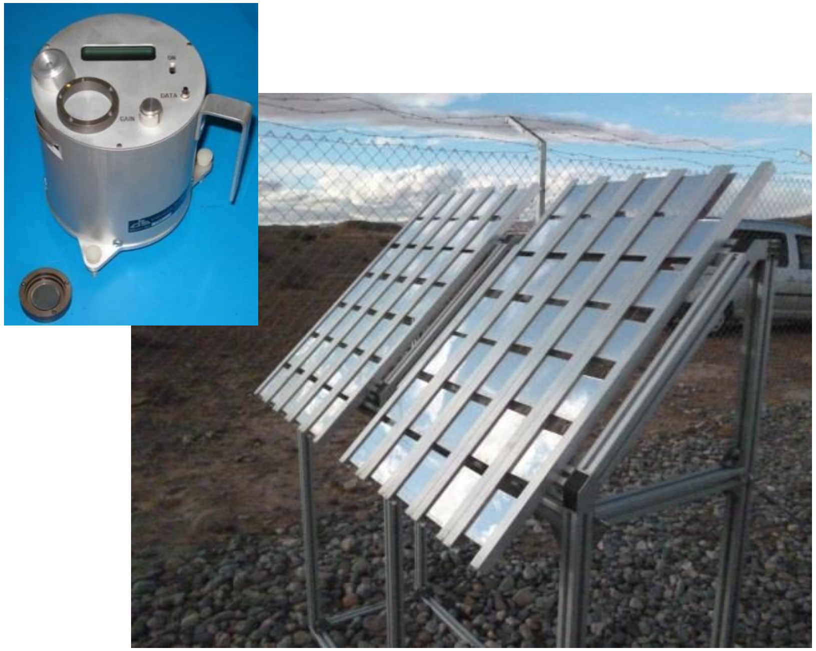

Beam attenuation in tower plants

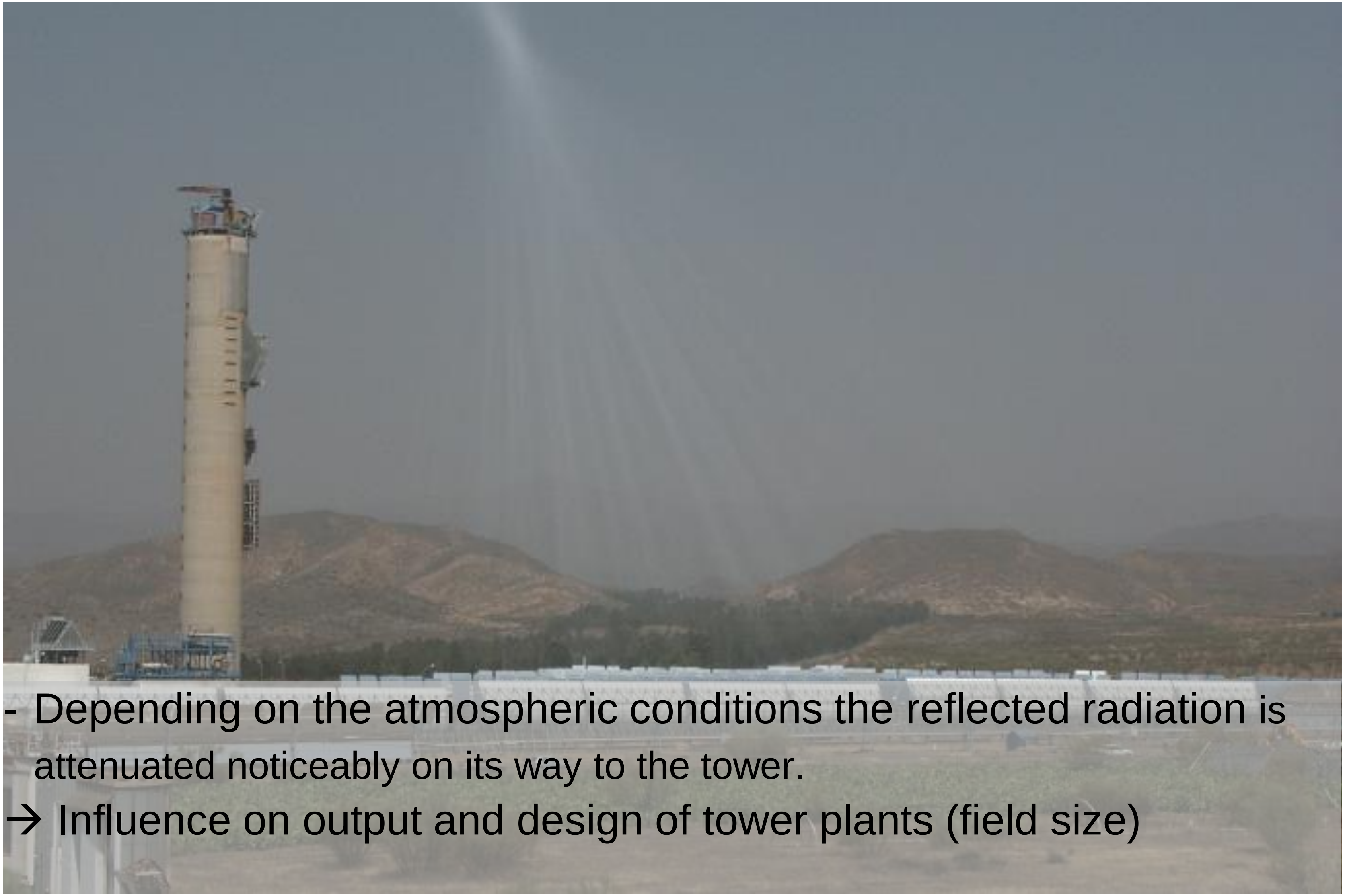

- Depending on the atmospheric conditions the reflected radiation is attenuated noticeably on its way to the tower.

→ Influence on output and design of tower plants (field size)

Image shows CESA-1 at Plataforma Solar de Almeria (Owned by the Spanish research centre CIEMAT)

Beam attenuation measurements

Options based on visibility sensors

Vaisala FS11 scatterometer
(NIR, no absorption)

Optec LPV-4 transmissometer (532 nm)

libRadtran

Absorption & Broadband Correction (ABC)

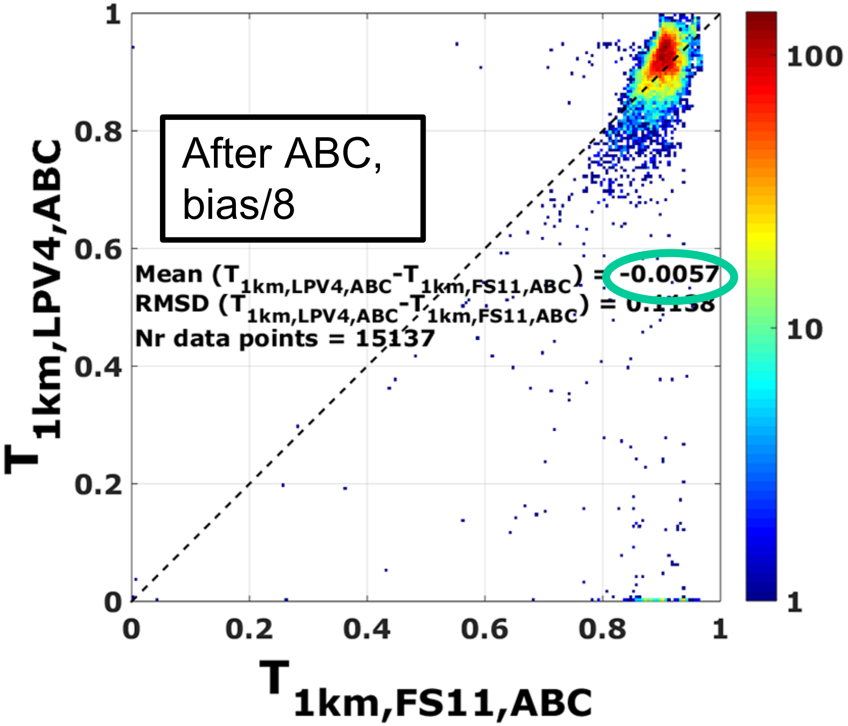

After ABC, bias/8

1 year processed data
10 min time resolution

→ ABC improves coincidence between both sensors!

Hanrieder, N., S Wilbert, R Pitz-Paal, C Emde, J. Gasteiger, B Mayer, and J. Polo. 2015. "Atmospheric extinction in solar tower plants: absorption and broadband correction for MOR measurements." *Atmos. Meas. Tech.* no. 8:3467-3480. doi: 10.5194/amt-8-3467-2015.

Beam attenuation measurements

- Camera based differential method from Ballestrin et al. that reduces calibration errors

$$T_{740m} = 1 - A_{740m} = \frac{I_2}{I_1}$$

with: $I_1 = I_{1W}-I_{1B}$ from camera 1
and $I_2 = I_{2W}-I_{2B}$ from camera 2

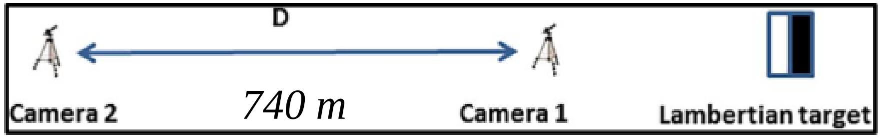

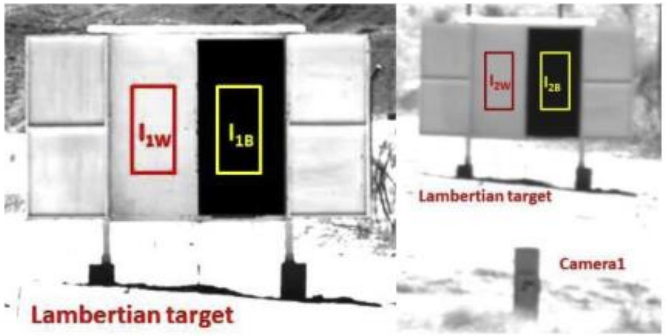

Images: Ballestrin et al (2018)

- Method based on nephelometer (Freud et al.)
  - measures the concentration of suspended particulates in a liquid or gas colloid (-> here air + particles = aerosol)
  - Applies corrections similar to those for visibility sensors

Ballestrin et al (2018), “Solar extinction measurement system based on digital cameras. Application to solar tower plants”, Renewable Energy 125, pp. 648-654.
Eyal Freud, Morag Am-Shallem and Rotem Hayut. 2020. Measuring in-field light transmittance in a tower CSP plant. SolarPACES conference 2020.

Attenuation models

Compare clear sky DNI measurement
to
clear sky DNI for one fixed atmosphere without aerosol

=> Estimate of aerosol effect

Assume that aerosol height profile is known

=>extinction coefficient close to ground

Similar models based on aerosol optical depth also available

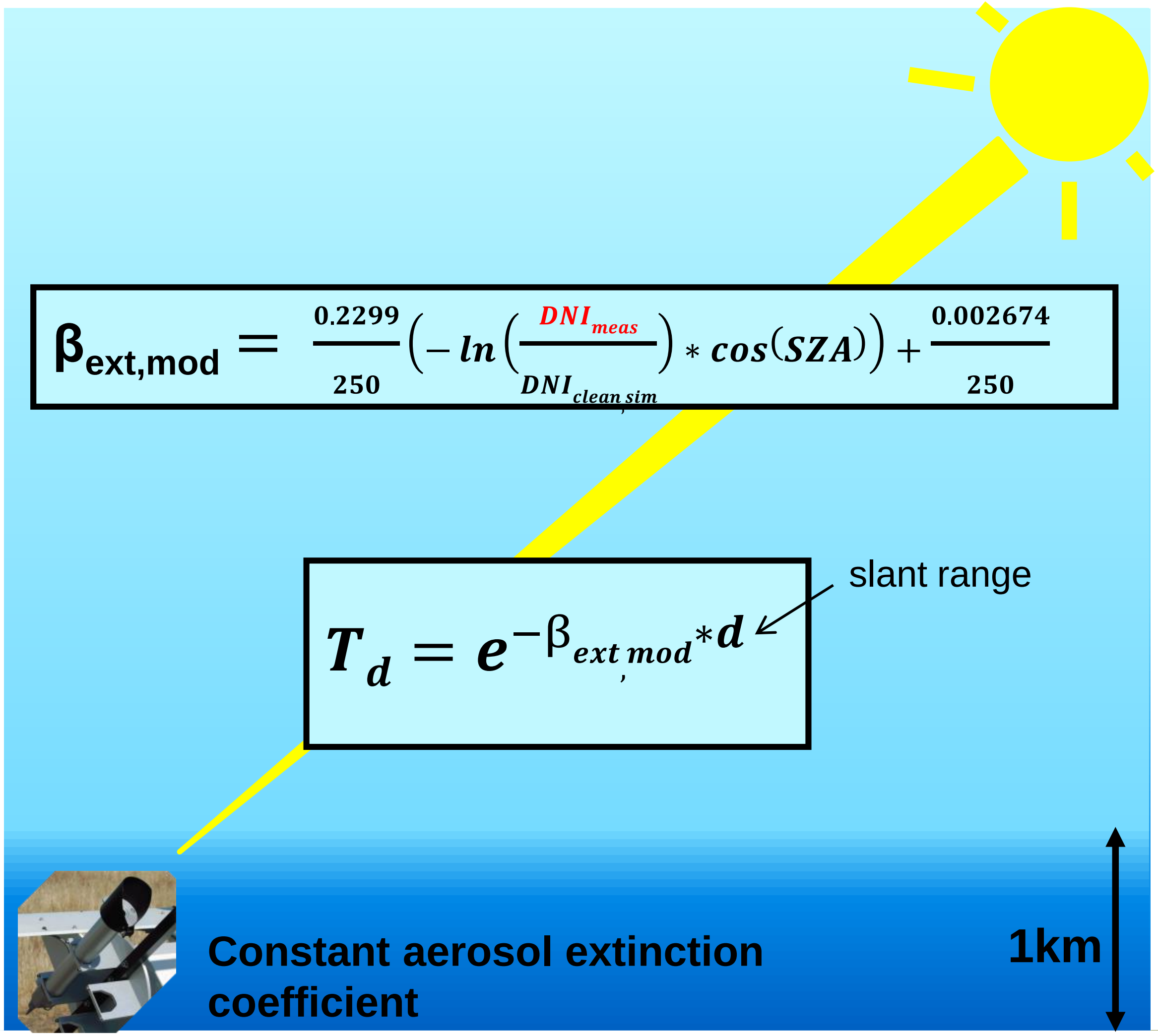

$$\beta_{\text{ext,mod}} = \frac{0.2299}{250}\left(-ln\left(\frac{DNI_{meas}}{DNI_{clean,sim}}\right) * cos(SZA)\right) + \frac{0.002674}{250}$$

$$T_d = e^{-\beta_{ext,mod} * d}$$

-Sengupta, M., Wagner, M., 2011: “Impact of aerosols on atmospheric attenuation loss in central receiver systems”. SolarPACES conference, Granada, Spain.
-N. Hanrieder, A. Ghennioui, S. Wilbert, M. Sengupta and L. F. Zarzalejo. AATTENUATION - The Atmospheric Attenuation Model for CSP Tower Plants: A Look-up table for Operational Implementation. Energies 2020
-J. Polo, J. Ballestrín, J. Alonso-Montesinos, G. López-Rodriguez, J. Barbero, E. Carra, et al.. Solar Energy 2017 Vol. 157 Pages 803-810. DOI: https://doi.org/10.1016/j.solener.2017.09.003

Durability

Power plants in desert environments

Relevant for:
-cheaper components
-high temperatures

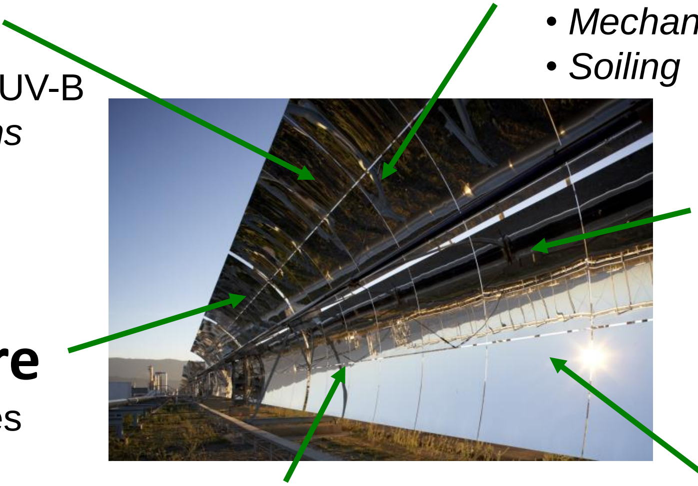

Radiation

- especially UV-A, UV-B
- *Chemical reactions*

Wind

- *Mechanical loads*
- *Soiling*

Aerosols

- Salt, dust, industrial emissions
- *Soiling*
- *Chemical reactions, especially on hot surfaces*

Temperature

- Diurnal changes
- frost
- *Mechanical stress*

Humidity

- Air humidity, dew, rain
- *Chemical reactions*
- *Soiling*

Sandstorms

- *Abrasion*

Measurement best practices - station design

- Measurement site must be representative of the conditions relevant for the power plant (shading by horizon ok, but not by small objects)
- Location of sensors relative to each other important
- Basics: no shading, stable mounts, well defined height above ground, …
- Security of station to avoid theft or vandalism (e.g. fence)
- Grounding and shielding
- Compatible with maintenance requirements
- Data connection for at least daily data control
    - Logger memory to avoid data loss
- *Some information in standards (ISO 9901, ASTM G183)*
    - *More in WMO CIMO guide, BSRN manual*

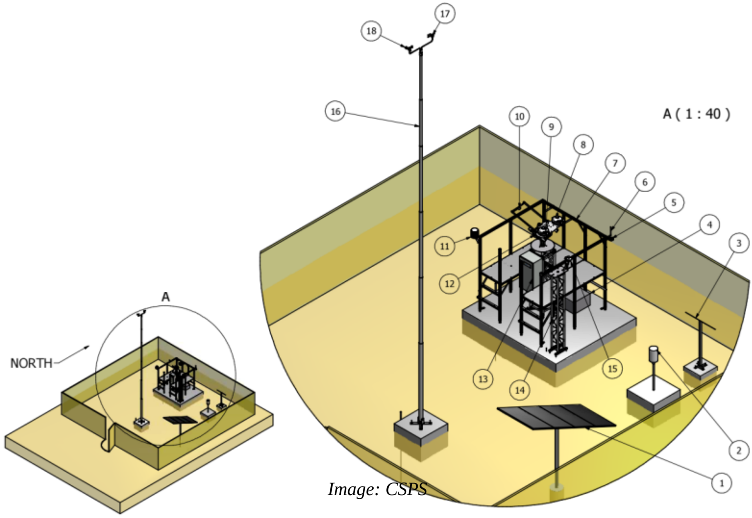

Image: CSPS

Quality control and flagging of solar data

Knowledge for Tomorrow

Deutsches Zentrum
für Luft- und Raumfahrt e.V.
in der Helmholtz-Gemeinschaft

Motivation

Why is data screening and flagging necessary?

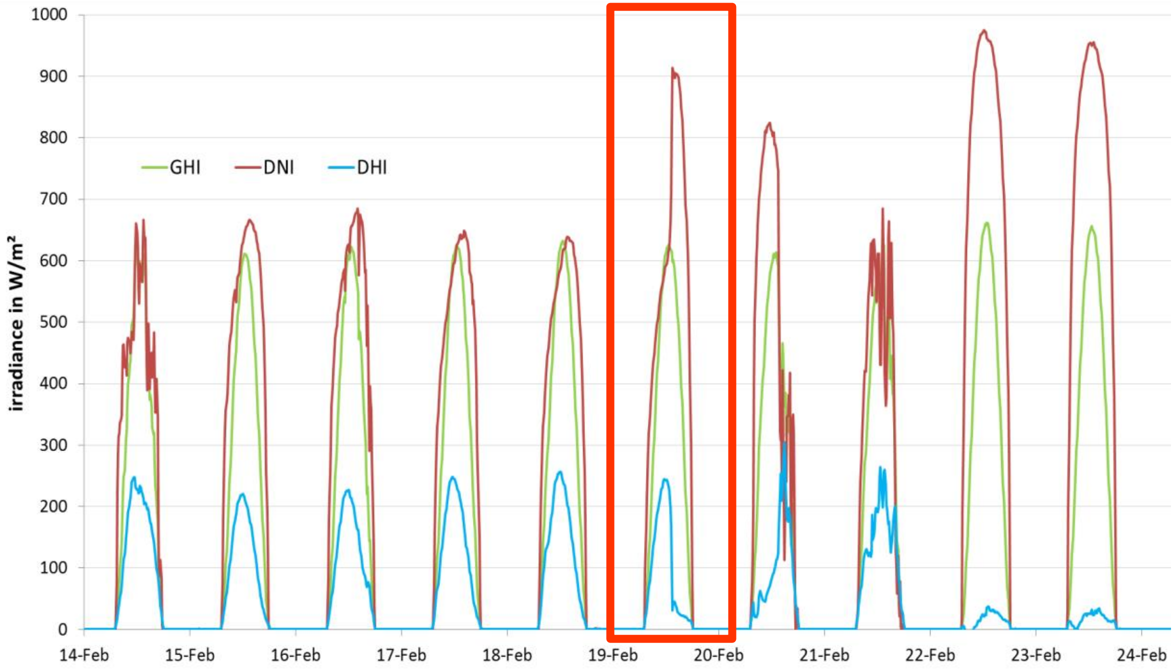

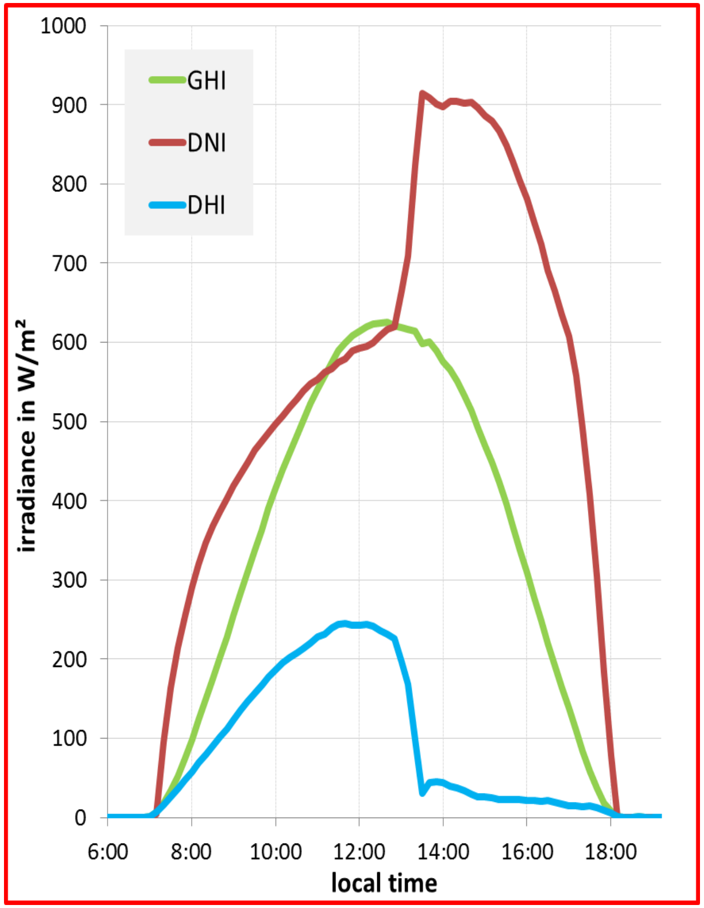

Many errors can occur while collecting meteo data

Errors observed on data sets received for evaluation: tracking error occurred, but long time not detected

Geuder, N., F. Wolfertstetter, S. Wilbert, D. Schüler, R. Affolter, B. Kraas, E. Lüpfert, and B. Espinar. 2015. "Screening and Flagging of Solar Irradiation and Ancillary Meteorological Data." Energy Procedia no. 69 (0):1989-1998. doi: http://dx.doi.org/10.1016/j.egypro.2015.03.205.

Automatic data screening

Meteorological measurements are often screened automatically for:

- *Missing values (data gaps)*
- *Physical limits of the measurements*
- *Plausibility of measured values, K-value tests*
- *Redundancy and coincidence check of irradiance measurements*
- *Operational checks for sun tracker or shadowband rotation*

further automatic tests:

- *Typical/maximal gradients and change rates*
- *Coincidence of sensor and ambient temperature*
- *Battery or voltage checks*
- *Are there text comments available for the timestamp?*

Geuder, N., F. Wolfertstetter, S. Wilbert, D. Schüler, R. Affolter, B. Kraas, E. Lüpfert, and B. Espinar. 2015. "Screening and Flagging of Solar Irradiation and Ancillary Meteorological Data." Energy Procedia no. 69 (0):1989-1998. doi: http://dx.doi.org/10.1016/j.egypro.2015.03.205.

Automatic data screening

Example: physical limits

Meteorological values are within <u>physical</u> limits:

- *Irradiance:* *0 to ~1400 W/m² (depending on component and duration)*
- *Temperature:* *-30 to 50°C (site dependent)*
- *Bar. Pressure:* *acc. to altitude ±30 hPa*
- *Rel. humidity:* *0 to 100 %*
- *Wind speed:* *0 to ~50 m/s*
- *Wind dir.:* *0 to 360°*

Also <u>rare limits</u> are defined.

Several limits exist in the literature:

  - *Limits and tests should be discussed and standardized*

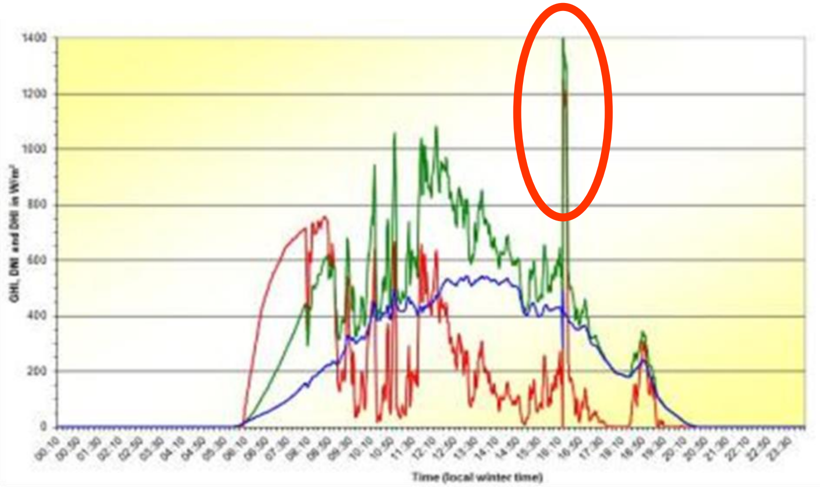

Geuder, N., F. Wolfertstetter, S. Wilbert, D. Schüler, R. Affolter, B. Kraas, E. Lüpfert, and B. Espinar. 2015. "Screening and Flagging of Solar Irradiation and Ancillary Meteorological Data." Energy Procedia no. 69 (0):1989-1998. doi: http://dx.doi.org/10.1016/j.egypro.2015.03.205.

Automatic data screening

Example: Redundancy and signal coincidence

- Redundancy checks and intercomparison limits:

With perfect measurements: $\frac{GHI}{DHI+DNI*\cos(z)} = 1$

Limit for different zenith angles z : 0.92 to 1.08 (z < 75°)

0.85 to 1.15 (z > 75°)

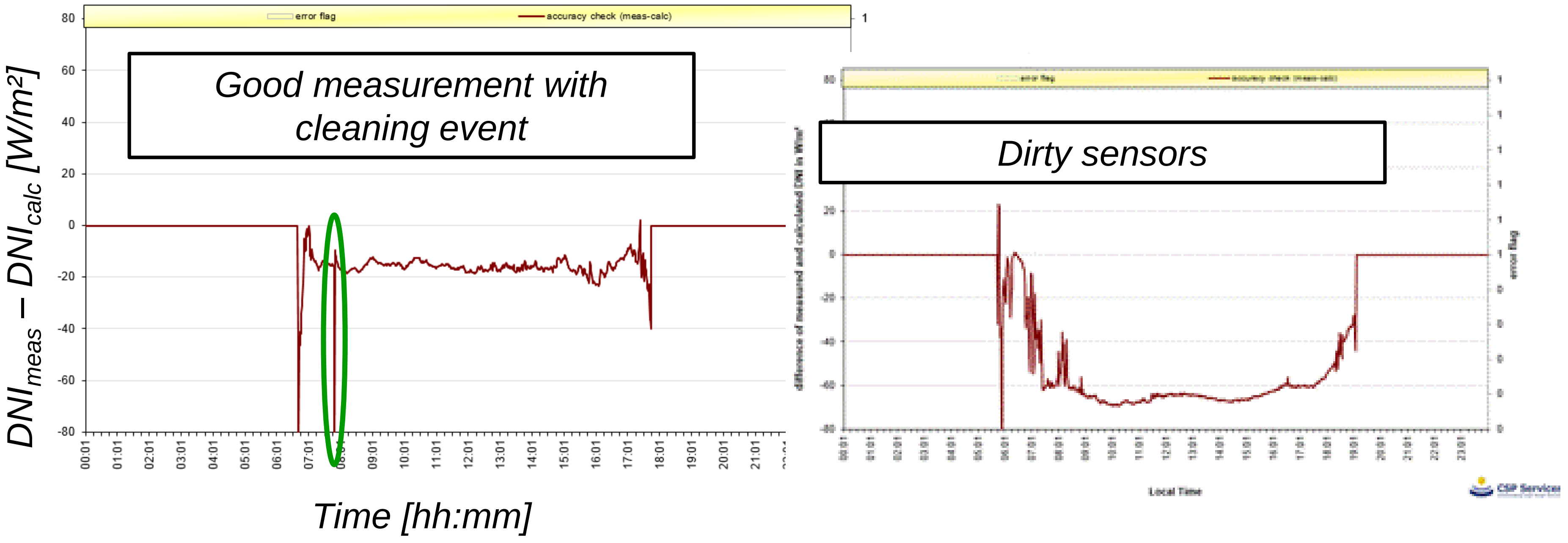

Good measurement with cleaning event

Dirty sensors

Geuder, N., F. Wolfertstetter, S. Wilbert, D. Schüler, R. Affolter, B. Kraas, E. Lüpfert, and B. Espinar. 2015. "Screening and Flagging of Solar Irradiation and Ancillary Meteorological Data." Energy Procedia no. 69 (0):1989-1998. doi: http://dx.doi.org/10.1016/j.egypro.2015.03.205.

Automatic data screening

Example: Gradient-tests

- Step test: change rates of measurement parameters
  implausibly rapid changes or constant values

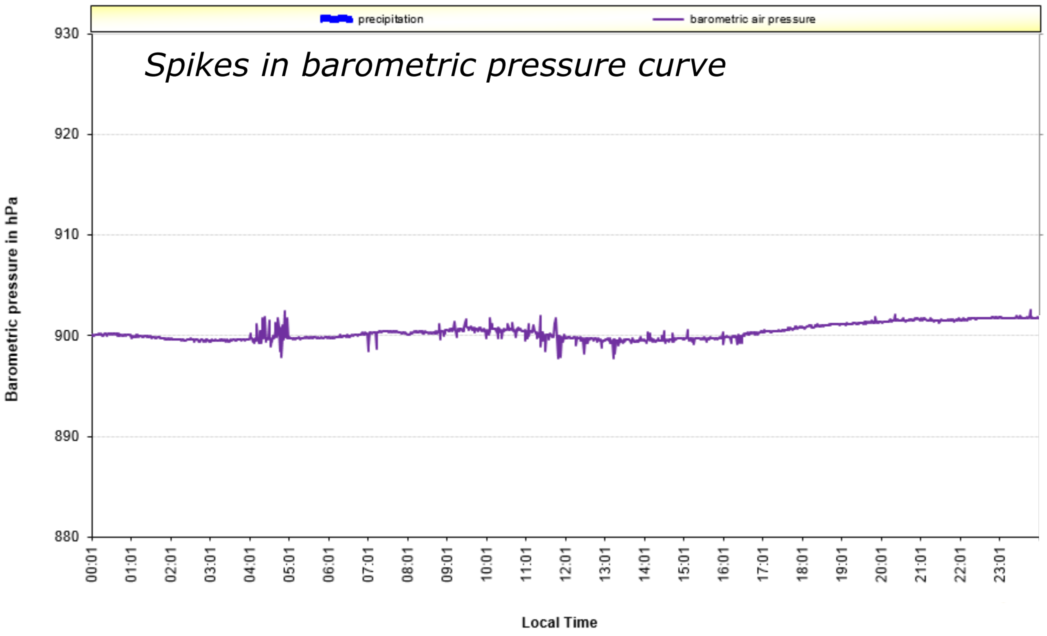
Spikes in barometric pressure curve

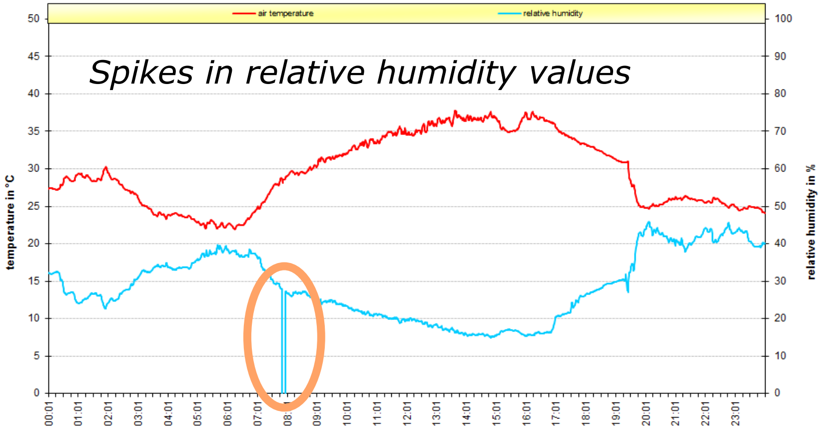
Spikes in relative humidity values

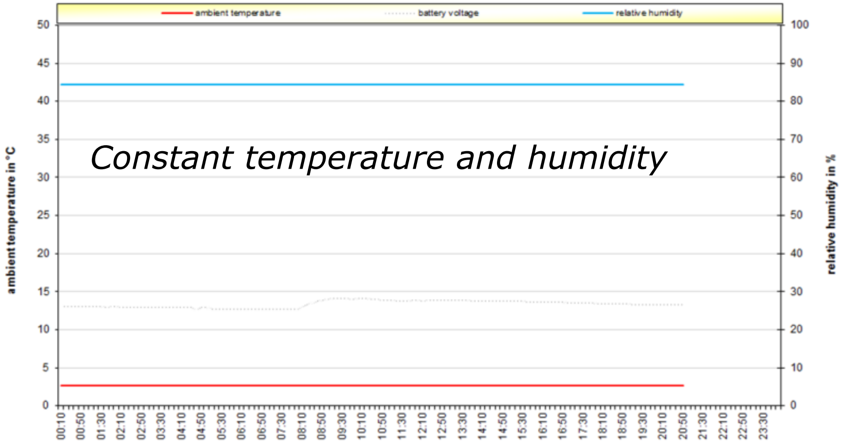
Constant temperature and humidity

Geuder, N., F. Wolfertstetter, S. Wilbert, D. Schüler, R. Affolter, B. Kraas, E. Lüpfert, and B. Espinar. 2015. "Screening and Flagging of Solar Irradiation and Ancillary Meteorological Data." Energy Procedia no. 69 (0):1989-1998. doi: http://dx.doi.org/10.1016/j.egypro.2015.03.205.

Visualization of flags, data treatment

Enabling error detection, interpretation and correction

Visual examination by an experienced user is necessary:

- *Some errors are not automatically detected.*
- *Automatically flagged data can be correct (e.g. only measured GHI affected).*
- *Correct interpretation of the flagged data can allow its correction.*

- *The thus found information and correction must be documented!*

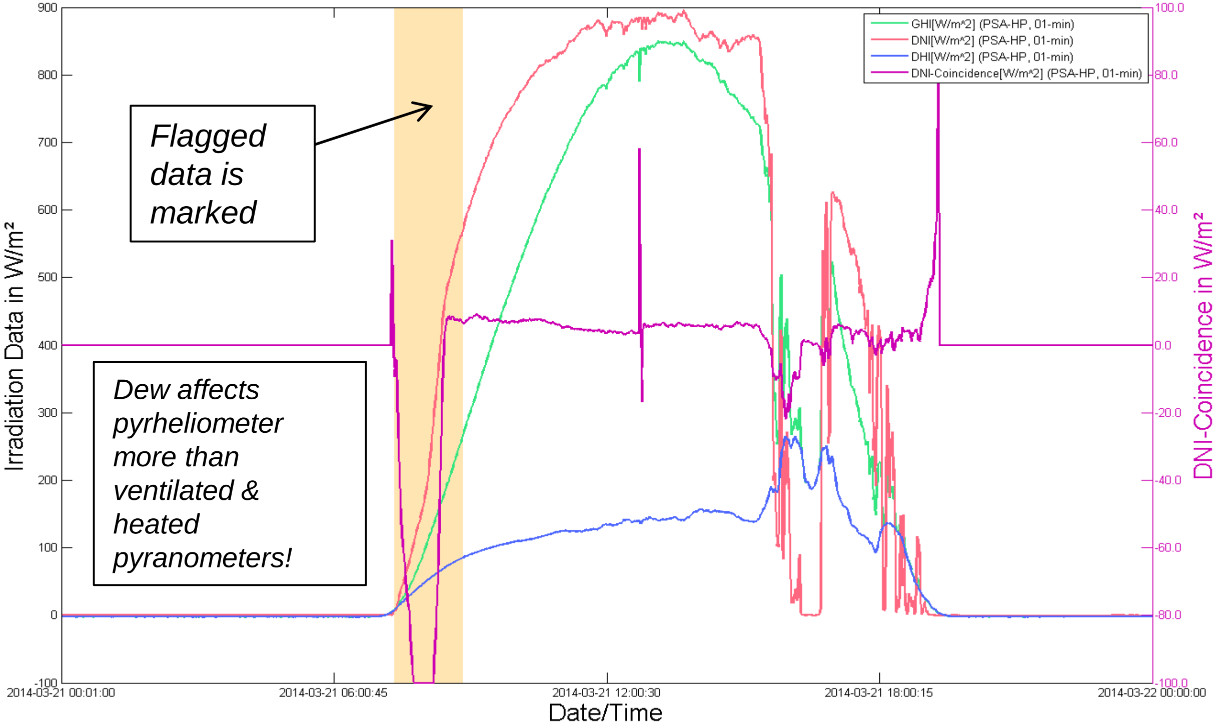

Flagged data is marked

Dew affects pyrheliometer more than ventilated & heated pyranometers!

Geuder, N., F. Wolfertstetter, S. Wilbert, D. Schüler, R. Affolter, B. Kraas, E. Lüpfert, and B. Espinar. 2015. "Screening and Flagging of Solar Irradiation and Ancillary Meteorological Data." Energy Procedia no. 69 (0):1989-1998. doi: http://dx.doi.org/10.1016/j.egypro.2015.03.205.

Endorse Visual QC

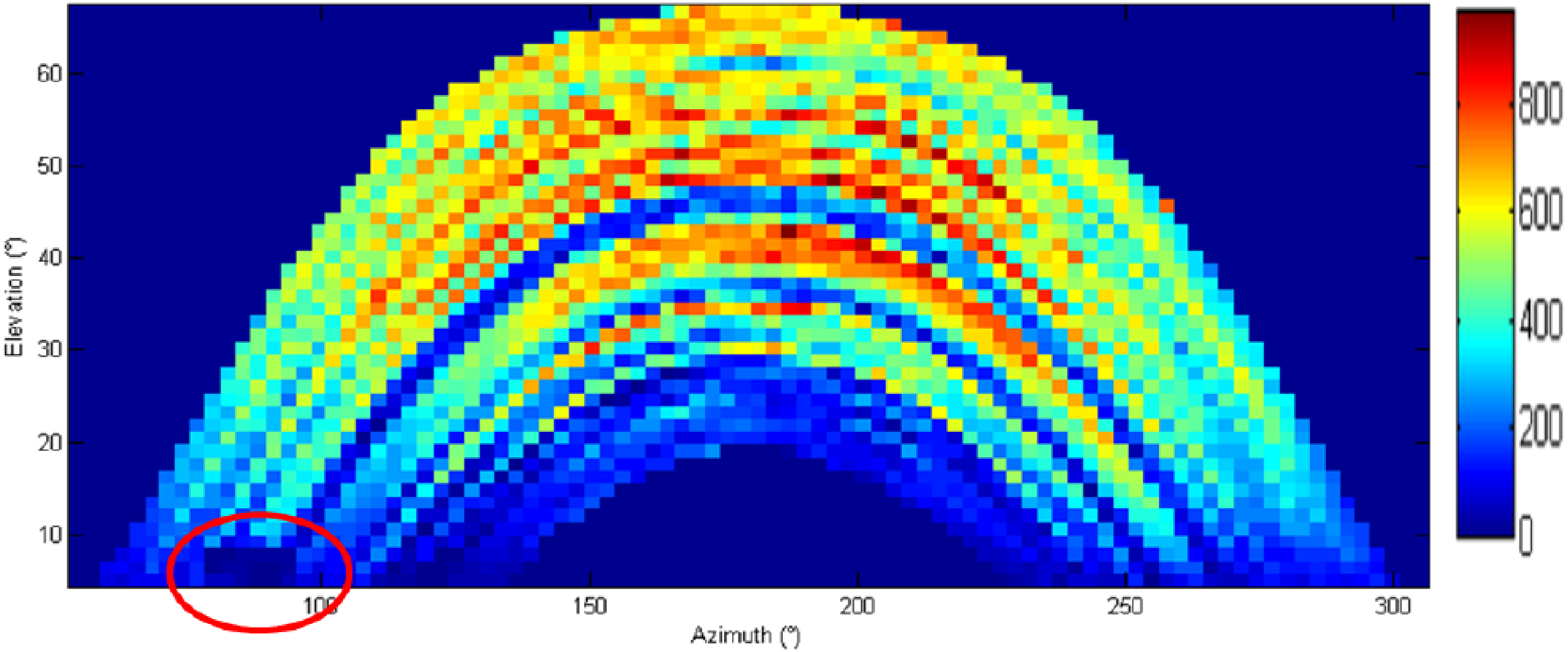

Figure B-11: Horizon derived from 1-min time series of normal direct solar irradiance (W m^{-2}) from the BSRN station of Payerne (Switzerland) in 2009, 1-min average data. The red circle shows the very low values likely associated to an obstacle in the sunlight path in the mornings.

Bella ESPINAR, Lucien WALD, Philippe BLANC, Carsten HOYER-KLICK, Marion SCHROEDTER-HOMSCHEIDT Thomas WANDERER, ENDORSE. D3.2. Report on the harmonization and qualification of meteorological data. 2011

Endorse Visual QC

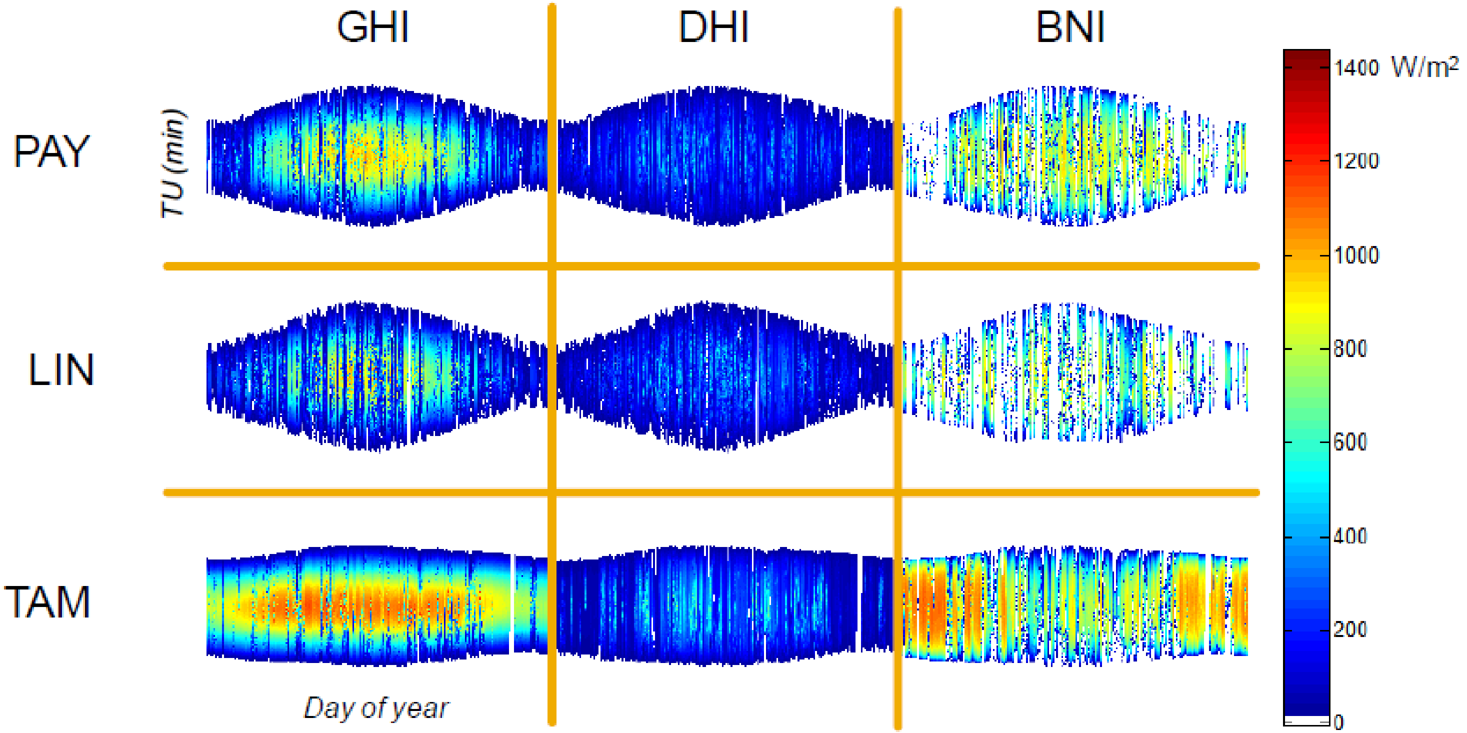

Figure A-14: Example of one year of 1-min average time series of GHI, DHI and BNI (in columns) for the three selected BSRN ground stations PAY, LIN, TAM (in rows). For each of the 3x3 squares, x-axis corresponds to days in the year and y-axis to Universal Time within a day.

Bella ESPINAR, Lucien WALD, Philippe BLANC, Carsten HOYER-KLICK, Marion SCHROEDTER-HOMSCHEIDT Thomas WANDERER, ENDORSE. D3.2. Report on the harmonization and qualification of meteorological data. 2011

Examples for sets of automatic QC tests

- BSRN: http://www.bsrn.awi.de/fileadmin/user_upload/redakteur/Publications/BSRN_recommended_QC_tests_V2.pdf
- MESOR
- SERI http://rredc.nrel.gov/solar/pubs/seri_qc/
- ENDORSE http://www.endorse-fp7.eu/science_harmonization
- Geuder, N., F. Wolfertstetter, S. Wilbert, D. Schüler, R. Affolter, B. Kraas, E. Lüpfert, and B. Espinar. 2015. "Screening and Flagging of Solar Irradiation and Ancillary Meteorological Data." *Energy Procedia* no. 69 (0):1989-1998. doi: http://dx.doi.org/10.1016/j.egypro.2015.03.205.

Summary

Summary

- Accurate measurement of the solar resource and meteorological conditions is possible, but requires a lot of work
  - Maintenance, documentation and quality control are very important
- The best instrument selection depends on the requirements (project phase/type), the available maintenance personnel
- Calibration is important
- Not only radiation must be measured

- Further reading: Best Practices Handbook for the Collection and Use of Solar Resource Data for Solar Energy Applications: Third Edition - IEA-PVPS

SFERA-III
Solar Facilities for the European Research Area

THANK YOU FOR YOUR ATTENTION!
ANY QUESTIONS?

Stefan.Wilbert@dlr.de

GOBIERNO DE ESPAÑA MINISTERIO DE CIENCIA, INNOVACIÓN Y UNIVERSIDADES Ciemat Centro de Investigaciones Energéticas, Medioambientales y Tecnológicas
ENEA
DLR Deutsches Zentrum für Luft- und Raumfahrt
UNIVERSIDADE DE ÉVORA
ESTELA
The Cyprus Institute
instituto imdea energía
Fraunhofer ISE
euronovia
LNEG
METU
ETH zürich
UNIVERSIDAD DE ALMERÍA
cnrs
cea

DLR
SFERA Solar Facilities for the European Research Area

SFERA-III
Solar Facilities for the European Research Area

Solar Facilities for the European Research Area

2nd Training for Industries “Optimization of CST plant output by optical and thermal characterization and target-oriented O&M”
26 – 29 April 2022, Plataforma Solar de Almería, Spain

Nowcasting
Stefan Wilbert, DLR, 28.4.22

NETWORKING

THIS PROJECT HAS RECEIVED FUNDING FROM THE EUROPEAN UNION’S HORIZON 2020 RESEARCH AND INNOVATION PROGRAMME UNDER GRANT AGREEMENT NO **823802**

Overview

- Overview of nowcasting options
- Introduction to nowcasting methods, mainly based on the example using All Sky Imagers (ASI)
- Validation of nowcasts
- Combination of forecasts

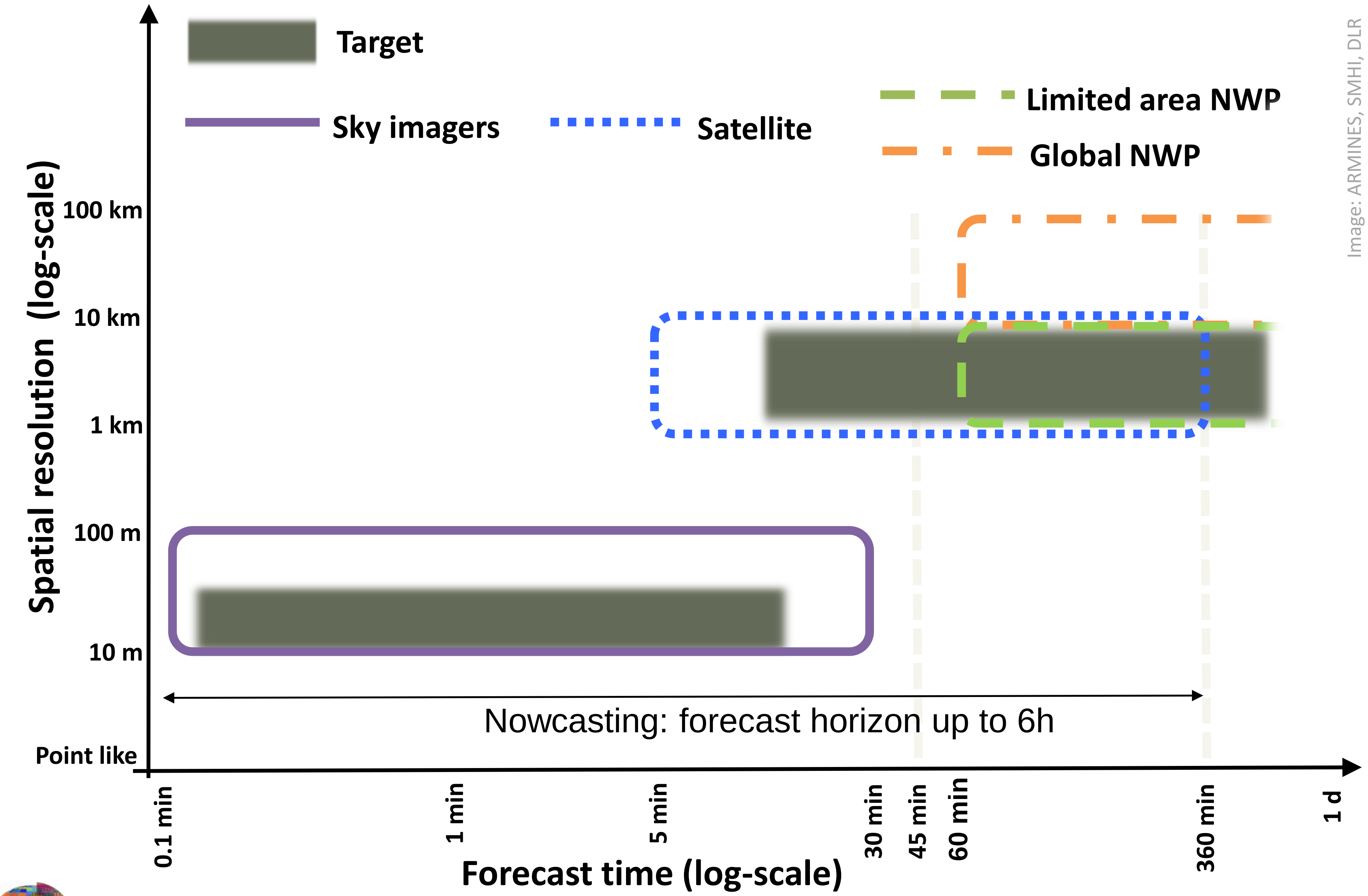

Image: ARMINES, SMHI, DLR

Overview ASI nowcasting approach: setup

Sky images from ≥1 ASI

Cloud detection

Cloud modelling

Cloud tracking

Shadow projection

Allocation of cloud transmittance

Irradiance forecast

- All sky images of at least one camera (e.g. fish eye lens)
- irradiance information from at least one ground based measurement station (e.g. pyranometer, pyrheliometer)

Overview ASI nowcasting approach: cloud detection

Sky images from ≥1 ASI

Cloud detection

Cloud modelling

Cloud tracking

Shadow projection

Allocation of cloud transmittance

Irradiance forecast

- E.g. clear sky library for cloud detection [Kuhn et al. 2017]
  - = data base which stores the red to blue ratio (RBR) of each camera pixel from a large amount of raw images with clear sky conditions for Pixel zenith angle, sun pixel angle, air mass and Linke turbidity

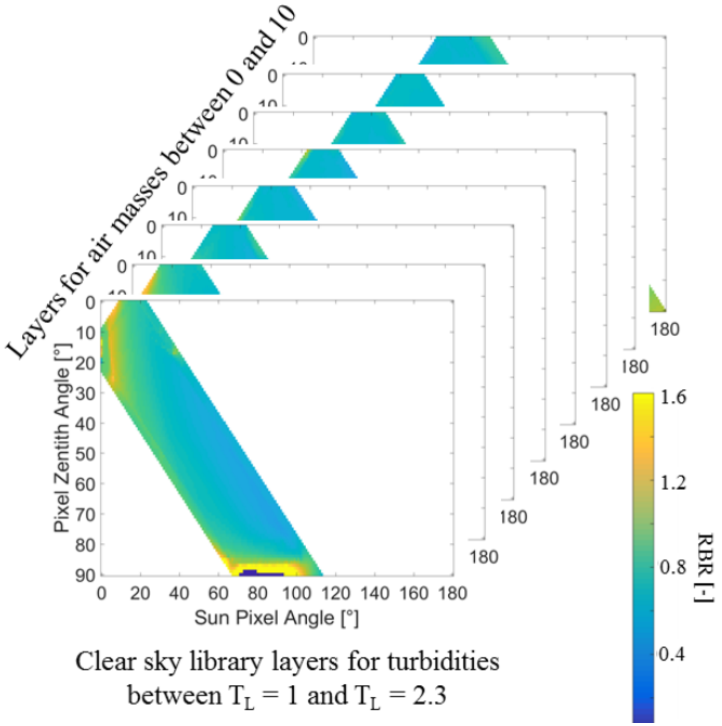

Clear sky library layers for turbidities between $T_L = 1$ and $T_L = 2.3$

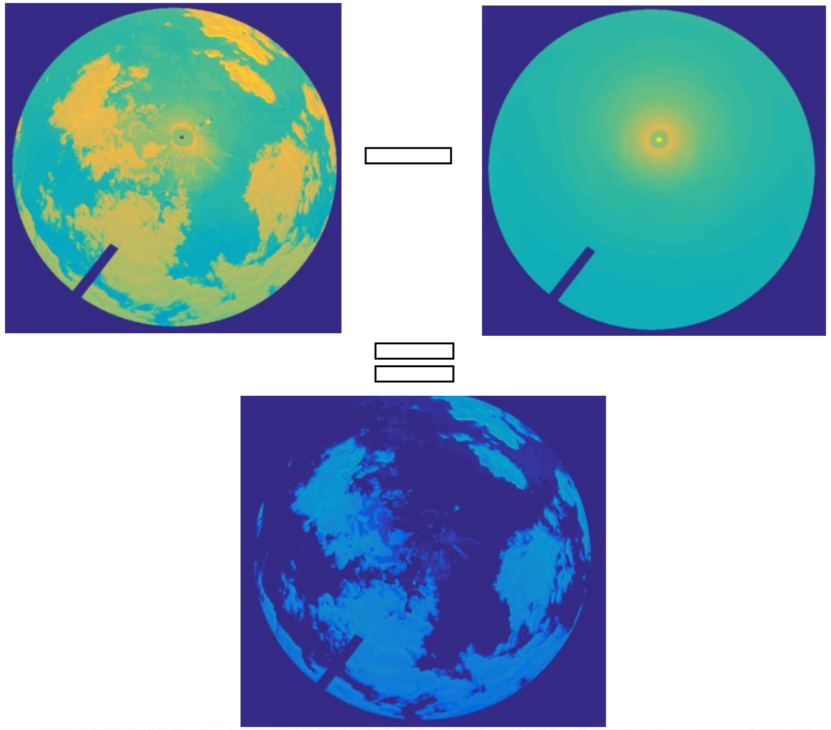

Overview ASI nowcasting approach: cloud detection

- Sky images from ≥1 ASI
- Cloud detection
- Cloud modelling
- Cloud tracking
- Shadow projection
- Allocation of cloud transmittance
- Irradiance forecast

- AI as alternative
- E.g. semantic cloud segmentation via Convolutional Neural Network in four classes [Fabel et al. 2022]

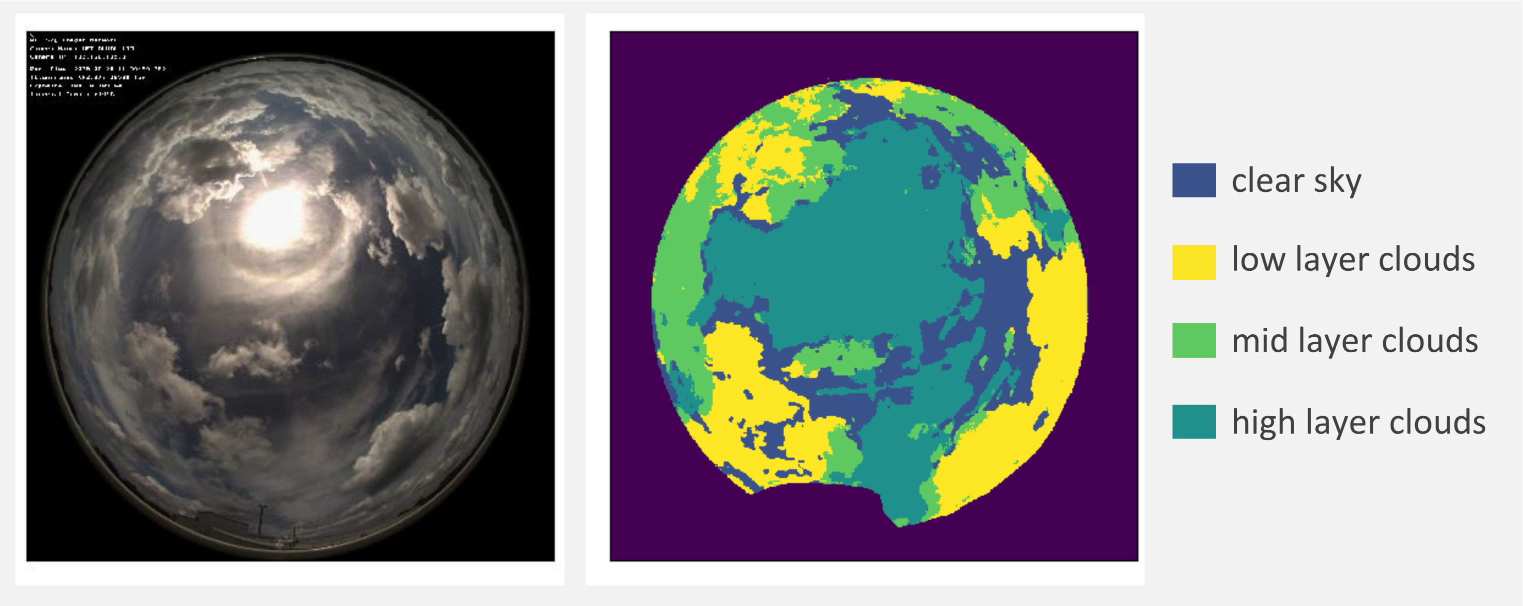

Overview used nowcasting approach: cloud modelling and tracking

Sky images from ≥1 ASI
Cloud detection
Cloud modelling
Cloud tracking
Shadow projection
Allocation of cloud transmittance
Irradiance forecast

- If only 1 RGB ASI is used:
  - no determination of cloud height
  - cloud speed derived from image series, but only in „pixel per second“
  - forecast only for the location of the camera

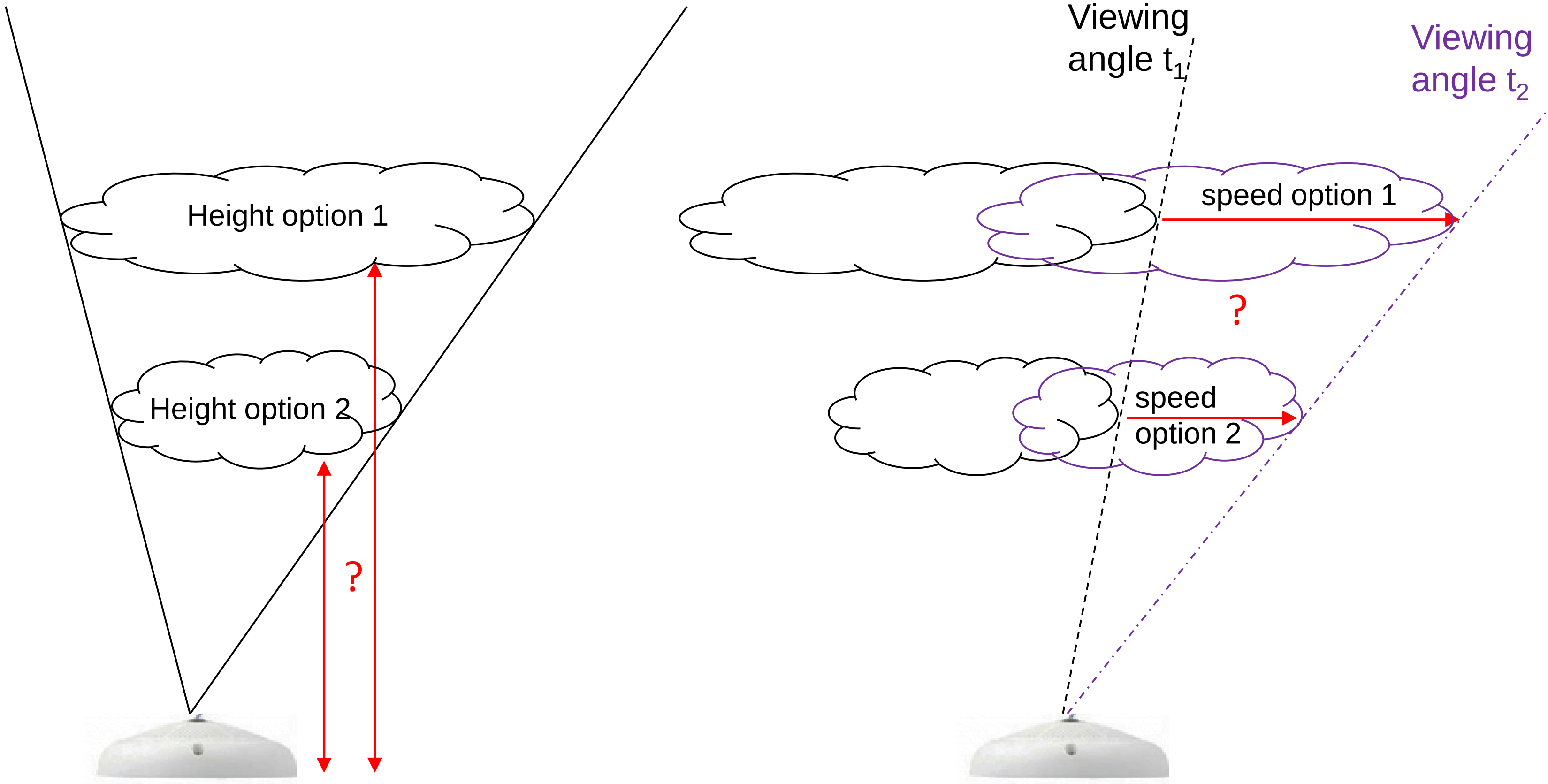

Overview used nowcasting approach: cloud modelling and tracking

Sky images from ≥1 ASI

Cloud detection

Cloud modelling

Cloud tracking

Shadow projection

Allocation of cloud transmittance

Irradiance forecast

- Cloud height and speed tracking in absolute units via stereoscopic approach from image series of multiple cameras [Nouri et al., Kuhn et al. 2019], ceilometers or IR camera
- -> calculation of irradiance maps, also for positions a few km away from the camera

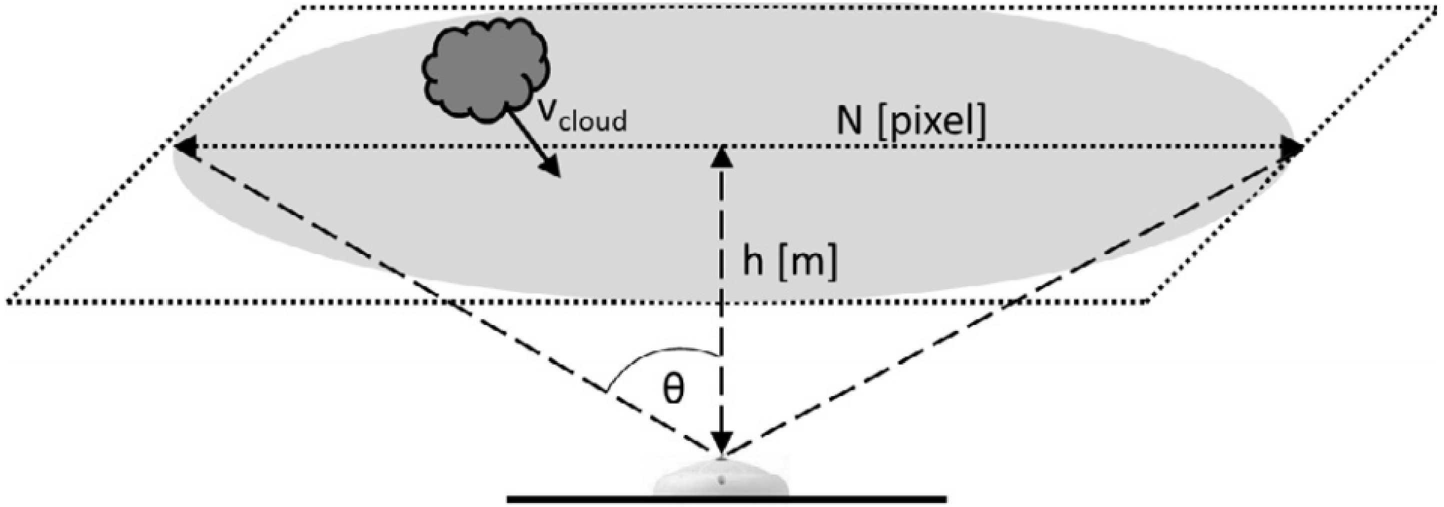

Overview used nowcasting approach: shadow projection

- Sky images from ≥1 ASI
- Cloud detection
- Cloud modelling
- Cloud tracking
- **Shadow projection**
- Allocation of cloud transmittance
- Irradiance forecast

If cloud height is derived: shadow projection e.g. via ray tracing and topographical information (e.g. TanDEM-X global elevation model (DLR Microwaves and Radar Institute)) [Nouri et al. 2018]

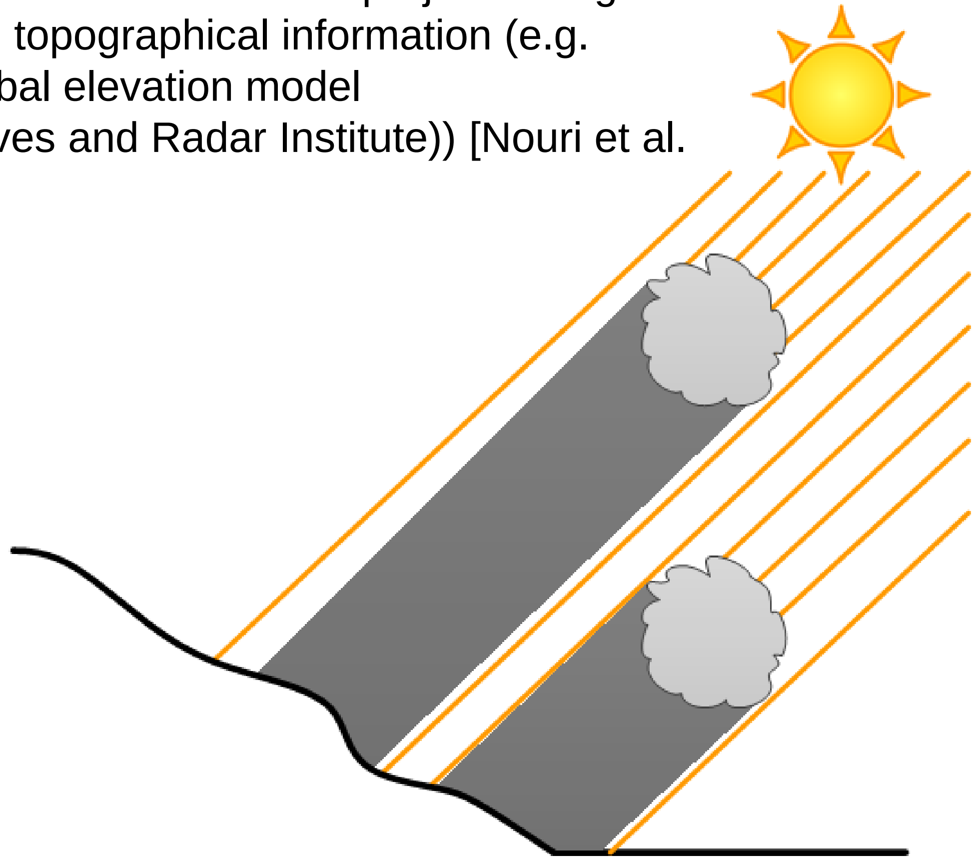

Overview used nowcasting approach: cloud radiative effect

Sky images from ≥1 ASI

Cloud detection

Cloud modelling

Cloud tracking

Shadow projection

Allocation of cloud transmittance

Irradiance forecast

Cloud radiative effect is determined by ground-based irradiance measurements, e.g. if DNI is measured:

$$\tau = \frac{DNI_{shaded}}{DNI_{clear}}$$

However, the majority of clouds remain without a transmittance measurement

- Transmittance estimation: e.g. based on results of a probabilistic analysis and recent cloud height and transmittance measurements [Nouri et al. 2019b]

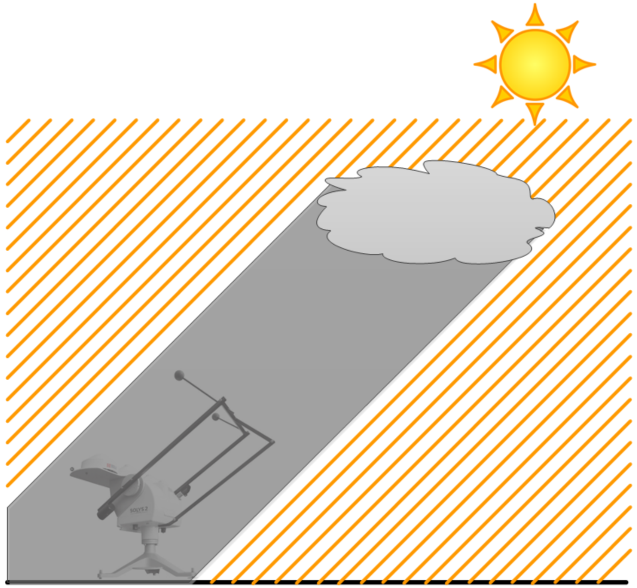

Overview used nowcasting approach: irradiance maps

Sky images from ≥1 ASI

Cloud detection

Cloud modelling

Cloud tracking

Shadow projection

Allocation of cloud transmittance

Irradiance forecast

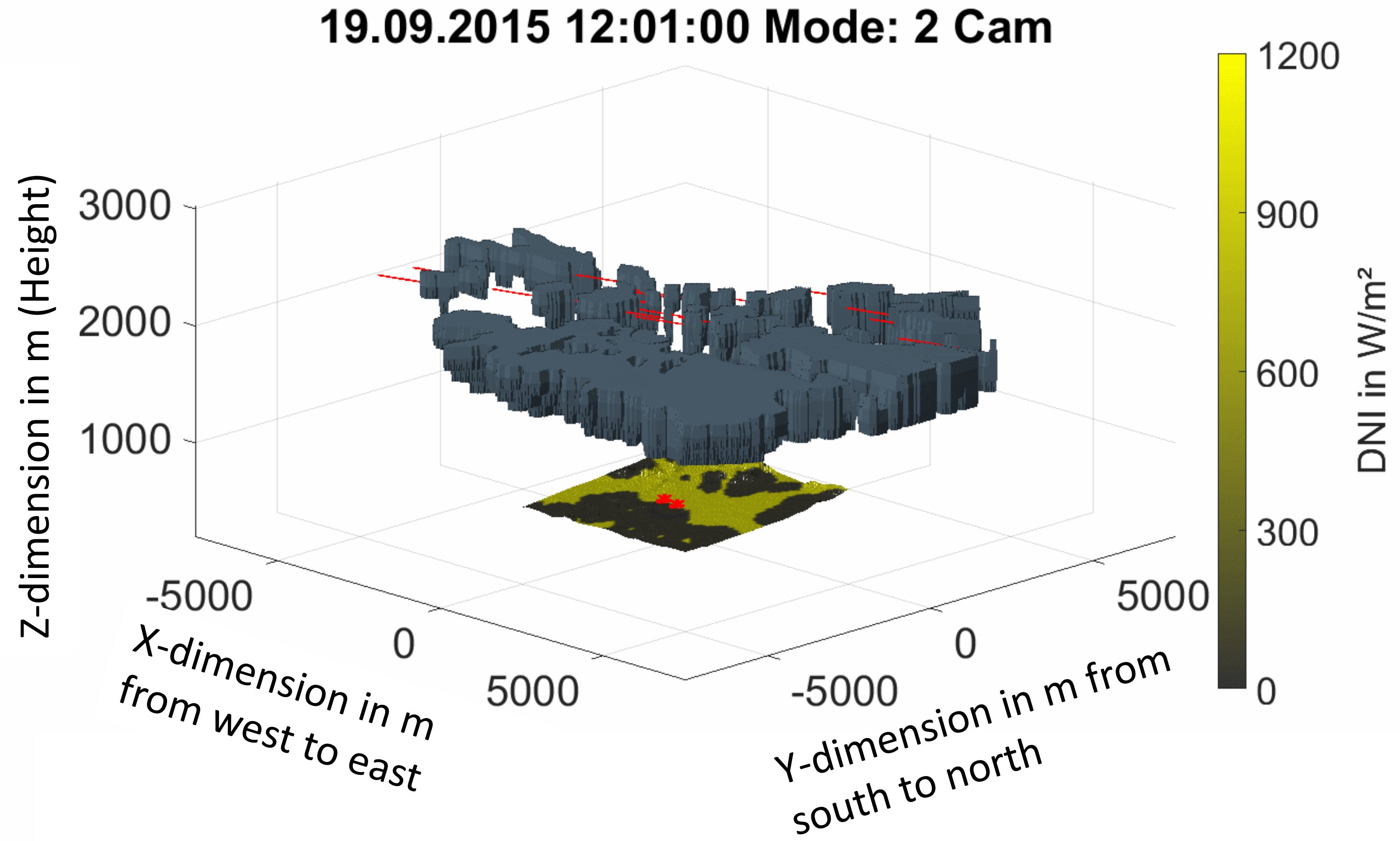

Overview ASI nowcasting approach: application of artificial intelligence

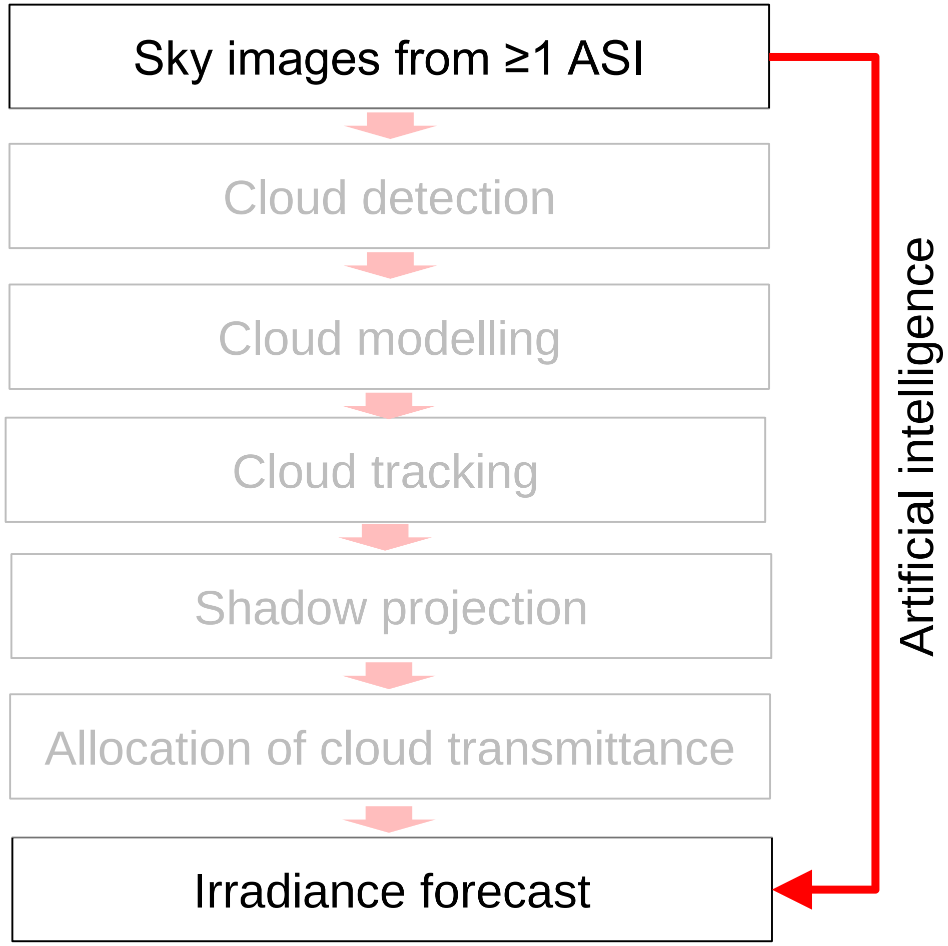

Sky images from ≥1 ASI

Cloud detection

Cloud modelling

Cloud tracking

Shadow projection

Allocation of cloud transmittance

Irradiance forecast

Artificial intelligence

- AI can be used in individual processing steps (e.g. cloud segmentation, tracking)
- But AI also option to avoid individual steps (e.g. Pierer & Remund, 2019)
- AI also an option to provide forecasts based only on irradiance measurements (-> limited accuracy e.g. for ramp detection)

Calculation of Solar Radiation from satellite images – example Heliosat method

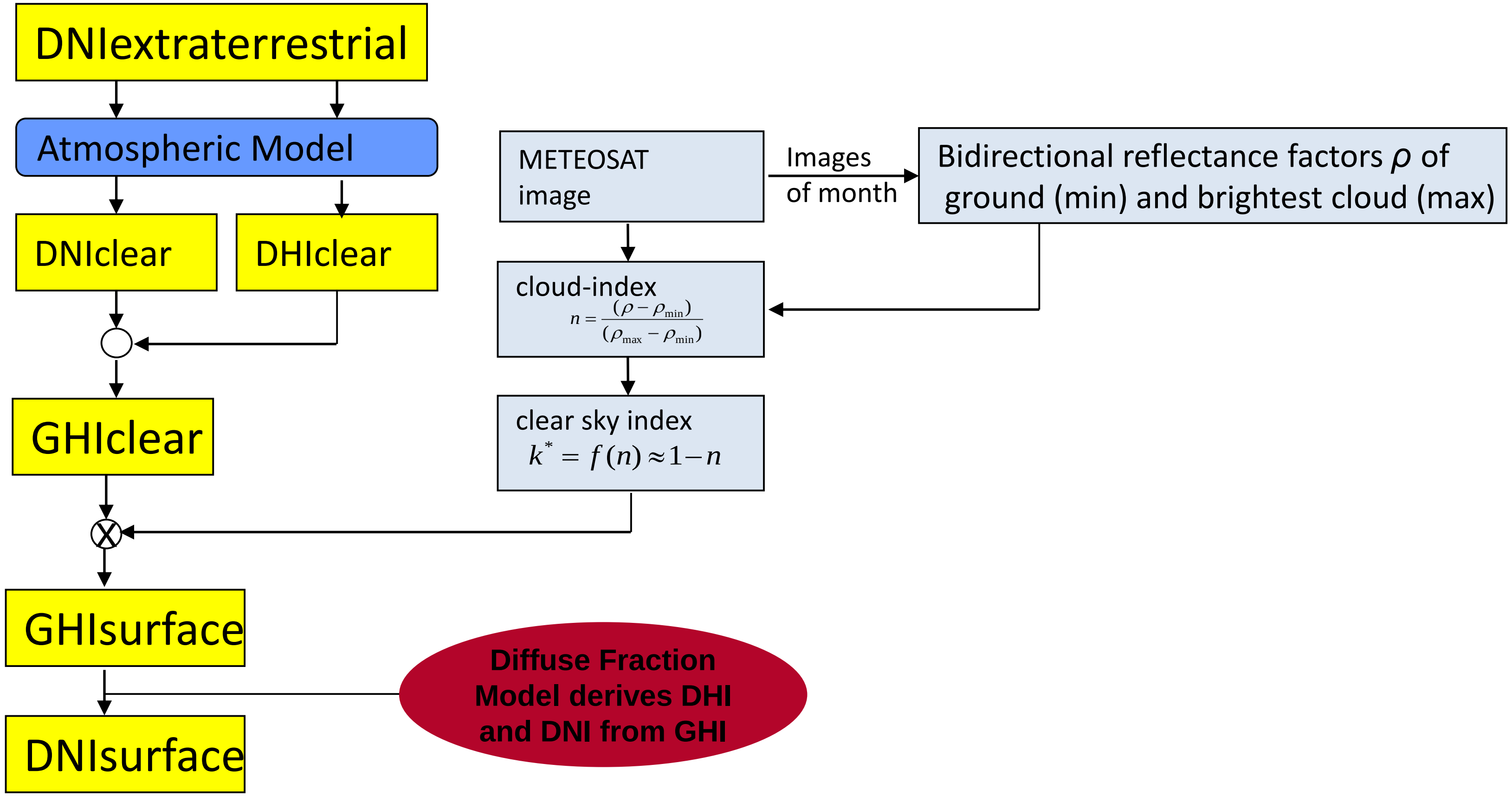

DNIextraterrestrial

Atmospheric Model

DNIclear

DHIclear

GHIclear

GHIsurface

DNIsurface

METEOSAT image

Images of month

Bidirectional reflectance factors ρ of ground (min) and brightest cloud (max)

cloud-index

$$n = \frac{(\rho - \rho_{\min})}{(\rho_{\max} - \rho_{\min})}$$

clear sky index

$$k^* = f(n) \approx 1 - n$$

Diffuse Fraction Model derives DHI and DNI from GHI

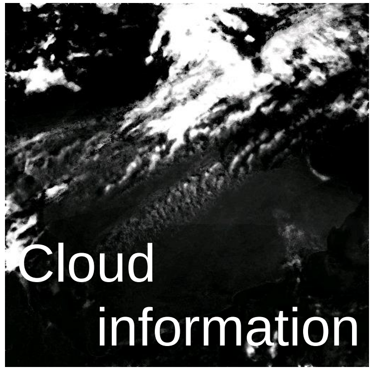

- Cloud height might come from infrared channels of satellite, but parallax effect might not be considered (-> cloud above (x,y) affects radiation at ground at (x,y))
- Cloud tracking in image series and prediction of future sat. image -> forecast

Numerical weather prediction (NWP) summary

- NWP models are designed for forecasting of weather conditions several days ahead, but some also provide data for next ~6h
- NWP models based on dynamical equations predicting the evolution of the atmosphere
  - calculations and inputs are done on a 3D grid
  - New forecasts typically 2/d to 4/d, e.g. 0, 6, 12 and 18 UTC
  - start conditions come from different meteo measurements incl. satellite
- Different model types
  - global models cover the whole planet 40 - 90km resolution
  - Mesoscale or limited area models use higher resolution and cover a smaller area (e.g. continent, country)
    - boundary conditions come from the global models

Validation of nowcasts

- Validation using common metrics such as Root mean square deviation, mean absolute deviation, bias, skill scores
- Also important application specific evaluations, e.g. ramp prediction accuracy, economic evaluations
- Validation results depend also on site and conditions during the validation

Site	Validation period
PSA, ESP	Whole years 2016, 2017 and 2018
La Africana, ESP	Whole year 2017
Évora, POR	42 days from May 2017 to March 2018
Jülich, GER	80 days from June to August 2019
Oldenburg, GER	86 days from April to June 2019

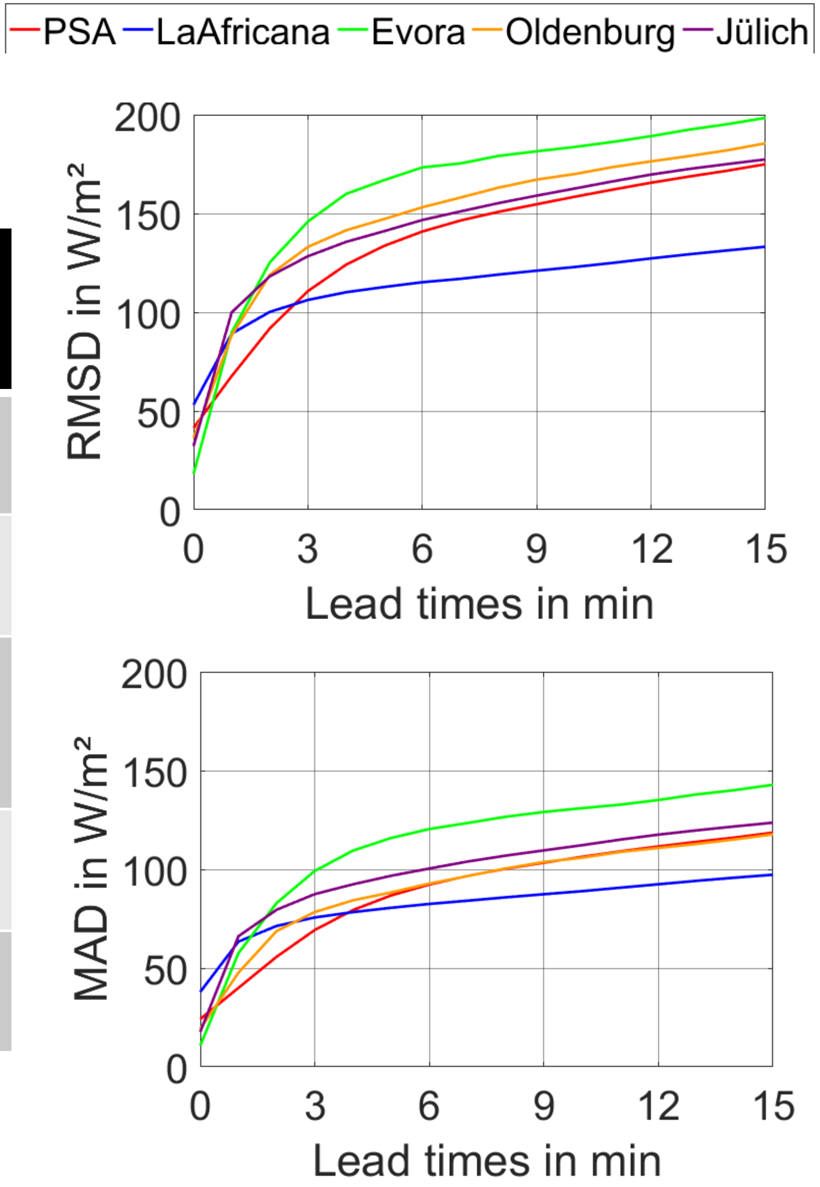

Nouri et al. 2020.

Validation of nowcasts

- Separation of data set in e.g. variability classes helps to describe errors better

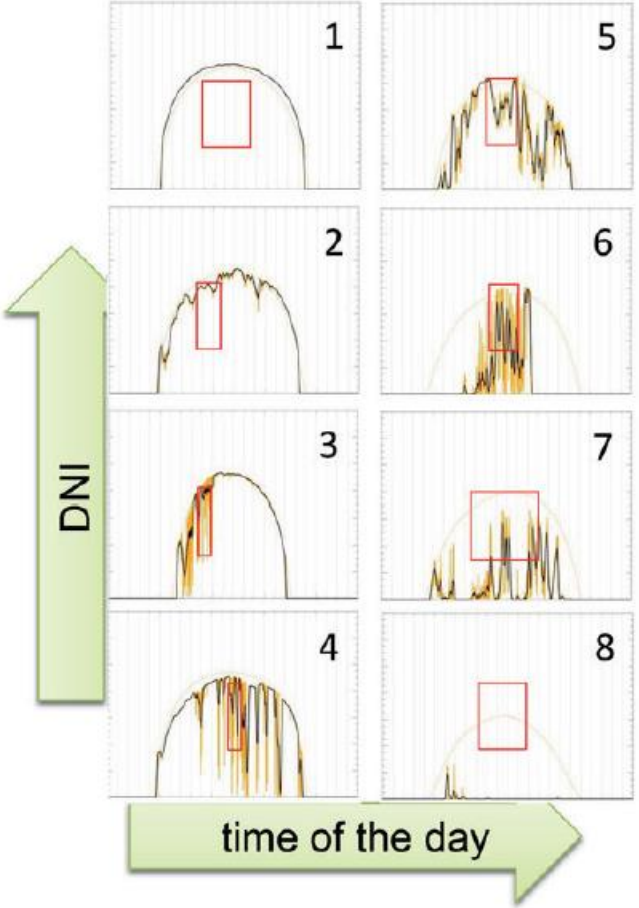

Schroedter-Homscheidt, et al., 2018.

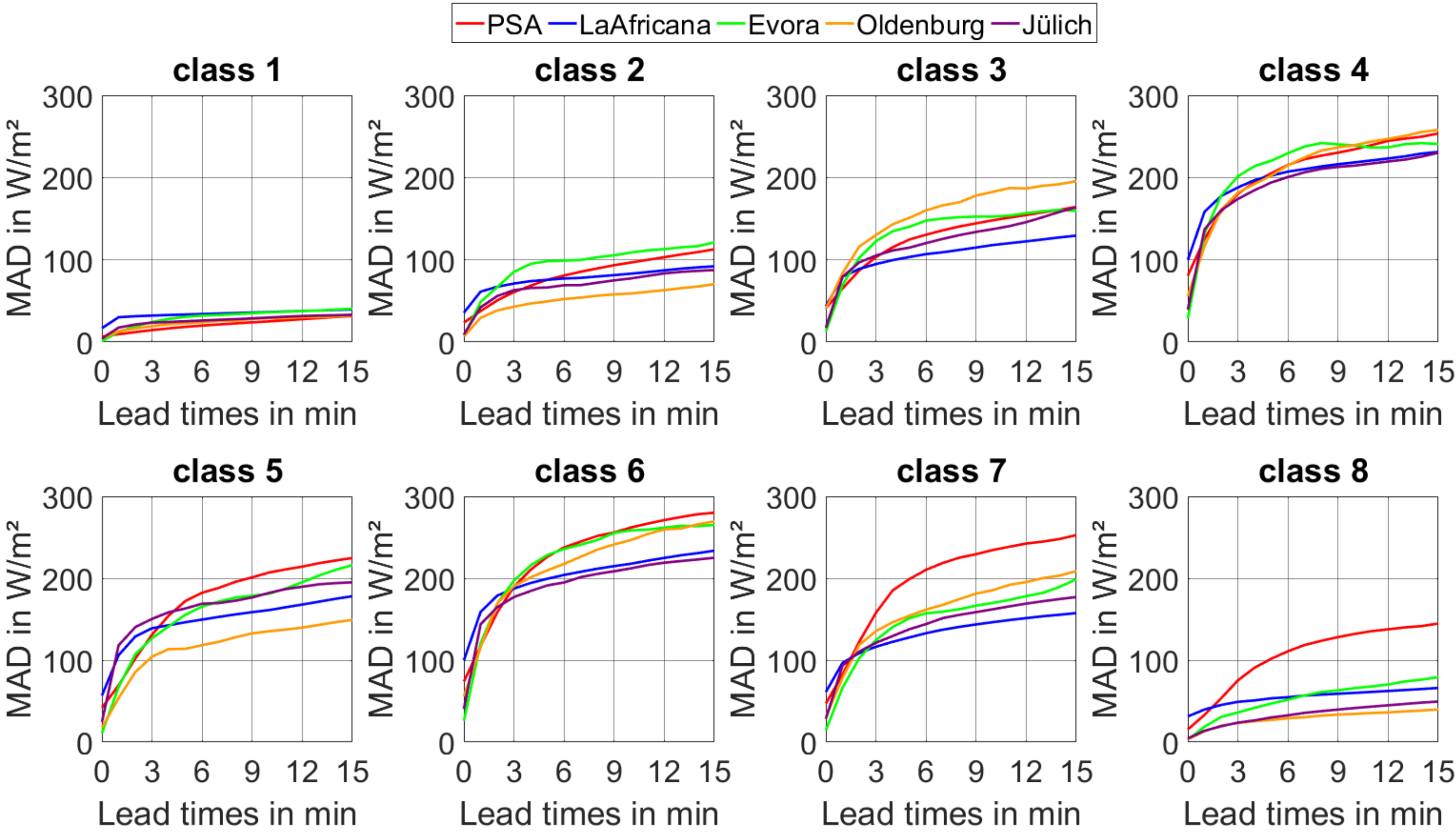

B. Nouri et al. 2020.

Validation of ASI systems

- Comparability of different forecasting systems is complex
  - Best solution is to compare systems operating at the same sites for the same time intervals
    - Comparison with simple systems (persistence)
    - E.g. ASI benchmark with different forecasting systems operated in parallel at the same site (A. Kazantzidis)

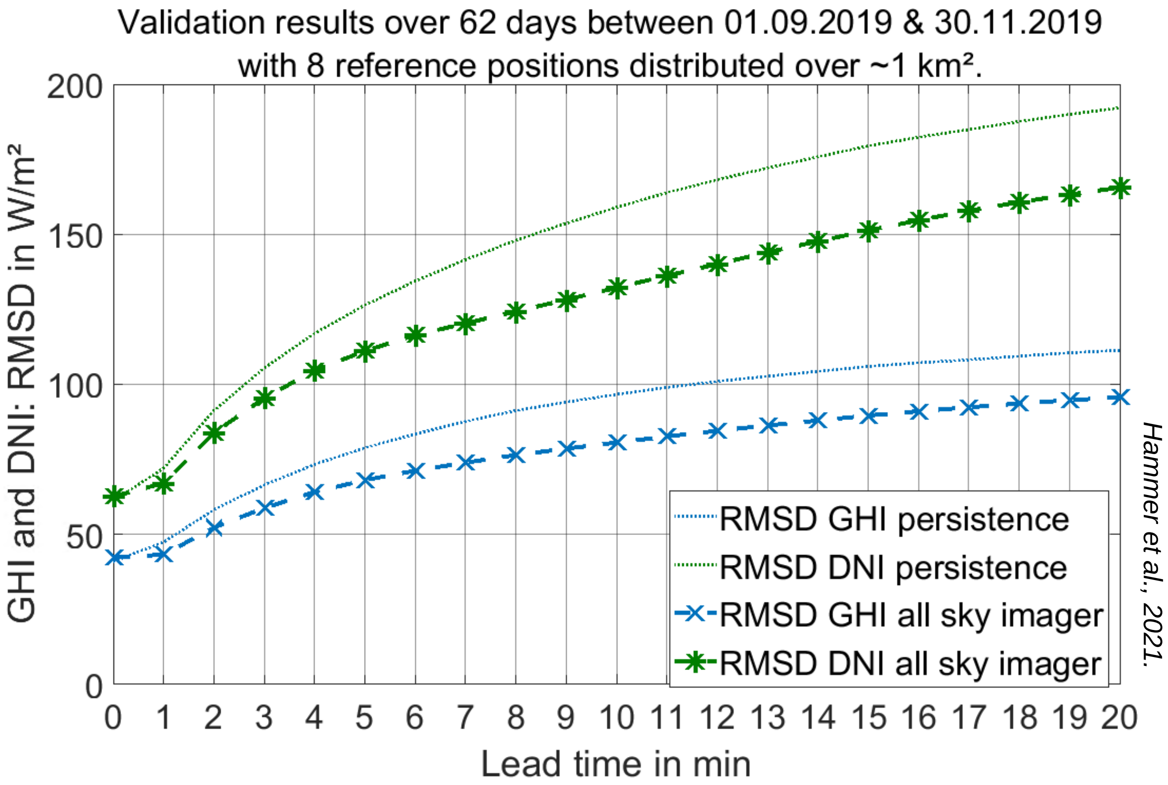

Hammer et al., 2021.

Accuracy of sat and NWP method - overview

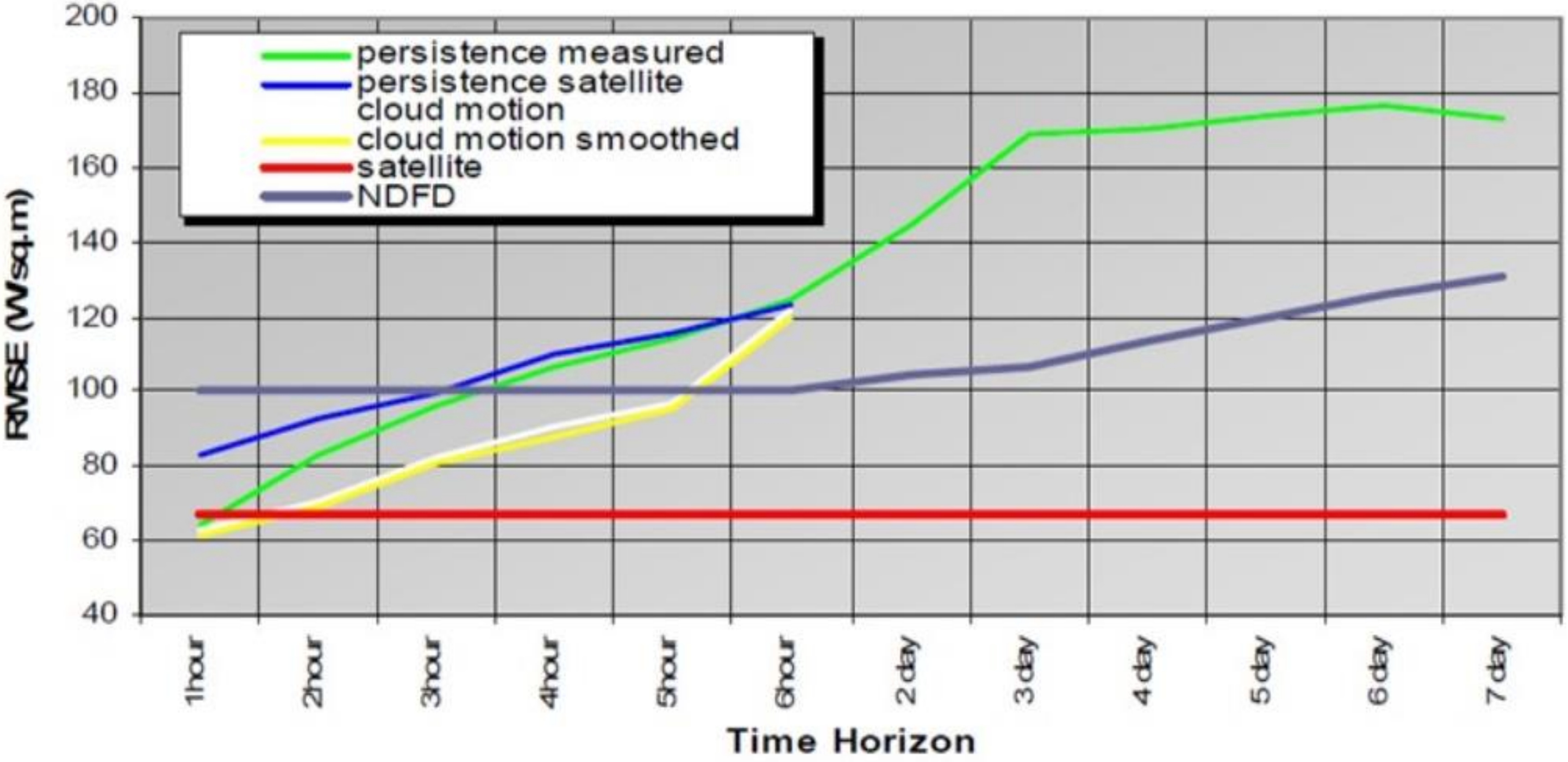

- ASI achieve best accuracy at least in the first ~10 minutes, comparison in this graph not possible due to much lower time resolution used in this slide

Pelland et al.. Photovoltaic and Solar Forecasting: State of the Art. IEA PVPS T14 report. 2013

Combination of forecasts to achieve best forecast for full horizon of interest

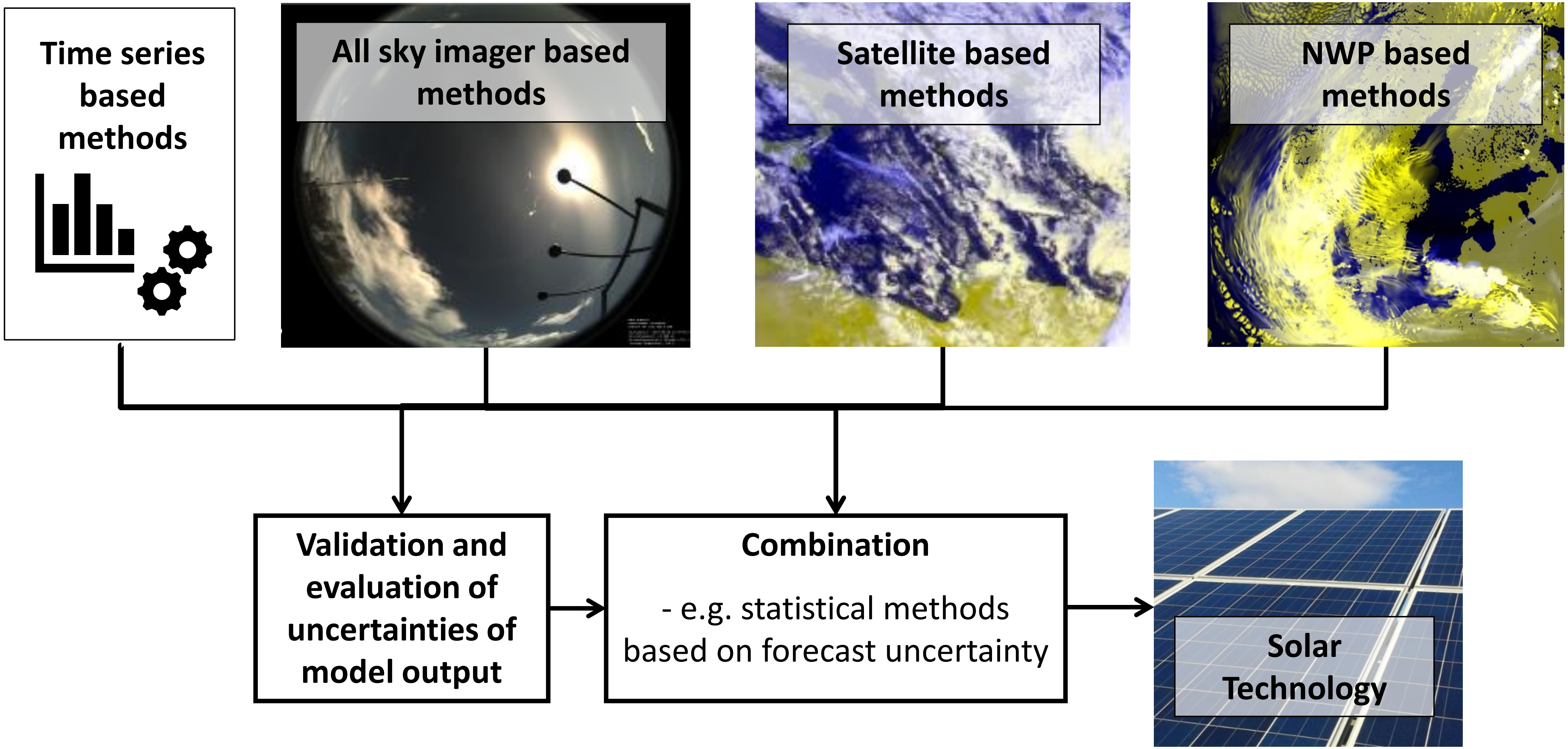

Time series based methods

All sky imager based methods

Satellite based methods

NWP based methods

Validation and evaluation of uncertainties of model output

Combination

- e.g. statistical methods based on forecast uncertainty

Solar Technology

Summary

- Nowcasts can be delivered using time series analysis, ASIs, satellites and NWP

- All sky imagers can deliver nowcasts
  - of irradiance at the camera site or
  - maps of the irradiance for several km^2 around the camera(s) if cloud height is derived
  - maps of irradiance covering thousands of km^2 if ASI networks are used

- The different methods have different advantages and disadvantages
  - combination with other forecasting methods is common

- Validation of methods at many sites and for different applications is needed

References

Kuhn, P., et al., 2017. Validation of an all-sky imager-based nowcasting system for industrial PV plants. Prog. Photovolt.: Res. Appl. doi: 10.1002/pip.2968.
Fabel, Y., et al. (2022). Applying self-supervised learning for semantic cloud segmentation of all-sky images. *AMT*
Nouri, B., et al. 2019. Cloud height and tracking accuracy of three all sky imager systems for individual clouds. Sol. Energy 177, 213–228. doi: 10.1016/j.solener.2018.10.079
Kuhn, P., et al., 2019. Determination of the optimal camera distance for cloud height measurements with two all-sky imagers. Sol. Energy., 179, 74–88 (2019). doi: 10.1016/j.solener.2018.12.038.
Nouri, B., et al., 2018. Nowcasting of DNI Maps for the Solar Field Based on Voxel Carving and Individual 3D Cloud Objects from All Sky Images, AIP Conference Proceedings. Vol. 2033. doi:10.1063/1.5067196
Nouri, B., et al., 2019b, Determination of cloud transmittance for all sky imager based solar nowcasting. Sol. Energy, 181, 251–263. doi: 10.1016/j.solener.2019.02.004.
B. Nouri et al. 2020. "Evaluation of an All Sky Imager Based Nowcasting System for Distinct Conditions and Five Sites." 2020. AIP Proceedings of SolarPaces Daegu 2019
Nouri, B. 2019c. Real-Time Uncertainty Specification of All Sky Imager Derived Irradiance Nowcasts. Remote Sens. 2019, 11, 1059. https://doi.org/10.3390/rs11091059
Noureldin, K., 2019. Modelling and Control of Transients in Parabolic Trough Power Plants with Single-Phase Heat Transfer Fluids, Ph.D. thesis, Fakultät für Maschinenwesen der Rheinisch-Westfälischen Technischen Hochschule Aachen, Aachen Germany
Pierer, Jörg and Remund, Jan 2019. SKYCAM Lokale Vorhersage der Sonneneinstrahlung. Report Bundesamt für Energie BFE, Forschungsprogramm Solare Hochtermperaturenergie (SI/5ß1515-1) https://www.aramis.admin.ch/default?DocumentID=50306&Load=true
Ryu, Anto, Hideo Ishii, and Yasuhiro Hayashi. "Battery Smoothing Control for Photovoltaic System Using Short-Term Forecast with Total Sky Images." Electric Power Systems Research 190 (2021/01/01/ 2021): 106645. https://doi.org/https://doi.org/10.1016/j.epsr.2020.106645.
Schmidt, T., et al., 2019. Energiemeteorologisches Wolkenkameranetzwerk für die hochaufgelöste Kurzfristprognose der solaren Einstrahlung. DACH-Tagung Garmisch Partenkirchen.
M. Schroedter-Homscheidt, et al., 2018. Classifying ground-measured 1 minute temporal variability within hourly intervals for direct normal irradiances. Met. Z., 27, 161-179.
Blum, et al. (2021) *Cloud height measurement by a network of all-sky imagers.* Atmospheric Measurement Techniques (AMT), 14 (7), 5199-5224. Copernicus Publications. doi: 10.5194/amt-14-5199-2021. ISSN 1867-1381.
Hammer, A. and Nouri, B., 2021. ISGAN–International Smart Grid Action Network. Smart4RES webinar on Advanced weather forecasting for RES applications – Part 2.
Pelland et al.. Photovoltaic and Solar Forecasting: State of the Art. IEA PVPS T14 report. 2013

THANK YOU FOR YOUR ATTENTION!
ANY QUESTIONS?

Stefan.Wilbert@dlr.de

SFERA-III
Solar Facilities for the European Research Area

Solar Facilities for the European Research Area

2nd Training for Industries “Optimization of CST plant output by
and thermal characterization and target-oriented O&M”
26 – 29 April 2022, Plataforma Solar de Almería, Spain

Use of nowcasting system to optimize the yield in parabolic trough power plants

Tim Kotzab, German Aerospace Center, DLR (tim.kotzab@dlr.de)

NETWORKING

THIS PROJECT HAS RECEIVED FUNDING FROM THE EUROPEAN UNION’S HORIZON 2020 RESEARCH AND INNOVATION PROGRAMME UNDER GRANT AGREEMENT NO **823802**

Control of parabolic trough solar fields

The control of solar field outlet temperature can be achieved through two parts:

1. Collector focus controller
2. Mass flow controller

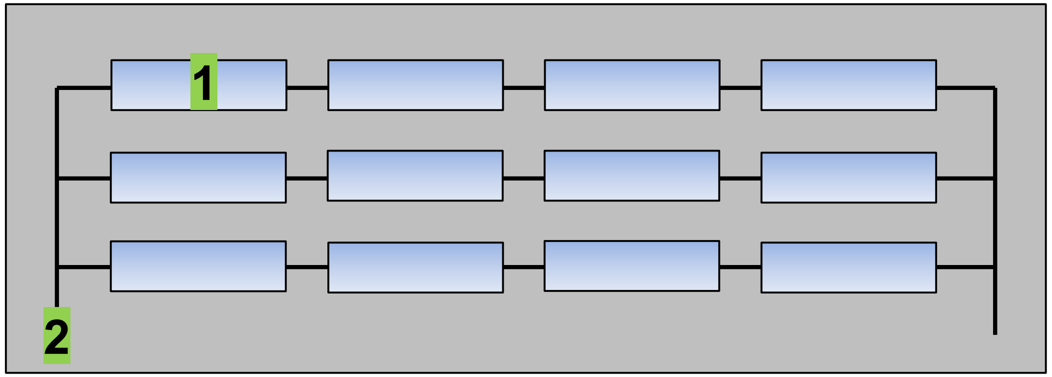

Current status of mass flow control:
- DNI spot measurements (2…5)

Our approach:
- Use of spatially resolved DNI maps
- Improvement of automatic control even in cloudy conditions

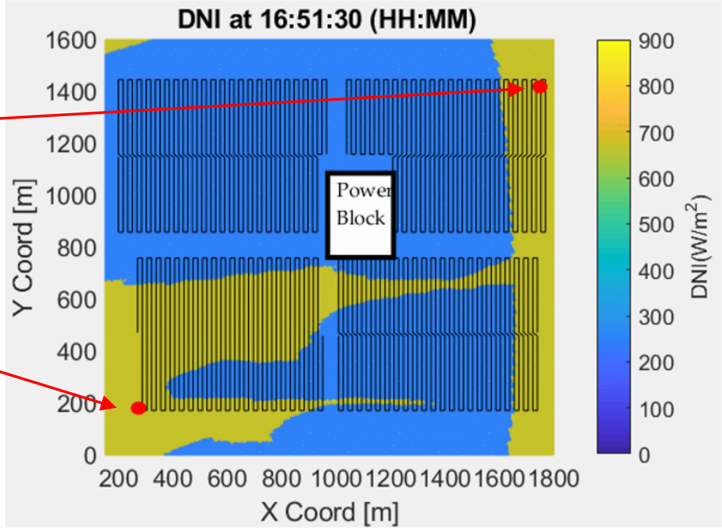

The Virtual Solar Field (VSF)

Virtual Solar Field (VSF) is a dynamic simulation program which models a complete parabolic trough solar field with high level of detail and adequate computation time.

Main features of VSF:

- Mass flow distribution
- Spatially variable irradiance can be modelled
- Flexible solar field layout
- Implementation of different solar field controller

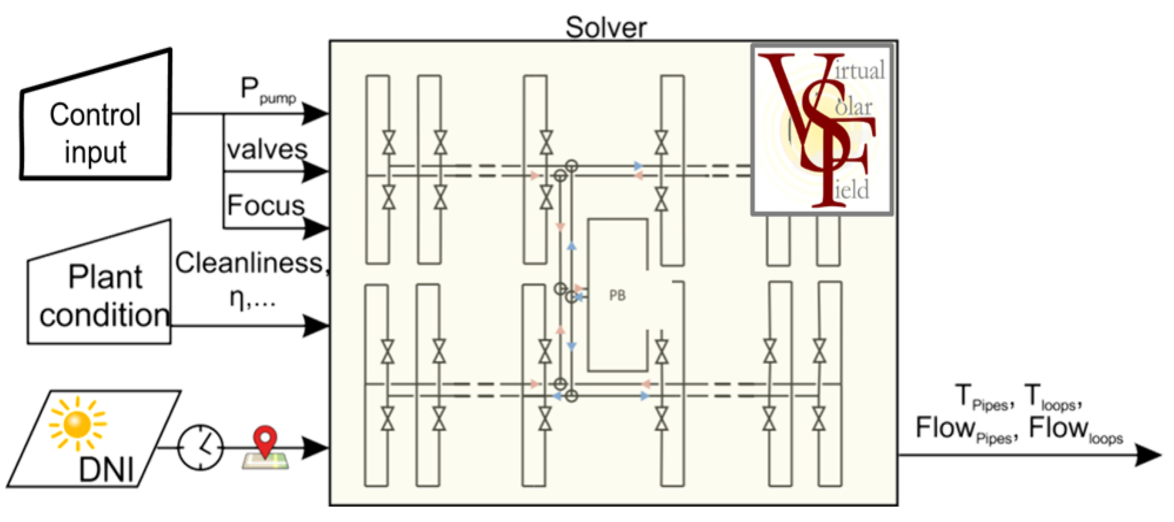

State of the art solar field controller

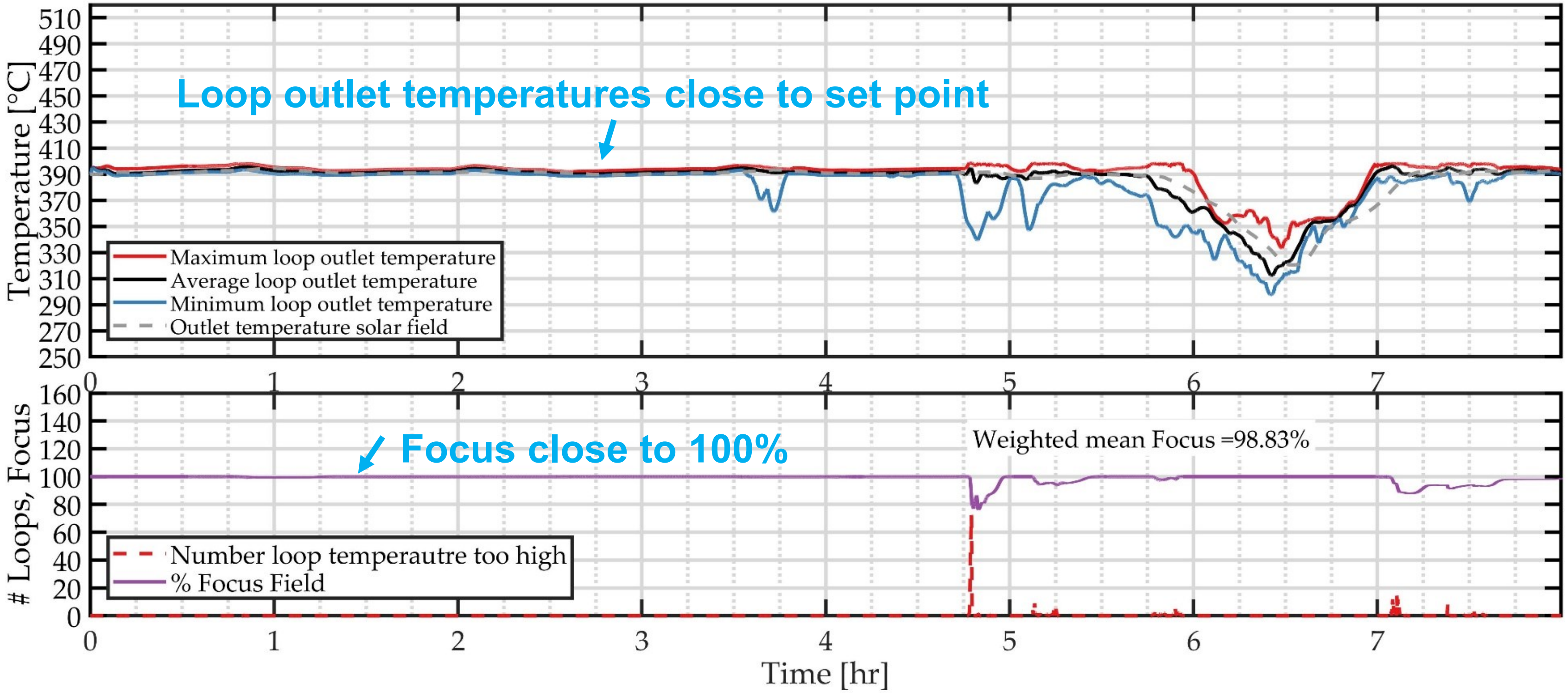

Loop outlet temperatures close to set point

Focus close to 100%

Reference controller can adjust the output temperature and field focus in the first 5 to 6 hours during clear sky conditions

State of the art solar field controller

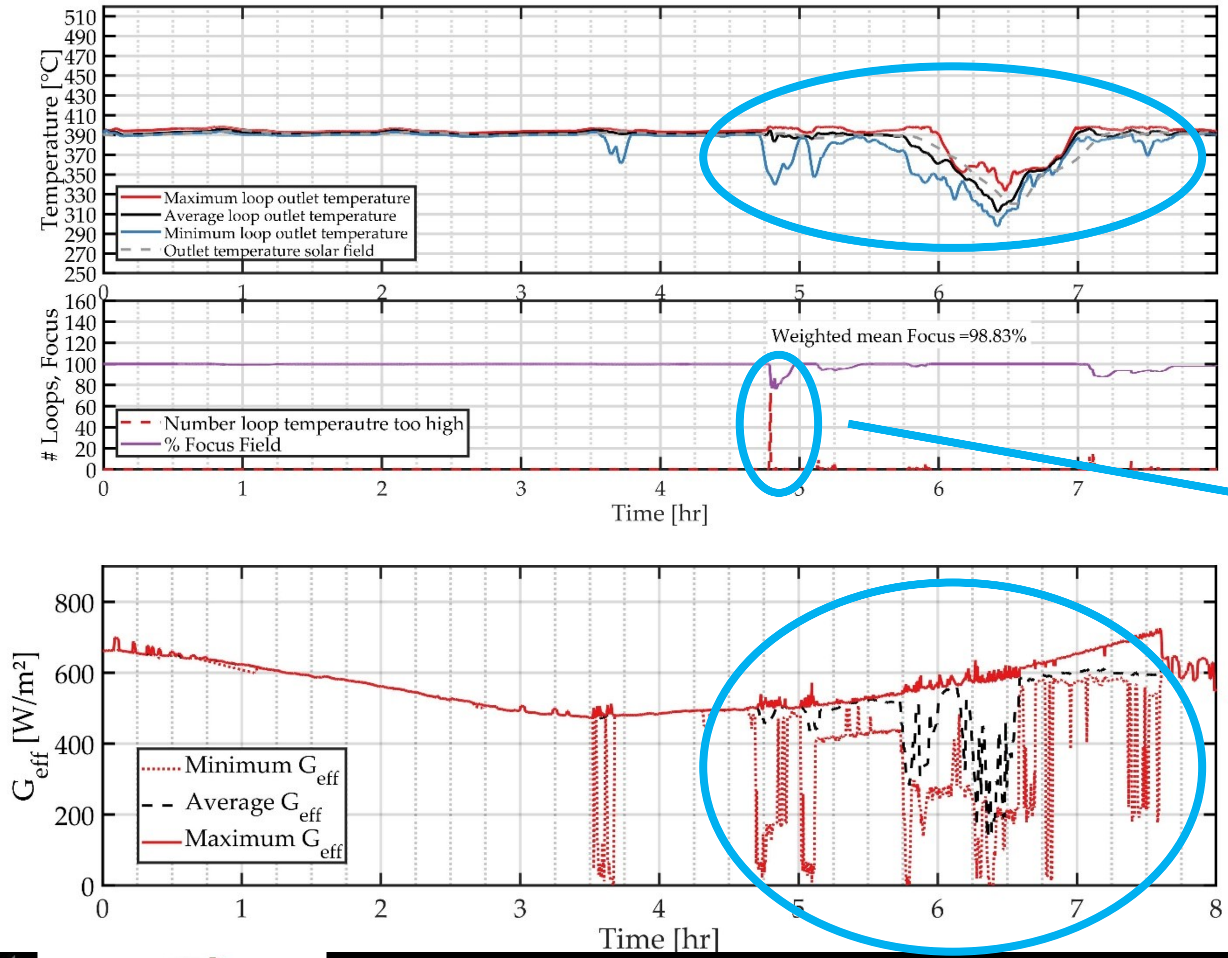

Strong deviations in outlet temperatures under cloud passage

Strong defocusing induced by over-temperatures

Improvements with nowcasting system and all sky imager approach

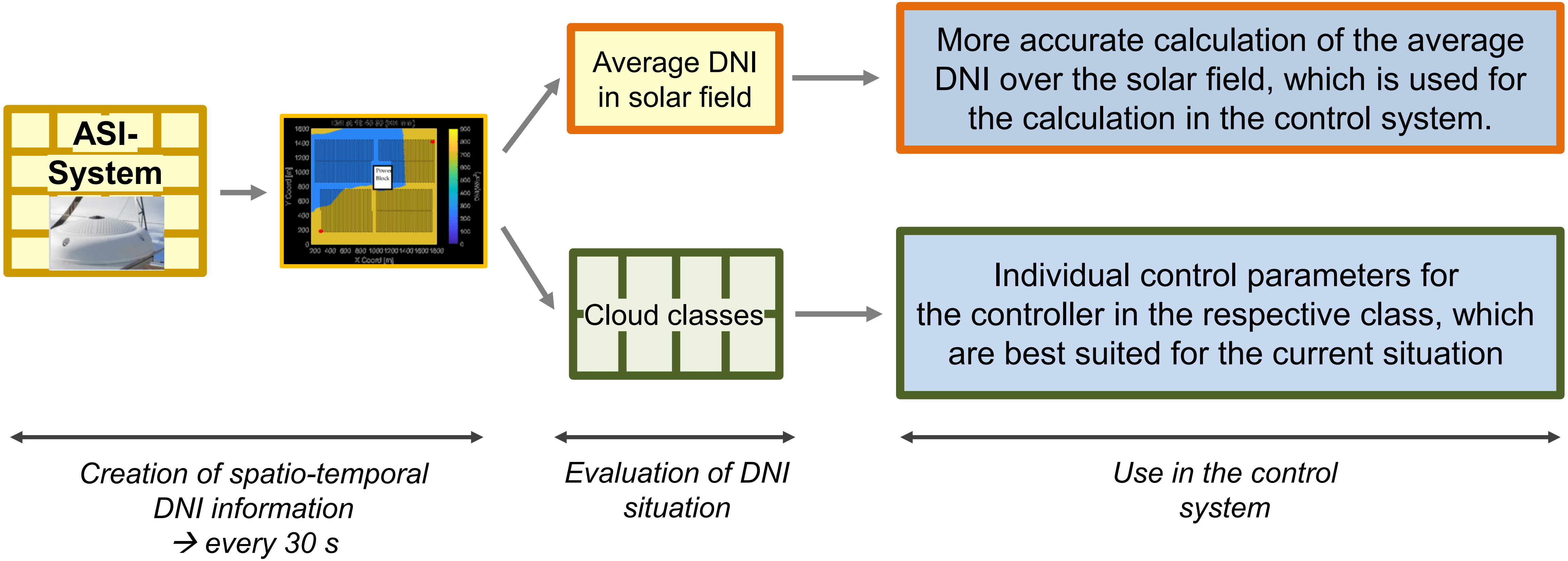

ASI-System

Average DNI in solar field

More accurate calculation of the average DNI over the solar field, which is used for the calculation in the control system.

Cloud classes

Individual control parameters for the controller in the respective class, which are best suited for the current situation

Creation of spatio-temporal DNI information → every 30 s

Evaluation of DNI situation

Use in the control system

Comparison of control concepts

State of the art controller

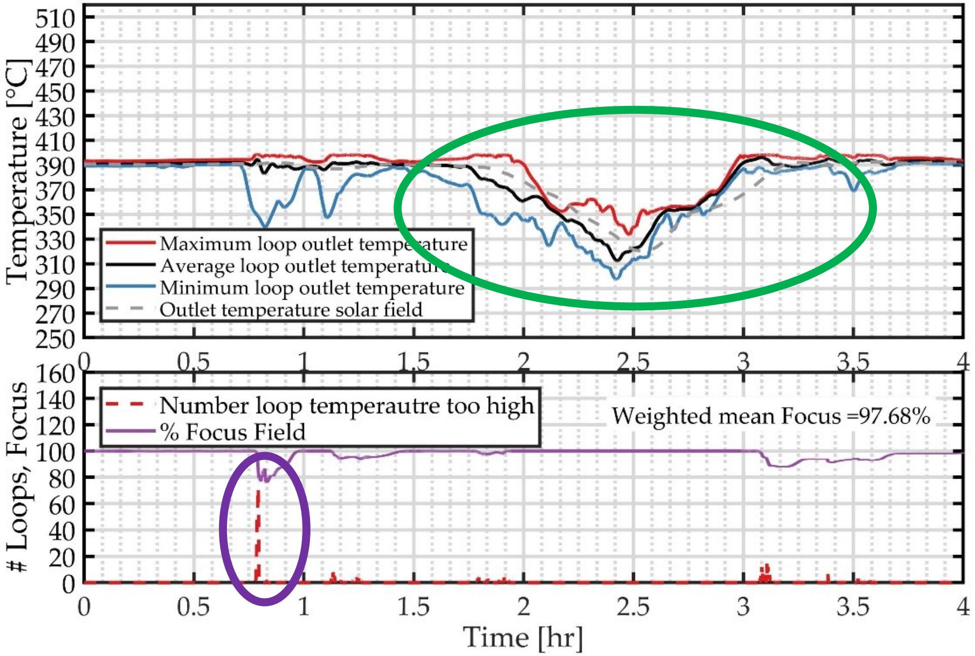

Increase of average outlet temperature

New control concept

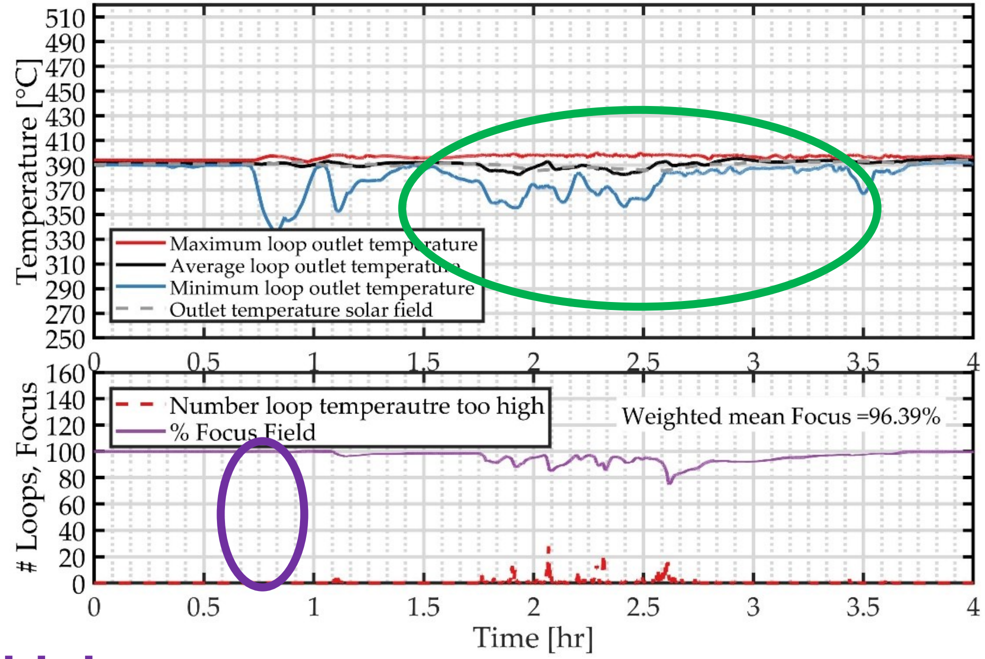

Reduction of high peak temperatures of individual loops

Further investigations under realistic conditions

Simulations with VSF

Differences to real solar field

- Soiling of collectors
- Uncertainties in nowcasting system
- Solar field inlet temperature

Simulations carried out to analyze real behavior:
- Simulation of uncertainties in DNI maps
- Change of solar field inlet temperature during the day
- Soiling of collectors
- Transferability of the control system to another solar field

Results of robustness analysis

Setup:

- Inhomogeneous soiling of the individual loops in the solar field.
- Variable change of solar field inlet temperature during the day.
- Uncertainties during the creation of DNI maps with nowcasting system

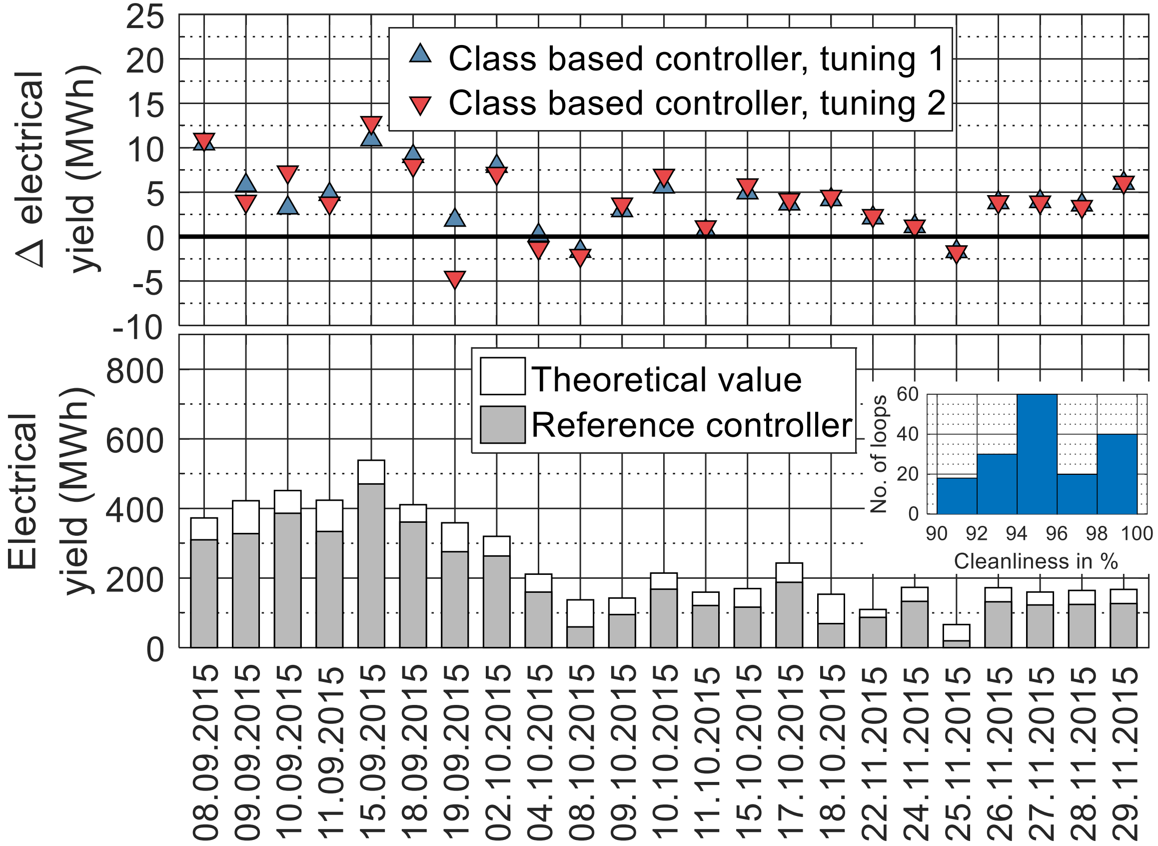

Results:

- Increase of electrical yield by 2%
- Increase average outlet temperature by 6% and solar field focus by 1%
- Decrease emergency defocusing events by 48%

Conclusion

Investigation of a control system for parabolic trough power plants with spatially resolved DNI maps.

- Better representation of the current irradiation in cloudy situations
- Classification of the current irradiation situation
- Performance improvements compared to actual control concepts

Investigation of the control behavior under "real" conditions (soiling, …)

Results:

- **Improvement of the control performance with the new system**
- **Increase of the average outlet temperature and focus**
- **Increase of the electrical yield up to 2% over all simulation days (to be achieved with the cost of a ASI system installation)**

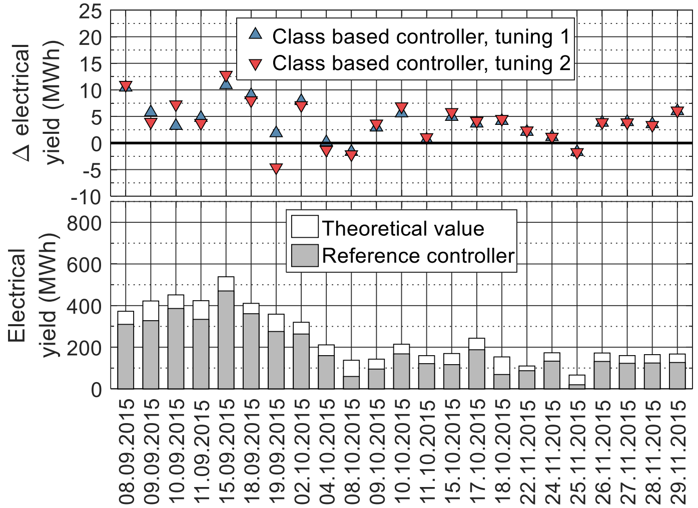

THANK YOU FOR YOUR ATTENTION!
ANY QUESTIONS?

GOBIERNO DE ESPAÑA
MINISTERIO DE CIENCIA, INNOVACIÓN Y UNIVERSIDADES
Ciemat
Centro de Investigaciones Energéticas, Medioambientales y Tecnológicas

ENEA

DLR Deutsches Zentrum für Luft- und Raumfahrt

UNIVERSIDADE DE ÉVORA

ESTELA

The Cyprus Institute

instituto imdea energía

Fraunhofer ISE

euronovia

LNEG

METU

ETH zürich

IN LUMINE SAPIENTIA UNIVERSITAS ALMERIENSIS
UNIVERSIDAD DE ALMERÍA

cnrs dépasser les frontières

DE LA RECHERCHE À L'INDUSTRIE
cea

Proposal for a demonstration at a real plant

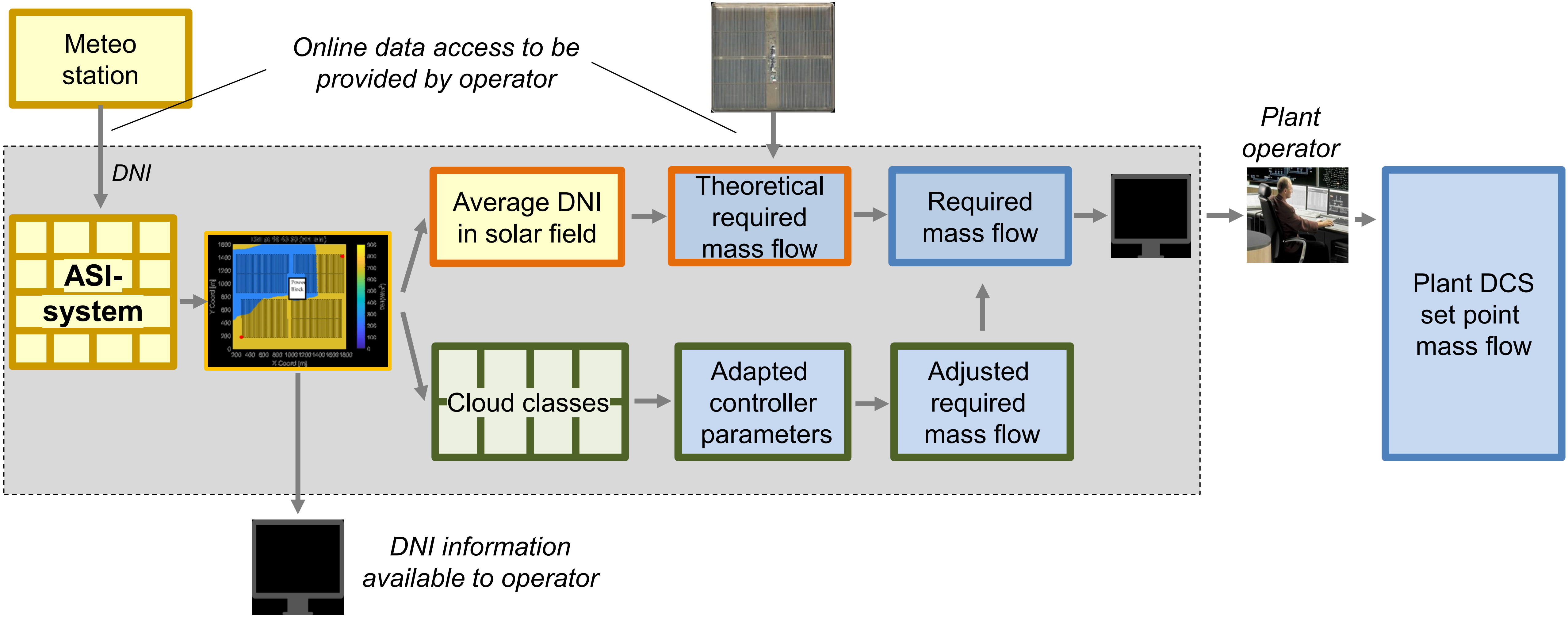

Meteo station

Online data access to be provided by operator

DNI

ASI-system

Average DNI in solar field

Theoretical required mass flow

Required mass flow

Plant operator

Plant DCS set point mass flow

Cloud classes

Adapted controller parameters

Adjusted required mass flow

DNI information available to operator

Developed control system with the ASI-System General concept

Feed-Forward:

Computes a required mass flow depending on:

- Current DNI Situation
- System parameters of the solar field

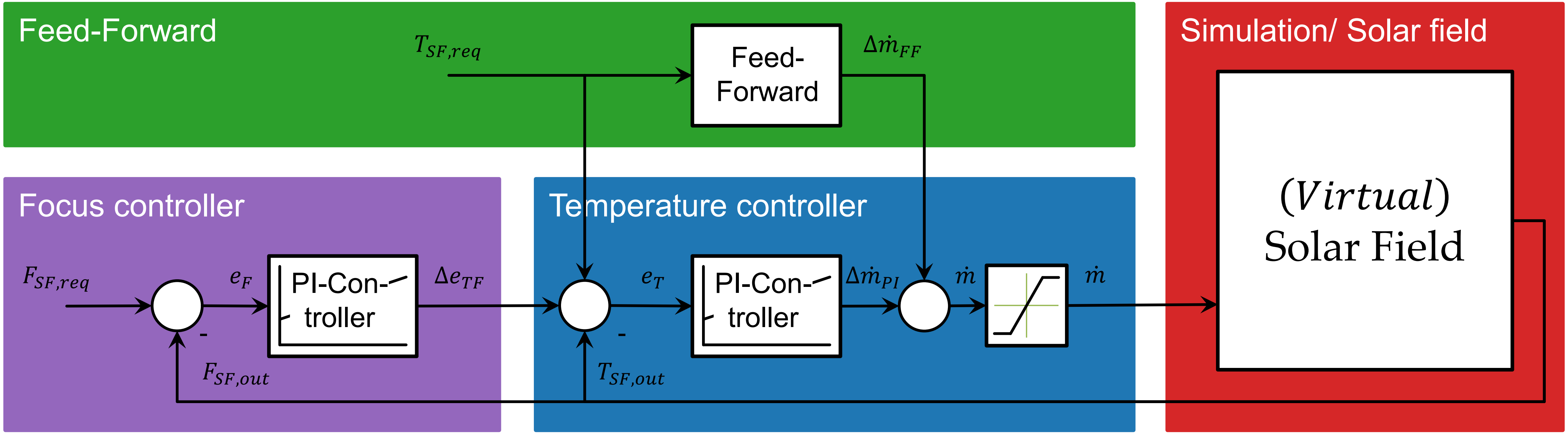

Feed-Back-Focus-Control:

Controls the whole solar field focus of the collectors

Feedback-Temperature-Control:

- Controls the solar field outlet temperature
- Adaptively computed control parameters depending on:
  - Solar energy input
  - Solar field thermodynamics state

Developed control system with the ASI-System
Use of ASI-System

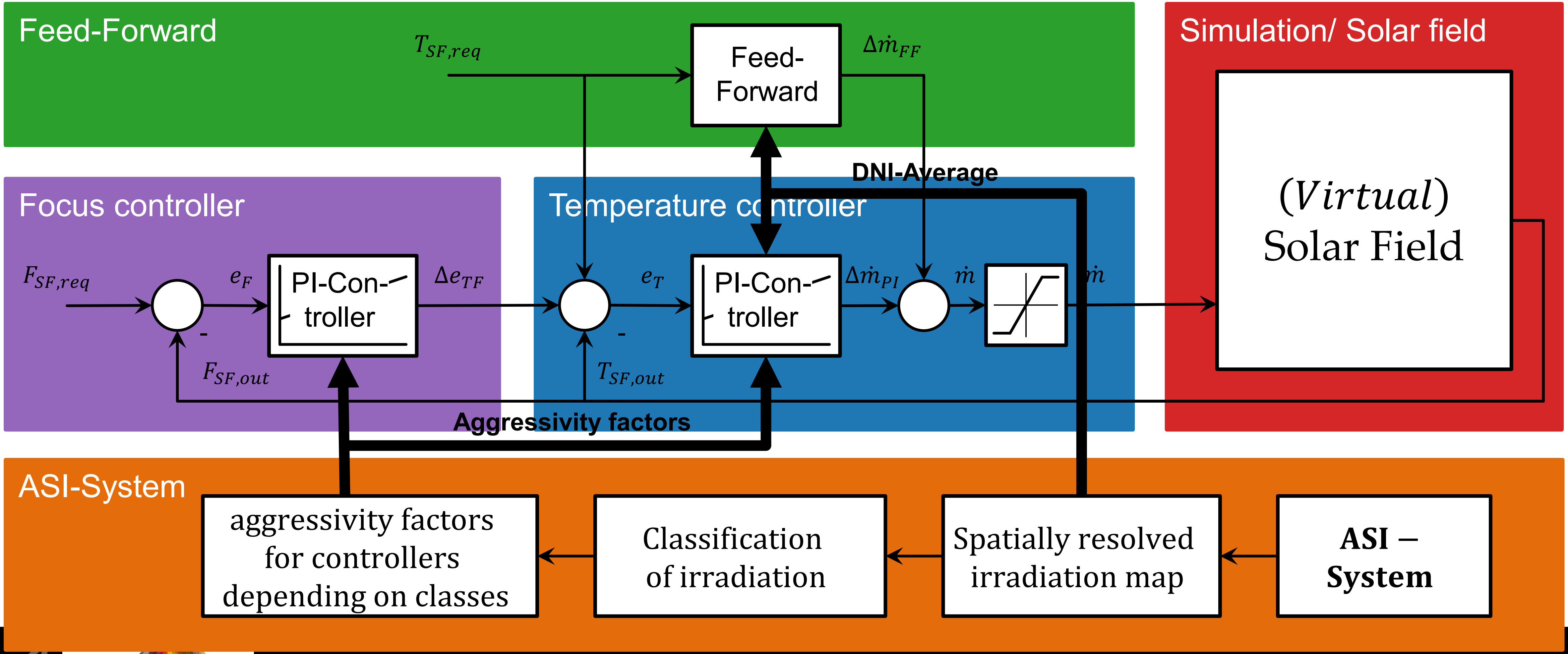

Integration possibilities of ASI- and Control System

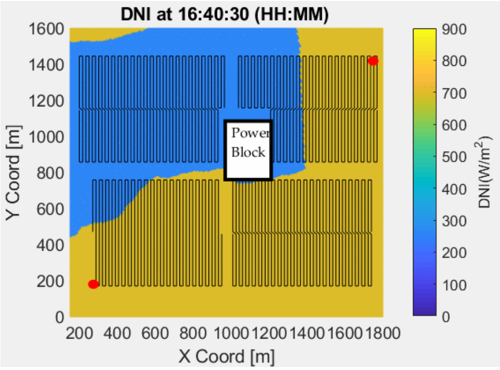

How can we use and integrate the ASI- and control system in a commercial power plant?

1. Information of operator: Use ASI system for a better overview of the DNI over the solar field

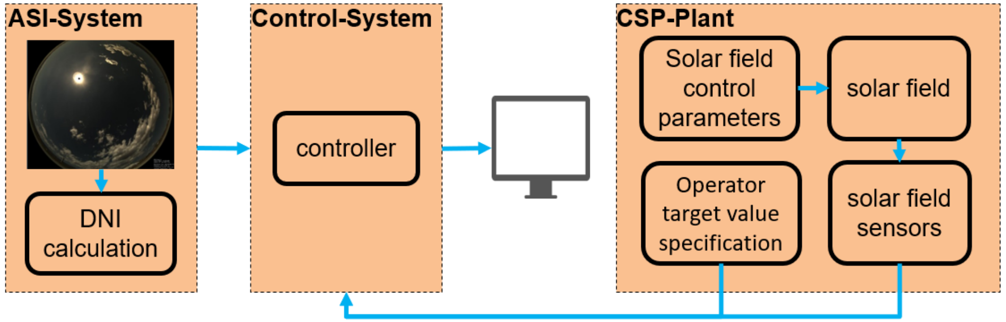

ASI-System

DNI calculation

Control-System

controller

CSP-Plant

Solar field control parameters

solar field

Operator target value specification

solar field sensors

2. Support operator: Use ASI + control system as assistance to support the mass flow adjustment in the solar field

3. Automation: Full integration of the systems for automatic control of the solar field

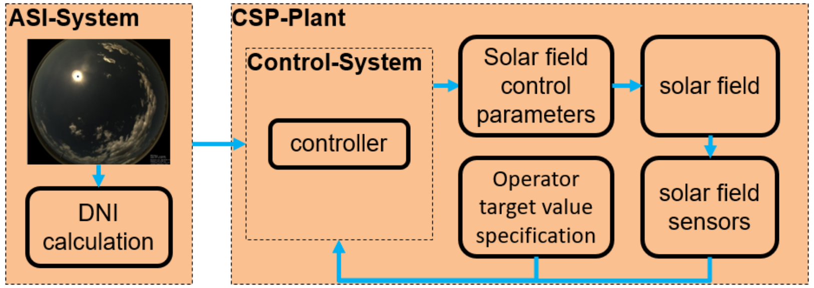

ASI-System

DNI calculation

CSP-Plant

Control-System

controller

Solar field control parameters

solar field

Operator target value specification

solar field sensors

SFERA-III

Solar Facilities for the European Research Area

Solar Facilities for the European Research Area

Training for Industries, Almería, 26. – 29.04.2022:
“Optimization of CST plant output by optical and thermal characterization and target-oriented O&M”

Measurement of optical properties (reflectance, absorptance, transmittance)

Florian Sutter, DLR
Arantxa Fernandez, CIEMAT

THIS PROJECT HAS RECEIVED FUNDING FROM THE EUROPEAN UNION’S HORIZON 2020 RESEARCH AND INNOVATION PROGRAMME UNDER GRANT AGREEMENT NO **823802**

Contents

- Reflectance
- Transmittance
- Absorptance
- Emittance
- Summary

SFERA-III
Solar Facilities for the European Research Area

Reflectance

Florian Sutter, DLR

2nd Training for Industries, Plataforma Solar de Almería

Near-specular reflectance

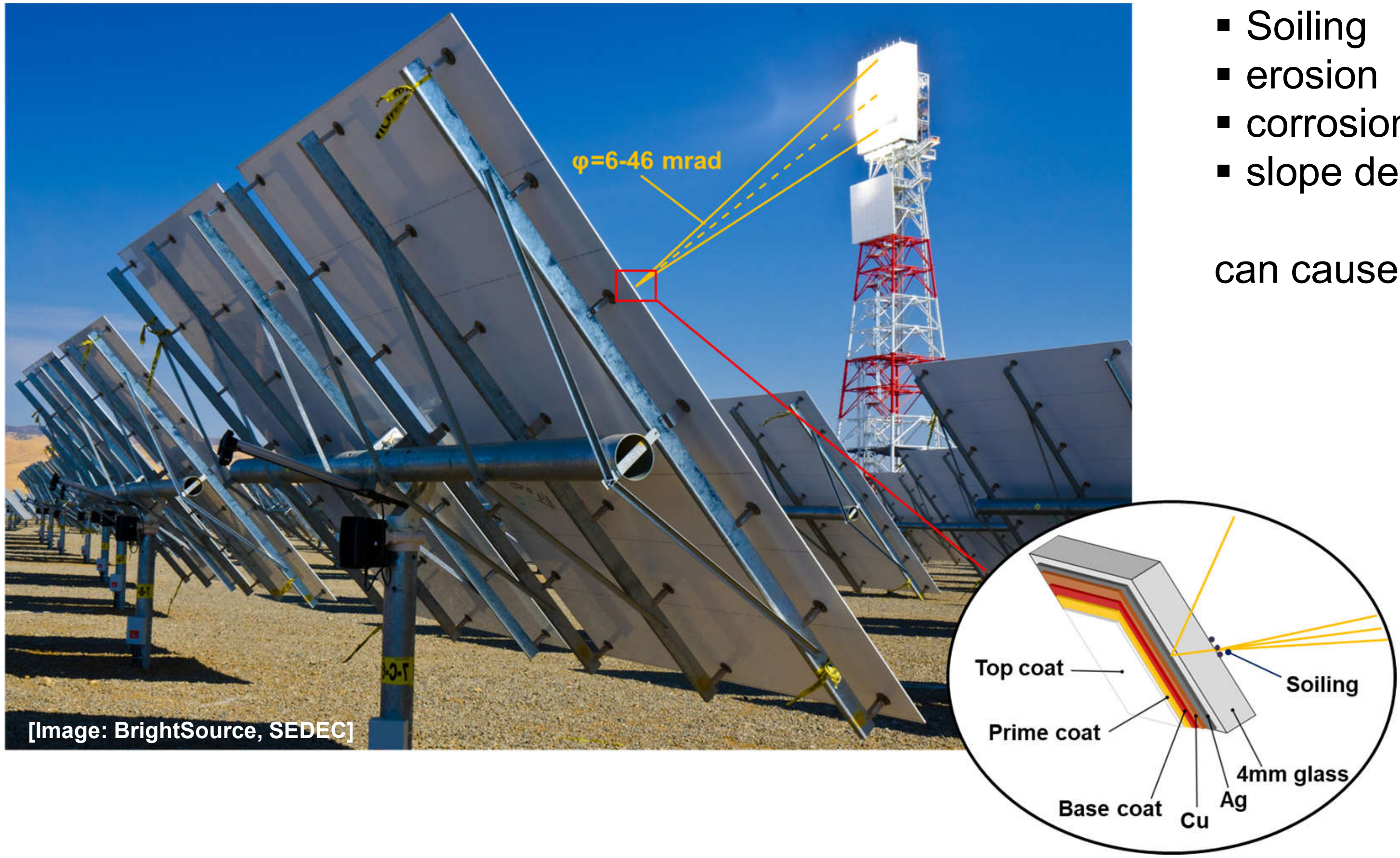

[Image: BrightSource, SEDEC]

- Soiling
- erosion
- corrosion
- slope deviation (shape)

can cause performance loss

Diffuse and specular reflectance

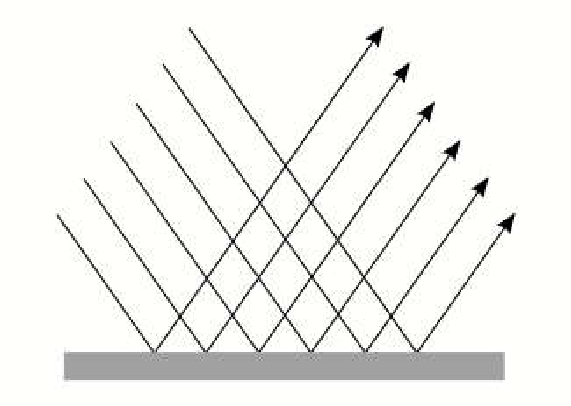

Perfect specular reflectance

$\theta_{\text{incidence}} = \theta_{\text{reflected}}$

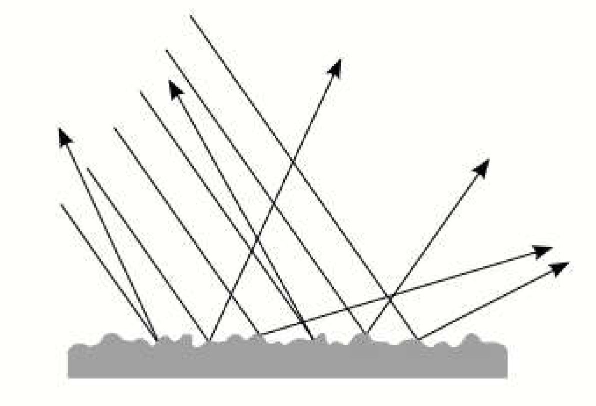

Diffuse reflectance

$\theta_{\text{incidence}} \neq \theta_{\text{reflected}}$

Hemispherical and specular reflectance parameters

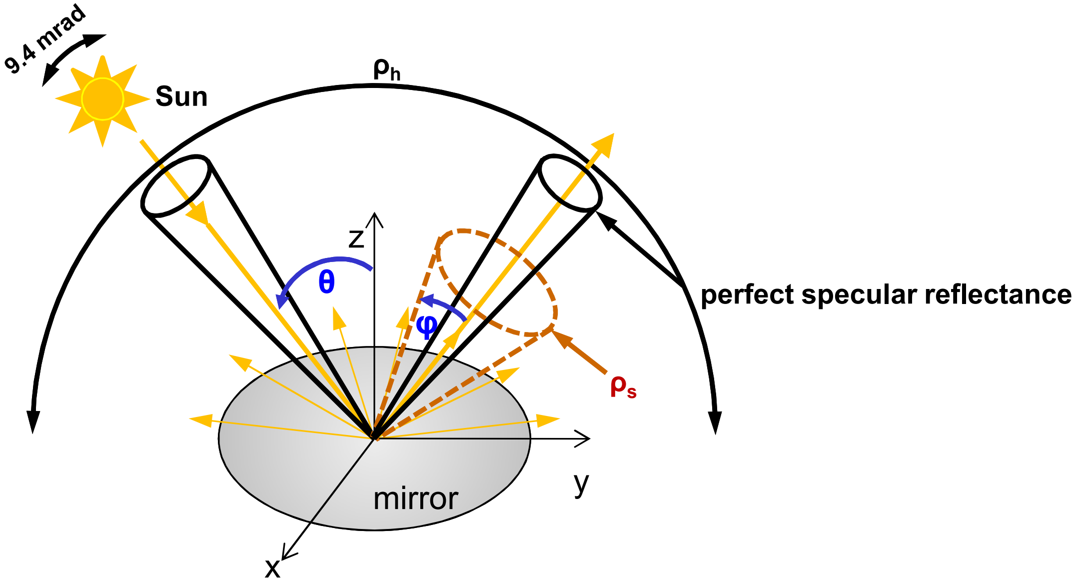

specular reflectance within acceptance angle φ

hemispherical reflectance (acceptance angle is complete hemisphere “φ=h”)

Fundamentals of reflectance

Every measured reflectance value needs to be declared in the format:

$$\boxed{\rho(\lambda, \theta_i, \varphi)}$$

λ	wavelength	[nm]
θ_i	incidence angle	[º]
φ	acceptance angle	[mrad]
(φ_i	beam divergence of the incident light	[mrad])* under discussion

To indicate solar weighted values use index s and indicate the wavelength range of the weighting instead of λ

To indicate hemispherical reflectance use “h” instead of φ

Examples: $\rho\,(660\ nm,\ 15º,\ 12.5\ mrad) = 95.3\%$

$\rho_s\,([280,2500nm],\ 8º,\ h) = 94.1\%$

Solar weighting of reflectance spectra

- Reflectance is wavelength dependent
- A suitable “mean value” of all relevant solar wavelengths is the solar weighted reflectance $\rho_s([\lambda_a,\lambda_b],\theta_i,\varphi)$

$$\rho_s([\lambda_a,\lambda_b],\theta_i,\varphi)=\frac{\sum_{i=0}^{i_{\max}}\rho(\lambda_i,\theta_i,\varphi)\cdot G_b(\lambda_i)}{\sum_{i=0}^{i_{\max}}G_b(\lambda_i)}$$

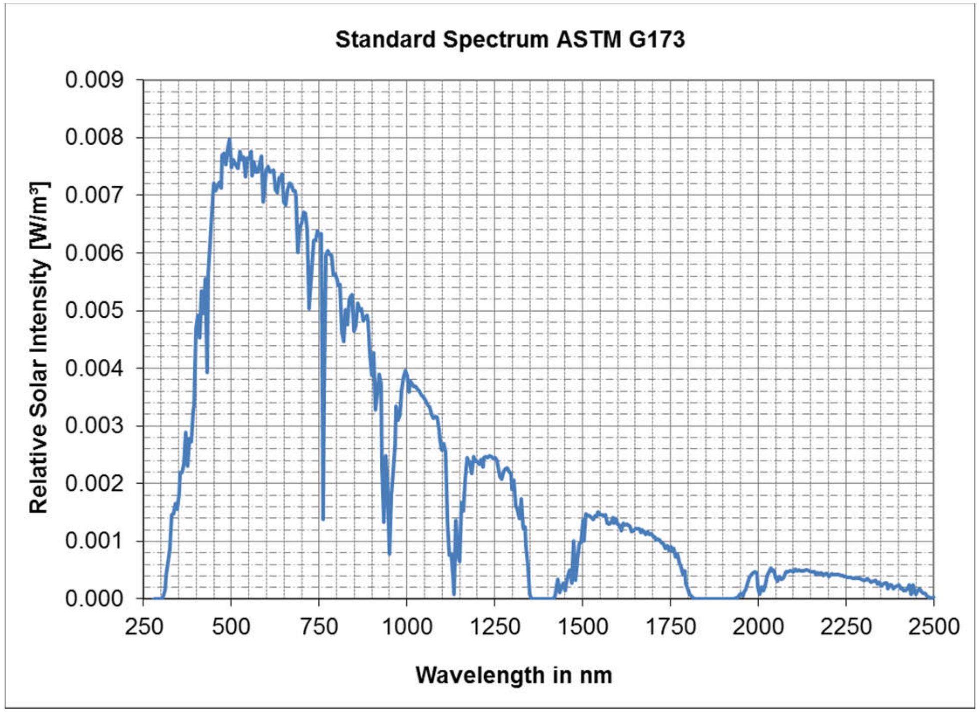

The spectral solar irradiance $G_b(\lambda_i)$ is obtained in 5 nm steps from a reference spectrum, e.g. ASTM G173 with air mass 1.5 and 1000 W/m²

The wavelength range to be considered is **[320, 2500]nm** (the far UV, UV-B and mid-infrared range have a negligible impact on $\rho_{s,h}$ and it is practically more convenient for the measurement equipment)

Examples of reflector measurements

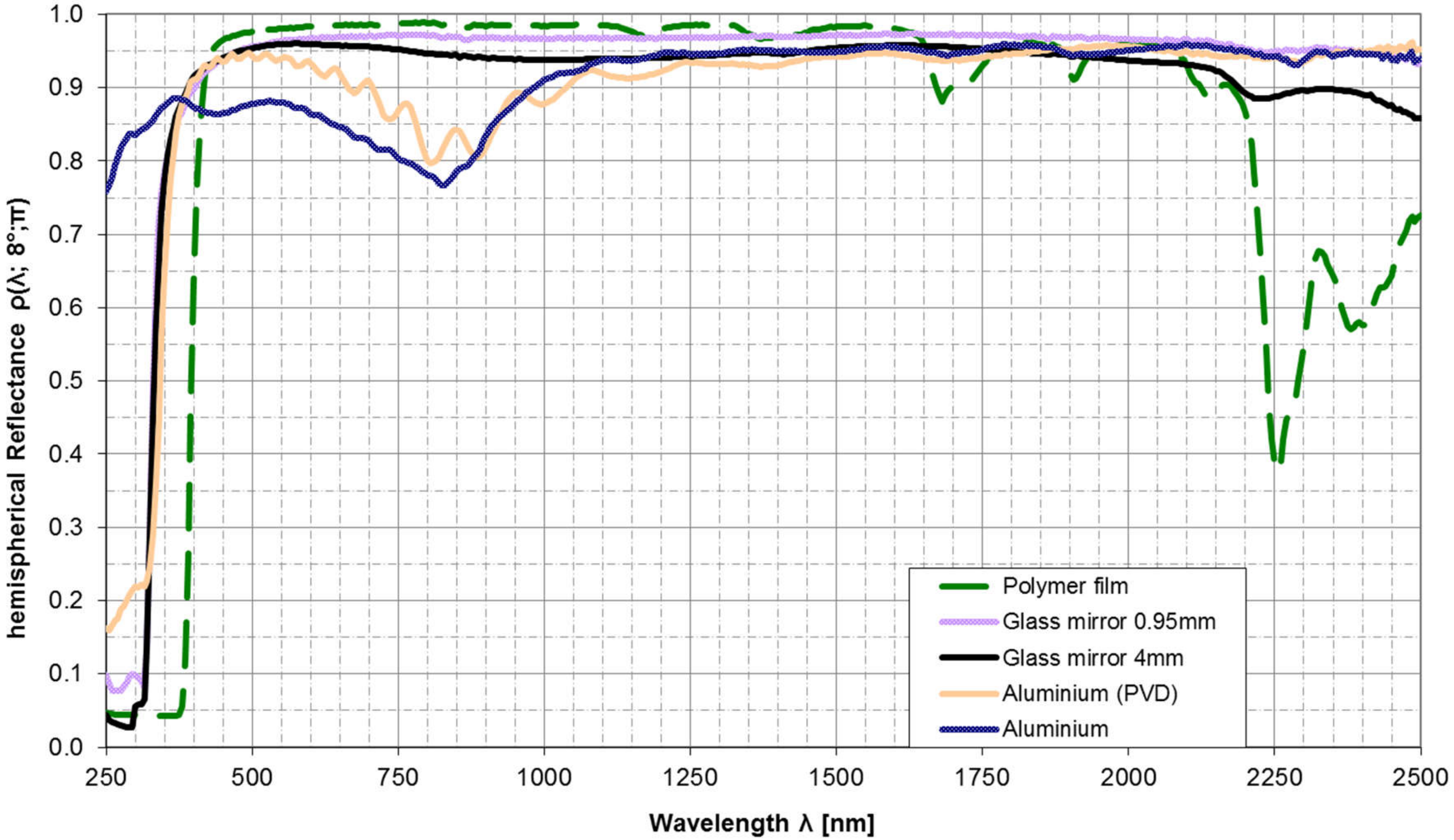

Reflectance parameters of different typical materials

	ρ_s([280-2500nm], 8º , h)	ρ(660nm, 8º, h)	ρ(660nm, 15º, 12.5mrad)
Glass mirror 0.95 mm	95.7	96.9	96.9
Glass mirror 4 mm	94.5	95.7	95.7
Polymer film	93.9	98.5	95.5
Aluminum (PVD)	90.0	90.6	85.1
Aluminum	87.2	84.2	79.6

Indication of scattering

Scattering solar reflector materials

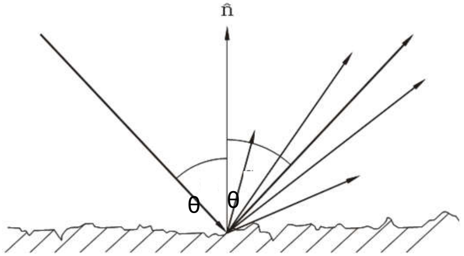

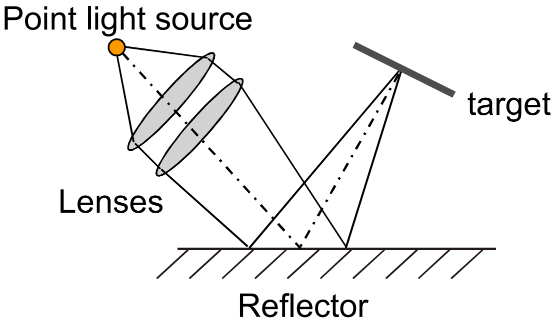

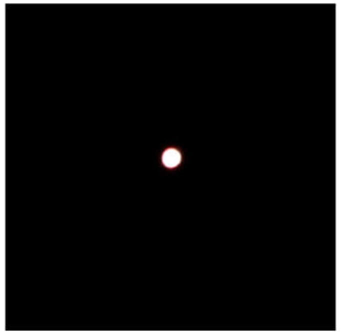

Silvered-glass reflector (0.95mm)

Polymer film

Aluminum (PVD)

Specularity

Specularity $$S_{\lambda,\varphi} = \frac{\rho_{\lambda,\varphi}}{\rho_{\lambda,h}}$$

is typically very high for silvered-glass reflectors (>0.996)

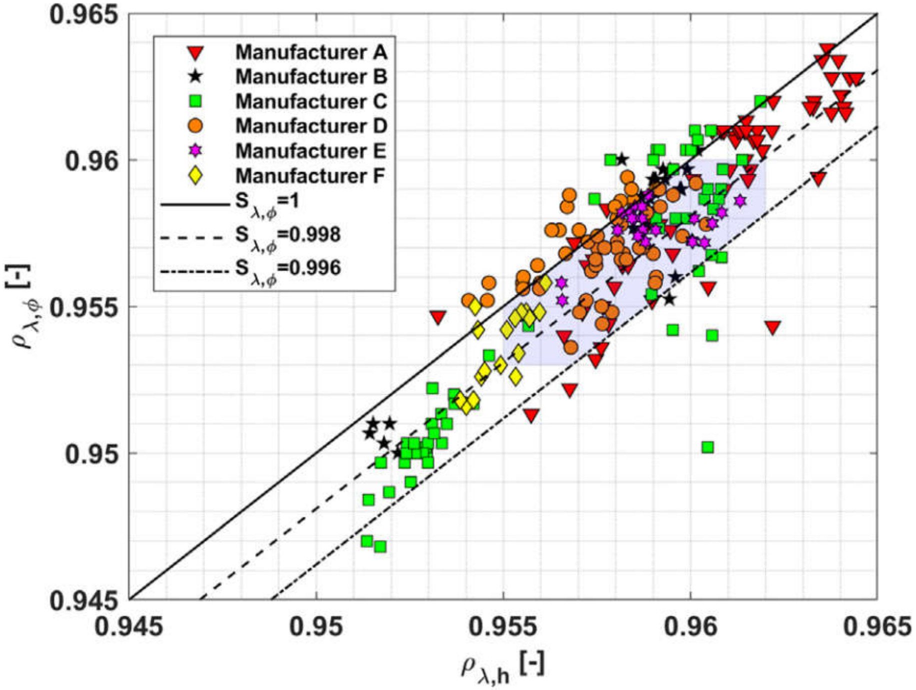

Fig. 3. Monochromatic near-normal hemispherical and monochromatic near-specular reflectance at λ = 660 nm of commercial 4 mm glass mirrors. The gray area can be considered as state of the art.

State of the art reflectance

Analysis of all relevant 4mm silvered-glass mirror manufacturers shows that

ρ_s([280-2500nm], 8º , h) = 94.5%

can be regarded as the state of the art.

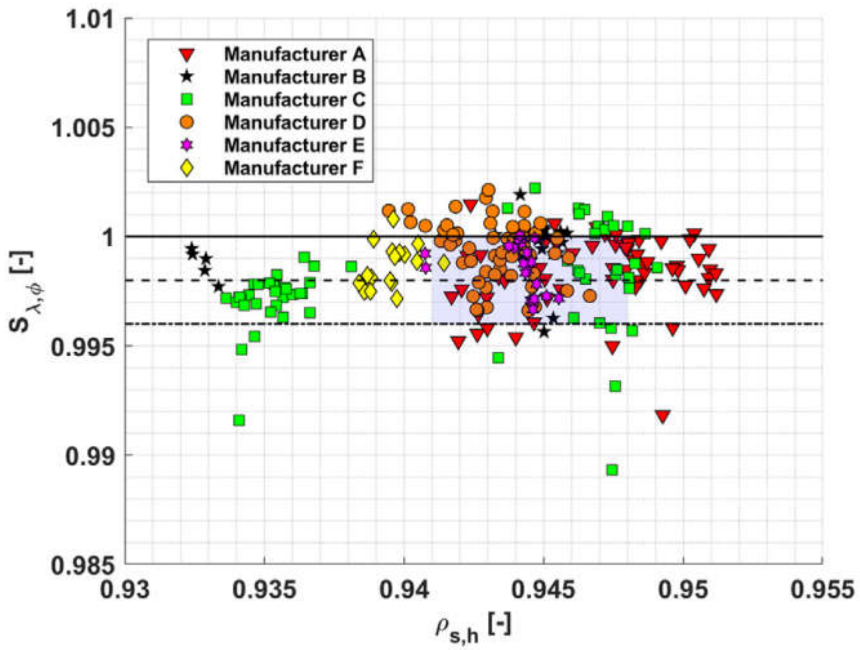

Fig. 4. Solar-weighted hemispherical reflectance, $\rho_{s,h}$, plotted over specularity, $S_{\lambda,\varphi}$, of commercial 4 mm silvered-glass mirrors. The gray area can be considered as state of the art.

Reflectance at a silvered glass mirror

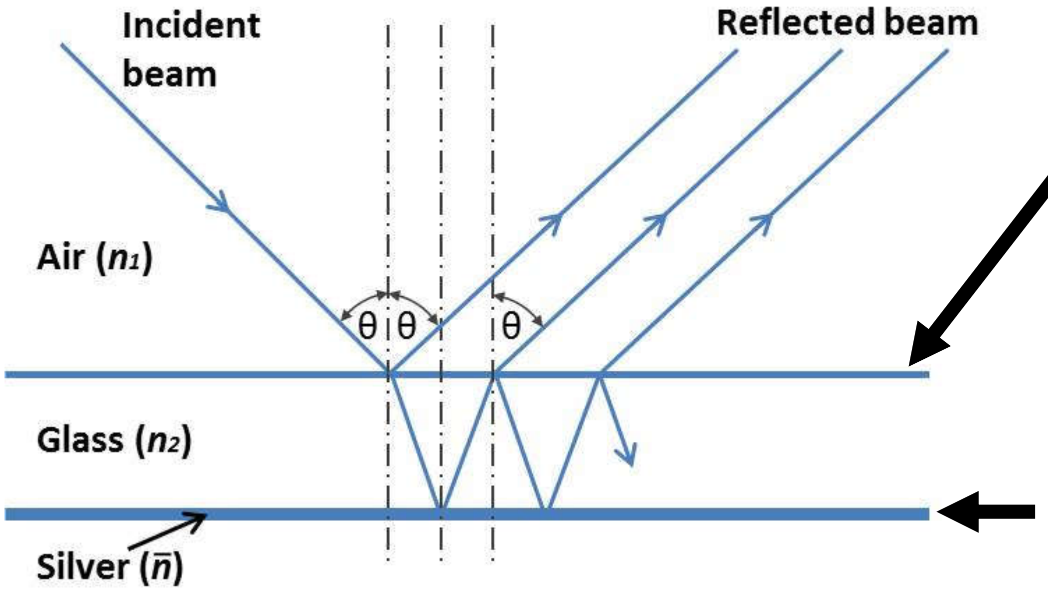

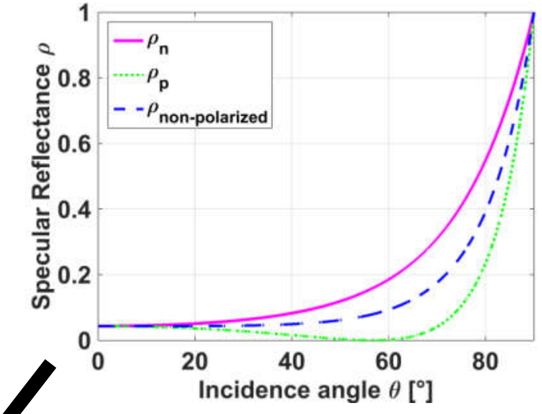

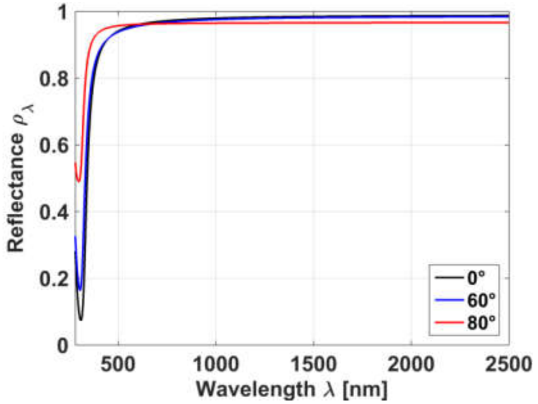

Reflectance at a silvered glass mirror

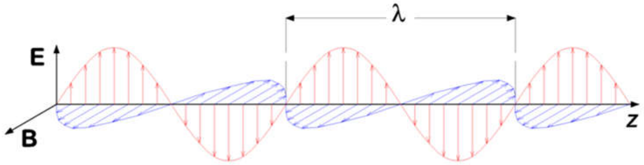

Fresnel formulae

Parallel polarized light

$$\rho_p = \left| \frac{n_2^2 cos(\theta) - n_1 \sqrt{n_2^2 - n_1^2\, sin^2(\theta)}}{n_2^2 cos(\theta) + n_1 \sqrt{n_2^2 - n_1^2\, sin^2(\theta)}} \right|^2$$

Perpendicular polarized light

$$\rho_s = \left| \frac{n_1\, cos(\theta) - \sqrt{n_2^2 - n_1^2\, sin^2(\theta)}}{n_1\, cos(\theta) + \sqrt{n_2^2 - n_1^2\, sin^2(\theta)}} \right|^2$$

$$\rho_{non-polarized} = \frac{1}{2}\left(\rho_p + \rho_s\right)$$

Refractive index for metals is complex.

The effect of incidence angle

- Near normal < 15°
- > 15° requires separate measurement of s- and p-polarization
- Near normal measurements are typically sufficient for silvered-glass mirrors

Location	Latitude	$\bar{\theta}$ [°]
Equator (PTC)	0°0‘	27.8
Aswan (PTC)	24°05‘	30.8
Ouarzazate (PTC)	30°56‘	32.8
PSA (PTC)	37°05‘	34.8
PSA (ST)	37°05‘	29.8

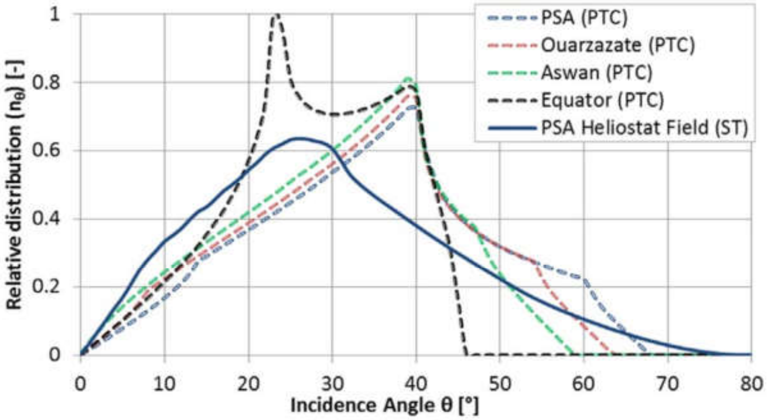

Fig. 4. Relative annual incidence angle distribution n_θ on mirror materials employed in parabolic trough collectors at PSA (Spain), Ouarzazate (Morocco), Aswan (Egypt) and the equator and in the heliostat field of the CESA-1 solar tower at PSA (Spain).

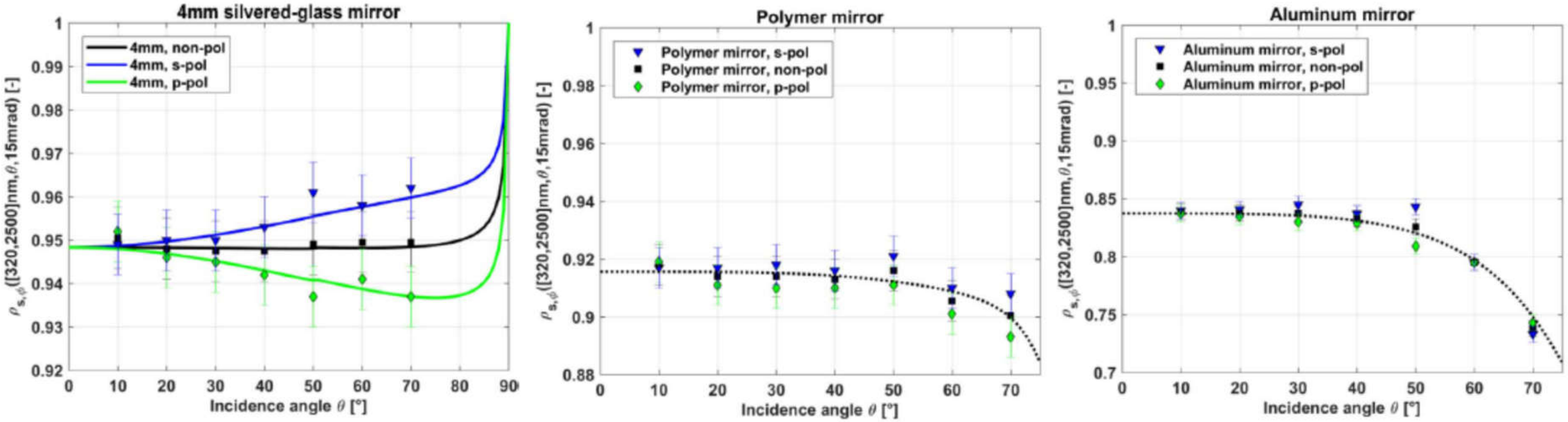

The influence of glass thickness

- Light travels twice through the glass, which causes absorption losses
- Solar-weighted reflectance as high as 96% was achieved with a 100µm thick front glass

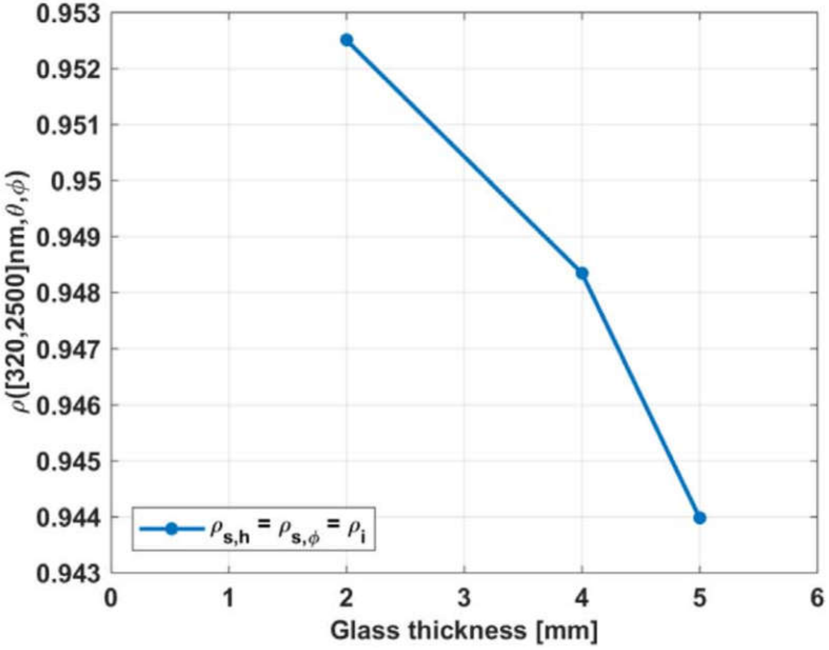

Three mirror types from the same manufacturer with different glass thicknesses

Important reflectance parameters for CSP

- Solar weighted values shall be used when comparing solar mirrors
- Relevant incidence angles are in the range of near normal to 70° (most frequent angles of incidence for PT and ST between 30° and 40°)
- Reflectance at incidence angles >20° must be measured separately for s- and p-polarization
- Acceptance angle is technology dependent

The parameters:

ρ_s([280,2500nm], 8º, h)
ρ(660 nm, 8º, h)
ρ(660 nm, 15º, 12.5 mrad)

are commonly used to characterize solar mirrors for parabolic troughs.

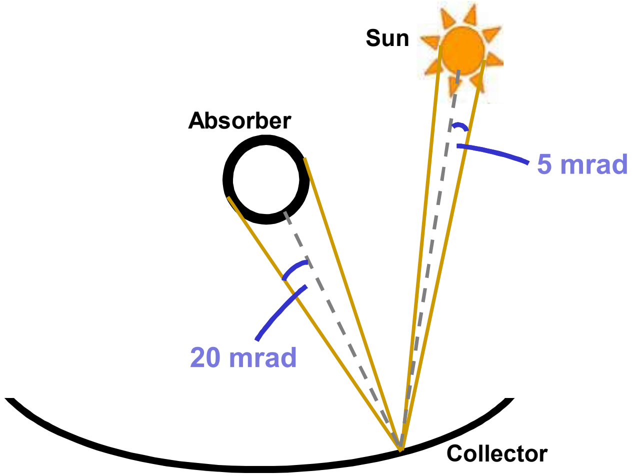

Specular reflectance in Power Tower applications

In power towers specularity is even more important! Acceptance angles down to φ= 6 mrad are relevant

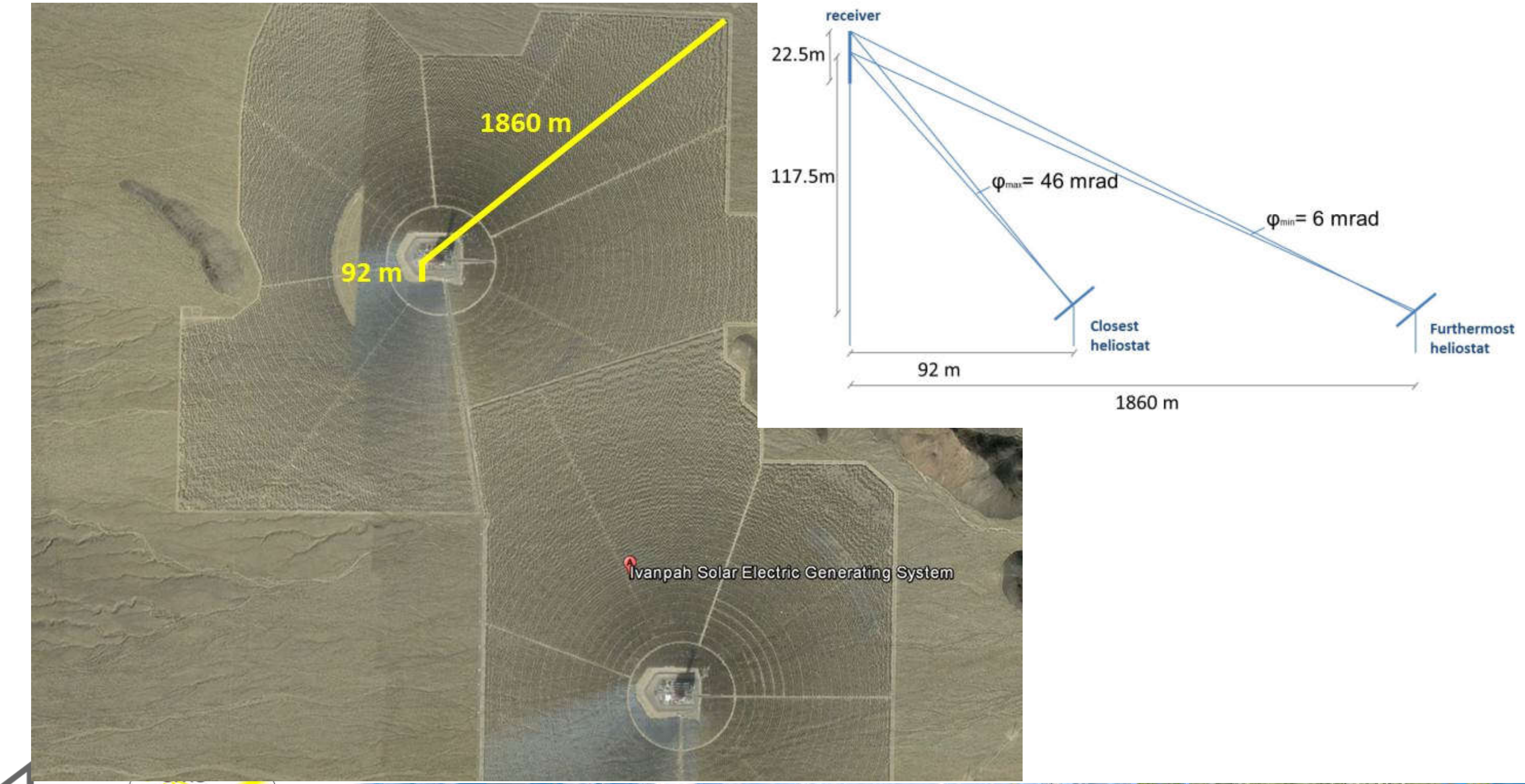

Typical instruments to characterize reflectance

Perkin Elmer Lambda 1050 spectrophotometer with integrating sphere accessory

Measures spectral hemispherical reflectance and transmittance

Devices and Services (D&S) Multiple Wavelength Portable Specular Reflectometer, Model 15R-RGB

Measures monochromatic specular reflectance

Perkin Elmer Lambda 1050 spectrophotometer

- Top class instrument
- Measures hemispherical reflectance and transmittance
- Wavelength of light source: λ= 250 - 2500 nm
- Incidence angle θ =8°
- High repeatability (<0.2%)

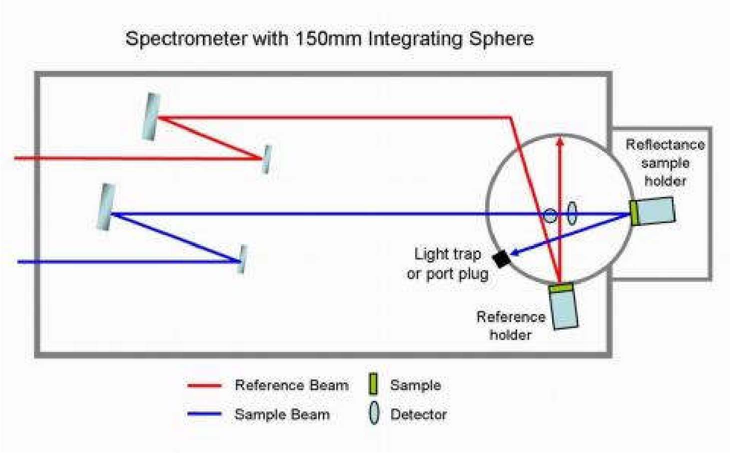

Disadvantages:

- Max. measurement spot 9x17mm²
- No specular measurements

Perkin Elmer Lambda 1050 spectrophotometer

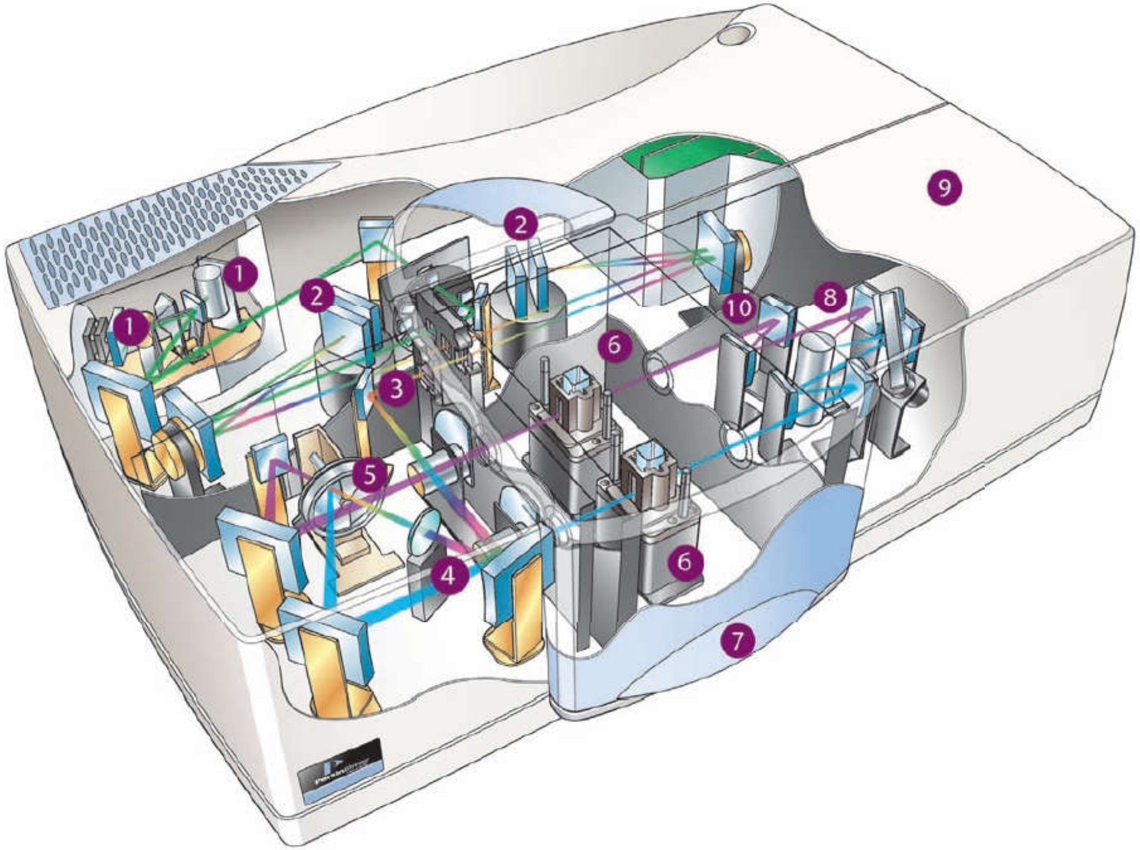

① **Deuterium and Tungsten Halogen Light Sources**
Prealigned and prefocused for quick replacement and maximum uptime. Source Doubling Mirror (LAMBDA 1050 only) for ultra-high sensitivity.

② **Double Holographic Grating Monochromators**
For ultra-low stray light performance.

③ **Common Beam Mask**
Allows precise adjustment of beam height to match samples of different dimensions.

④ **Common Beam Depolarizer**
Corrects for inherent instrument polarization to allow accurate measurements of birefringent samples (optional).

⑤ **Chopper**
Switches between sample and reference beam. Four-segment design provides individual blank readings for sample and reference, increasing measurement accuracy.

⑥ **Sampler and Reference Beam Attenuators**
For extremely sensitive and accurate measurements on highly absorbing samples.

⑦ **Largest Sample Compartment in the Industry**
Allows easy access to a wide variety of sampling accessories and sample types.

⑧ **High-sensitivity Photomultiplier and Peltier-controlled PbS Detectors**
Provides full range UV/Vis/NIR coverage from 175 to 3300 nm (LAMBDA 950).

⑨ **Second Sampling Area**
Houses a range of snap-in sampling modules including transmission optics (shown), 60 mm and 150 mm integrating spheres and the Universal Reflectance Accessory for high-precision absolute reflectance measurements.

⑩ **High-sensitivity Photomultiplier, Peltier-controlled InGaAs and PbS Detectors**
Provides full range UV/Vis/NIR coverage from 175 to 3300 nm (LAMBDA 1050 only).

The integrating sphere attachment

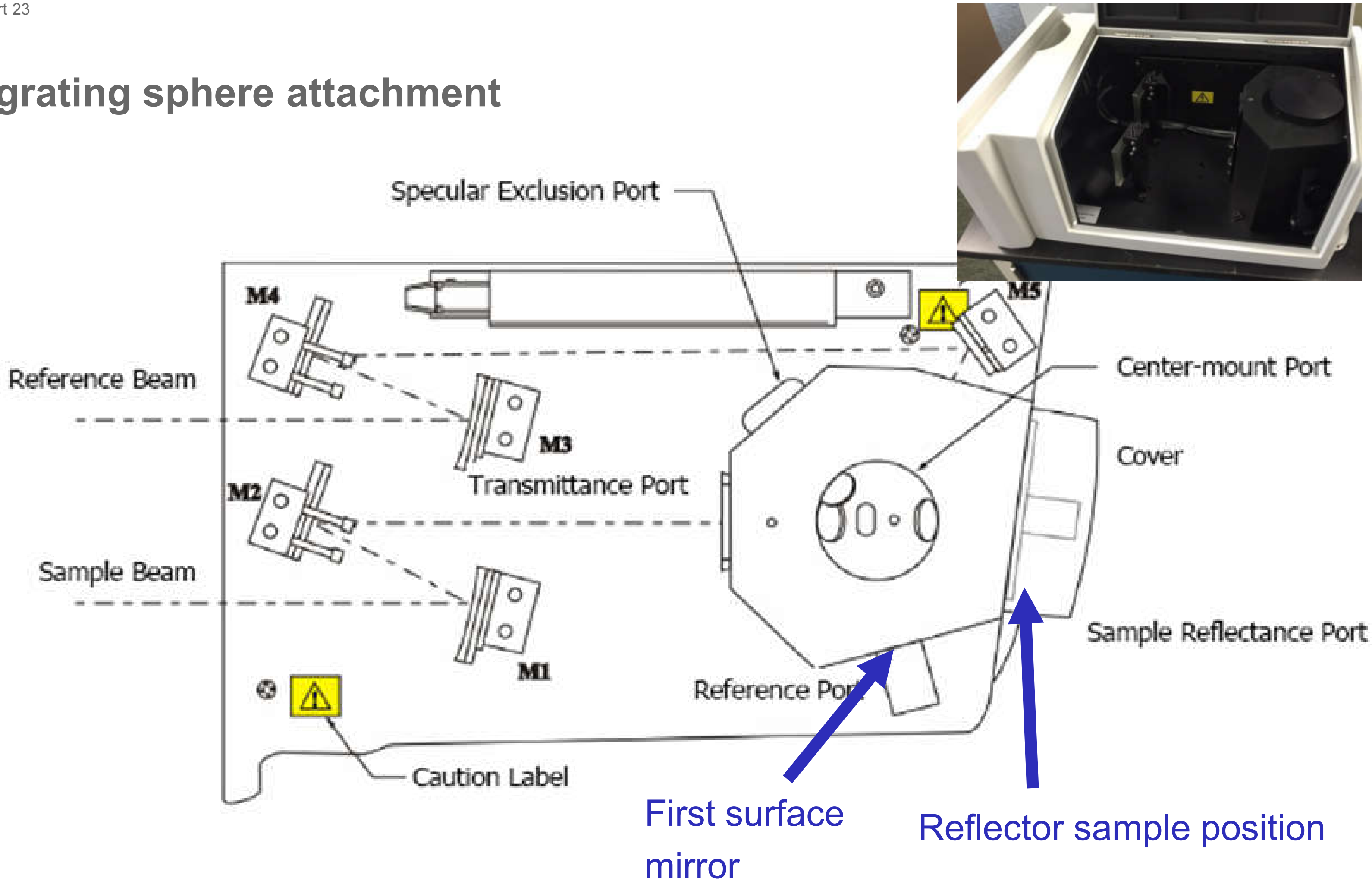

Measurement of the hemispherical reflectance

One measurements consists of:

- Zeroline
- Baseline (measurement of *working standard*)
- Sample measurement

$$\rho_{sample}(\lambda;8°;h) = \frac{I_{sample}(\lambda;8°;h) - Zeroline(\lambda;8°;h)}{I_{WorkingStd}(\lambda;8°;h) - Zeroline(\lambda;8°;h)} \cdot \rho_{WorkingStd}(\lambda;8°;h)$$

Measurement of specular reflectance

Spectral measurement of specular reflectance is not possible at the state of the art!!

Only monochromatic measurements are possible

Devices & Services – Multiple Wavelength Portable Specular Reflectometer Model 15R-RGB

- Acceptance angles φ= 2.3, 3.5, 7.5, 12.5, 23 mrad
- Wavelength of light source: λ= 460, 550, 650, 720nm
- Incidence angle θ =15°
- Repeatability: +/- 0.002 reflectance units for glass mirrors
- Lower repeatability for flexible mirror samples : +/- 0.004
- Expected uncertainty including reference mirror: +/- 0.007 or +/- 0.009

Measurement of the specular reflectance

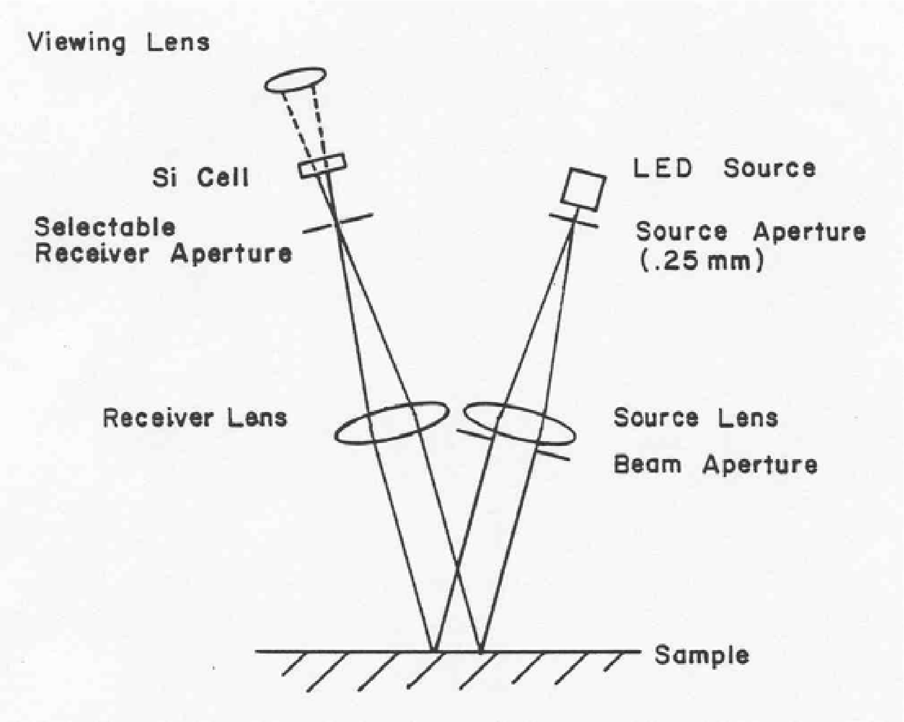

Beam is manually aligned until reflected light is centered to middle of aperture using 2 screws at instrument legs

Calibration of the D&S

Standard calibration mirror

Reference value

Needs to be adjusted until reference value is reached

Calibration with external reference mirror also possible and recommended!

Calibration of D&S at small acceptance angles

When using the small acceptance angles (φ=2.3 and 3.5 mrad) reproducibility is extremely challenging. The precision reference mirror shall be used!

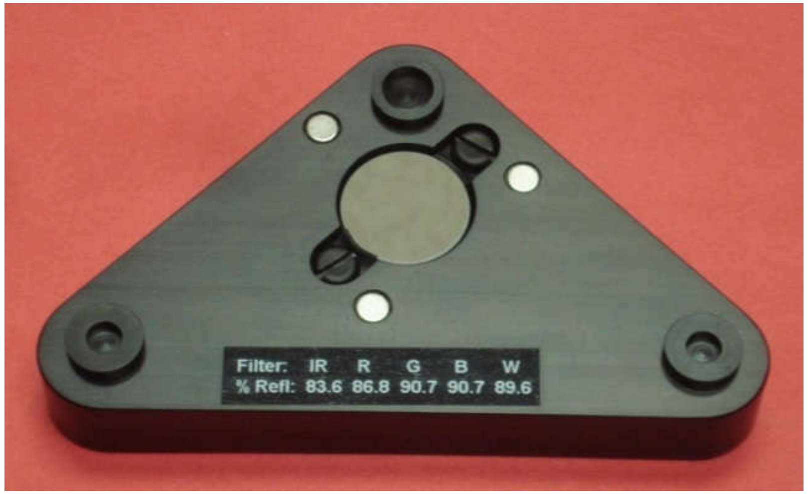

Filter:	IR	R	G	B	W
% Refl:	83.6	86.8	90.7	90.7	89.6

Precision reference mirror with calibrated reflectance values for the 15R-RGB with spacers installed.

Calibration of D&S

- For each **aperture (acceptance angle)** a new instrument calibration has to be carried out
- For each **wavelength** a new instrument calibration has to be carried out
- Ensure that the calibration has not shifted due to operating temperature or battery voltage in regular intervals during measurement (every 30 minutes recommended)

Portable reflectometers

Manufacturer	Surface Optics	Devices & Services Co		Aragon Photonics	Konica Minolta	PSE AG
Developer	Surface Optics	Devices & Services Co		Abengoa & University of Zaragoza	Konica Minolta	Fraunhofer ISE
Model	410 Solar	15R-USB	15R- RGB	Condor	CM-700d/600d	pFlex 2.1
Type of measurement	Hemispherical and diffuse (specular computable)	Monochromatic near specular		Monochromatic near specular and solar-weighted with 6 λ	Hemispherical and diffuse, gloss	Monochromatic near specular and cleanliness
Light source	Tungsten	LED		LED	Xenon	LED
Incidence angle, θ_i (°)	20	15		12	8	8
Diameter of measurement spot (in mm)	6.35	10.00		6 measurements with varying diameter, total area of 230mm^2	3 (model 700d) 8 (model 700d and 600d)	10
Wavelength, λ (nm)	7 bands between 300 y 2500	Peak at 660	460 (±50), 550 (±50), 650 (-40 +150), 720 (-40 +100)	435, 525, 650, 780, 940 and 1050, solar-weighted	400-700 (in10nm steps)	470 (±25), 525 (±25), 625 (±25)
Acceptance half-angle, φ (mrad)	52.4	3.5, 7.5, 12.5, 23.0	2.3, 3.5, 7.5, 12.5, 23.0	145.0	*	67

Reference mirrors

- The Master mirror shall be used to calibrate working standards for daily use
- Working standards need to be replaced when scratched or visually degraded
- Master mirror shall be stored in soft cloth and hard case
- Master mirror expanded uncertainty is typically 0.003 (level of confidence of 95%)

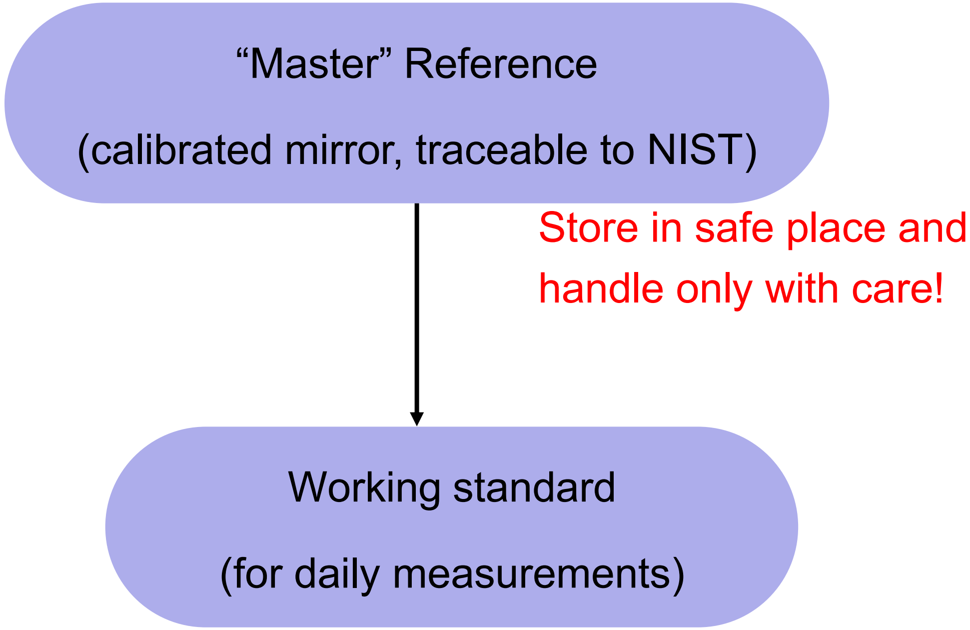

"Master" Reference

(calibrated mirror, traceable to NIST)

Store in safe place and handle only with care!

Working standard

(for daily measurements)

SolarPaces Task III reflectance guideline

- Several measurements shall be taken per sample to get statistically meaningful results

- Check the current recommended measurement procedure (Version 3.1) available at:

https://www.solarpaces.org/wp-content/uploads/202004_SolarPACES-Reflectance-Guidelines-V3.1.pdf

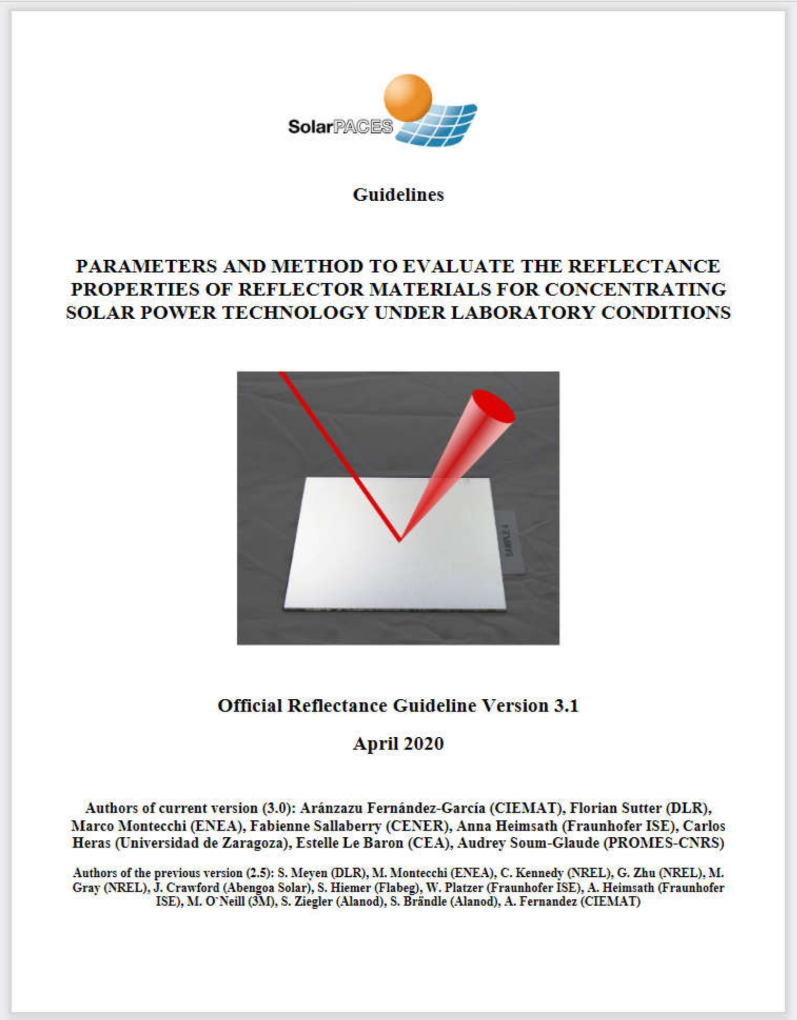

SolarPACES

Guidelines

PARAMETERS AND METHOD TO EVALUATE THE REFLECTANCE
PROPERTIES OF REFLECTOR MATERIALS FOR CONCENTRATING
SOLAR POWER TECHNOLOGY UNDER LABORATORY CONDITIONS

Official Reflectance Guideline Version 3.1

April 2020

Authors of current version (3.0): Aránzazu Fernández-García (CIEMAT), Florian Sutter (DLR), Marco Montecchi (ENEA), Fabienne Sallaberry (CENER), Anna Heimsath (Fraunhofer ISE), Carlos Heras (Universidad de Zaragoza), Estelle Le Baron (CEA), Audrey Soum-Glaude (PROMES-CNRS)

Authors of the previous version (2.5): S. Meyen (DLR), M. Montecchi (ENEA), C. Kennedy (NREL), G. Zhu (NREL), M. Gray (NREL), J. Crawford (Abengoa Solar), S. Hiemer (Flabeg), W. Platzer (Fraunhofer ISE), A. Heimsath (Fraunhofer ISE), M. O`Neill (3M), S. Ziegler (Alanod), S. Brändle (Alanod), A. Fernandez (CIEMAT)

Scattering – comparison of specular and hemispherical reflectance

Silvered-glass mirrors

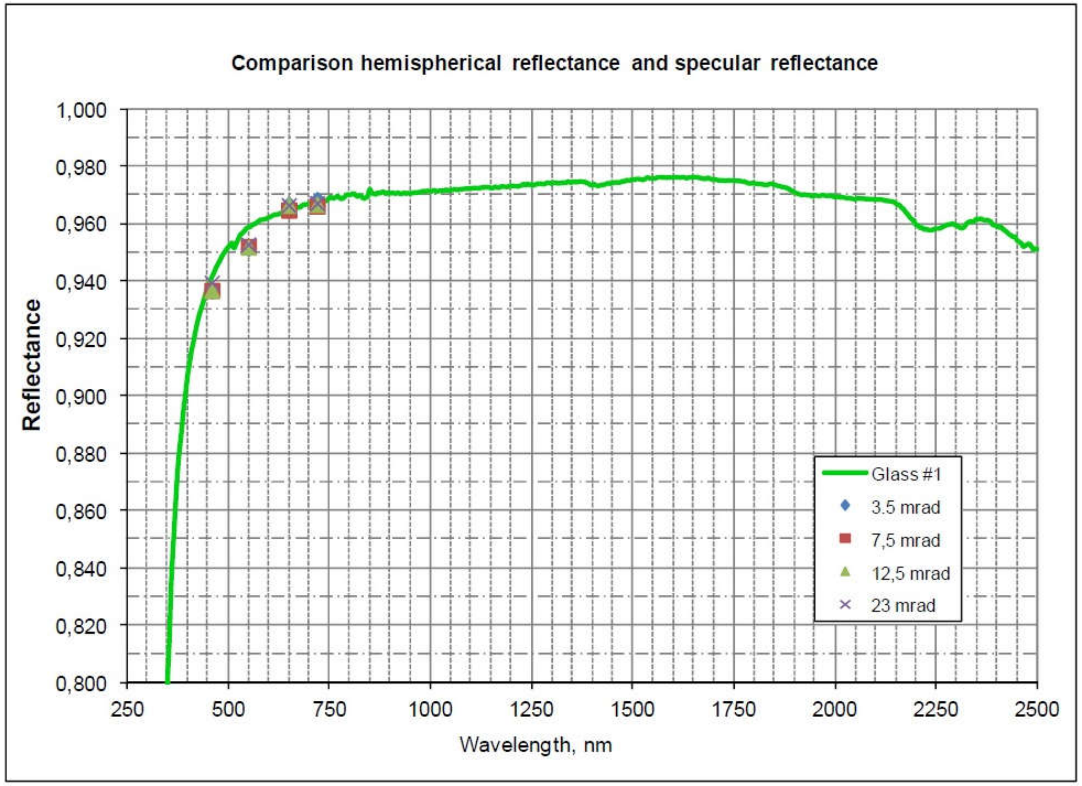

Scattering – comparison of specular and hemispherical reflectance

Aluminum mirrors

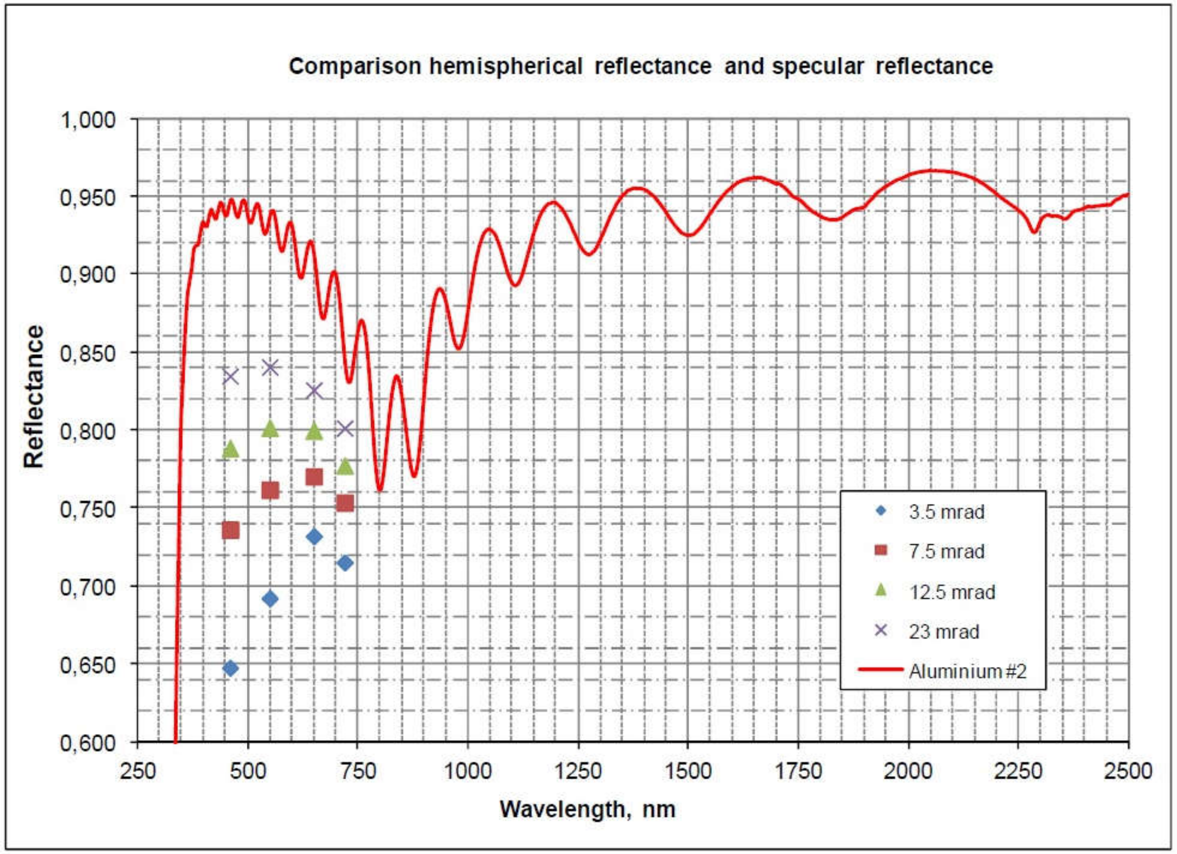

Measurement of solar reflector materials

State of the art

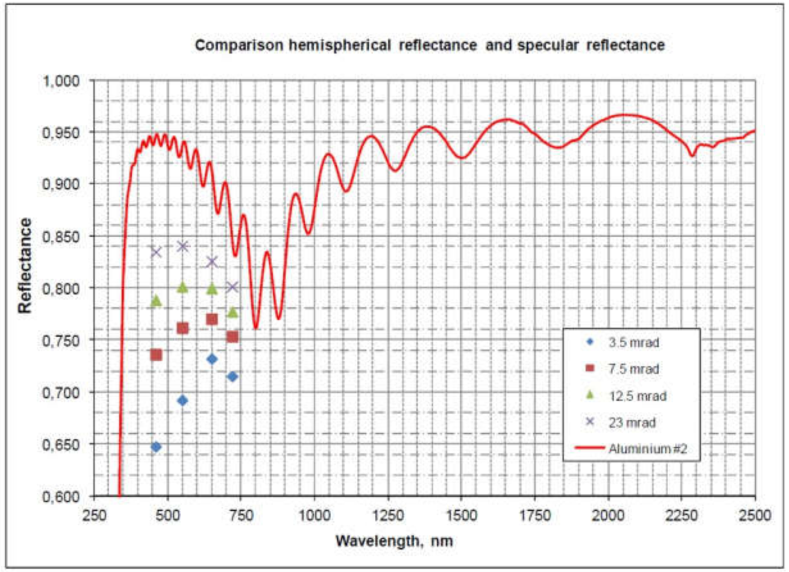

Spectral measurement of hemispherical reflectance and monochromatic measurement of specular reflectance

Target

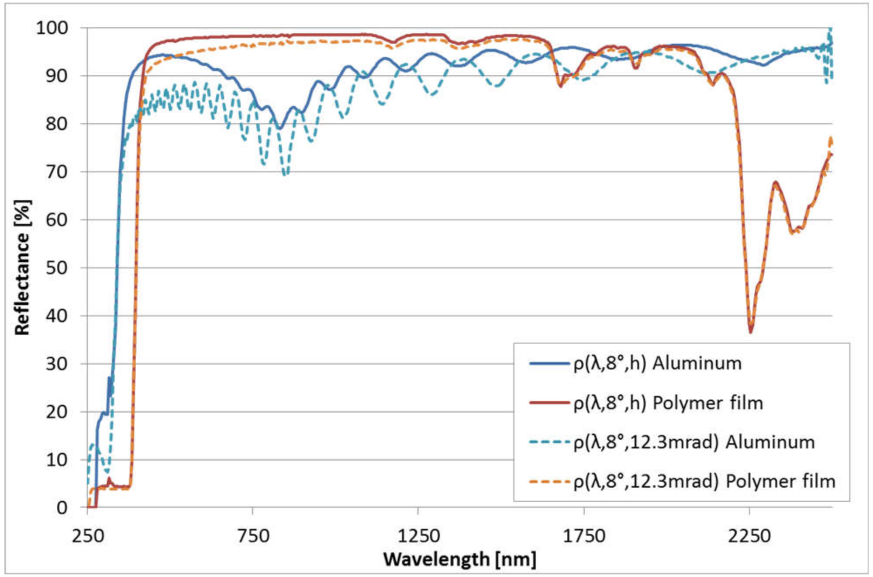

Spectral measurement of hemispherical **AND** specular reflectance

Spectral Specular Reflectance Accesory (S2R)

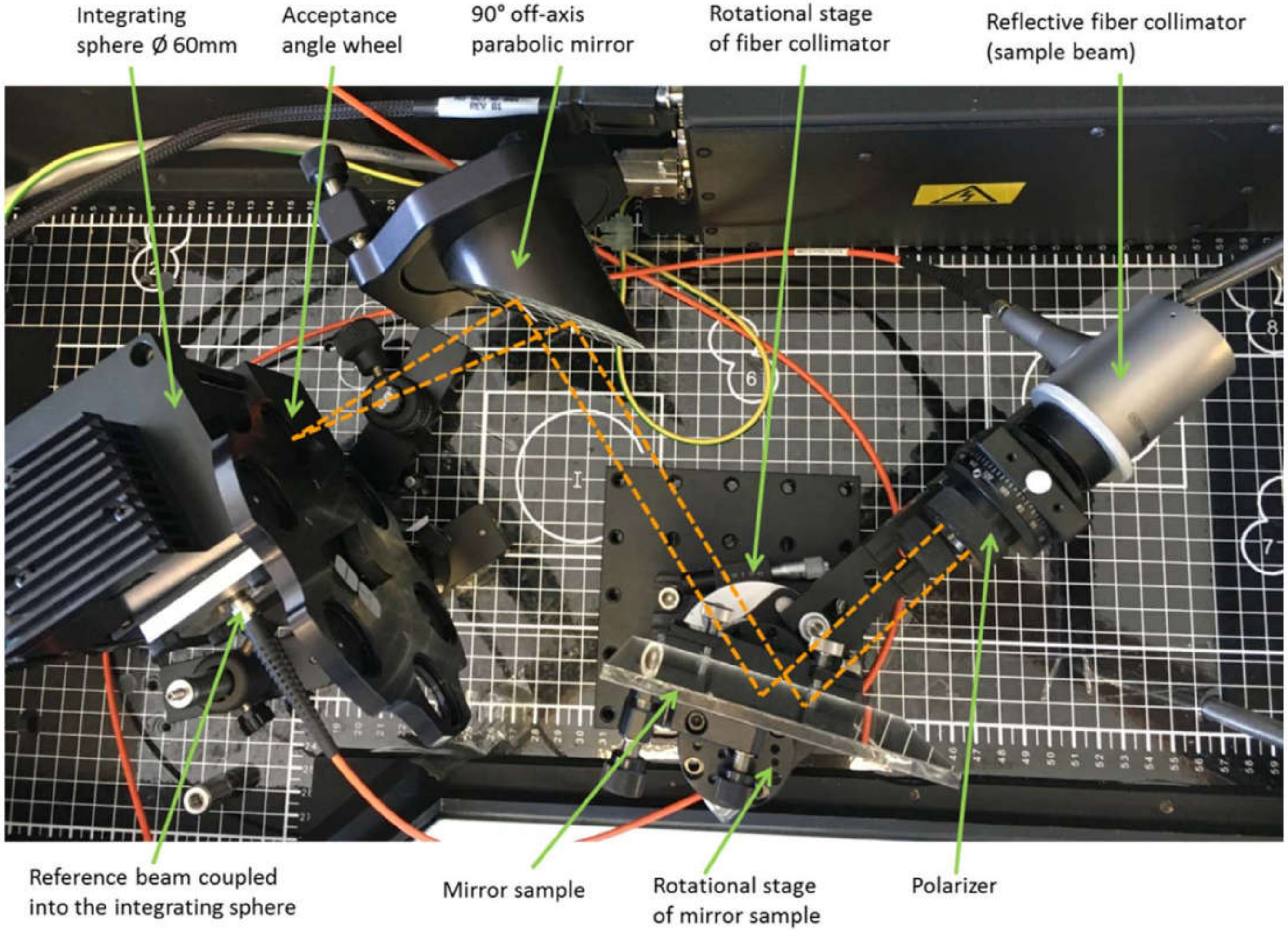

Spectral Specular Reflectance Accesory (S2R)

Complete overlapping of hemispherical and 12.3 mrad spectra for silvered-glass mirrors. This proofs the high specularity of glass mirrors.

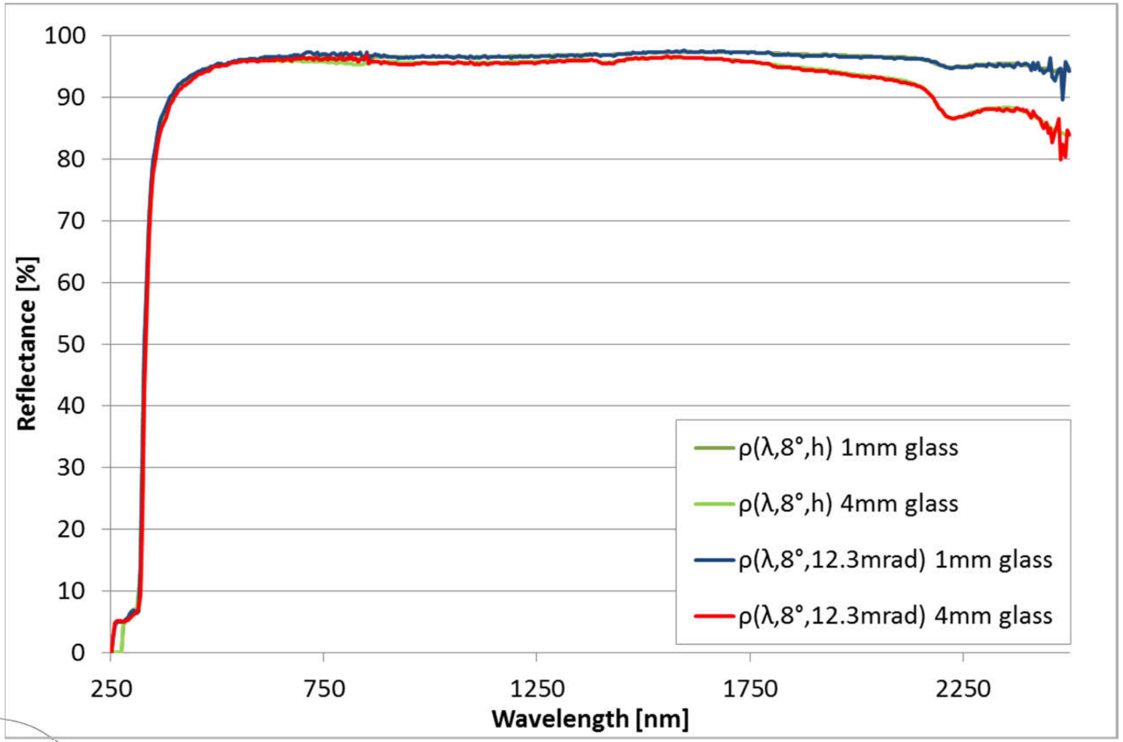

Spectral Specular Reflectance Accesory (S2R)

Scattering losses of ~2pp for polymeric mirrors and ~10pp for aluminum mirrors detected in the visible range.

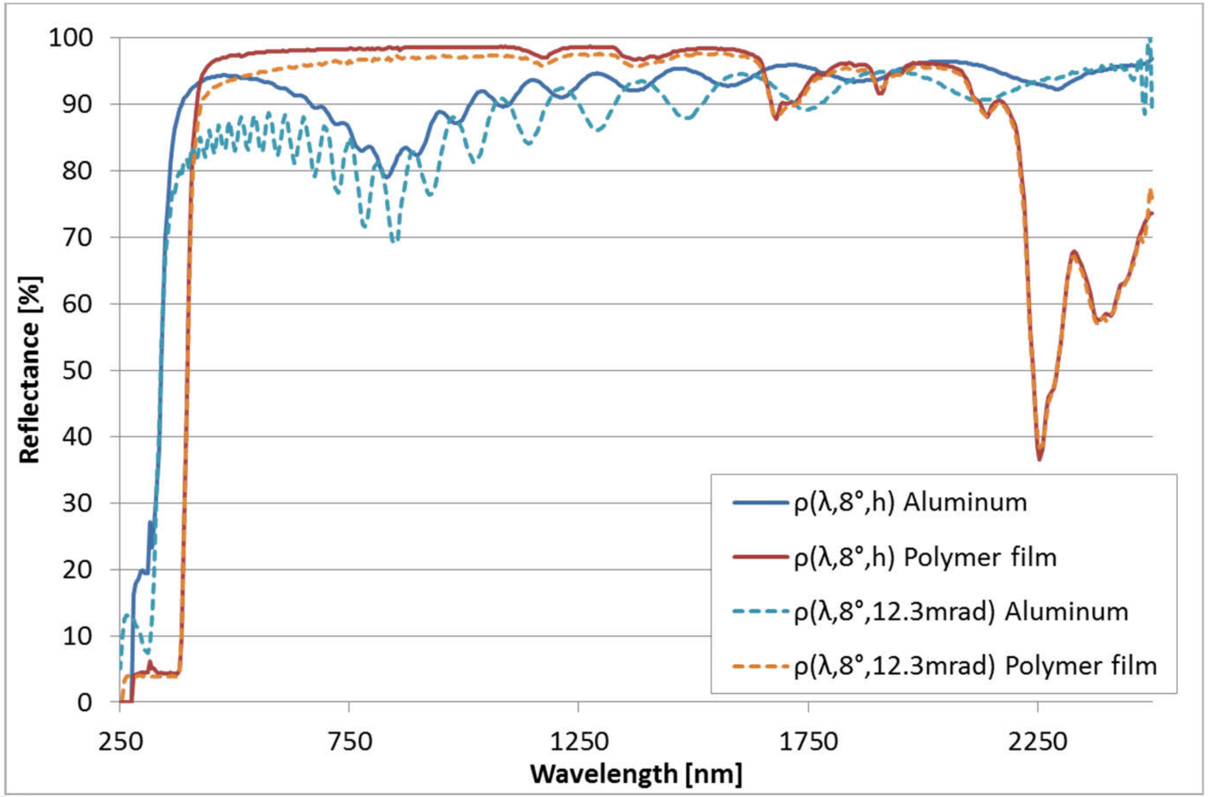

Spectral Specular Reflectance Accesory (S2R)

Measured spectra and computed solar weighted values at different acceptance angles for an aluminum reflector

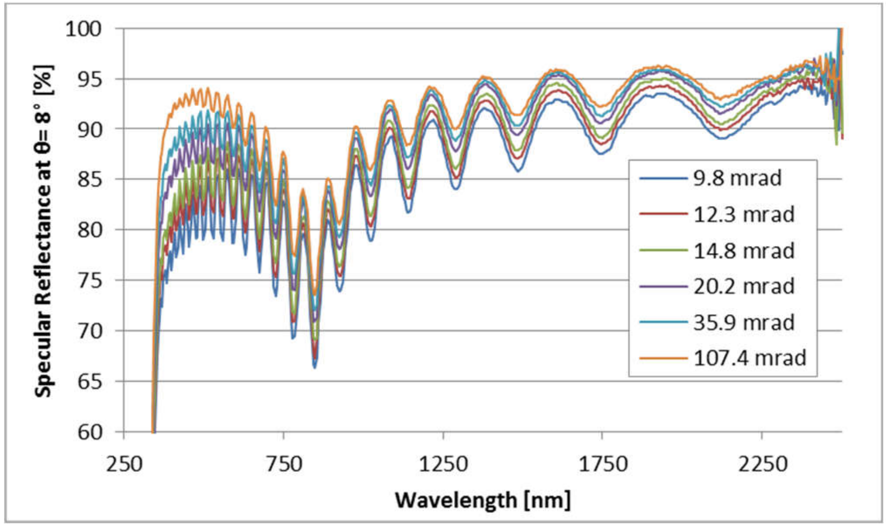

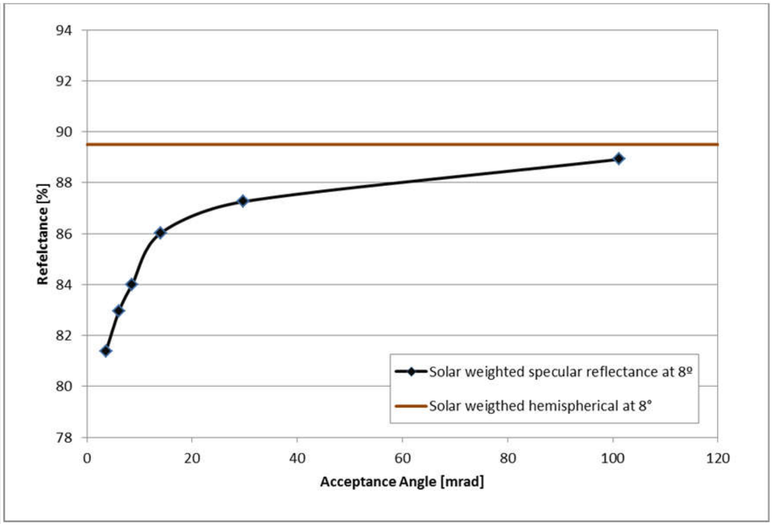

Spectral Specular Reflectance Accesory (S2R)

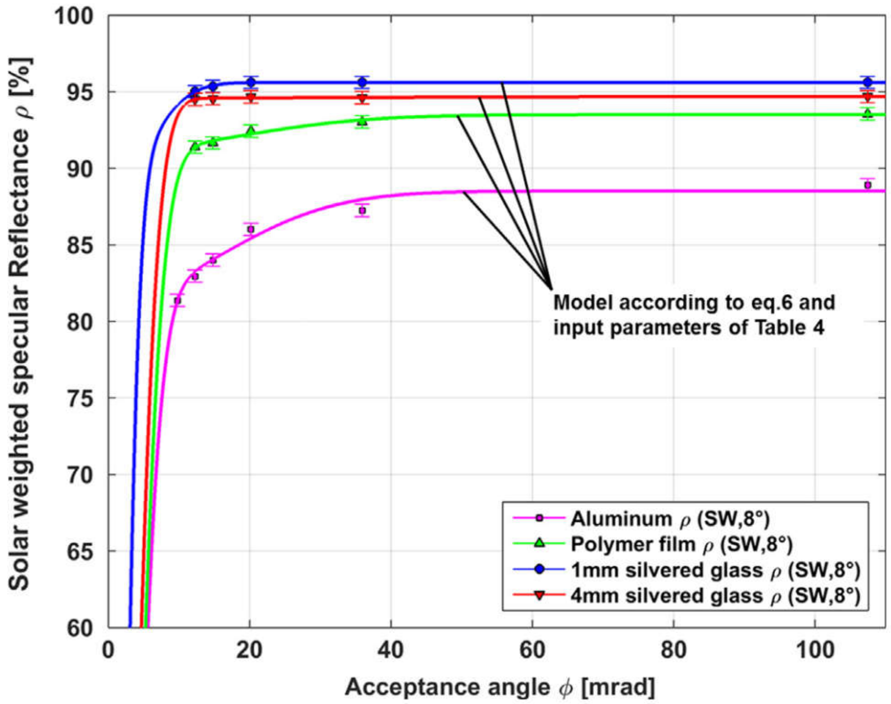

Fitting function used to model the specular behaviour

$$\rho(\lambda,\theta,\varphi) = \rho(\lambda,\theta,h)\cdot\left[1 - K\exp\left(-\frac{\varphi^2}{2\sigma_1^2}\right) - (1-K)\cdot\exp\left(-\frac{\varphi^2}{2\sigma_2^2}\right)\right]$$

Measurements at low acceptance angles <10mrad not trustworthy due to alignment issues

→ In such regions it is better to measure with CCD sensors of cameras

MIRA (Mirror Reflection Analyzer)

Measurement principle

- Allows to compute reflectance as function of φ
- Variable incidence angle θ = 6° - 60°
- White light or λ = 450, 500, 550, 650, 700, 850, 940 nm

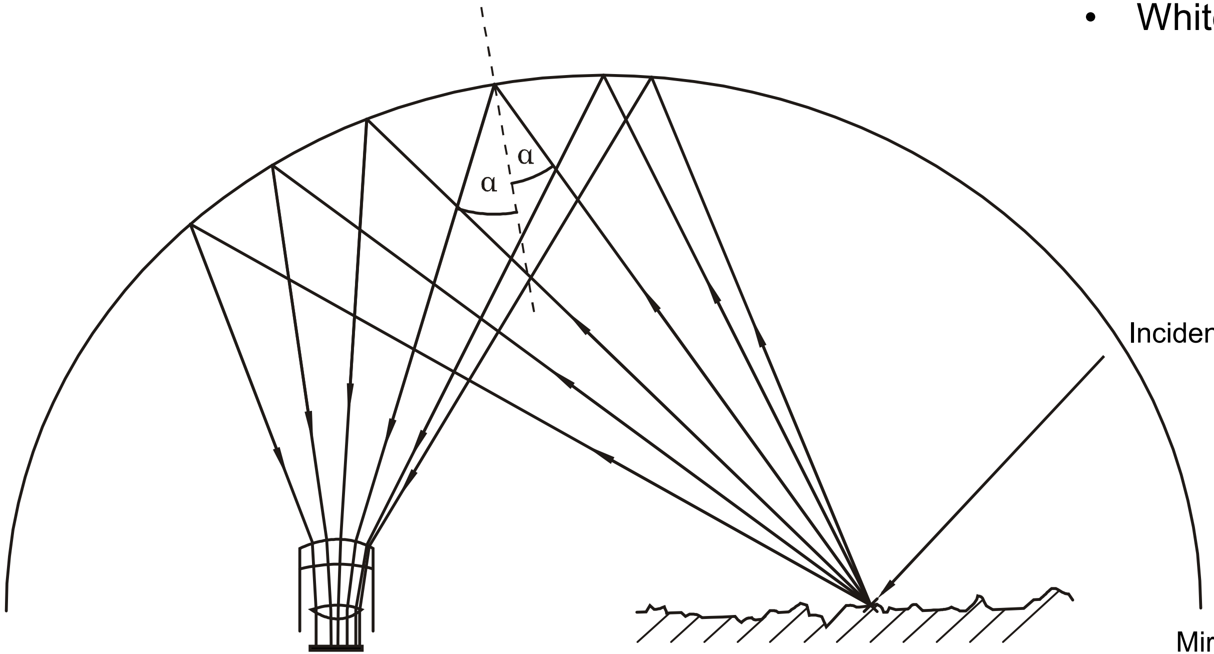

Incidence Beam

Mirrored ellipsoid

Fisheye lens,
camera and CCD-array
serve as detector
2nd focal point

Rough mirror
sample

1st focal point

Every pixel represents one scattering angle → BRDF

Data evaluation

Mirror characteristic

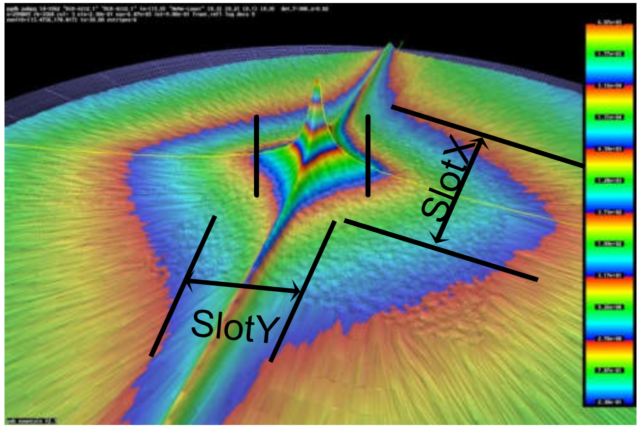

BRDF measurement

Calculation of specular reflectance as function of acceptance angle with virtual, continuous aperture (circular or slot)

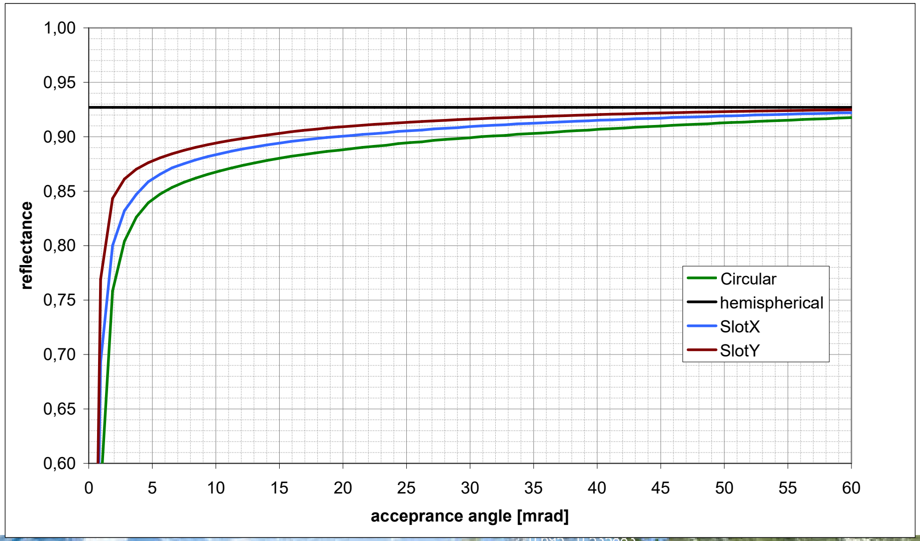

Space resolved specular reflectometer (SR)^2

- Measurement of specular reflectance with spatial resolution
- φ = 3.5 , 7.5 , 12.5 mrad
- θ = 15°
- λ = 410, 500, 656 nm
- Spot size: 50 mm in diameter
- Automatic detection of degradation
- Calculation of degraded area

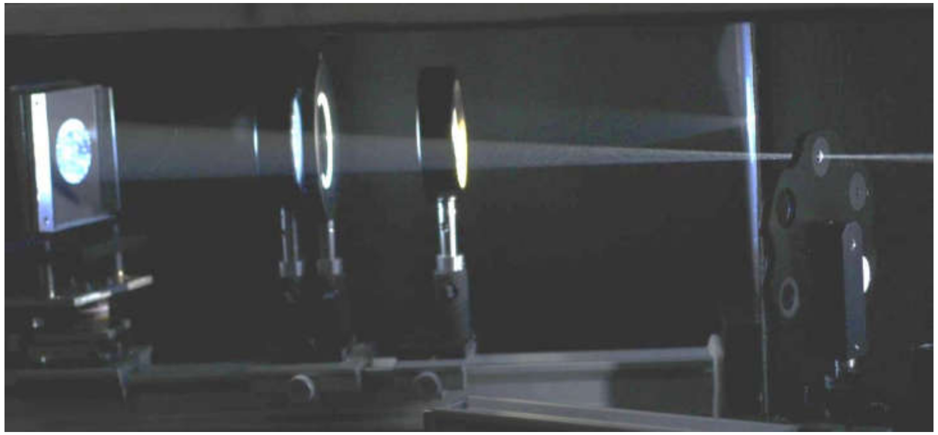

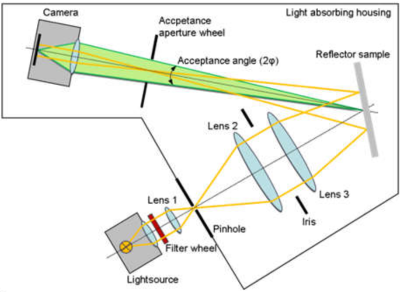

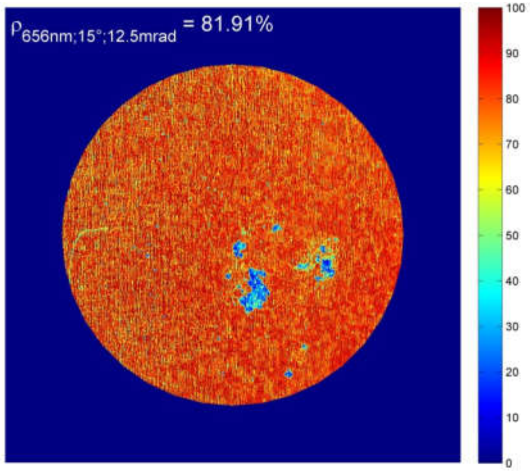

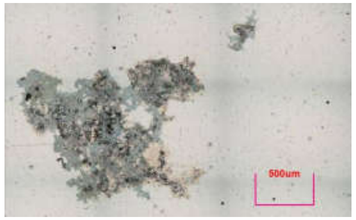

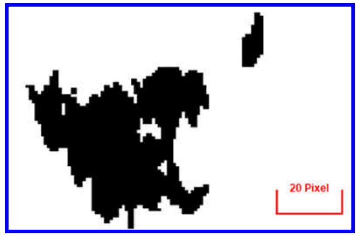

Transmittance

Florian Sutter, DLR

2nd Training for Industries, Plataforma Solar de Almería

Introduction

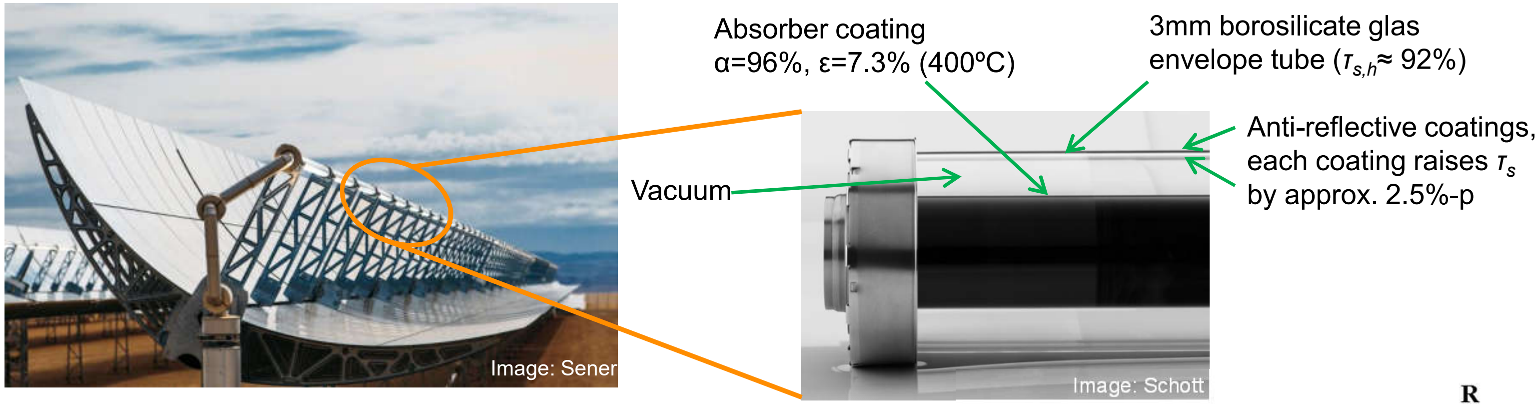

Image: Sener

Absorber coating
α=96%, ε=7.3% (400ºC)

3mm borosilicate glas
envelope tube ($\tau_{s,h}\approx$ 92%)

Anti-reflective coatings,
each coating raises τ_s
by approx. 2.5%-p

Vacuum

Image: Schott

→ transmission of 3 mm borosilicate glass tube can be raised by approx. 5%-p if:

1. R1 and R2 have the same amplitude
   $$\rightarrow \; n_c = \sqrt{n_1 \cdot n_g} = \sqrt{1 \cdot 1.52} = 1.23$$
2. Phase shift of π between R1 and R2
   $$\rightarrow \; d = \frac{\lambda_0}{4n_c} = \frac{550nm}{4{\cdot}1.23} = 112nm$$

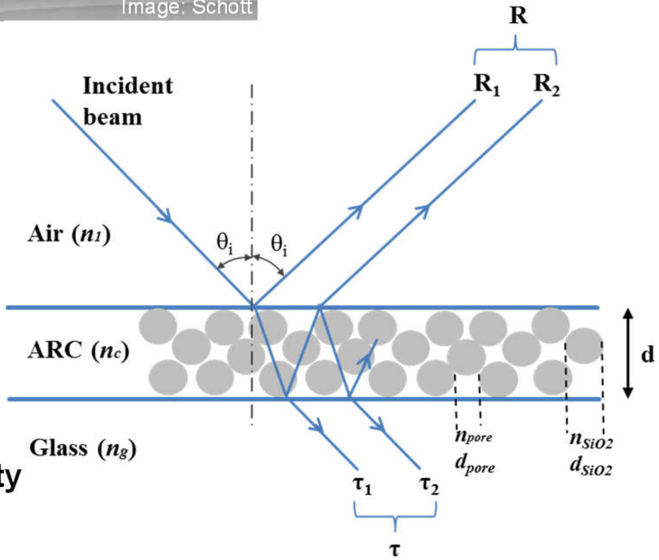

Problem: mechanical stability of the coating due to its porosity

Energy conservation law

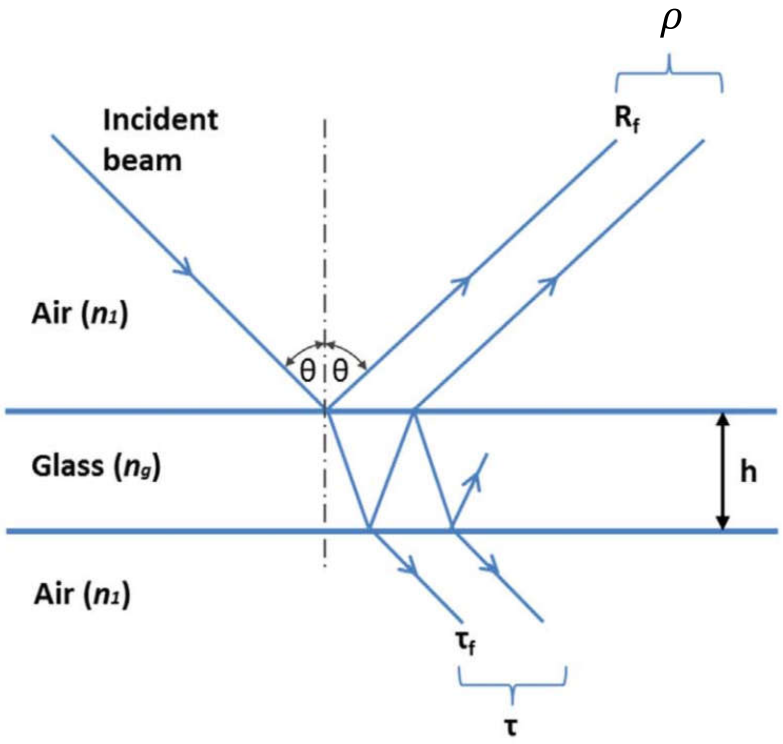

$$\rho + \tau + \alpha = 1$$

Typical solar transmittance values

Sample	τ([280,2500nm],8°) [%]
4 mm conventional soda-lime glass	82 - 86
4 mm solar glass (low iron content)	91 - 92
3 mm AR-coated solar glass for parabolic trough receiver	96 - 97

Transmittance spectra

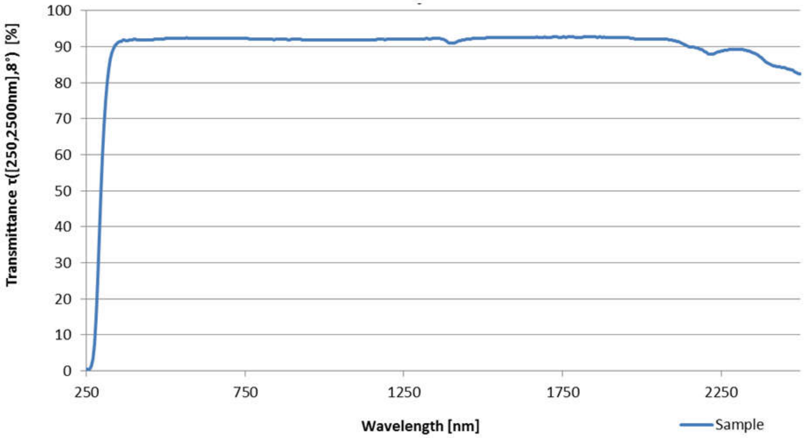

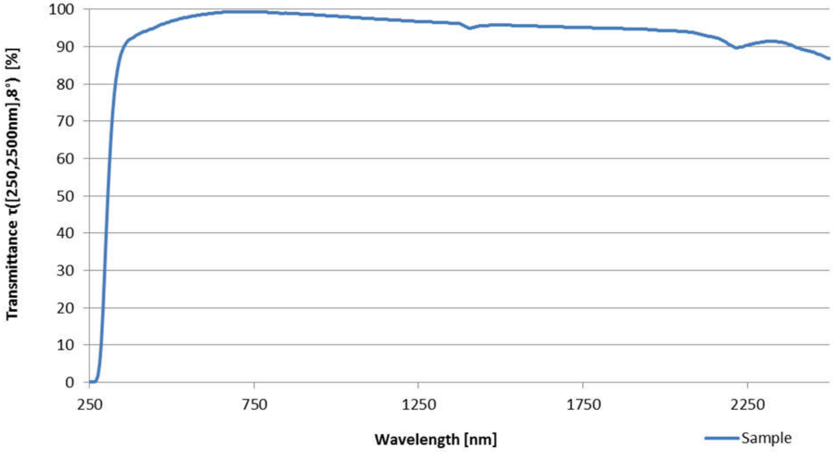

Typical 3 mm solar glass (low iron) used for mirrors (no anti-reflective coating)

Typical anti-reflective coated glass envelope tube for parabolic trough receivers

Transmittance in pristine state

Anti-reflective coatings of all relevant receiver tube manufacturers were measured

State of the art: **$\tau_{s,h}$= 96.8%**

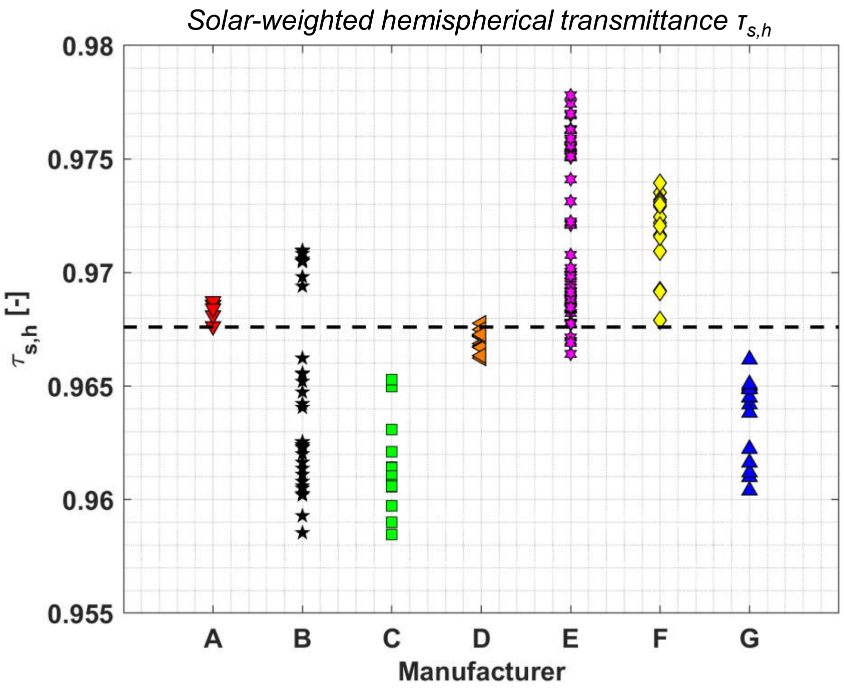

Cleaning of anti-reflective coated glass samples before measurement

Anti-reflective coated glass samples: Cleaning of anti-reflective coated glass samples is performed in ethanol in order to clean the porous structure of the coating from gaseous molecules from the ambient that are adsorbed by the pores and decrease the transmittance. Clean the sample by rinsing with ethanol and employing a very soft paper tissue with very little pressure to not scratch the coating. After that place the sample during 5 minutes in a beaker filled with ethanol. Then take the sample out and use filtered compressed air to dry the sample.

All other glass samples: can be cleaned with demineralized water and soft tissue

The integrating sphere attachment

Perkin Elmer Lambda 1050 spectrophotometer with integrating sphere accessory

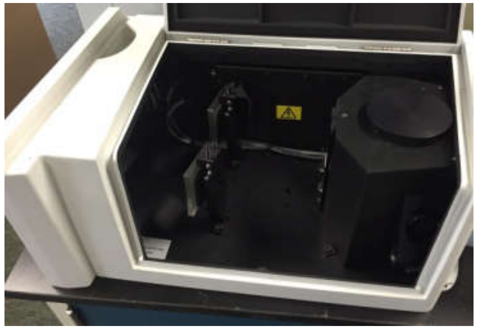

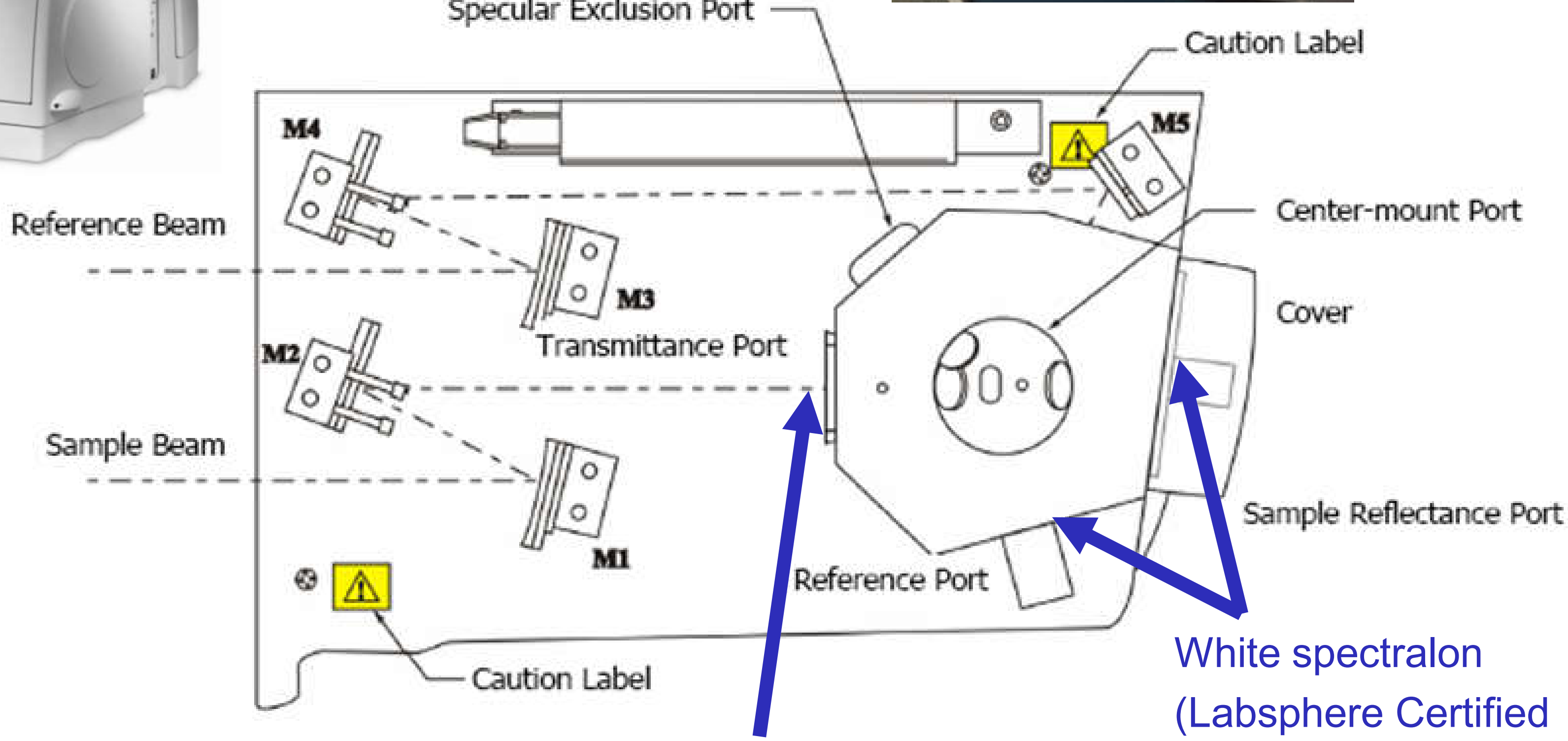

Sample position

White spectralon (Labsphere Certified Reflectance Standard)

Sample position: hemispherical transmittance

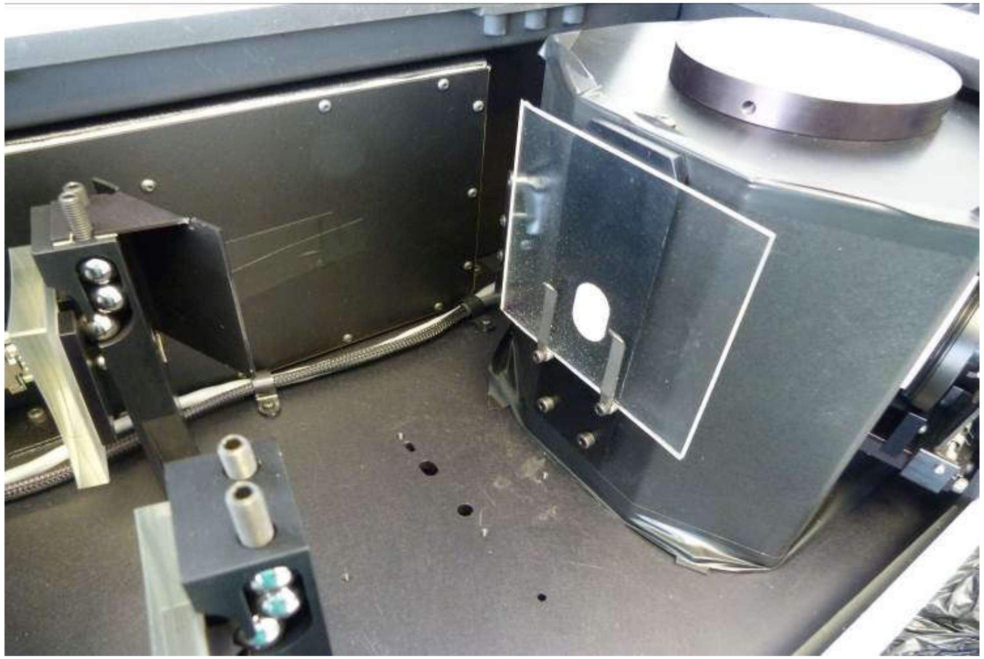

Sample position: specular transmittance

By positioning the sample away from the transmittance port, the specularity of the sample can be examined.

The acceptance angle can be computed from the distance of the sample to the port and the port dimensions.

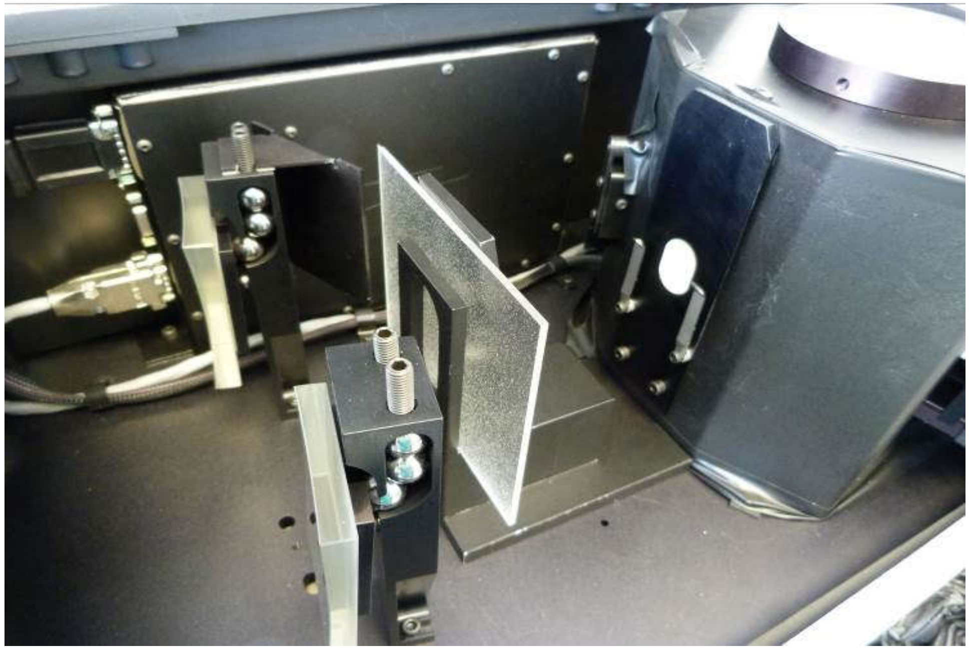

Measurement of the hemispherical transmittance

One measurements consists of:

- Zeroline
- Baseline (measurement in air as 100% reference)
- Sample measurement

$$\tau_{sample}(\lambda;8^\circ) = \frac{I_{sample}(\lambda;8^\circ) - Zeroline(\lambda;8^\circ)}{I_{Air}(\lambda;8^\circ) - Zeroline(\lambda;8^\circ)}$$

No reference sample needed!

Solar weighting of transmittance spectra

- Transmittance is wavelength dependent
- A suitable “mean value” of all relevant solar wavelengths is the solar weighted transmittance $\tau([\lambda_a, \lambda_b], \theta_i)$

$$\tau([\lambda_a, \lambda_b], \theta_i) = \frac{\sum_{i=0}^{i_{\max}} \tau(\lambda_i, \theta_i) \cdot G_b(\lambda_i)}{\sum_{i=0}^{i_{\max}} G_b(\lambda_i)}$$

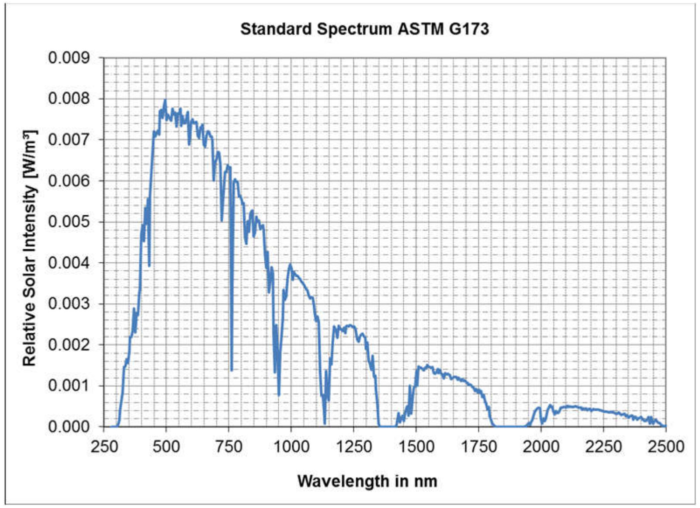

The spectral solar irradiance $G_b(\lambda_i)$ can be obtained in 5 nm steps from a reference spectrum, e.g. ASTM G173 with air mass 1.5 and 1000 W/m²

Aging of anti-reflective coatings

Degradation rates after accelerated aging testing (AAT), outdoor exposure testing (OET), in-service testing (IST)

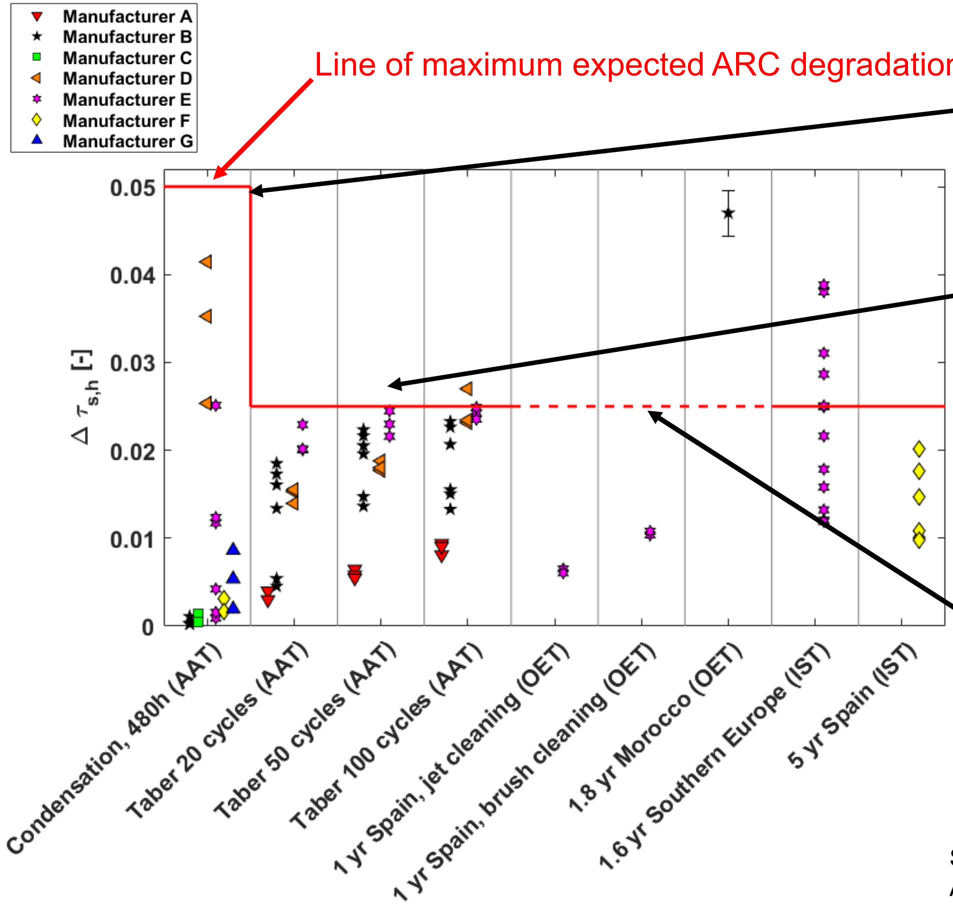

Line of maximum expected ARC degradation

Exposure from both sides, maximum expected transmittance loss is $\Delta\tau_{s,h} \approx$ 5%-p (glass substrate is resistant against humidity)

Exposure on one side, maximum expected transmittance loss is $\Delta\tau_{s,h} \approx$ 2.5%-p (glass substrate is not damaged by MIL-E-12397 abrasor)

Predominant exposure on one side, (cleaning only performed on front side, wind direction in Morocco predominant on front side) small degradation from back coating can not be excluded

Sutter et al. Durability of anti-reflective coatings for parabolic trough receivers
AIP Conference Proceedings 2303, 150015 (2020); https://doi.org/10.1063/5.0028751

SFERA-III
Solar Facilities for the European Research Area

Absorptance

Florian Sutter, DLR

2nd Training for Industries, Plataforma Solar de Almería

Solar Facilities for the European Research Area

Absorptance of solar radiation

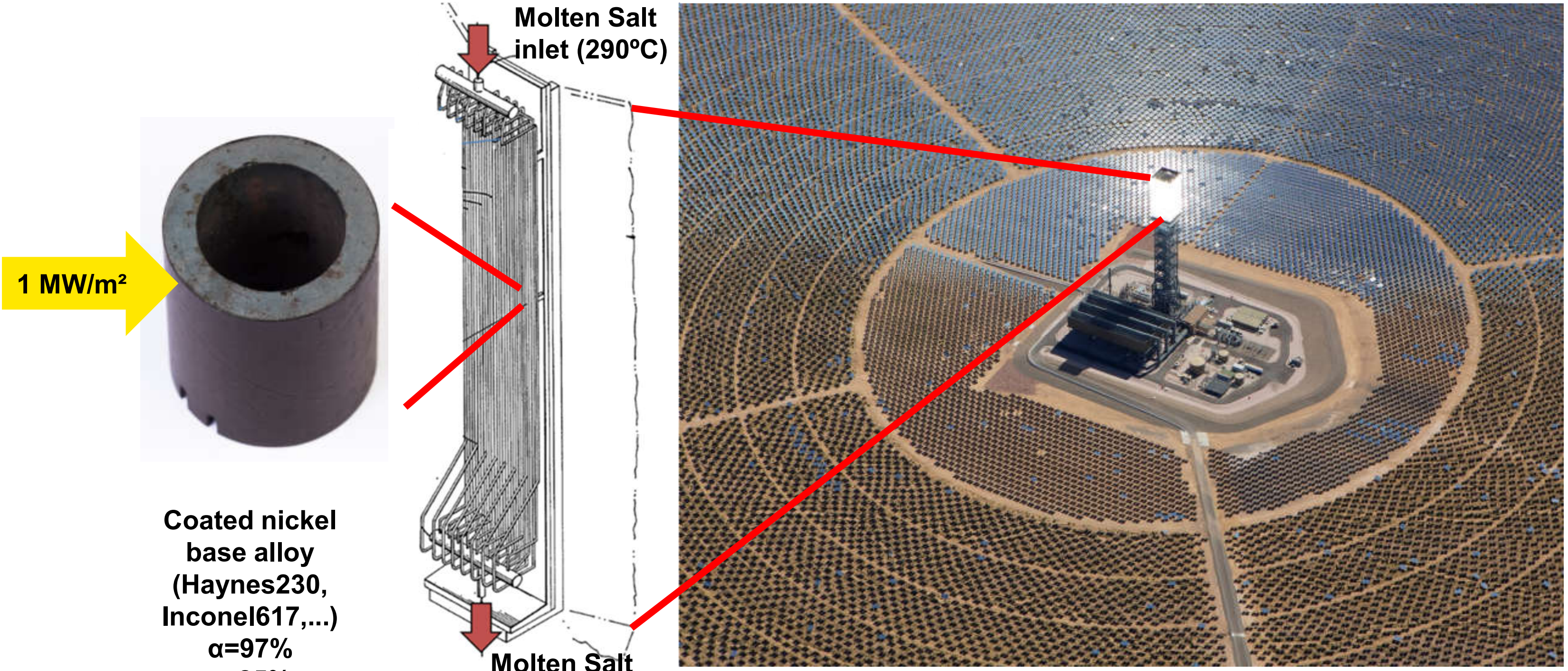

1 MW/m²

Molten Salt inlet (290ºC)

Molten Salt outlet (565ºC)

Coated nickel base alloy (Haynes230, Inconel617,...)
α=97%
ε=85%

[Image: BrightSource, Ivanpah plant, operated with steam instead of molten salt]

Absorptance measurement

- Absorptance is determined by measuring reflectance and

  $\alpha = 1 - \rho$ (for opaque materials)

- Same procedures as for reflectance measurements apply
- BUT: the calibration coupon used should be of similar reflectance characteristics than the sample to be measured

  → for spray-coated samples (e.g. for solar towers) a diffuse absorber reference should be used

  → for selective absorber coatings on polished substrates (e.g. in parabolic trough receivers) a specular absorber reference should be used

- Best is to send a couple of diffuse and specular absorber coupons to a calibration institute and use the provided reference spectra for calibration of the instrument

Curved vs. flat samples

- Curvature changes the reflected direction
- Results between flat and curved samples should not differ significantly
- It is good practice to measure flat and curved samples of same coating to check
- Curved samples shall be calibrated with curved reference absorbers

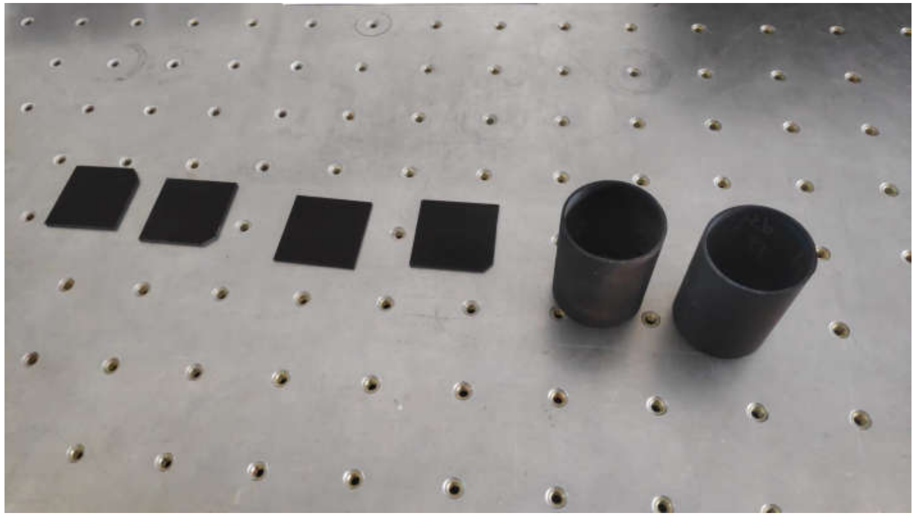

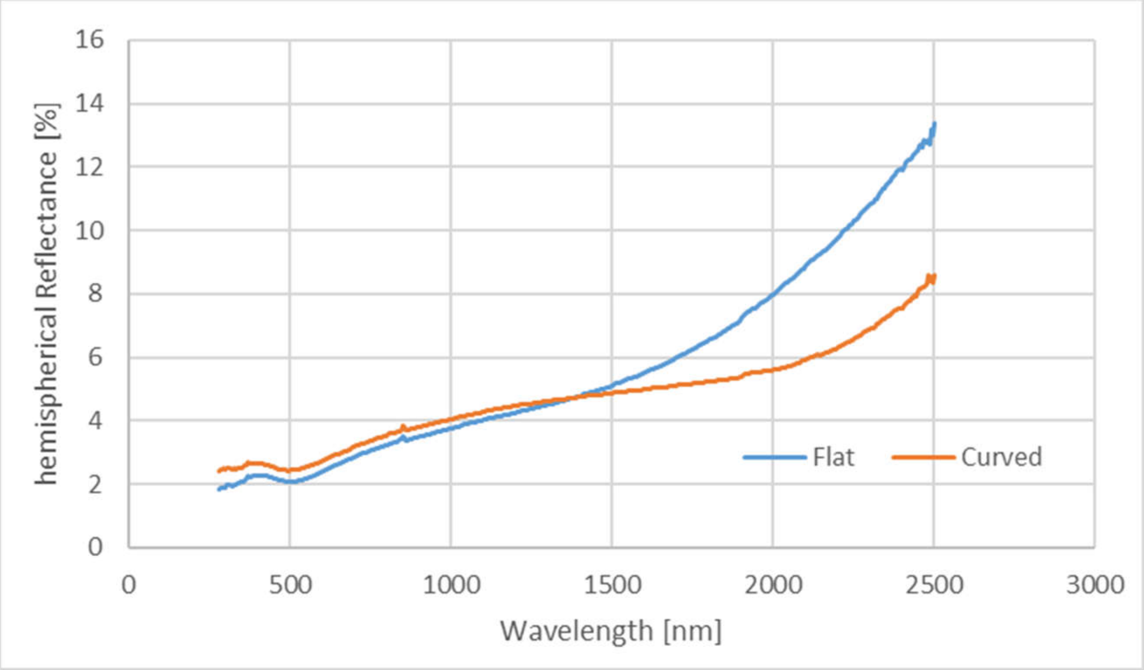

Particle samples

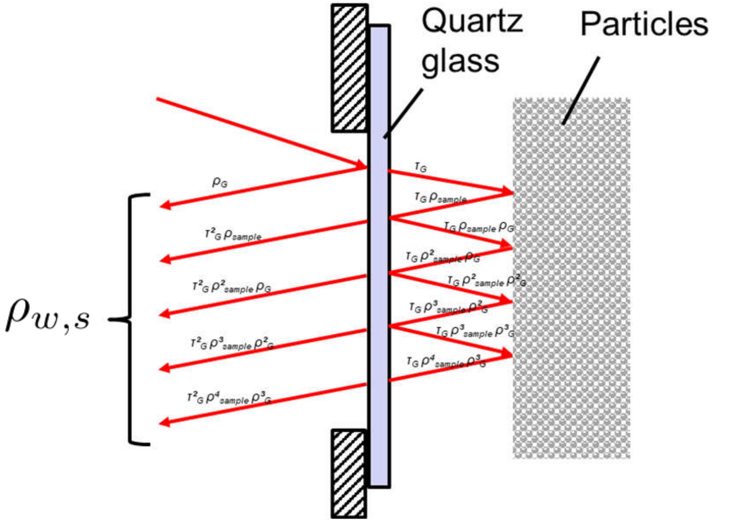

- Particles are investigated as absorber material
- They need to be measured trough a window (for non-beam down spectrophotometers)
- The influence of the window needs to be corrected from the measurements by the formula

$$R_s = \frac{\rho_{w,s} - \rho_w}{\tau_w^2 + \rho_w(\rho_{w,s} - \rho_w)}$$

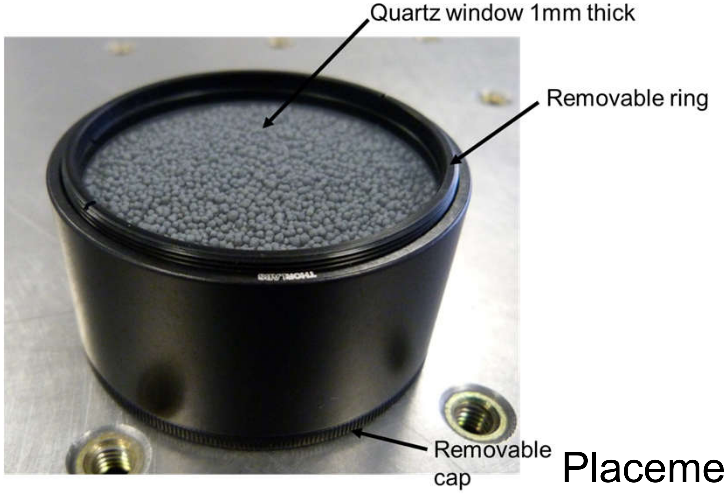

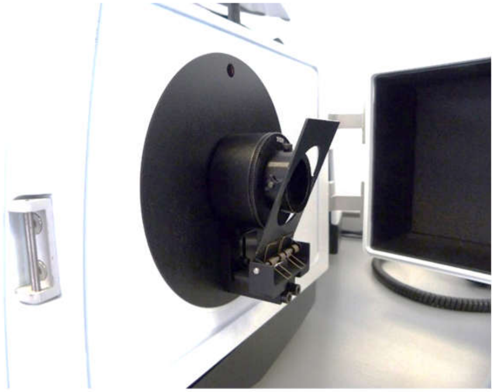

Placement of sample holder in spectrophotometer

SFERA-III

Solar Facilities for the European Research Area

Emittance

Florian Sutter, DLR

2nd Training for Industries, Plataforma Solar de Almería

Solar Facilities for the European Research Area

Kirchhoff's law of thermal radiation

Emittance is equal to absorptance at any given wavelength and temperature (for opaque bodies)

$$\varepsilon(\lambda,T) = \alpha(\lambda,T)$$

Knowledge of the emittance allows to compute the radiative heat loss of the receiver using Stefan Boltzman‘s law

$$E= \varepsilon(T)\ A\ T^4$$

Determination of ε(T)

- ε(λ) is determined with FTIR spectrometers by measuring reflectance typically in the range 2-16µm at room temperature (!)

  → ε(λ) = α(λ) = 1 – ρ(λ)

- The measured spectrum is weighted with the emitted energy of a blackbody at temperature T

$$\varepsilon(T) = \frac{\int_{\lambda_{min}}^{\lambda_{max}} \left(1 - \rho(\lambda)\right) \cdot E_{bb}(\lambda, T) d\lambda}{\int_{\lambda_{min}}^{\lambda_{max}} E_{bb}(\lambda, T) d\lambda}$$

where the emitted energy of the blackbody is computed with Planck‘s law $E_{bb}(\lambda, T) = \frac{2\pi h c^2}{\lambda^5 \left[e^{\left(\frac{hc}{\lambda k T}\right)} - 1\right]}$

Example of FTIR spectrometer

PerkinElmer Frontier FTIR CSI

PIKE Mid-IR IntegratIR

Example of integrating sphere

- **PIKE Mid-IR IntegratIR**

Upward-looking IntegratIR

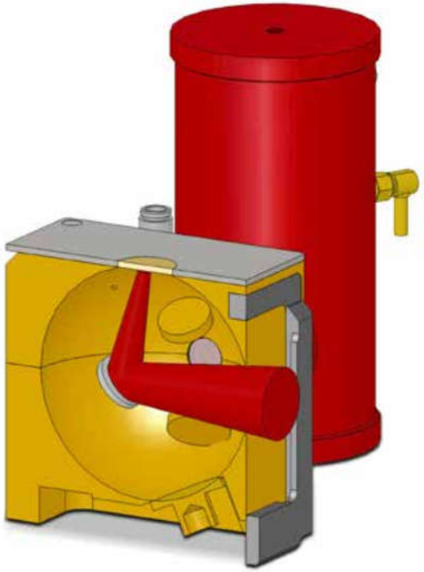

- Spectral emittance (2 -16 µm)
- Incidence angle 12°
- Hemispherical measurements
- Internal deflector allows to perform background correction
- Detector needs to be cooled with liquid nitrogen

Examples of FTIR measurement of particles

Measurement of particles trough ZnSe window

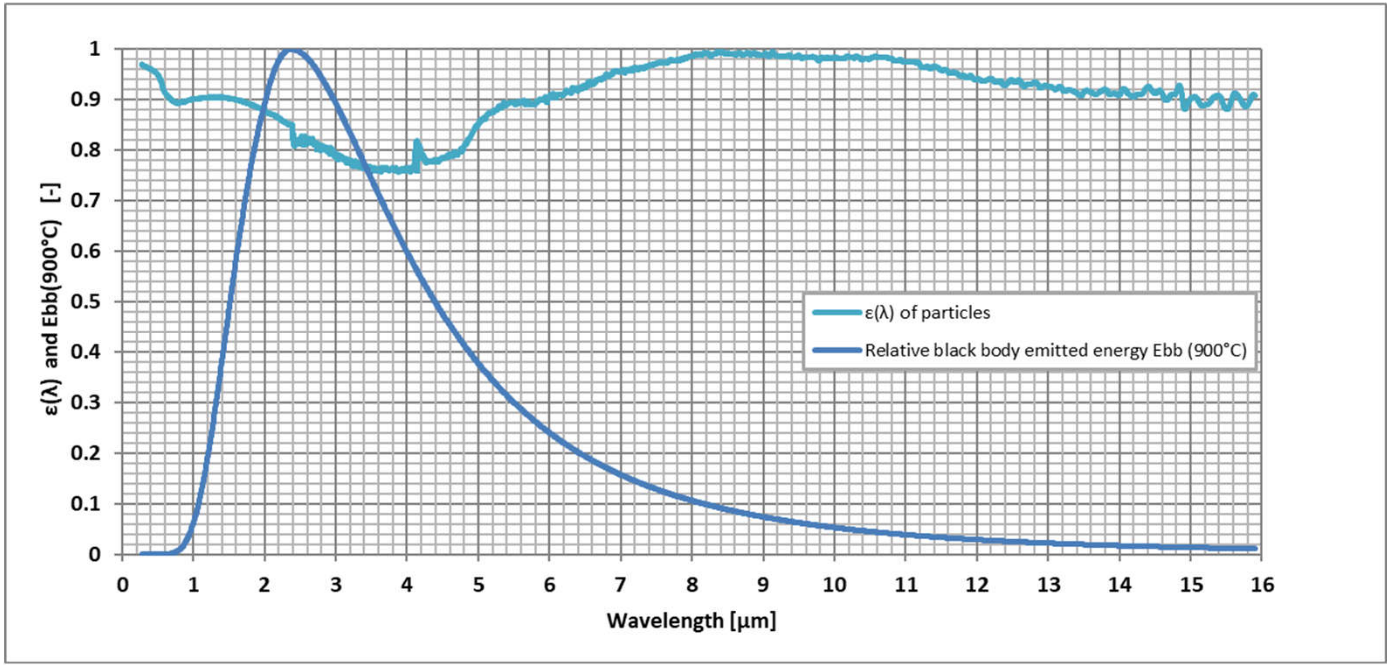

After weighting with blackbody spectrum → ε(900°) = 84.5%

Some take-away messages

- Spectral reflectance is typically measured hemispherically and specular reflectance only monochromatically. Specialized equipment is needed to determine spectral specular reflectance. Measurement at small acceptance angles becomes challenging.
- Transmittance measurements do not require the use a reference mirror. Ethanol to measure AR-coatings
- Absorptance is determined by measuring reflectance and $\alpha = 1 - \rho$. Absorber references shall be used for calibration.
- $\varepsilon(\lambda)$ is measured at ambient T and spectrum is weighted with blackbody spectrum of a certain temperature.
  → assumes that $\varepsilon(\lambda)$ is not dependent of T, which is not the case for all materials.
- Good care needs to be taken with the reference mirrors/absorbers. They should be traceable to NIST and not be used for daily measurements. The accuracy of the measurements depends strongly on the reference mirror!
- Round Robin Testing with other institutes is a good way to cross check that no systematic errors are happening

THANK YOU FOR YOUR ATTENTION!

Florian.Sutter@dlr.de
afernandez@psa.es

SFERA-III
Solar Facilities for the European Research Area

Training for Industries, Almería, 26. – 29.04.2022:
“Optimization of CST plant output by optical and thermal characterization and target-oriented O&M”

Aging of mirrors

Aránzazu Fernández-García, CIEMAT
Florian Sutter, DLR

THIS PROJECT HAS RECEIVED FUNDING FROM THE EUROPEAN UNION’S HORIZON 2020 RESEARCH AND INNOVATION PROGRAMME UNDER GRANT AGREEMENT NO **823802**

Contents

- Introduction
- Comparative tests
- Lifetime prediction tests
- Other R&D tests

Introduction

Introduction

Importance of mirror aging

1. The concentrator is the first element in CST technologies that interacts with solar radiation

2. Direct effect in the plant efficiency

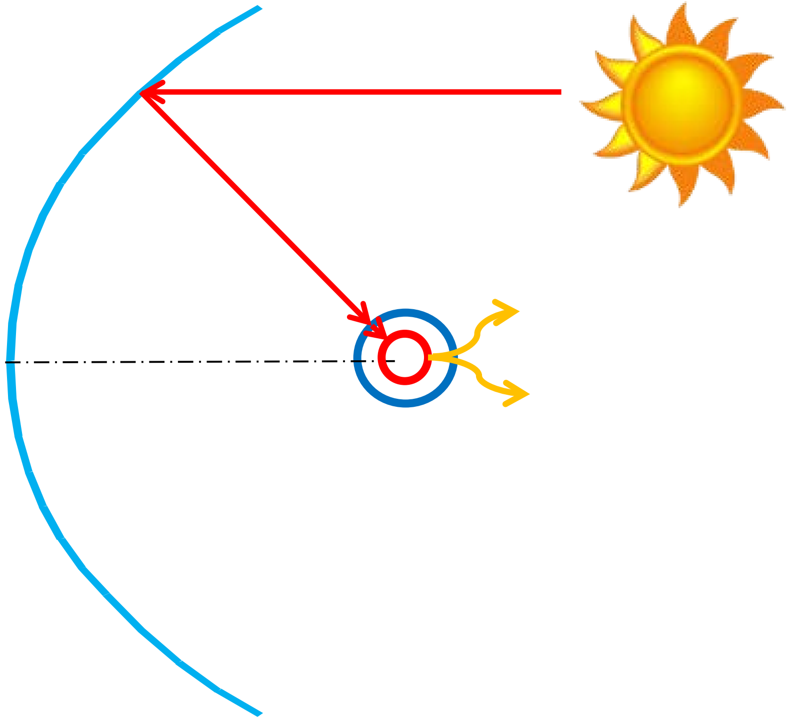

$$\eta = \boxed{\rho} \cdot \gamma \cdot \tau \cdot \alpha - \frac{\dot{Q}_l}{\dot{Q}_s}$$

Introduction

Importance of mirror aging

3. High surface covered by mirrors

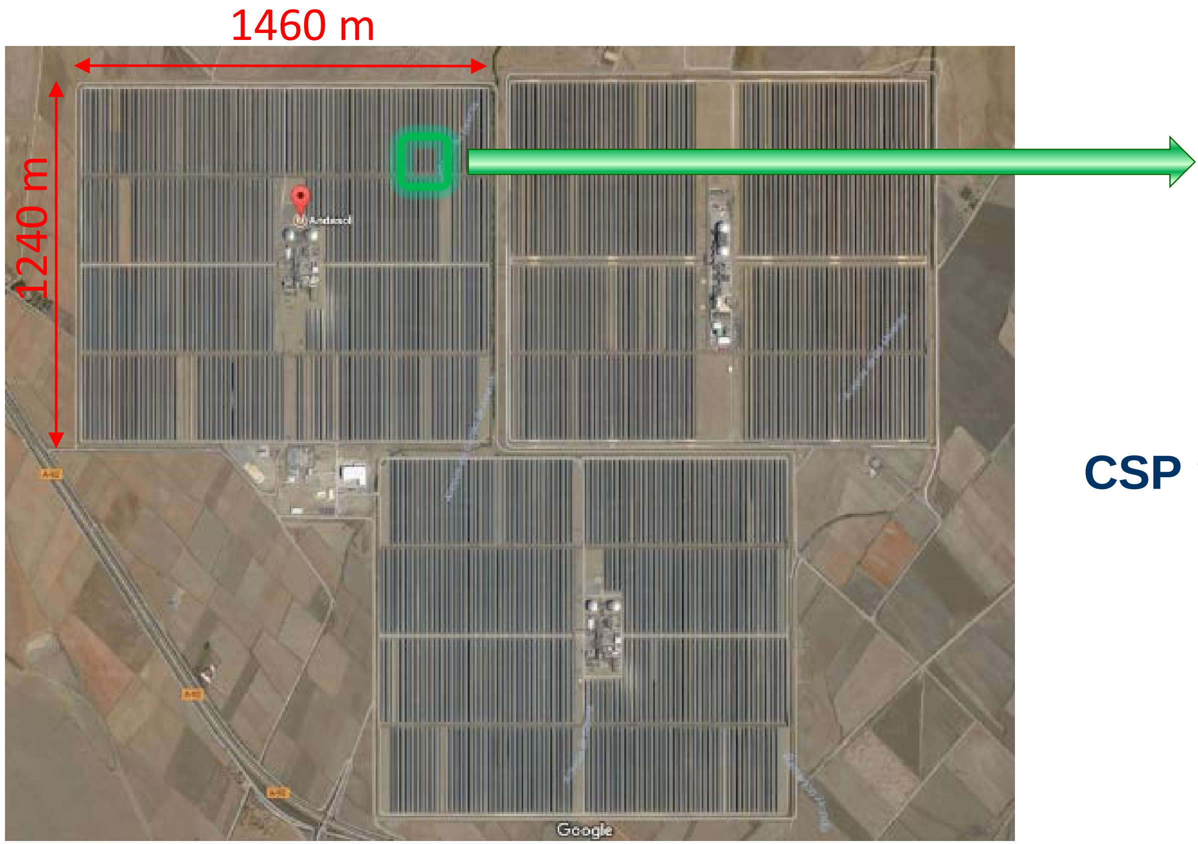

CSP plant with parabolic-trough collectors (PTC)

Each plant: 50 MW_e
Solar field ≈ 510,000 m^2

Introduction

Importance of mirror aging

3. High surface covered by mirrors

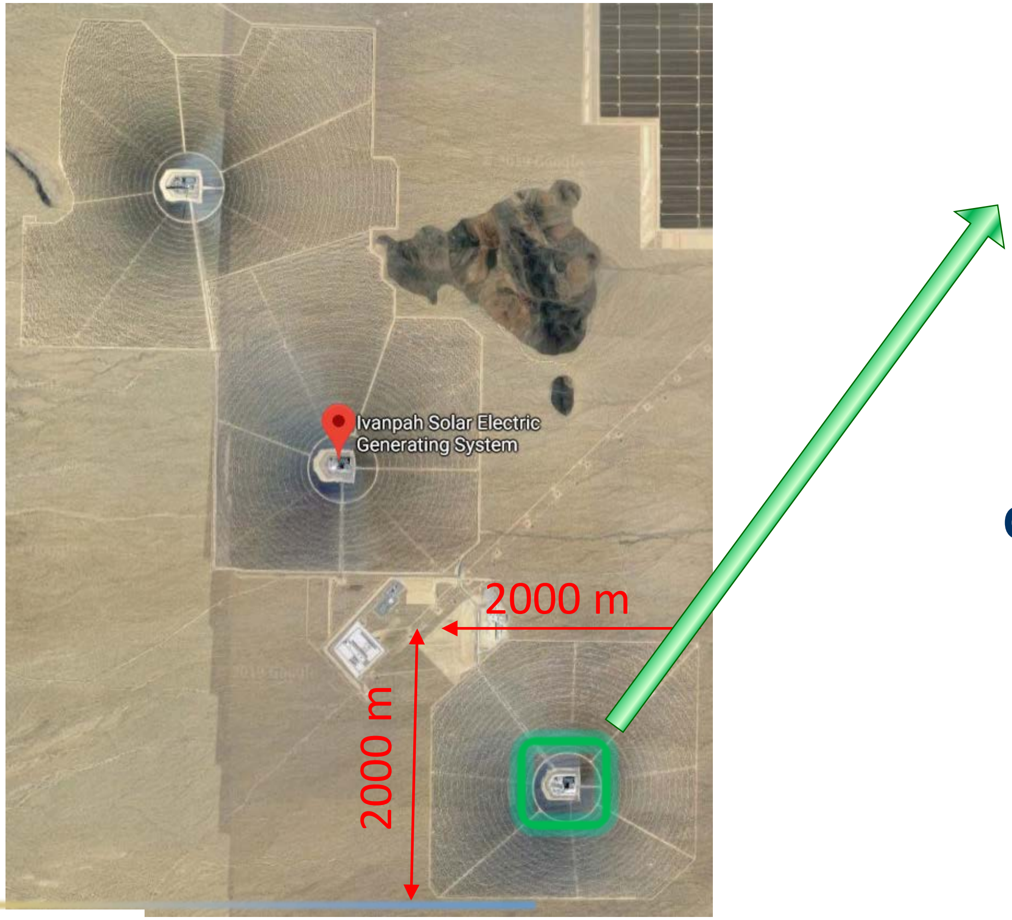

CSP plant with solar tower (ST) technology

Each plant: 126 MW_e
Solar field ≈ 870,000 m^2

Introduction

Degradation sources

→ **Non permanent: soiling** (Fabian's speech)

→ **Permanent: degradation**

Temperature
- Day/night
- Frost
- *[Secondaries]*

Radiation
Specially UV

Abrasion
- Cleaning
- Handling

Erosion
- Particles

Humidity
- RH
- Dew
- Rain, snow

Pollutants
- Sea
- Industries
- Particles

[A. García-Segura et.al, Renew Sust Energy Reviews 143 (2021) 110879]

Introduction

Degradation types

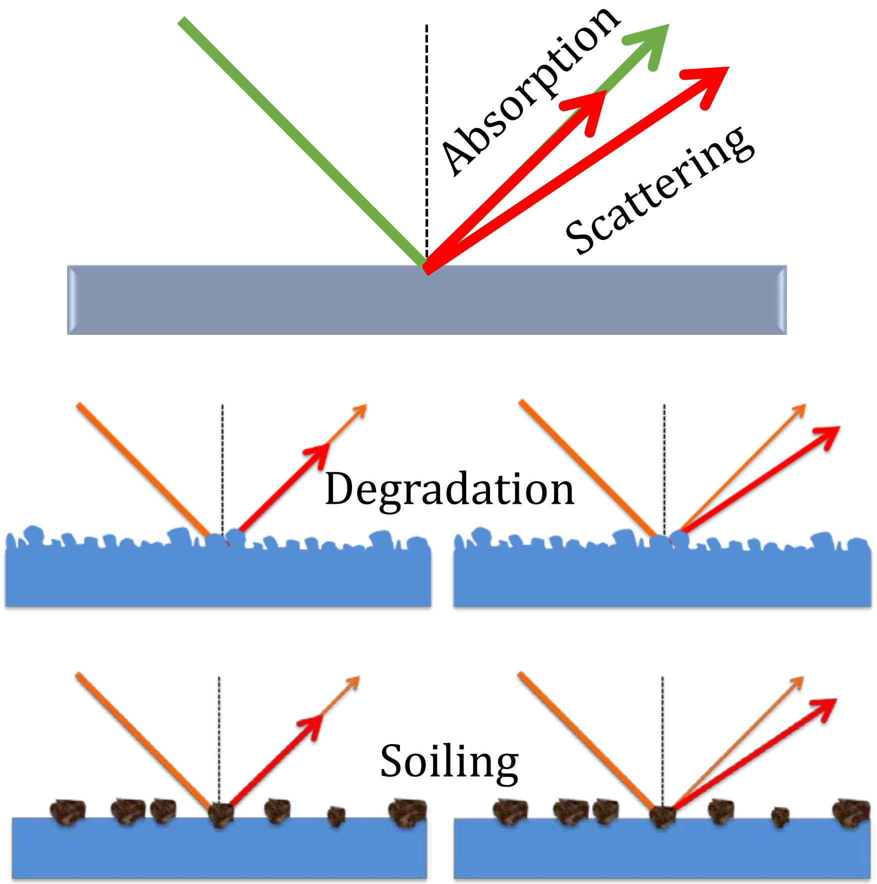

Comparative tests

Comparative testing

Type of tests

Comparative testing

Lifetime prediction (LTP) testing

- **Ranking of materials**: helps to select the most durable materials for operation, comparison with state of the art. Plant developers
- **Quality control:** monitors the quality of and to detect eventual issues in the running production. Manufacturers
- **Material development:** performance tool when the chemistry of coatings or manufacturing parameters are to be optimized. Material developers

Comparative testing

AENOR standard UNE 206016:2008

No.	Short name	Test name	Summary of testing conditions	Minimum duration
1	NSS	Neutral Salt Spray ISO 9227	T= 35±2ºC, pH=[6.5-7.2] at 25ºC Sprayed NaCl solution of 50 ± 5 g/l	480 h
2	CASS	Copper Accelerated Acetic Acid Salt Spray ISO 9227	T=50±2°C, pH=[3.1-3.3] at 25°C Sprayed NaCl solution of 50 ± 5 g/l and 0.26 ± 0.02 g/l $CuCl_2$	120 h
3	COND	Condensation ISO 6270-2 CH	T=40±3°C; RH: 100%	480 h
4	TCH	Thermal Cycling / Humidity	4 h at T=85°C, 4 h at T=-40°C, Method A: 16 h at T= 40°C and 97±3% RH Method B1: 16 h at T=85°C and RH=85±3% Method B2: 40 h at T=65°C and RH=85±3%	10 cycles
5	UVH	UV / Humidity ISO 16474-3	1 cycle: 4h at UV exposure at 60±3°C followed by 4h at 100% RH at 50±3°C	1000 h (front side) + 1000 h (back side)
6	ABR	Abrasion ISO 9211-4	Abradant of diameter ¾" producing mild abrading action, pushed with a force of 3.4 N on the reflector (0.012 N/mm^2), 25 cycles per minute and stroke length of 8 ± 2 cm	1000 cycles

Comparative testing

State-of-the-art criteria

	$\Delta\rho_{s,h}$	$\Delta\rho_{\lambda,\phi}$	l_c	d_c	Blistering level
NSS, 480h	≤0.004	≤0.004	≤ 0.1 cm	≤ 0.01 cm^{-2}	0(S1)
CASS, 120h	≤0.002	≤0.002	≤ 0.1 cm	≤ 0.01 cm^{-2}	0(S1)
Condensation, 480h	≤0.002	≤0.002	≤ 0.1 cm	≤ 0.01 cm^{-2}	≤1(≤S4)
TCH, 10 cycles	≤0.002	≤0.002	≤ 0.1 cm	≤ 0.01 cm^{-2}	≤1(≤S4)
UVH, 2000h	≤0.004	≤0.004	≤ 0.1 cm	≤ 0.01 cm^{-2}	≤1(≤S4)

These criteria were obtained in OPAC according to our experience with state-of-the-art mirrors
They are currently under study to include mirrors with low/free lead paints

l_c: Maximum penetration depth of corrosion starting from the original edge
d_c: Number of corrosion spots in the reflective surface with a diameter 1mm ≥ d_C ≥ 200 µm per sample area (excluding edge corrosion area)

[F. Sutter et al., Sol Energy Mat Sol Cells 193 (2019) 361-371]

Comparative testing

Analyzed parameters

Degradation results		
Maximum edge corrosion penetration (cm)	Number of corrosion spots >200µm per 300 cm² in the silver layer	Number of bubbles per 300 cm² in the paint layer
0.3	4	56

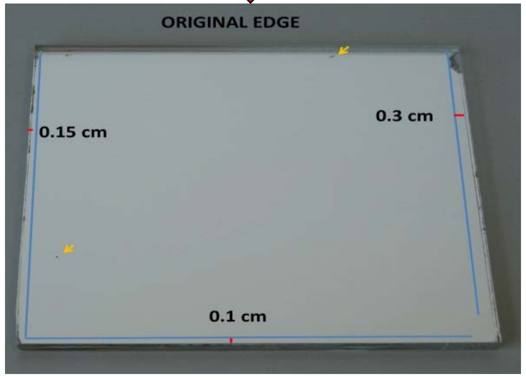

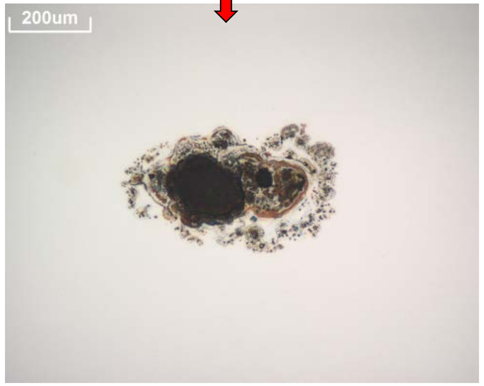

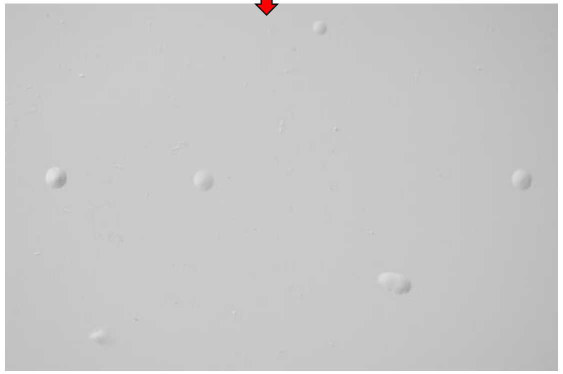

Comparative testing

IEC PT 62862-3-6: under preparation

No	Short name	Test name	Specific conditions	Duration	$\Delta\rho_{s,h}$*	$\Delta\rho_{\lambda,\varphi}$*	d_{c200}*	l_c*
1	NSS	Neutral Salt Spray ISO 9227		480 h*	≤0.005	≤0.005	≤0.03 cm^{-2}	≤0.1 cm
2	CASS	Copper Accelerated Acetic Acid Salt Spray ISO 9227	1 cycle: 120 h test + 24 h lab conditions	Low corrosivity sites (C2): 4 c Higher corrosivity sites (C4): 8 c	≤0.005	≤0.005	≤0.05 cm^{-2}	≤0.5 cm
3	COND	Condensation ISO 6270-2 CH		960 h	≤0.005	≤0.005	≤0.02 cm^{-2}	≤0.1 cm
4	TCH	Thermal Cycling / Humidity	Method A	40 cycles	≤0.005	≤0.005	≤0.02 cm^{-2}	≤0.1 cm
5	DH	Damp Heat IEC 62108	T=65 ± 2°C, RH=85 ± 5%	2000 h	≤0.005	≤0.005	≤0.02 cm^{-2}	≤0.1 cm
6	UVH	UV / Humidity ISO 16474-3		1000 h (front side) + 1000 h (back side)	≤0.010	≤0.010	≤0.02 cm^{-2}	≤0.1 cm
7	ALT	Alternate Exposure ISO 16474-3 & ISO 21207*		480 h UVH + 8 cycles	≤0.005	≤0.005	≤0.02 cm^{-2}	≤0.1 cm
8	ABR	Abrasion ISO 9211-4		1000 cycles	-	≤0.017	-	-
9	SE	Sand Erosion	Blowing dust/sand particles specified in MIL-STD-810, impinging with 20 m/s on the 45° tilted reflector surface.	Low erosivity sites (E1): m_d=0.03 g/cm²; m_s=0.00 g/cm² Higher erosivity sites (E2): m_d=0.08 g/cm²; m_s=0.37 g/cm²	-	E1: ≤0.007 E2: ≤0.032	-	-

* Under discussion

Lifetime prediction tests

LTP testing

Type of tests

Comparative testing

Lifetime prediction (LTP) testing

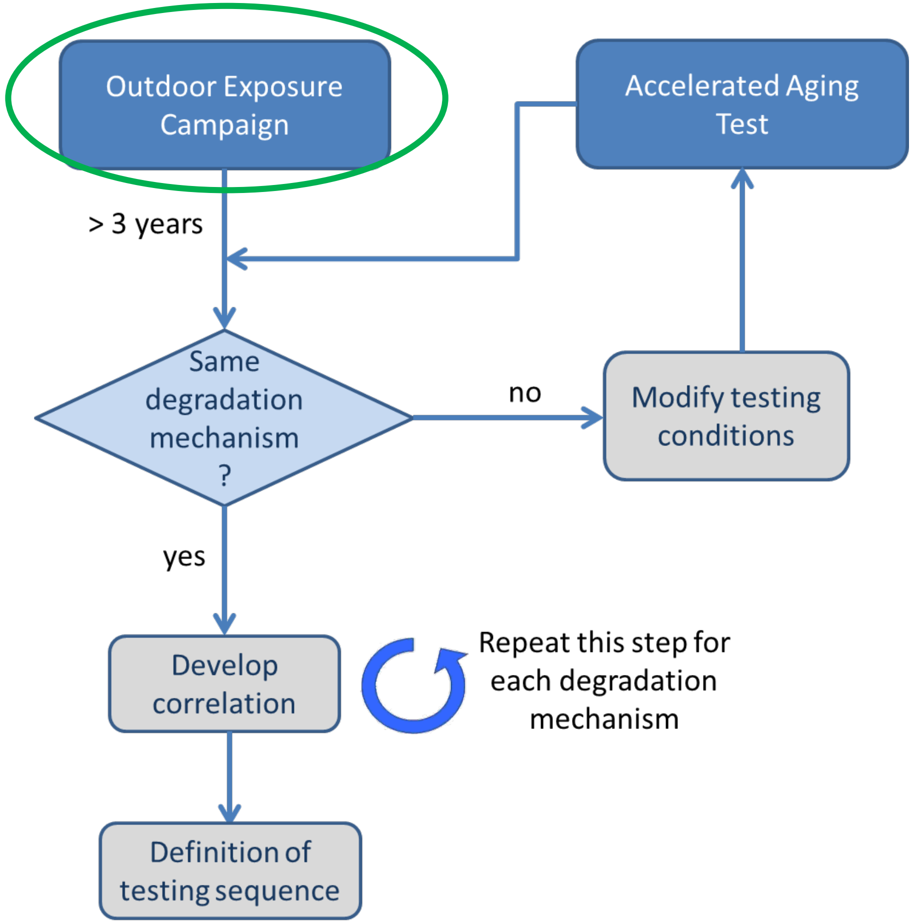

Outdoor Exposure Campaign

Accelerated Aging Test

> 3 years

Same degradation mechanism ?

no

Modify testing conditions

yes

Develop correlation

Repeat this step for each degradation mechanism

Definition of testing sequence

LTP testing

Outdoor exposure testing


Missour


Erfoud


Zagora


Canary Islands

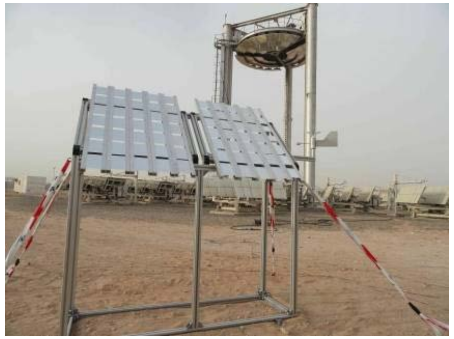
Abu Dhabi


Tabernas PSA


Almería

LTP testing

Outdoor exposure testing

- Galvanic separation sample-rack
- Facing towards equator
- 45° tilt angle

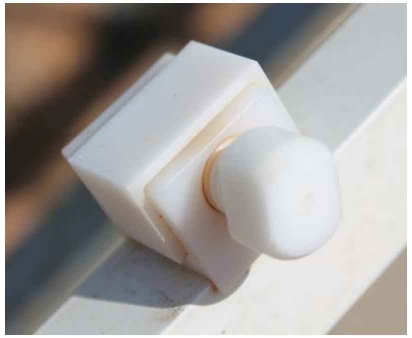

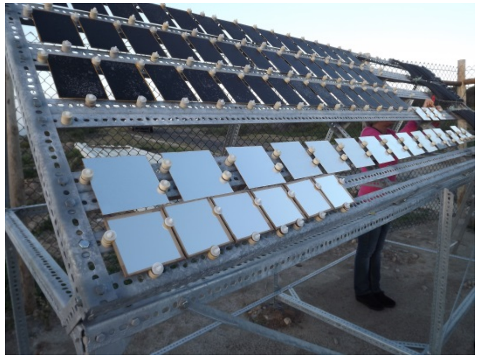

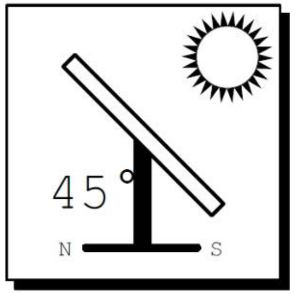

45 degree tilt angle, facing South.

LTP testing

Site corrosivity

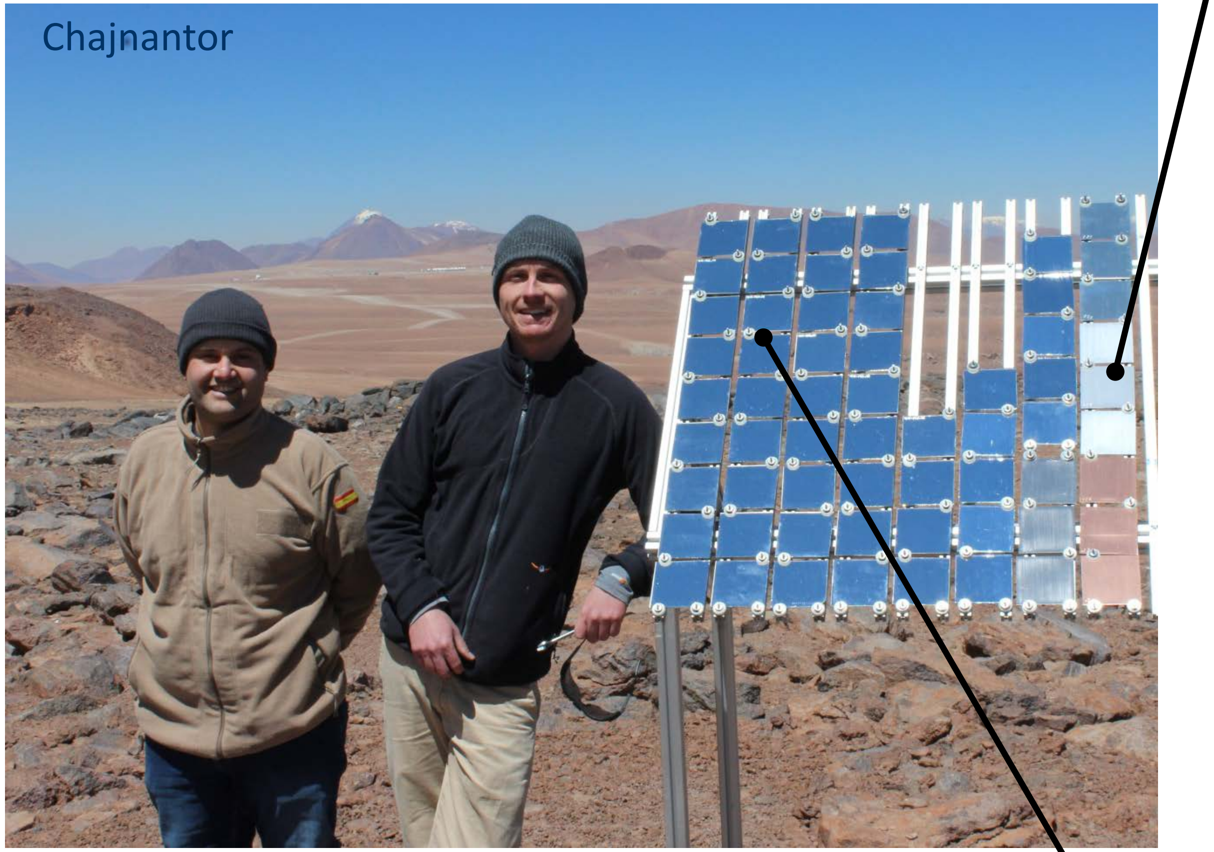

Zinc, Aluminum, Steep and Copper materials to determine the corrosivity class according to ISO 9223:2012

C1: very low

C2: low

C3: medium

C4: high

C5: very high

CX: extreme

Reflector samples

[ISO 9223, 2012]

LTP testing

Accelerated outdoor testing

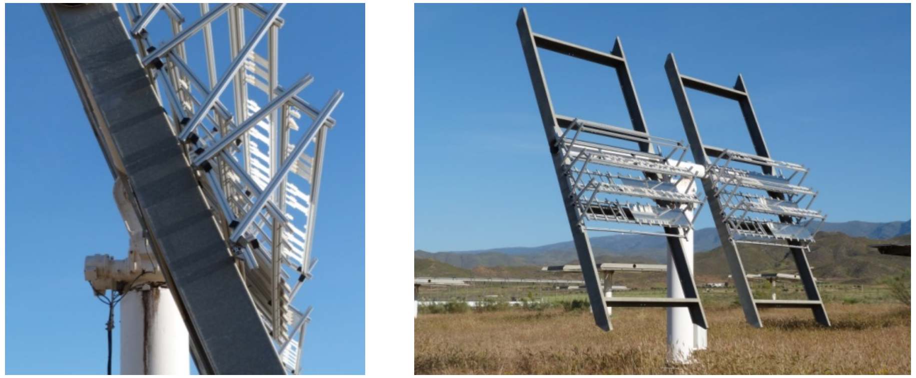

Blocking test bench

- Test mounted in a heliostat on PSA and tracked continuously
- Samples receiving radiation from the back to simulate the blocking in a heliostat field

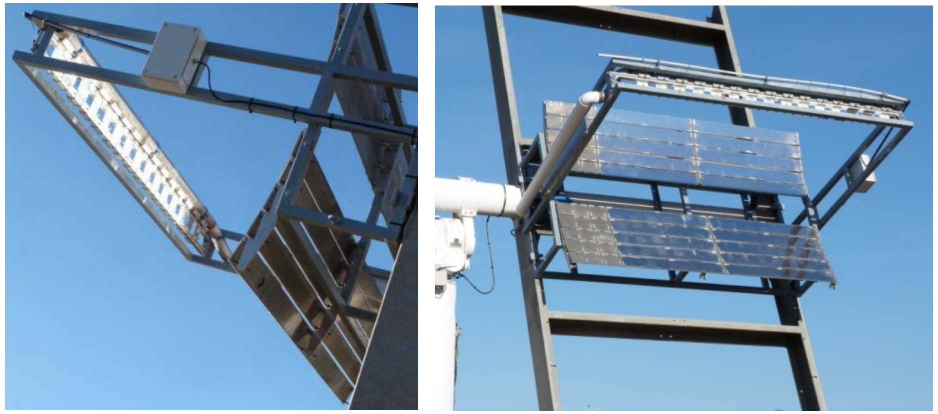

Concentrating radiation test bench

- Test mounted in a heliostat on PSA and tracked continuously
- Increased solar radiation testing in the entire solar spectrum (C-factor 10)
- Ambient parameters
- Cooling system available

LTP testing

Lifetime prediction (LTP) testing

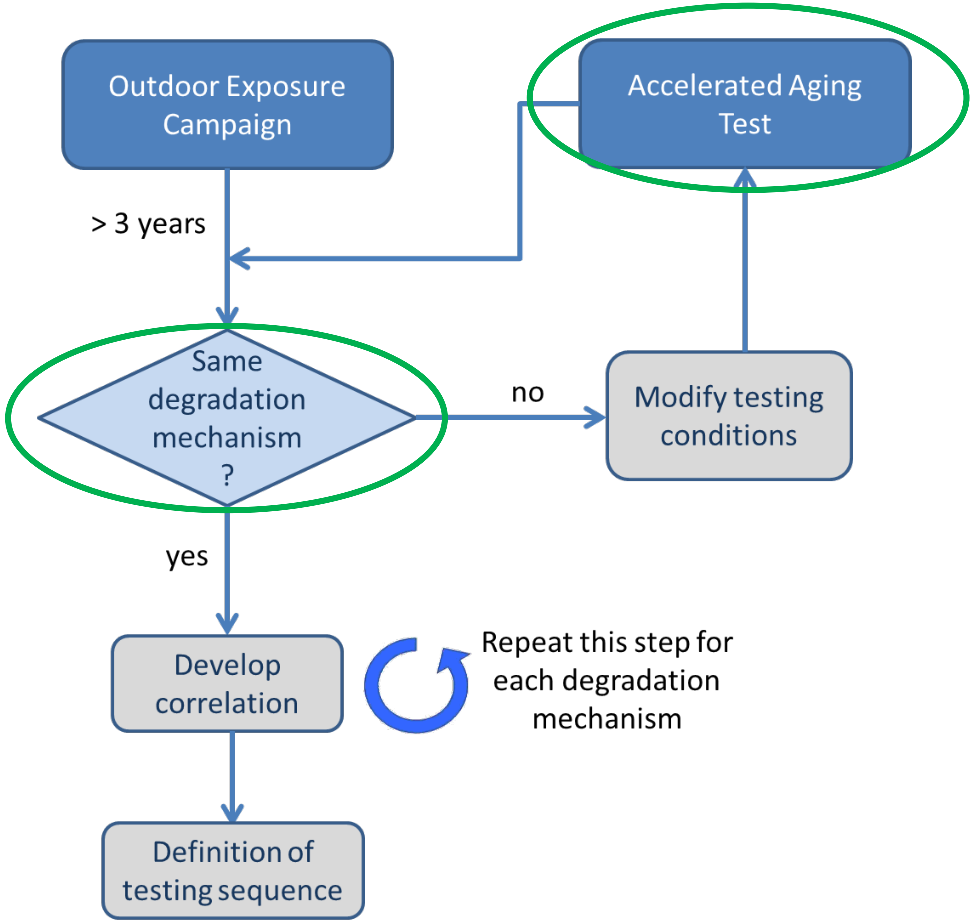

LTP testing

Degradation mechanisms: example of Al mirrors

Top coating erosion | **PVD-layer corrosion** | **Pitting corrosion** | **Micropitting PVD-layer** | **Deposits**

Outdoor test

Accelerated aging tests

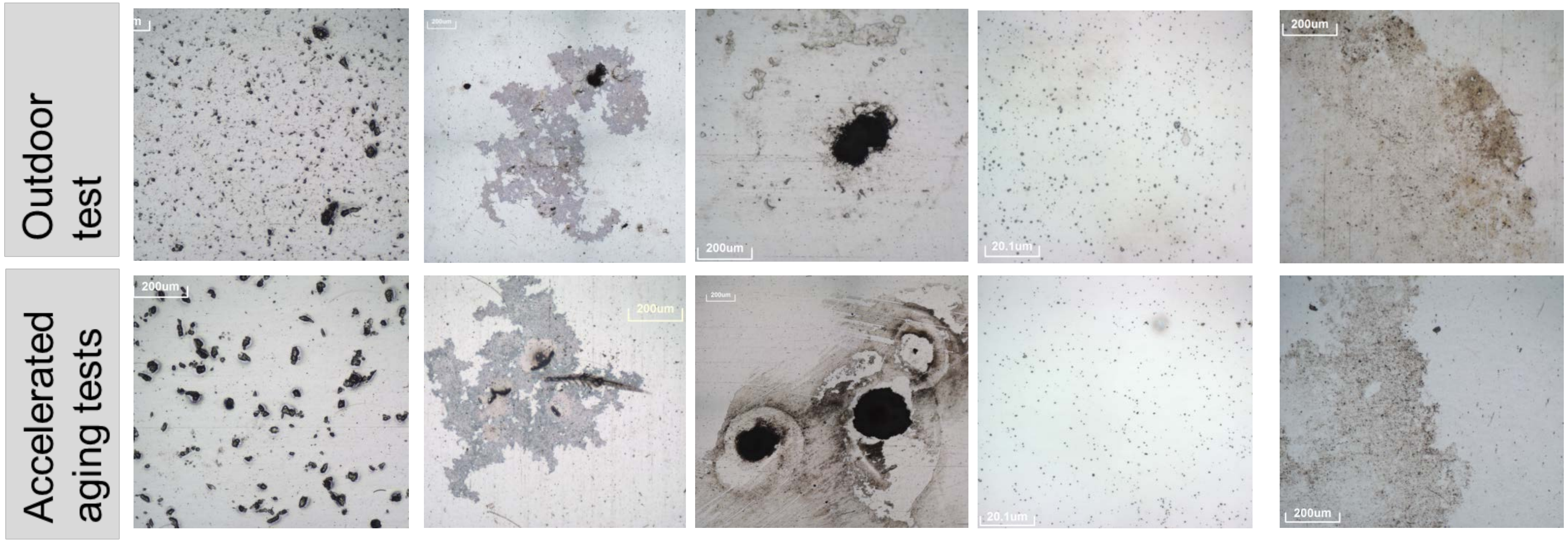

Sand storm (Acetube) | **Sand trickling + ISO 9227 CASS** | **ISO9227 CASS** | **ISO11507 UV/humidity** | **soiled surface + ISO11507**

[J. Wette et al., Energies 9 (2016) 916-16]

LTP testing

Lifetime prediction (LTP) testing

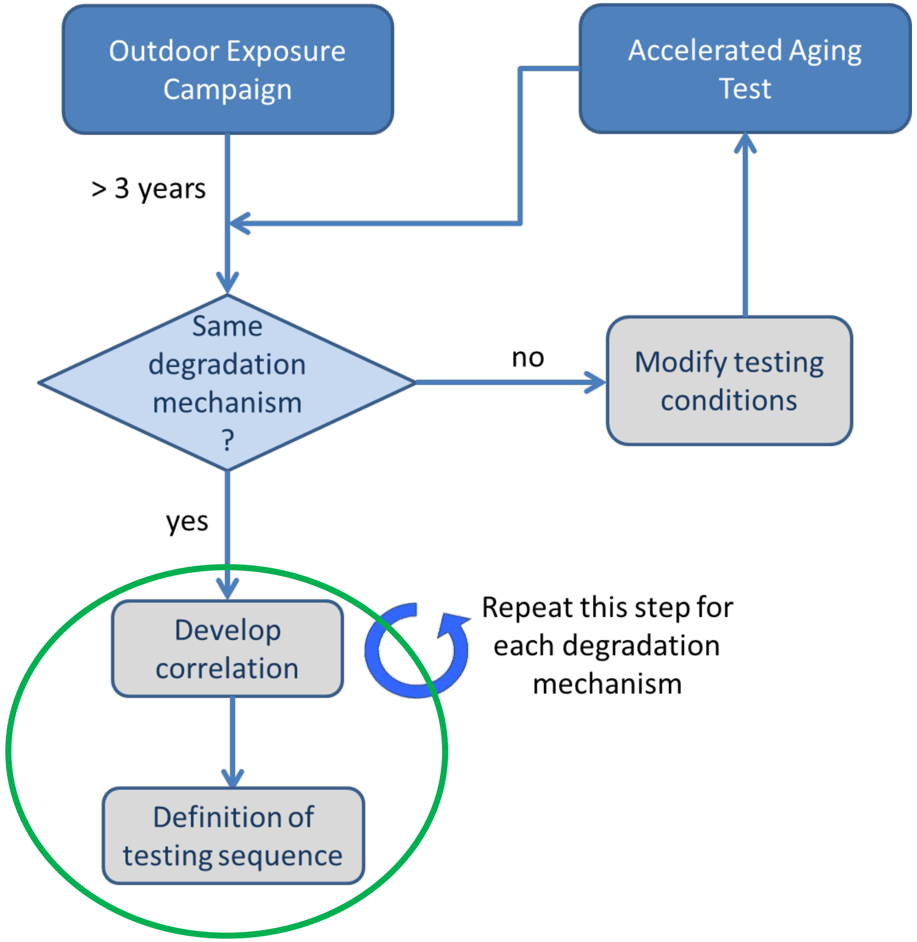

Outdoor Exposure Campaign

Accelerated Aging Test

> 3 years

Same degradation mechanism ?

no

Modify testing conditions

yes

Develop correlation

Definition of testing sequence

Repeat this step for each degradation mechanism

LTP testing

Correlations: example of aluminum mirrors

Accelerated aging step			3b	4
Simulated reference site	GHI T v r.H.	Sim late yea	SO9227: CASS esting time in h]	ISO 16474-3, Method A, cycl No. 1 [testing time in h
Extreme Desert	2174 kWh/m²/a 23.9 °C 3.8 m/s 23.4 %	3	2	480
		10	8	480
Desert	1965 kWh/m²/a 19.5 °C 3.3 m/s 45.9 %	3	8	480
		10	24	480
Coastal	1925 kWh/m²/a 19.7 °C 5.3 m/s 71.3 %	3	8	480
		10	24	480

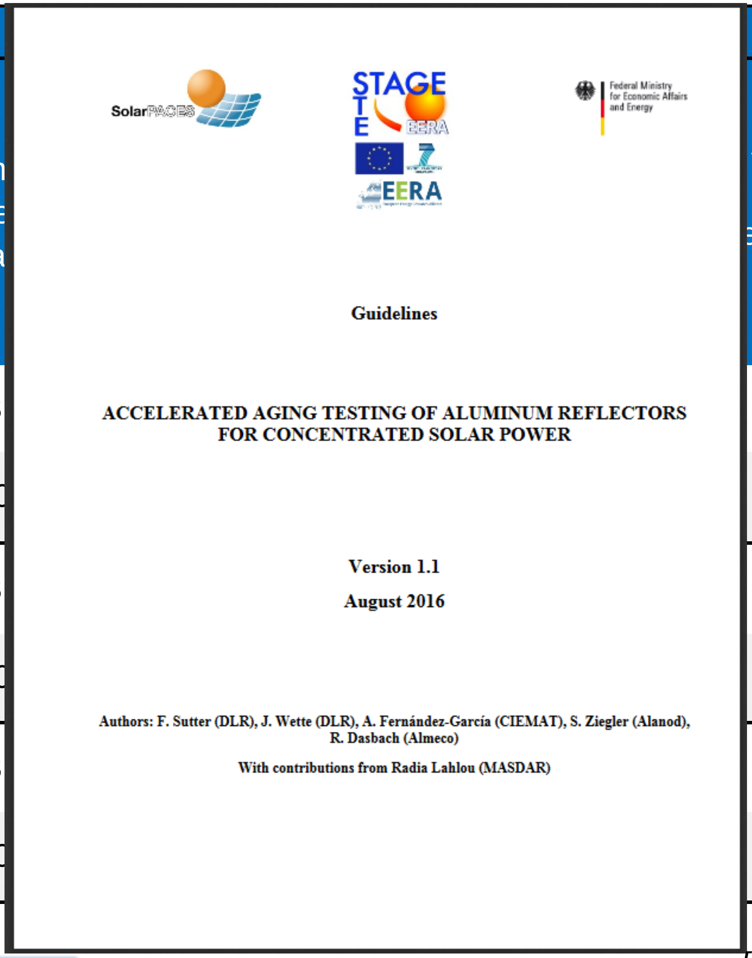

Guidelines

ACCELERATED AGING TESTING OF ALUMINUM REFLECTORS
FOR CONCENTRATED SOLAR POWER

Version 1.1

August 2016

Authors: F. Sutter (DLR), J. Wette (DLR), A. Fernández-García (CIEMAT), S. Ziegler (Alanod), R. Dasbach (Almeco)

With contributions from Radia Lahlou (MASDAR)

[F. Sutter et al., Sol Energy 2018;174:149–163]

LTP testing

Correlation: Erosion (silvered-glass mirrors)

- Scope: reproducing the erosion defects in size and density of reflector samples exposed at a height of 1.5 m above ground not surrounded by a wind fence, collectors or any other barriers, in two types of desert environments, named as E1 and E2.
- Method: Erosion is tested with sand blasting devices or wind tunnels with particle flow. v= 20m/s, α=45°

	Environment in which reflector shall be employed	
CASE	E1	E2
Guidance **t_t= 20 yrs**	m_d= 0.12 g/cm² m_s= 0 g/cm² $\Delta\rho_{\lambda,\phi}$ < 0.025	m_d= 0.32 g/cm² m_s= 1.46 g/cm² $\Delta\rho_{\lambda,\phi}$ < 0.125

m_d Impacting mass density of MIL-STD-810 blowing dust particles (97-99% quartz, diameter 1-150µm)
m_s Impacting mass density of MIL-STD-810 blowing sand particles (>95% quartz, diameter 149-850µm)

E2 sites fulfill at least 2 of the following criteria: (a) the soil exhibits a significant proportion of fine sand (0.063-0.2 mm), (b) the average relative humidity over a meteorological year lies below 30%, (c) events with wind velocities stronger than 10m/s are taking place at least 300 hours per year.
E1 sites are less erosive and only one of the above listed criteria applies.

[F. Wiesinger et.al, Applied Energy 268 (2020) 114925]

LTP testing

Correlation: Erosion (silvered-glass mirrors)

Measured defect densities in E1, E2, E3 after 12 months of exposure and corresponding laboratory simulation

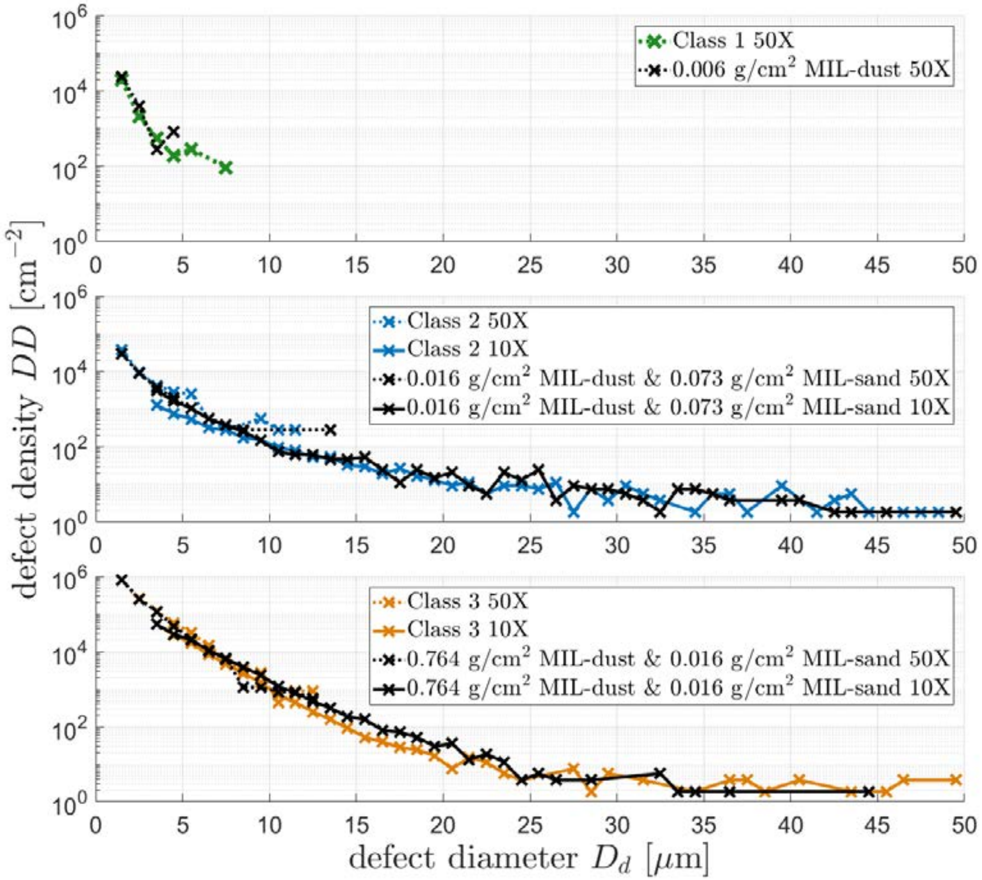

→ 20 years E1 exposure is simulated by m_d= 0.12 g/cm²
(linear behavior is assumed)

→ 20 years E2 exposure is simulated by m_d= 0.32 g/cm² and m_s= 1.46 g/cm²

E3 environment is not included in IEC draft – this site is extremely aggressive causing annual reflectance losses of more than 4%

[F. Wiesinger et.al, Applied Energy 268 (2020) 114925]

LTP testing

Correlation: Corrosion (silvered-glass mirrors)

- Scope: This test aims at reproducing the corroded area A_c, excluding edge corrosion, of mirror samples exposed in environments of corrosivity class C2, C3 and C4 according to ISO 9223.
- Method: Corrosion is tested according to the CASS test. The time in outdoor conditions (for the different corrosivity classes) reproduced with the CASS test, and the corresponding acceleration factors, is listed below in the table

		Time [years] reproduced for the different corrosivity class (according to ISO 9223)		
CASE	**t [h] in CASS**	**C2**	**C3**	**C4**
CASS test	120 (1 cycle)	5.6	4.2	2.8
	480 (4 cycles)	22.2	16.7	11.1
a_f*		400	300	200

* Calculated with an optimization of the data presented in the next slide

[F. Buendía et.al, Sol Energy Mat & Sol Cells 224 (2021) 110996]

LTP testing

Correlation: Corrosion (silvered-glass mirrors)

$$\rho = \left(\rho_0 - a \cdot t_{outdoor}\right) \cdot \left(e^{-b\left(\frac{t_{outdoor}}{a_f}\right)^c}\right)$$

Measured corroded area A_c during CASS test

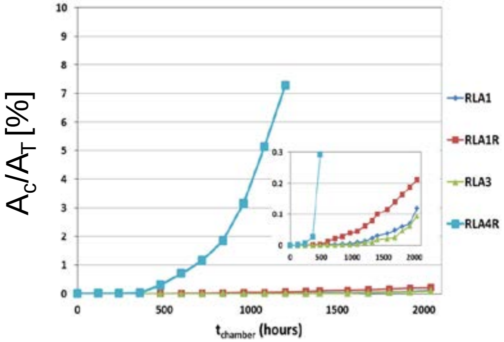

Measured corroded area A_c after three years of outdoor exposure testing

Material<	Site (corrosivity class)			
	Almería (C4)	Tabernas (C3)	Atacama Desert (C3)	Missour and Erfoud (C2)
	Ac [-]	Ac [-]	Ac [-]	Ac [-]
RLA1	0.000001	1.5E-7	2E-7	-
RLA1R	0.000007	0.000002	0.000002	1.9E-7
RLA3	0.000037	0.000004	0.000001	-
RLA4R	0.000210	0.000021	0.000055	-

Time in chamber to produce the same A_c after approximately 3 years of outdoor exposure and the acceleration factor (a_f) between the CASS test and outdoor exposure, depending on the material and site.

Material	Site (corrosivity class)							
	Almería (C4)		Tabernas (C3)		Atacama Desert (C3)		Missour and Erfoud (C2)	
	t (h)	a_f (-)	t (h)	a_f(-)	t (h)	a_f(-)	t (h)	a_f(-)
RLA1	234	106	118	204	131	200	-	-
RLA1R	230	108	130	185	144	182	60	400
RLA3	935	27	493	48	331	79	-	-
RLA4R	280	88	157	153	201	131	-	-

[F. Buendía et.al, Sol Energy Mat & Sol Cells 224 (2021) 110996]

Other R&D tests

Other R&D durability tests

Corrosion in industrial sites

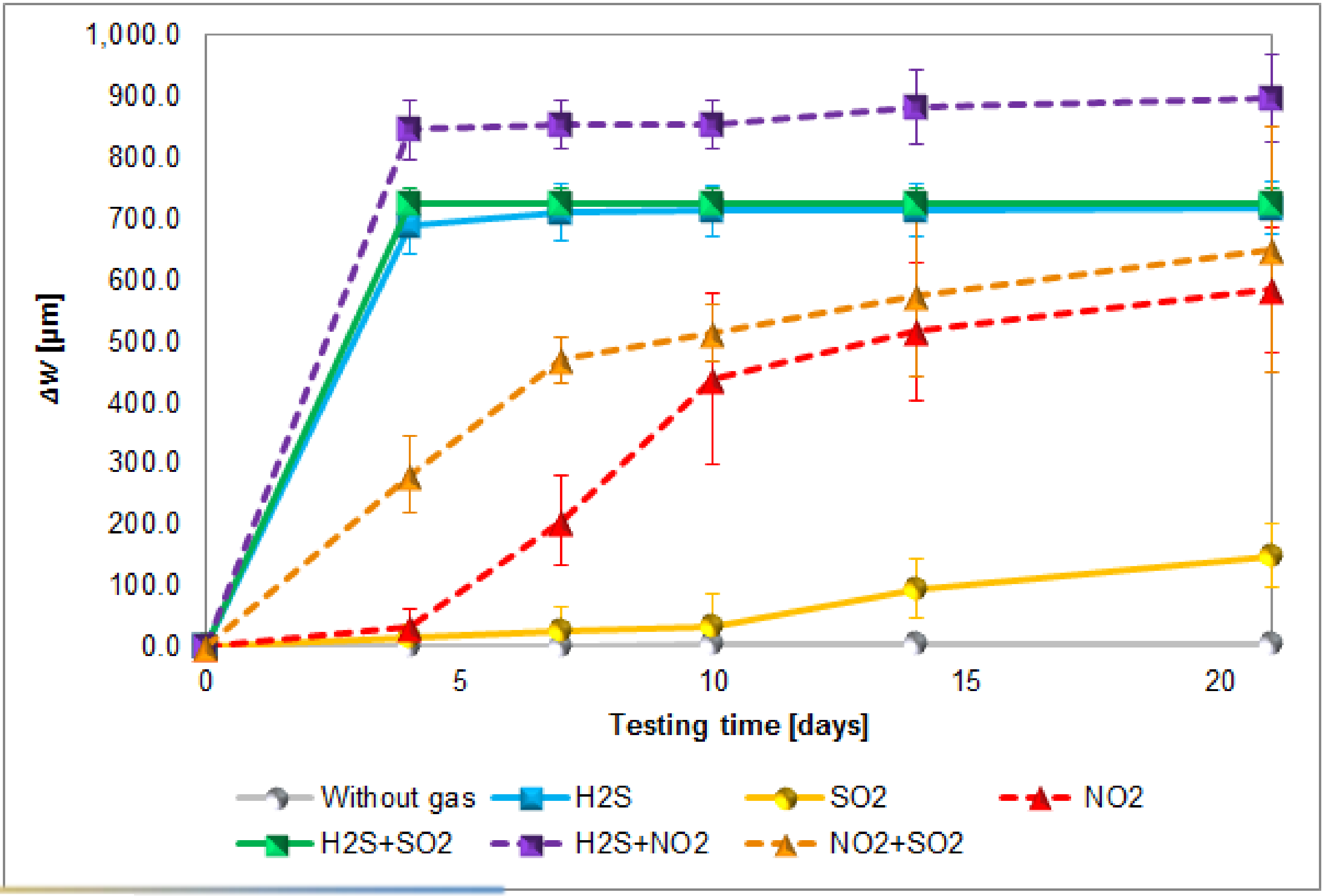

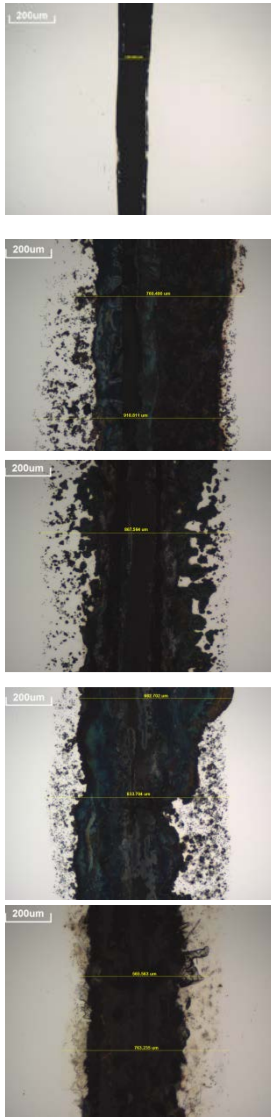

[A. García Segura et al., Sol Energy Mater Sol Cells. 200 (2019) 109955]

Other R&D durability tests

Abrasion due to cleaning

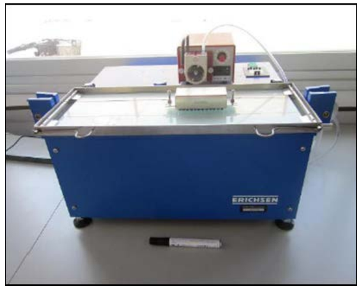

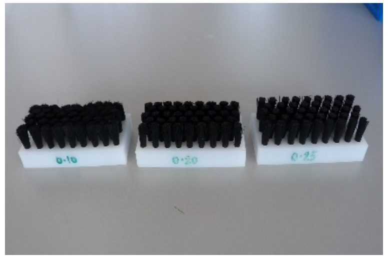

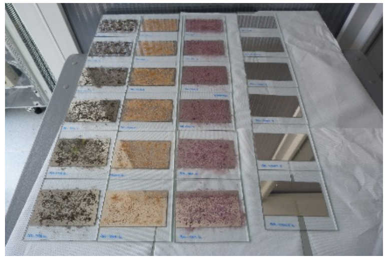

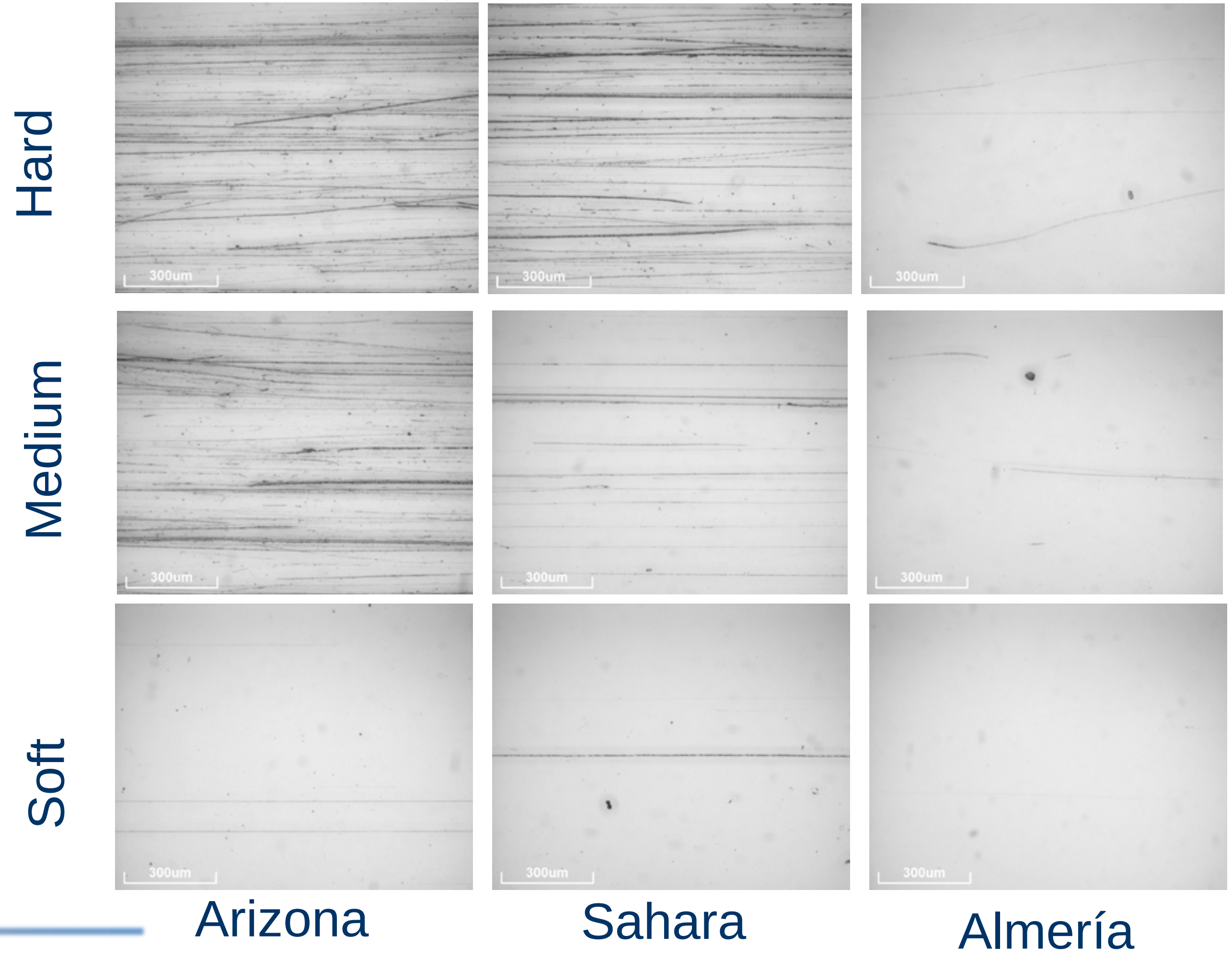

[C. Sansom et al., Energies 9 (2016) 1006-12]

Other R&D durability tests

Degradation due to sand

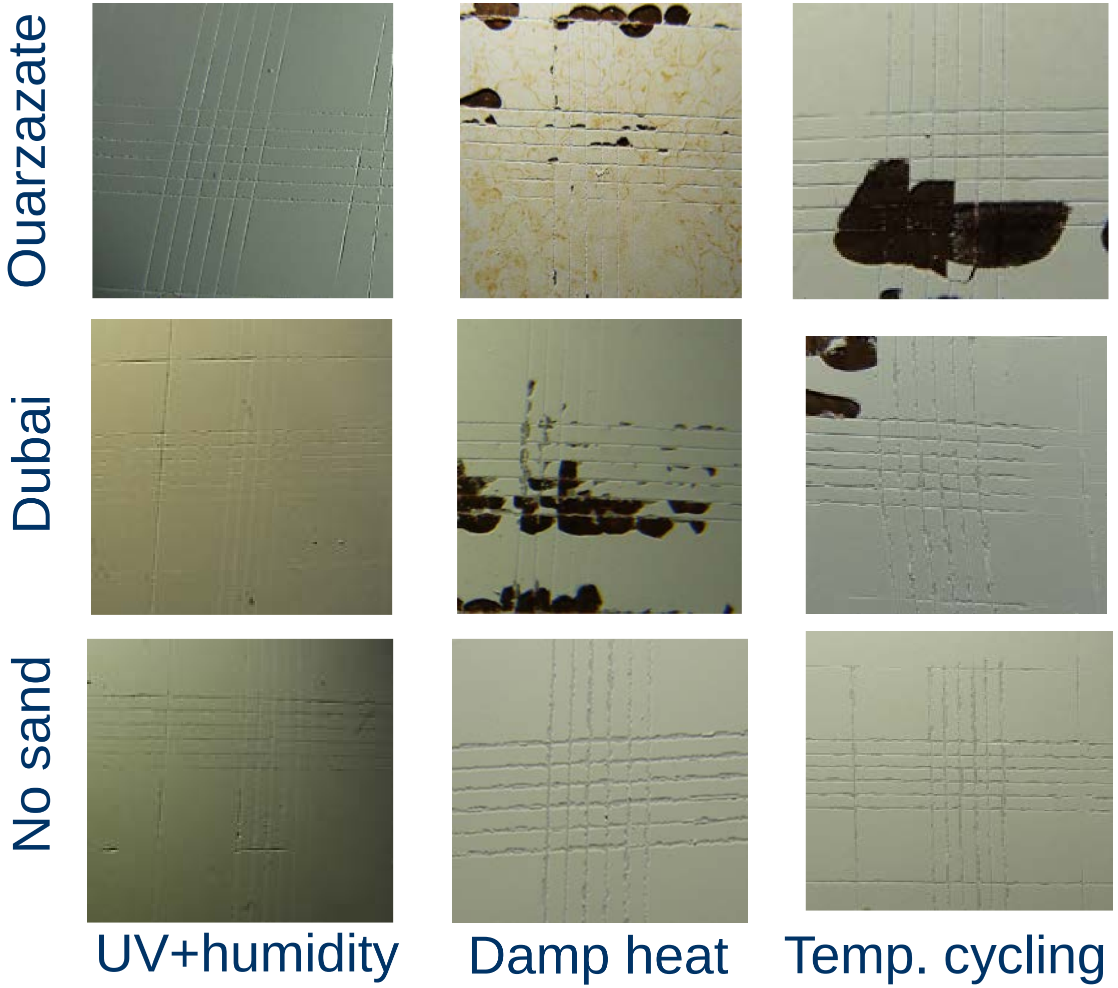

[A. Fernández-García et al., Energies 11(2018) 808]

Other R&D durability tests

Secondary concentrators

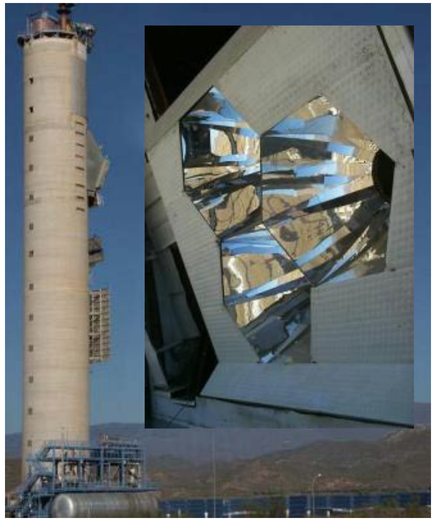

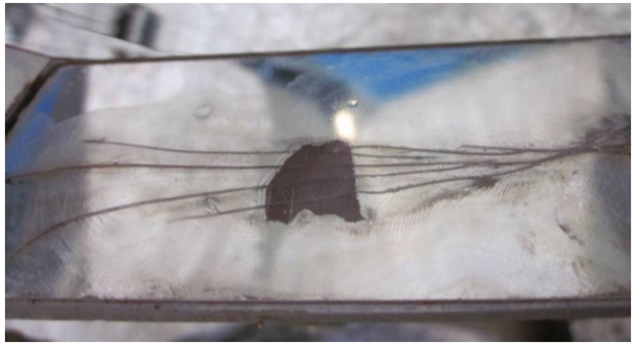

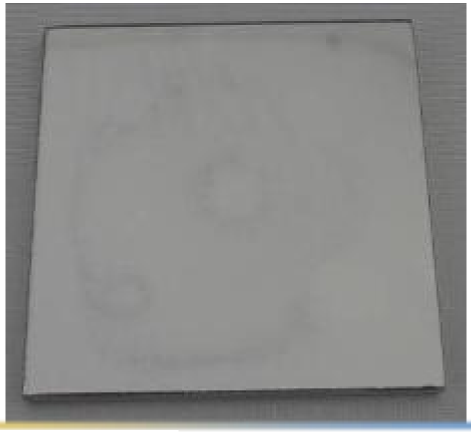

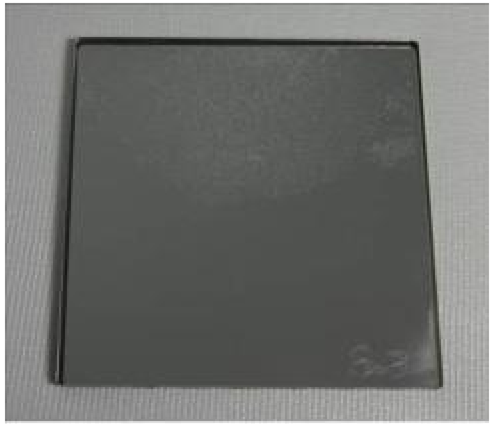

[A. Fernández-García et al., Sol Energy Mater Sol Cells 130 (2014) 51-63]

THANK YOU FOR YOUR ATTENTION!

arantxa.fernandez@psa.es
Florian.Sutter@dlr.de

SFERA-III
Solar Facilities for the European Research Area

Solar Facilities for the European Research Area

2nd Training for Industries “Optimization of CST plant output by optical and thermal characterization and target-oriented O&M”
26 – 29 April 2022, Plataforma Solar de Almería, Spain

Components aging: Receiver coatings
Simon Caron (DLR)

NETWORKING

THIS PROJECT HAS RECEIVED FUNDING FROM THE EUROPEAN UNION’S HORIZON 2020 RESEARCH AND INNOVATION PROGRAMME UNDER GRANT AGREEMENT NO **823802**

Outline

- **Introduction**
- **Materials and Methods**
  - Substrates and Coatings
  - Optical Characterization
  - Durability Test Program
- **Results and Discussion**
  - Solar Cycling Tests
  - Climate Chamber Tests
  - Summary for Gen 2 Coatings
- **Conclusion & Outlook**

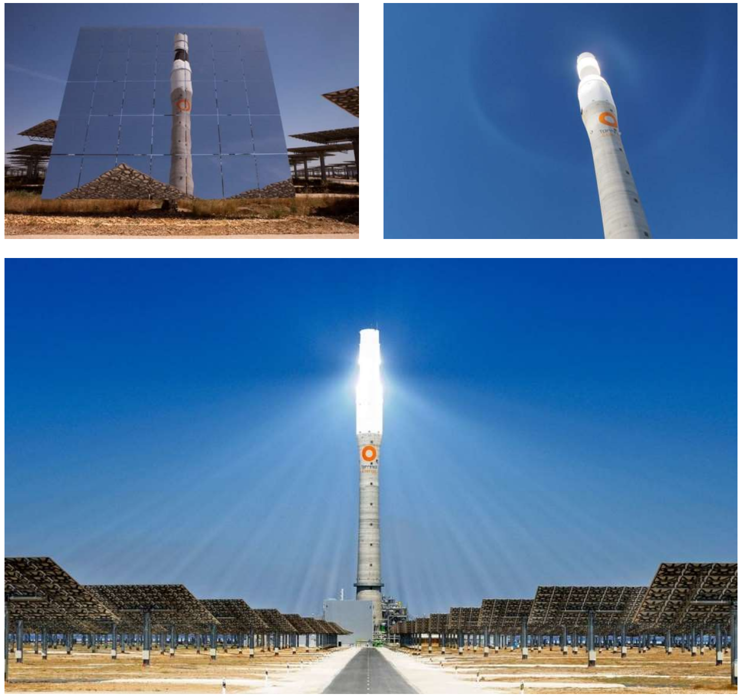

https://torresolenergy.com/gemasolar/

Introduction

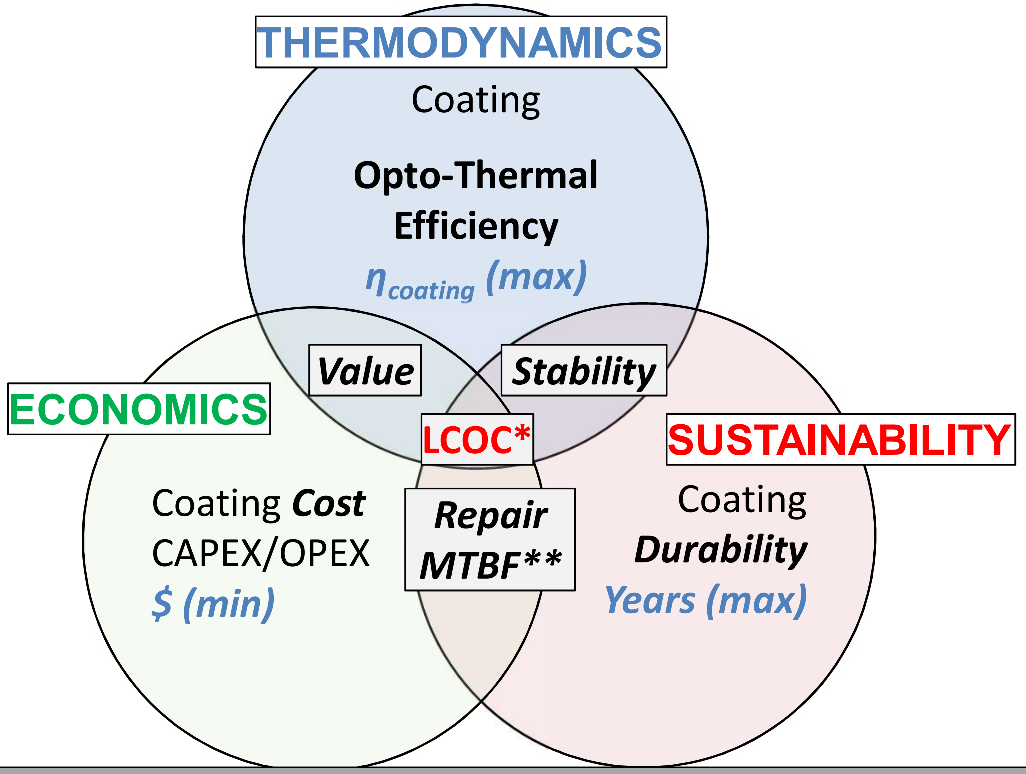

THERMODYNAMICS

Coating

Opto-Thermal Efficiency

$\eta_{coating}$ (max)

Value

Stability

ECONOMICS

LCOC*

SUSTAINABILITY

Coating ***Cost***
CAPEX/OPEX
$ (min)

Repair
MTBF**

Coating
Durability
Years (max)

Metrological inspection system
(Solar absorptance, thermal emittance, Skin temperature)

*LCOC**: Levelized Cost of Coating
(Ho et al., Sol. Energy 108 (2014) 315-321)

*MTBF***: Mean Time Between Failure
(Optimization of Recoating interval)

Materials and Methods
Substrates

- SRSG* (Water/steam)
  - Ferritic-martensitic alloys
  - Manufactured by Vallourec
  - Standard Boiler technology
  - Max. Temp. 600 – 650 °C
  - Cheap alloys, require coatings

T91/P91 (X10CrMoVNb9-1)

VM12-SHC

vallourec

*SRSG**: **Steam** Receiver Super Generator

- <u>MSR** (Molten Salt)</u>
  - Nickel-Chromium superalloys
  - Inconel 617 (**Inc617**); Haynes 230 (**H230**) Aerospace Industry, Gas Turbines
  - High Temp. (1000 – 1150 °C)
  - Expensive alloys, but less corrosion

SPECIAL METALS

HAYNES International

*MSR***: **Molten Salt** Receiver

http://www.vallourec.com/fossilpower/EN/Products/Pages/tp91.aspx
http://www.vallourec.com/fossilpower/EN/Products/Pages/vm12-shc.aspx

Materials and Methods

Coatings

- A ceramic spray consisting of a primer coating and a high solar absorptance (HSA) top coating (Coating A)
- A slurry aluminide primer coating protecting the steel substrate from hot oxidation, in combination with the above ceramic HSA top coating (Coating B)
- A magnetron-sputtered multi-layered thin film cermet solar selective coating (SSC) applied on a polished substrate (Coating C)
- A multi-metallic Cr-Mn diffusion coating applied with the pack cementation process (Coating D)
- A combination of the above slurry aluminide primer *(b)* with a thin film cermet SSC on top (Coating E)
- A combination of the multi-metallic diffusion coating *(d)* as a primer coating combined with the ceramic HSA top coating *(a)* (Coating F)

Coating/Substrate	**T91**	**VM12**	**Inc617**	**H230**
Coating A	Yes	Yes	Yes	Yes
Coating B	Yes	Yes	No	No
Coating C	Yes	No	Yes	No
Coating D	Yes	Yes	Yes	No
Coating E	Yes	No	Yes	No
Coating F	No	Yes	No	No

Coating A

Coating B

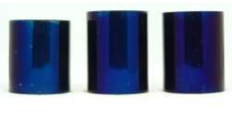

Coating C

Coating D

Coating E

Coating F

Coating	Substrate	Thickness (DFT, μm)	Selective ?	Surface preparation	Coating application	Thermal treatment
A	T91 | VM12 Inc617 | H230	55 (Primer) 35	No	Grit blasting	Spraying	Curing
B	T91 | VM12	85 | 55	No	Grit blasting	Spraying	Curing (x2)
C	T91 | Inc617	0.6	Yes	Polishing, mirror finish	Sputtering	-
D	T91 | VM12 | Inc617	35	No	Glass bead blasting	Cementation	Pre-oxidation
E	T91 | Inc617	~ 65	No	Polishing of primer coating (B)	Spraying + Sputtering	-
F	VM12	~ 70	Yes	Glass bead blasting	Cementation + Spraying	Pre-oxidation + Curing

Materials and Methods

Optical characterization

Room Temperature (RT)
Discrete meas. (points)

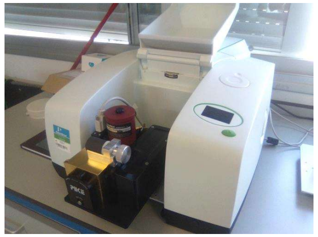

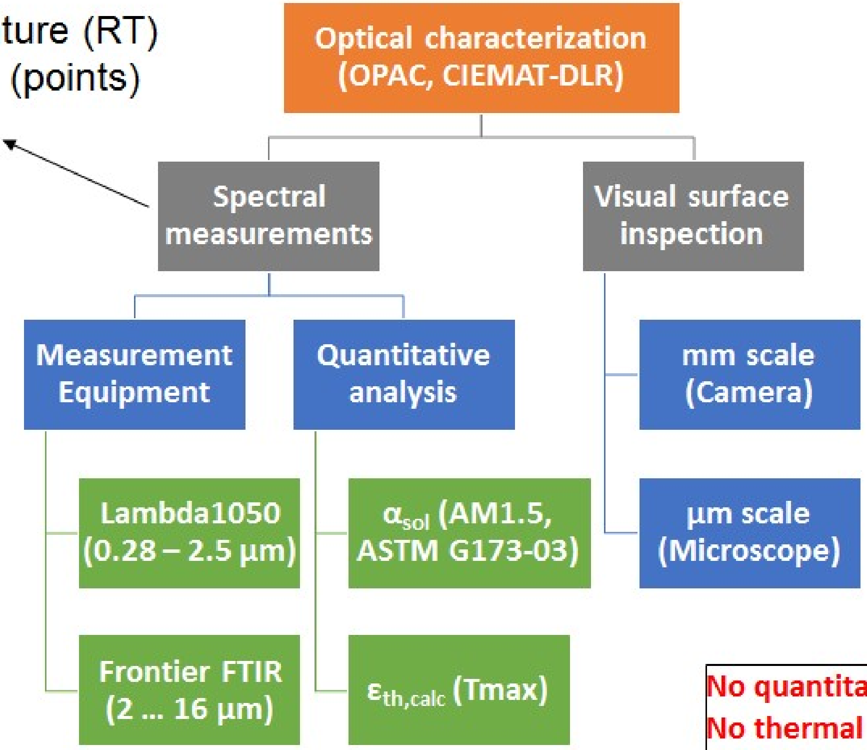

Optical characterization (OPAC, CIEMAT-DLR)

- Spectral measurements
  - Measurement Equipment
    - Lambda1050 (0.28 – 2.5 µm)
    - Frontier FTIR (2 … 16 µm)
  - Quantitative analysis
    - α_{sol} (AM1.5, ASTM G173-03)
    - $\varepsilon_{th,calc}$ (Tmax)
- Visual surface inspection
  - mm scale (Camera)
  - µm scale (Microscope)

No quantitative adhesion test
No thermal conductivity data
No metallographic analysis

Materials and Methods

Spectral measurements

- **Baseline calibration**

$$\rho_{sample}(\lambda) = \frac{R_{sample,meas}(\lambda)}{R_{baseline,meas}(\lambda)} \cdot \rho_{baseline,ref}(\lambda)$$

SDHR: Spectral Directional –Hemispherical Reflectance

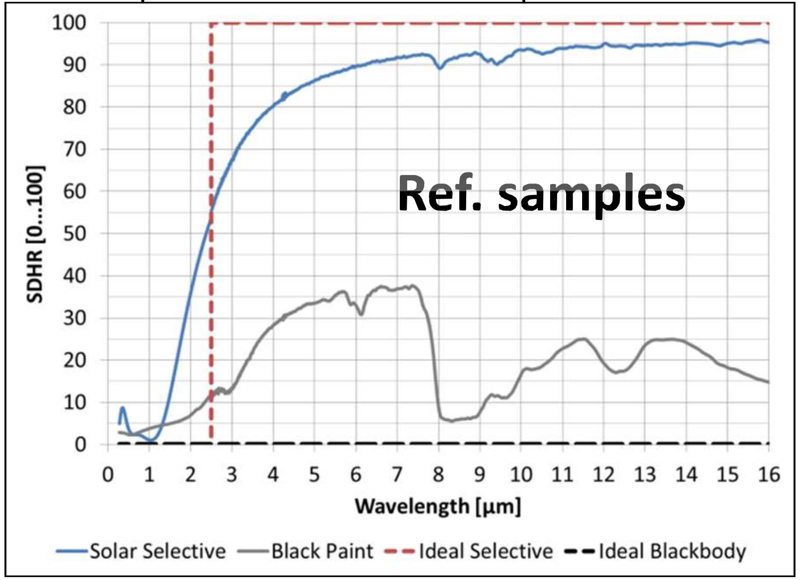

- **Weight functions**:
  - α_{sol}: ASTM G173-03 direct, AM1.5
  - ε_{th}: Blackbody spectrum (650/750 °C)
  - 8-12° incidence angle (Near normal)

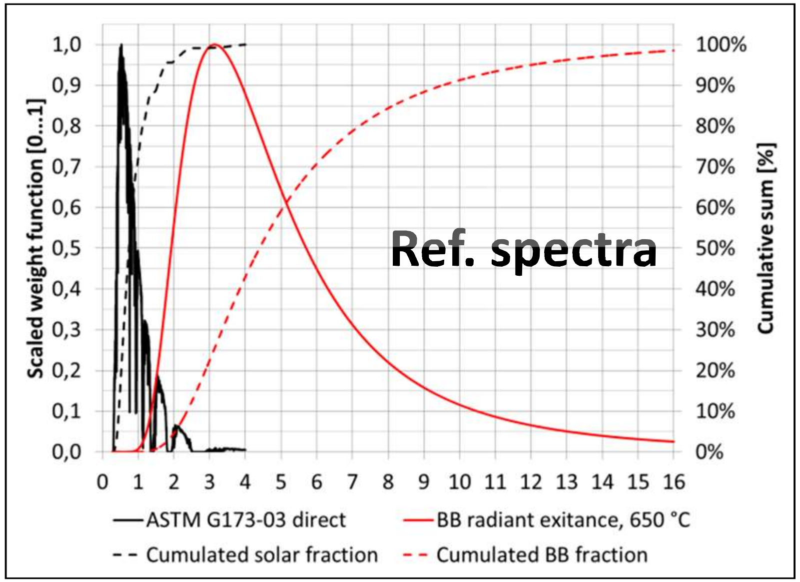

Materials and Methods

Solar absorptance and thermal emittance

- Solar absorptance α_{sol}
  - HSA: High Solar Absorptance (> 96%)

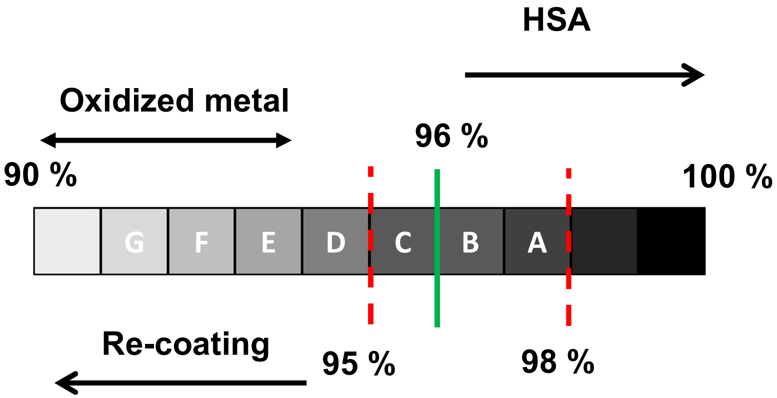

- Thermal emittance ε_{th} (T)

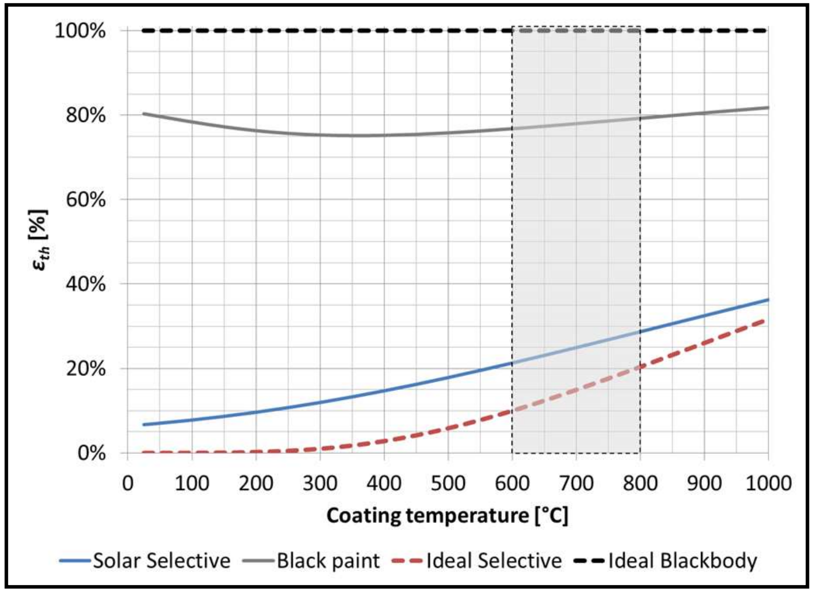

Materials and Methods

Opto-thermal coating efficiency

- Opto-thermal efficiency:

$$\eta_{coating} \approx \frac{\alpha_{sol} \cdot \dot{q}''_{sol} - \varepsilon_{th}(T_{abs}).\sigma.T_{abs}^4}{\dot{q}''_{sol}}$$

- Trade-off factor Z:

$$Z = \frac{\Delta\alpha_{sol}}{\Delta\varepsilon_{th}} = -\frac{\dot{q}''_{sol}}{\sigma.T_{abs}^4}$$

- Solar absorptance predominant for Central Receiver System (CRS)

- Allowable Flux Density (AFD)

  Vant-Hull, *J. Sol. Energy Eng*. 2002, 124(2): 165-169
  - for Molten Salt HTF (Corrosion)
  - ***High Flux*** & ***Low Temp***,
    Low Flux & ***High Temp***.

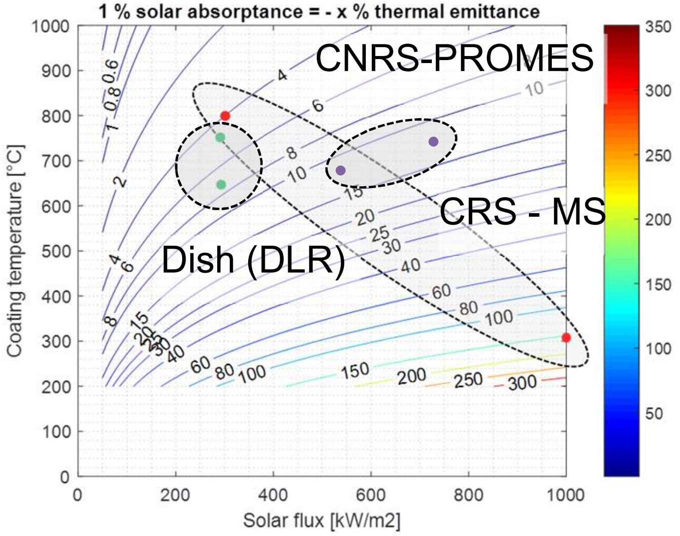

Materials and Methods

Durability Test Program

Solar cycling: ✓
CIEMAT-DLR
CNRS-PROMES

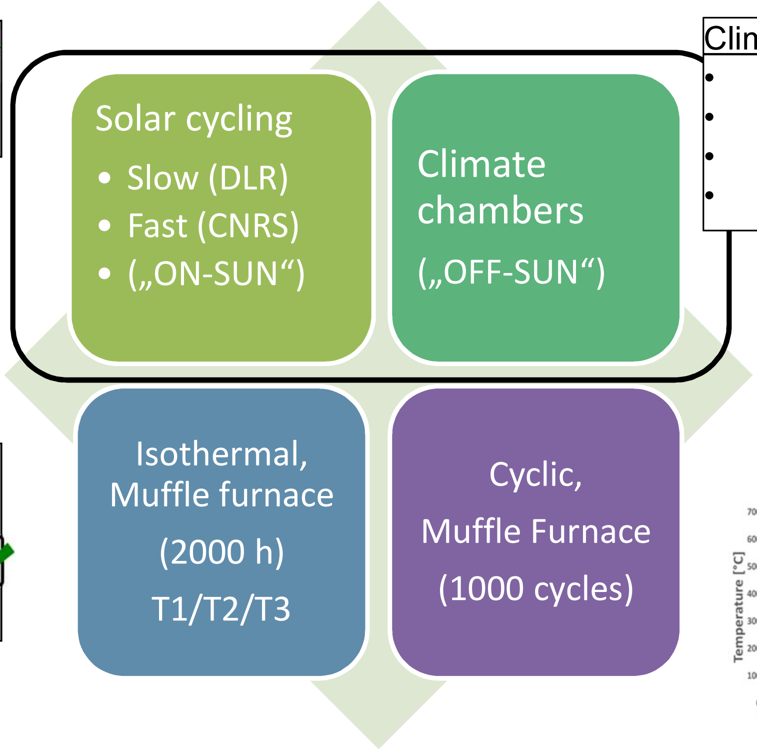

Solar cycling

- Slow (DLR)
- Fast (CNRS)
- („ON-SUN")

Climate chambers

(„OFF-SUN")

Isothermal, Muffle furnace

(2000 h)

T1/T2/T3

Cyclic,

Muffle Furnace

(1000 cycles)

Climate chambers (CIEMAT-DLR)

- Damp Heat (DH)
- Humidity Freeze (HF)
- ***Neutral Salt Spray (NSS)***
- ***Sand Erosion (SE)*** ✓

T91/VM12:
600/620/650 C
Inc617/H230: ✓
680 / 710 / 750 C

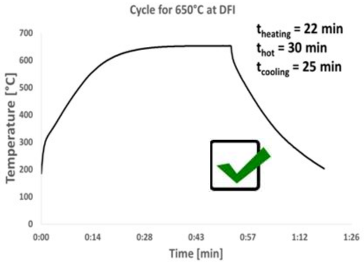

Materials and Methods

Solar Cycling Tests (1)

- CNRS-PROMES (Odeillo, France)
  - SAAF: Solar Accelerated Aging Facility

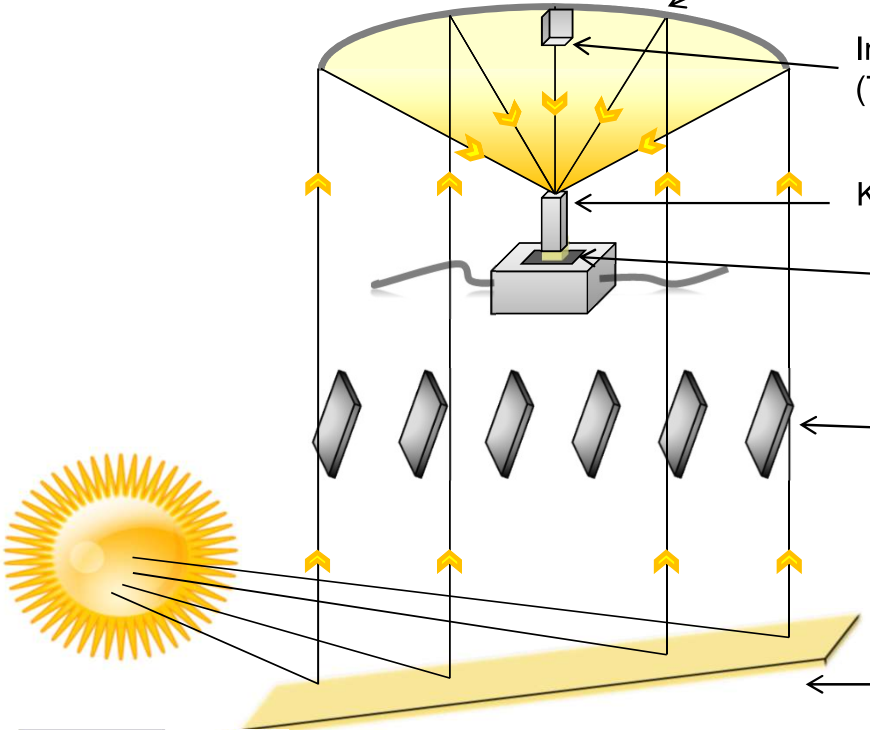

Concentrator
C=15000 (max.)
Diameter=1,5m

Infrared Pyrometer
(Temp. Measurement)

Kaleidoscope to homogenize the flux

Flat sample mounted
on cooled sample holder

Shutter
Fully open in 0,7s

Heliostat

Materials and Methods

Solar Cycling Tests (2)

2 strategies

200 short cycles

40 long cycles

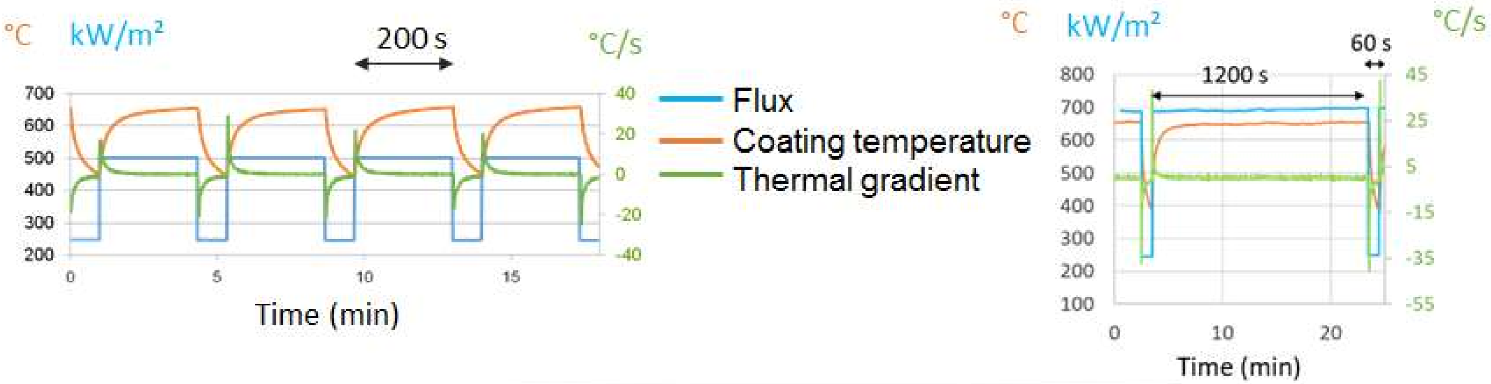

& nominal conditions

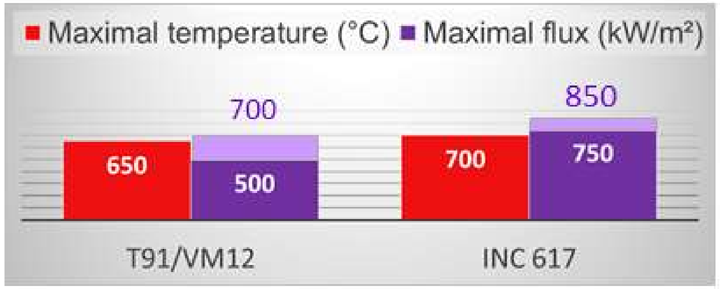

& higher flux

Steam receiver
super generator

Molten salt receivers

Materials and Methods

Solar Cycling Tests (3)

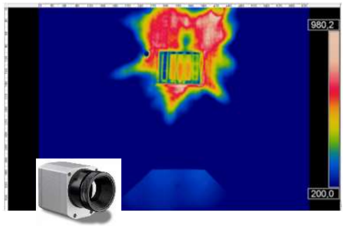

- **The Distal II facility is located at Plataforma Solar de Almeria, owned by the Spanish research center CIEMAT.**

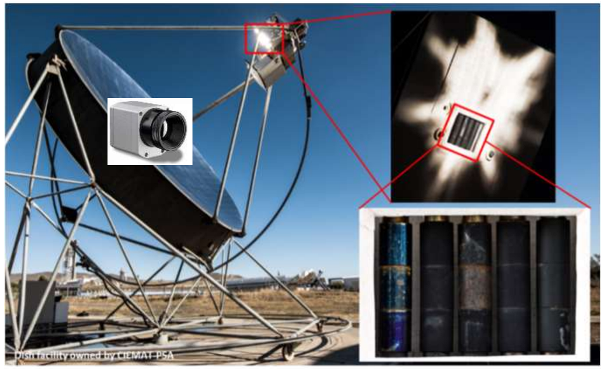
Dish facility owned by CIEMAT-PSA

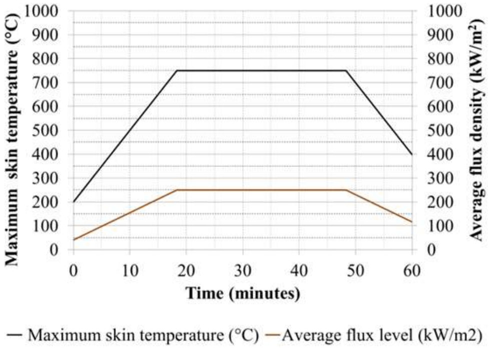

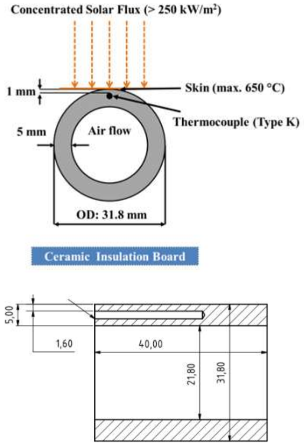

Initial

1000 h, 650/750 C, muffle furnace

50 dish cycles (650/750 C)

100 hours cond.

50 dish cycles (650/750 C)

Materials and Methods

Climate Chamber Tests

- Standard climate chamber tests performed on flat absorber samples

Test	DH	HF	NSS	SE
Standard	IEC 62108, Test 10.7b	IEC 62108, Test 10.8	ISO 92237	Based on MIL-STD 810 G
Duration	1000 hours	1500 hours	120, 480 hours	-
Parameters	T_{amb}: 65 °C RH: 85 %	T_{amb}: -40 to 65 °C RH: max. 85%	T_{amb}: 35 °C pH 6.5 to 7.2 at 25 °C	20 m/s; 3x 70 g std blowing dust

Site characterization:
a. Corrosivity class
b. Erosivity class

DH, HF

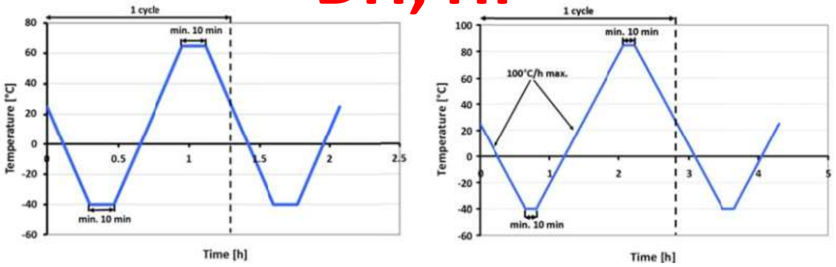

NSS

SE

Results and discussion
Pristine State (before test)

Coating	Substrate	Thickness (DFT, µm)	Selective ?	Surface preparation	Coating application	Thermal treatment
A	T91 | VM12 Inc617 | H230	55 (Primer) 35	No	Grit blasting	Spraying	Curing
B	T91 | VM12	85 | 55	No	Grit blasting	Spraying	Curing (x2)
C	T91 | Inc617	0.6	Yes	Polishing, mirror finish	Sputtering	-
D	T91 | VM12 | Inc617	35	No	Glass bead blasting	Cementation	Pre-oxidation
E	T91 | Inc617	~ 65	No	Polishing of primer coating (B)	Spraying + Sputtering	-
F	VM12	~ 70	Yes	Glass bead blasting	Cementation + Spraying	Pre-oxidation + Curing

Coating\Substrate	Optical characterization Measurand	Units	T91	VM12	Inc617	H230
			Tmax = 650 °C		*Tmax = 750 °C*	
Coating A (BSII)	α_{sol} (AM1.5, direct)	[%]	96,4%	96,2%	97,2%	97,1%
	ε_{th} (Tmax)	[%]	78,4%	76,4%	89,5%	89,5%
Coating B (INTA+BSII)	α_{sol} (AM1.5, direct)	[%]	96,6%	96,2%	*N.A.*	*N.A.*
	ε_{th} (Tmax)	[%]	76,0%	77,2%	*N.A.*	*N.A.*
Coating C (Fraunhofer)	α_{sol} (AM1.5, direct)	[%]	94,9%	*N.A.*	94,7%	*N.A.*
	ε_{th} (Tmax)	[%]	26,8%	*N.A.*	30,6%	*N.A.*
Coating D (Dechema)	α_{sol} (AM1.5, direct)	[%]	94,6%	94,7%	95,3%	*N.A.*
	ε_{th} (Tmax)	[%]	85,9%	84,8%	87,3%	*N.A.*
Coating E (INTA+Fraunhofer)	α_{sol} (AM1.5, direct)	[%]	96,2%	*N.A.*	95,7%	*N.A.*
	ε_{th} (Tmax)	[%]	41,6%	*N.A.*	38,9%	*N.A.*
Coating F (Dechema+BSII)	α_{sol} (AM1.5, direct)	[%]	*N.A.*	96,8%	*N.A.*	*N.A.*
	ε_{th} (Tmax)	[%]	*N.A.*	78,9%	*N.A.*	*N.A.*

Coating A

Coating B

Coating C

Coating D

Coating E

Coating F

Results and discussion

Solar Cycling Tests / Inc617 & H230

Inc617 (**A**,**C**,D,**E**)
H230 (**A**)

CNRS-PROMES

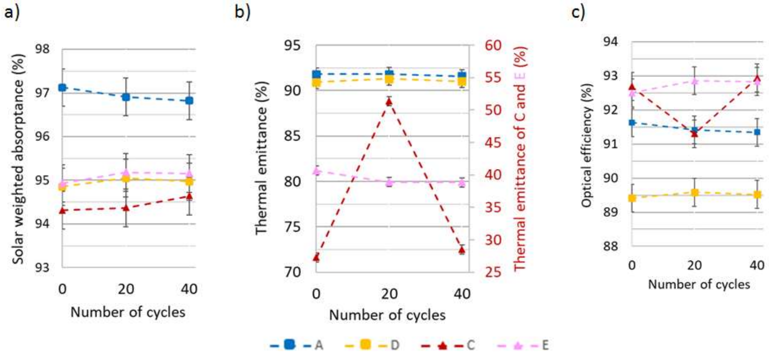

Figure 12: Optical characteristics (%) of Inconel 617 samples with 3 coatings after high flux accelerated aging tests

CIEMAT-DLR

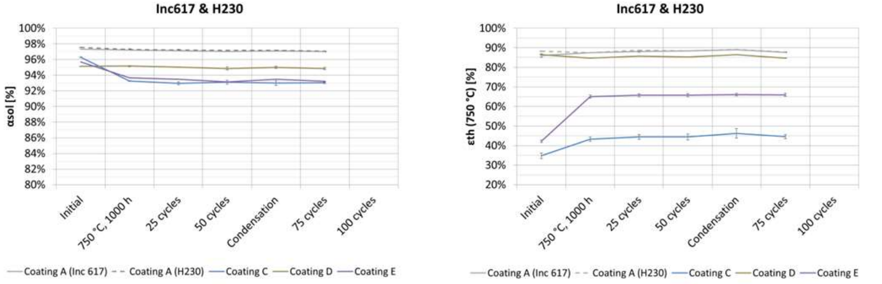

(a) Combined testing, Inc617 and H230 substrates, α_{sol} (b) Combined testing, Inc617 and H230 substrates, ε_{th} (750°C)

Figure 18: Optical characterization of Inc617 and H230 coated samples over the solar cycling test sequence at DLR. (a) Evolution of solar absorptance over the test sequence. (b) Evolution of thermal emittance over the test sequence.

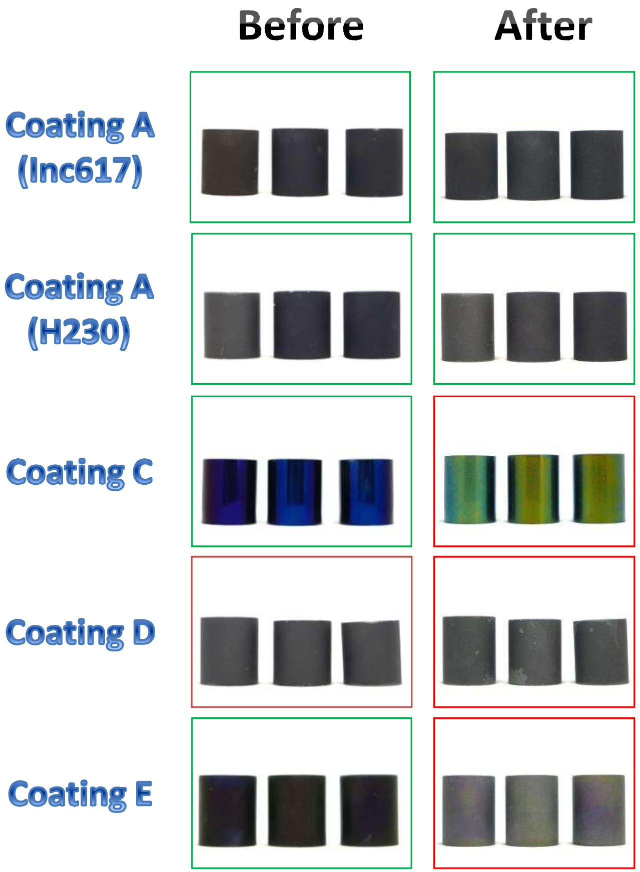

Results and discussion

Climate Chamber Tests / Inc617 & H230

Inc617 (**A**,**C**,D,**E**)
H230 (**A**)

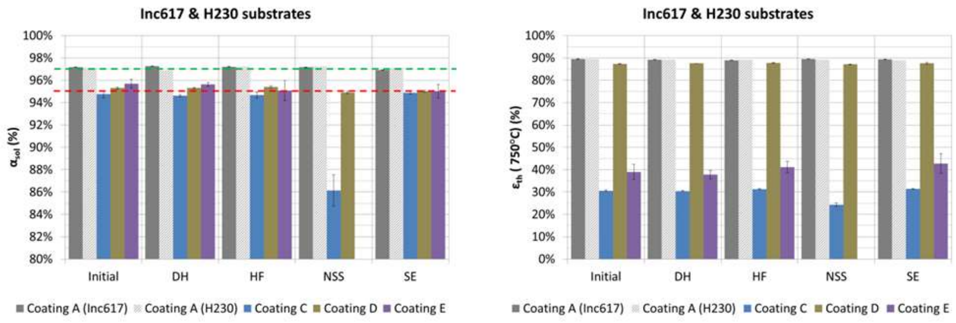

(a) Combined testing, Inc617 and H230 substrates, α_{sol} (b) Combined testing, Inc617 and H230 substrates, ε_{th} (750°C)

Figure 29: Optical characterization of Inc617 and H230 flat coated samples before and after climate chamber tests. (a) Evolution of solar absorptance over the test sequence. (b) Evolution of thermal emittance over the test sequence.

Coating A (Inc617)

Coating A (H230)

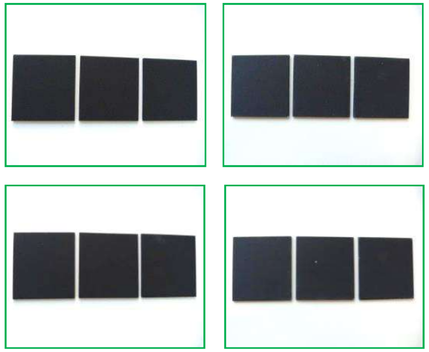

	Coating A (Inc617)	**Coating A (H230)**	**Coating C**	**Coating D**	**Coating E**
Before					
NSS (480 h)					**120 h**

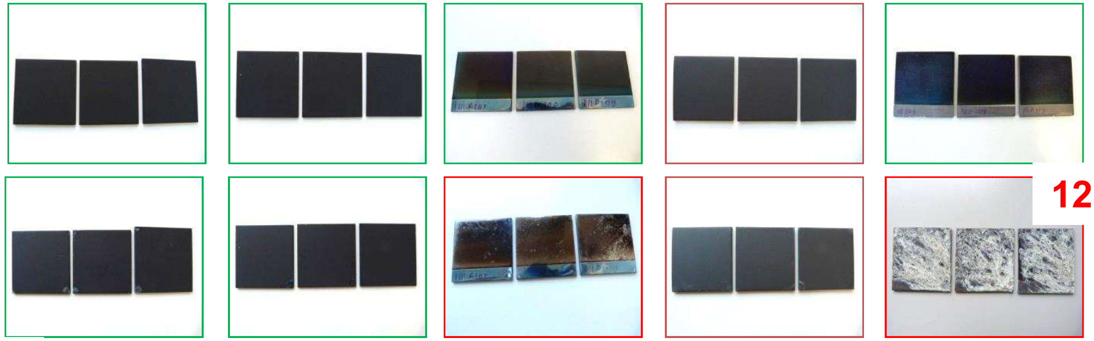

Results and discussion

Summary for Gen2 Coatings (1)

- Inc617 / H230

Variation in solar absorptance $\Delta\alpha_{sol}$			Initial value	Solar cycling		Isothermal, 2000 hours			500 cycles	Climate chambers			
Generation	Substrate	Coating	α_{sol}	SC-DLR	SC-CNRS	T1	T2	T3	Cyclic	DH	HF	NSS	SE
Gen 2	Inc617	A (BSII, Inc617)	97,2%	-0,4%	-0,3%	-0,3%	-0,4%	-1,1%	On going	0,1%	0,0%	0,0%	-0,3%
Gen 2	H230	A (BSII, H230)	97,1%	-0,4%	On going	N.A.	N.A.	On going	On going	0,1%	0,1%	0,0%	-0,2%
Gen 2	Inc617	C (Fraunhofer)	94,7%	-4,2%	0,3%	-2,2%	-5,7%	-9,9%	On going	-0,1%	-0,1%	-8,6%	0,1%
Gen 2	Inc617	D (Dechema)	95,3%	-0,2%	0,1%	-0,1%	-0,3%	-0,9%	On going	0,0%	0,1%	-0,4%	-0,3%
Gen 2	Inc617	E (INTA+Fraunhofer)	95,7%	-2,3%	0,2%	-0,3%	-2,7%	-1,4%	On going	-0,1%	-0,6%	FAIL	-0,7%

Variation in thermal emittance $\Delta\varepsilon_{th}$			Initial value	Solar cycling		Isothermal, 2000 hours			500 cycles	Climate chambers			
Generation	Substrate	Coating	ε_{th} (750 °C)	SC-DLR	SC-CNRS	T1	T2	T3	Cyclic	DH	HF	NSS	SE
Gen 2	Inc617	A (BSII, Inc617)	89,5%	1,0%	-0,2%	0%	0%	0%	N.A.	-0,3%	-0,5%	0,0%	-0,1%
Gen 2	H230	A (BSII, H230)	89,5%	0,4%	On going	N.A.	N.A.	On going	On going	-0,2%	-0,2%	-0,5%	-0,3%
Gen 2	Inc617	C (Fraunhofer)	30,6%	9,5%	1,3%	11%	10%	12%	N.A.	-0,1%	0,7%	-6,2%	0,8%
Gen 2	Inc617	D (Dechema)	87,3%	-1,3%	0,1%	0%	0%	-1%	N.A.	0,3%	0,5%	-0,2%	0,3%
Gen 2	Inc617	E (INTA+Fraunhofer)	38,9%	25,7%	-1,8%	23%	22%	26%	N.A.	-1,2%	2,2%	FAIL	3,8%

Ranking:

Inc617 (A,C,D,E)

H230 (A)

Inc617/Gen 2 - Solar absorptance

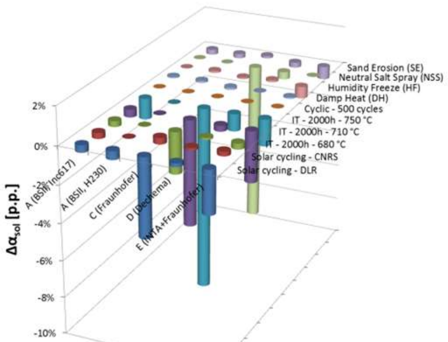

Inc617/Gen 2 - Thermal emittance

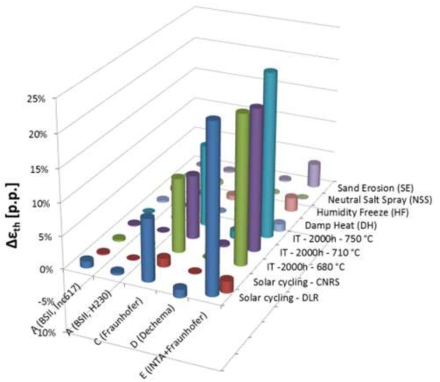

Results and discussion

Summary for Gen2 Coatings (2)

- T91

Variation in solar absorptance $\Delta\alpha_{sol}$			Initial value	Solar cycling		Isothermal, 2000 hours			500 cycles	Climate chambers			
Generation	Substrate	Coating	α_{sol}	SC-DLR	SC-CNRS	T1	T2	T3	Cyclic	DH	HF	NSS	SE
Gen 2	T91	A (BSII)	96,4%	-0,3%	-0,2%	0,1%	0,0%	0,0%	-0,4%	0,0%	-0,1%	-1,4%	-0,8%
Gen 2	T91	B (INTA+BSII)	96,6%	-0,1%	0,0%	0,1%	-0,1%	-0,1%	-0,7%	0,0%	0,1%	-0,2%	-1,3%
Gen 2	T91	C (Fraunhofer)	94,9%	-6,8%	-0,3%	0,0%	-0,9%	-1,0%	On going	-0,4%	-0,2%	FAIL	-0,4%
Gen 2	T91	D (Dechema)	94,6%	-0,4%	0,1%	-0,4%	-0,4%	-0,5%	-0,5%	0,1%	0,2%	-0,5%	-0,3%
Gen 2	T91	E (INTA+Fraunhofer)	96,2%	-3,6%	0,5%	-0,2%	-0,6%	-0,7%	On going	0,1%	0,1%	FAIL	-1,4%

Variation in thermal emittance $\Delta\varepsilon_{th}$			Initial value	Solar cycling		Isothermal, 2000 hours			500 cycles	Climate chambers			
Generation	Substrate	Coating	ε_{th} (650 °C)	SC-DLR	SC-CNRS	T1	T2	T3	Cyclic	DH	HF	NSS	SE
Gen 2	T91	A (BSII)	78,4%	-0,2%	0,1%	**N.A.**	**N.A.**	**N.A.**	**N.A.**	-0,6%	-1,4%	-0,1%	0,0%
Gen 2	T91	B (INTA+BSII)	76,0%	0,1%	-0,5%	**N.A.**	**N.A.**	**N.A.**	**N.A.**	-0,3%	0,0%	-0,9%	-0,5%
Gen 2	T91	C (Fraunhofer)	26,8%	5,8%	0,7%	**N.A.**	**N.A.**	**N.A.**	**N.A.**	0,4%	0,1%	FAIL	0,4%
Gen 2	T91	D (Dechema)	85,9%	-2,3%	-0,1%	**N.A.**	**N.A.**	**N.A.**	**N.A.**	-0,3%	0,6%	0,3%	0,4%
Gen 2	T91	E (INTA+Fraunhofer)	41,6%	11,0%	-1,3%	**N.A.**	**N.A.**	**N.A.**	**N.A.**	0,5%	-0,6%	FAIL	-2,6%

T91/Gen 2 - Solar absorptance

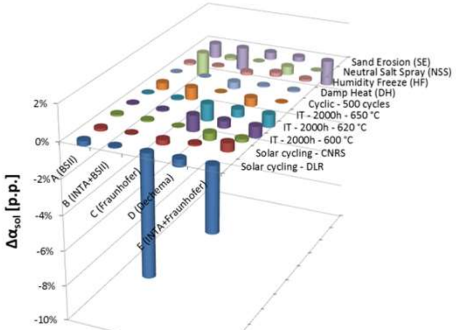

T91/Gen 2 - Thermal emittance

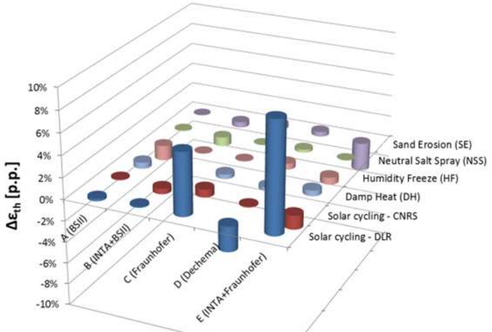

T91 (A,B,C,D,E)

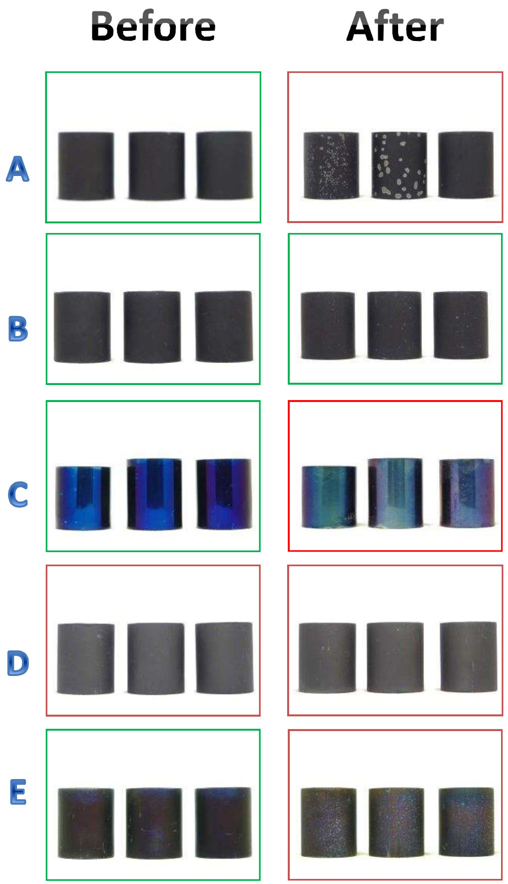

Conclusion and Outlook

- Conclusions:

- Inc617/H230:
  - Best coating: Coating A
  - Brightsource (commercial): $\alpha_{sol} \geq 97$ %
- T91/VM12:
  - Slurry aluminide primer coating protects metal substrate better against corrosion (NSS).
  - Most durable Coating : B *(INTA+Brightsource)*
  - Best α_{sol} value: Coating F (>96.5%) *(Dechema + Brightsource)*

- Coating D stable, but lower efficiency
- Solar selective coatings C/F efficient … but not durable (isothermal, NSS)

- Outlook:
  - **Coating A commercialized**
  - Aging models in development, Service Lifetime Prediction (SLP)
  - Estimation of LCOC (*Levelized Cost of Coating)*

THANK YOU FOR YOUR ATTENTION!
ANY QUESTIONS?

HELIOSTAT CALIBRATION

R. Monterreal
CIEMAT-PSA

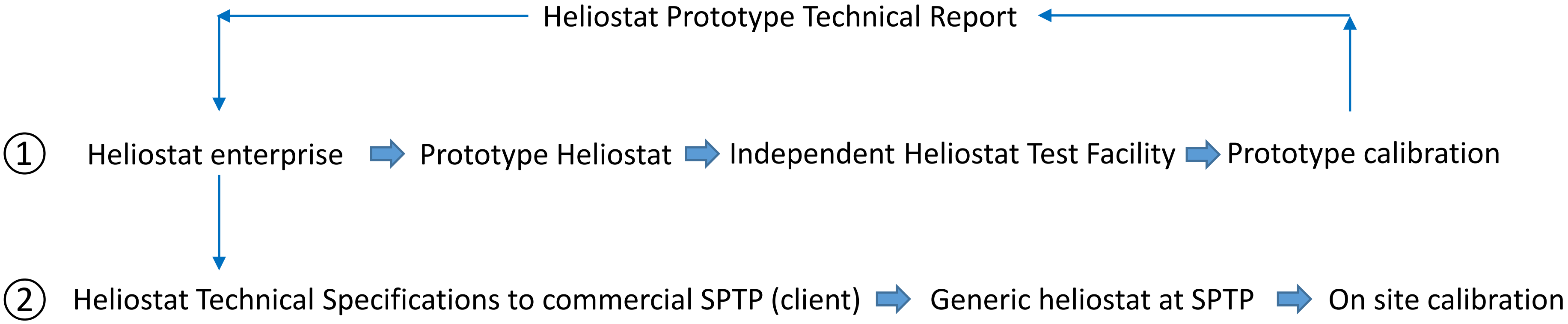

Heliostat Prototype Technical Report

① Heliostat enterprise ➡ Prototype Heliostat ➡ Independent Heliostat Test Facility ➡ Prototype calibration

② Heliostat Technical Specifications to commercial SPTP (client) ➡ Generic heliostat at SPTP ➡ On site calibration

Simplified block diagram of Solar Power Tower Plant (SPTP) heliostat calibration process

But what does *calibration* mean?

Basically, it means *to compare something with a benchmark and provide a quality number for that comparison.*

☞ Let's see how to “calibrate” a heliostat in above point ①

① Prototype calibration (at Test Facility)

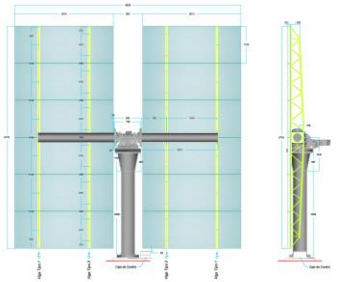

Paradigm heliostat

Prototype heliostat

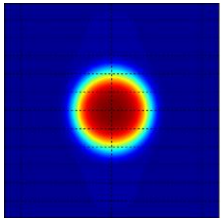

Benchmark: paradigm heliostat reflected sun-image on target (synthetic, software made)

Comparison

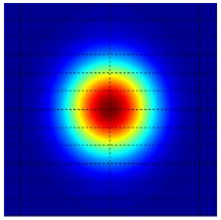

Under testing: prototype heliostat reflected sun-image on target (real, from outdoor test)

Tools, methods

- High quality Test Facility
- Highly qualified staff
- Highly qualified instrumentation
- A strict Test Protocol
- Adequate evaluation method
- Technical report

Calibration at Test Facility

Goal: Get prototype heliostat quality parameters :

- Optical Quality: **Slope-error** (ε)
- Tracking Quality: **Tracking error** (τ)

☞ Let's see how to “calibrate” a heliostat in above point ② :

② On site heliostat calibration (at SPTP)

Heliostat prototype <u>quality parameters</u> {ε, τ}

Generic solar field heliostat at SPTP

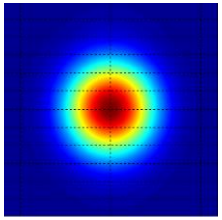

Benchmark: <u>synthetic</u> prototype heliostat reflected sun-image on target with quality (ε, τ)

Comparison

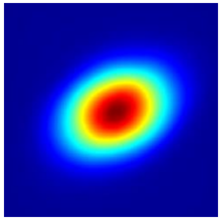

Under testing: <u>generic</u> solar field heliostat reflected sun-image on target (<u>real,</u> from outdoor test)

Tools, methods

- Adequate instrumentation
- Adequate evaluation method

Calibration at SPTP

Goal: Get <u>generic</u> heliostat quality parameters:

- Optical Quality: **Slope-error** (ε′)
- Tracking Quality: **Tracking error** (τ′)

What we should have now…

Calibration results at Test Facility

Prototype heliostat quality parameters

- Optical Quality: **Slope-error** (ε)
- Tracking Quality: **Tracking error** (τ)

Calibration results at SPTP

Generic heliostat quality parameters

- Optical Quality: **Slope-error** (ε')
- Tracking Quality: **Tracking error** (τ')

Has anyone ever checked this two issues on a commercial SPTP site?:

a) Prior to SPTP commissioning → check if: $\varepsilon' = \varepsilon \pm d\varepsilon$, $\tau' = \tau \pm d\tau$

b) As a routine task throughout the useful life of the plant → check if: $\varepsilon' \approx cte$, $\tau' \approx cte$

If not, things like these can fail in any commercial SPTP project:

a) From the beginning: **Initial deviation** from the **nominal** behavior of the plant regarding to :
- Solar plant efficiency, profitability
- Irradiance distribution on the receiver
- Pointing strategies on the receiver
- Receiver operation and safety protocols, etc.

b) With time: **Progressive deviation** from the **nominal** behavior of the plant regarding to:
- Solar plant efficiency, profitability
- Irradiance distribution on the receiver
- Pointing strategies on the receiver
- Plant operation and safety protocols, etc.

- So, the **calibration of heliostats**, both in the **Test Facility** and in the **commercial SPTP**, are necessary and must be carefully performed.

How to understand and quantify the quality of any heliostat throughout the calibration process

✋ **Remember heliostat “functional” features:**

- **Concentrating** capacity of the reflected sun light onto a fix target (solar receiver)
- **Pointing** capacity of the reflected sun light onto a fix target (solar receiver)

✋ **Heliostat qualification (calibration) →** it is necessary to find out a **“quality number”** for both functional features:

☼ **Concentrating capacity →** quality number: **Optical quality** (also called slope-error, beam dispersion error, beam quality). Units: mrad.

☼ **Pointing capacity →** quality number: **Tracking quality** (also called tracking error). Units: mrad.

Fast understanding of heliostat optical quality (I)

Heliostat surface as seen from the CESA-1 Tower

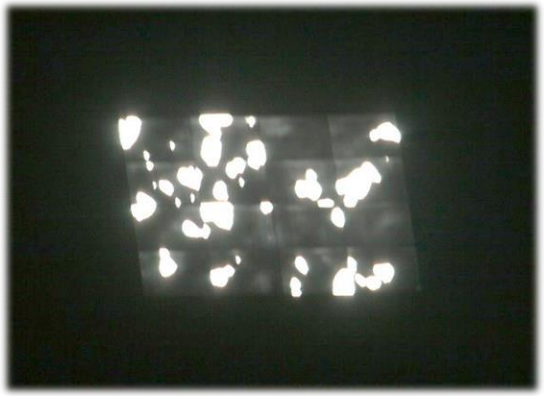

Heliostat surface as seen from the focal point. Reflection errors are evident just by sight.

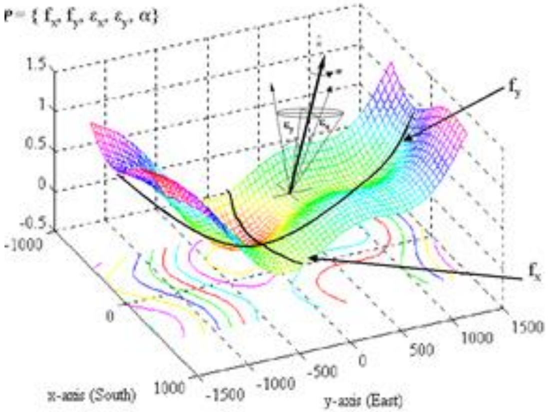

Math model: normal vector of each elemental mirror areas are *deviated* from the theoretical one

Fast understanding of heliostat optical quality (II)

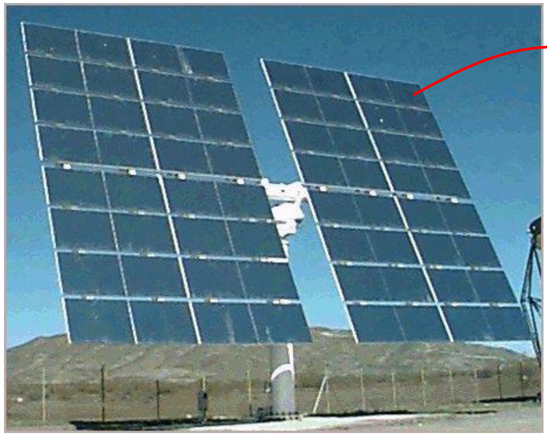

ΔS_k = mirror elemental reflecting surface (k = 1,…, n)

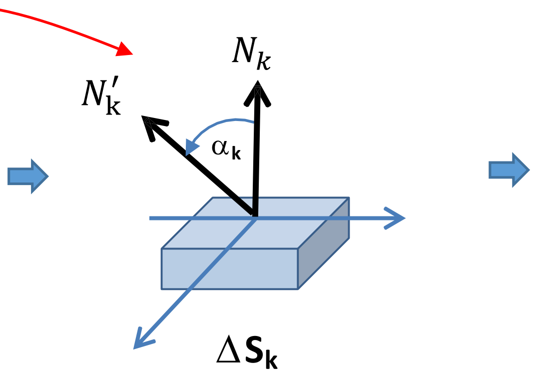

Mirror close-up view at ΔS_k (local deviations of normal vector)

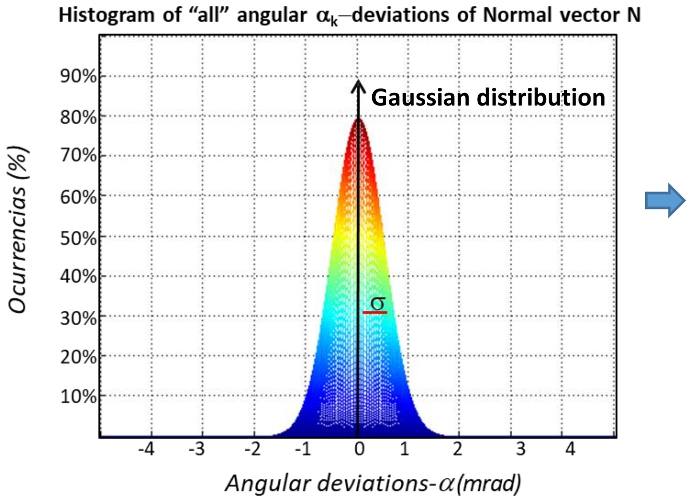

This is our postulate…

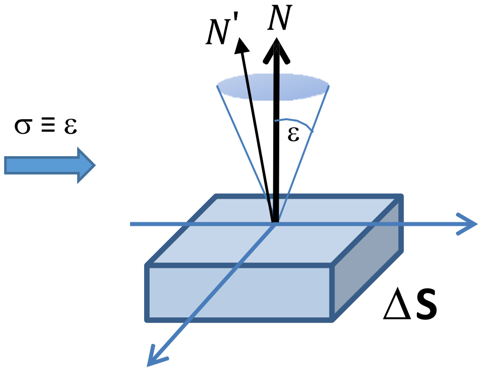

<u>Interpretation</u>: at any place on the heliostat reflecting surface the probability that the normal vector N deviates an angle less than **ε** is 68.27% (1-std). **ε** is called "heliostat slope-error".

Fast understanding of heliostat optical quality (III)

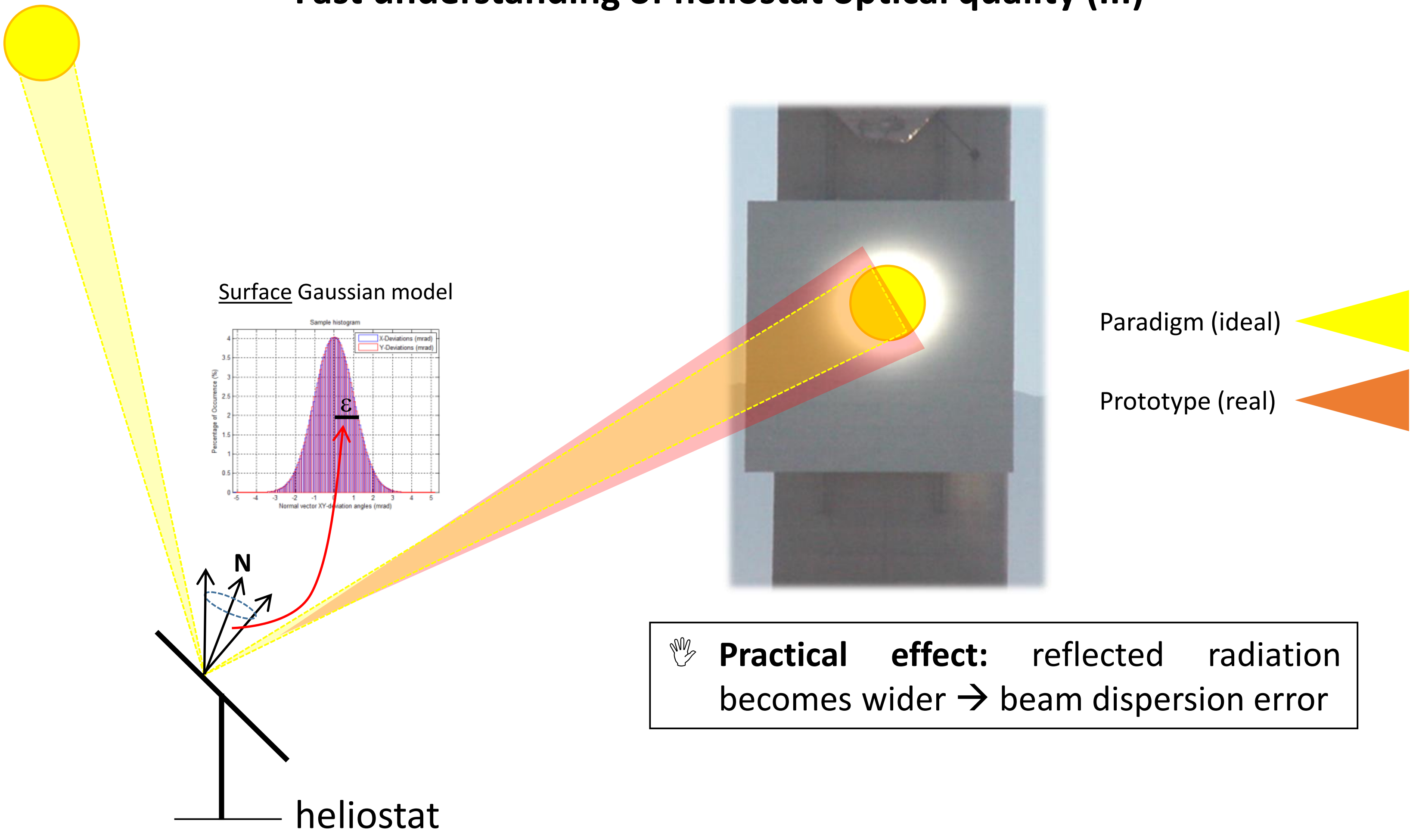

✋ **Practical effect:** reflected radiation becomes wider → beam dispersion error

Fast understanding of heliostat tracking quality (tracking-error)

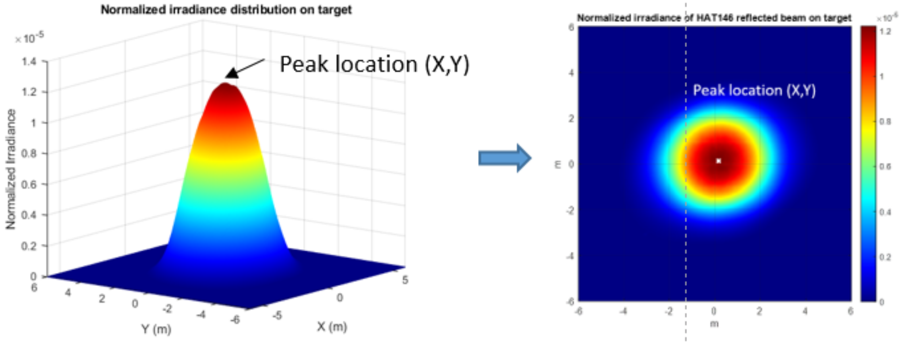

Within this red zone, the probability of finding the heliostat peak is 68.27%.

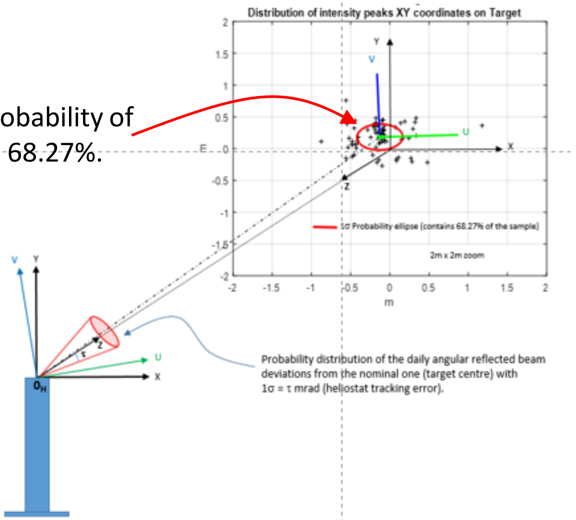

Probability distribution of the daily angular reflected beam deviations from the nominal one (target centre) with 1σ = τ mrad (heliostat tracking error).

Positioning Gaussian model

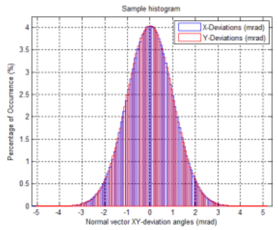

What TRK-error do we need
for our solar tower plant?

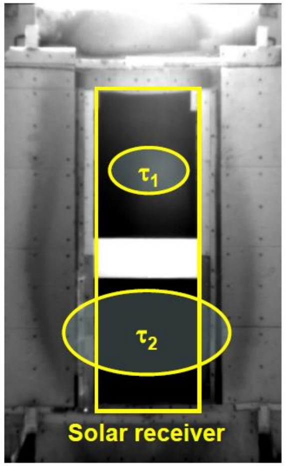

TRK-error τ_1 is OK

TRK-error τ_2 is rejected

Practical effect: In both pointing areas on the receiver, the probability of finding the heliostat image is 68.27%. So tracking-error of τ_2 mrad is not acceptable because the heliostat image (peak) could be out of the receiver during its daily operation (spillage).

Some recommendations concerning heliostat calibration for SPTP

1. Be sure you have a professional Prototype Heliostat Technical Report with the numerical values of optical and tracking quality.

2. Prior to plant commissioning, check on site a statistically significant sample of heliostats quality. I must fit with the Prototype Heliostat Technical Report.

3. During the SPTP useful life, check periodically the optical and tracking quality of a statistically significant sample of heliostats.

4. To achieve points 2 and 3 contract external professional services or provide your facility with the tools to do it yourself. Among other things, the efficiency of your plant depends a lot on it.

Thank you very much

SFERA-III
Solar Facilities for the European Research Area

2nd Training for Industries “Optimization of CST plant output by optical and thermal characterization and target-oriented O&M”
26 – 29 April 2022, Plataforma Solar de Almería, Spain

Recent Developments in Airborne Heliostat Calibration
Julian Krauth, DLR

NETWORKING

THIS PROJECT HAS RECEIVED FUNDING FROM THE EUROPEAN UNION’S HORIZON 2020 RESEARCH AND INNOVATION PROGRAMME UNDER GRANT AGREEMENT NO **823802**

Motivation

- Heliostats **collect the input energy** for the power plant
- The efficiency of the heliostat field depends on many factors
    - Heliostat tracking offsets (heliostat calibration)
    - Shape deviations
    - Soiling
    - Mirror-reflectivity
- Classical calibration method (camera-target method) takes months
- **Airborne calibration is fast and efficient** (but requires a **big effort in development**).

SSPS installation at Plataforma Solar de Almeria (Owned by the Spanish research centre CIEMAT)

Background Information

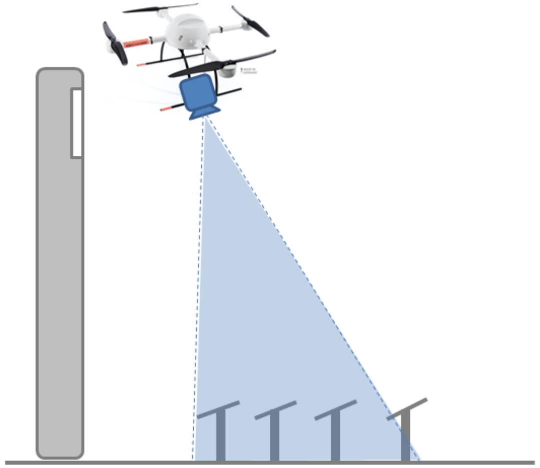

- **Calibration** means here:
  1. Measurement of an heliostat orientation for at least one “position”
  2. Comparison of *measured* data to the *set* values
  3. Calculation of calibration parameters or direct orientation correction of the heliostat.
- Different types of **heliostat tracking**:
  - Closed-loop: calibration parameters only used for coarse alignment
  - Open-loop: calibration needs to be precise, typically measured once after setup.

  We consider the latter, common for smaller to medium size heliostats.
- Characteristics of **Heliostat fields**:
  - Up to 100 000 Heliostats with distances to central receiver of up to 1.7 km.
  - Accurate alignment of all heliostats below 1mrad without calibration system is very difficult to achieve.
  - Traditional calibration of such an heliostat field can take many valuable months

Overview Calibration Techniques

Camera(s) on ground

Camera(s) on tower or UAV

Central laser or radar-based measurement

Solar focus position detection with cameras or sensors on tower

Cameras or sensors on each heliostat

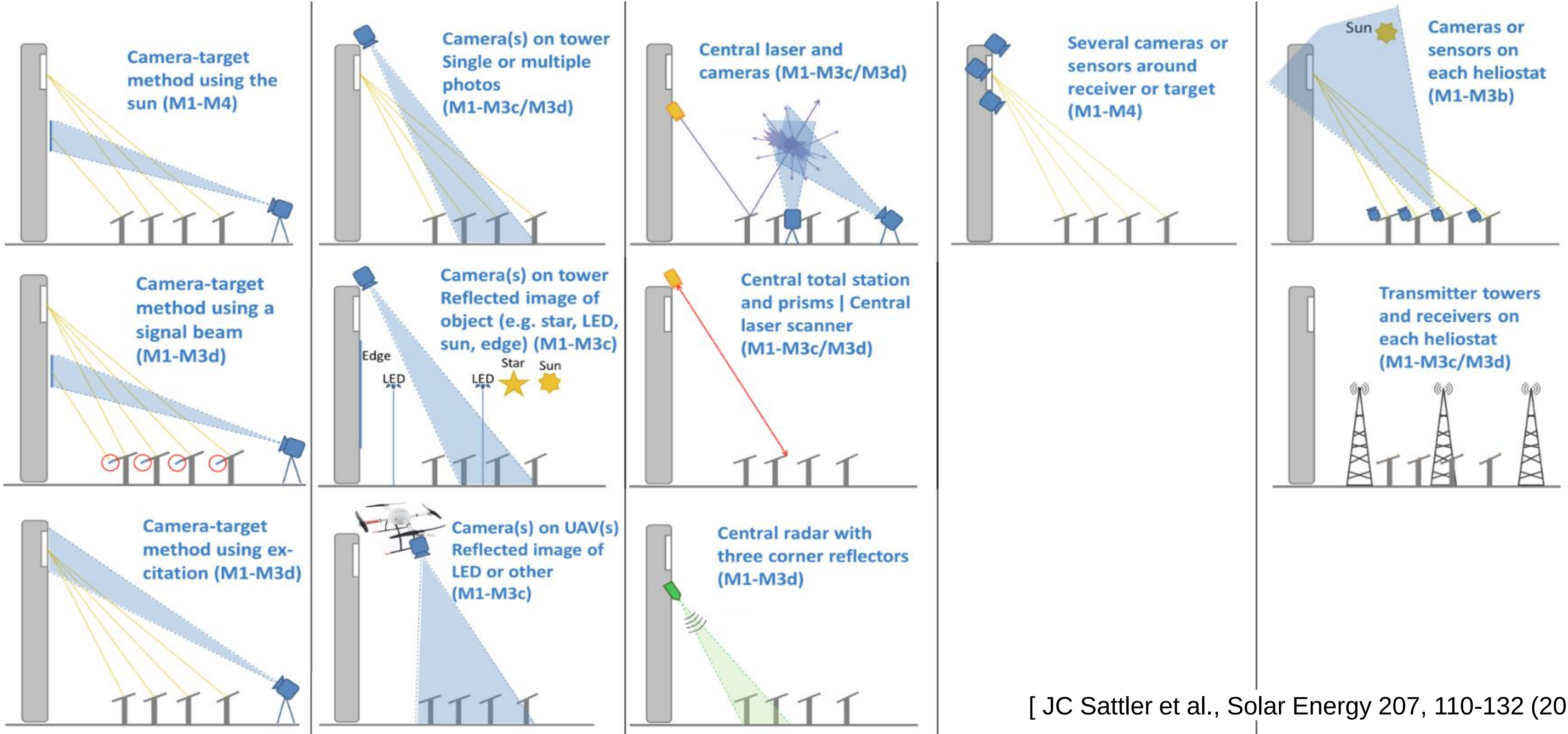

[JC Sattler et al., Solar Energy 207, 110-132 (2020)]

Airborne heliostat calibration

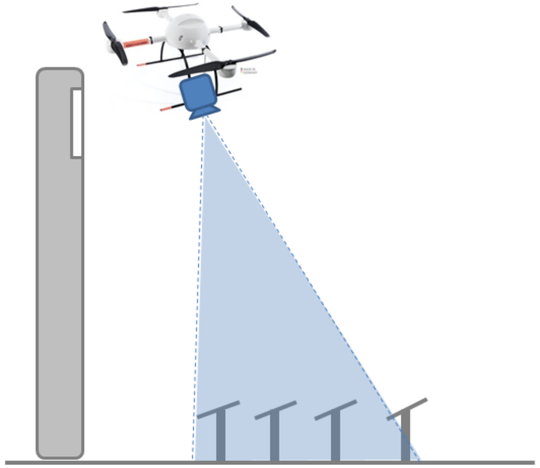

Pros and cons

+ Arbitrary positioning of measurement device (LED, camera, …)
+ Independent of infrastructure (tower, target)
+ Fast (allows shorter ramp-up phase of new solar tower plants)
+ Also works on cloudy days
+ Different methods can be used (photogrammetry, reflex-based, …)

- Drone operator needed (for now, but projects for autonomous flights are planned)
- No closed-loop ability (also here, real-time data evaluation is planned for the future)

Airborne heliostat calibration

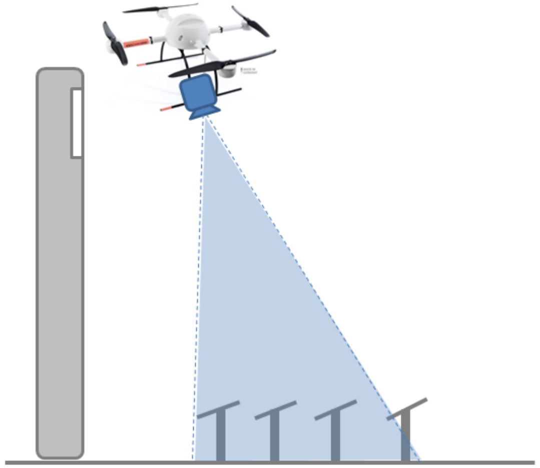

We develop such methods in the projects **HelioPoint** and **HelioPoint-II** with support

Economic Affairs and Climate Action

Federal Ministry
for Economic Affairs
and Climate Action

2 main methods are available/ in development at DLR (together with CSP Services)

1. **Photogrammetry** (obtain information about: position, orientation, canting)
2. **Reflex-based calibration** measurements (obtain information about: precise orientation, canting)

DLR is not the only one: NREL/SANDIA also develop airborne heliostat calibration.

Photogrammetric (coarse) calibration

[cinecommunities.org]

Procedure:

- Flight for image acquisition from different perspectives on the heliostat field
- Edge recognition and corner recognition
- All evaluated corners of mirror panels of heliostats are used for a bundle adjustment
- Obtain 3d coordinates of heliostat corners and derive heliostat orientation

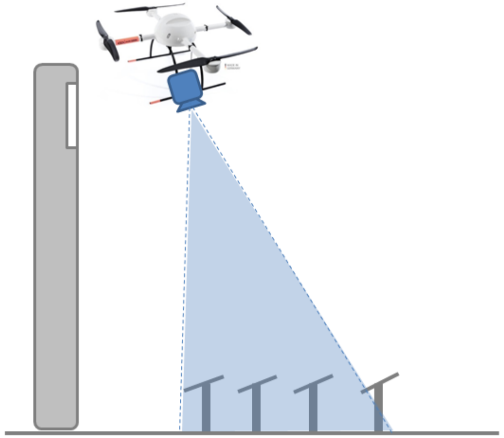

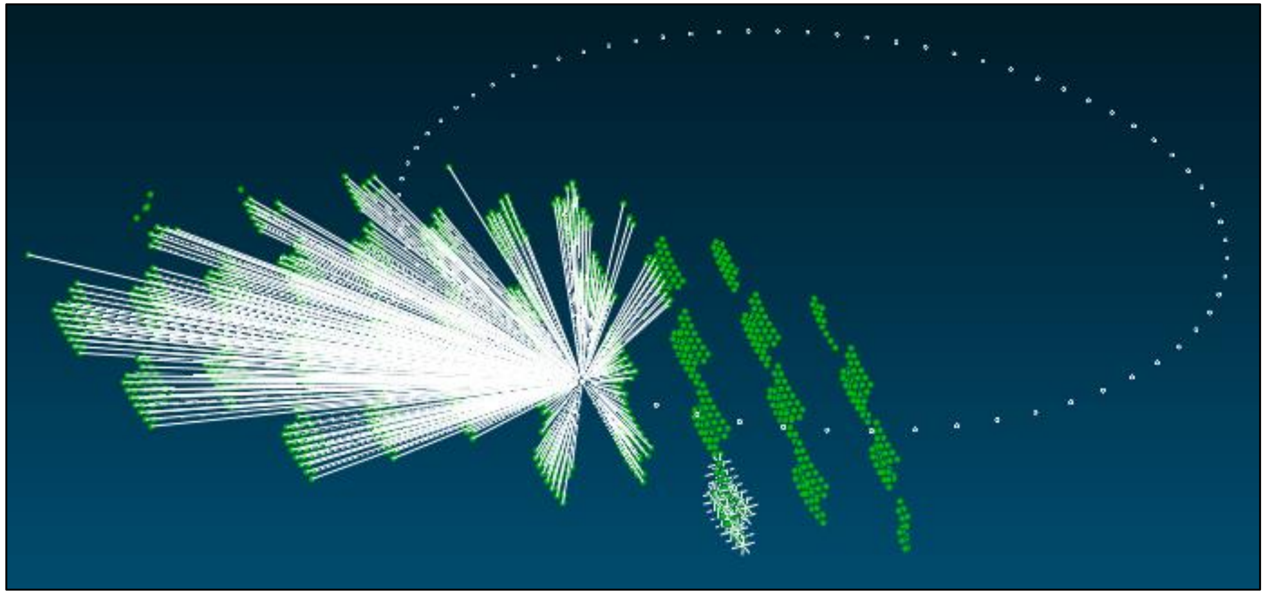

Photogrammetric (coarse) calibration

Corner detection

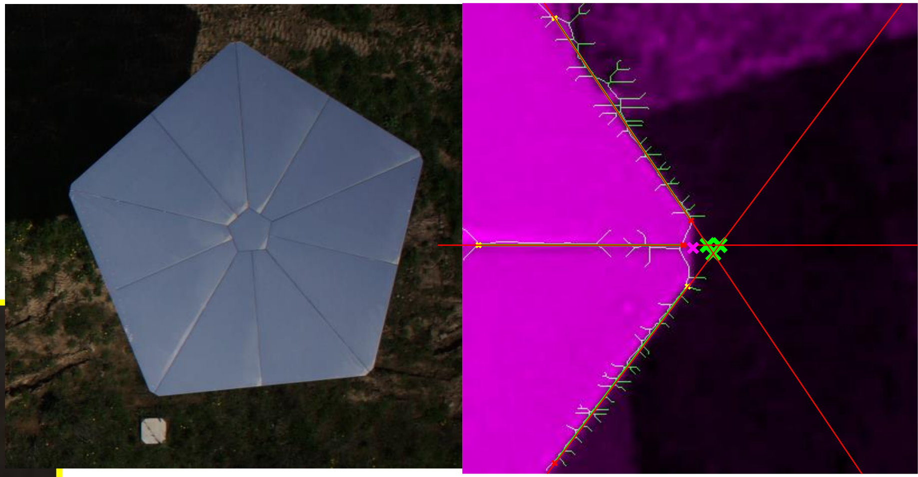

Detected corner on Stellio type

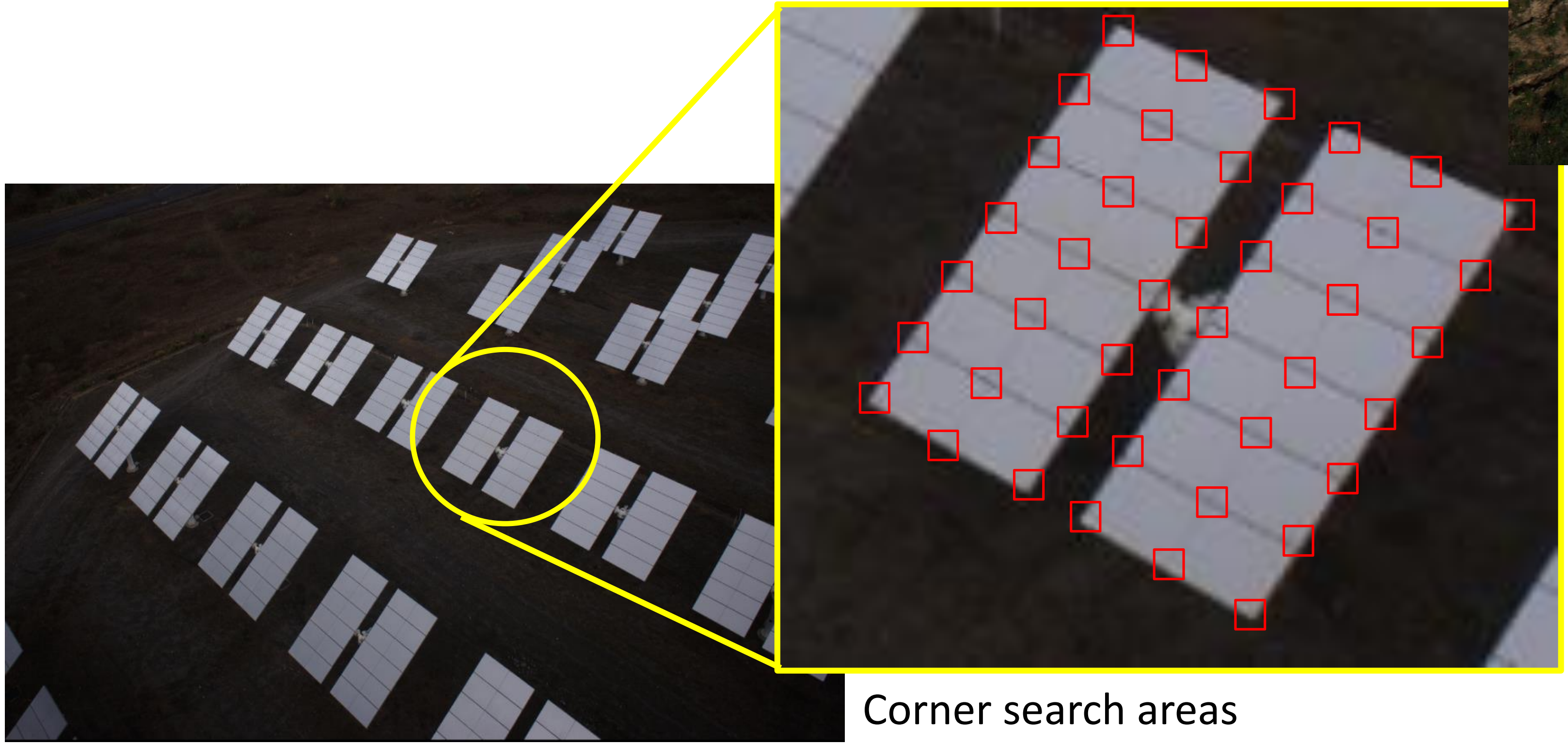

Corner search areas

Images show Plataforma Solar de Almeria (owned by the Spanish research centre CIEMAT.) and Research Center Jülich (owned by DLR). (Source: DLR)

Photogrammetric (coarse) calibration

Image registration (for correct corner identification)

Intensity - based

Feature - based

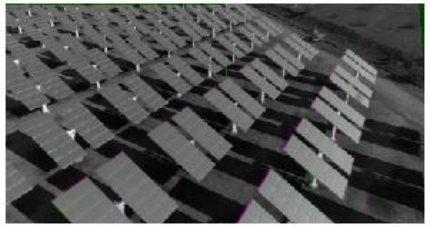

Image overlay

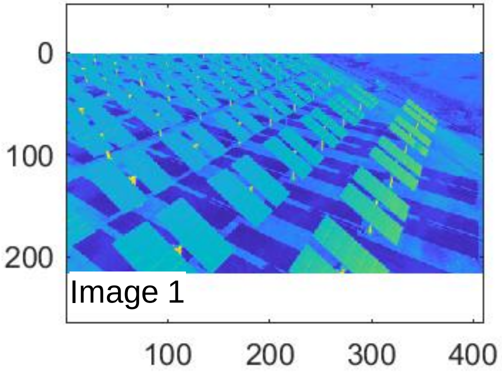

Image 1

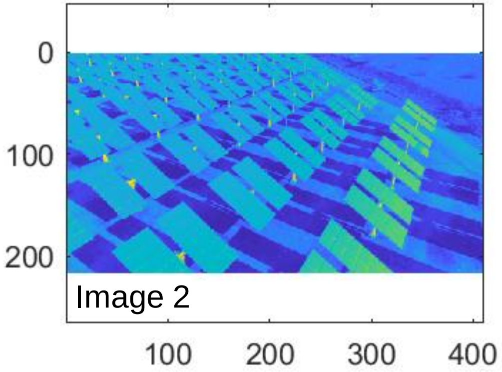

Image 2

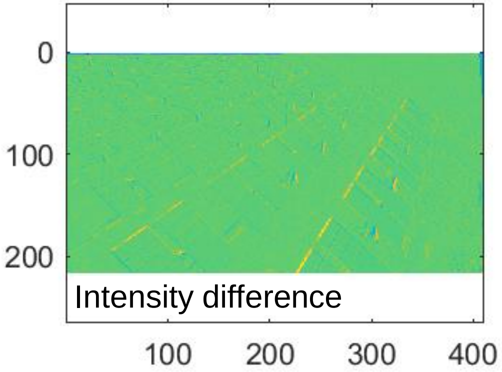

Intensity difference

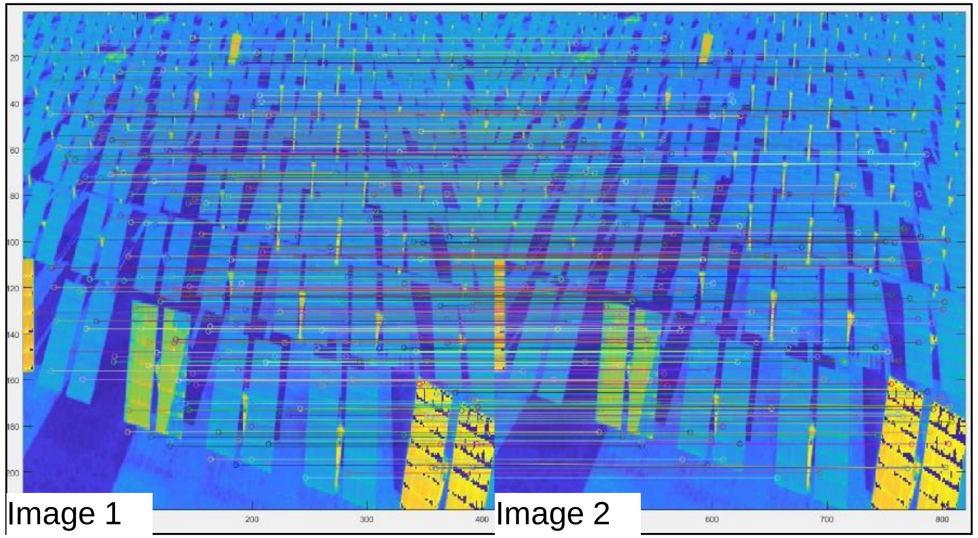

Image 1

Image 2

Photogrammetric (coarse) calibration

Bundle adjustment (Aicon) yields global coordinates

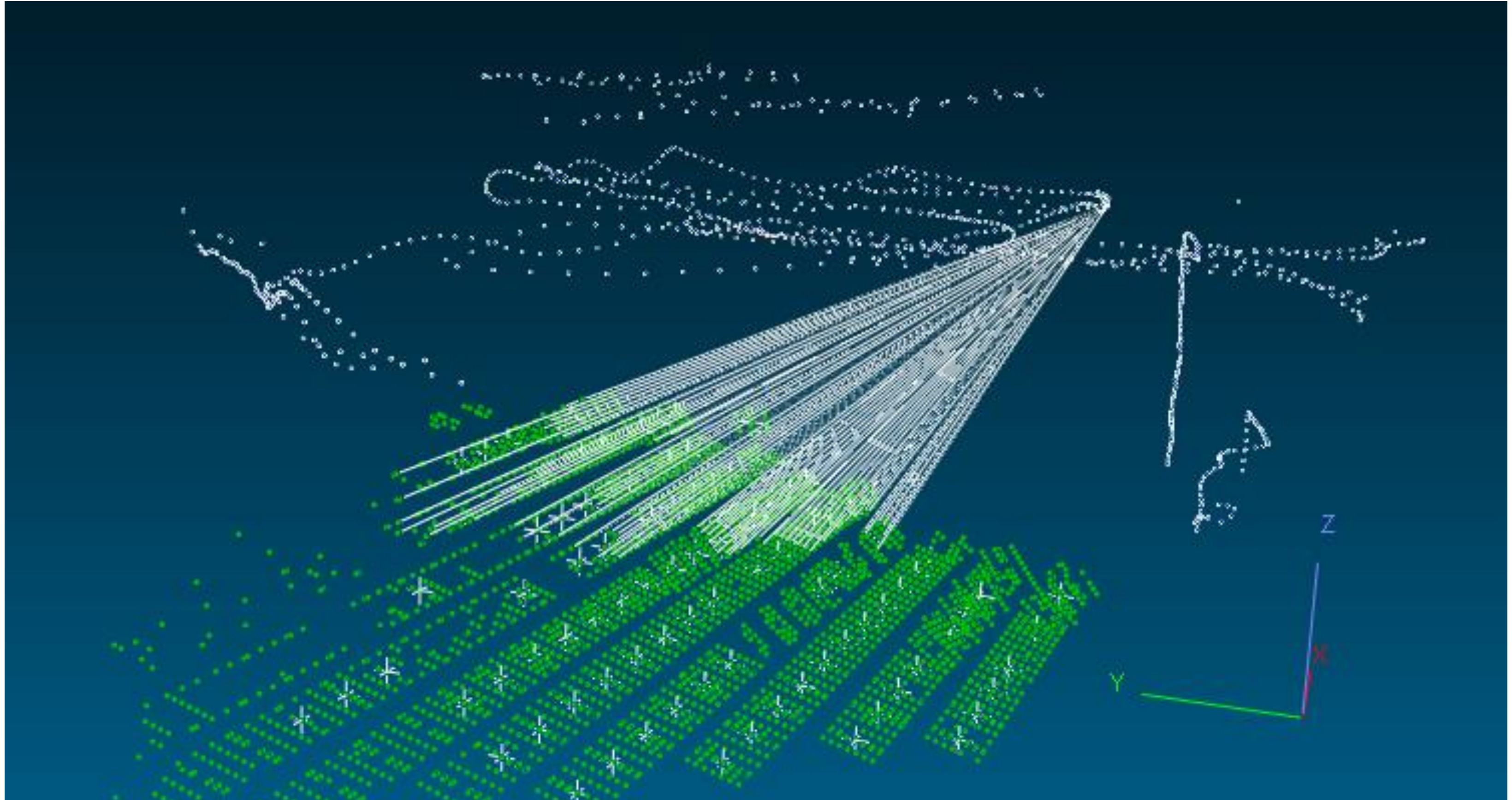

Important parameters:

-Orientation measurement accuracy: ~5 mrad.

-Measurement speed: days (instead of months)

Reflex-based (fine) calibration

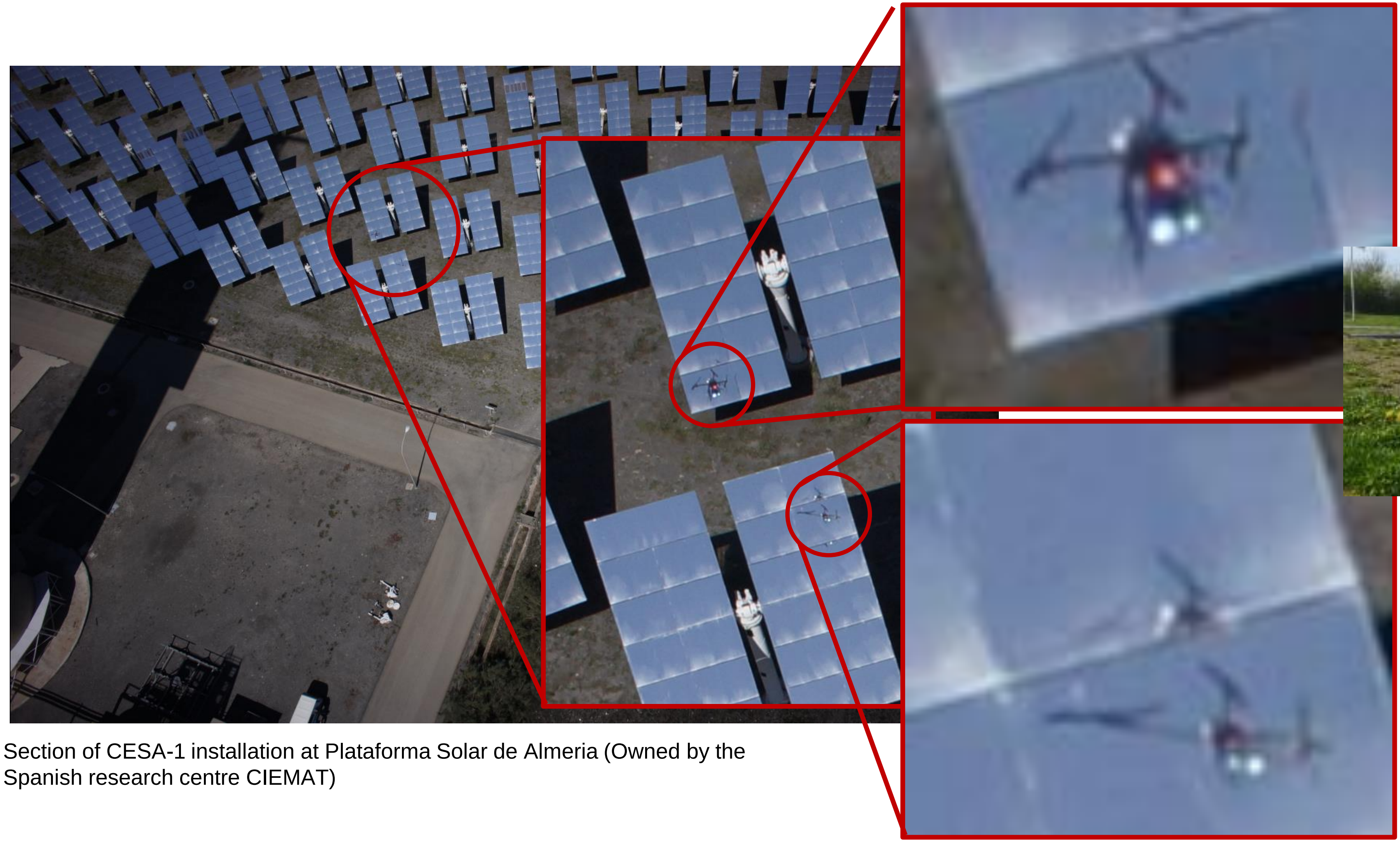

Section of CESA-1 installation at Plataforma Solar de Almeria (Owned by the Spanish research centre CIEMAT)

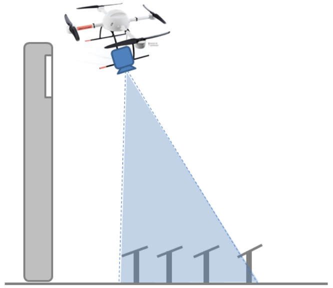

Reflex-based (fine) calibration

Measurement principle

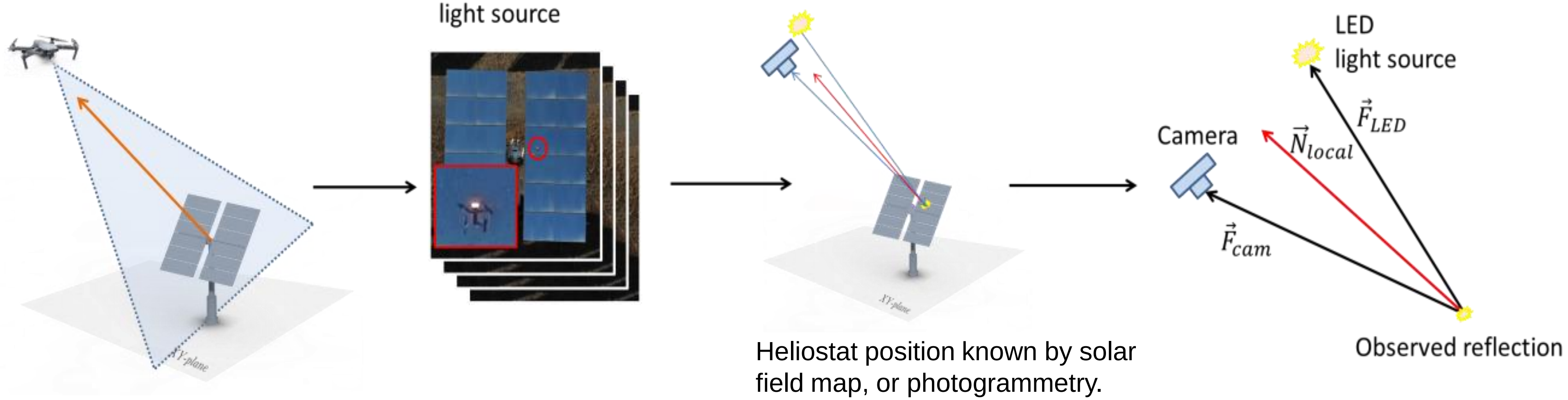

Precise UAV positioning near
the mirror‘s estimated normal vector

Images with reflection
of the mounted LED
light source

UAV position known via
photogrammetry, RTK, …

Heliostat position known by solar
field map, or photogrammetry.

Orientation precisions of <1 mrad can be achieved.
Expected measurement speed: 10 000 heliostats in a few hours

Reflex-based (fine) calibration

Scaling-up

Idea:

1. Set heliostat orientation such that normal vectors cross in one point.
2. UAV flies a scanning route through that zone
3. On each image the visible reflections on the heliostats will show if they are oriented towards the UAV
4. Drone and heliostat position is known by photogrammetry or a combination of RTK and heliostat coordinates provided by operator
5. By repeating the measurement with different heliostat orientations more calibration points can be obtained

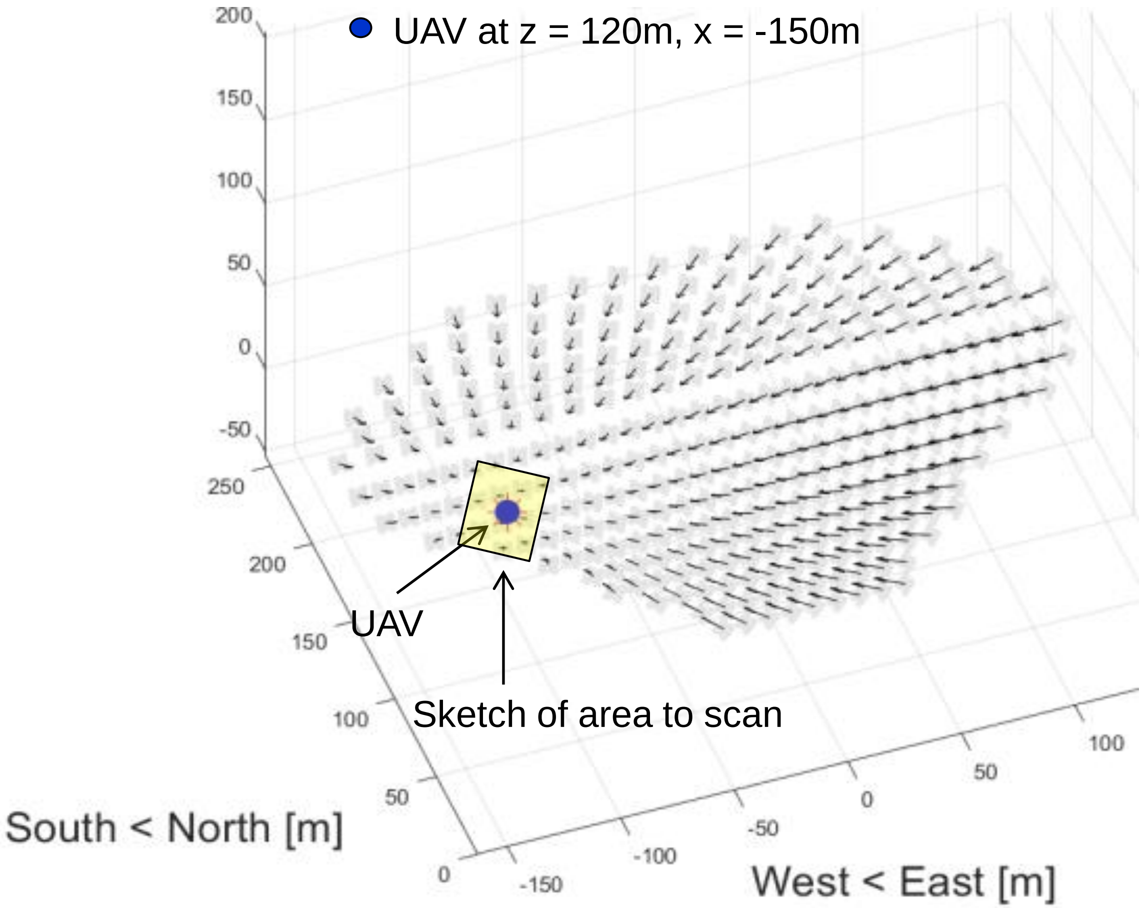

● UAV at z = 120m, x = -150m

UAV

Sketch of area to scan

Reflex-based (fine) calibration

Scaling-up

Blue: theoretical point where normals cross

🟨 : area to scan with a UAV

Idea:

1. Set heliostat orientation such that normal vectors cross in one point.
2. UAV flies a scanning route through that zone
3. On each image the visible reflections on the heliostats will show if they are oriented towards the UAV
4. Drone and heliostat position is known by photogrammetry or a combination of RTK and heliostat coordinates provided by operator
5. By repeating the measurement with different heliostat orientations more calibration points can be obtained

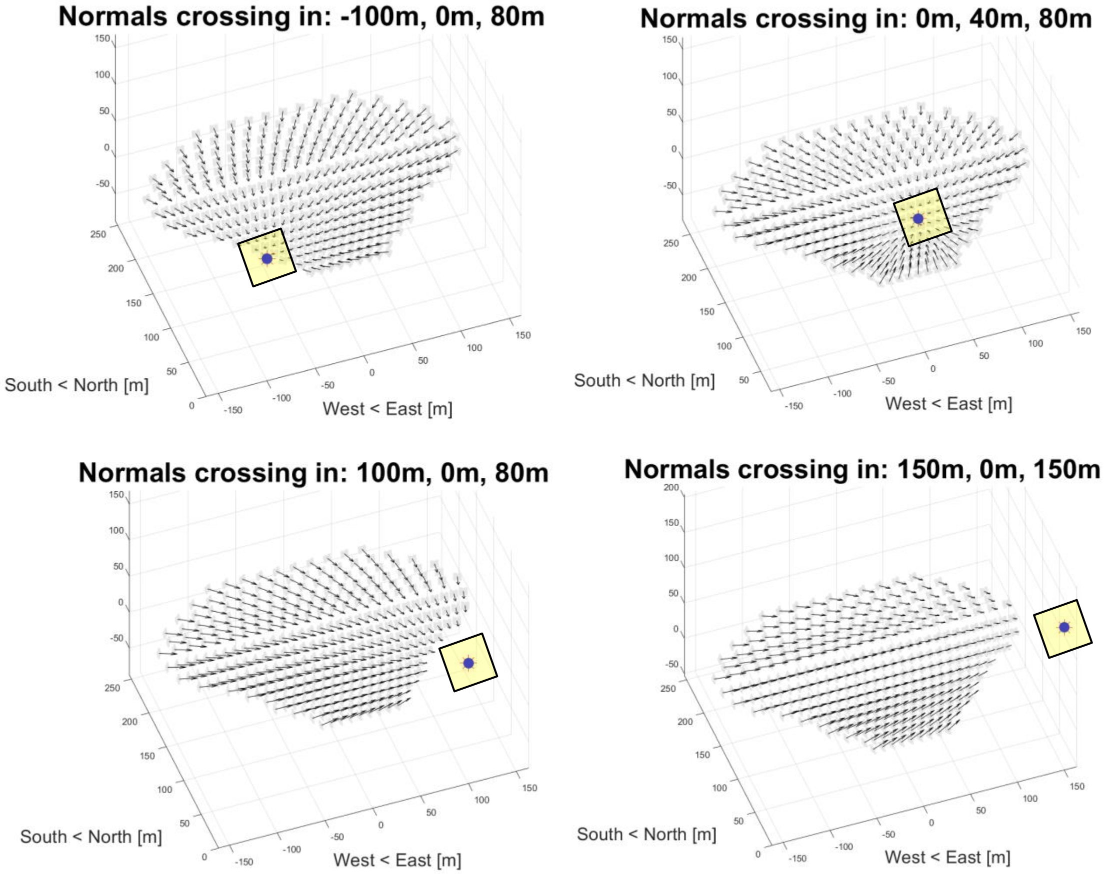

Challenges

- Need high-density of images -> slow flight speed due to limited images/sec
- Limitations of UAV positions:
  - Altitude limited by law
  - Distance to heliostat limited by resolution of images
- Low altitude leads to heliostats covering each other on the image
- Different heliostats need different calibration points because they have different orientations throughout the whole year.

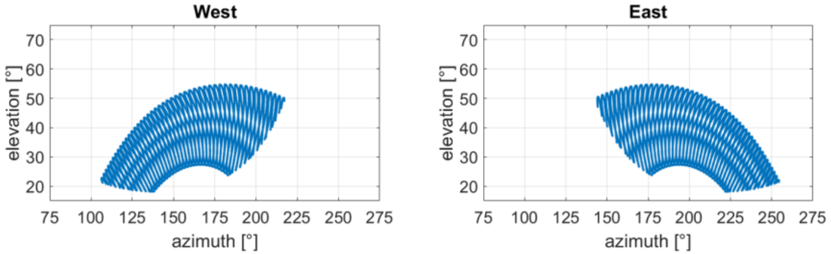

CESA-1 installation at Plataforma Solar de Almeria (Owned by the Spanish research centre CIEMAT)

- Flight routes have potential for optimization but many parameters are involved (different requirements for different methods, sun position, possible grouping of heliostats can differ, flight regulations, …)

Flight route design

Photogrammetry example at CESA I (CIEMAT-PSA)

Blue: camera positions
Red: reference heliostats

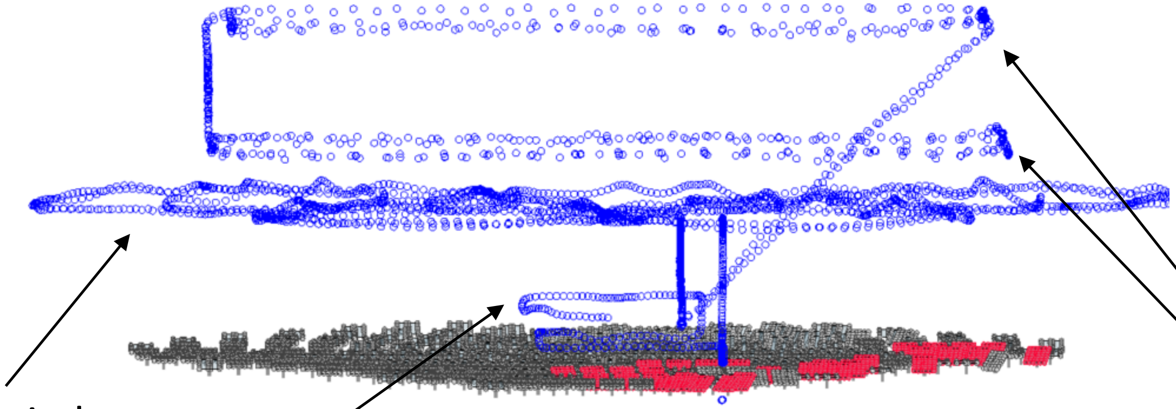

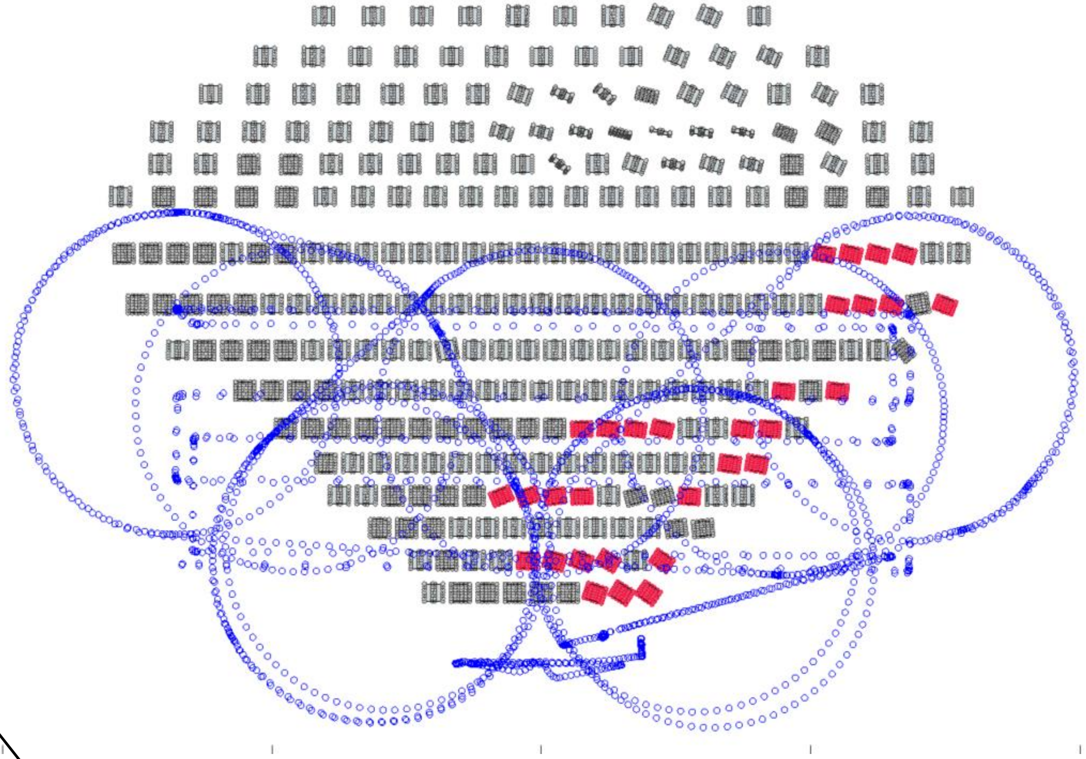

Flying circles

Flying in nadir mode at high altitude to strengthen the photogrammetric network.

Flying a spiral at the beginning for initialization of photogrammetry

Flight route design

Perspective orientation example at CESA I (CIEMAT-PSA)

Different positions relative to the heliostats yield different detection rates.

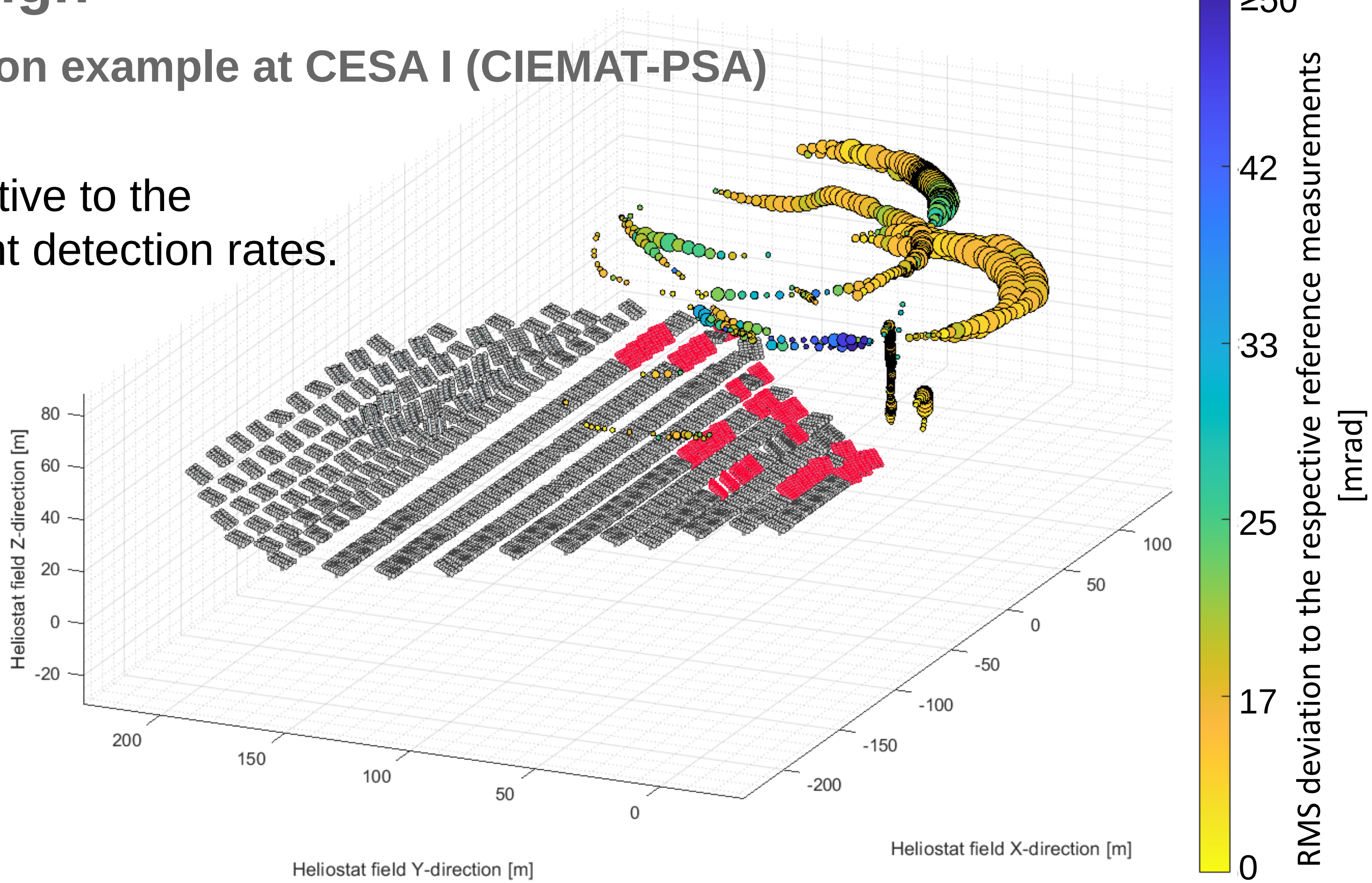

Bubble diameter:
Number of oriented heliostats per image.

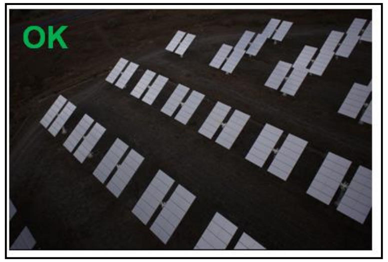

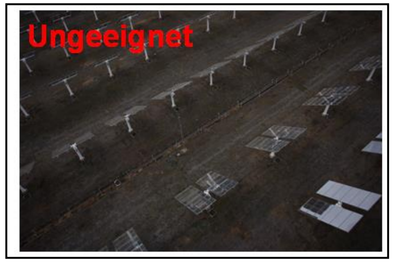

Flight route optimization

Simulating flights for photogrammetry to find the best path and orientations

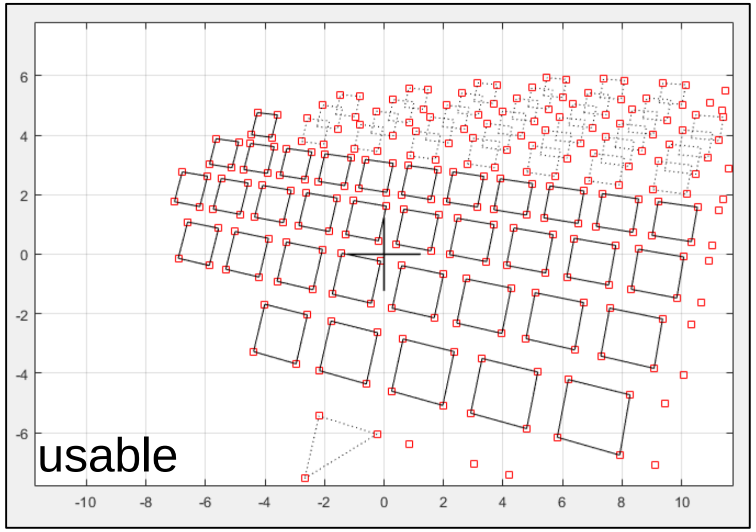

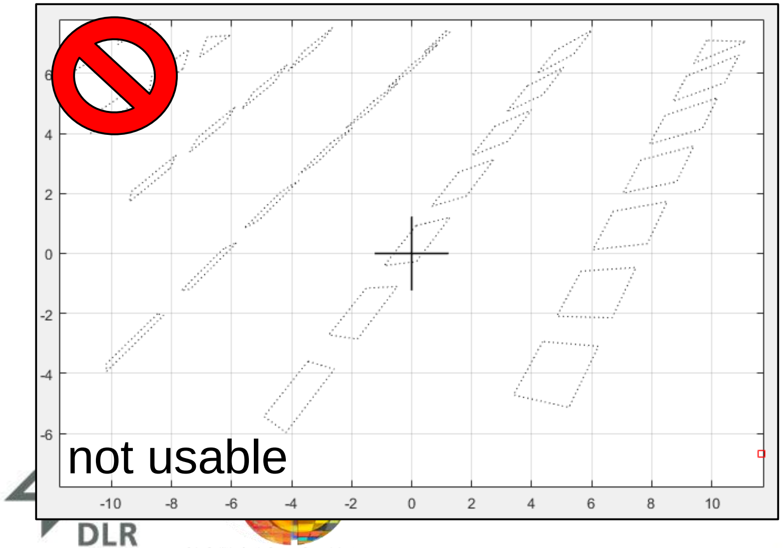

Possible flight route

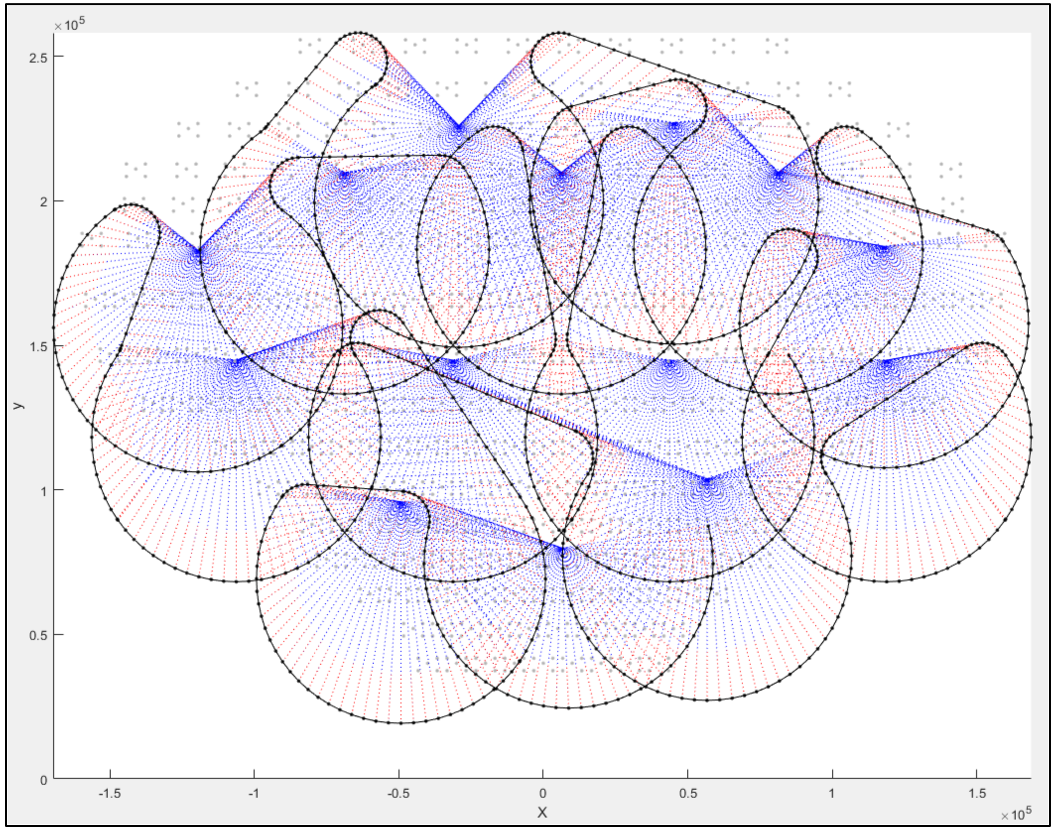

Black: Path of UAV
Blue and red: Camera orientation at time of image

Summary and Outlook

- Methods for calibrating entire heliostat fields are in heavy development (several projects in process and planned)
- First tests show successfully their capabilities (**Project HelioPoint and HelioPoint II**).
- Calibration methods with interactive flight routes and autonomous flight routes will be developed in the next years (e.g. **Project 5hine** - using 5G in the solar field)
- New methods for a more robust heliostat detection are being developed (e.g. **Project AuSeSol2** – using deep learning and CNNs)

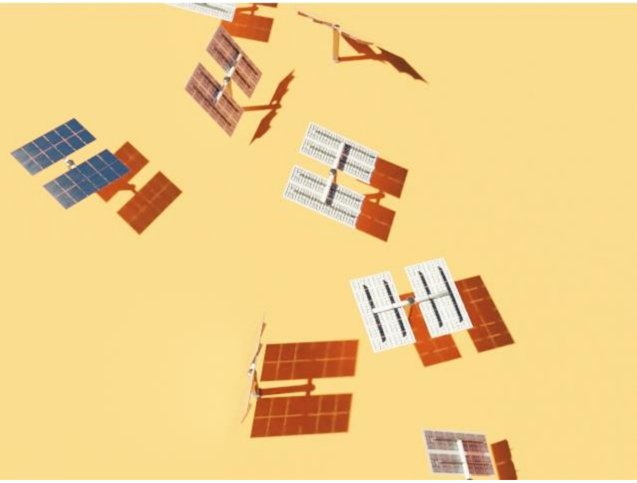

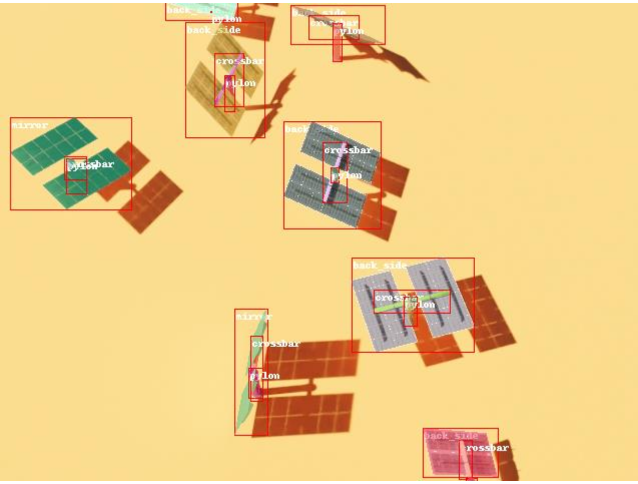

SFERA-III
Solar Facilities for the European Research Area

THANK YOU FOR YOUR ATTENTION!
ANY QUESTIONS?

Flux Density Measurement

Christian Raeder

SFERA-III Training
Optimization of CST plant output by optical and thermal characterization and target-oriented O&M
Plataforma Solar de Almería, Spain, April 2022

Measuring High Intensity Radiation (5 - 4000 kW/m²)

- Gardon-gauge
- Kendall-cavity
- Sun-catch
- Gardon-gauge Combined with Camera and Lambertian Target
- Radiometer- and scan method and reflection off the absorber

Gardon-gauge

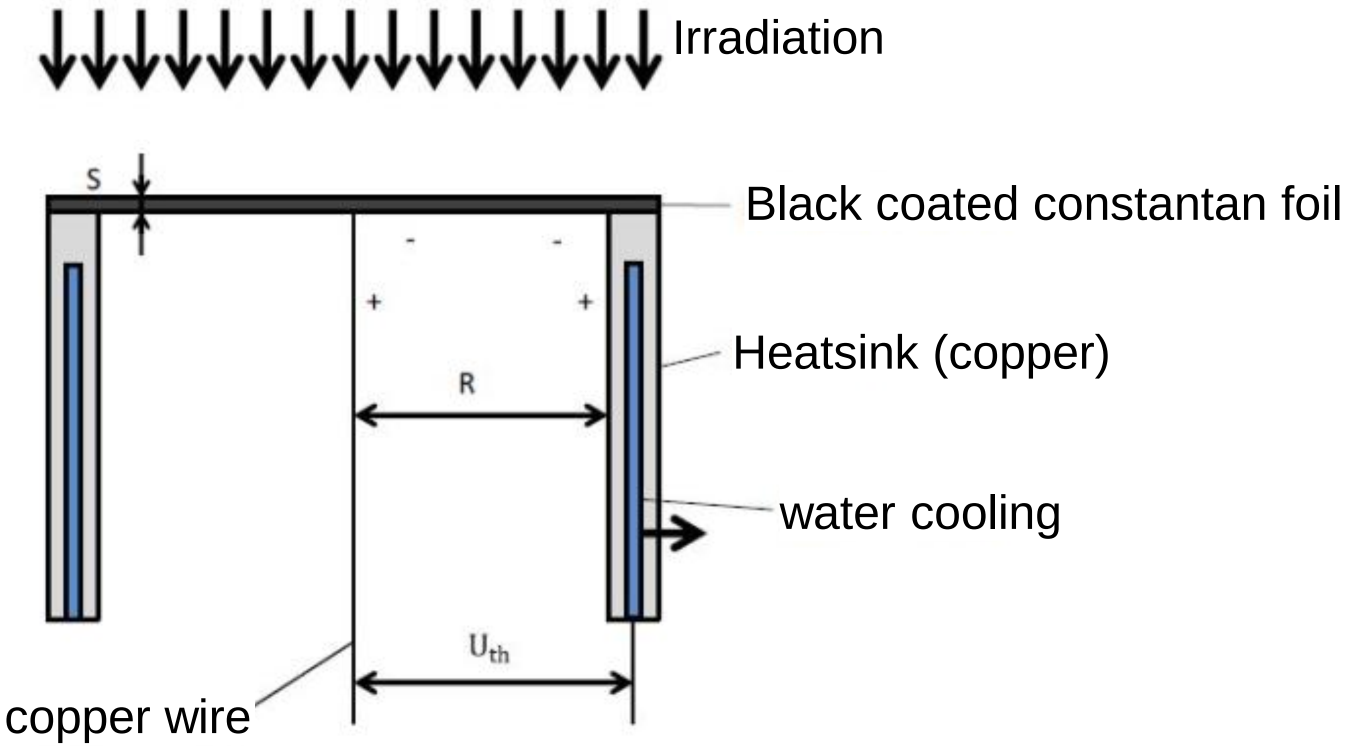

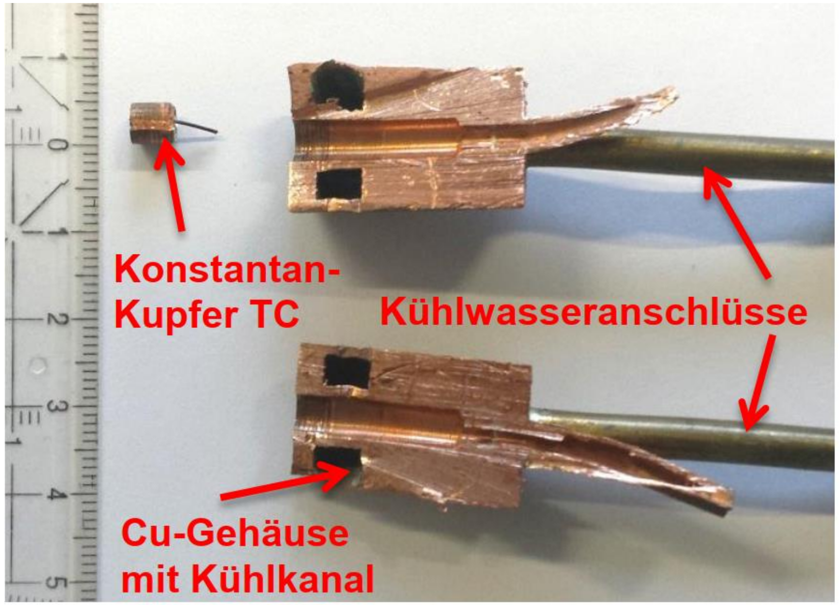

Robert Gardon; An Instrument for the Direct Measurement of Intense Thermal Radiation, Review of Scientific Instruments **24**, 366 (1953); doi: 10.1063/1.1770712

Kendall-Cavity

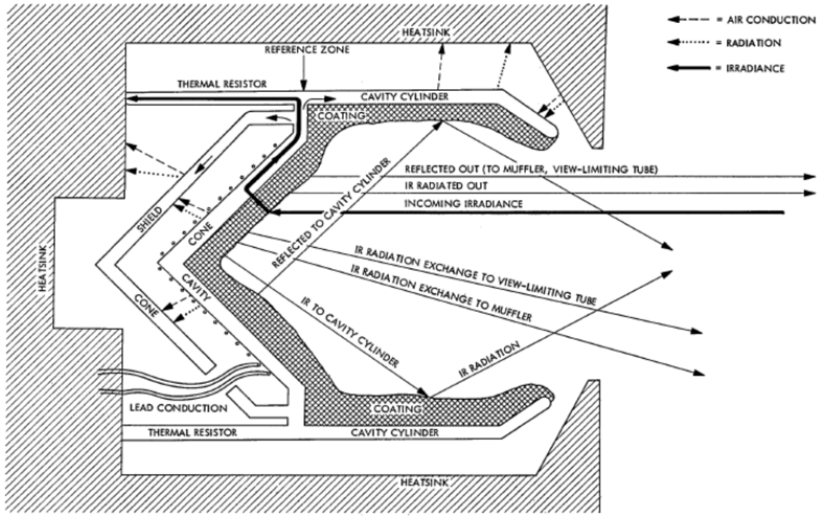

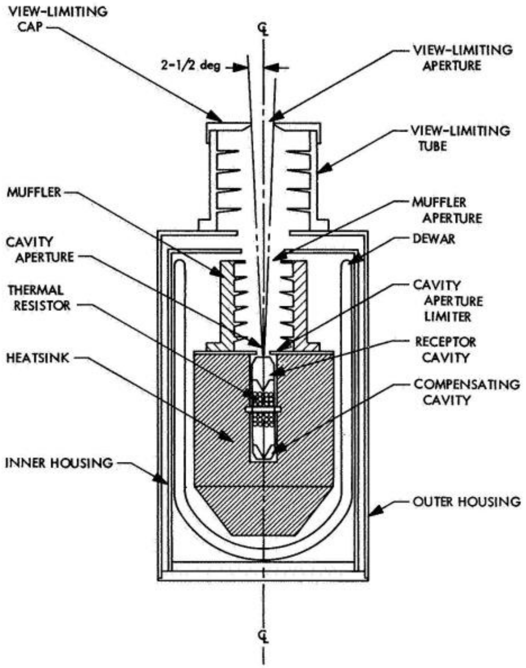

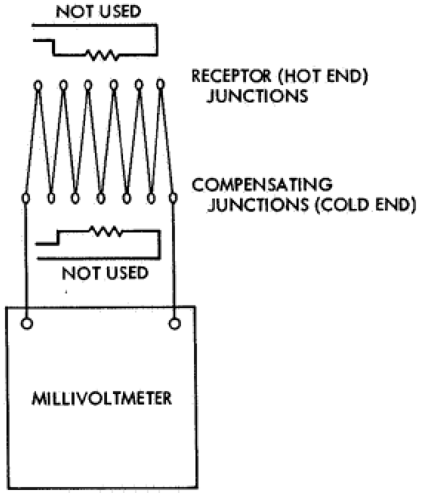

- Cavity is heated by incident irradiation
- Causes the thermopile to emit a voltage signal
- Compensating cavity is electrically heated
- Until thermopile signal is zero
- With P = U × I and the diameter of the aperture the irradiation in W/m² can be calculated

J. M. Kendall, Sr; *Primary Absolute Cavity Radiometer; Technical Report 32-139;* jet propulsion laboratory california institute of technology, Pasadena, California*; July 15, 1969*

Response Time

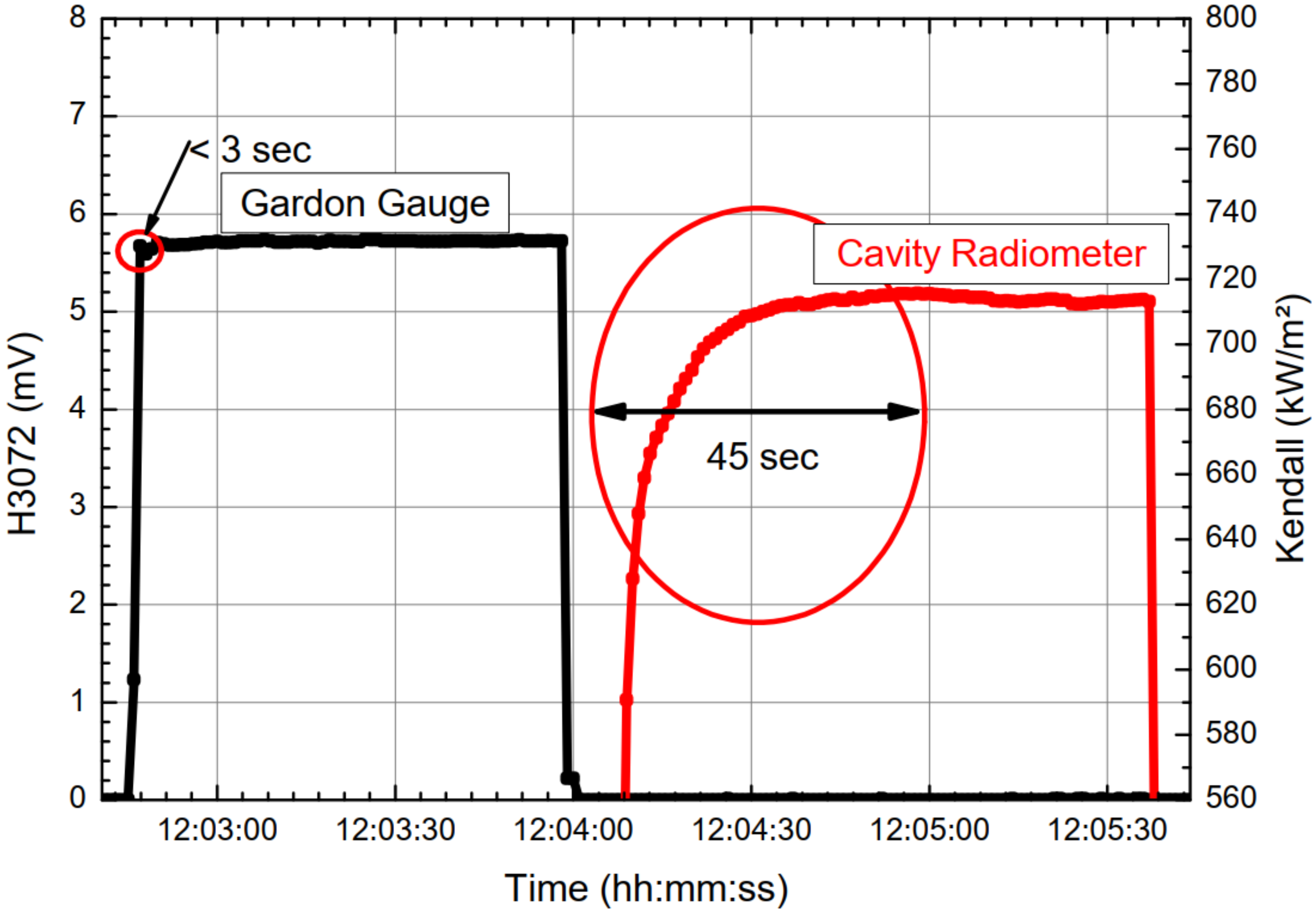

Sun-Catch

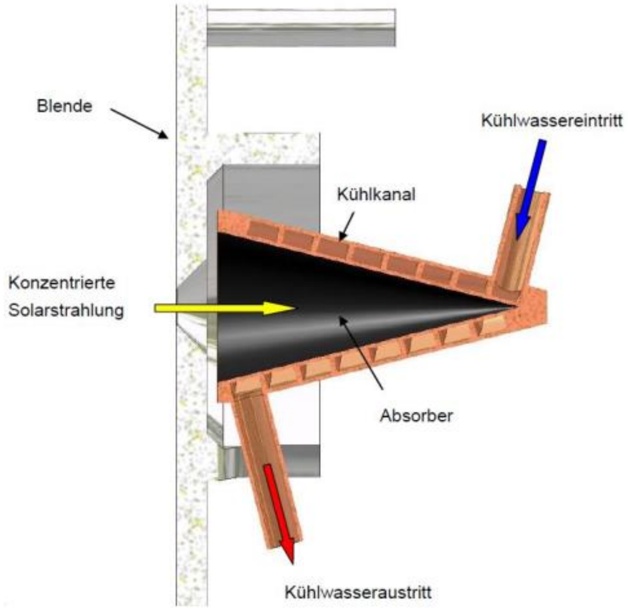

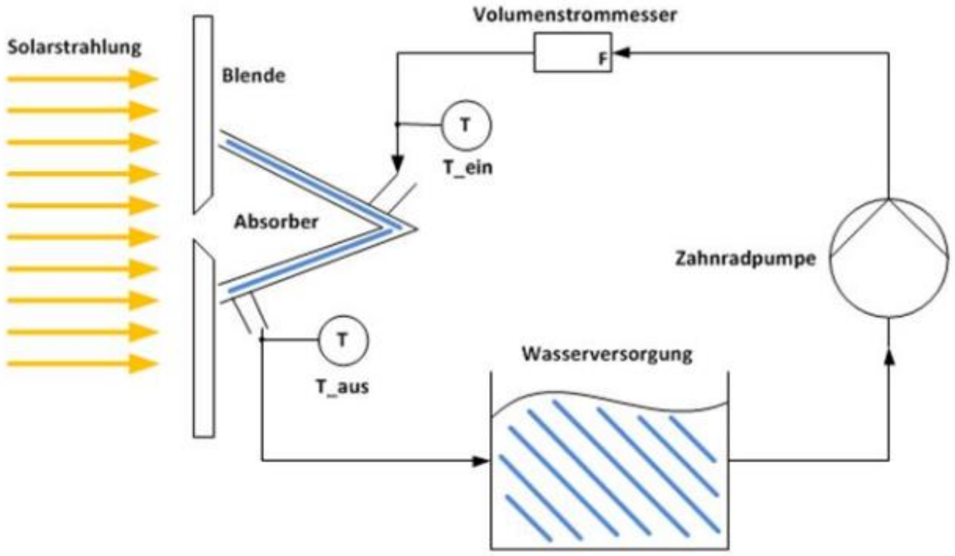

$$\dot{Q} = \dot{V}\,\rho\,c_p\,\Delta T$$

Response time: > 2 min

Temperature dependent

Flux density distribution measurement acquisition system: FMAS

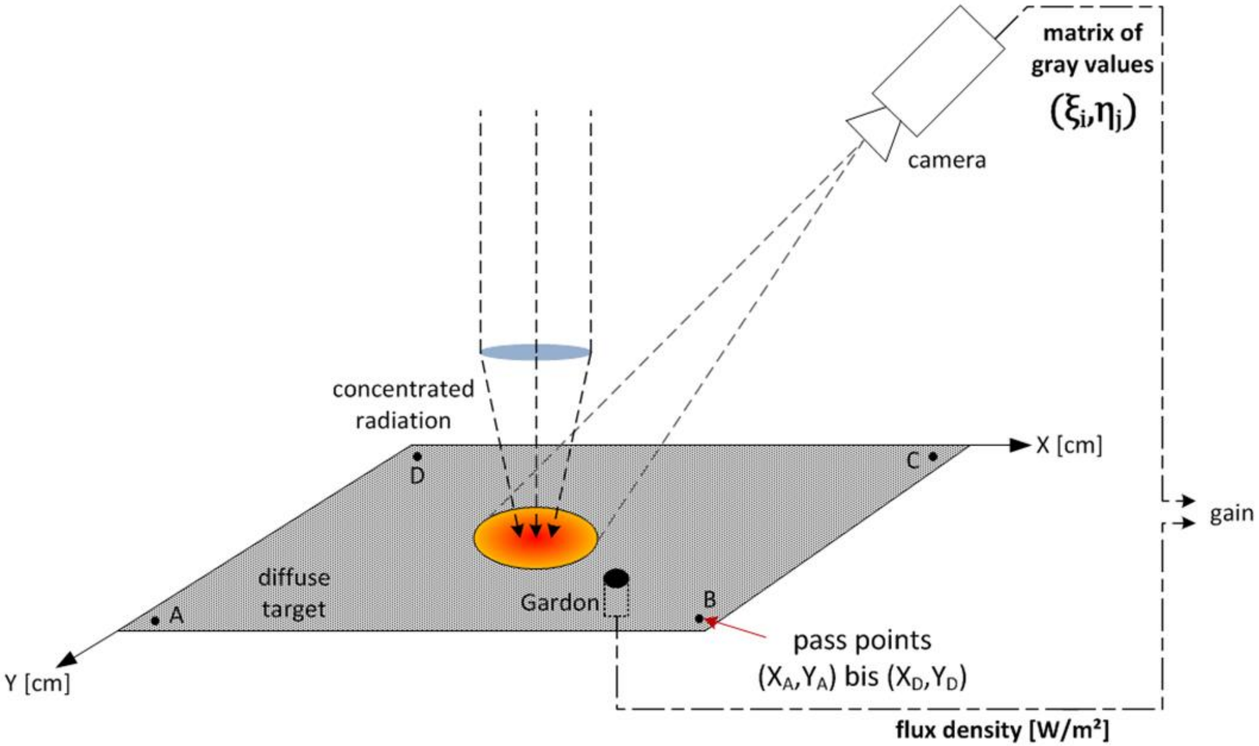

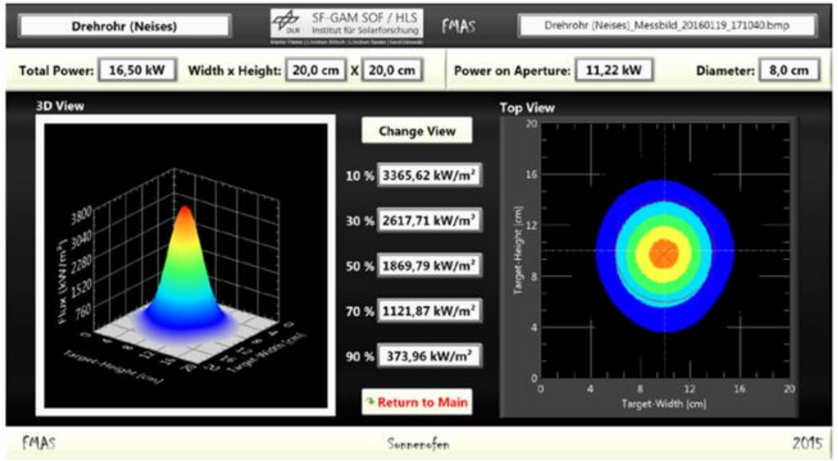

Drehrohr (Neises)

Drehrohr (Neises)_Messbild_20160119_171040.bmp

Total Power: 16,50 kW

Width x Height: 20,0 cm X 20,0 cm

Power on Aperture: 11,22 kW

Diameter: 8,0 cm

10 % 3365,62 kW/m²

30 % 2617,71 kW/m²

50 % 1869,79 kW/m²

70 % 1121,87 kW/m²

90 % 373,96 kW/m²

M. Thelen; Entwicklung eines optischen Messsystems für Strahlungsflussdichteverteilung und Verifizierung anhand hochkonzentrierter Solarstrahlung; Master Thesis; Rheinische Fachhochschule Köln; 2016

Moving bar

Moving bar installed at the test receiver Solar tower Jülich

Radiometer method (Focus shift)

process

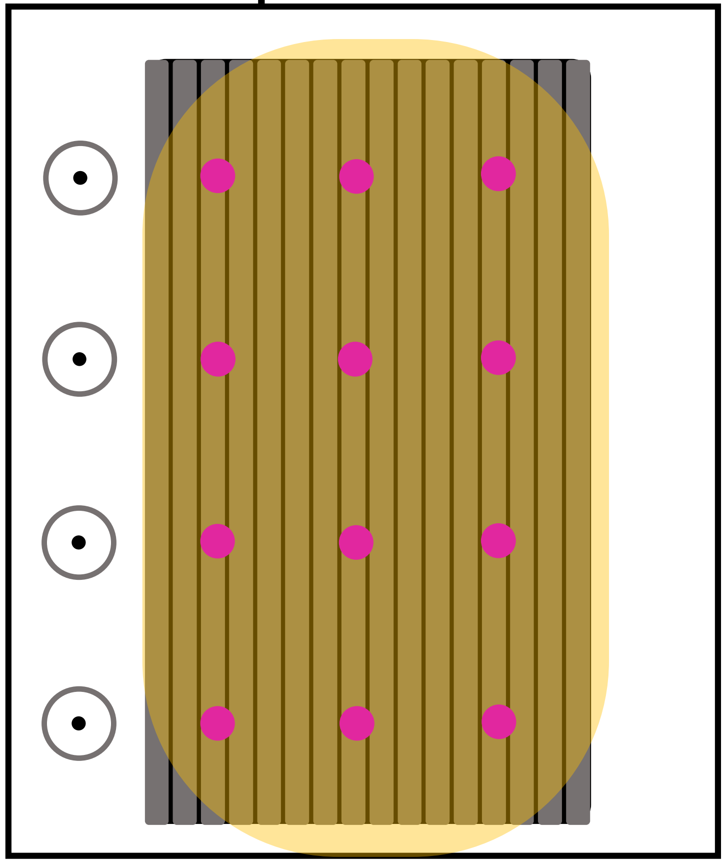

data of radiometers

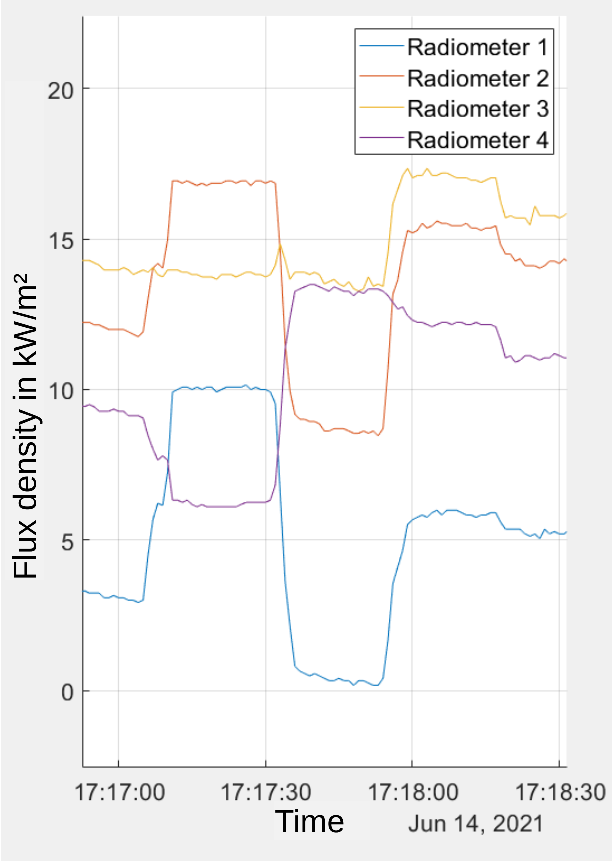

result

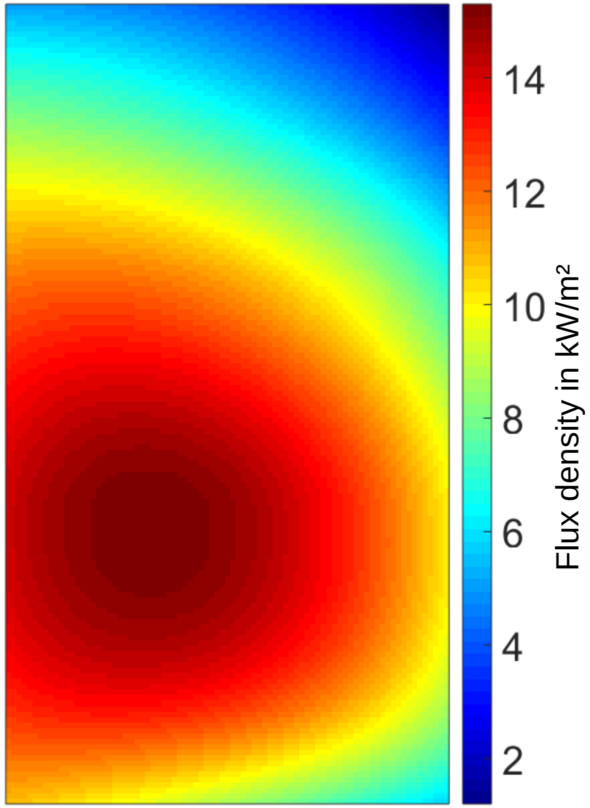

Matthias Glinka; Flux density measurement using reflection off solar towers - commissioning and usage of a water-cooled tube receiver; Bachelor Thesis; RWTH Aachen; 2021

Reflection off the absorber

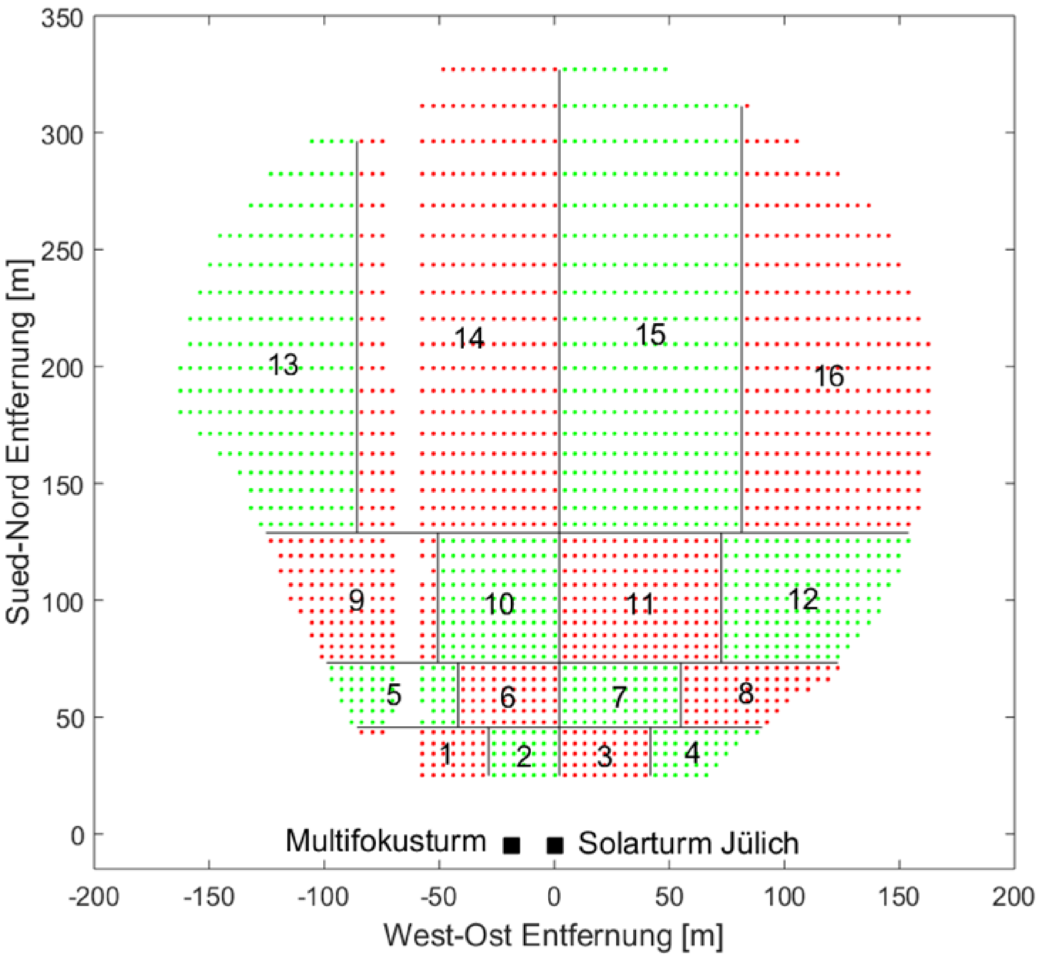

- C Raeder, M Offergeld, M Röger, A Lademann, J Zöller, M Glinka, J Escamilla and A Kämpgen; Proof of Concept: Real-Time Flux Density Monitoring System on External Tube Receivers for Optimized Solar Field Operation; Solar Paces 2021
- M Offergeld, M Röger, H Stadler, et al.; Flux density measurement for industrialscale solar power towers using the reflection off the absorber; AIP Conference Proceedings 2126, 110002 (2019)

Scan method

Determination of the Reflection Properties

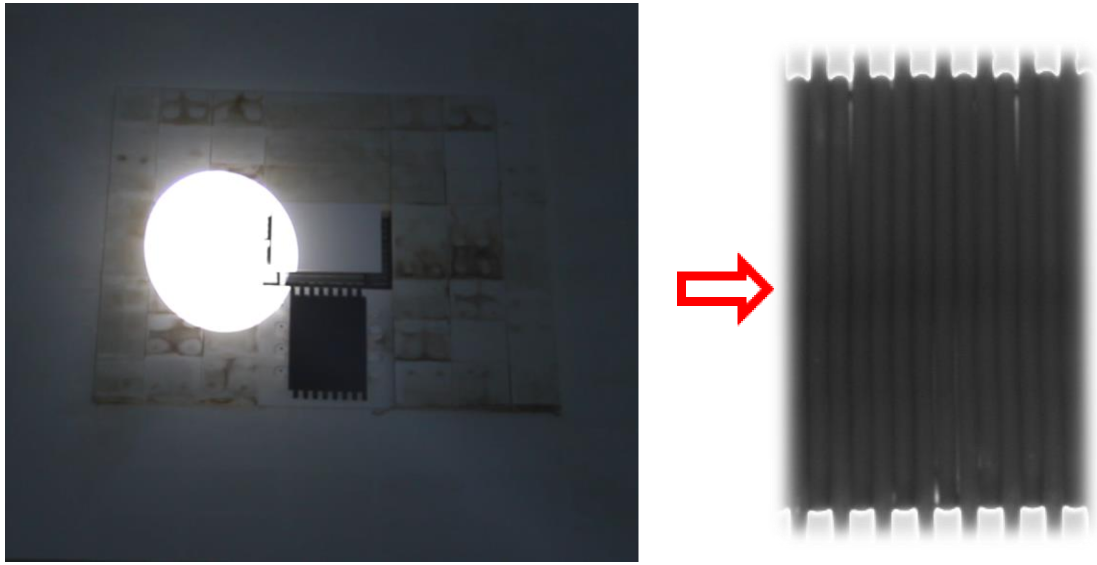

- Meander-shaped path of the light spot
- Simultaneous high-frequency series image recording
- Determination of maximum image ⇨ virtual image of a homogenously illuminated receiver

Comparison: Reflection off the absorber – Radiometer method

- 24 Heliostaten aus den Gruppen 10,11,12
- Überwiegend gute Übereinstimmung, insbes. im zentralen Bereich
- Lokale Abweichungen im unteren & seitlichen Randbereich

Judith Zöller; Flux Density Measurement Using Reflection at Solar Tower Tube Receivers – Image Acquisition and Software-Based Image Processing; Bachelor Thesis; RWTH Aachen; 2021

Kamerabasierte Messung

Relatives Differenzbild

Radiometermessung

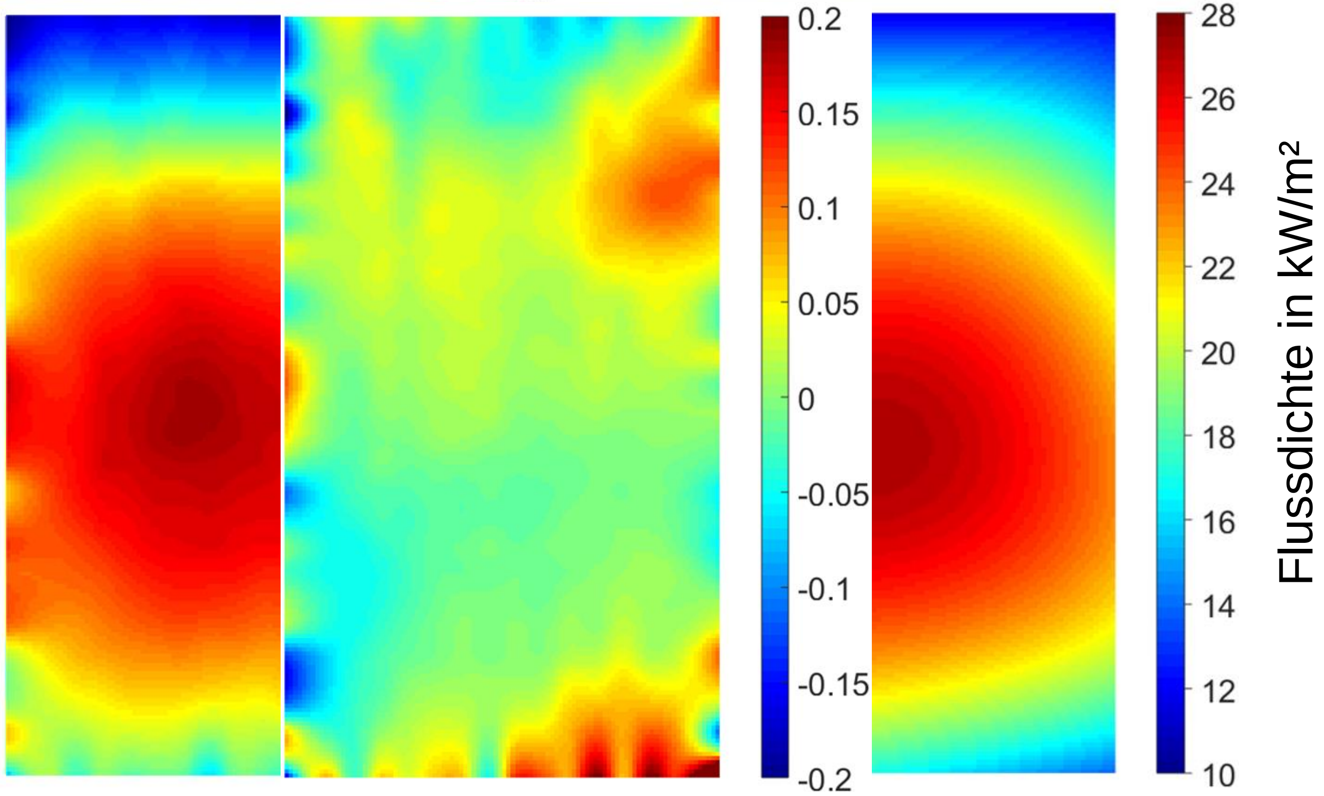

$\dot{Q}_{\mathrm{kam}} = 18{,}52\ \mathrm{kW}$ $\Delta\dot{Q} = 0{,}9\ \%$ $\dot{Q}_{\mathrm{ref}} = 18{,}34\ \mathrm{kW}$

Thank You !

Solar Facilities for the European Research Area

SFERA-III

Solar Facilities for the European Research Area

2nd Training for Industries "Optimization of CST plant output by optical and thermal characterization and target-oriented O&M"
29 April 2022, Plataforma Solar de Almería, Spain

Optimized Cleaning Strategies for CSP

Fabian Wolfertstetter, DLR

NETWORKING

THIS PROJECT HAS RECEIVED FUNDING FROM THE EUROPEAN UNION'S HORIZON 2020 RESEARCH AND INNOVATION PROGRAMME UNDER GRANT AGREEMENT NO **823802**

Outline

- Introduction
- Soiling related measurements
- Solar field model and comparison parameter
- Condition based cleaning strategies:
  - Strategy definition,
  - Case studies and results
- Reinforced learning algorithms
  - Creation of synthetic data series
  - Performance of ANN strategies

Cleaning and soiling

- Cleaning operators have to find the best trade-off between reduced **cleaning costs** and increased optical **solar field efficiency**
- Cleaning performance has to be quantified **financially**
- **Time resolved** analysis and **realistic soiling** rate dataset is crucial

Soiled trough at PSA
(Infrastructure owned by the
Spanish research centre CIEMAT)

Cleaning optimization: solar field model

- Solar field model tracks cleaning vehicles and each troughs cleanliness
- Assumption: all troughs soil with same soiling rate
- Output: net profit = project‘s profit – cleaning cost

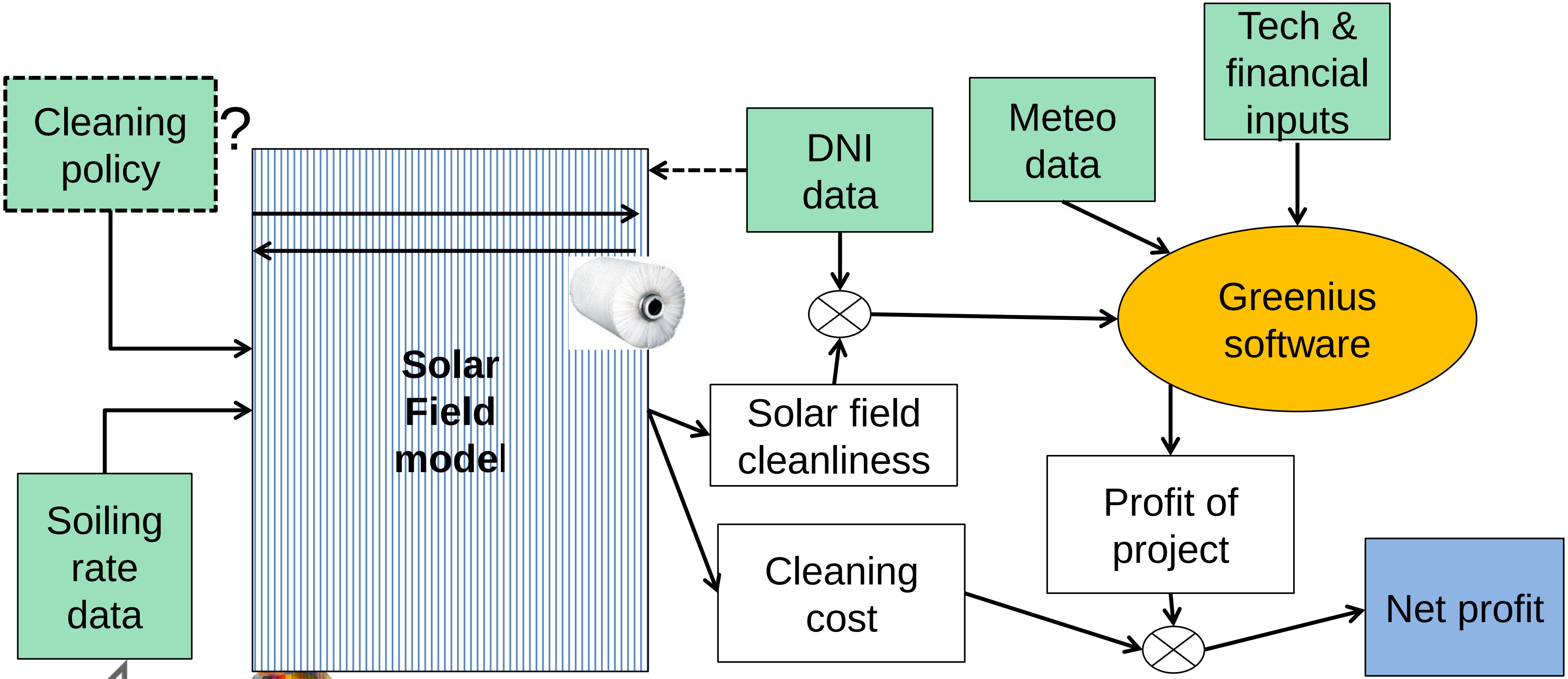

Cleaning optimization: scenario & inputs

- 50 MW plant with 7.5 h storage
- Water and brush based cleaning vehicles
- Cleaning related technical and financial parameters (see table)
- Cleaning costs:
  - Labor, water, fuel, depreciation of cleaning vehicles
- **5 years** of soiling rate measurement data at PSA
- >**28 years** of irradiance and weather data

Parameter	Value
Nominal turbine power	49, 9MW
Number of loops in Solar Field	156
Aperture area of solar field	510.000 m^2
Thermal storage	7.5 h
Cooling	water
Planned lifetime	25 years
DNI-yearly sum at PSA	2388 kWh/m^2/a
Equity ratio	30 %
Specific operating costs	1.8 EUR/m^2/a
Feed-in tariff	0.27 EUR/kWh
Cleaning velocity for one unit	9 loops / shift
Number of personnel per vehicle	1
Cleaning vehicle fuel consumption	6 – 8 l/loop
Cleanliness after cleaning	0.986
Demin. water consumption of cleaning unit	1 m^3/loop
Estimated lifetime of cleaning unit	15 years

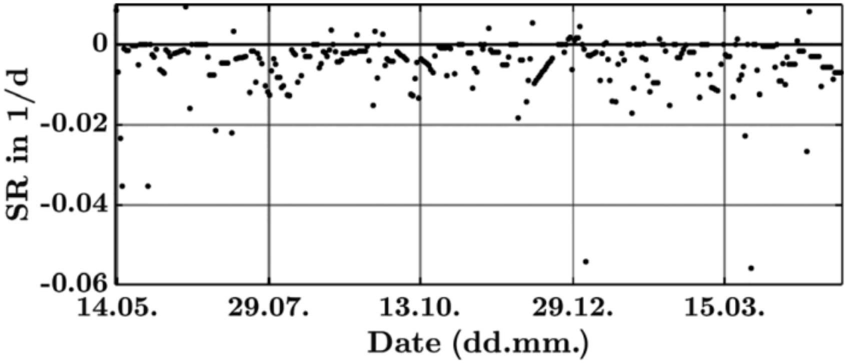

Wolfertstetter, F., Wilbert, S., Dersch, J., Dieckmann, S., Pitz-Paal, R., & Ghennioui, A. (2018). Integration of Soiling-Rate Measurements and Cleaning Strategies in Yield Analysis of Parabolic Trough Plants. *Journal of Solar Energy Engineering*, *140*(4), 041008.

Cleaning optimization: policy comparison

- A **reference cleaning strategy** is chosen as a reference point: constant, daily cleaning in one shift with 1 vehicle
- Cleaning policies are compared to reference by **relative profit increase (RPI)**
- **First study**: condition based cleaning policies:
    - Vary number of vehicles and cleanliness threshold

Wolfertstetter, F., Wilbert, S., Dersch, J., Dieckmann, S., Pitz-Paal, R., & Ghennioui, A. (2018). Integration of Soiling-Rate Measurements and Cleaning Strategies in Yield Analysis of Parabolic Trough Plants. *Journal of Solar Energy Engineering*, *140*(4), 041008.

- **Second study**: reinforced learning including soiling forecast

Terhag, F., Wolfertstetter, F., Wilbert, S., Hirsch, T., & Schaudt, O. (2019, July). Optimization of cleaning strategies based on ANN algorithms assessing the benefit of soiling rate forecasts. In *AIP Conference Proceedings* (Vol. 2126, No. 1, p. 220005). AIP Publishing LLC.

Condition based cleaning strategies

- Strategies oriented on operational practices. Strict rules are followed and simulated in solar field model

- **Constant d**: Clean at a constant rate only during the night shift with all available CU
- **Constant dn:** Clean at a constant rate during day and night shifts. This is the **reference strategy** when 1 CU is utilized.
- **Threshold n/dn:** Clean with all CU only if average field cleanliness is lower than a threshold nlim
- **Assisted n/dn:** Similar to threshold, but additional manual cleaning teams are hired if field cleanliness falls below a second threshold
  value

- Tested for different cases:
  - With thermal storage “AS” and without “IP”
  - Cost parameters for Morocco and Spain

Condition based strategies "constant"

- Profit increases are highest with Moroccan cost parameters
- Storage favors cleaning
- More cleaning units needed if only nightly cleaning

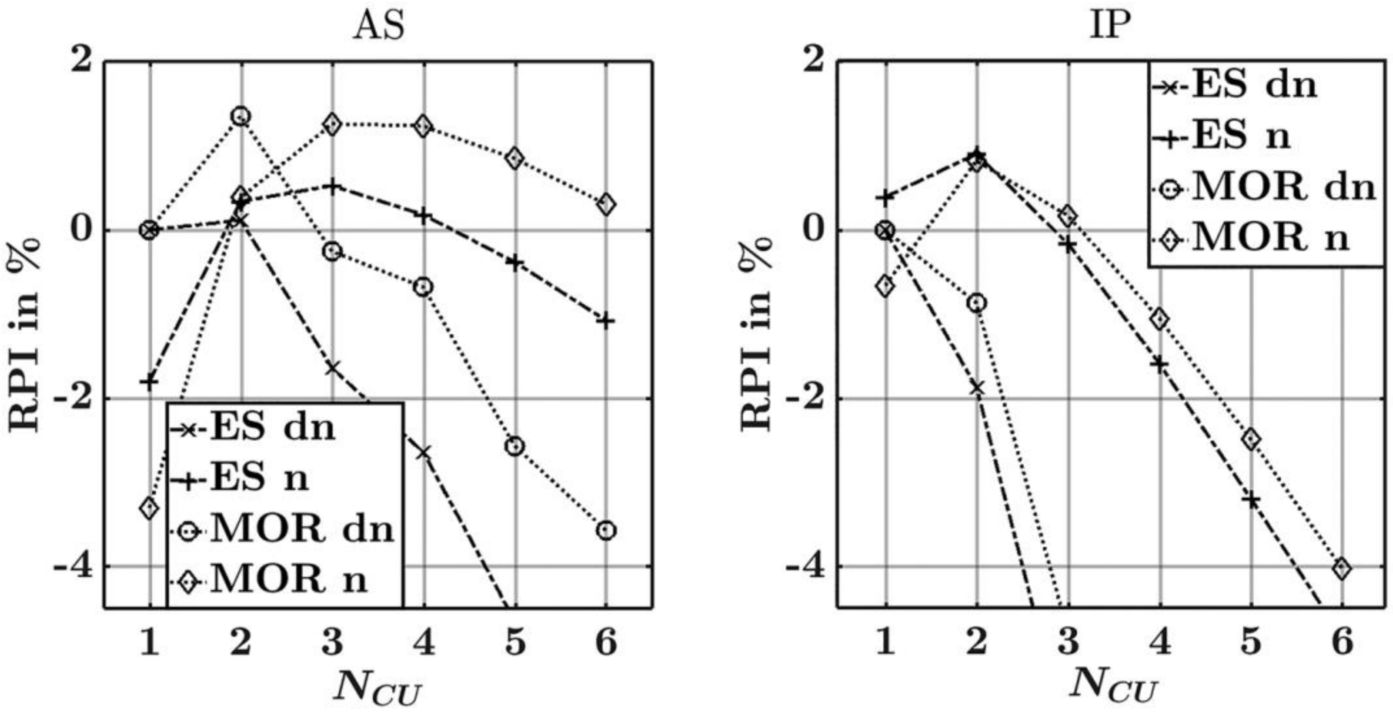

Condition based strategies "constant"

- Profit increases are highest with Moroccan cost parameters
- Storage favors cleaning
- More cleaning units needed if only nightly cleaning
- Dumping!

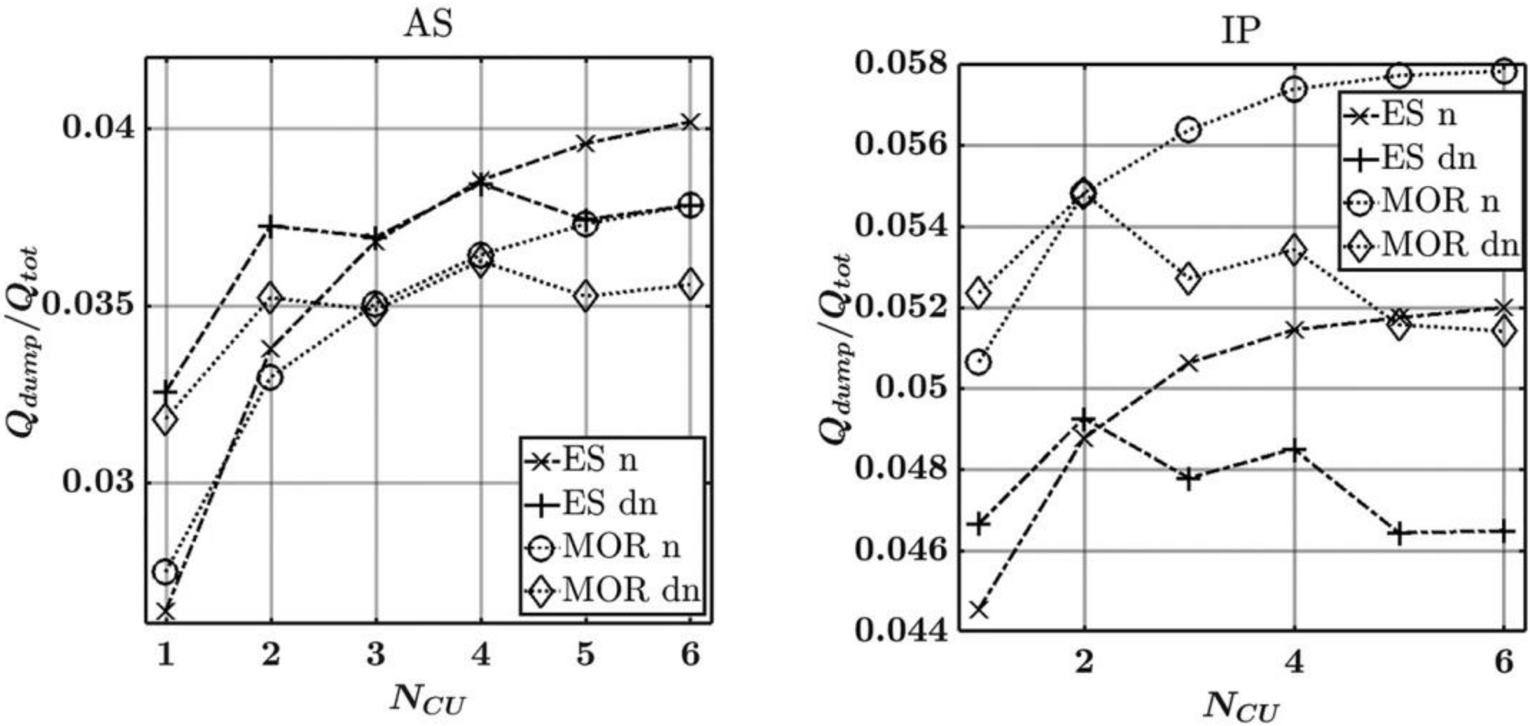

Condition based strategies

- With Moroccan cost parameters and storage, more cleaning is incentivized
- Cleaning can increase profit by 1.36%
- Storage makes plants more robust against wrong cleaning decisions

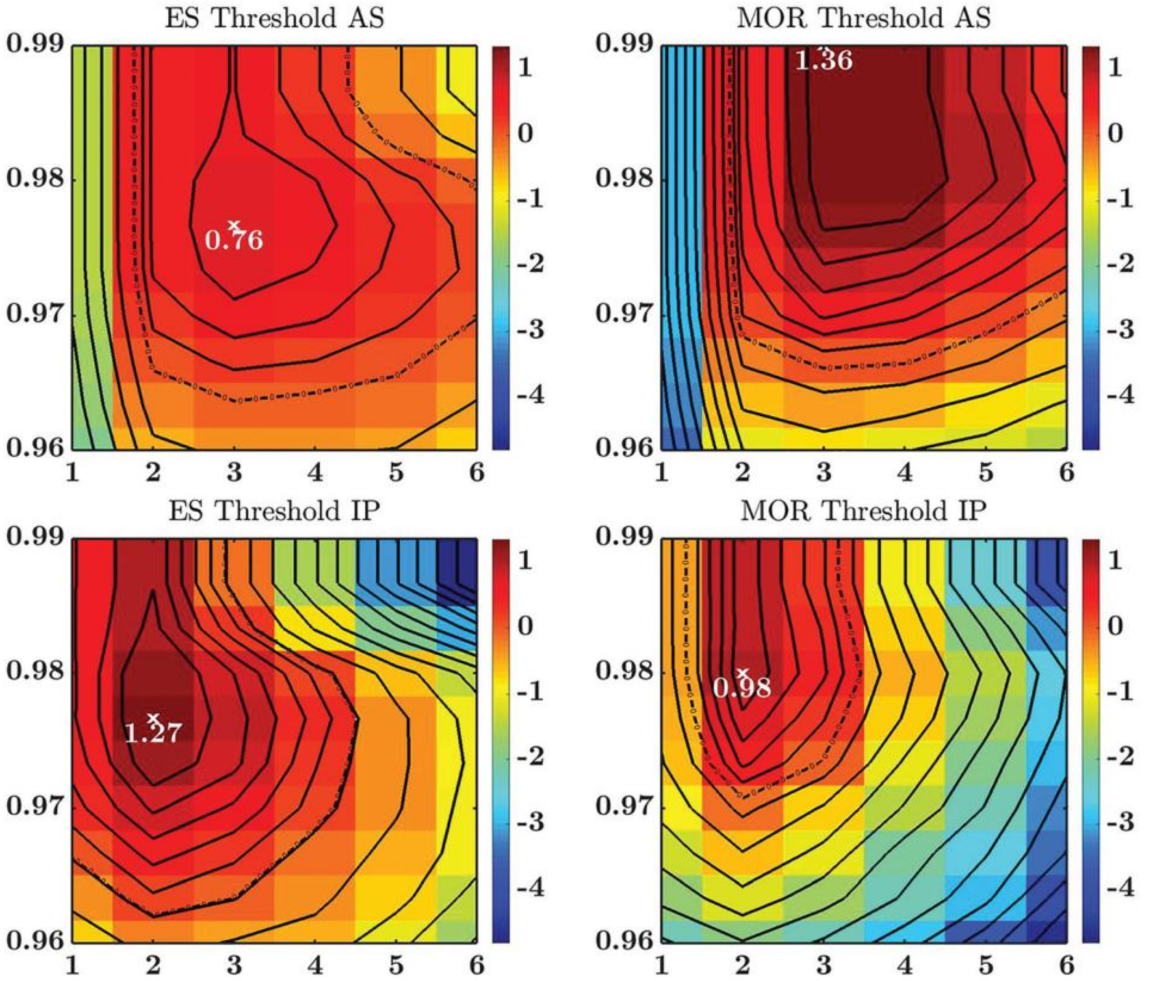

Condition based strategy with constant soiling rate

- Simulation for constant soiling rate:
- It is important to have a soiling time series for representative yield analysis and cleaning optimization

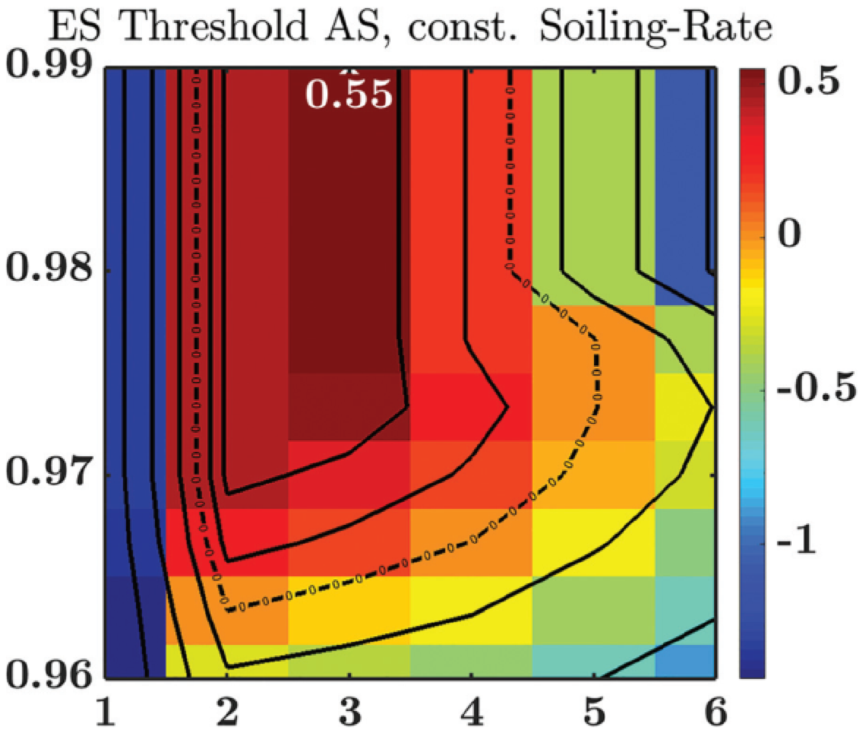

Fig. 7 Simulated RPIs shown in color for the CS threshold in ES and AS, where the *x*-axis shows the number of CU employed and ξ_{lim} is shown on the y-axis. The soiling-rate dataset used was set to the average soiling rate of −0.0052/d of the dataset acquired at PSA for every day of the year. The depicted scenario is the same as shown in the upper left graph of Fig. 5 with the only difference that here the SR has been assumed as constant in time with the mean value of the measured SR from PSA here.

Condition based cleaning with high soiling events

- The soiling rate dataset has been extended by 5 heavy soiling events
- Intelligent cleaning becomes more profitable
- Assisted strategy does not increase profit significantly

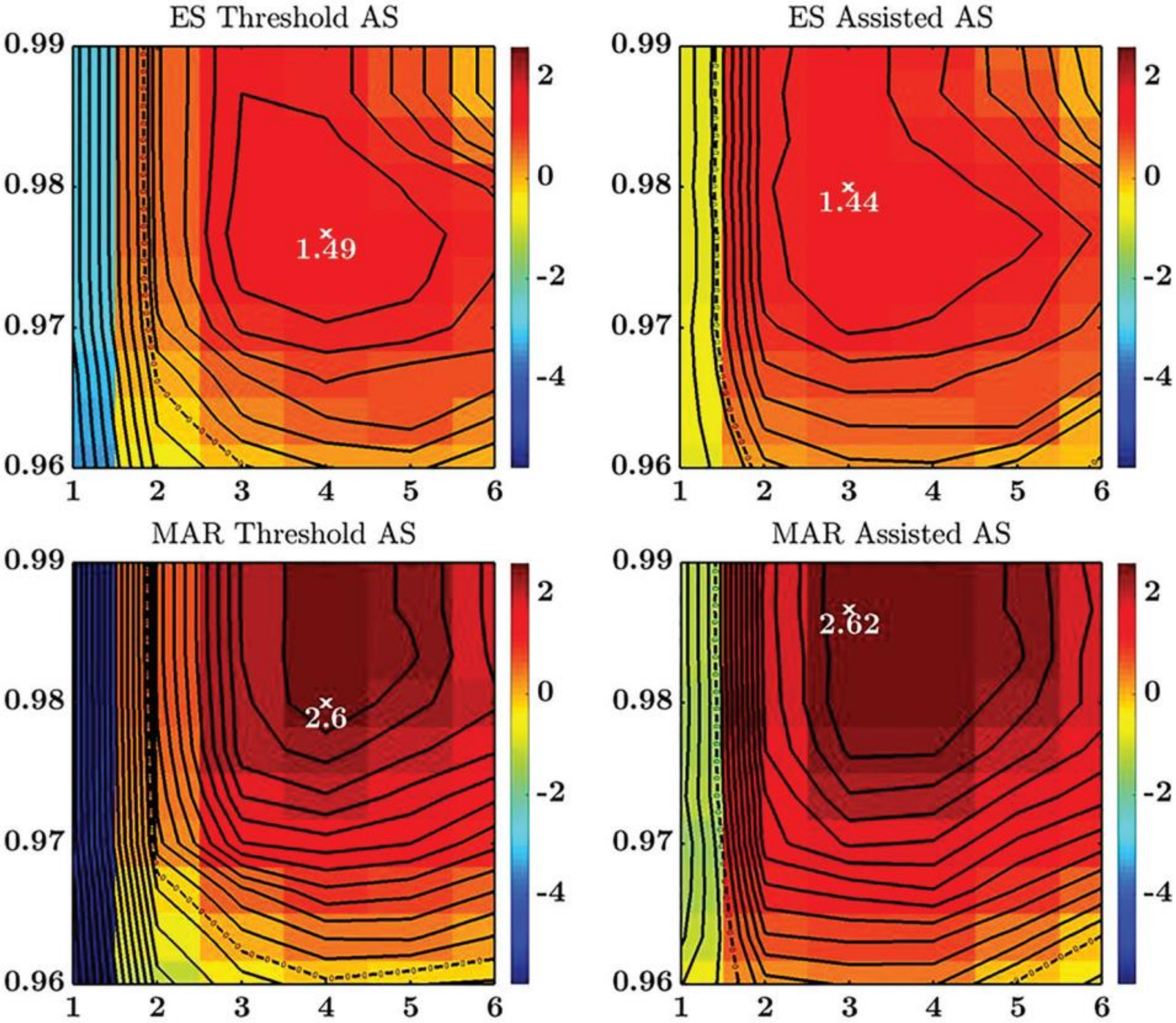

Condition based strategies conclusions

- Cleaning costs correspond to 1-3% of profit
- Lower cleaning costs incentivize cleaning despite lower feed in tariffs
- Time resolved soiling information necessary for accurate estimation of plant yield

Next: reinforced learning strategy development

- Can artificial neural networks increase cleaning strategy performance?
- Can **soiling forecasts** increase performance further?

Literature on soiling model development:
http://wascop.eu/wp-content/uploads/2018/06/WASCOP_deliverable_3.2_final_plainText.pdf

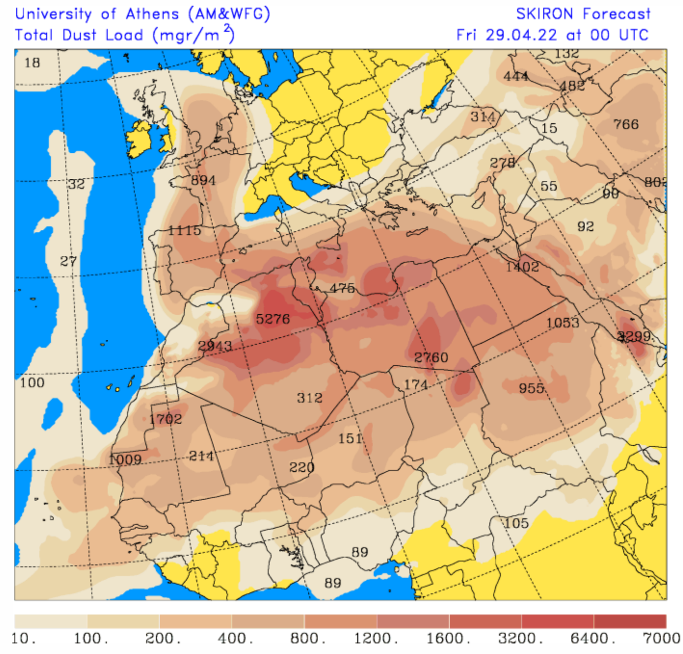

Artificial Neural Networks: Reinforced learning

- Agent takes action depending on the environment

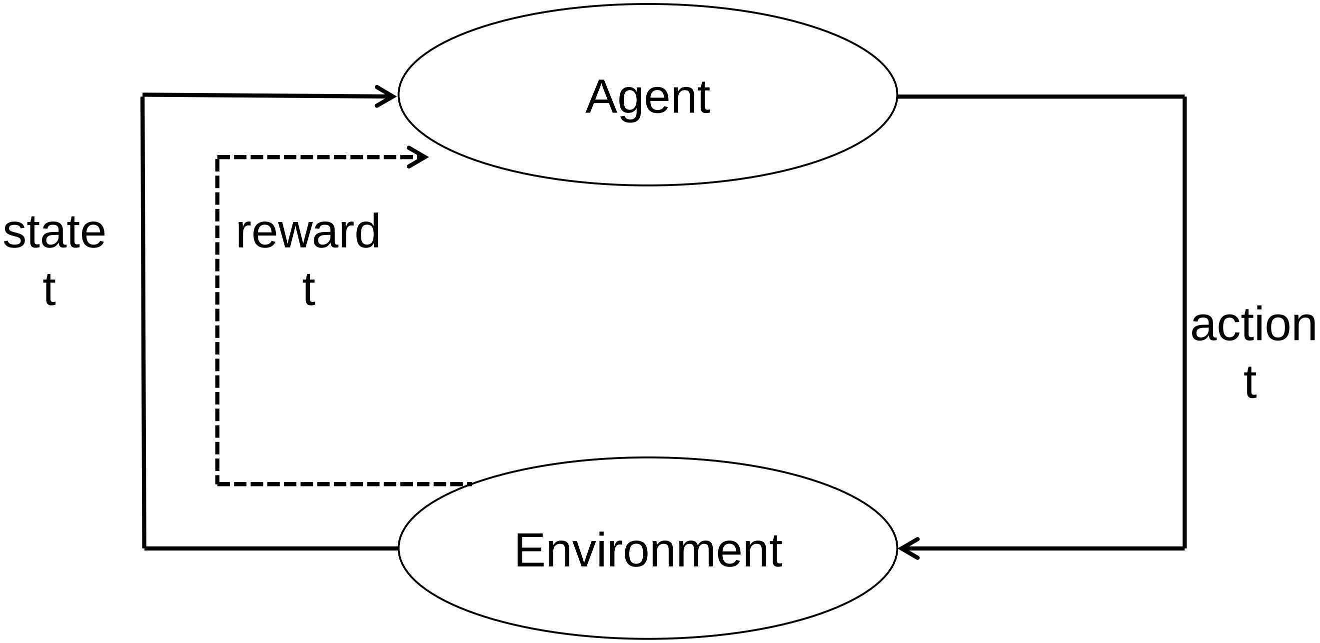

Artificial Neural Networks: Reinforced learning

- Agent takes action depending on the environment
- Actions influence environment and creates a reward feedback
- **Learning process**: Agent is updated after each run => negative or positive feedback on current policy according to reward
- The fully trained agent can be applied to any new environment to deliver high reward

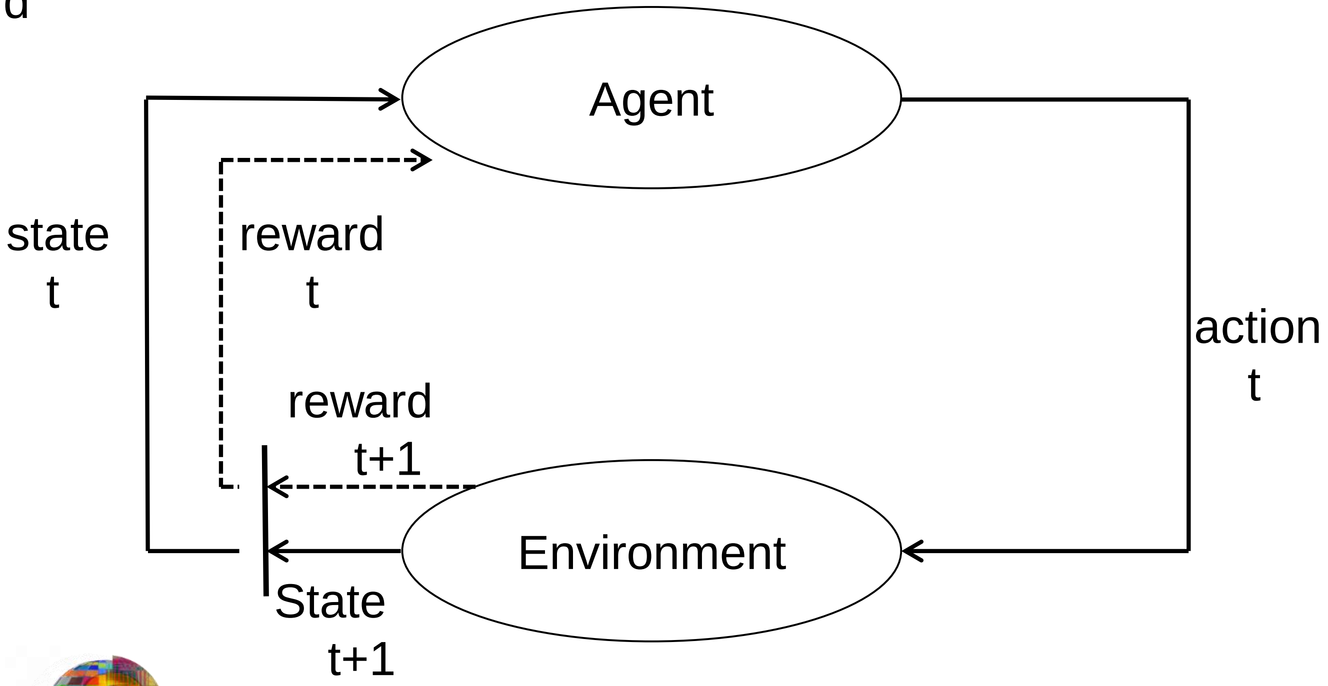

Artificial Neural Networks: Reinforced learning

- agent = cleaning policy
- action = daily cleaning decision
    - Clean with 0 – 2 vehicles in 1 or 2 shifts each
- state = solar field cleanliness, weather data, optional: **forecast** for irradiance class and high/low soiling rate
- Reward = RPI

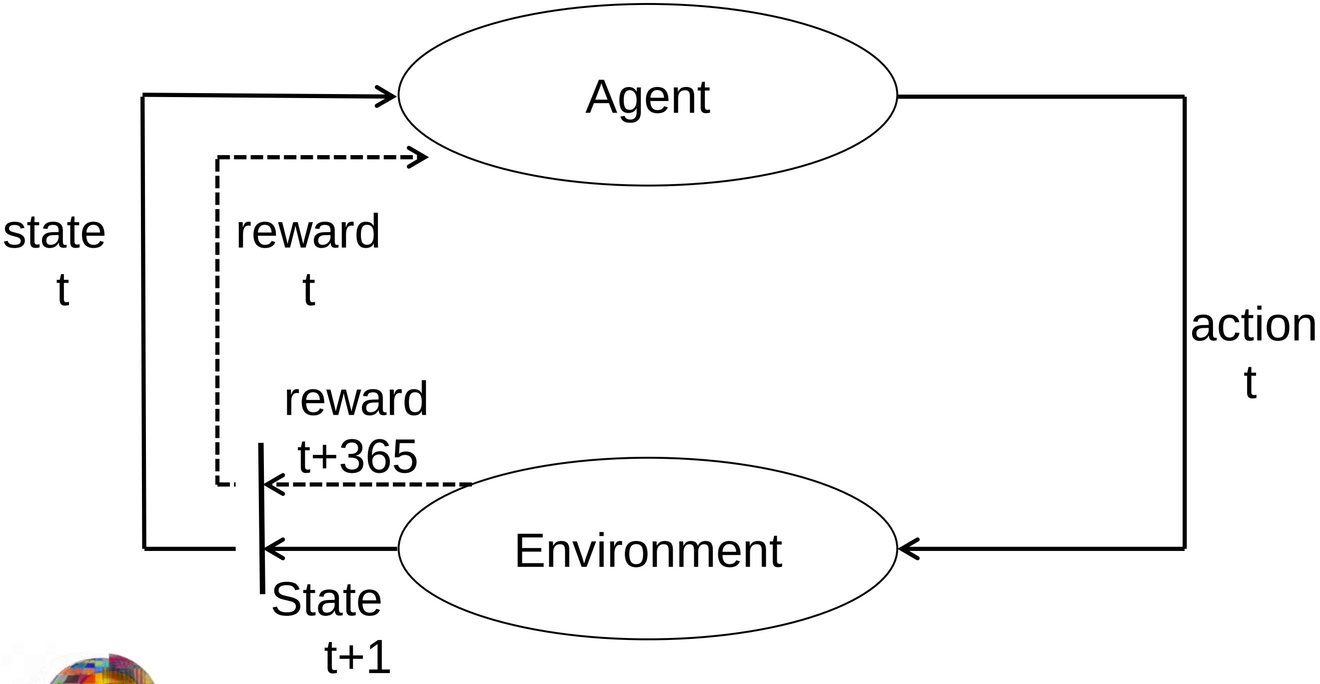

Reinforced Learning: Reward and training

- Each training run involves full simulation year, i.e. 365 states and cleaning decisions
- Option to provide agent with soiling rate and weather forecast information
- Training of reinforced learning agent requires a **large amount of data**
- 5 years of soiling data and 28 years of weather data is **not enough** for reinforced learning

=> need to increase database by **synthetic data extension**

Synthetic data extension: weather

- Measurement days are classified for **DNI variability** (clear sky, intermittent, cloudy) [1]
- **Transition probabilities** are determined
- Original measurement days are drawn from a 14 day time window according to transition probabilities
- >5,000 data years are created

Average DNI variability class distribution over 28 years at PSA

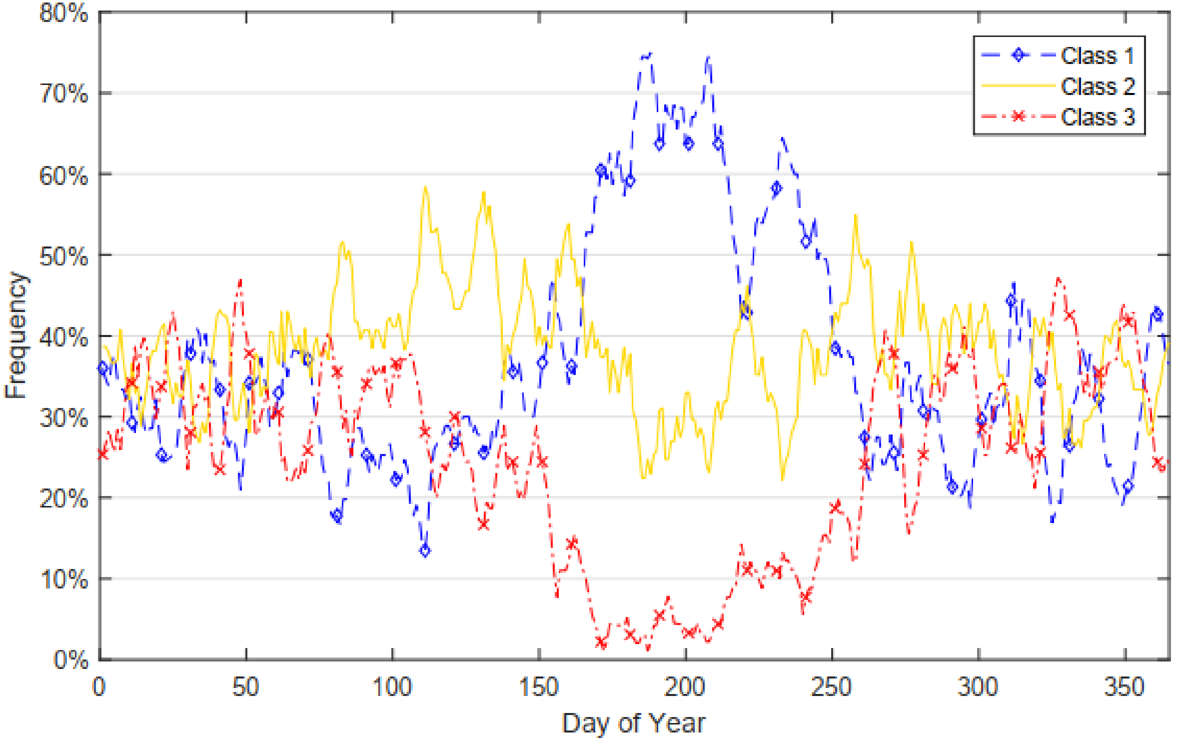

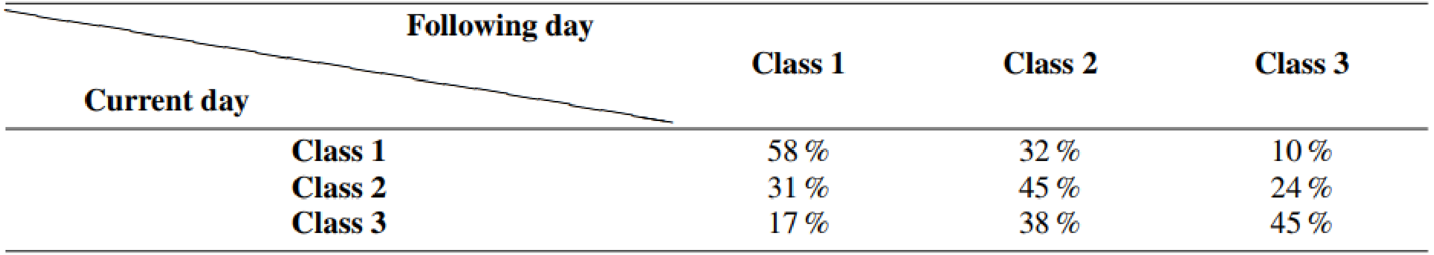

Following day Current day	Class 1	Class 2	Class 3
Class 1	58 %	32 %	10 %
Class 2	31 %	45 %	24 %
Class 3	17 %	38 %	45 %

---

[1] M. Schroedter-Homscheidt, M. Kosmale, S. Jung, and J. Kleissl, “Classifying ground-measured 1 minute temporal variability within hourly intervals for direct normal irradiances,” *Meteorologische Zeitschrift*, 2018.

Synthetic data extension: soiling rate and natural cleaning

- Soiling rate is drawn according to probability for each variability class
- Rain cleaning action quantified in cleaning efficiency

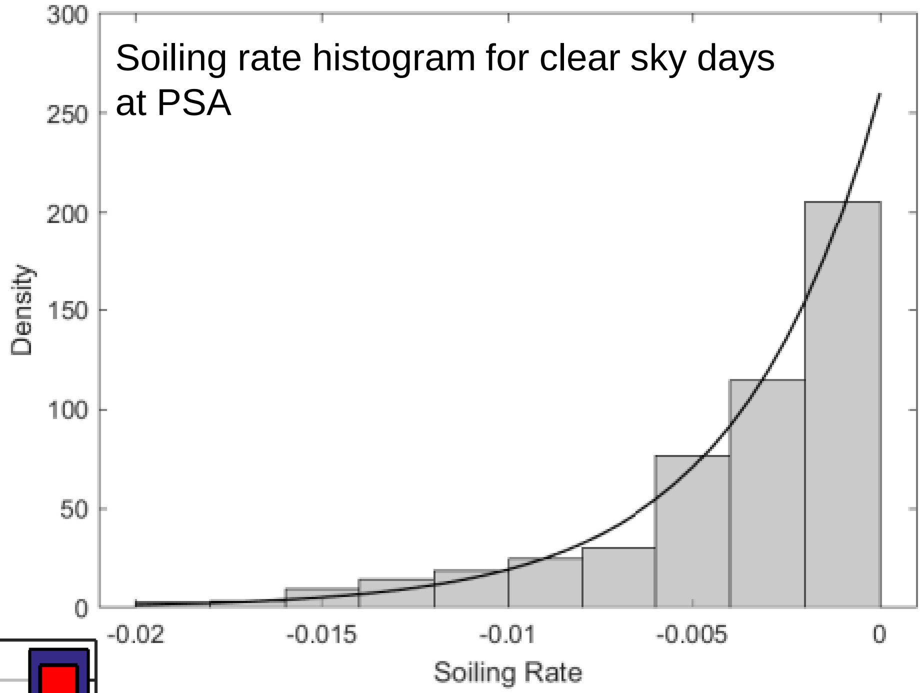
Soiling rate histogram for clear sky days at PSA

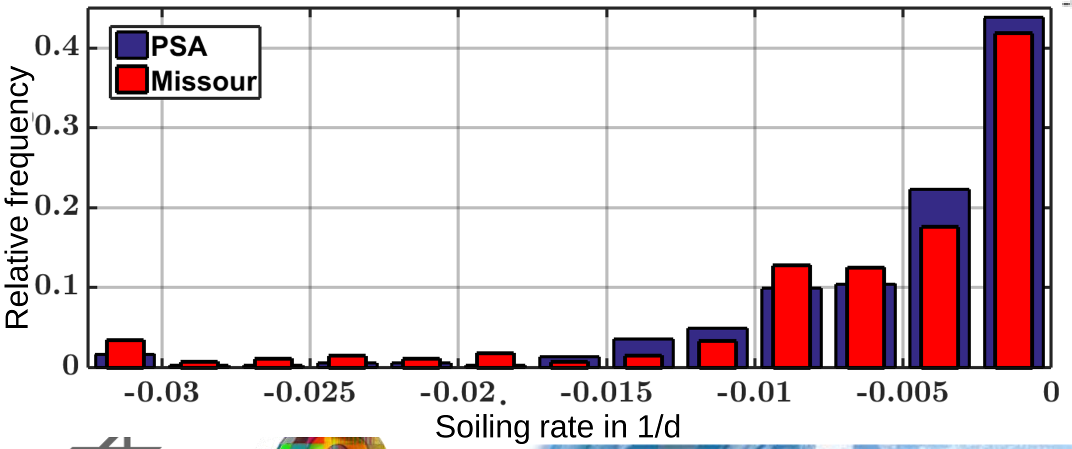

Soiling rate histograms for PSA and Missour, Morocco and all classes

Learning progress

- Agent begins with **random strategy**
- **Agent is updated** after each training year according to reward
- Repeat 10 times on each test year and 15 different years (**training run**)
- **Validation set**: fix dataset of 20 years
- **Agent is tested** on validation set after each training run
- RPI increases with training run
- **Exit condition**: no RPI-improvement in the last 20 training runs
- Resulting agent is the final cleaning policy

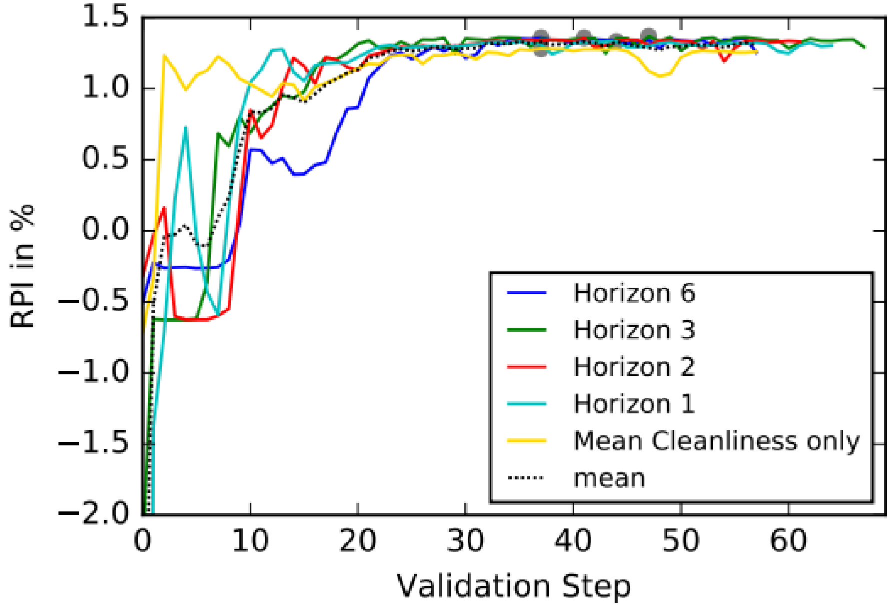

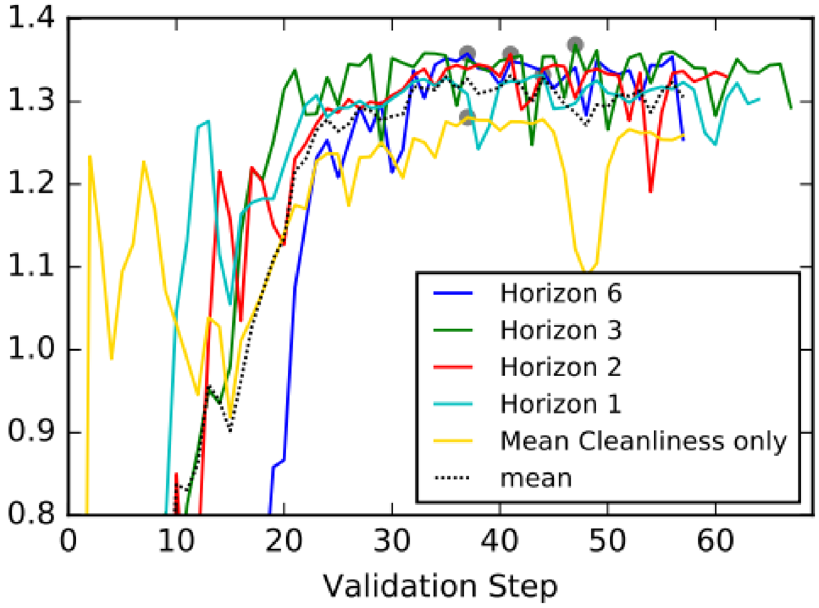

Application of soiling forecast in cleaning policy: results

- Reinforcement learning strategy nearly doubles the RPI of the condition based strategy if no forecast is provided
- Reinforcement learning strategies achieve RPI of 1.3 % if no forecast is provided
- RPI of 1.4% with forecast information

- Note: PSA is not a heavy soiling location
- Much higher results are expected for regions with higher dust loads

Forecast Horizon in days	**RPI in [%]**
ø	1.28
1	1.33
2	1.36
3	1.37
6	1.36

Evolution of soiling and cleaning in solar field

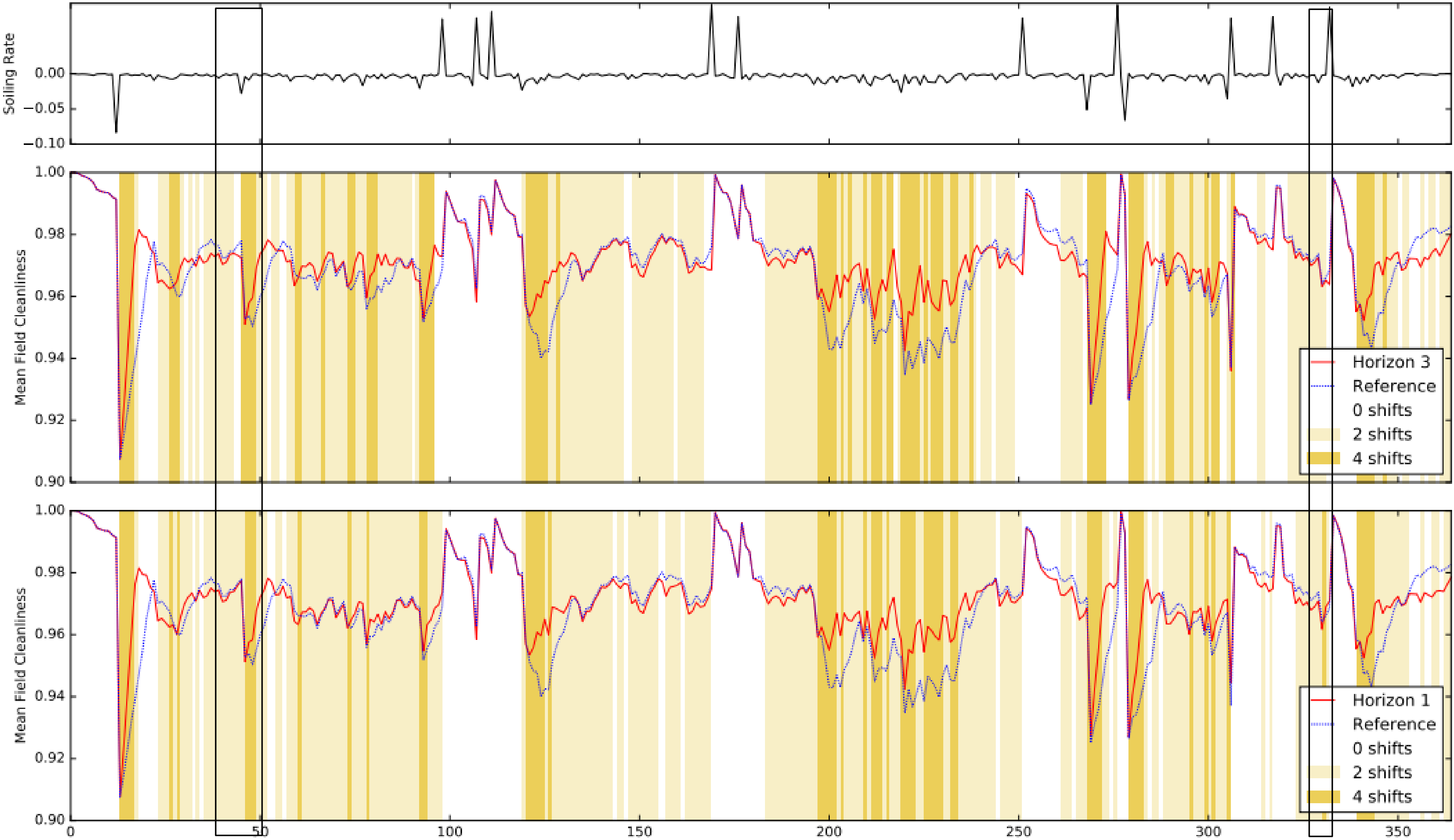

Wolfertstetter, F., Wilbert, S., Dersch, J., Dieckmann, S., Pitz-Paal, R., & Ghennioui, A. (2018). Integration of Soiling-Rate Measurements and Cleaning Strategies in Yield Analysis of Parabolic Trough Plants. *Journal of Solar Energy Engineering*, *140*(4), 041008.

Conclusion reinforced learning strategies

- Solar field cleaning model as an add on to yield analysis software such as greenius
- Data extension algorithm for training of reinforcement learning algorithms
- Reinforcement learning applied to cleaning optimization
- Reinforcement learning agent nearly **doubles the profit increase** compared to condition based cleaning strategies
- Inclusion of forecast for high/low soiling rate and irradiance class can further increase the profit
- Better results expected for sites with higher soiling load

Thank you for your attention

fabian.wolfertstetter@dlr.de

more details can be found in these two studies:

Terhag, F., Wolfertstetter, F., Wilbert, S., Hirsch, T., & Schaudt, O. (2019, July). Optimization of cleaning strategies based on ANN algorithms assessing the benefit of soiling rate forecasts. In *AIP Conference Proceedings* (Vol. 2126, No. 1, p. 220005). AIP Publishing LLC.

Wolfertstetter, F., Wilbert, S., Dersch, J., Dieckmann, S., Pitz-Paal, R., & Ghennioui, A. (2018). Integration of soiling-rate measurements and cleaning strategies in yield analysis of parabolic trough plants. *Journal of Solar Energy Engineering*, *140*(4).

Literature on soiling model:
http://wascop.eu/wp-content/uploads/2018/06/WASCOP_deliverable_3.2_final_plainText.pdf

Soiling rate

- Soiling rate = reduction of cleanliness over time
- Soiling rate is dependent on time and location
- Not (yet) a standard measurement parameter
- Little information available in target regions for so

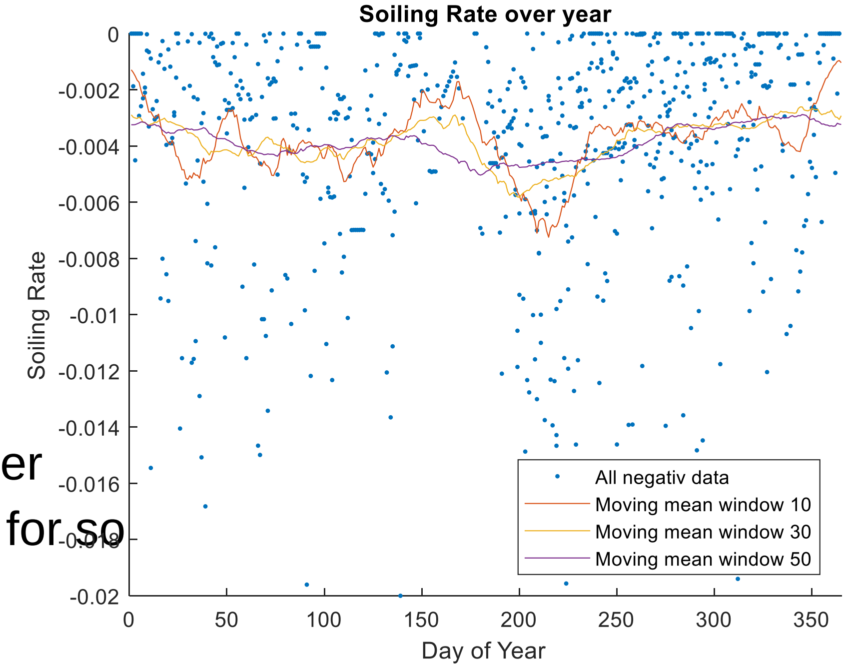

Source: Google Eatrth

SFERA-III
Solar Facilities for the European Research Area

THANK YOU FOR YOUR ATTENTION!
ANY QUESTIONS?

CSP – markets, services and future

Gonzalo Martin – Secretary General
gonzalomartin@protermosolar.com
29 April 2022

About Solar Concentra

The technological Platform SOLAR CONCENTRA is a forum build up by the most representative agents in the Solar Thermal / Concentrating Solar sector.

It's an active tool that fosters the R&D activities in the sector and has the goal to implement this activities in Spain.

The outcomes are achieved due to the wide structure that holds the platform and the working groups that gather entities across the complete value chain

The technological platform began its activities in 2010.
Currently it is managed by Protermosolar.

Agenda

1. Introduction
2. Worldwide outlook
3. The future

1. Introduction

CSP is the alternative to fossil fuels dependence

a

CSP is not an alternative to the use of PV → CSP is actually an alternative to *fossil fuels*

b

Neither an "expensive" RES → indeed CSP improve the cost dynamics of the system

CSP is a dispatchable RES that, together with other dispatchable RES such as hydro or biomass, shall provide the necessary back-up to intermittent RES to fully decarbonize the electricity generation

List of acronyms:
CSP: Concentrating Solar Power
PV: Photovoltaics
RES: Renewable Energy Source

1. CSP is already cheaper than fossil fuels in some locations

CSP competes against fossil fuels and other dispatchable RES (Biomass and Hydro)

CSP, due to its solar resource needs, has lower growth potential than PV affecting its global installed capacity

However, for the same installed capacity, the cost reduction is almost 2x

CSP has still a significant potential for cost reduction, not only coming from R&D but also from greater installed capacity.

Nonetheless, PV and CSP will not compete but complement each other.

Figure ES.2 Global LCOEs from newly commissioned, utility-scale renewable power generation technologies, 2010-2020

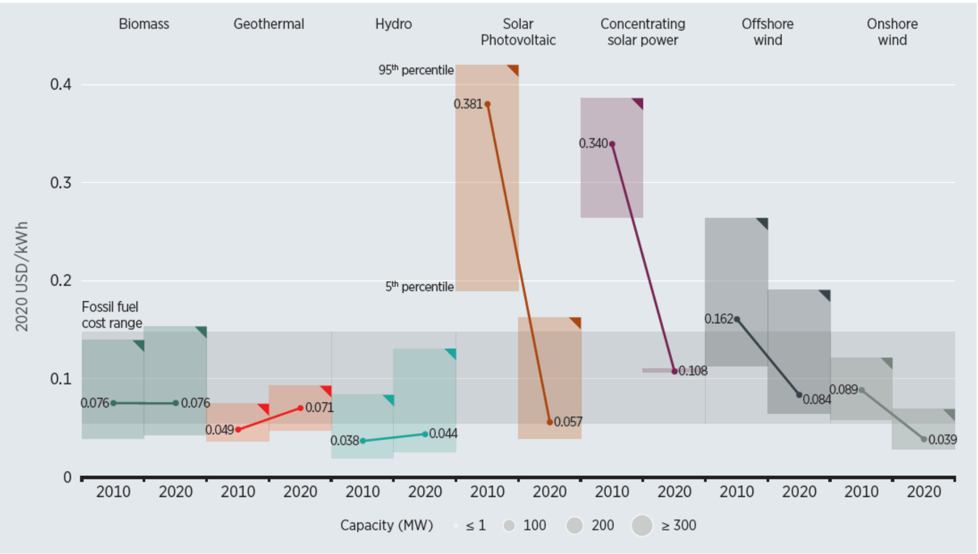

Source: IRENA Renewable Cost Database

Note: This data is for the year of commissioning. The thick lines are the global weighted-average LCOE value derived from the individual plants commissioned in each year. The project-level LCOE is calculated with a real weighted average cost of capital (WACC) of 7.5% for OECD countries and China in 2010, declining to 5% in 2020; and 10% in 2010 for the rest of the world, declining to 7.5% in 2020. The single band represents the fossil fuel-fired power generation cost range, while the bands for each technology and year represent the 5th and 95th percentile bands for renewable projects.

Figure ES.1 Global weighted-average LCOE from newly commissioned, utility-scale solar and wind power technologies, 2019-2020

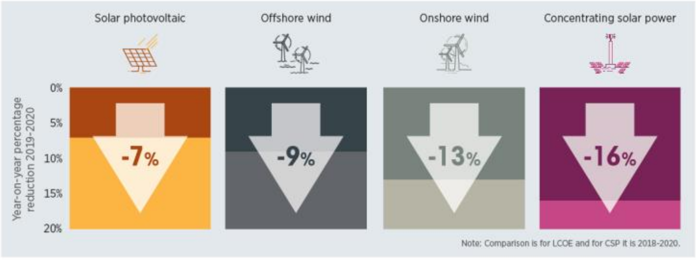

Note: Comparison is for LCOE and for CSP it is 2018-2020.

Source: IRENA Renewable Cost Database

PV

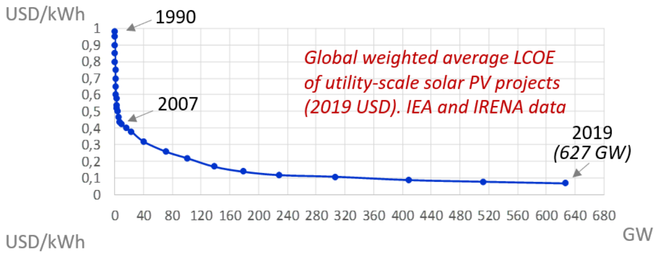

Global weighted average LCOE of utility-scale solar PV projects (2019 USD). IEA and IRENA data

WIND

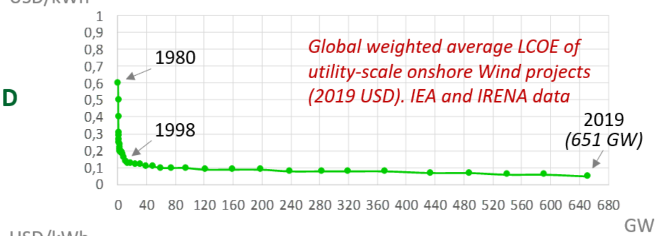

Global weighted average LCOE of utility-scale onshore Wind projects (2019 USD). IEA and IRENA data

CSP

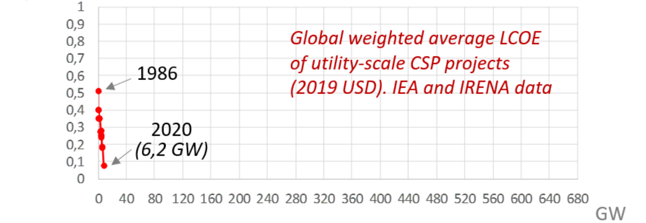

Global weighted average LCOE of utility-scale CSP projects (2019 USD). IEA and IRENA data

Source: Julian Blanco. PSA
Internal working document

1. CSP shall become the back-up for intermittent RES

Savings are in the pool price, also by no longer keeping excessive fossil fuels plants.

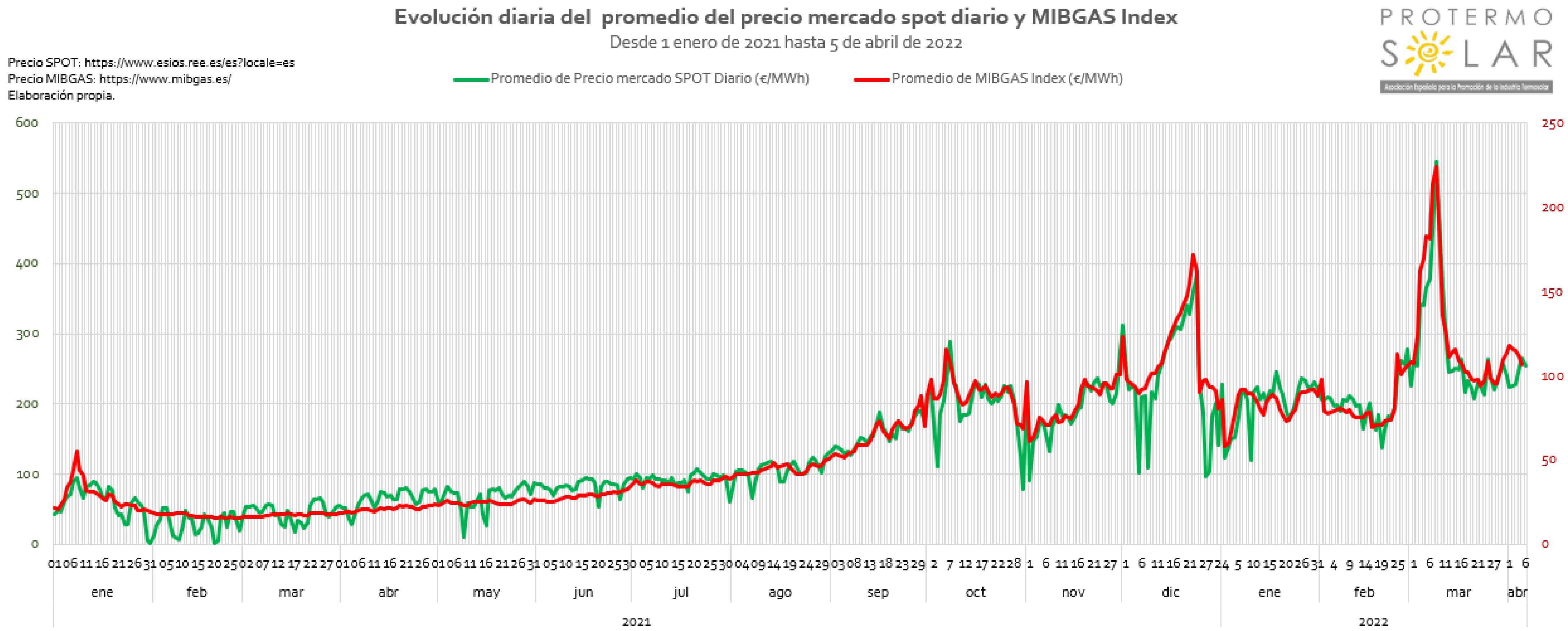

Spain

Spain has the most significant shares of excess capacity of all the countries included in this report, where 13 GW or 36% of fossil fuels installed in the country was not required to service peak demand in 2019.

Retiring excess fossil fuel capacity would yield total annual savings of €425 million EUR ($476 million USD) from FOM costs. The early retirement of the aging coal capacity alone would save nearly €361 million EUR ($405 million USD) per year.

Source: Ripe for Closure: Accelerating the energy transition and saving money by reducing excess fossil fuel capacity. September 2021. Centre for Research on Energy and Clean Air.

1. The real contribution of fossil fuels

PROTERMO SOLAR
Asociación Española para la Promoción de la Industria Termosolar

Natural gas CC generates less than 25% almost always matching demand

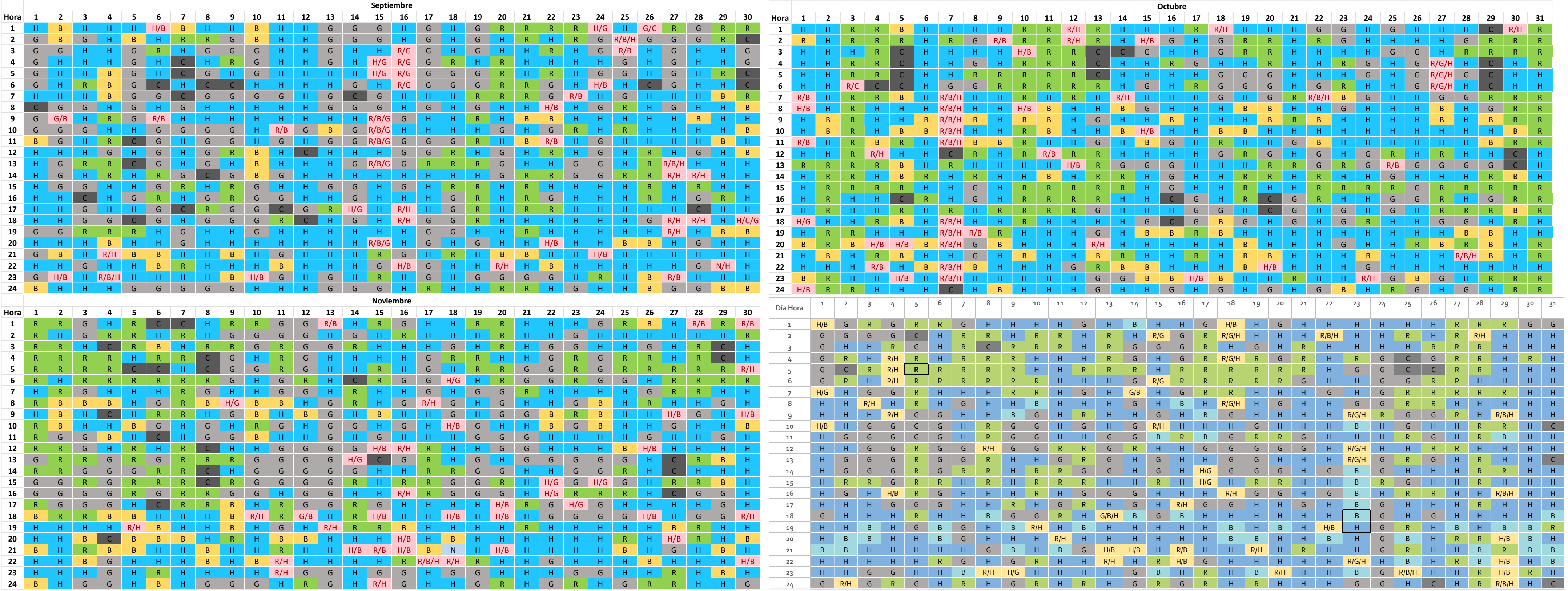

Month	Day	Night	Subtotal
Sep	20,16%	24,79%	22,47%
Oct	17,24%	22,21%	20,14%
Nov	24,52%	27,02%	26,08%
Dec	19,12%	19,84%	19,57%
Jan	20,75%	22,88%	22,17%
Feb	18,33%	22,57%	20,80%
Subtotal	19,94%	23,16%	21,86%

	CC generation [MWh]	CC contribution [%]
Sep	1.353.537,62	24,40%
Oct	616.721,98	24,85%
Nov	1.618.940,90	28,80%
Dec	1.186.561,71	22,27%
Jan	1.325.841,92	23,91%
Feb	949.405,43	22,53%
Subtotal	7.051.009,56	24,53%

1. Photovoltaics must be complemented every day

Photovoltaics (PV) only/mainly produce when the Sun is shinning

PV Generation in Spain

Cumulative per hour in 2019

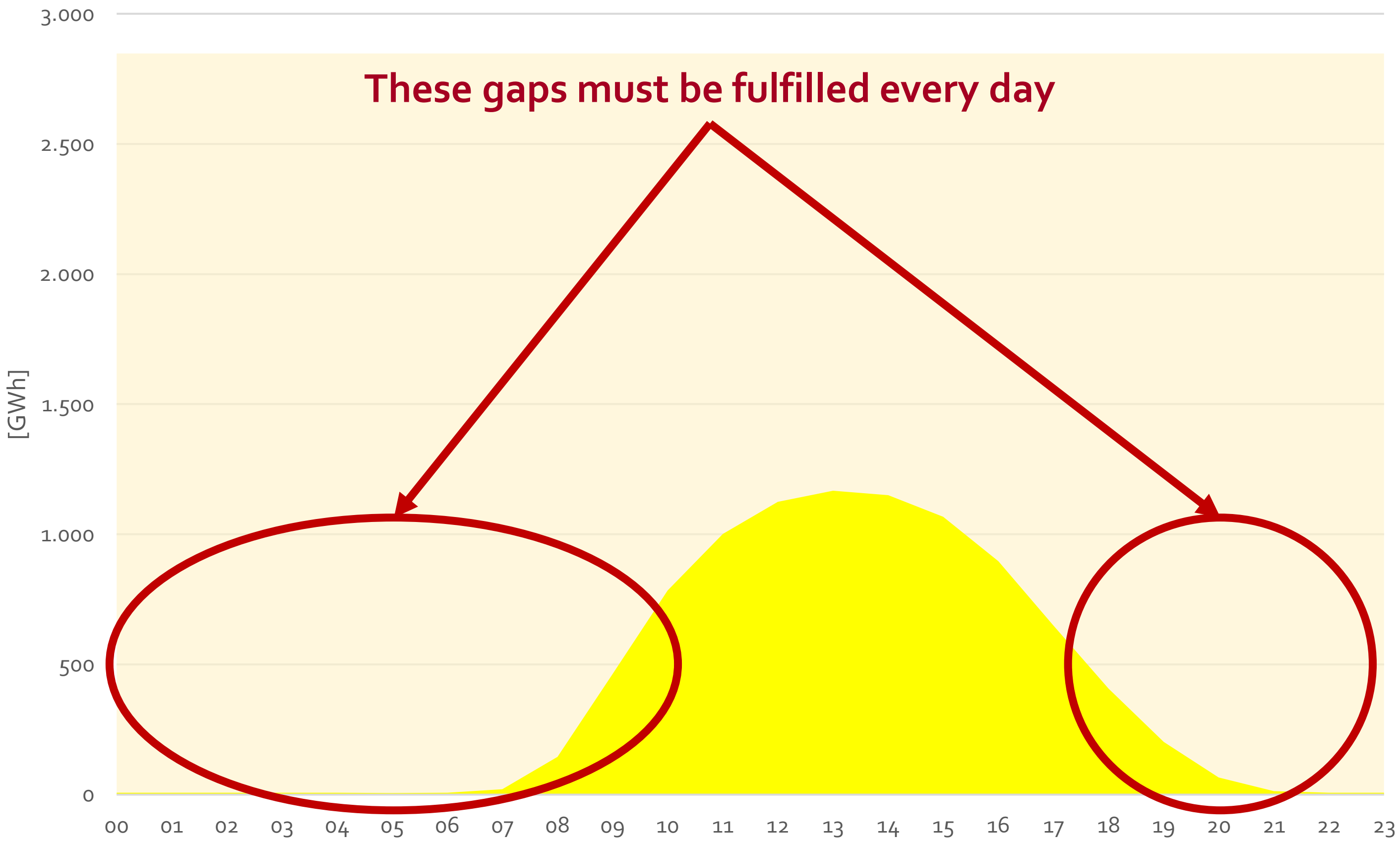

1. Intermittent RES pose a risk to the electricity market

The electricity market might present dysfunctionalities with lack of dispatchable RES

Duck curve 2030 - Spain

Source: Made by PwC with data from REE

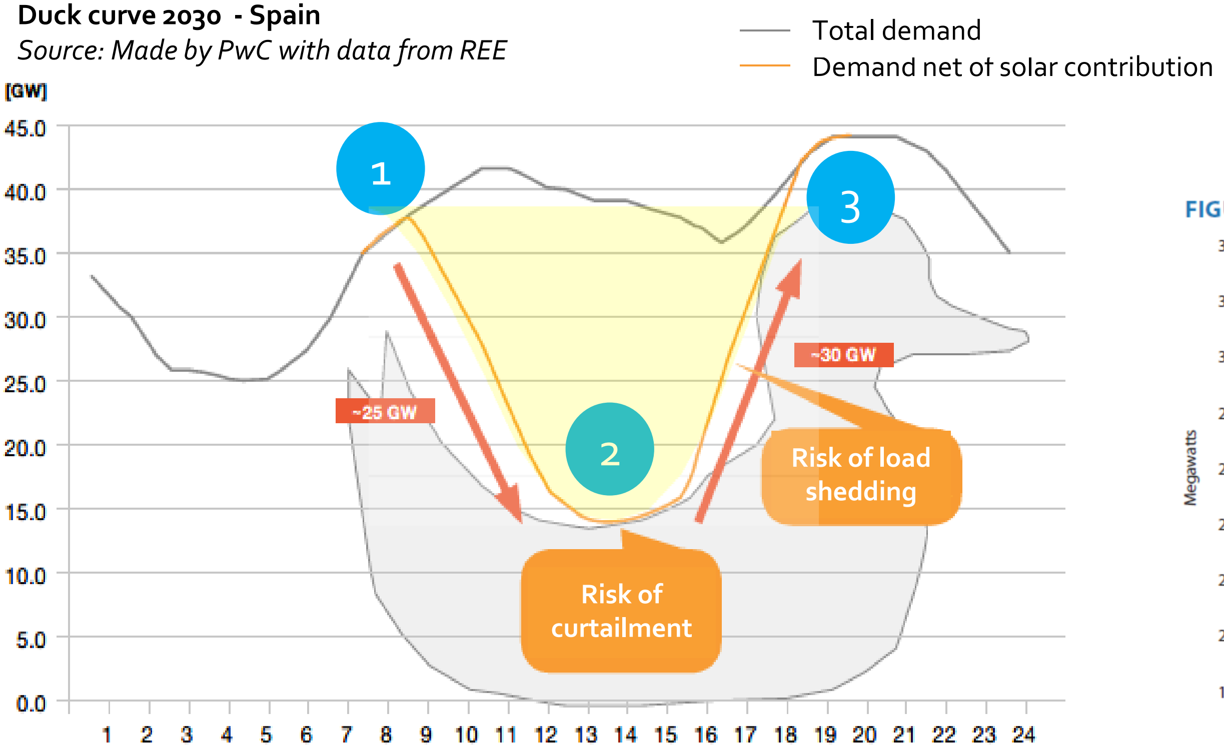

FIGURE 1.5 Peak times of daily net electricity load (after solar PV): California's "duck curve"

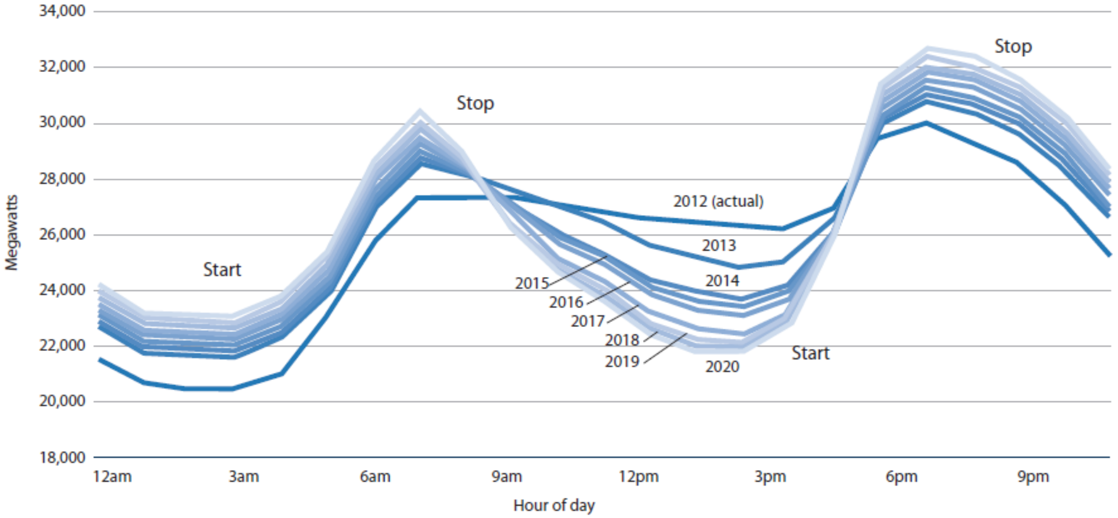

Source: CAISO 2016.

https://www.fundacionnaturgy.org/publicacion/integracion-de-las-tecnologias-renovables-en-la-transicion-energetica/

World Bank. 2021. Concentrating Solar Power: Clean Power on Demand 24/7. Washington, DC: World Bank.

A large penetration of intermittent or non-dispatchable **Renewable Energy Sources (RES)** might create a significant dysfunctionality in the electricity market:

1. Need to decouple night energy supply during the morning.
2. Risk of curtailment/excess of energy and therefore prices close to zero.
3. Difficulties to reach the demand increase at sunset.

1. CSP is the technology to complement PV

CSP with storage for night supply is the natural complement to daily PV generation

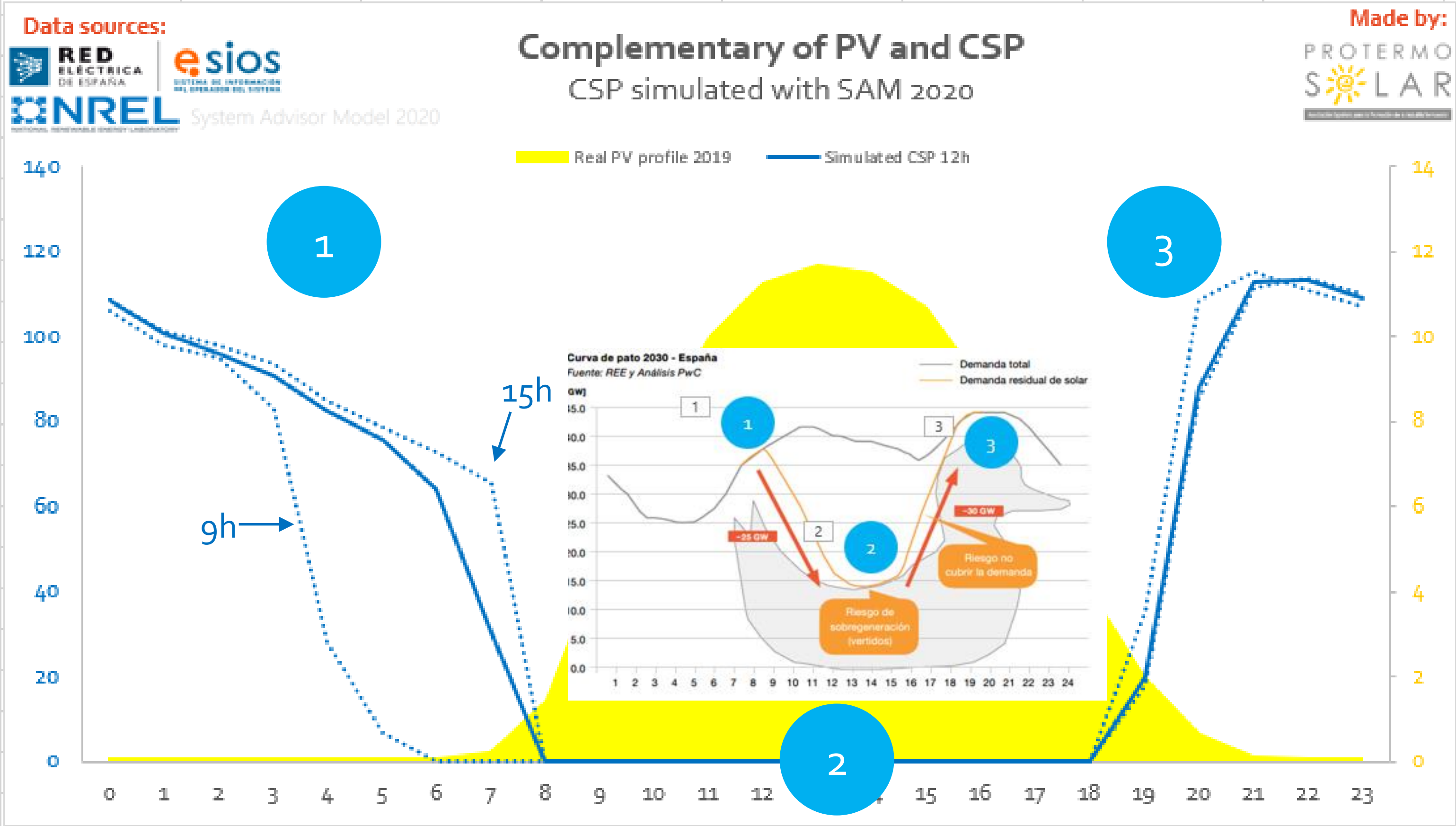

Simulation parameters:

- Location: village in Spain with most CSP
- Forced to zero from 8h to 18h
- Parabolic trough
- Solar multiple 2.5x (can be adjusted)
- Capacity 150 MW (irrelevant)
- Values in MWh

Simulated with SAM 2020 from NREL

PV real profile:

- Location: Spain
- Time series: Full year 2019
- Values in 0.1·GWh
- Actual cumulative hourly generation

Data obtained from REE

- New CSP will include large storage >9h
- Complementary Operation to PV, helping to mitigate the duck curve
- Capacity greater than 50 MW
- Lessons learnt after one decade of operation

1. Other services that CSP could provide to the system

PROTERMO SOLAR
Asociación Española para la Promoción de la Industria Termosolar

Strategic reserve, price arbitration and thermal battery

1

With the appropriate price signal:
- <u>Reserve</u> for the yearly 100h peak hours
- > 3,5 GWhe currently available (could be x2) in winter to store energy for days until the system demands it

2

Optional:
- Price arbitration
- Curtailment collection for later dispatch

(simply adding a electrical heater)

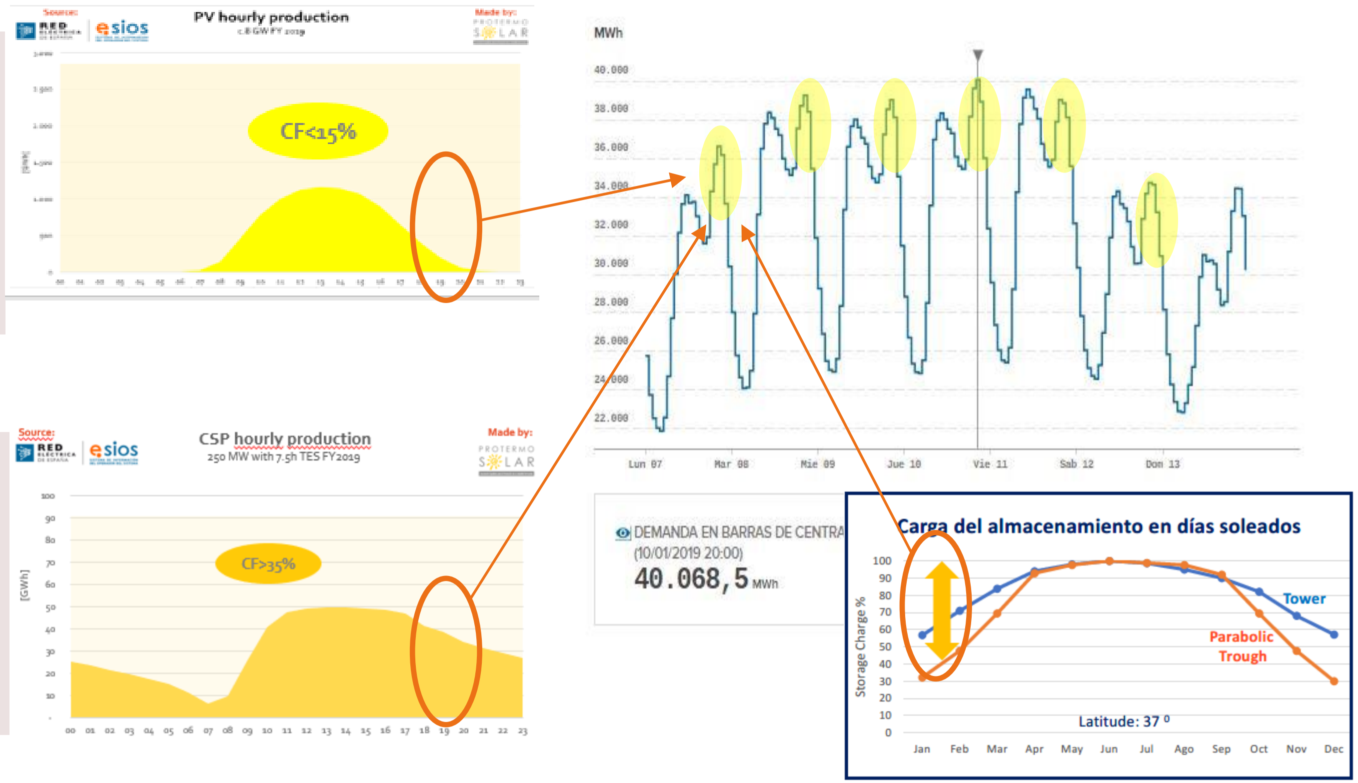

There are >7 GWhe already available, easily expandable to 12-14 GWhe and in 2030, according to the NECP, will be more than 60 GWhe. This storage can provide additional services to the system at a low cost.

1. CSP does not increase the system cost

Reduces curtailments by keeping same electricity cost

Example of the study carried out in Portugal

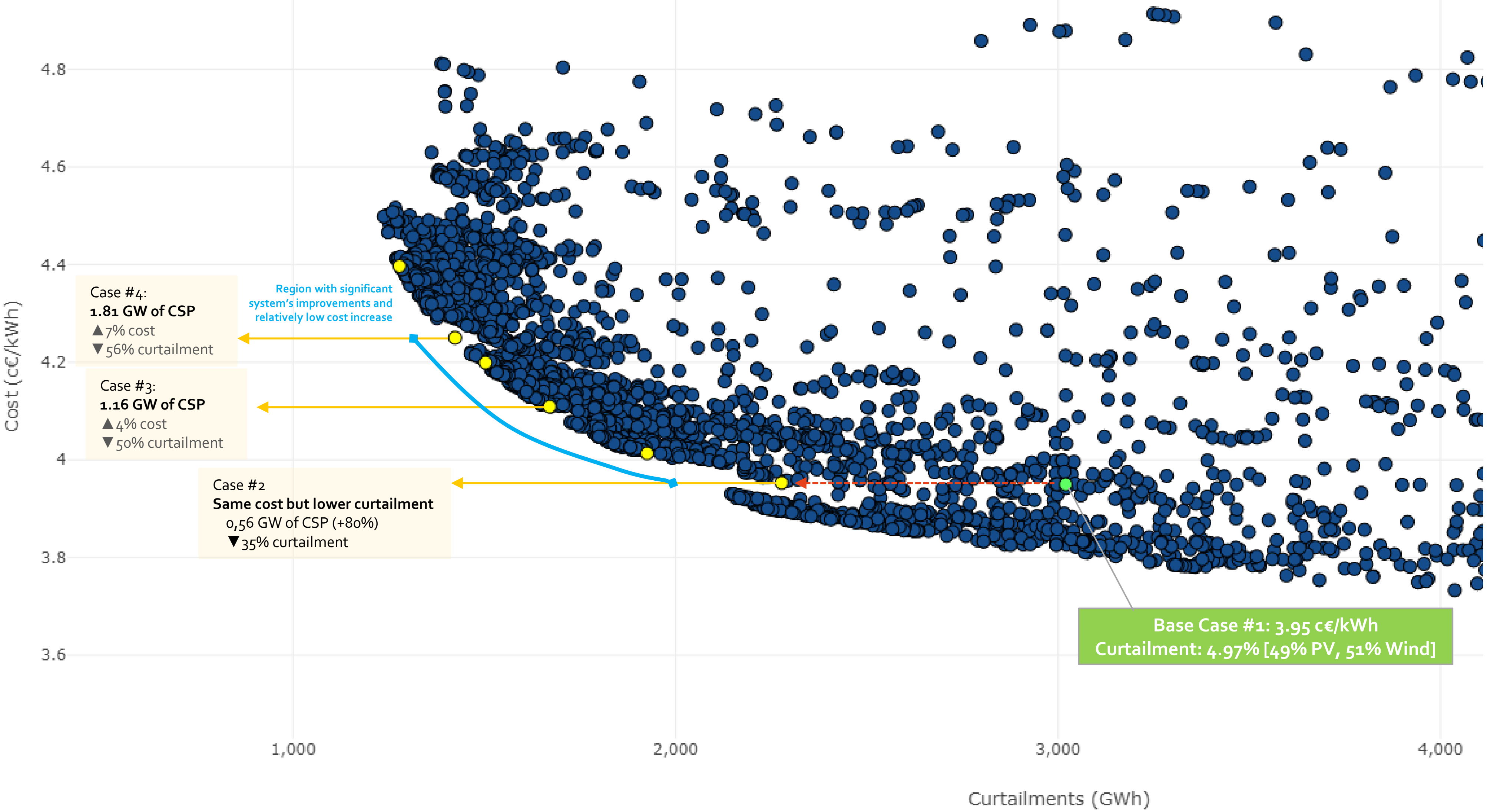

Case #4:
1.81 GW of CSP
▲7% cost
▼56% curtailment

Region with significant system's improvements and relatively low cost increase

Case #3:
1.16 GW of CSP
▲4% cost
▼50% curtailment

Case #2
Same cost but lower curtailment
0,56 GW of CSP (+80%)
▼35% curtailment

Base Case #1: 3.95 c€/kWh
Curtailment: 4.97% [49% PV, 51% Wind]

1. Introduction

Besides Hydro, TES in CSP was the most deployed technology in 2017…

Figure ES8: Global operational electricity storage power capacity by technology, mid-2017

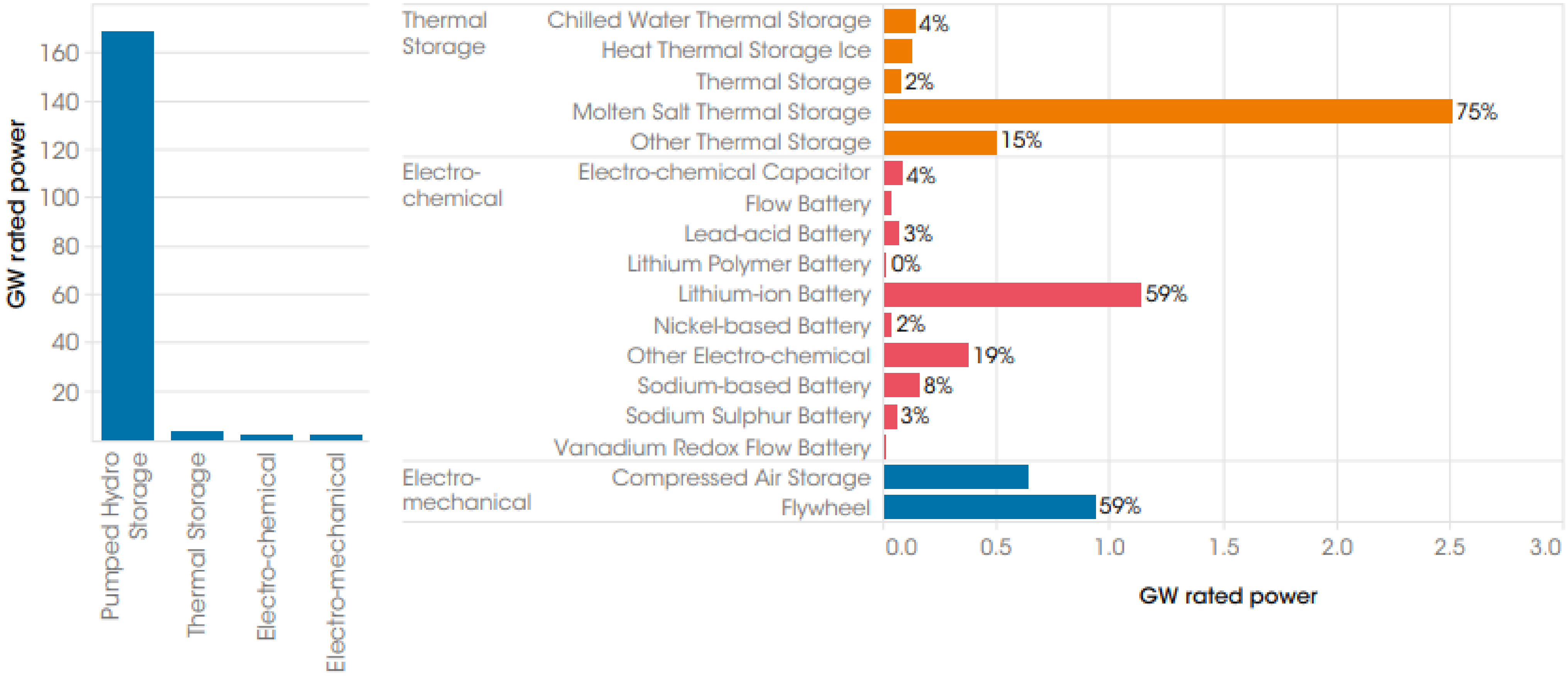

Source: IRENA (2017), Electricity Storage and Renewables: Costs and Markets to 2030, International Renewable Energy Agency, Abu Dhabi

1. Introduction

…with promising growth perspectives

Figure ES3: Electricity storage energy capacity growth by source, 2017-2030

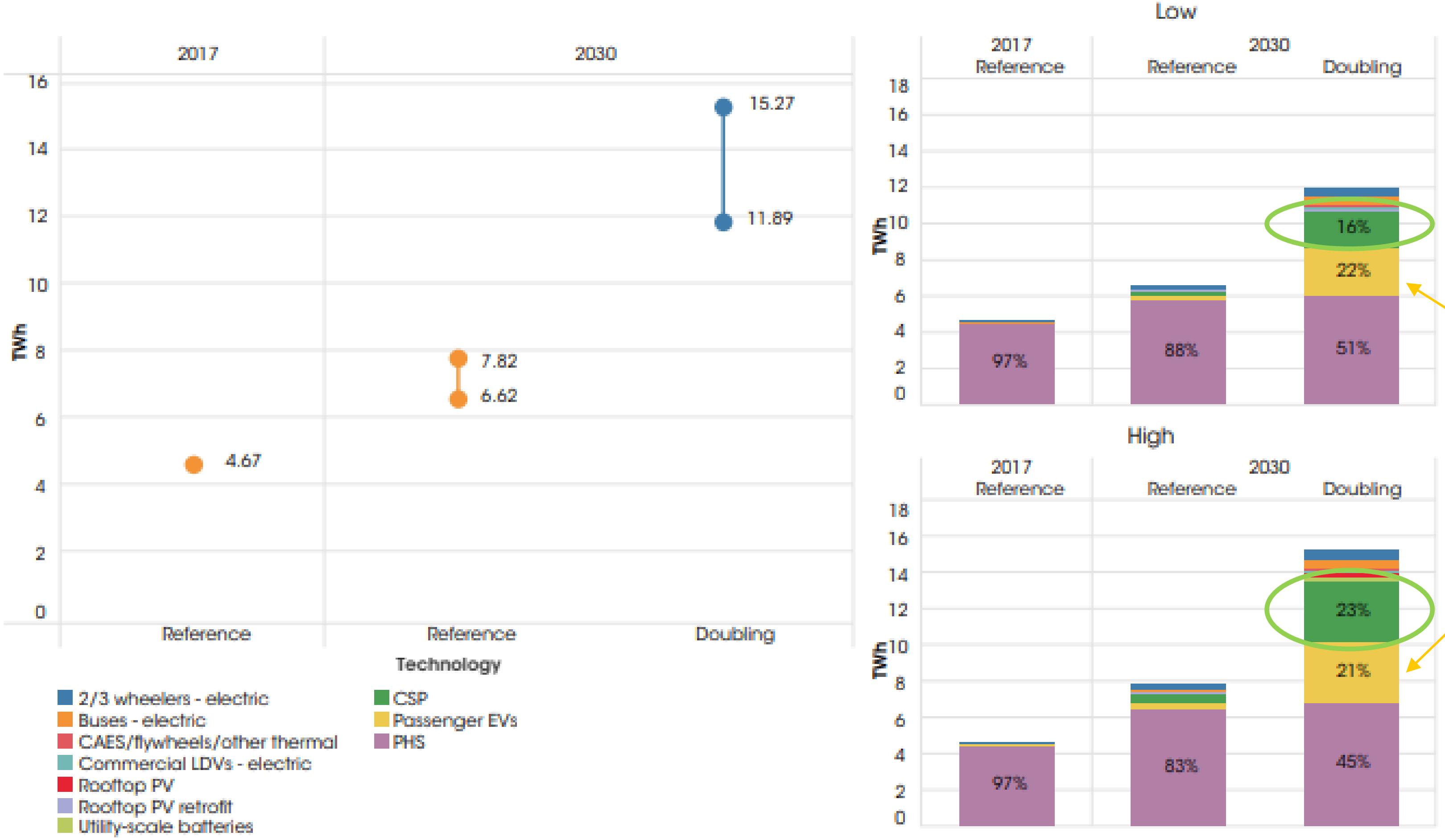

Not utility-scale storage

Source: IRENA (2017), Electricity Storage and Renewables: Costs and Markets to 2030, International Renewable Energy Agency, Abu Dhabi

Agenda

1 Introduction

2 Worldwide outlook

3 The future

2. Recognition of the value provided by CSP storage

Solar Concentra

Spain foresees 5 GW of new CSP until 2030

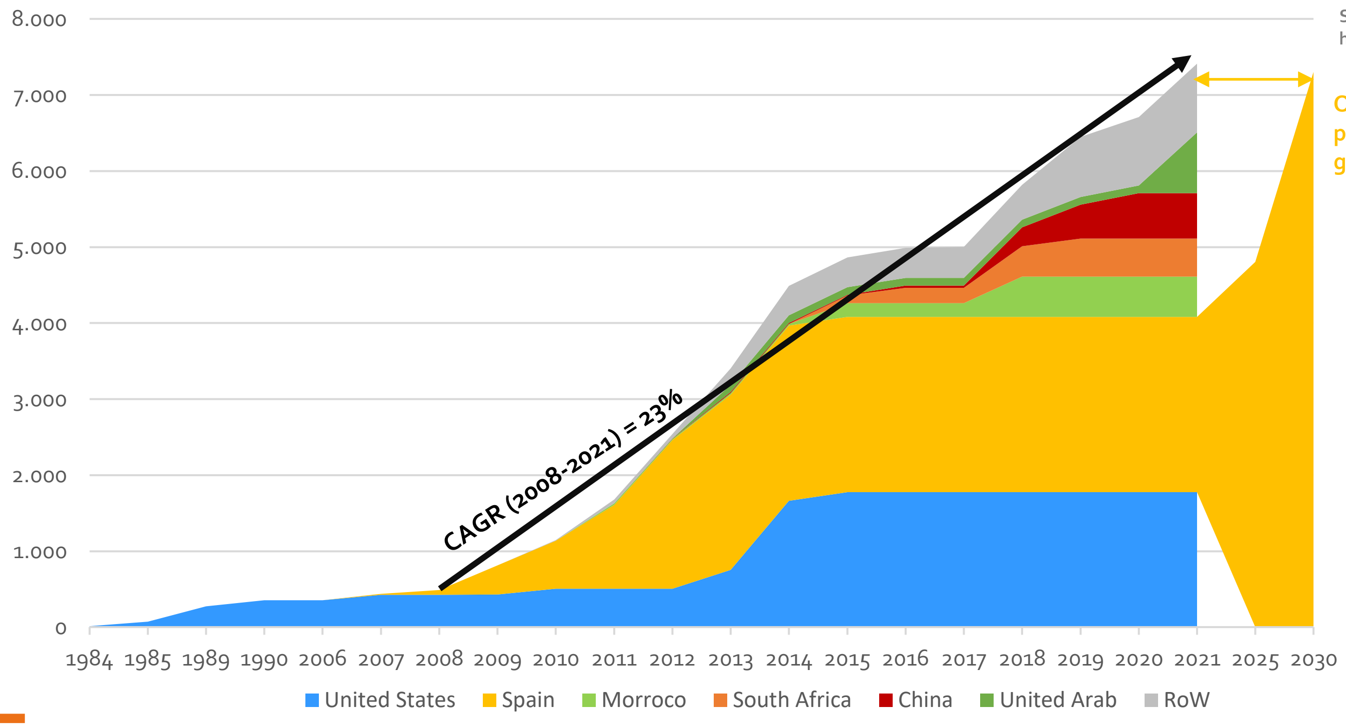

Concentrating Solar Thermal Power Global Capacity [MW]

Includes 154 MW non-operational and 860 MW under construction with expected COD in 2021

Period 2021-2030 only includes the 5 GW of the Spanish national plan

Edited by:

PROTERMO SOLAR

Source:
https://csp.guru/

Only the Spanish plan represents a global CAGR of 6%

1 Spain led the CSP global growth in 2008-2013 with 2.3 GW

2 Despite the Spanish stoppage in 2014, other countries kept installing CSP

3 Spain has submitted to the EC* its plan to reduce CO2 emissions in 2030; which includes 5 GW of new CSP.

4 This "new" CSP must include a significant storage to reach a number of operating hours >3.000 and up to 4.000 per year

Thanks to its massive storage, CSP is the perfect complement to PV to generate 24/7 using Solar energy at a very low price.

---

*European Commission

2. Spanish plan to install 5 GW of new CSP

Solar Concentra

The plan was submitted to the European Commission on the 31 March 2020

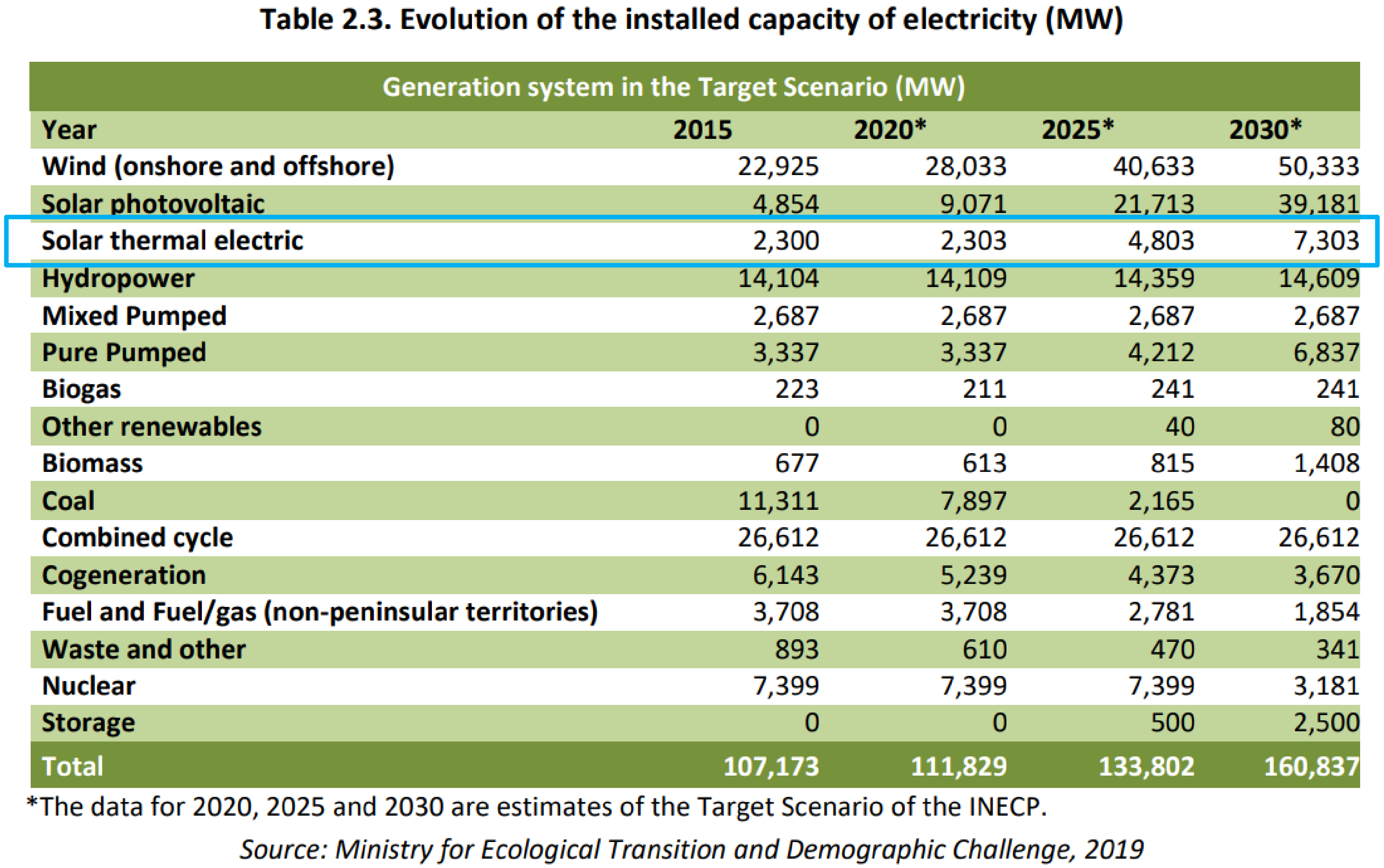

Table 2.3. Evolution of the installed capacity of electricity (MW)

Generation system in the Target Scenario (MW)				
Year	**2015**	**2020***	**2025***	**2030***
Wind (onshore and offshore)	22,925	28,033	40,633	50,333
Solar photovoltaic	4,854	9,071	21,713	39,181
Solar thermal electric	2,300	2,303	4,803	7,303
Hydropower	14,104	14,109	14,359	14,609
Mixed Pumped	2,687	2,687	2,687	2,687
Pure Pumped	3,337	3,337	4,212	6,837
Biogas	223	211	241	241
Other renewables	0	0	40	80
Biomass	677	613	815	1,408
Coal	11,311	7,897	2,165	0
Combined cycle	26,612	26,612	26,612	26,612
Cogeneration	6,143	5,239	4,373	3,670
Fuel and Fuel/gas (non-peninsular territories)	3,708	3,708	2,781	1,854
Waste and other	893	610	470	341
Nuclear	7,399	7,399	7,399	3,181
Storage	0	0	500	2,500
Total	**107,173**	**111,829**	**133,802**	**160,837**

*The data for 2020, 2025 and 2030 are estimates of the Target Scenario of the INECP.

Source: Ministry for Ecological Transition and Demographic Challenge, 2019

Downloaded from: https://ec.europa.eu/energy/sites/default/files/documents/es_final_necp_main_en.pdf

2. Worldwide outlook

Solar Concentra

The global trend is bigger plants with presence of PV

Mature

+

-

NooRo I, II y III (Marruecos) → 510 MW

PPA 25 years

CCP: 160 MW + 3h @ 18c$/kWh

CCP: 200 MW + 7h @ 13c$/kWh

MST: 150 MW + 7h @ 15c$/kWh

700 MW + 250 MW← Noor I (DEWA, EAU)

PPA 35 years, 15h storage

3x200 MW CCP

1x100 MW MST

250 MW PV

7,3c$/kWh CSP y 2,4c$/kWh PV

Midelt (Marruecos) → 800 MW

PPA 25 years

PV integrated into TES

7 c$/kWh

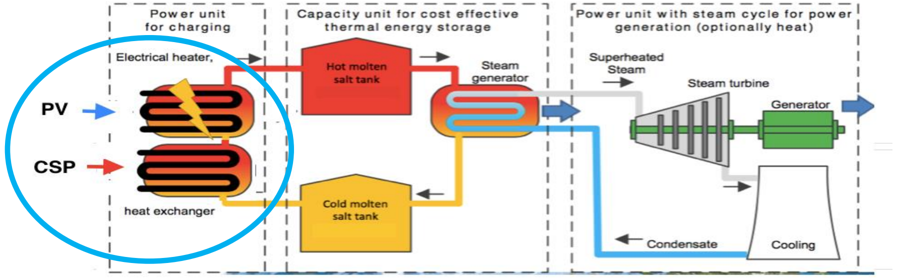

Redstone (Sudáfrica) → 100 MW
Torre con 12h almacenamiento
Tarifa 20 años con perfil horario

Likana (Chile)
Contrato financiero
PV diurna, CSP nocturna

China
5*100 MW
Adjudicados en octubre

2. Significant increase in size

The economies of scale are significant in the latest projects

DEWA

Solar Field Plot

Agenda

Solar Concentra

1. Introduction
2. Worldwide outlook
3. The future

3. CSP vs Batteries storage cost

CSP with storage is and remains cheapest for more than 4 hours storage

<u>Results</u>:

1. PV+BESS is cheaper than CSP+TES for short storage durations up to 2–3 hours.

2. CSP+TES is and remains cheapest for more than 4 hours storage except in the low-cost PV+BESS case where very strong PV+BESS learning is assumed, and the tipping point moves to 10 storage hours.

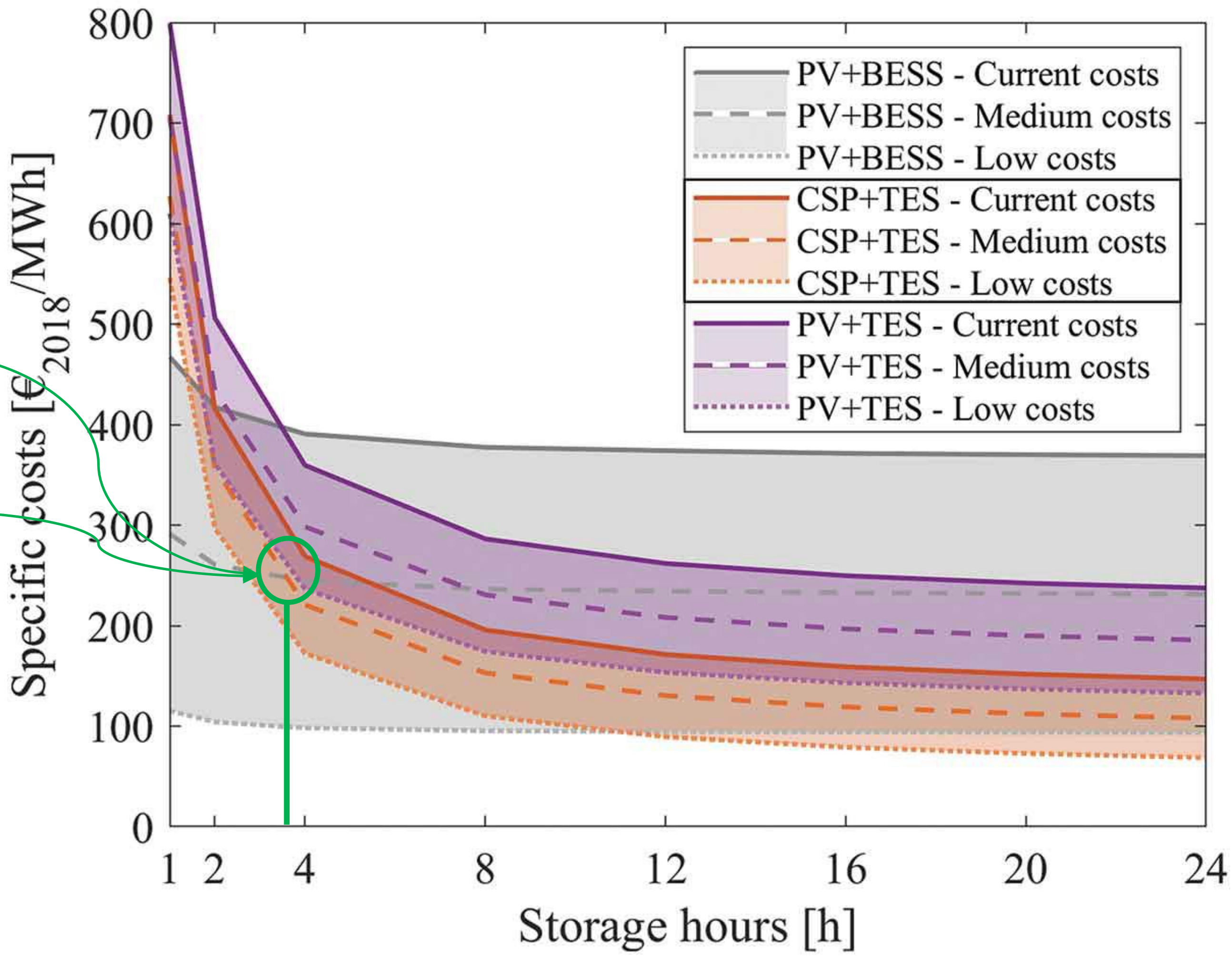

A very recent paper (2021) contrasted the cost of:

- PV + utility-scale Li-Ion batteries (PV+BESS)
- CSP + two-tank molten-salt (CSP+TES)
- TES using electric heater (PV+TES)

The reference case is a continuous load of 100MW during the pre-specified period (from 1 to 24h after sunset).

Franziska Schöniger, Richard Thonig, Gustav Resch & Johan Lilliestam (2021) Making the sun shine at night: comparing the cost of dispatchable concentrating solar power and photovoltaics with storage, Energy Sources, Part B: Economics, Planning, and Policy, DOI: 10.1080/15567249.2020.1843565
https://www.tandfonline.com/doi/full/10.1080/15567249.2020.1843565

3. TES potential in Spain

The potential TES capacity in 2030 would exceed the 60 GWhe

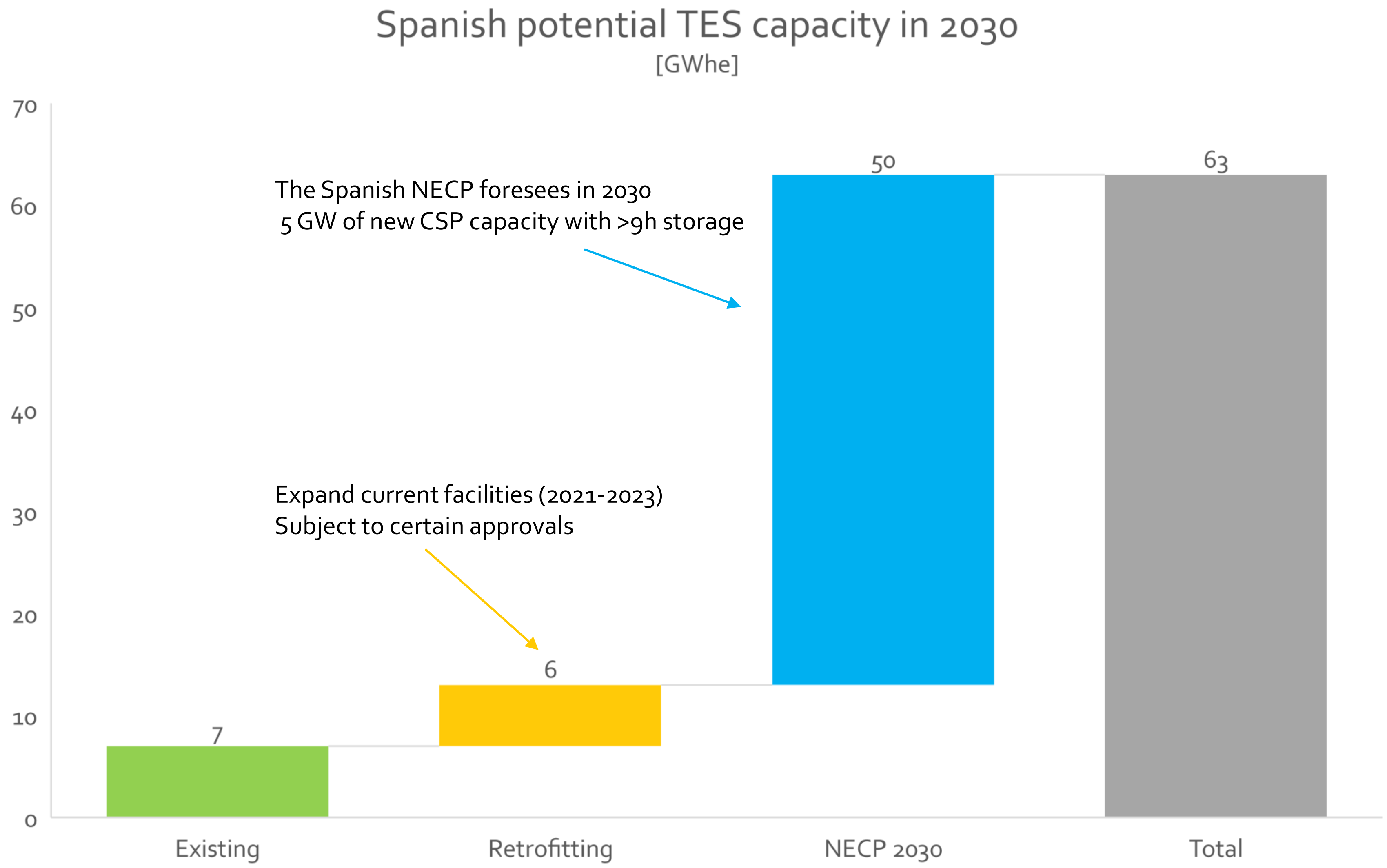

The Spanish NECP foresees in 2030
5 GW of new CSP capacity with >9h storage

Expand current facilities (2021-2023)
Subject to certain approvals

3. CSP is in the *España Vaciada*

The current TES capacity in Spain is 7 GWhe

Spain

- 49 plants with a stable yearly generation of c. 5 TWh
- GDP contribution >1.450 M€ (2018) and > 5k jobs (source: APPA Renovables)
- Supply chain from the entire country (Asturias, País Vasco, Cataluña, Madrid…)
- Each plant is the economic drive of the region

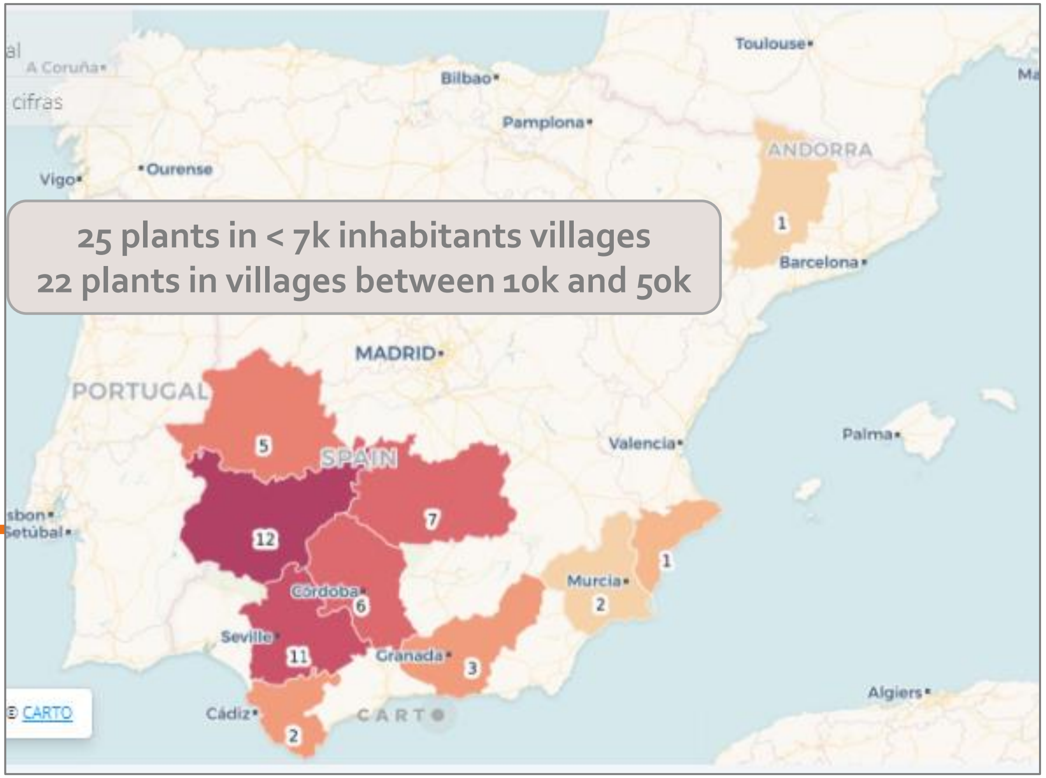

25 plants in < 7k inhabitants villages
22 plants in villages between 10k and 50k

Type	Plants	Power (MW)
Parabolic Trough 50 MW without Storage	27	1350
Parabolic Trough 50 MW With storage	17	850
Saturated Steam Tower	2	31
Molten Salt tower with storage	1	20
Fresnel	1	30
Hybrid Solar/Biomass	1	22
TOTAL	**49**	**2303**

3. Double the TES capacity by retrofitting

Many existing plants are designed for a TES add-on

CSP and PV are mature as separate technologies, however there is plenty of room to implement as a single unit.

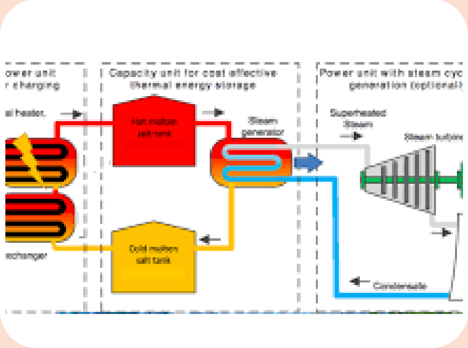

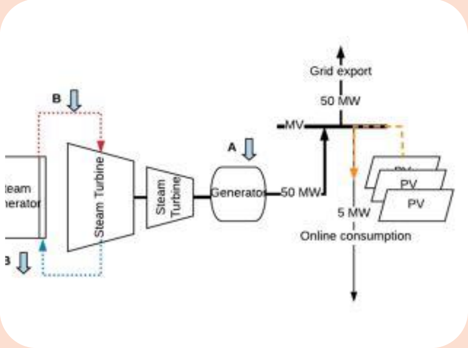

Generation to the grid

1. Improve design considering annual operating hours and capacity factors

2. Control system to keep max load to the grid

3. Improvement on the CSP fraction (new solar field designs)

Integration into the process (TES)

4. Analysis of PV integrated into the TES system – develop new systems for electrical charge

5. Research on control system to allow thermal and electrical load

6. Impact on tanks foundations

Auxiliary consumption

7. New electrical designs of the facility

8. Technology integration, use of PV, floating PV, batteries, etc. into the balance of plant.

Prototypes are needed as debt lenders and financing institutions would not facilitate a FOAK at commercial scale

Concentrating Solar Power plays a crucial role into the world electricity system to allow for a real decarbonization while decreasing the total system costs by phasing-out fossil fuels.

Solar Concentra

1 **Definition**

- CSP is the alternative to the use of fossil fuels.
- CSP does not cannibalize PV but, on the contrary boost its development.
- While using comprehensive tools, CSP results into a lower system cost.

2 **Services**

- Night-time base load / back-up to intermittent RES
- Strategic reserve
- Price arbitration
- End user of curtailments

3 **Storage maximization**

- With the use of European funds, the existing storage can be doubled implying savings for the consumers.
- All new CSP plants will include at least 6h of storage.

Solar Concentra

Thanks

Follow us:

gonzalomartin@protermosolar.com